UNIVERSITY OF OKLAHOMA

GRADUATE COLLEGE

RHODIUM CARBENOID INITIATED CASCADES FOR THE SYNTHESIS OF DIVERSE MEDIUM-SIZED HETEROCYCLES

A DISSERTATION

SUBMITTED TO THE GRADUATE FACULTY

In partial fulfillment of the requirements for the

Degree of Doctor of Philosophy (Ph.D.)

By

NICHOLAS P. MASSARO

Norman, Oklahoma

2019

RHODIUM CARBENOID INITIATED CASCADES FOR THE SYNTHESIS OF DIVERSE MEDIUM-SIZED HETEROCYCLES

A DISSERTATION APPROVED FOR THE DEPARTMENT OF CHEMISTRY AND BIOCHEMISTRY

BY

Dr. Indrajeet Sharma, Chair

Dr. Steven C. Crossley

Dr. Daniel T. Glatzhofer

Dr. Adam S. Duerfeldt

Dr. Anthony W. Burgett

Dedication

I dedicate this thesis to my wife for her overwhelming support throughout our journey here in Oklahoma.

Abstract

Medium-sized rings (8–12 membered) are a unique class of cyclic molecules. These structures are present within a plethora of relevant natural products often possessing enhanced pharmacokinetic properties due to their dynamic structures. However, these molecules are drastically underrepresented due to the challenges associated with their construction. For this reason, more efficient methods to synthesize medium-sized rings may increase their presence in future drug scaffolds. The research presented in this thesis provides a highly convergent strategy to access diverse medium-sized heterocycles. The strategy relies on ambiphilic rhodium vinylcarbenoid precursors and dual-purpose nucleophile/electrophile synthons, which allow for smaller ring construction followed by subsequent ring expansion. The initial ring annulation occurs via a heteroatom insertion into a highly electrophilic rhodium carbenoid, derived from diazo synthons, generating a reactive zwitterionic intermediate. This intermediate then undergoes an intramolecular aldol cyclization to provide an oxy-Cope capable synthon primed for ring expansion which, upon thermal treatment, yields the highly functionalized medium-sized ring. This approach has been applied to O–H and N–H nucleophiles. Furthermore, this zwitterionic portion of the cascade was further extended to tolerate carboxylic acids, different ring sizes and the use of earth abundant iron catalysts. In addition to the synthesis of medium-sized rings, these products proved to be versatile substrates for serendipitous ring contraction cascades, leading to relevant bioactive natural product cores, such as highly functionalized quinolines and cyclopentanes in a diastereoselective manner. As a final remark, many of the products produced have been submitted for high throughput screening which has allowed for the

identification of hit molecules that are now being further studied in the Sharma Research Group.

Acknowledgements

First and foremost, I would like to express my appreciation for the graduate education my advisor Dr. Indrajeet Sharma has instilled upon me. He has provided untiring support throughout my PhD. He has always encouraged me to strive for success and I am confident that without his wonderful mentorship, I would not have reached as far as have today.

I would also like to thank my committee members Professor Adam Duerfeldt, Professor Anthony Burgett, Professor Daniel Glatzhofer, and Professor Steven Crossley for their valuable advice and time spent throughout my PhD, for this dissertation and for this defense.

I also want to extend a warm appreciation to my undergraduate and masters advisor Professor Fehmi Damkaci. Not only did Fehmi lead me to the path of graduate school, but he also continues to inspire me and many others. Fehmi is a great mentor and friend, and I aspire to be an educator as qualified and passionate as him in the future.

Furthermore, I could not have done this research without the support of OU Chemistry and Biochemistry Department. With special thanks to Research Support Services staff. Specifically: Dr. Susan Nimmo for help with NMR; Dr. Douglas Powell for help with X-ray crystallography; Dr. Steven Foster for help with Mass Spec; Carl Van Buskirk and Jeff Jackson with help on fixing equipment; Erin Mayberry with fixing glassware; and DeAnna Stone for helping with shipments, packaging, and supplies.

I would also like to express my gratitude to Dr. Kiran Chinthapally and Dr. Suneel Chepuri. Throughout my PhD, I learned so much from both of them and I greatly appreciate their encouragement and help. It was always a pleasure working with them in the lab, having the privilege of listening to Suneel sing or being able to joke around with Kiran while we were working on numerous projects together. It wouldn't have been the same without them. Furthermore, I would also like to extend my thanks to other group members in the Sharma Research Group for continuing suggestions in the lab and during group meetings.

Also, I am thankful for my parents Karen and Peter Massaro. They have taught me countless life lessons throughout my life that have truly impacted every action I have done to reach this point. Their love, support, and sacrifice has made me the man I am today, and I hope to continue making them proud now and in the future.

Finally, I would like to extend my greatest appreciation to my wife Vesela for her love and support throughout our journey in New York and Oklahoma. I could not have achieved my goals without her and I am so happy to call myself her husband and the father of our newborn daughter Viktoria. Truly, family is everything, and I could not be any happier.

Table of Contents

List of Figures

List of Tables

List of Schemes

List of Abbreviations

acac = acetylacetonate

BF_4 = tetrafluoroborate

Boc = *tert*-butyloxycarbonyl

Bn = benzyl

CCDC = Cambridge Crystallographic Data Centre

CH_2Cl_2 = dichloromethane

C_6H_5Cl = chlorobenzene

CM = complex mixture.

CSA = camphor sulfonic acid

$(CuOTf)_2$•benzene = copper (I) triflate benzene complex

$(CuOTf)_2$•Tol = copper (I) triflate toluene complex

DBU = 1,8-diazabicyclo[5.4.0]undec-7-ene

DCE = 1,2-dichloroethane

DMAP = 4-dimethylaminopyridine

Dmb = 2,4-dimethoxybenzyl

DMPU = N,N'-dimethylpropylene urea

DMSO = dimethyl sulfoxide

DOSP = [1-[[4-alkyl(C_{11}-C_{13})phenyl]sulfonyl]-(2*S*)-pyrrolidinecarboxylate

E = entgegen (opposite)

EDC – 1-ethyl-3-(3-dimethylaminopropyl)carbodiimide

EDG = electron-donating group

esp = $\alpha,\alpha,\alpha',\alpha'$-tetramethyl-1,3-benzenedipropionic acid

Et_3N = triethylamine

EtOH = ethanol

EWG = electron-withdrawing group

Fe(TPP)TFA = 5,10,15,20-tetraphenyl-21*H*,23*H*-porphine iron (III) trifluoroacetate

Fmoc = fluorenylmethyloxycarbonyl

HFB = heptafluorobutyrate

HFIP = hexafluoro-2-propanol

HMPA = hexamethylphosphoramide

K_2CO_3 = potassium carbonate

KH = potassium hydride

LDA = lithium di-isopropyl amide

LG = leaving group

$LiAlH_4$ = lithium aluminum hydride

LiHMDS = lithium bis(trimethylsilylamide)

MeCN = acetonitrile

MnO_2 = manganese dioxide

MS = molecular sieves

$NaBH_4$ = sodium borohydride

nOe = nuclear Overhauser effect

NaOH = sodium hydroxide

NR = no reaction

OAc = acetate

OTf = triflate

p-ABSA = 4-acetamiobenzenesulfonyl azide

PF_6 = hexafluorophosphate

$PhI(OAc)_2$ = (diacetoxyiodo)benzene

$POCl_3$ = phosphoryl chloride

p-TsOH = 4-methylbenzene-1-sulfonic acid

py = pyridine

RCM = ring-closing metathesis

$Rh_2(oct)_4$ = rhodium (II) octanoate dimer

$Rh_2(TFA)_4$ = rhodium (II) trifluoroacetate dimer

SAR = structure activity relationships

SbF_6 = hexafluoro antimonate

$Sc(OTf)_3$ = scandium (III) triflate

$SOCl_2$ = thionyl chloride

TBAF = tetrabutylammonium flouride

TBS = *tert*-butyldimethylsilyl

Temp. = temperature

TFA = trifluoroacetic acid

TFE = 2,2,2-trifluoroethanol

THF = tetrahydrofuran

TPA = triphenylacetate

TPP = 5,10,15,20-tetraphenyl-21*H*,23*H*-porphine

Z = zusammen (together)

Chapter 1. Introduction

A convergent cascade approach to access diverse medium-sized rings.

1.1 Medium-Sized Rings

Medium-sized rings (8–12 membered) are important structural motifs that possess unique synthetic challenges associated with their construction compared to small and macrocyclic structures. These ring scaffolds exist within a plethora of relevant natural products exhibiting favorable bioactivity through enhanced bioavailability, potency, selectivity, and cell permeability due to their rotational and conformational restrictions.[1-2]

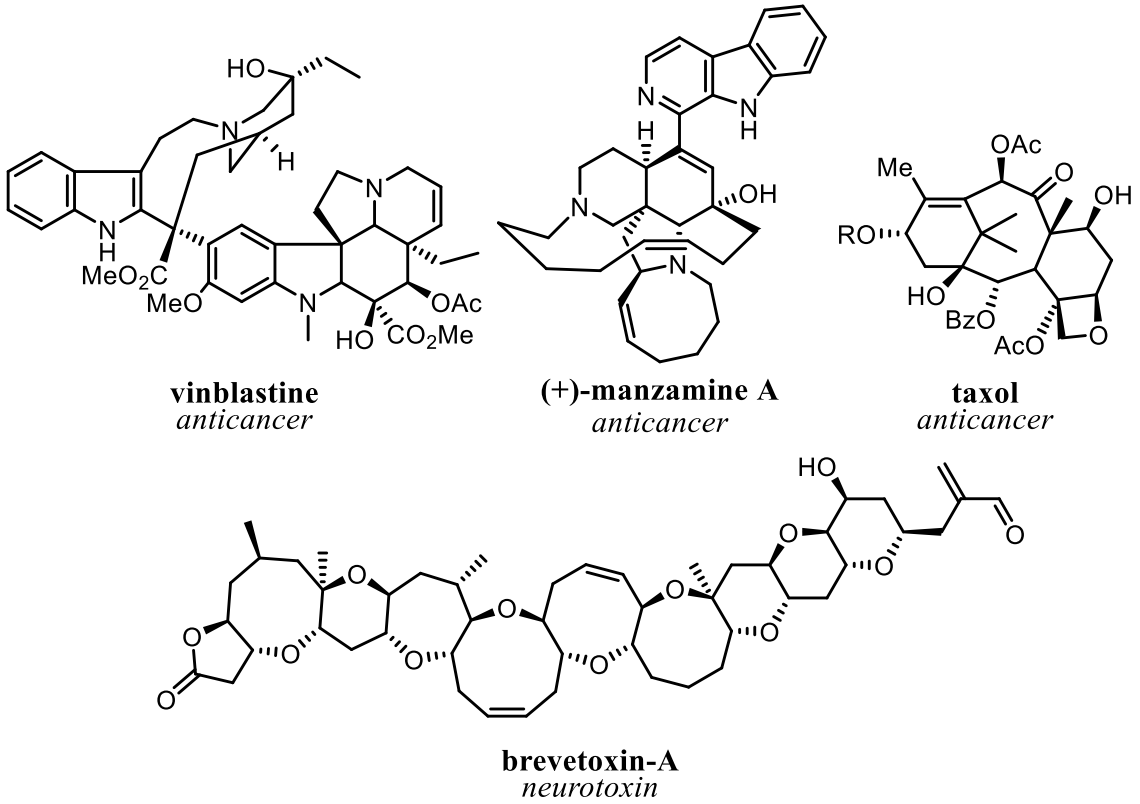

Figure 1. Examples of medium-sized natural products

Key examples include vinblastine,[3] (+)-manzamine A,[4] brevetoxin-A,[5] and taxol (Figure 1).[6] Although, when considering these and other examples, only taxol and vinblastine have been commercialized as pharmaceuticals. Furthermore, taxol is the only

drug possessing a medium-sized ring within the top 200 most prescribed pharmaceuticals in the market.[7-8] In addition, the production of taxol is accomplished through a semisynthetic route that bypasses the synthesis of the medium-sized carbocycle.[9] This scarcity of commercialized medium-sized ring construction can be linked to difficulties associated with accessing these cores, which has created a significant rift in current structure activity relationship data for biological targets with respect to medium-sized rings ligands.[10] The general structure and stability of these compounds is often dictated by transannular interactions within the molecule as well as substituents and heteroatoms present within the ring scaffold. Furthermore, these interactions often play a pivotal role in the synthesis of medium-sized rings, as intramolecular interactions often inhibit or prevent synthetic methods used for cyclization. Currently there are a variety of methods to access medium-sized rings, the most common approaches involve end-to-end cyclizations, and rearrangement strategies. Unfortunately, current methods generally require high dilution conditions or the preparation of highly complex precursors, limiting their utility for general application. Thus, the development of a convergent strategy to synthesize functionalized medium-sized rings will provide direct access to diverse scaffolds difficult to access through traditional approaches.

1.2 End-to-End Cyclization Strategies

The most conventional approach to access medium-sized rings is via an end-to-end cyclization strategy. This direction has led to beautiful examples of medium-sized ring construction utilizing coupling reactions,[11] alkene metathesis,[12] addition reactions,[13] radical cyclization,[14] Diels–Alder cyclizations.[15] These strategies are often dependent on substituents introducing conformational constraint to promote cyclization.[16] Furthermore,

these linear approaches require highly dilute conditions and often have high risk of polymerization side reactions.[17-19] Andrus and co-workers exhibited these limitations during their synthesis of octalactin lactone and side chain. While performing a systematic study for their key lactonization step using EDC/DMAP conditions, they realized that substituents situated on their precursors (**1a**–**1c**) played a significant role in product formation (**2a**–**2c**). When the corresponding substituents were removed, they observed that the yield of intramolecular cyclization drastically decreased with each deletion and ultimately led to no formation of product **2c** (Scheme 1).

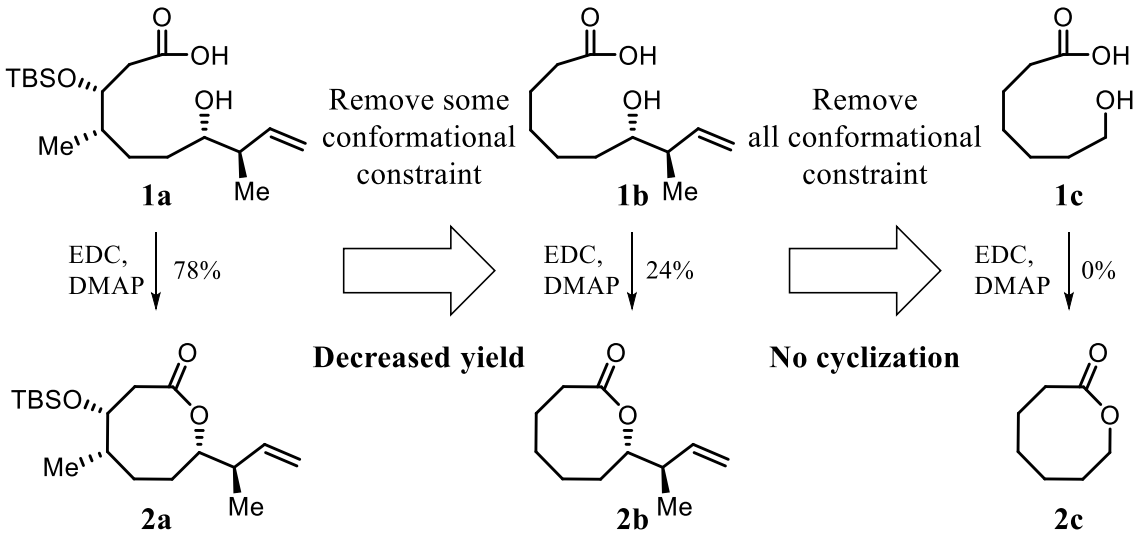

Scheme 1. Substrate dependence for lactonization strategies

Although coupling reactions are not the only victims of decreased reaction rates; a similar substrate dependence trend can be associated with alkene metathesis too. Lubell and co-workers, using precursor **3a**, successfully performed ring-closing metathesis (RCM) to form medium-sized ring **4a**, clearly showing constraint dependence. By simply removing a dimethoxybenzyl protecting group from the amide nitrogen, Lubell and co-workers showed that **3b** failed to cyclize under typical metathesis conditions (Scheme 2).[20]

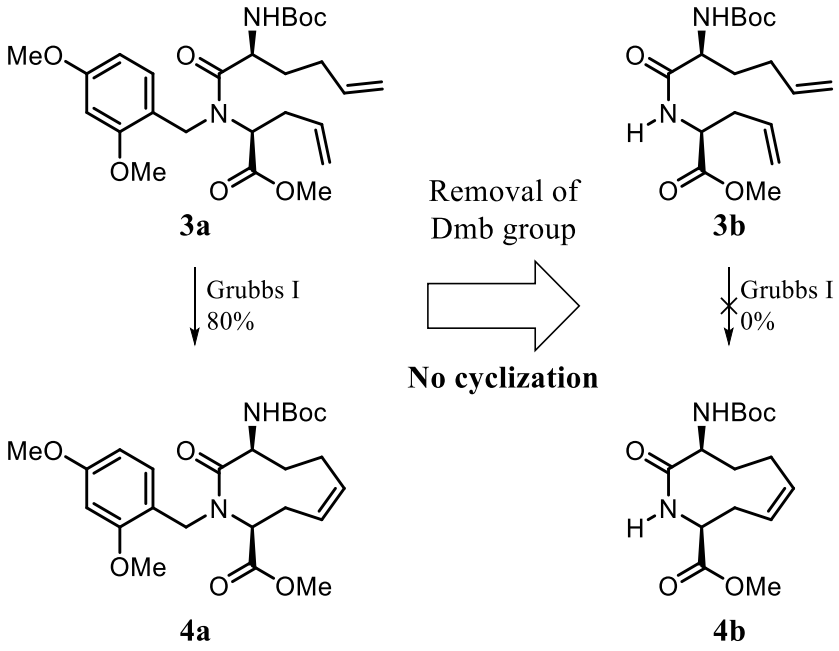

Scheme 2. substrate dependence in olefin metathesis

In addition to substituents, ring size can also play a significant role on the rate of cyclization. Danishefsky and co-workers showed that intramolecular Suzuki couplings with **5** resulted in low yield of **6**, likely due to entropic and enthalpic barriers associated with medium-sized head-to-tail cyclizations (Scheme 3). Furthermore, they determined that ring sizes of greater than 13 proved to cyclize as expected, thus highlighting the unique characteristics of medium-sized ring systems.[21]

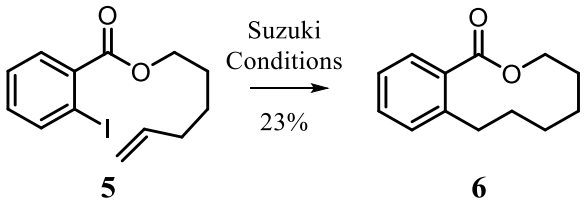

Scheme 3. Suzuki coupling substrate dependence

Insight into the phenomena associated with medium-sized rings has been provided by a systematic study performed by Illuminati and co-workers. By tabulating the rate of

intramolecular cyclization of bifunctional chain molecules, they identified that intramolecular cyclization occurs slowest with ring sizes 8 through 12 (Figure 2).

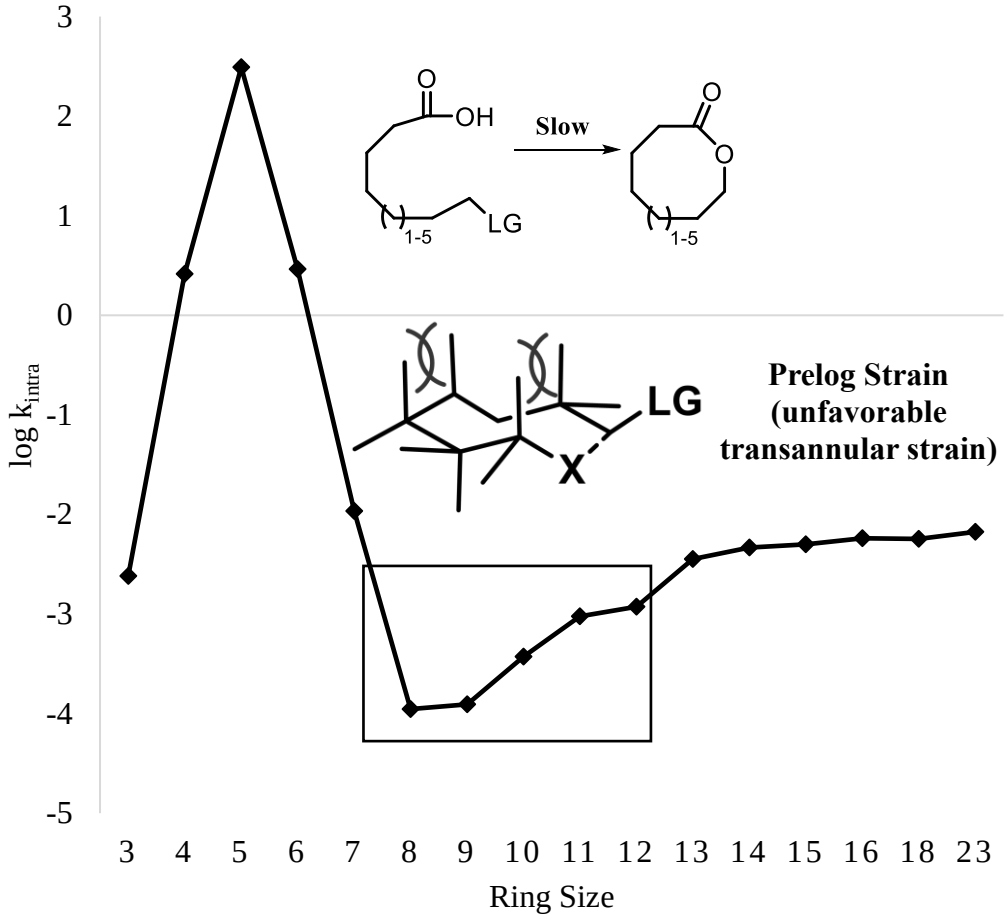

Figure 2. Rate of lactonization versus ring size[21]

The main reason for this decrease in rate is due to unfavorable transannular interactions also known as Prelog strain. In addition, torsional strain and negative entropy also inhibit the formation of medium-sized rings.[17, 22]

1.3 Rearrangement and Ring Expansion Strategies to Synthesize Medium-Sized Rings

Alternative to the common head-to-tail cyclization approaches, many researchers have been developing rearrangement and ring expansion strategies which circumvent the entropic and enthalpic barriers associated with medium-sized ring formation as well as the necessity for high dilution factors. One of the most common employments of bond migration is through homologation, usually facilitated by reacting a diazo compound (**8**) with a ketone (**7**) to yield a transient β-hydroxy diazo compound which then undergoes a homologation to yield medium-sized ring **9**.

a) Diazo mediated homologation by Kingsbury et al.[19]

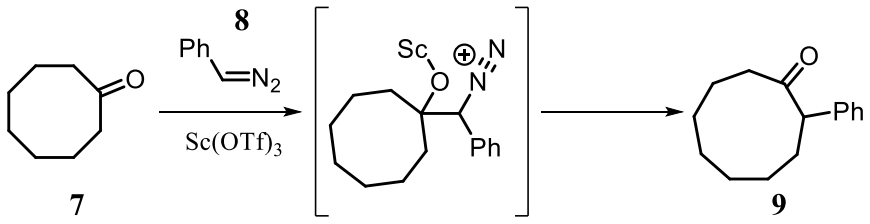

b) Translactonization strategy by Corey et al.[20]

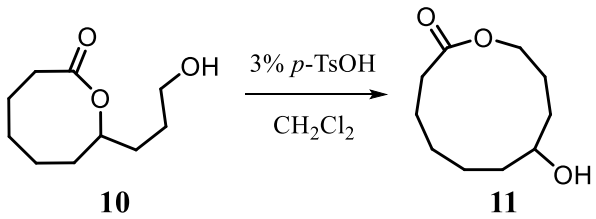

Scheme 4. Bond migration and ring expansion strategies

This transformation often proceeds with high stereo- and chemoselectivity. Because of one carbon homologation, it is necessary to have a medium-sized ring precursor to access 9- through 12-membered rings with this transformation, so this method fails to provide a robust solution to medium-sized ring construction (Scheme 4a).[23] There are

alternative medium-sized ring expansions such as translactonization strategy developed by Corey et al. (Scheme 4b).[24] However, translactonization of medium-sized rings **10** to **11** suffers from similar drawbacks as homologation as well as equilibrium dependencies. Other methods of ring expansion have also been developed to access medium-sized rings via Grob fragmentation, which was accomplished by Paquette et al. for the synthesis of diterpenoids jatrophatrione and citlalitrione. The key step of the synthesis incorporated a Grob fragmentation of **12** to yield intermediate **13** (Scheme 5).[25]

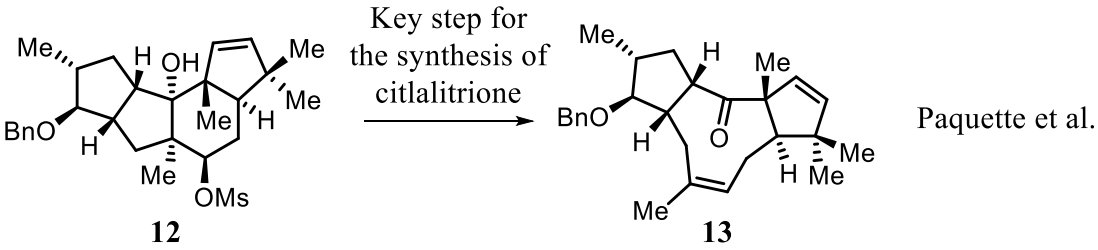

Scheme 5. Example of Grob fragmentation

In addition to Grob fragmentation, other ring expansion methods have been utilized, such as β-hydroxy retro aldol cascades. A perfect example of this type of chemistry is shown by Unsworth and co-workers where acylation of lactam **14** with the bifunctional acid chloride **15** provided precursor **16**, which is capable of undergoing a base-initiated ring expansion to yield heterocycle **17**. This two-step method provides access to medium-sized rings, as well as successive ring expansions to yield macrocycles (Scheme 6).[26-28]

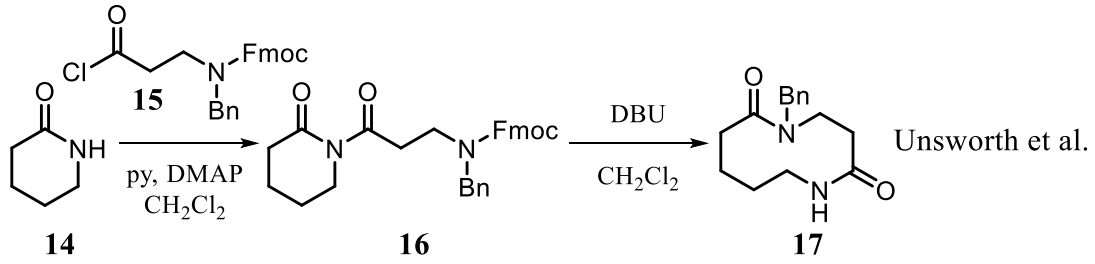

Scheme 6. β-hydroxy carbonyl ring expansion[26-28]

Other two-step protocols for ring expansion methods have been developed where oxidation of the phenol precursor **18** allows for a dearomatization cyclization to form the intermediate quinone **19**, which is capable of undergoing an acid catalyzed rearomatization ring expansion sequence to yield **20** (Scheme 7).[8]

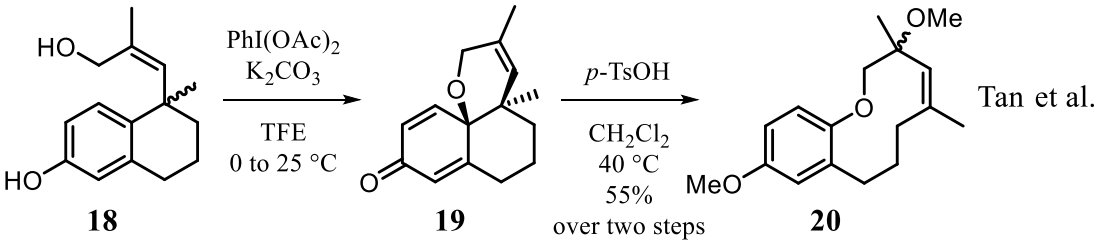

Scheme 7. Oxidative ring expansion sequence

Comparison of these methods to access medium-sized rings, reveals that they often require multistep procedures and complex starting materials. To diverge from previous strategies, development of a highly convergent strategy to access medium-sized rings from readily available synthons could provide a more suitable foundation for a diversity-oriented synthesis of medium-sized ring libraries for drug discovery; a research program aim of the Sharma Research Group.

1.4 A Concise Retrosynthesis of Medium-Sized Rings

We envisioned that medium-sized rings could be constructed from a convergent cascade reaction yielding the desired product in a single step from two readily available fragments. Retrosynthetic analysis identified our first disconnection as an oxy-Cope reaction providing a divinyl ring-contracted intermediate. Our second disconnection incorporated a X–H insertion/aldol cascade that utilizes a two-bond disconnection leading to two readily available starting materials (Scheme 8).

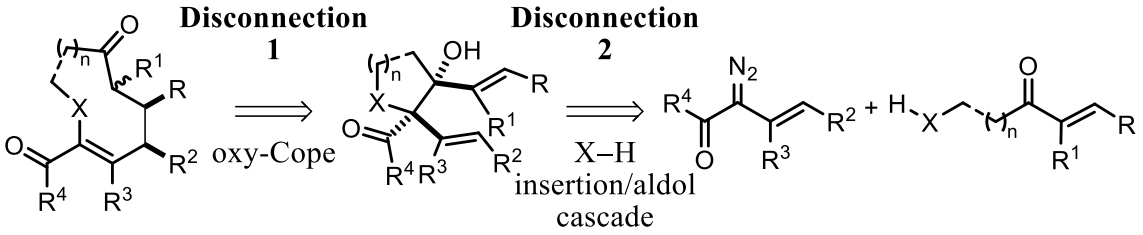

Scheme 8. Retrosynthetic disconnection of medium-sized rings

To further support the feasibility of this strategy, there were literature reports validating this synthetic route. Regarding our first retrosynthetic disconnection, Shair and co-workers formed medium-sized ring **22** through a similar divinyl ring intermediate **21** via an anionic oxy-Cope reaction (Scheme 9).[29]

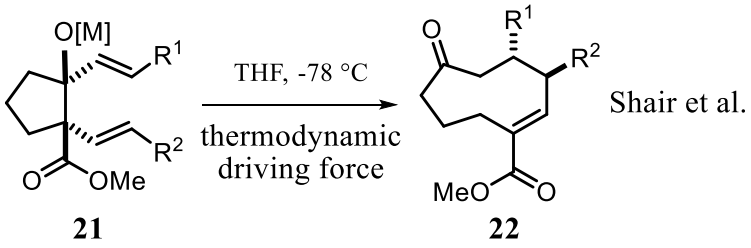

Scheme 9. Anionic oxy-Cope ring expansion

Our second retrosynthetic disconnection was corroborated by a very mild and efficient method to access a variety of tetrahydrofurans and pyrrolidines developed by Moody and co-workers.(Scheme 10).[30-31]

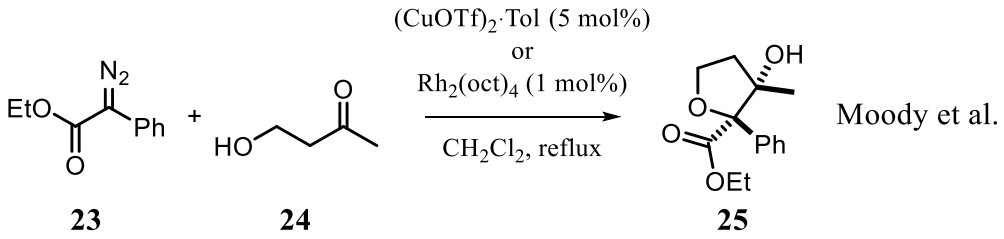

Scheme 10. Representation of diverted X–H insertion developed by Moody[30-31]

The cascade involved the decomposition of a donor/acceptor diazo **23** with a transition metal catalyst (Rh or Cu) generating a metal carbenoid capable of reacting with *β*-hydroxy ketone **24** to generate highly functionalized 5-membered heterocycles; although no divinyl products were ever synthesized.[30-31]

Inspired from these literature reports, we decided to focus our efforts towards the extension of this diverted X–H insertion, developed by Moody, to operate with vinyl diazoacetate and *β*-hydroxy vinyl ketone precursors, which would provide direct access to intermediates capable of undergoing oxy-Cope ring expansions to provide medium-sized rings.

1.5 Diazo Chemistry

The diazo N–N bond was first discovered by Peter Griess in 1858, over a 100 years ago when he accomplished the diazotization of anilines.[32] The motif itself is a unique wonder of elemental reactivity because of the atoms involved. Normally, when considering two elements such as carbon and nitrogen, carbon can possess reactivity in a variety of fashions, while dinitrogen alone ordinarily exists as an inert substance. Although when dinitrogen is combined with carbon, the subsequent molecule possesses augmented

reactivity arising from its resonance character. Furthermore, diazo surrogates such as triazoles have also been identified as possessing similar resonance qualities (Figure 3).[33]

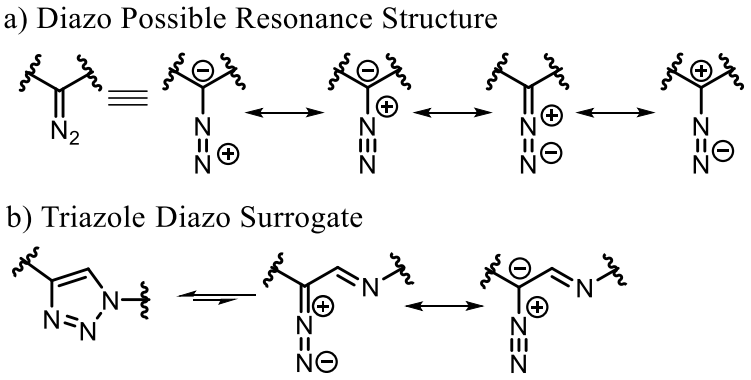

Figure 3. Diazo resonance structures and diazo surrogates

1.6 Diazo Structure and Reactivity

More recent applications of the diazo motif are seen at the α-position of carbonyl compounds. The electronic nature of the α-center strongly dictates the reactivity of the diazo compound. In fact, there are three categories of diazo compounds, termed as acceptor/acceptor, acceptor and acceptor/donor with their corresponding stabilities as most stable, stable, and least stable, respectively. Acceptor (A) groups withdraw electron density while donor (D) groups release electron density; R substituents are neutral in nature and leave the electron density unperturbed (Figure 4).[34]

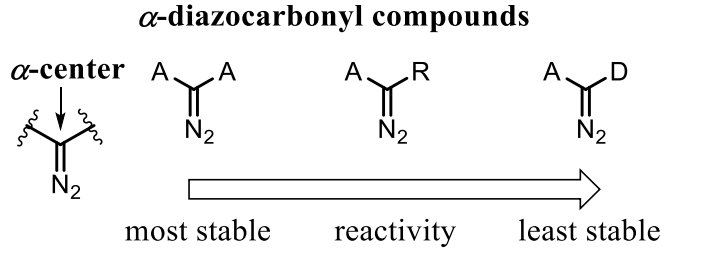

Figure 4. General stability of diazo precursors[34]

1.7 Application of α-Diazocarbonyl Compounds

For more than 40 years, α-diazocarbonyl precursors have been exploited for their ability to generate reactive carbenes and metal carbenoids.[35] These transient intermediates inspired diverse reactions such as the Wolff rearrangement, homologation, cyclopropanation and cyclopropenation, dipolar cycloadditions,[36-42] C–H insertion,[34, 43-44] ylide formation,[45] heteroatom insertion.[46-50] From these applications, the two focused most in this research will be heteroatom insertion and ylide generation chemistry will be the focus of research reported herein (Figure 5).

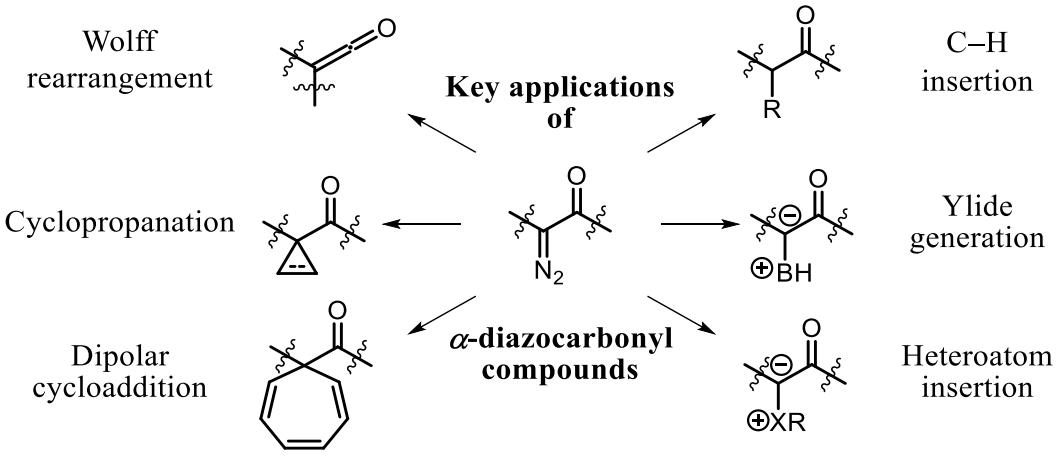

Figure 5. Versatility of α-diazocarbonyl compounds[35]

1.8 Preparation of Diazo Compounds

Arguably, the most common method of preparation for α-diazocarbonyl compounds is via diazo transfer reagents, but a variety of methods exist such as diazotization, dehydrogenation, acylation, substitution or cross-coupling, and deacylative diazo transfer (Figure 6).[35] For the research performed in this thesis, most α-carbonyl diazo compounds were prepared utilizing diazo transfer reagents, which are most widely used due to their stability, robustness, and ease of removal during workup procedures. One diazo

transfer reagent utilized most often due to these benefits is 4-acetamidobenzenesulfonyl azide (*p*-ABSA) developed by Huw Davies.[51]

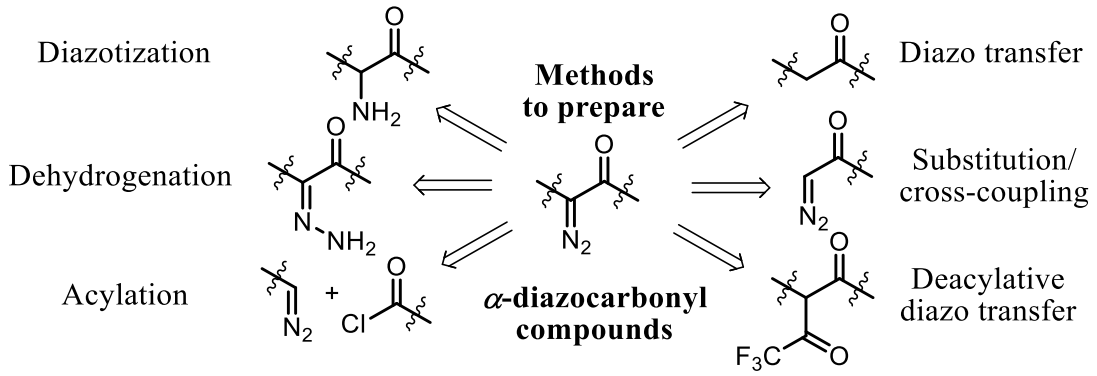

Figure 6. Common methods to prepare α-diazocarbonyl precursors

1.9 Carbenoids

The most common application of diazo precursors arises from their ability to decompose into a corresponding metal carbenoid, meaning that a metal-carbon double bond is formed while subsequently evolving N_2 gas; which are quite different than a free carbene. A free carbene is a carbon with two unpaired valence electrons that can exist in either a singlet or a triplet state.

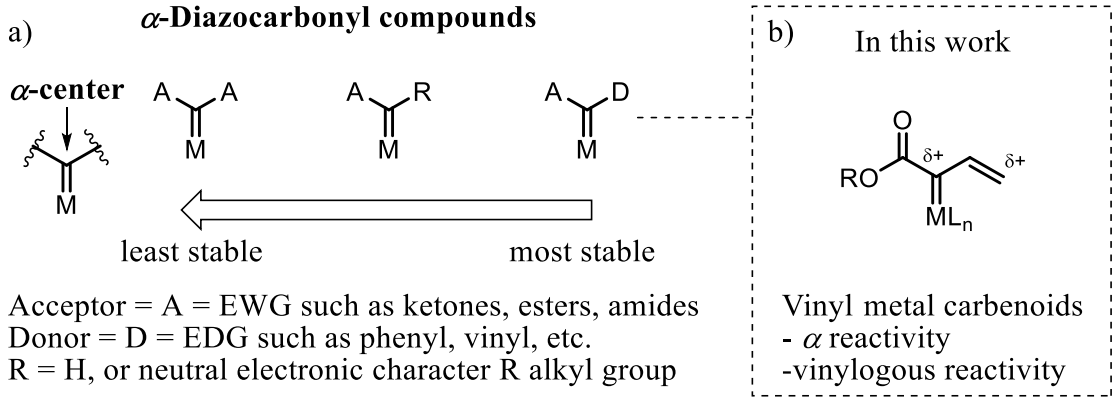

Figure 7. General stability of carbenoid intermediates

Carbenoids, on the other hand, are carbenes stabilized by transition metal catalysts either existing as a Fisher or Schrock carbene; Fisher carbenes tend to be electrophilic in nature while Schrock carbenes tend to be nucleophilic. With respect to this research, we will focus on electrophilic Fischer carbenoids. Interestingly, the reactivity of the carbenoids is reverse compared to the diazo precursors based on substituents (Figure 7a). Even though donor/acceptor diazo synthons may be the most unstable of these three types, the corresponding carbenoid generated is most stable. In order to synthesize medium-sized rings, we envisioned the use of vinyl metal carbenoids which would provide one of the necessary vinyl groups for ring expansion. Vinyl metal carbenoids, however, possess a multitude of reaction possibilities and potential side reactions due to their electrophilicity at both the α and vinylogous positions (Figure 7b).[52] For this reason, it is necessary to understand the reactivity of metal vinylcarbenoids to facilitate our desired heteroatom insertion/aldol cascade to access medium-sized rings.

1.10 Different Transition Metal Carbenoids for Heteroatom Insertion Reactions

C–X bonds are found in numerous natural products and direct methods to form these bonds are of high value to the synthetic community. One such way is through heteroatom insertion reactions, most commonly accomplished via diazo derived transition metal carbenoids. The first examples were performed with copper catalysts.[46] Although these initial reports were racemic, ligand incorporation soon lead to enantioselective variants.[53] Despite these advancements, the overall development of X–H insertion reactions remained stagnant due to more focus on C–H functionalization and cyclopropanation chemistry.[54] This chemistry has had some development with other metal catalysts such as rhodium, gold, silver and iron, as well (Figure 8).

Fe	Co	Ni	Cu
Ru	Rh	Pd	Ag
Os	Ir	Pt	Au

Figure 8. Catalysts used in heteroatom insertion chemistry relative to scale of symbol[52]

Specifically, rhodium and copper have been the main focus of heteroatom insertion as they tend to react through similar mechanisms, allowing for their use in cascade reactions, such as transition metal carbenoid-initiated intermolecular heteroatom insertion/ylide trapping by Hu and co-workers.[54-55] Rhodium catalysts have become increasingly popular due to their high turnover rates and low catalyst loading.

1.11 Rhodium Catalysis

Rhodium catalysts have been a mainstay in carbenoid chemistry. [56-57] This arises from the capabilities of dirhodium catalysts to decompose diazo precursors to form reactive rhodium carbenoids with extremely low catalyst loadings, broad substrate scope, high chemoselectivity, and often potential diastereo- and enantioselective induction.

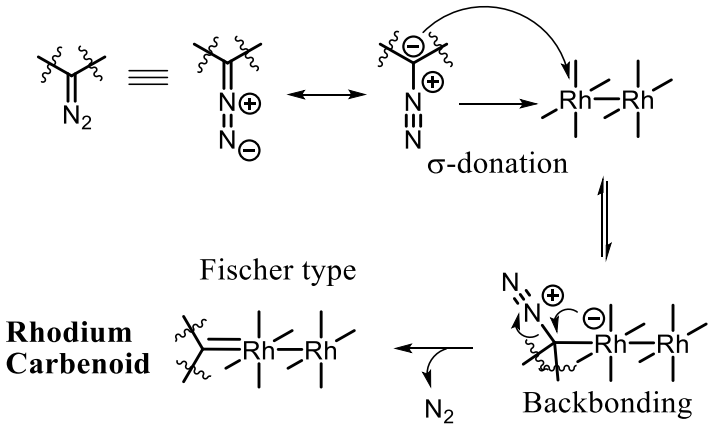

Figure 9. Simplified mechanism of rhodium carbenoid generation from diazo precursors and Rh catalysts

A simplified mechanism for the formation of rhodium carbenoids involves the σ donation of a diazo synthon to the dirhodium center followed by back bonding resulting in the evolution of N_2 gas, which can often be visualized due to the high turnover rate of these catalysts (Figure 9).[58] These carbenoids initially exhibit extreme electrophilicity that facilitates a variety of insertion type reactions. Upon insertion, a reactive ylide or zwitterion is formed with nucleophilic character that can often be trapped by an electrophile. Thus, the dual character of these rhodium carbenoids is defined as ambiphilic reactivity.[59]

1.12 Types of Rhodium (II) Catalysts Utilized in Diazo Chemistry

In terms of the rhodium catalysts for diazo decomposition, rhodium (II) paddle wheel complexes have been most utilized. There are a variety of different types carboxylate ligands that attenuate the rate of decomposition of diazo precursors, as well as provide a steric environment capable of inducing diastereo- and enantioselectivity (Figure 10).

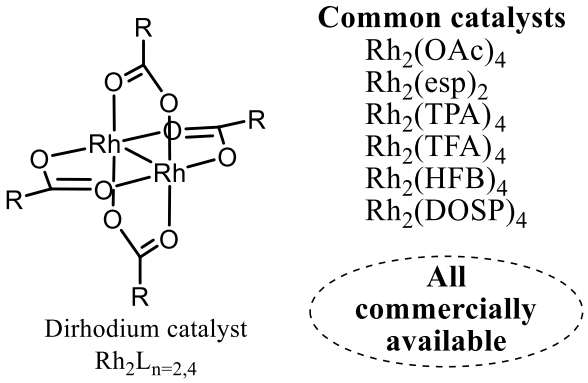

Figure 10. Common types of rhodium catalysts

Furthermore, these rhodium complexes perform well under extremely low catalyst loadings; usually as low as 1 to 0.1 mol%. Thus, even though the price of rhodium is high, costs are not prohibitive.

1.13 Metal Carbenoid Reactions

Ambiphilic metal carbenoid is a modern term labeling the dual character reactivity of the metallocarbenoid; often best termed as ylide formation.[60] The formation of the ylide followed by ylide trapping is the foundation for many cascades that employ diazo derived carbenoids.[61] This dual character has been implemented into dipolar cycloaddition reactions along with various intra- and inter-molecular cascades. Whenever a X–H insertion is the initial stage of a cascade sequence, there is always a risk of protodemetalation via 1,2-proton transfer of the transient zwitterionic or ylide intermediate, yielding an insertion byproduct (Figure 11). With suitable reaction conditions and catalyst selection this protodemetalation can be avoided to facilitate a cascade reaction. This strategy for X–H insertion initiated cascades has been implemented into our approach to medium-sized rings as well as the ylide based cascades developed by the Moody and Hu

research groups.[30-31, 54, 62] Our envisioned approach compliments the methodologies by Moody by extending this cascade to vinylcarbenoids derived from vinyl diazo precursors.

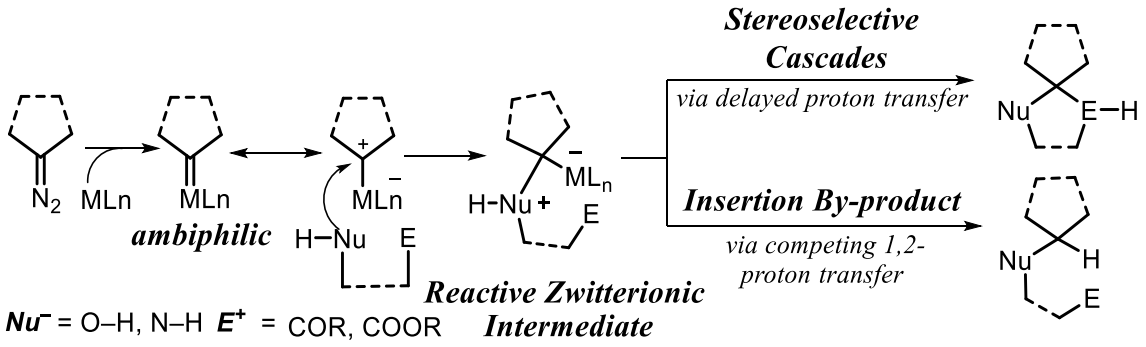

Figure 11. Two pathways of carbenoid cascades initiated by X–H insertions

Furthermore, we expected to utilize this method in tandem sequence with a compatible oxy-Cope ring expansion to yield the medium-sized rings.

1.14 Cascades Involving Sigmatropic Ring Expansion Reactions

Sigmatropic ring expansions have been integrated in cascade sequences and applied to the construction of a variety of complex molecules. This strategy is often seen through transient intermediates such as ylides and zwitterions formed in situ. In addition, the [3,3] rearrangements most utilized for these expansions are the Cope rearrangement promoted by ring strain or the oxy-Cope variation that provides a thermodynamic sink by forming a subsequent ketone. A perfect example of a rhodium carbenoid initiated cyclopropanation ring expansion incorporating a strain release Cope rearrangement was developed by Padwa et al. (Scheme 11). The mechanism involves an initial carbenoid formation from diazo **26**, followed by olefin metathesis and carbenoid transfer to yield intermediate **27**, which performs a cyclopropanation to produce intermediate **28** followed by ring expansion to arrive at the final complex molecule **29** in good yield.[63]

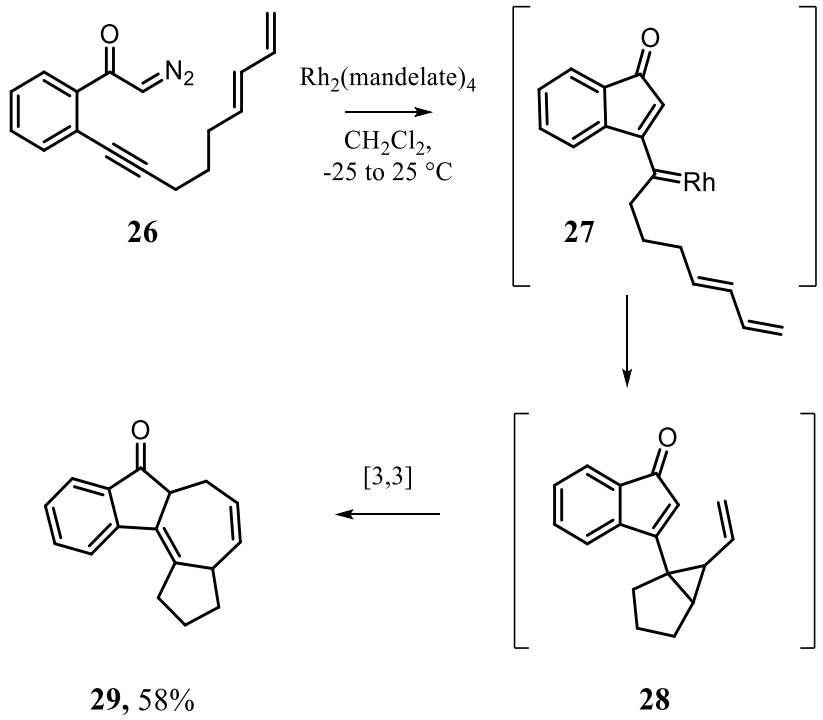

Scheme 11. Rhodium initiated cope cascade

Another example includes an anionic oxy-Cope ring expansion transannular ring cyclization (Scheme 12).[64] One key aspect to consider regarding the rhodium-initiated cascade developed by Padwa et al. was the use of sigmatropic rearrangements within the cascade sequence.

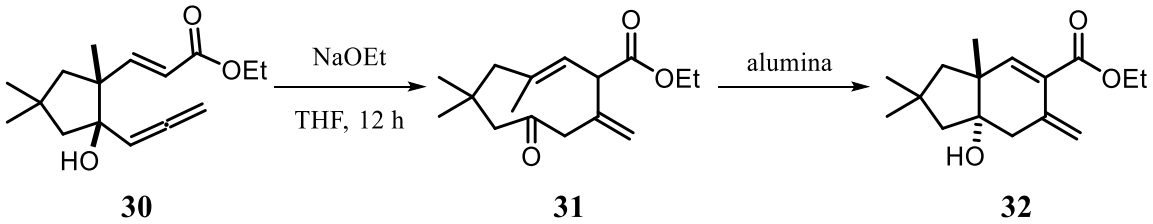

Scheme 12. Anionic oxy-Cope initiated cascade

Furthermore, Raja-gopalan et al. showed an example proving that oxy-Cope ring expansion cascades can provide medium-sized ring products such as **31** from allene **30**, but the generated product may further react due to internal strain leading to transannular ring

contraction product **32**; a possible future challenge associated with the construction of medium-sized rings. [65]

1.15 [3,3] Sigmatropic Rearrangements

Pericyclic reactions are defined as concerted reactions involving orbital symmetry of molecular components oriented in a cyclic transition state. Each of these examples have been incorporated into numerous syntheses via cascade strategies. Sigmatropic reactions are probably the most unique of these three types because the process retains the same number of each type of bond, such as double and single, unlike Diel–Alder and electrocyclizations that sacrifice π bonds for the formation of σ bonds.

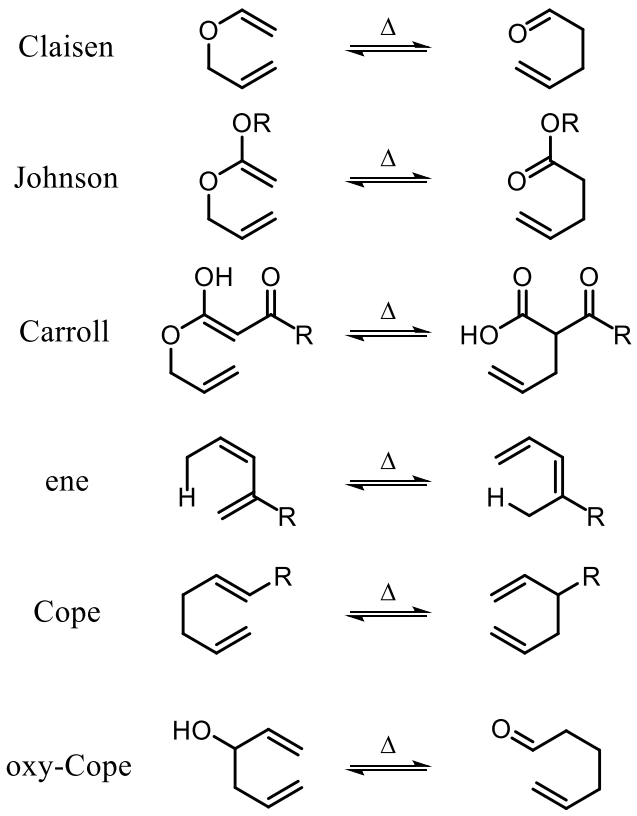

Figure 12. Examples of common [3,3] sigmatropic rearrangements

Furthermore, there are numerous varieties of [3,3] sigmatropic rearrangements available such as the Cope, oxy-Cope, anionic oxy-Cope, Claisen rearrangement, etc. with a number

of varieties in each of these subclasses (Figure 12). When comparing the Cope rearrangement alone, literature shows that catalytic efforts are generally needed to reduce the thermal temperature necessary to access the rearrangement. In addition, these rearrangements are always in a dynamic equilibrium, so it is quite pertinent to incorporate a thermodynamic sink to push the reaction in the forward generally through the formation of a carbonyl or by relieving ring strain.[66]

1.16 Oxy-Cope Rearrangement

The oxy-Cope rearrangement is disparate from other [3,3] sigmatropic rearrangements due to a hydroxy located at the 1 position.[67-70] In regards to the transition state itself, both the chair and the boat transition state are possible, although the energy difference (ΔG) is not significant in most cases; generally a difference of only 10 kcal/mol (Figure 13).[66]

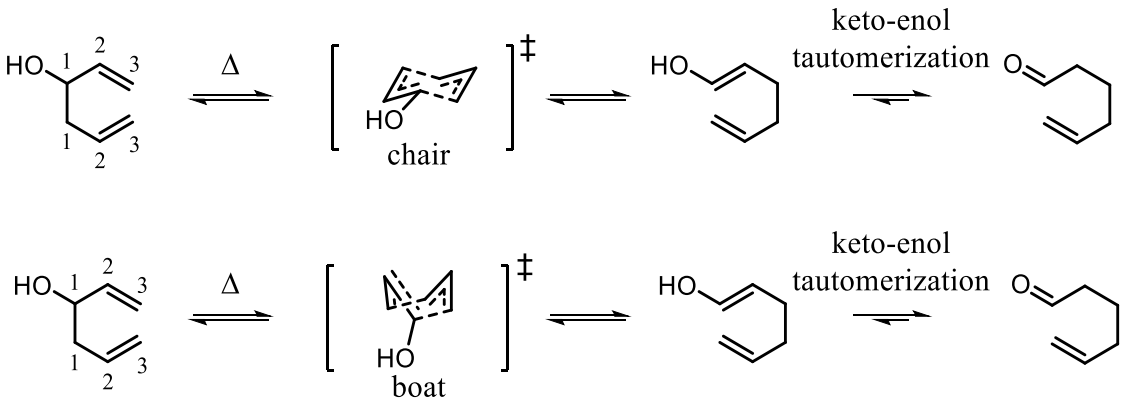

Figure 13. Two possible oxy-Cope transition states

Furthermore, oxy-Cope and Cope ring expansion reactions occur best when substrates are expanding smaller ring sizes such as cyclopropanes and cyclobutanes, and these examples tend to favor the boat transition state. When considering the thermodynamic driving

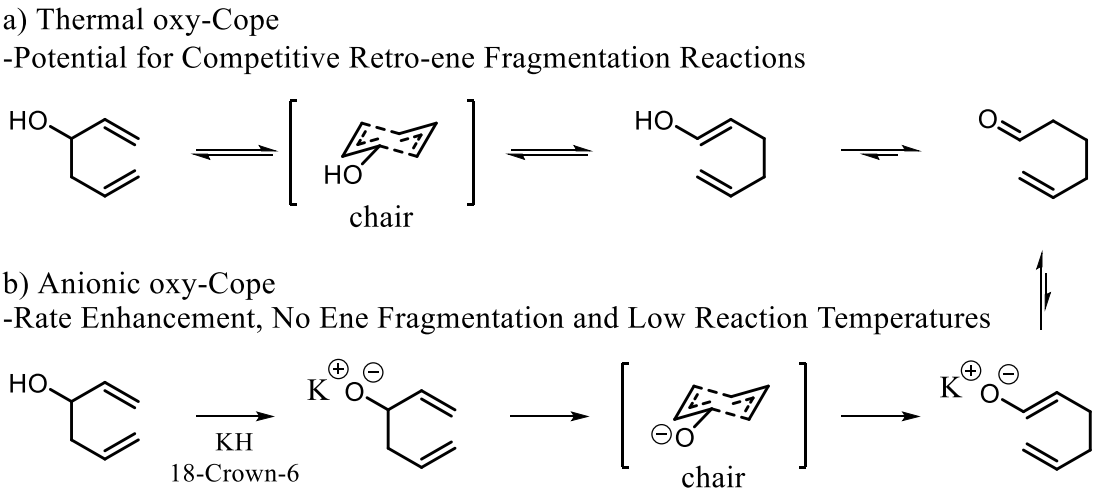

Figure 14. Comparison of thermal oxy-Cope and anionic oxy-Cope

force of the oxy-Cope rearrangements it is also necessary to consider the anionic oxy-Cope, which is generally induced by basic potassium salts. The anionic oxy-Cope has been a significant advancement in oxy-Cope reaction methodology and there are significant advantages often seen with this modification, such as rate enhancement and reduced reaction temperatures (Figure 14). However, depending on substrate and product stability, the anionic oxy-Cope can be an unsuitable method compared to thermal conditions. For example, **33** proceeds with greater success thermally to produce product **34** (Scheme 13a).[71-72] Another concerned voiced by Moody and co-workers was the potential risk of a retro-aldol fragmentation (Scheme 13b, **36**).[30]

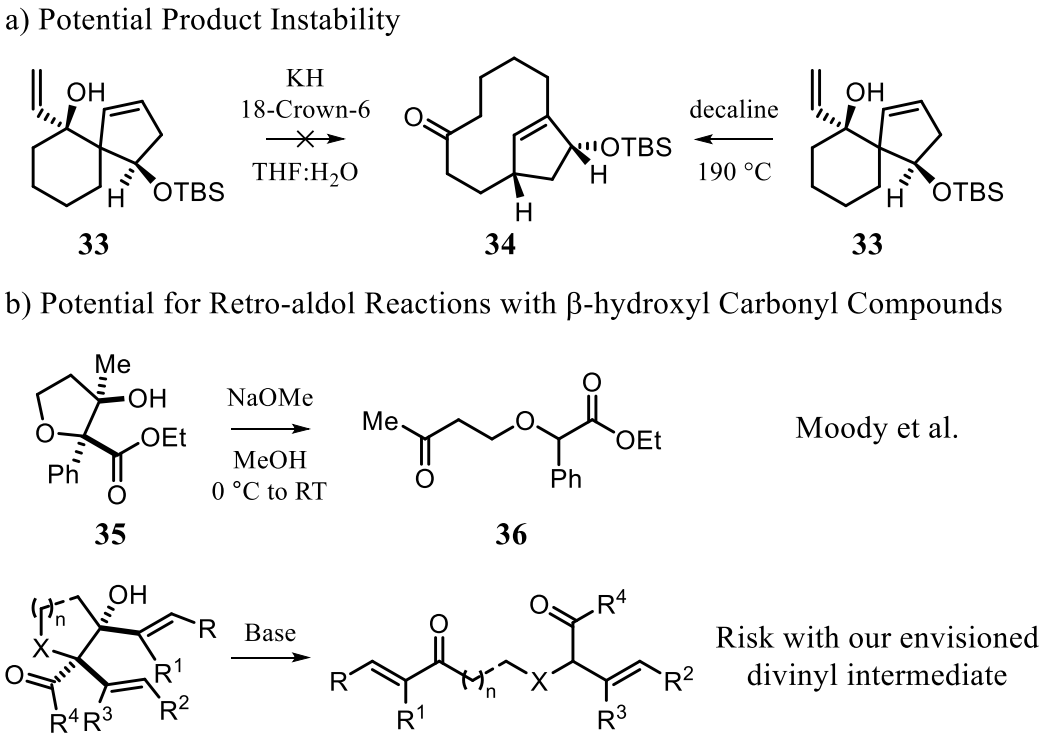

Scheme 13. Preference to use thermal oxy-Cope over anionic oxy-Cope

Aside from specific rearrangements of linear substrates, the Cope and oxy-Cope are often most implemented in ring expansion methods to access medium sized rings, but accessing the necessary starting materials to perform the desired ring expansions is often problematic.[73-75]

1.17 Goals of this Thesis

The work described in this thesis provides a highly convergent approach to medium-sized heterocycles. Our approach utilizes a rhodium-catalyzed heteroatom insertion/aldol cyclization that operates cohesively with oxy-Cope ring expansion to access medium-sized heterocycles in a single step. The cascade strategy incorporates various nucleophiles shown in previous reports of diverted heteroatom insertion as well as unprecedented variants. Chapter 2 describes the initial implementation of our rhodium

carbenoid initiated cascade strategy to access medium-sized oxacycles. In chapter 3, this cascade is further extended to incorporate ketoacid precursors for the synthesis of diverse lactones and medium-sized decanolides. Furthermore, earth abundant iron as a catalyst in the O–H insertion/aldol cyclization is investigated. Striving to move away from O–H to other heteroatoms such as N–H, chapter 4 delineates the synthesis of diverse quinoline scaffolds derived from initial attempts to access medium-sized azacycles. Finally, chapter 5 discusses how quinoline formation was avoided to effectively synthesize 9-membered medium-sized azacycles.

Chapter 2: Synthesis of Medium-Sized Oxacycles.

First example of insertion/aldol/oxy-Cope cascade

2.1 Introduction*

A significant source of unique medium-sized cyclic ethers is marine microorganisms.[76] Isolates from these bacteria and fungi have led to the discovery of bioactive compounds, such as the marine ladder toxins: ciguatoxins, brevetoxins, and other various derivatives of these macromolecular polycyclic frameworks, which often target the voltage ion channels of cells.[77] In addition, simpler metabolites have also been elucidated such as laurencin, obtusenyne and eunicellin, but many of these molecules have yet to be thoroughly screened for bioactivity (Figure 15).

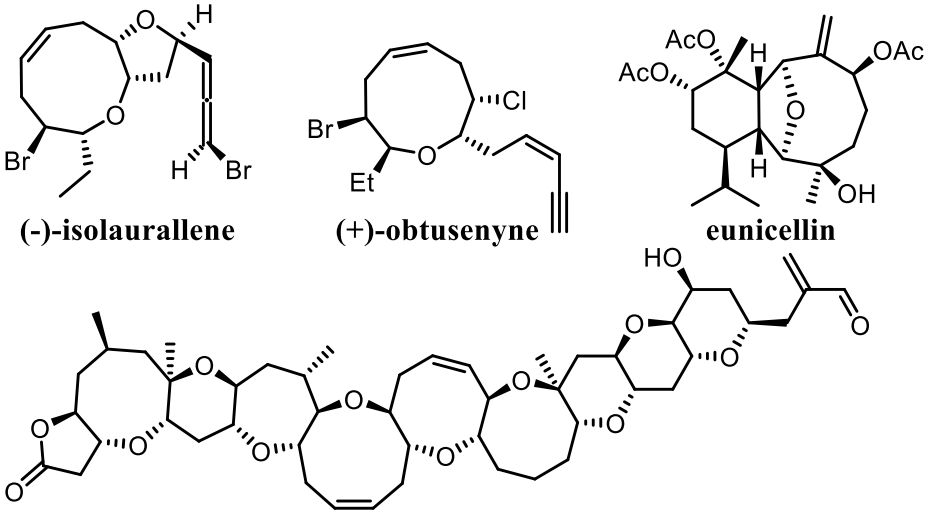

Figure 15. Oxacycle natural products

*Reproduced in part from "Rhodium Carbenoid Initiated O-H Insertion/Aldol/Oxy-Cop Cascade for the Stereoselective Synthesis of Functionalized Oxacycles." Kiran Chinthapally, Nicholas P. Massaro and Indrajeet Sharma. *Org. Lett.* **2016**, *18*, 24, 6340-6343 with permission from Organic Letters. *Copyright © American Chemical Society*. N.P.M. contributed by designing substrate scope, preparing precursors, product characterization, and manuscript preparation.

Even with the lack of biological data, their medium-sized ring scaffolds have attracted the attention of synthetic chemists due to the challenges associated with their construction.[78-81] This has inspired significant advancements in medium-sized ring construction, but there still remains a lack of convergent approaches capable of efficient library synthesis for drug discovery. For this reason, the core scaffolds found in many bioactive natural products remain underexplored.[82-85]

There have been several reports in literature for the synthesis of oxacycles through cyclization of an appropriate linear precursor (Scheme 14).[13-14, 86] The cyclization step often poses challenges due to entropic and enthalpic barriers as well as the necessity for high dilution conditions to avoid polymerization.[17-19] Current ring expansion reactions that are insensitive to substrate conformational effects provide an alternative to conventional cyclization strategy.[8, 87] However, the synthesis of an appropriate precursor for the ring expansion reactions requires multiple steps, and limits the synthetic utility.

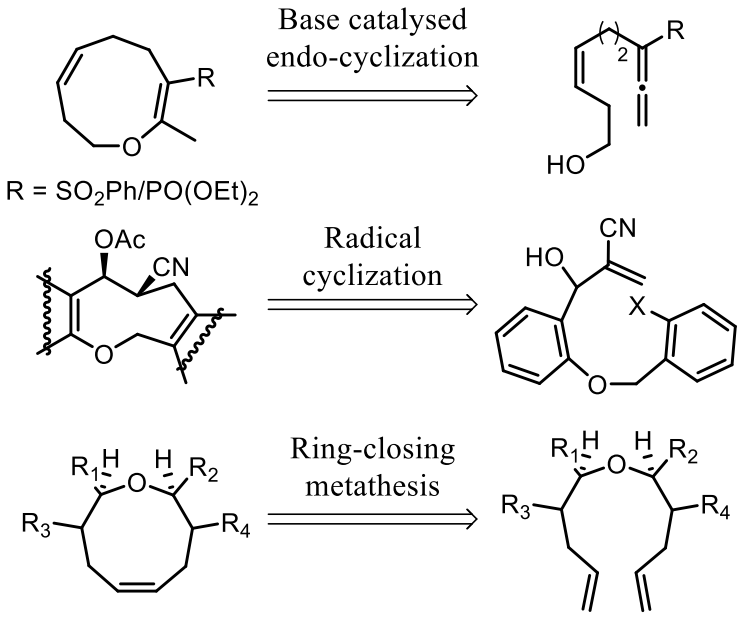

Scheme 14. Linear methods to access 9-membered cyclic ethers.

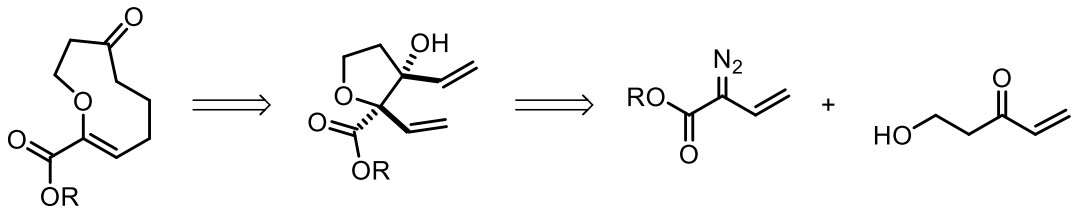

Scheme 15. Retrosynthetic analysis of 9-membered cyclic ethers

As discussed during chapter one, a cascade approach was envisioned that could produce medium-sized heterocycles such as cyclic ethers via a heteroatom insertion/aldol/oxy-Cope cascade to access 9-membered cyclic ethers.[30, 88-91] The focus of this chapter is to demonstrate the feasibility of this cascade with O-H nucleophiles to yield the desired 9-membered cyclic ethers. Originating from the disconnections shown in chapter one, a more specific retrosynthetic analysis involves an oxy-Cope reaction followed by aldol O–H insertion/aldol cyclization resulting from readily accessible vinyl diazoacetates and β-hydroxy vinyl ketones (Scheme 15).

2.2 Preparation of Model Substrates and Precursors

We chose *β*-hydroxy vinyl ketone **39a** (Figure 16) and vinyl diazobenzoate **48** as model substrates for optimization of this cascade. **39a** was synthesized using an efficient three-step route, enabling convenient diversification of the *β*-hydroxy vinyl ketone fragment to access a variety of oxacycles.

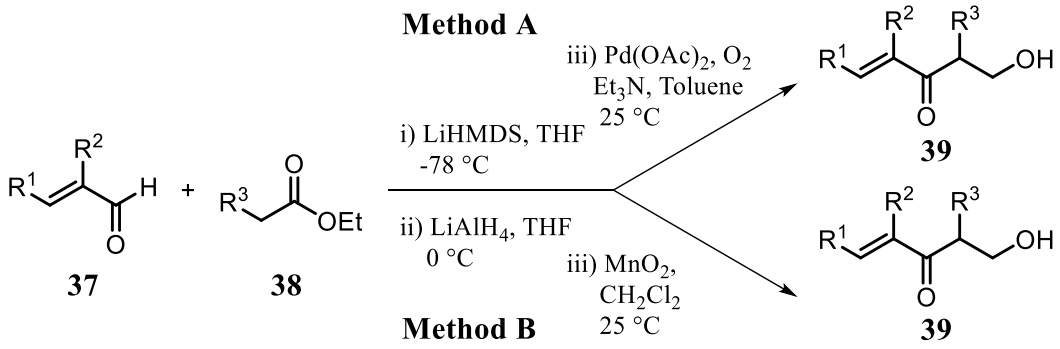

Scheme 16. General scheme for the preparation of β-hydroxy vinyl ketones

The route began with a conventional aldol reaction performed with LiHMDS followed by reduction with $LiAlH_4$ to a diol synthon that was then subjected to selective allylic oxidation using either MnO_2 or $Pd(OAc)_2$ in the presence of oxygen (Scheme 16). Using this three-step route, five primary β-hydroxy vinyl ketones were prepared (Figure 16).

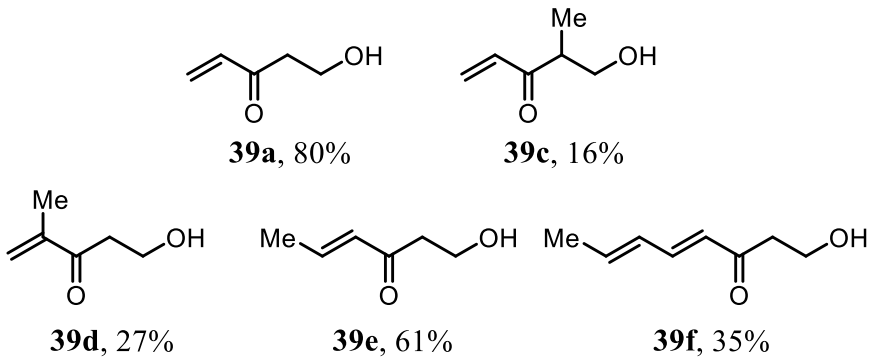

Figure 16. β-hydroxy vinyl ketone starting materials **39a**, **39c-39f**

Secondary β-hydroxy vinyl ketone **39b** was prepared by a different method (Scheme 17). Starting with ethyl acetate (**40**), an aldol reaction was performed on benzaldehyde (**41**) yielding benzyl alcohol **42**. This was subsequently transformed into Weinreb amide **44** using **43** and n-BuLi conditions. At this point, the amide product **44** was then subjected to a Grignard addition, selectively providing the β-hydroxy vinyl ketone **39b** in a single step.

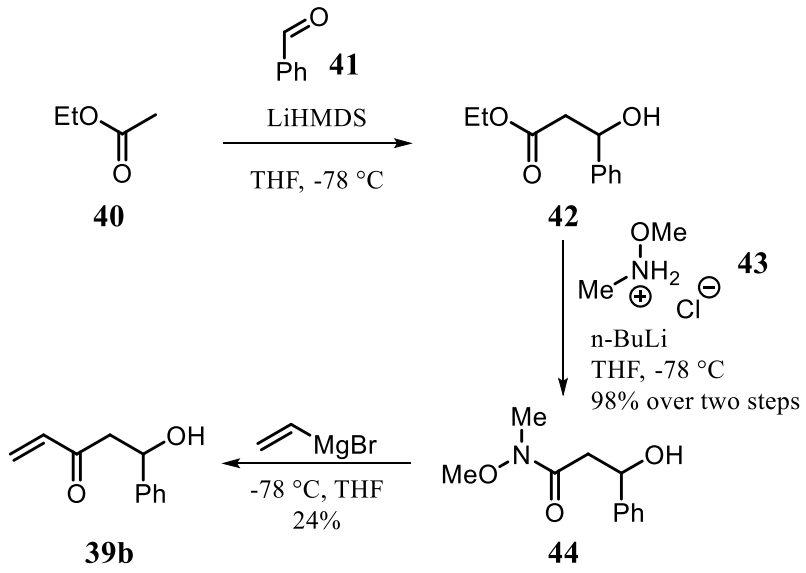

Scheme 17. Preparation of β-hydroxy vinyl ketone **39b**

The corresponding diazo precursors were also prepared via two separate three-step protocols. Benzyl 2-diazobut-3-enoate **48** was prepared by first synthesizing a very stable acceptor/acceptor diazo **46** from commercially available benzyl acetoacetate **45** using diazo transfer conditions. Then, **46** was selectively reduced with sodium borohydride to the corresponding secondary alcohol **47** which was then dehydrated to yield benzyl 2-diazobut-3-enoate **48** (Scheme 18).

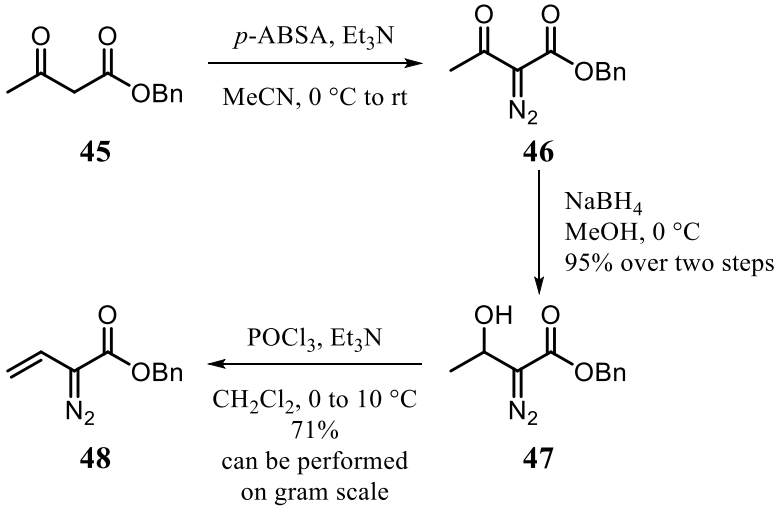

Scheme 18. Preparation of benzyl 2-diazobut-3-enoate **48**[92]

Methyl (*E*)-2-diazohexa-3,5-dienoate **52** was prepared with a different synthetic route starting from commercially available sorbic acid **49**, which was subjected to esterification conditions in methanol to yield the methyl sorbate **50**. Following this, **52** was accessed directly following deprotonation and selective α-diazo transfer with *p*-ABSA. Better yields were eventually obtained with a two-step process, starting with isomerization of methyl sorbate **50** to the deconjugated diene **51** followed by diazo transfer to yield methyl (*E*)-2-diazohexa-3,5-dienoate **52** (scheme 19).

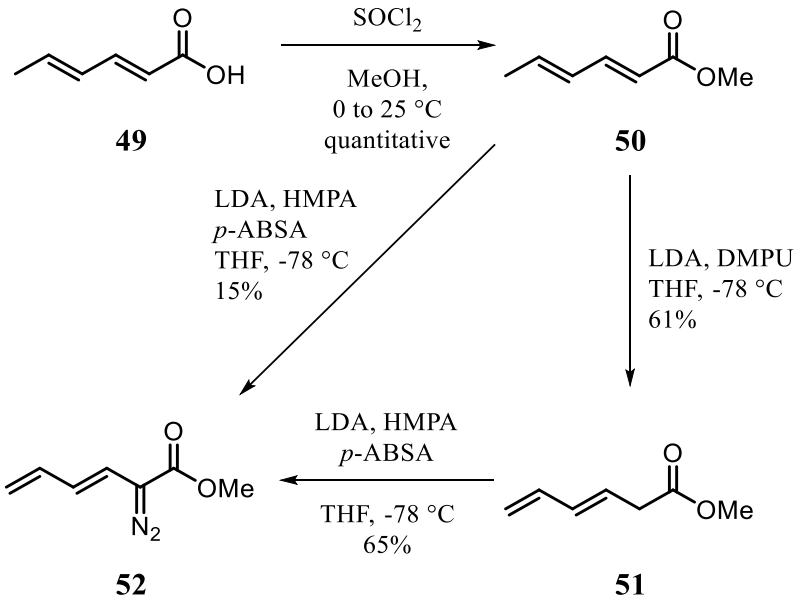

Scheme 19. Preparation of methyl (*E*)-2-diazohexa-3,5-dienoate **52**[93]

2.3 Reaction Setup

From our initial attempts and previous literature reports, diazoacetate precursors often exhibit a high level of reactivity and thermal instability that results in complex mixtures.[30-31] For this reason, we introduced our diazo precursors to the reaction mixture via slow addition over several hours. To accommodate this, a basic but effective apparatus shown in figure 17 was utilized for all of the cascades shown in this and the following

chapters unless otherwise stated. As shown in figure 17, the reaction pot contained the β-hydroxy vinyl ketone **39** and catalyst in refluxing solvent while a solution of vinyl diazoacetate (**48**/**52**) was added via syringe pump through a 12" needle fixed through the reflux condenser. It is important to note that the needle needed to be above the line of reflux to avoid diazo decomposition in the needle.

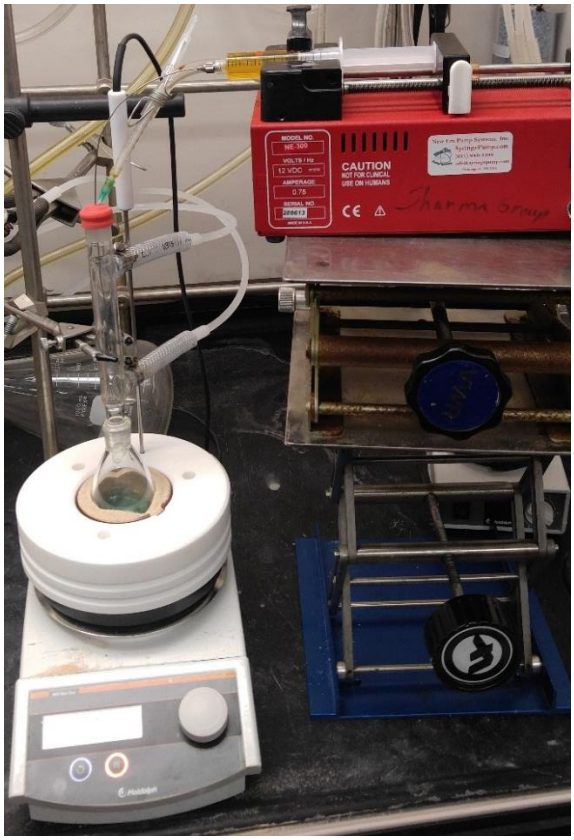

Figure 17. Slow addition reaction setup

2.4 Reaction Optimization

For the initial optimization, model substrates **48** and **39a** were screened with $Rh_2(esp)_2$ due to this catalyst's efficient performance in O–H insertion reactions.[49] At the outset, $Rh_2(esp)_2$ in CH_2Cl_2 at 25 °C resulted in chemoselective O–H insertion followed by

an aldol cyclization to yield **53** but did not proceed through the oxy-Cope rearrangement to complete the third step of the envisioned cascade sequence (Table 1, entry 1).

Table 1. Efficiency of metal-salts in carbene O—H insertion/aldol/oxy-Cope cascade

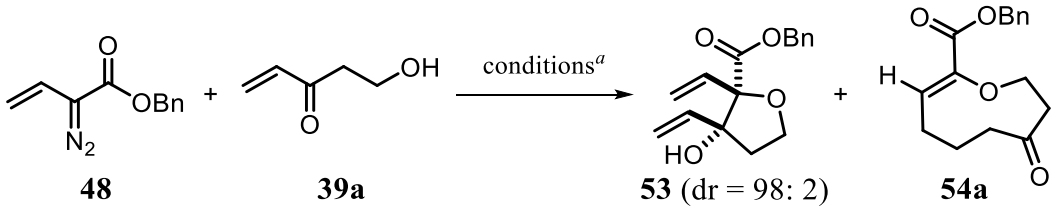

48 **39a** **53** (dr = 98: 2) **54a**

entry	reagent	solvent, temp (°C)	product yield (%)[b]
1	$Rh_2(esp)_2$	CH_2Cl_2, 25 °C	**53**, 45
2	$Rh_2(esp)_2$	CH_2Cl_2, reflux	**53**, 72
3	$Rh_2(esp)_2$	DCE, reflux	**53**, 71
4	$Rh_2(esp)_2$	toluene, reflux	**54a**, 42
5	**$Rh_2(OAc)_4$**	**toluene, reflux**	**54a, 68**
6	$Rh_2(TFA)_4$	toluene, reflux	**54a**, 26
7	$Rh_2(HFB)_4$	toluene, reflux	**54a**, 29
8	$Rh_2(OAc)_4$	trifluorotoluene, reflux	**54a**, 67
9	$Rh_2(OAc)_4$	chlorobenzene, reflux	**54a**, 68
10	$Cu(acac)_2$	toluene, reflux	CM
11	$Cu(OAc)_2$	toluene, reflux	CM
12	Cu(OTf)	toluene, reflux	CM

[a]All optimization reactions were performed by adding a 0.38 M solution of **48** (1.5 equiv) into a 0.17 M solution of **39a** (1 equiv) with catalyst (1 mol %) over 3 h *via* a syringe pump, after the addition of diazo compound, all reactions were refluxed for an additional 1 h. [b]Isolated yields after column chromatography.

Furthermore, the yield of aldol product **53** obtained was quite low (45%) with a high account of insertion byproduct. Due to the tendency of $Rh_2(esp)_2$ to lead to protodemetalation quickly, these results were not surprising, but it required us to solve two problems sequentially. First, we sought to identify whether ring expansion would occur. Since it is known that oxy-Cope rearrangements can be thermally driven[75, 94] we focused our attention toward identifying an appropriate solvent and temperature that would induce the ring expansion. We initially attempted refluxing conditions in CH_2Cl_2 (b.p. 40 °C) yielding good results for aldol product **53**, but still no trace of medium-sized ring **54a** (entry 2). We elevated the refluxing temperature further by screening dichloroethane (DCE, b.p. 84 ºC) which resulted in similar aldol conversion, suggesting that further thermal enhancement of the O–H insertion/aldol step was not plausible (entry 3). Furthermore, we still had not obtained medium-sized ring **54a** at 84 °C. To our delight, when we performed the same reaction in toluene (b.p. 110 °C), we obtained the medium-sized ring **54a** in 42% yield (entry 4). These encouraging results led us to screen other Rh (II)-salts (entries 5–7) using refluxing toluene temperatures. Among them, $Rh_2(OAc)_4$ was found to be the most efficient catalyst for the cascade sequence (entry 5). We then screened solvents with varying levels of polarity and boiling points with no improvement in the overall yield of **54a**. With hope to achieve the cascade sequence with earth abundant transition metal catalysts known to effectively form carbenoid intermediates, we also screened various Cu-salts,[95] but only observed a complex mixture of different products (entries 10–12). Interestingly, the copper salts utilized by Moody et al.[30] failed to even provide aldol product **53** suggesting that the vinylcarbenoid derived from **48** possess different reactivity compared to the aryl diazoacetate counterparts.

2.5 Substrate Scope of Aldol/Oxy-Cope/Cascade

With optimized conditions in hand, we then moved to test the substrate scope of this cascade. To our delight, this cascade tolerated substituents on all positions of the *β*-hydroxy vinyl ketone fragment in good yield providing exclusively *Z*-olefin oxacycles. Specifically, the cascade tolerated both primary and secondary *β*-hydroxy vinyl ketones (Scheme 20, **54a**, **54b**).

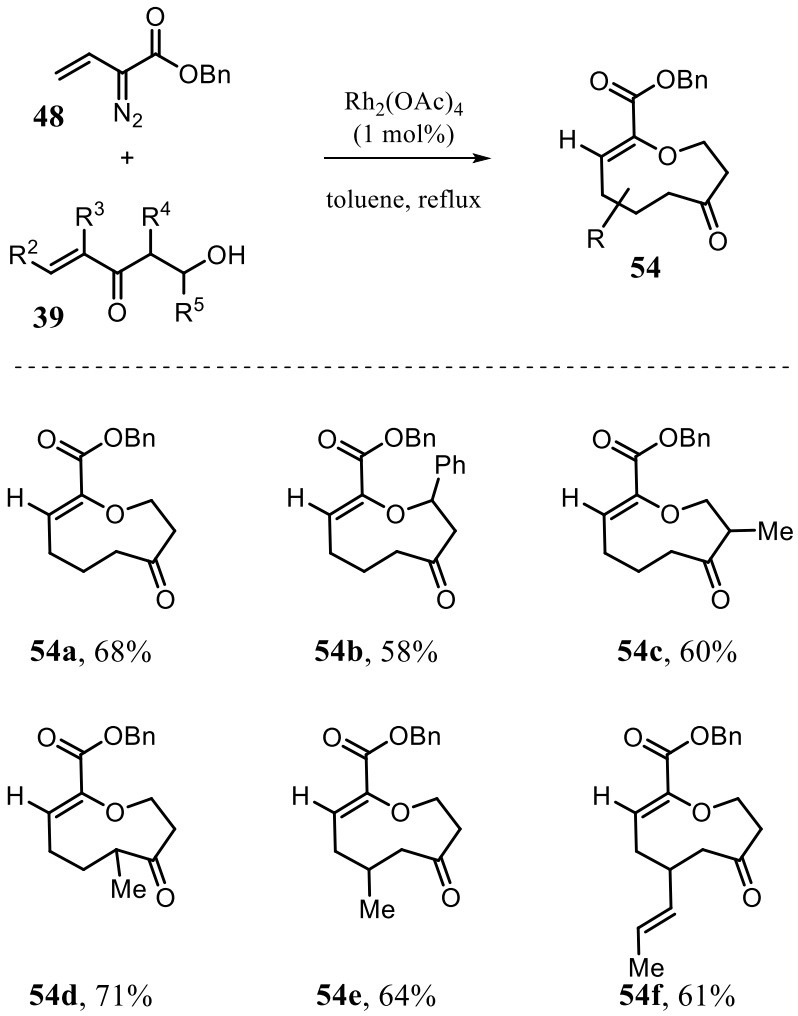

Scheme 20. Scope of $Rh_2(OAc)_4$-catalyzed carbene-OH insertion/aldol/oxy-Cope cascade: modifying the keto-alcohol fragment

Furthermore, the reaction tolerates a variety of different methyl substituents (**39c**–**39e**) as well as a vinyl substituent (**39f**) providing medium-sized oxacycles **54c**–**54f** respectively in good yield. Methyl (*E*)-2-diazohexa-3,5-dienoate **52** performed the desired cascade chemoselectively with most aforementioned *β*-hydroxy vinyl ketones (Scheme 21).

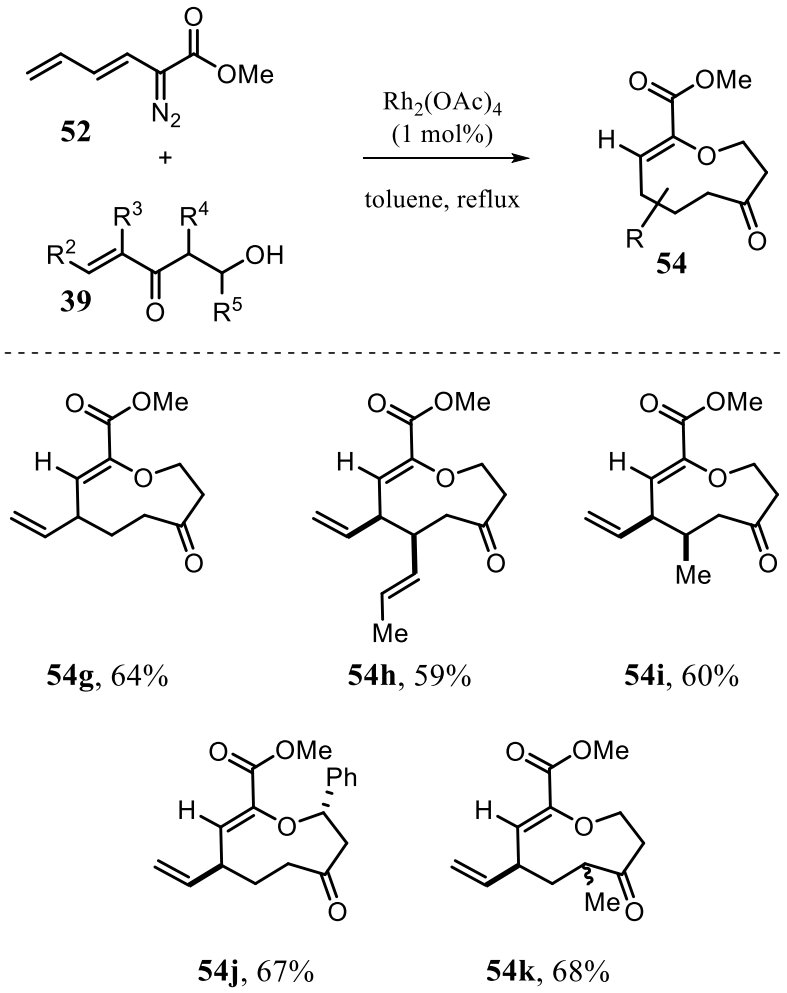

Scheme 21. Scope of $Rh_2(OAc)_4$-catalyzed carbene-OH insertion/aldol/oxy-Cope cascade with methyl (*E*)-2-diazohexa-3,5-dienoate **52**

Upon treatment with substituted vinyl keto alcohols, **52** underwent the desired cascade sequence smoothly to obtain the corresponding oxacycle in good yields with complete stereoselectivity (Scheme 21, **54g-k**). Remarkably, methyl (*E*)-2-diazohexa-3,5-dienoate

52 underwent the desired cascade with no observed C–H activation or cyclopropanation diversions, attesting to the chemoselectivity of this reaction. The rest of the β-hydroxy vinyl ketone precursors were then screened with this diene diazo exhibiting similar yields (scheme 21). In addition, this diazo also allowed us to demonstrate the diastereoselectivity of the cascade sequence. We obtained a single diastereomer in all cases except **54k**, which is explained by the reaction mechanism further in this chapter. Furthermore, we hypothesized that **54h** could undergo further ring expansion via subsequent Cope reaction to form a 13-membered oxacycle (Scheme 21). Unfortunately, this expansion did not occur under thermal conditions or with the use of catalysts know to induce Cope rearrangements, such as bisbenzonitrile palladium dichloride.[96]

2.6. Probing the Mechanism of the Reaction

The stereochemical arrangement of substituents and *Z*-configuration of olefin was determined based on the nOe correlations and was further confirmed by the single crystal structure of **54i** using X-ray diffraction (Figure 18).

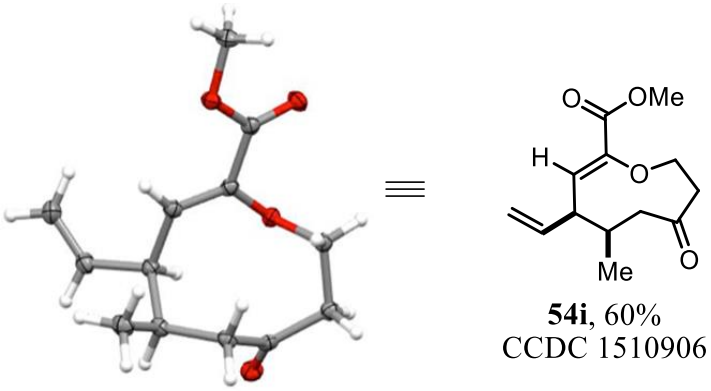

Figure 18. X-ray crystal structure of oxacycle **54i**

For further insights into the reaction mechanism, additional experiments were carried out. First, the intermediate aldol product **53**, isolated as a single diastereomer, was exposed to

$Rh_2(OAc)_4$ in refluxing toluene. As expected, we observed a clean formation of oxy-Cope rearrangement product **54a** in excellent yield (Table 2, entry 1). Next, **53** was refluxed in toluene without $Rh_2(OAc)_4$ to rule out the involvement of Rh-metal in the oxy-Cope rearrangement. As expected, the reaction took the same time to afford product **54a** suggesting a thermally driven oxy-Cope rearrangement (Table 2, entry 2). Since oxy-Cope rearrangements can be catalyzed under basic conditions,[70, 72] aldol product **53** was subjected to different bases known to promote an anionic oxy-Cope rearrangement. Unfortunately, we observed significant decomposition without any trace of desired oxacycle **54a** (Table 2, entry 3, 4).

Table 2. Oxy-Cope rearrangement of compound **53** into **54a** control experiments

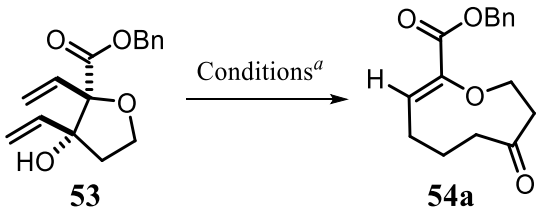

53 **54a**

entry	reagent	solvent, temp (ºC), *t*	yield (%)[b]
1	$Rh_2(OAc)_4$	toluene, reflux, 2 h	88
2	-	toluene, reflux, 2 h	90
3	KH, 18-crown-6	THF, 0 ºC, 5 min	CM
4	LiHMDS	THF, 0 ºC, 15 min	CM
5	CSA	toluene, 25 °C to reflux, 2 h	CM

[a]All optimization reactions were performed with 0.1 M solution of **53**;
[b]Isolated yields after column chromatography.

We also attempted acidic conditions to catalyze the oxy-Cope rearrangement but did not observe any desired product (Table 2, entry 5). These findings allow us to propose the reaction mechanism shown in Scheme 22.

First, diazo compound **48/52** is decomposed by the $Rh_2(OAc)_4$ to form an ambiphilic Rh-carbenoid that undergoes a chemoselective O–H insertion reaction with *β*-hydroxy vinyl ketone **39** (Scheme 22). The resulting insertion intermediate then undergoes a 5-*exo*-trig aldol cyclization to provide the tetrahydrofuran intermediate **53** with high diastereoselectivity.[30, 88-91].

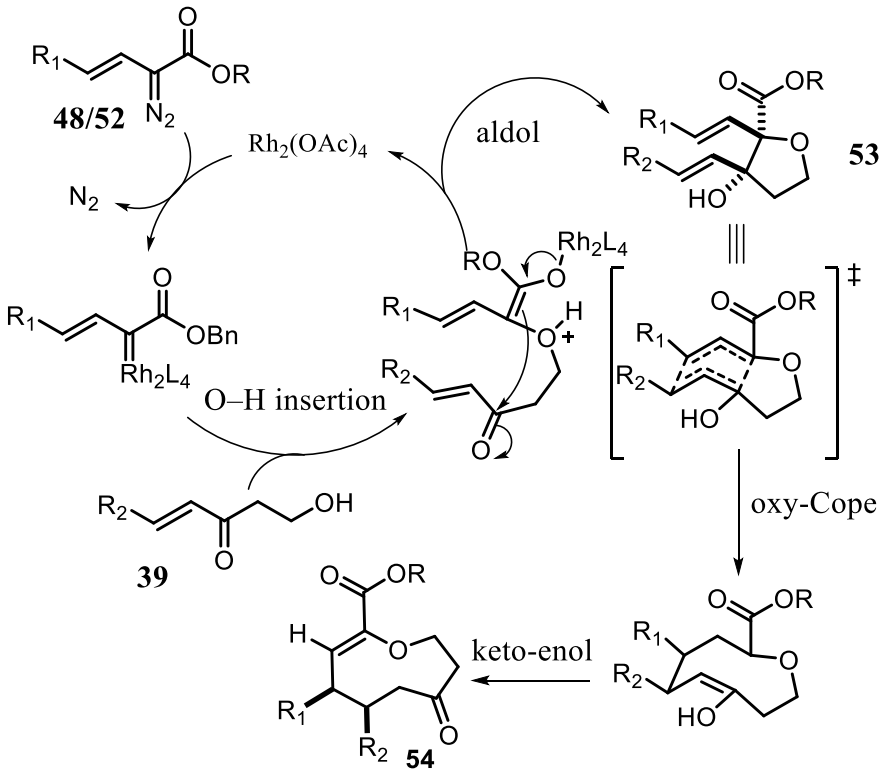

Scheme 22. Proposed reaction mechanism for $Rh_2(OAc)_4$-catalyzed diazo-OH insertion/aldol/oxy-Cope cascade

The divinyl tetrahydrofuran **53** sets the stage for a thermally driven, concerted oxy-Cope rearrangement via a boat-type transition state, which results in an enol product with the substituents *syn* to each other. The enol-form then tautomerizes to provide the thermodynamically more stable keto-tautomer **54**. The boat transition state of this oxy-Cope rearrangement was confirmed due to the retention in *syn* stereochemistry from aldol intermediate **53** to oxacycle product **54**. Otherwise, a chair transition state would have caused an inversion in stereochemistry. With the proposed mechanism, the observed decrease in diastereoselectivity (dr = 3:1) with **54k** (Scheme 21) can be explained. This is attributed to the keto-enol tautomerism of the final cascade product. The concerted oxy-Cope rearrangement initially leads to the enol-form, which rearranges to the thermodynamic keto-form under the reaction conditions racemizing this stereocenter (Scheme 22).

2.7 Conclusion and Future Directions

In conclusion, the reported diazo-OH insertion/aldol/oxy-Cope cascade sequence is convergent in nature and uses readily accessible starting materials to access highly functionalized 9-membered oxacycles.

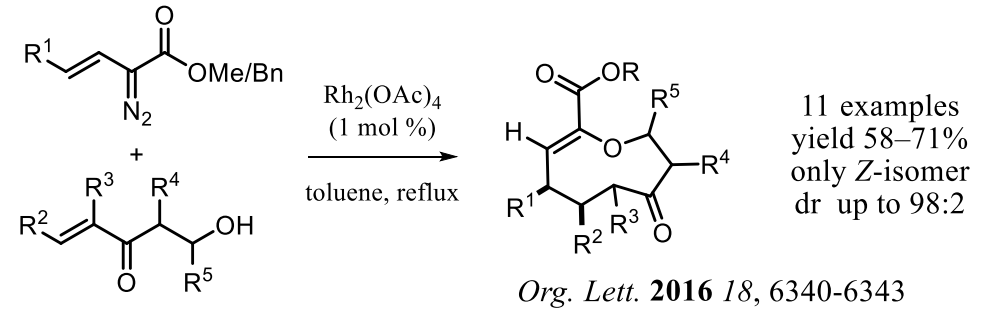

Scheme 23. Synthesis of oxacycle by ring expansion strategy

An important feature of this transformation is its excellent regio- and stereo-selectivity. This work was published in *Organic Letters* and was highlighted in an Organic Chemistry blog established by Professor Douglas Taber known as *Organic Chemistry Portal* (Scheme 23). Furthermore, the compounds synthesized in this chapter were submitted for high-through-put screening for fungicide properties. Unfortunately, none of the molecules reported herein resulted in any hit compounds.

Thus, the future direction of this medium-sized ring construction strategy is to incorporate new nucleophiles and/or attain different ring sizes. During the initial optimization of this work, we often observed competitive protodemetalation, yielding the major insertion byproduct. However, with proper catalyst selection, alcohol synthons were capable of cascade transformations due to their lower tendency of 1,2-proton transfer. Conversely, carboxylic acid nucleophiles only lead to insertion products when reacted under similar conditions. We speculate that the lower pKa of carboxylic acids compared to alcohols prevents the zwitterionic intermediate from reacting in a productive manner by always leading to the insertion byproduct. Thus, in the next chapter, we show that this problem can be circumvented to provide a diverse array of lactones in a diastereoselective fashion.

Chapter 3. Stereoselective Synthesis of Diverse Lactones

Stereoselective Synthesis of Diverse Lactones through a Cascade Reaction of Rhodium Carbenoids with Ketoacids

3.1 Introduction*

Spanning the realm of complexity that exists within natural and synthetic organic frameworks, the lactone motif is unquestionably prominent, useful, and attractive to the scientific community.[97] With ring sizes ranging from 3 to 60, the lactone ring is present in food additives,[98] perfumes,[99-100] pharmaceuticals,[101] and exists in more than 10% of natural products often possessing significant bioactivity or synthetic utility.[102-105] Due to the importance of the lactone motif, their synthesis remains an area of current interest to the chemical community.

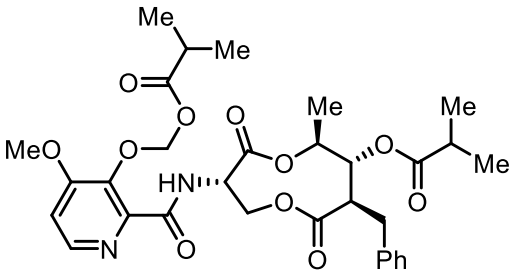

fenpicoxamid
(Inatreq™), 2016
Fungicide
EC_{50} = 0.051 mg L^{-1}

Figure 19. A potent fungicide diolide

* Reproduced in part from, "Stereoselective Synthesis of Diverse Lactones through a Cascade Reaction of Rhodium Carbenoids with Ketoacids." Nicholas P. Massaro, Joseph C. Stevens, Aayushi Chatterji and Indrajeet Sharma. *Org. Lett.* **2018**, 20, 23, 7585–7589 with permission from Organic Letters. *Copyright © American Chemical Society*. N.P.M. developed cascade sequence, performed optimization, designed and synthesized substrate scope, characterized all unknown compounds, prepared manuscript and developed iron cascade.

Furthermore, fenpicoxamid had been launched by Corteva as a potent fungicide (Figure 19).[106] The utility of this 9-membered diolide inspired us to extend our previously developed strategy to accommodate carboxylic acids in order to synthesize medium-sized lactones.[35, 53] In comparison to the previously known reports of alcohol O–H insertion/aldol cyclization in literature for the synthesis of tetrahydrofurans (Scheme 24a),[30, 107] we presumed that the incompatibility of carboxylic acids in carbene cascade reactions may be attributed to the competing insertion reaction via proton transfer resulting from low pKa values of protonated carboxylic acids in the zwitterionic intermediate (Scheme 24b).

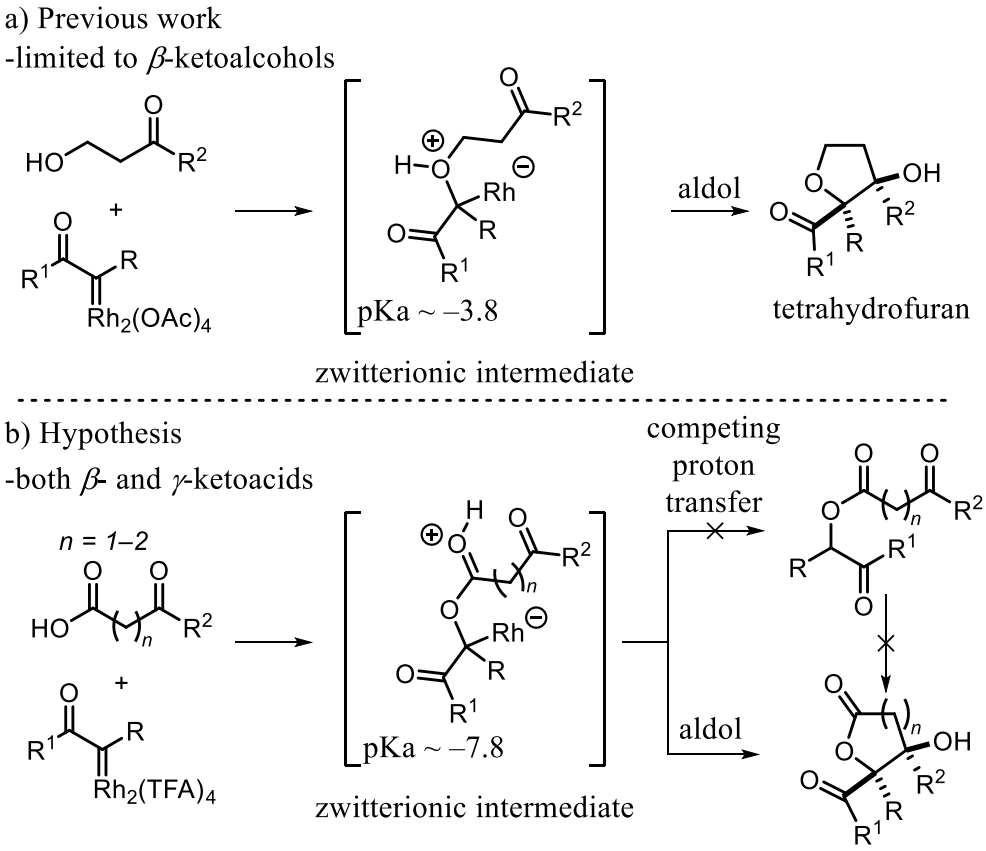

Scheme 24. Recent Applications of O-H insertion/aldol Cyclization

Thus, we made a hypothesis that proton transfer could be delayed by promoting a Zimmerman-Traxler transition state by changing the electronics of the catalyst that forms

the diazo-derived rhodium carbenoid (Scheme 24b), leading to aldol cyclization. This would provide valuable γ-lactones which are important, complex building blocks. For example, 3-hydroxybutyrolactone has been utilized as an enantiopure precursor for both Pfizer's Lipitor® and AstraZeneca's Crestor (Figure 20).[108-109]. In addition to this, we envisioned that these synthons could also be ring-expanded to the nine membered lactones. However, as will be stated in this chapter, the necessary *β*-keto-acid precursors were less suitable for this expansion cascade due to thermal instability, so the reaction was adjusted to incorporate a 6-membered *exo*-trig cyclization via aromatic ring constraint which provided direct access to functionalized, benzannulated valerolactones and the ring expanded 10-membered lactones. This was quite

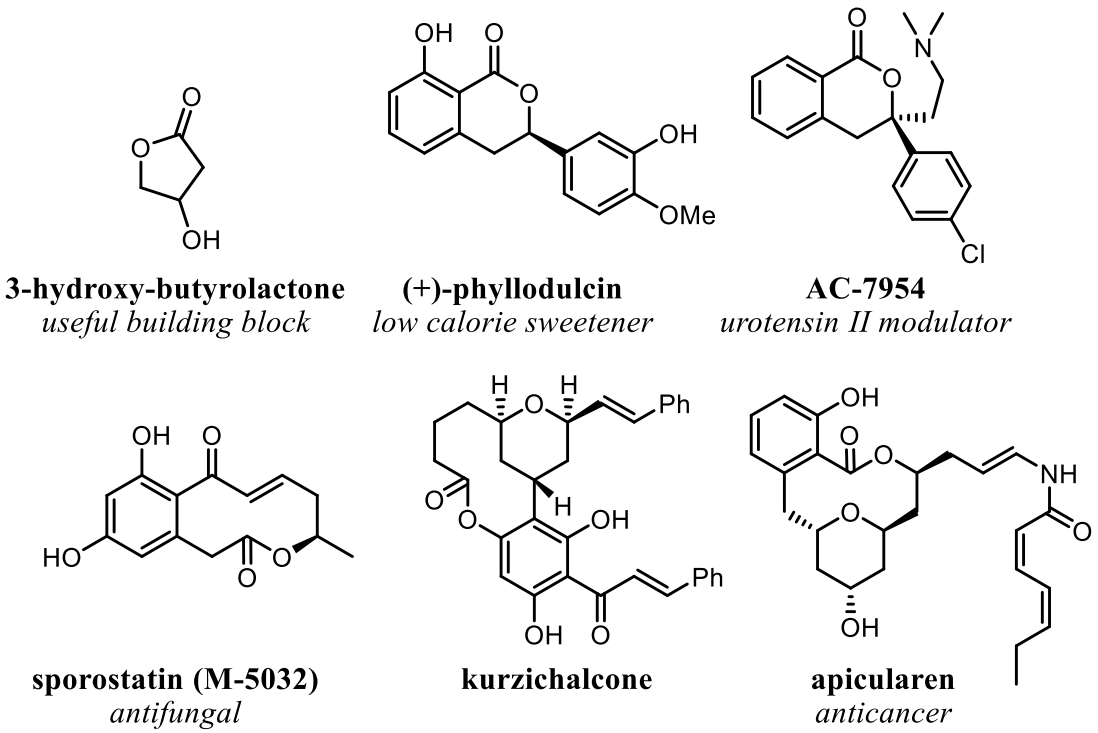

Figure 20. Examples of natural and synthetic lactone products

useful because benzannulated lactones represent an interesting class of medium-sized heterocycles such as sporostatin and apicularen that have biological and industrial relevance (Figure 21).[110-112]

3.2 Optimization of Acid Insertion/Aldol Cascade

When developing the carboxylic acid insertion/aldol cascade, it was a significant challenge to determine a viable model substrate for which to base our optimization efforts. Initially, *β*-ketoacid **55** and aryl diazoacetate **56a** were chosen as model substrates. We performed an initial screening of catalyst conditions as shown in Table 3. As expected, both $Rh_2(OAc)_4$ and $Rh_2(esp)_2$ provided insertion product exclusively (Table 3, entries 1–2).

Table 3. Initial optimization of acid insertion/aldol cascade

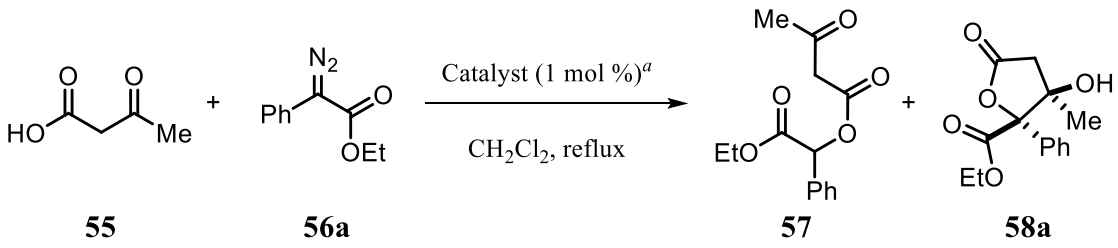

55 **56a** **57** **58a**

entry	catalyst	ratio **57**:**58a** (%)[b]
1	$Rh_2(OAc)_4$	100:0
2	$Rh_2(esp)_2$	100:0
3	$Rh_2(TPA)_4$	100:0
4	**$Rh_2(TFA)_4$**	**37:63**
5	$Rh_2(HFB)_4$	50:50

[a]All optimization reactions were performed by adding a 0.24 M solution of **56a** (24.0 mg, 0.12 mmol, 2.0 equiv.) into a 0.12 M solution of **55** (15.0 mg, 0.06 mmol, 1.0 equiv.) with catalysts via a syringe pump for 1.5 h, after the addition of diazo, all reactions were refluxed for an additional 30 min.
[b]The percent ratio of **57** and **58a** was determined by crude ^{1}H NMR.

We then turned our attention to more sterically encumbering catalysts such as $Rh_2(TPA)_4$ but did not observe promising results of aldol formation (Table 3, entry 3).

Table 4. Optimization of γ-ketoacid O–H insertion/aldol cascade with diazoacetate **56a**

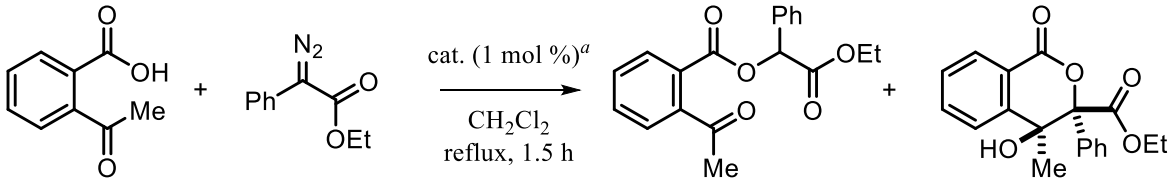

59a **56a** **60a** **61a** (dr = 98: 2)

entry	catalyst	solvent, temp (°C)	ratio **60a**:**61a**[b]	yield **61a** (%)[c]
1	$Rh_2(OAc)_4$	CH_2Cl_2, reflux	100:0	0
2	$Rh_2(esp)_2$	CH_2Cl_2, reflux	100:0	0
3	$Rh_2(TPA)_4$	CH_2Cl_2, reflux	100:0	0
4	**$Rh_2(TFA)_4$**	**CH_2Cl_2, reflux**	**37:63**	**60**
5	$Rh_2(HFB)_4$	CH_2Cl_2, reflux	50:50	46
6	$(CuOTf)_2$•benzene	CH_2Cl_2, reflux	100:0	0
7	$Cu(acac)_2$	CH_2Cl_2, reflux	100:0	0
8	Fe(TPP)Cl	CH_2Cl_2, reflux	100:0	0
9	–	CH_2Cl_2, reflux	100:0	0

[a]All optimization reactions were performed by adding a 0.24 M solution of **56a** (24.0 mg, 0.12 mmol, 2.0 equiv.) into a 0.12 M solution of **59a** (15.0 mg, 0.06 mmol, 1.0 equiv.) with catalysts via a syringe pump for 1.5 h, after the addition of diazo, all reactions were refluxed for an additional 30 min.
[b]The percent ratio of **60a** and **61a** was determined by crude ^{1}H NMR.
[c]Isolated yields of **61a** obtained after column chromatography.

Then two our delight, we decided to screen more electron deficient catalysts such as $Rh_2(TFA)_4$ and $Rh_2(HFB)_4$ which both provided aldol product **58a**; although $Rh_2(TFA)_4$

provided slightly superior results. These results were encouraging, but the isolated yield of **58a** was only 54%. We then realized that the *β*-ketoacid precursor **55** was prone to decarboxylation.[113]

We then decided to initiate our optimization reaction with *γ*-ketoacids which provided a new challenge to overcome. First, the acid insertion/aldol cascade was not known aside from our preliminary result stated earlier. Secondly, the desired aldol reaction was now expanded to a 6-*exo*-trig cyclization, which was not previously accomplished in literature reports with rhodium ylide chemistry. For the second optimization, commercially available 2-acylbenzoic acid **59a** and aryl diazoacetate **56a** were selected as model substrates and subjected to a similar catalyst screening.[48] As anticipated, $Rh_2(OAc)_4$, $Rh_2(esp)_2$, and $Rh_2(TPA)_4$, in refluxing CH_2Cl_2 provided exclusively insertion product **60a** (Table 4, entry 1–3). To our delight, when we moved to our previously identified catalyst systems $Rh_2(TFA)_4$ and $Rh_2(HFB)_4$, we obtained similar insertion to aldol product ratio, but with much higher isolated yield, likely because **59a** exhibits higher thermal stability than **55** (Table 4, entry 4–5). With the hope to achieve the cascade sequence with earth abundant transition metal catalysts known to effectively decompose diazo compounds, we also screened copper and iron salts but failed to observe any desired product (entries 6–8).[95, 114] Finally, the cascade was attempted under metal-free conditions in refluxing CH_2Cl_2,[115] which led to diazo decomposition to provide exclusively the insertion product **60a** (entry 9). Due to the overall goal of synthesizing medium-sized rings, a similar optimization table was performed to test the applicability of vinyl starting materials (Table 5). When this was performed, an interesting enhancement in aldol production was observed with almost all rhodium catalysts screened except for $Rh_2(TPA)_4$,

which did not provide insertion (**60b**) or aldol (**61g**) products (Table 5, entry 3). As expected, the best results were obtained with $Rh_2(TFA)_4$, which provided aldol product **61g** exclusively in excellent yield.

Table 5. Optimization of γ-ketoacid O–H insertion/aldol cascade with diazoacetate **48**

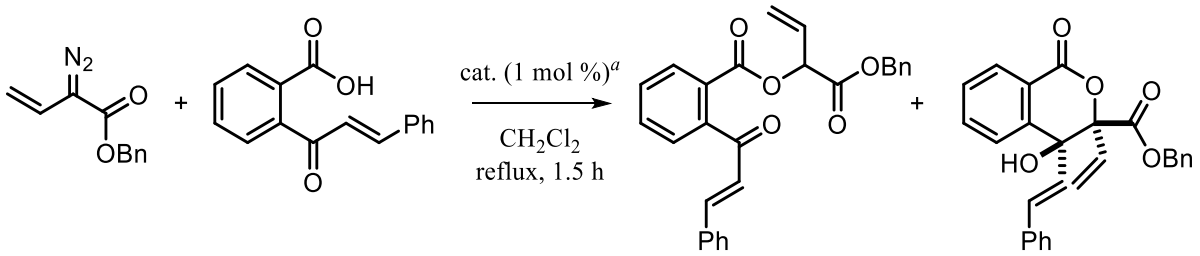

48 **59b** **60b** **61g** (dr = 98: 2)

entry	catalyst	solvent, temp (°C)	ratio **60b**:**61g**[b]	yield **61g** (%)[c]
1	$Rh_2(OAc)_4$	CH_2Cl_2, reflux	19:81	79
2	$Rh_2(esp)_2$	CH_2Cl_2, reflux	35:65	65
3	$Rh_2(TPA)_4$	CH_2Cl_2, reflux	-	0
4	**$Rh_2(TFA)_4$**	**CH_2Cl_2, reflux**	**0:100**	**97**
5	$Rh_2(HFB)_4$	CH_2Cl_2, reflux	0:100	67
6	$(CuOTf)_2$•benzene	CH_2Cl_2, reflux	CM	0
7	$Cu(acac)_2$	CH_2Cl_2, reflux	100:0	0
8	Fe(TPP)Cl	CH_2Cl_2, reflux	NR	0

[a]All optimization reactions were performed by adding a 0.24 M solution of **48** (24.0 mg, 0.12 mmol, 2.0 equiv.) into a 0.12 M solution of **59b** (15.0 mg, 0.06 mmol, 1.0 equiv.) with catalysts via a syringe pump for 1.5 h, after the addition of diazo, all reactions were refluxed for an additional 30 min.
[b]the percent ratio of **60b** and **61g** was determined by crude ^{1}H NMR.
[c]Isolated yields of **61g** obtained after column chromatography.

3.3 Synthesis of Readily Available Starting Materials

As stated in subsection 3.1, during the initial development of this cascade, *β*-ketoacid **55** was initially utilized. The preparation of this *β*-ketoacid was achieved by saponification of ethyl acetoacetate **62** with NaOH, yielding 3-oxobutanoic acid **55** as a white solid (Scheme 25).

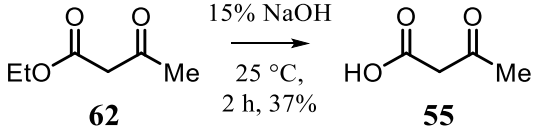

Scheme 25. Synthesis of *β*-ketoacid **55**[116]

In order to synthesize 9-membered lactones, (*E*)-3-oxo-5-phenylpent-4-enoic acid **67** was synthesized. The preparation of **67** was achieved via a three-step protocol with 52% overall yield (Scheme 26). First, the addition of *tert*-butyl acetate (**63**) to cinnamyl aldehyde (**64**) was accomplished followed by allylic oxidation of the secondary alcohol **65** with MnO_2 yielding *tert*-butyl (*E*)-3-oxo-5-phenylpent-4-enoate **66** in 95% over two steps.

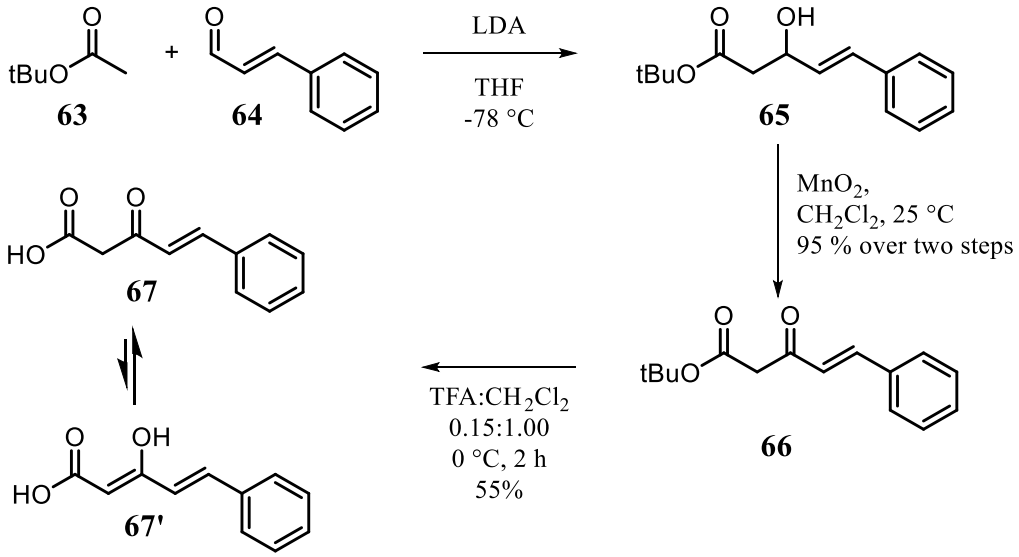

Scheme 26. Synthesis of vinyl *β*-ketoacid

Then *tert*-butyl (*E*)-3-oxo-5-phenylpent-4-enoate **66** was efficiently deprotected by stirring in a 1:1 ratio of TFA:CH_2Cl_2 yielding (*E*)-3-oxo-5-phenylpent-4-enoic acid **67** as the keto-enol tautomeric mixture (Scheme 26).

The second optimization table utilized commercially available 2-acylbenzoic acid **59a**. This starting material provided efficient access to ketoacid chalcones which were also utilized for the third optimization table and substrate scope of this cascade. These chalcones were achieved via a Claisen-Schmidt condensation with 2-acylbenzoic acid **59a** with various aryl aldehydes **68** (Scheme 27).

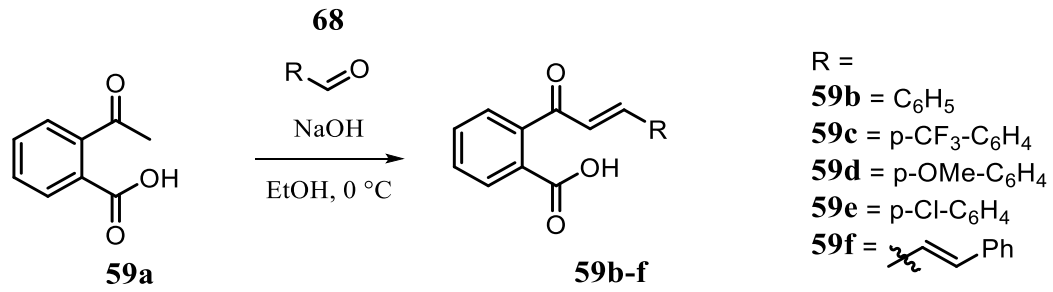

Scheme 27. Chalcone carboxylic acid synthesis[117]

Since this insertion/aldol cascade was not previously explored with rhodium carbenoids, we felt it was appropriate to test the substrate scope of this 6-*exo*-trig cyclization. Thus, we needed to prepare a variety of aryl diazoacetates as well.

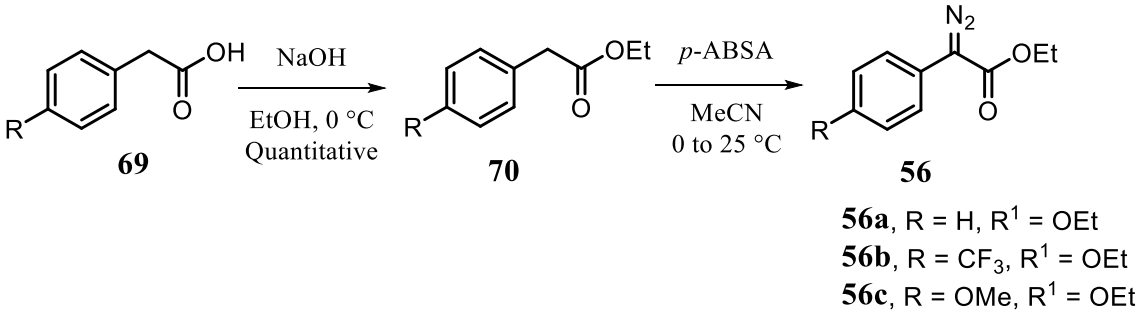

Scheme 28. Synthesis of aryl diazoacetates **56a**-**56c**[118-121]

Diazo starting materials **56a-c**, were synthesized via known diazo transfer conditions with *p*-ABSA (Scheme 28). 1-diazo-1-phenylpropan-2-one **72** was prepared through a similar method starting from commercially available phenylacetone **71** and performing a diazo transfer reaction with *p*-ABSA and DBU in acetonitrile to furnish the desired product in good yield (Scheme 29).

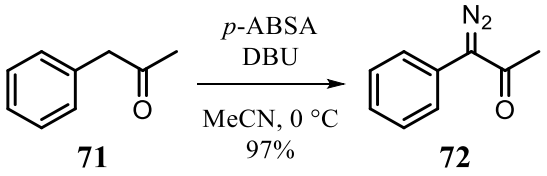

71 **72**

Scheme 29. Synthesis of 1-diazo-1-phenylpropan-2-one **72**

3-diazo-1-methylindolin-2-one **75**, was synthesized using a known literature protocol, converting N-methylisatin **73** into the tosylhydrazone **74** which could be exposed to basic conditions to generate 3-diazo-1-methylindolin-2-one **75** (Scheme 30).[122]

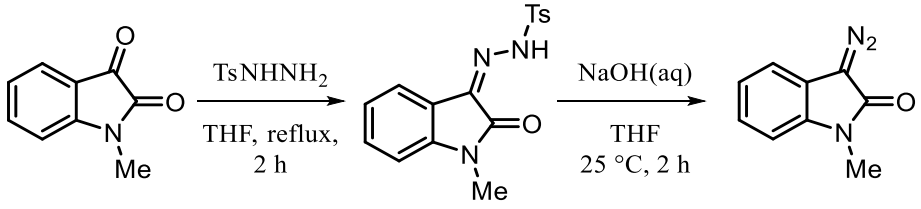

73 **74** **75**

Scheme 30. Synthesis of 3-diazo-1-methylindolin-2-one **75**[122]

Ethyl (*E*)-2-diazopent-3-enoate **78** was synthesized in a 70% overall yield following an aldol addition of ethyl diazoacetate **76** to propanal and subsequent elimination of the secondary alcohol **77** with phosphoryl chloride and triethylamine (Scheme 31).[40]

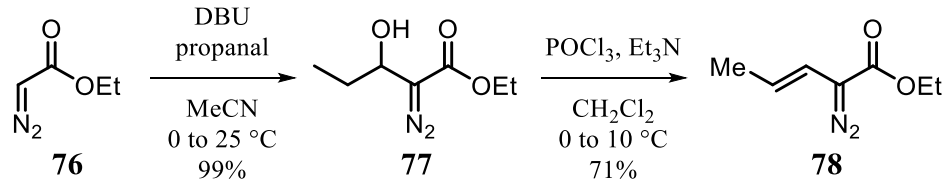

Scheme 31. Synthesis of Ethyl (*E*)-2-diazopent-3-enoate **78** [40]

3.4 Substrate Scope of Acid/Insertion Aldol Cascade

With optimized conditions in hand, we then investigated scope of the carbene cascade (Scheme 32). The cascade proceeds in good and excellent yield to produce **61a** and cinnamoyl derivative **61b,** respectively (Scheme 32) presumably due to the less steric interference of the styryl substituent compared to the methyl group in regard to A-values.[123] Electron-withdrawing and -donating groups are both tolerated on the aromatic ring of the diazoacetate fragments (Scheme 32, **61c**, **61d**). The decrease in aldol yield for ethyl 2-diazo-2-(4-(trifluoromethyl)phenyl)acetate **59b** is presumably due to electron deficiency at the carbenoid carbon, reducing its capability to perform the subsequent aldol cyclization compared to electron-rich carbenoid precursors like ethyl 2-diazo-2-(4-methoxyphenyl)acetate **56c**. Notably, the cascade reaction also accommodates α-diazoketones (**72**), which are prone to undergo the Wolff rearrangement, providing **61e** in good yield (Scheme 32).[124] The cascade reaction proceeds in good yield with 3-diazo-1-methylindolin-2-one **75** to provide the corresponding spirocyclic oxindole (Scheme 32, **61f**).

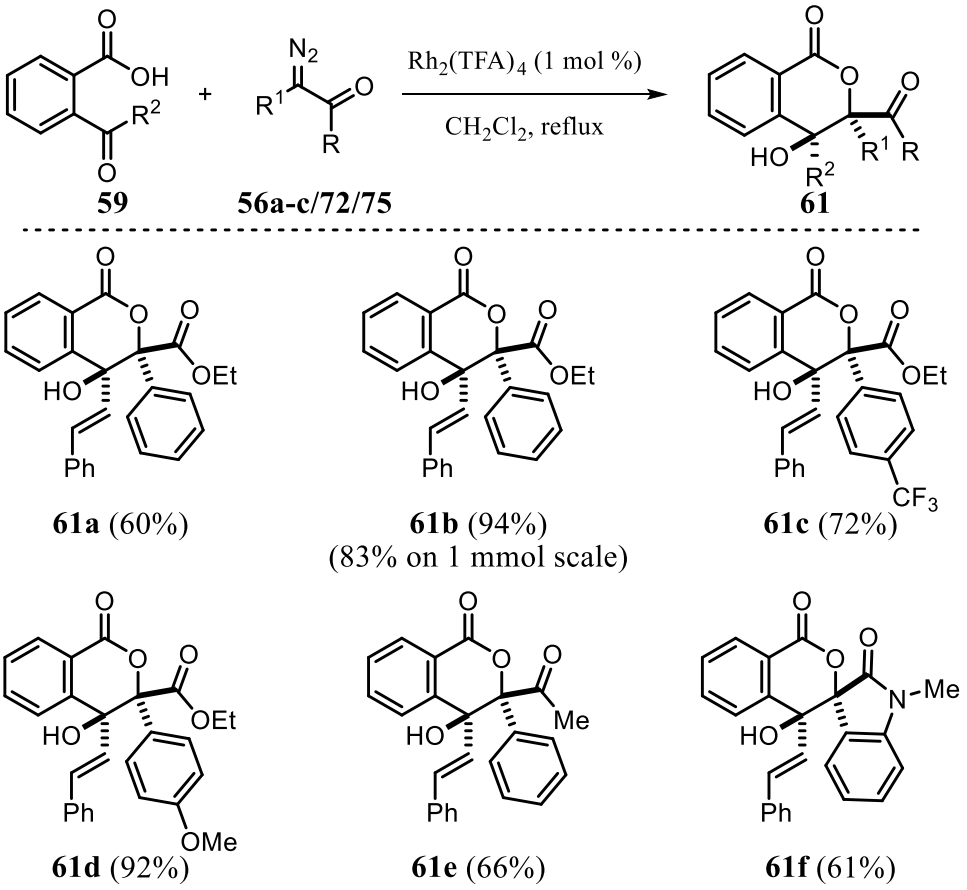

Scheme 32 Scope of $Rh_2(TFA)_4$-catalyzed carbene carboxylic acid O–H insertion/aldol cascade sequence with aryl diazoacetates

Relative stereochemistry of the spirocyclic oxindole **61f** was determined using single crystal X-ray diffraction (Figure 21). As expected, the resulting hydroxyl group and carbonyl moiety of the diazo were found to be in a *cis* configuration as reported in chapter two and previously in literature.[30, 48] This encouraged us to extend our cascade to vinyl

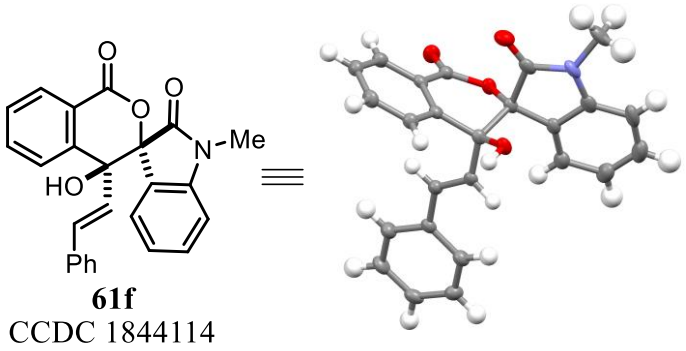

61f
CCDC 1844114

Figure 21. Crystal structure of **61f**

diazoacetates,[125-126] which would result in aldol products having divinyl motifs capable of undergoing a thermally induced oxy-Cope ring expansion[48] to provide access to 10-membered benzannulated lactones.

3.5 Substrate Scope of Acid Insertion/Aldol/oxy-Cope Cascade

To our delight, benzyl 2-diazobut-3-enoate **48** exhibited analogous reactivity to the aryl diazoacetates utilized in scheme 32. In this case, we modified the electronic nature of the chalcone ketone motif. The cascade performed well with 2-cinnamoylbenzoic acid **59b** obtaining an excellent yield (**61g**, Scheme 33). The reaction also operates in excellent yield with electron withdrawing groups attached to the chalcone ring (**61h**, Scheme 33). Conversely, when an electron donating group was installed, the ketone becomes less electrophilic resulting in a decreased yield of aldol product **61i**. The cascade also tolerated the presence of halogens as well as a cinnamyl group (Scheme 33, **61j**, **61k**).

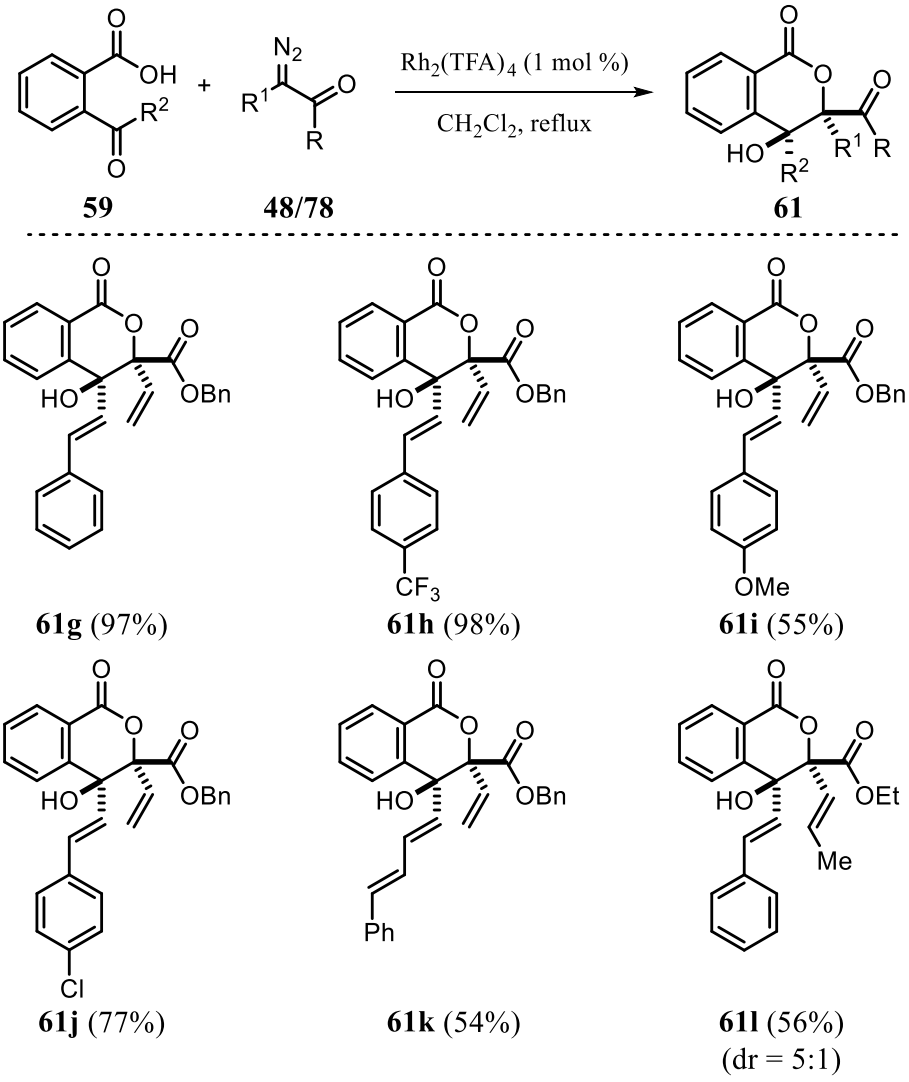

Scheme 33 Scope of $Rh_2(TFA)_4$-catalyzed carbene carboxylic acid O–H insertion/aldol cascade sequence with vinyl diazoacetates

With regard example **61k**, we envisioned incorporating methyl (*E*)-2-diazohexa-3,5-dienoate **52**, utilized in chapter 2, to provide a tetraene product capable of successive Cope ring expansion to yield 14-membered rings. Unfortunately, when we attempted the reaction with diazo **52**, no product was observed. Although, the cascade did tolerate ethyl (*E*)-2-diazopent-3-enoate **78** to access δ-lactone **61l** in respectable yield with a slightly reduced

diastereoselectivity. With this small library of oxy-Cope capable precursors, we decided to expand these 6-membered lactones to their corresponding 10-membered decanolides. δ-lactones **61g**–**61l** were subjected to thermally induced oxy–Cope ring expansion conditions in refluxing toluene (b. p. 110 ºC), similar to conditions reported in chapter 2.[48]

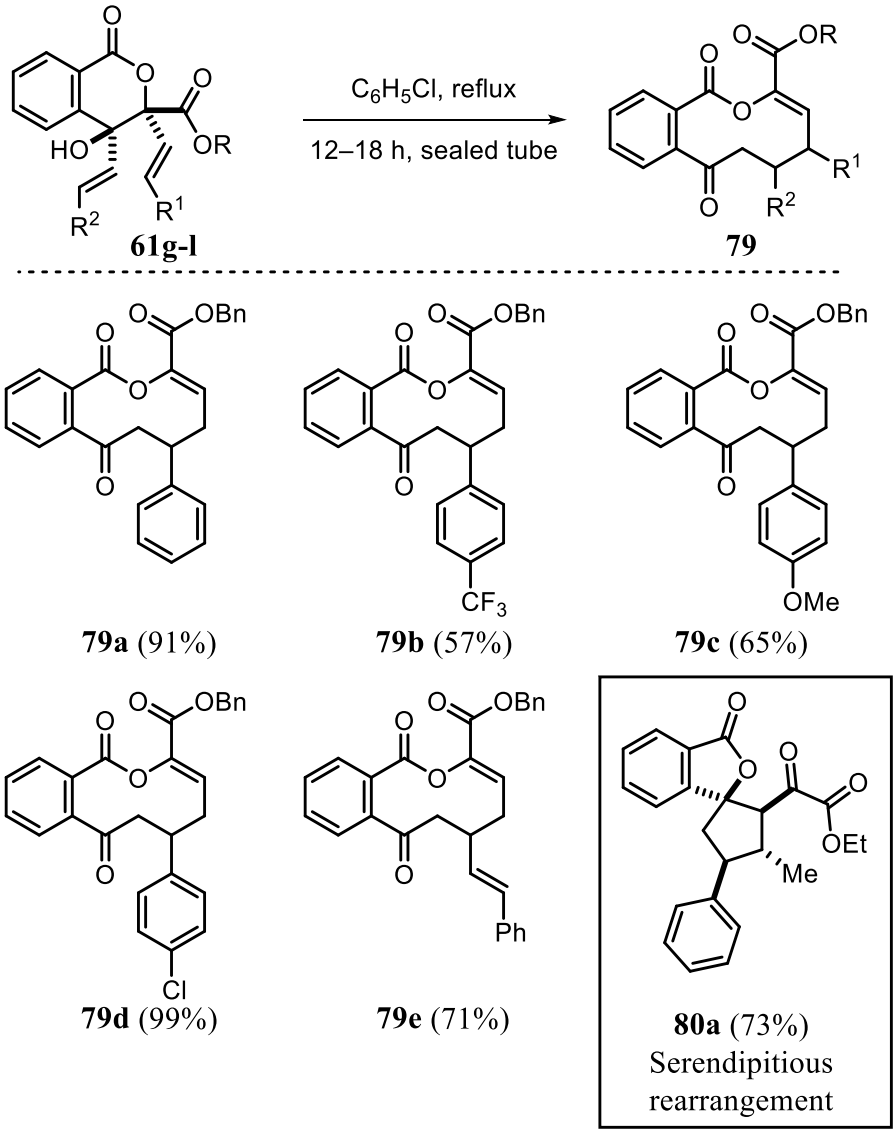

Scheme 34. Scope of thermal oxy-Cope ring expansion strategy

Ring expansion occurs under these solvent conditions, although the reaction is quite sluggish, and we continuously observed a unique side reaction between the starting

material and toluene that produced an unidentified set of by-products, causing a reduction in isolated yield. We suspect that radical oxidation of toluene may be occurring. To circumvent this unexpected problem, the solvent was changed to chlorobenzene in a sealed tube and the reaction was maintained under nitrogen atmosphere. The benefit of utilizing this solvent is that it is more deactivated due to the chlorine substituent, and has a higher boiling point (b. p. 131 ºC) to further promote the ring expansion. To our delight, the oxy-Cope ring expansion proceeds cleanly in good yield to the corresponding benzannulated decanolides (Scheme 34, **79a**–**79e**).

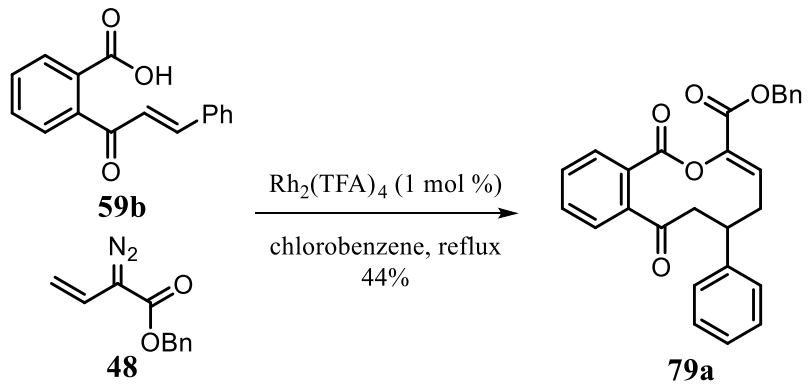

Scheme 35. One-pot synthesis of decanolide **79a**

Furthermore, we attempted the synthesis of decanolides as a one-pot cascade by performing the reaction in refluxing chlorobenzene. The synthesis of decanolide **79a** was successful, but the yield was diminished as compared to our two-step protocol (Scheme 35).

To our surprise, when the aldol product **61l** was subjected to the same reaction conditions, we obtained a spirophthalolactone bearing a highly functionalized cyclopentane ring (Scheme 34, **80a**).

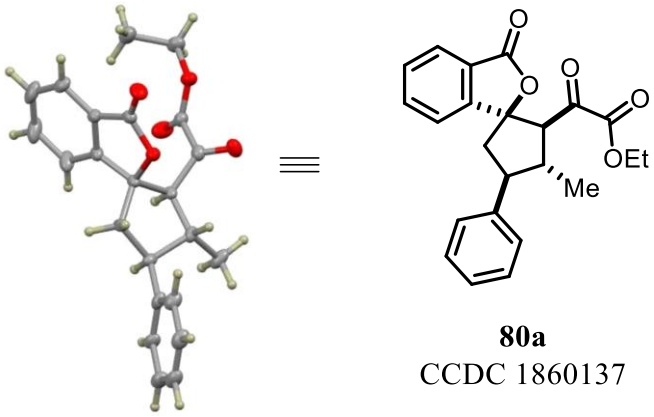

80a
CCDC 1860137

Figure 22. X-ray crystal structure of **80a**

The structure of **80a** was determined based on the nOe correlations and single crystal X-ray diffraction (Figure 22).

3.6 Serendipitous Rearrangement Yielding Spirophthalolactones

Since functionalized cyclopentanes are present in numerous bioactive natural products,[127-128] we decided to test the substrate scope of this serendipitous cascade. We synthesized aldol products **61m**–**61o** with high diastereoselectivity using ethyl (*E*)-2-diazopent-3-enoate **78**. As expected, the corresponding *δ*-lactones **61m**–**61o** underwent the rearrangement to form the desired cyclopentanes **80b**–**80d** (Scheme 36) in good yield as single diastereomers at 200 °C, albeit with prolonged reaction times needed of one to three days.

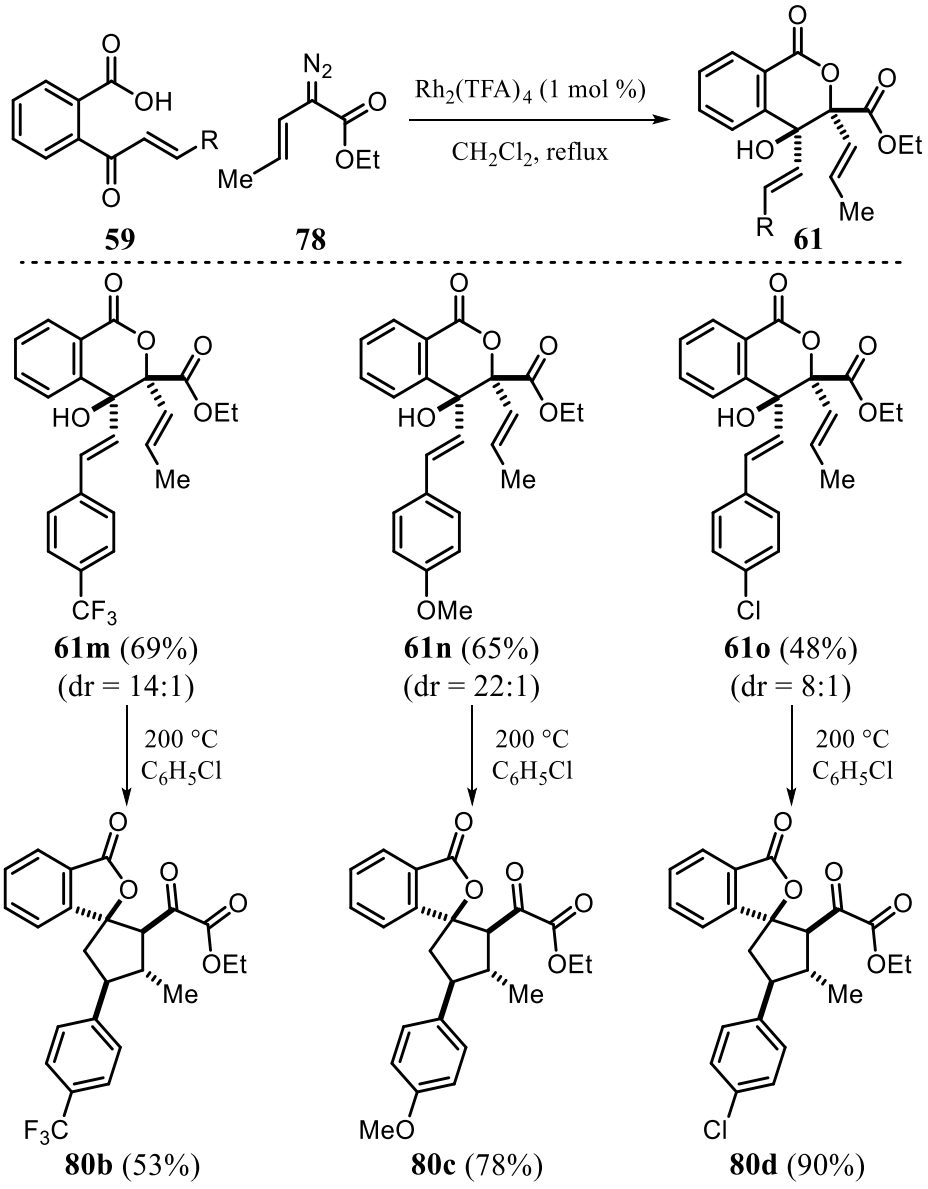

Scheme 36. Scope of rearrangement to access spirocyclic fused phthalolactones

3.7 Proposed Mechanism of Decanolide Synthesis

For further insights into the reaction mechanism of the ketoacid insertion/aldol cyclization, additional control experiments were carried out (Scheme 37). We attempted the same O–H insertion/aldol cascade with commercially available 3-benzoyl propionic acid **81** yielding exclusively the insertion product **82** (Scheme 37a). This result suggests

that the conformational constraint is necessary for a 6-*exo*-trig aldol cyclization. The aromatic ring brings the electrophilic ketone moiety in closer proximity of the rhoda-enolate in the zwitterionic intermediate lowering the entropic barrier of ring cyclization associated with the corresponding linear alternatives.[129-132] Next, we performed two experiments with the corresponding insertion product **60a** (Scheme 37b). We refluxed the insertion product in CH_2Cl_2 with $Rh_2(TFA)_4$ alone and with the addition of excess triethylamine. We did not observe any conversion of insertion product **60a** to aldol product **61a** suggesting that a rhodium bound zwitterionic intermediate is necessary for the aldol cyclization.[30, 35, 47-48, 89, 133]

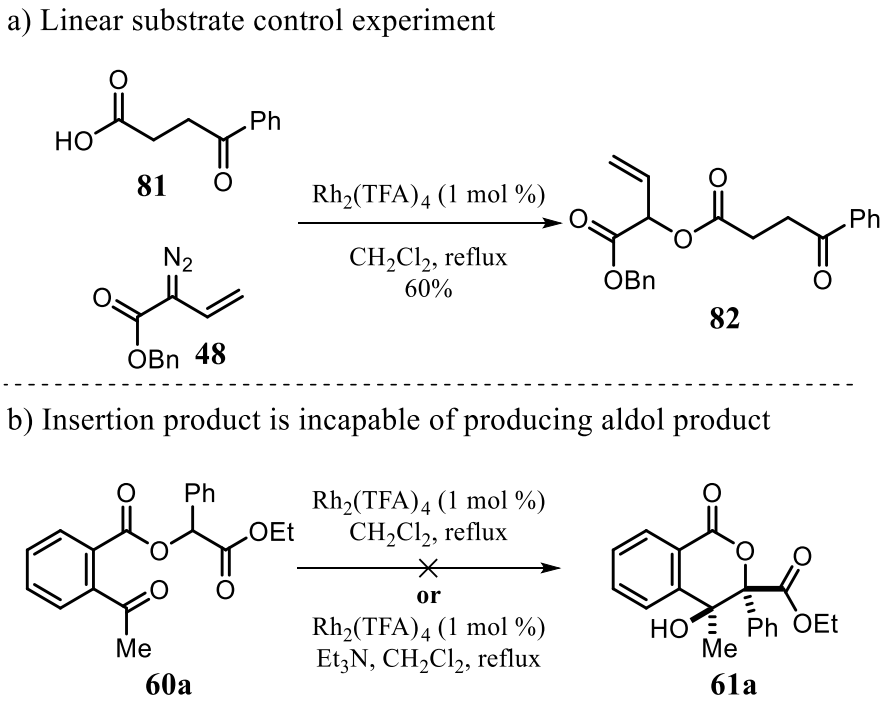

Scheme 37. Control experiments.

From these results we were able to propose a mechanism for this cascade sequence. Similar to previously developed method reported in chapter 2, the vinyl diazo substrate

(**48/78**) decomposes to the corresponding rhodium vinylcarbenoid that undergoes a regioselective O–H insertion with **59**, generating a ylide possessing a *Z*-rhoda-enolate capable of a enol-*exo*-6-*exo*-trig cyclization to yield *syn* aldol product **61** which is isolated or directly subjected to thermal expansion conditions to produce decanolide **79**. We presume that the *syn* aldol product stereochemistry occurs following the Zimmerman-Traxler model.

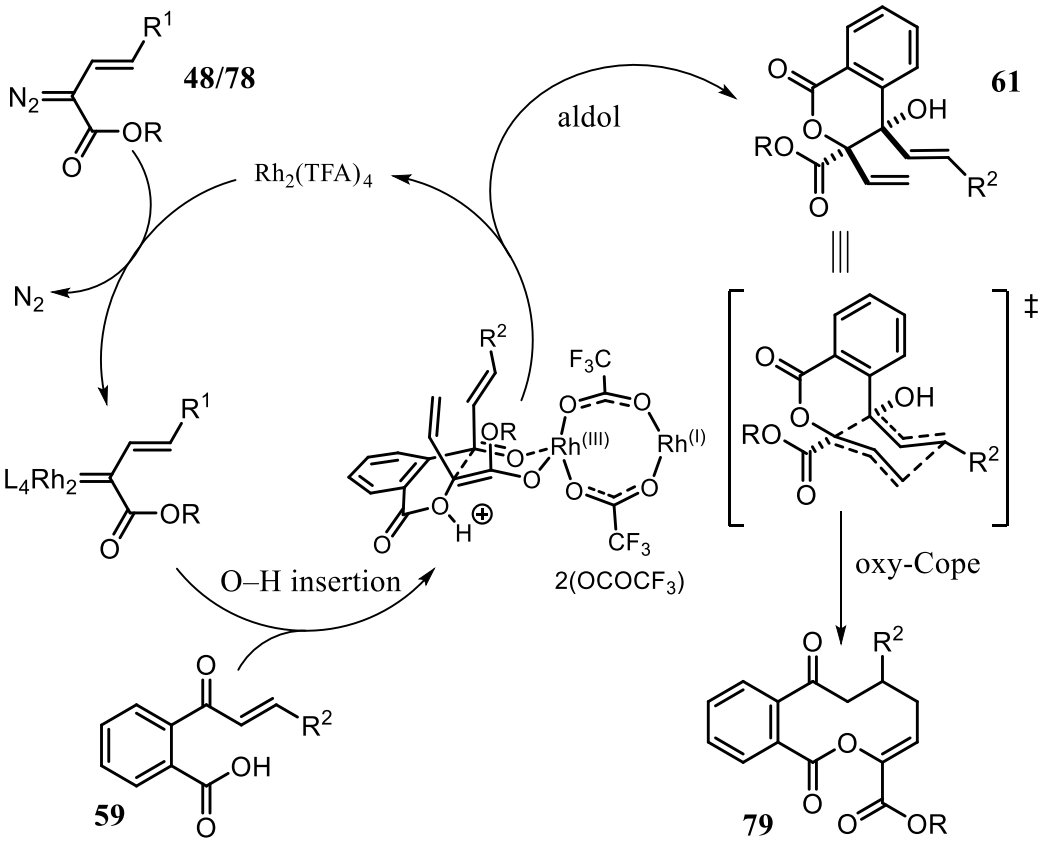

Scheme 38. Proposed mechanism of acid insertion/aldol/oxy-Cope cascade.

Furthermore, this transition state model also provides some reasoning for the diminished stereochemistry observed for aldol products **61m-61o**, because the additional methyl group on vinyl diazoacetate **78** may sterically disrupting the ordered Zimmerman-Traxler transition state or may affect the geometry of the rhoda-enolate. To further identify the

nature of the oxy-Cope rearrangement, we proposed a chair transition state. With the mechanism shown in scheme 38, both transition states are possible, but as will be discussed in the following subsection, we have discovered evidence suggesting that this mechanism operates via a chair transition state exclusively.

3.8 Proposed Mechanism of Serendipitous Rearrangement

When considering the cause of the serendipitous product **80a** formed during our attempt to synthesize a decanolide utilizing ethyl (*E*)-2-diazopent-3-enoate **78** (Scheme 34), we rationalized that the additional methyl substituent on the diazo fragment was key. When considering the stability of medium-sized rings, 9- and 10-membered rings tend to possess significantly high internal strain energy as shown in Figure 23.[17, 134]

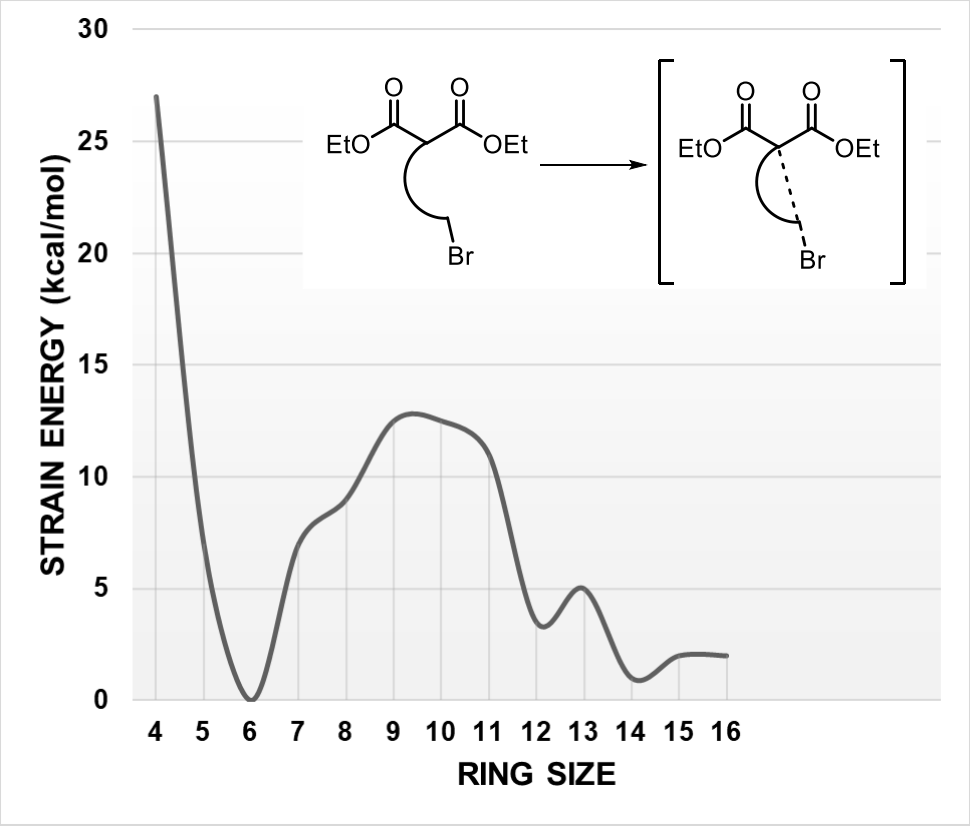

Figure 23. Transition state strain for the formation of medium-sized rings[17, 134]

Furthermore, this internal strain is enhanced with the addition of a methyl group. In fact, during two independent studies on the reactivity of cyclic ketones, it was shown empirically that cyclodecanones were the most unreactive in terms of reduction and nucleophilic addition. Reetz and Brown have both suggested that transition from a sp^2 to sp^3 carbon center causes a drastic increase in Prelog strain resulting in low or no conversion for their desired reactions[135-136] In regard to product **80**, it presumably forms through the planned oxy-Cope ring expansion to yield the desired decanolide **79**, an intermediate that likely suffers from significant Prelog strain[136-138] due to the additional methyl group, causing the decanolide to undergo an intramolecular aldol cyclization followed by translactonization to provide the spirophthalolactone **80** (Scheme 39).

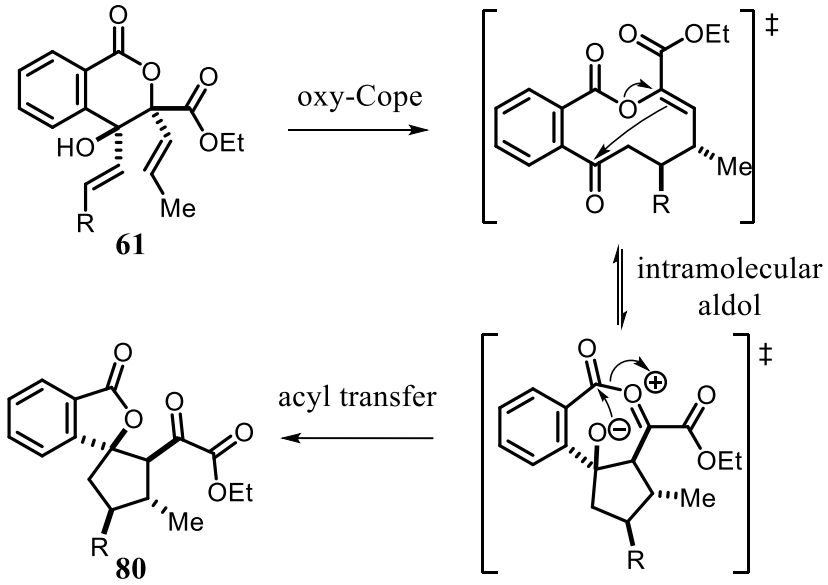

Scheme 39. Plausible mechanism of spirophthalolactone fused cyclopentanes.

The stereochemistry of **80** was confirmed by X-ray diffraction (Figure 22). Both the methyl and aryl substituents were found to be *anti* on the cyclopentane fragment of the spirophthalolactones suggesting that the proposed mechanism of the oxy-Cope ring

expansion shown in Schemes 38 and 39 must proceed via a chair-type transition state, which is opposite from our previous reports shown in chapter 2.[139]

3.9 Substrate Scope of 5-Membered Lactone Cascade

To further demonstrate the utility of this cascade, we also attempted the reaction with β-ketoacids, which are prone to decarboxylation.[113] To our delight, the cascade accommodates β-ketoacids with a wide range of diazo compounds to provide functionalized γ-butyrolactones (Scheme 40).

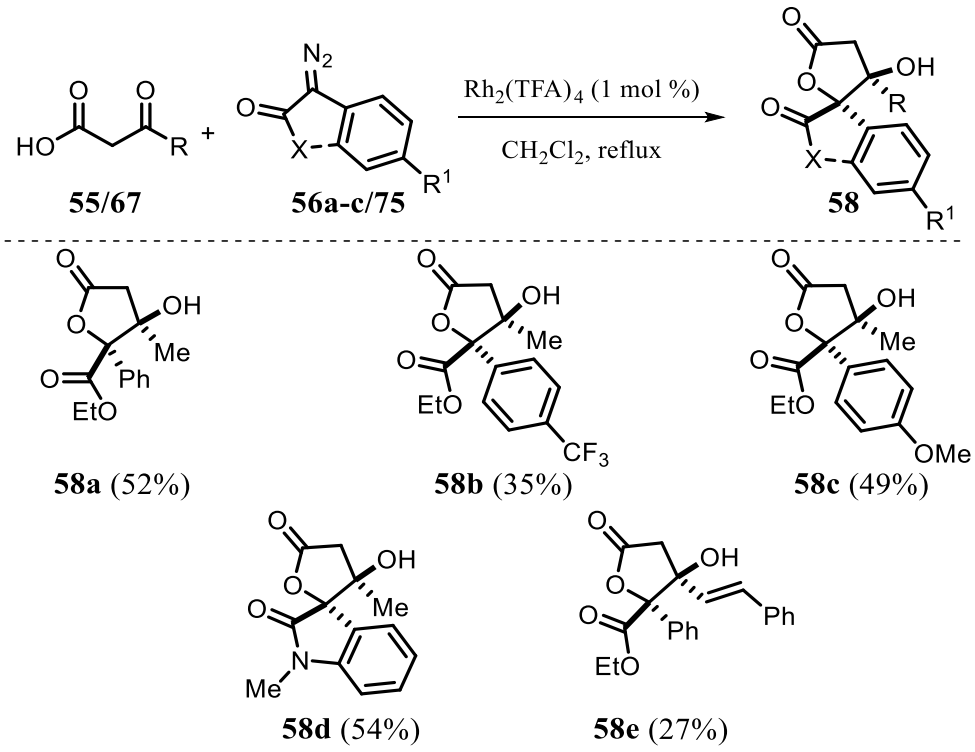

Scheme 40. Scope of $Rh_2(TFA)_4$-catalyzed carbene carboxylic acid O-H insertion/aldol cascade sequence for the synthesis of 3-hydroxy-γ-lactones

As anticipated, the cascade reaction proceeds in lower yield due to instability of the ketoacid starting materials under these reaction conditions. We also observe similar electronic trends involved with the carbenoid intermediates generated in Scheme 37.

Specifically, the electronically unperturbed substrate ethyl 2-diazo-2-phenylacetate **56a** undergoes the acid insertion/aldol cascade in good yield (Scheme 40, **58a**). However, the electron deficient rhodium carbenoid generated from **56b** undergoes the 5-*exo*-trig cascade in much lower yield (Scheme 40, **58b**). Conversely, electron rich aryl diazoacetate **56c** affords the desired cyclization in good yield (Scheme 40, **58c**). The cascade reaction also tolerates 3-diazo-1-methylindolin-2-one **75** to provide the corresponding spirocyclic oxindole (Scheme 40, **58d**). Relative stereochemistry of **58d** was determined using single crystal X-ray diffraction (Figure 24). As expected, the resulting hydroxyl group and the carbonyl moiety of diazo were found to be in a *syn* configuration similar to previous reports.[48]

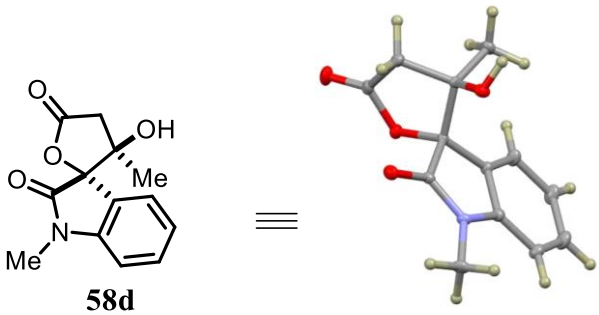

58d
CCDC 1844116

Figure 24. X-ray of **58d**

Against the overwhelming odds of precursor decarboxylation, we still explored medium-sized ring synthesis with these β-keto-acids. We performed the cascade with (*E*)-3-oxo-5-phenylpent-4-enoic acid **67** and ethyl 2-diazo-2-phenylacetate **56a** yielding 3-hydroxybutyrolactone **58e**. However, we quickly realized that (*E*)-3-oxo-5-phenylpent-4-enoic acid **67** was even more thermally unstable than 3-oxobutanoic acid **55**, as represented by the decreased yield (Scheme 40, **58e**).

3.10 Notable Byproducts Observed During the Development of this Cascade.

Even though we obtained lactone **58e** in low yield, we then attempted this cascade with ketoacid **67** and benzyl 2-diazobut-3-enoate **48**. During our attempts to synthesize 9-membered lactones, we realized that the method was incompatible with both starting materials due to thermal instability. This was further confirmed during our screening of conditions where a common byproduct observed was the thermal decarboxylation of **67** to cinnamyl ketone **83** (Scheme 41a). Furthermore, it was observed that in the absence of a nucleophile, the vinyl diazoacetate **48** undergoes a thermal [1,5] electrocyclization to produce **84** exclusively.[140]

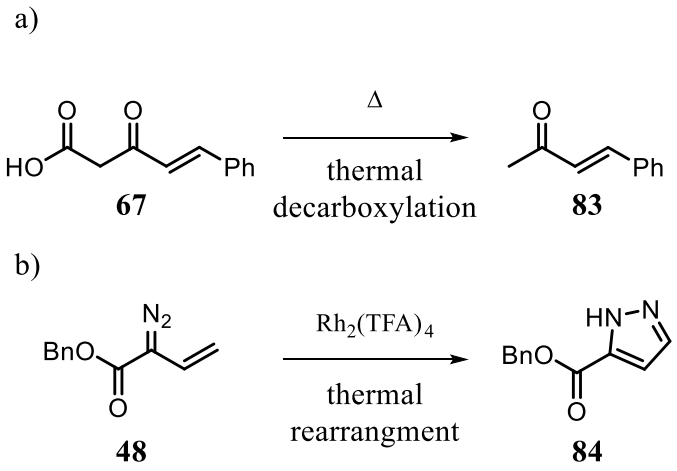

Scheme 41. Observed byproducts for 5-*exo*-trig cyclization

Interestingly, this vinyl diazoacetate had another byproduct pathway, which was observed during the optimization of this cascade (Table 5, entry 3). During this entry, the starting material 2-cinnamoylbenzoic acid **59b** was not consumed but one major byproduct was observed.

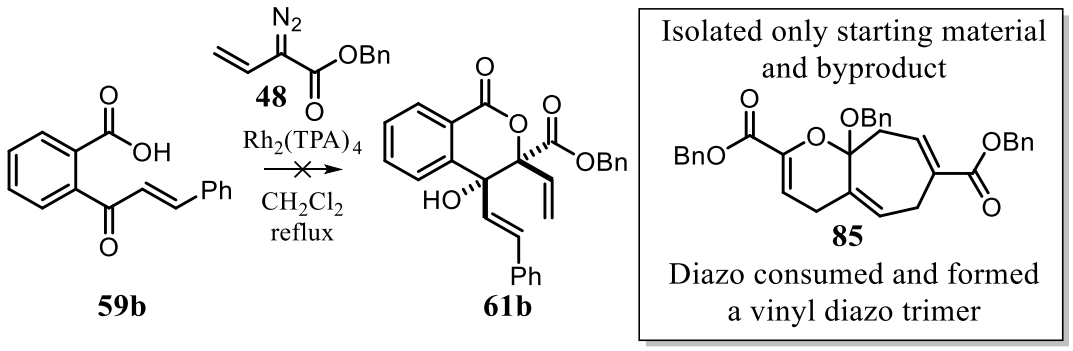

Scheme 42. Benzyl 2-diazobut-3-enoate **64** trimerization

The product was determined to be a vinyl diazo trimer, which was previously reported by Davies and co-workers (Scheme 42).

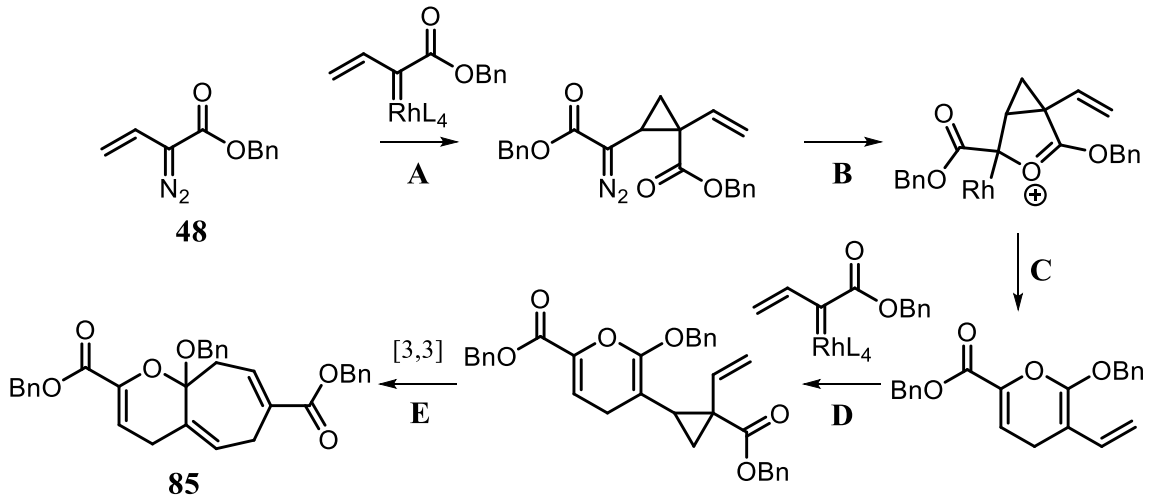

Scheme 43. Proposed mechanism of benzyl 2-diazobut-3-enoate **48** trimerization

The first stage of this mechanism involves the generation of rhodium carbenoid that undergoes a cyclopropanation reaction with another molecule of the vinyl diazoacetate (Scheme 43, A). This cyclopropane diazo, then forms a subsequent rhodium carbenoid, generating an oxonium ylide (Scheme 43, B) that leads to cyclopropane ring opening to generate a 1,4 skipped diene pyran (Scheme 43, C). Then another vinyl diazoacetate decomposes to the rhodium vinylcarbenoid capable of a cyclopropanation to the terminal

vinyl group of the pyran intermediate (Scheme 43, D) that subsequently performs a cope ring expansion to yield bicycle **100** (Scheme 43, E).[141] Davies and co-workers reported that this reaction performs best with $Rh_2(piv)_4$, which is bulkier compared to $Rh_2(OAc)_4$ and $Rh_2(TFA)_4$. However, when comparing the sterics of $Rh_2(TPA)_4$ and $Rh_2(piv)_4$, similar steric environments are noted, which seems to inhibit the O-H insertion reaction specifically with this keto-acid substrate (Figure 25).

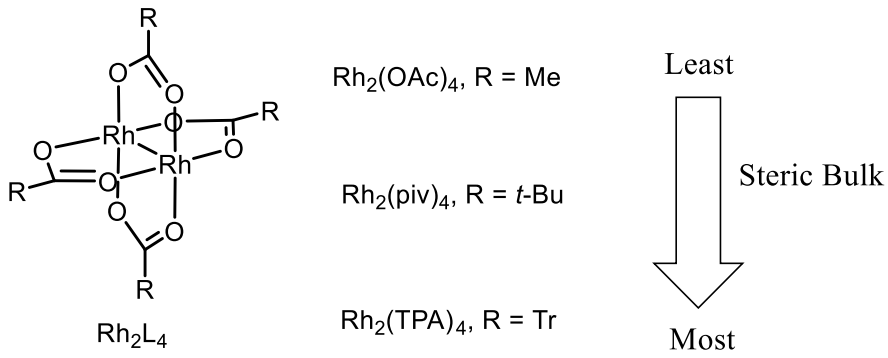

Figure 25. Comparison of rhodium catalyst sterics

3.11 Earth Abundant Alternatives for O-H Insertion/Aldol Cascade.

Our initial efforts to generate medium-sized rings all required the precious metal rhodium as a catalyst. Fortunately, the catalyst loading for these reactions are so minuscule that cost is not a concern. However, metals such as rhodium, ruthenium and iridium are not very abundant on the earth's crust and sustainability of their applications in chemistry is limited. There is an ongoing need for more earth abundant alternatives (Figure 26).

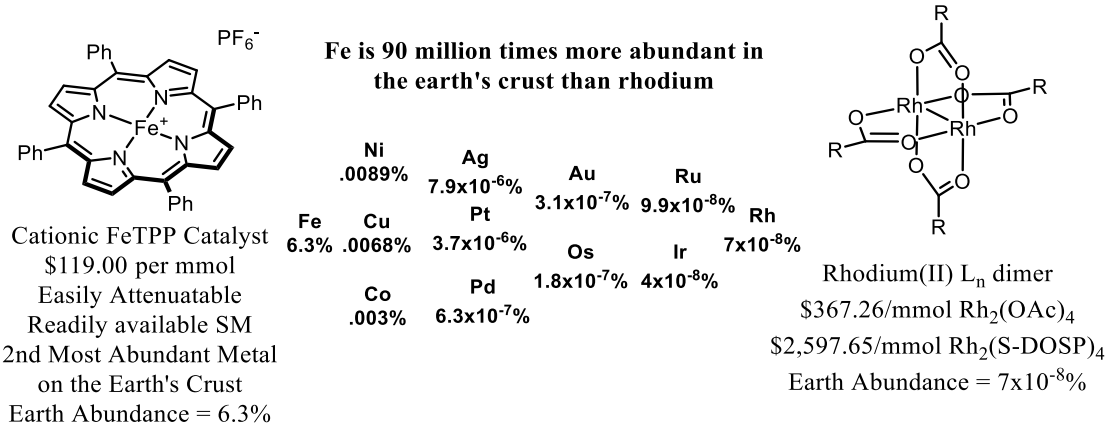

Figure 26. Iron earth abundance compared to rhodium

With that in mind, iron is an ideal sustainable catalyst source because it is the most abundant metal in the earth's crust and is capable of diverse chemical transformations due to its ability to exist in a variety of oxidation states. From a poetic perspective, these benefits of iron as a catalyst make it an ideal choice for further development of carbenoid chemistry. In reference to a poem shown below, iron is master of them all.

Gold is for the mistress – silver for the maid –
Copper for the craftsman cunning at his trade. "Good!" said the Baron, sitting in his hall, "But Iron – Cold Iron – is master of them all."
Rudyard Kipling, Cold Iron

Surprisingly with such reactivity, there are significant key gaps in iron carbenoid chemistry; specifically, in terms of cascade catalysis. Iron (III) porphyrin complexes are known to react with ethyl diazoacetate to form iron carbenoids capable of heteroatom insertion reactions.

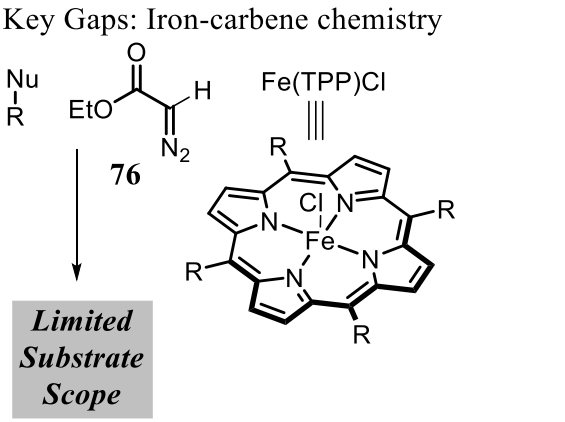

Figure 27. Key gaps in iron carbenoid cascades

Unfortunately, current methods are limited to ethyl diazoacetate, while also requiring high reaction temperatures and prolonged reaction times. Furthermore, prior to our work described herein, there are no examples of iron carbenoid initiated cascades.[142] Fortunately, we have developed cationic iron(III) porphyrin complexes capable of performing heteroatom insertion/aldol cascades under ambient temperatures with excellent diastereoselectivity, making these catalysts suitable alternatives to their precious rhodium counterparts.

3.12 Optimization of Iron Insertion/Aldol Cascade

We decided to focus our efforts towards commercially available iron (III) porphyrin complexes such as Fe(TPP)Cl; a catalyst known to react with ethyl diazoacetate (**76**). Prior to our work, attempts to utilize catalyst to generate iron carbenoids with donor/acceptor diazo precursors failed. We hypothesized that the covalently bound axial chloride ligand may be the reason for low reactivity. Previous reports state that reduction of Fe(TPP)Cl with cobaltocene increased the reactivity of the catalyst.[142] Furthermore, when considering

ethyl diazoacetate (**76**) as a molecule, it can also serve as a mild reductant,[143] thus it became apparent that making the axial coordination site of the Fe(TPP) catalyst more accessible to σ donation from a diazo, might facilitate carbenoid formation with donor/acceptor diazo precursors.

Table 6. Optimization of iron O-H insertion/aldol cascade

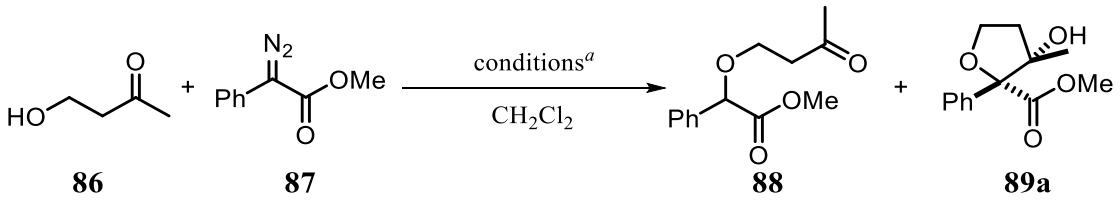

86 **87** **88** **89a**

Entry	Catalyst	Mol (%), t (h)	Temp. °C	Ratio 88:89a[b]	Yield (%)[c]
1	$Fe(TPP)SbF_6$	20.0, 1.5	40	-	30%
2	$Fe(TPP)SbF_6$	10.0, 1.5	40	0.19:1.00	-
3	$Fe(TPP)BF_4$	10.0, 1.5	40	1.63:1.00	-
4	$Fe(TPP)PF_6$	10.0, 1.5	40	0.00:1.00	76%
5	Fe(TPP)TFA	10.0, 1.5	40	0.10:1.00	75%
6	Fe(TPP)Cl	10.0, 1.5	40	0.00:0.00	NR
7	AgTFA	10.0, 1.5	40	0.38:1.00	-%
8	-	-, 1.5	40	0.00:0.00	NR
9	Fe(TPP)TFA	10.0, 24	25	0.00:1.00	69%
10	**$Fe(TPP)PF_6$**	**10.0, 24**	**25**	**0.00:1.00**	**77%**

[a]All reactions were performed by adding keto-alcohol **86** (10 μL, 0.1 mmol, 1.0 equiv) to a solution of FeTPPX in 450 μL CH_2Cl_2 (0.05 M) prepared in situ followed by addition of diazo **87** (20 mg, 0.1 mmol, 1 equiv).
[b]The percent ratio of **88** and **89a** was determined by crude ^1H NMR.
[c]Isolated yields of **89a** obtained after column chromatography.

For initial optimization, commercially available 4-hydroxybutan-2-one **86** and methyl 2-diazo-2-phenylacetate **87** were utilized as model substrates. Upon initial screening with Fe(TPP)SbF_6, we obtained promising results, isolating the aldol product **89a** in 30% yield (entry 1). Encouraged by these results, we decreased the catalyst loading due to the difficulty in removing catalyst impurities from the product and found a ratio of 0.19:1.00 insertion to aldol product (entry 2). We screened a variety of other noncoordinating counter anions and found that both Fe(TPP)PF_6 and Fe(TPP)TFA provide excellent results at reflux (entry 4 and 5). To prove that the silver additive was not responsible for the transformation we screened the reaction in absence of Fe(TPP)Cl, which provided **89a** but with a less than optimal ratio of insertion to aldol products, proving the iron carbenoid formation (entry 7). In addition, to prove this reaction is not occurring thermally as well, the reaction was performed without any additives, which resulted in no reaction. During this optimization, we realized that slow addition of the diazo precursor was not necessary because the rate of the iron carbenoid cascade appears to be slower compared to rhodium catalyzed reactions. Thus, we hypothesized that this cascade may occur at lower temperatures. To our delight, when the cascade was performed at 25 °C over 24 hours better results were obtained (Table 6, entry 10). This result is a significant discovery because it suggests that this process is occurring through an iron carbenoid at extremely mild conditions in comparison to a free carbene.

3.13 Substrate Scope of Iron Insertion/Aldol Cascade

With optimized conditions in hand, we then screened a variety of diazo precursors and quickly realized that electronic modification of the diazo synthon drastically inhibites the aldol cascade. The reaction proceeds well to provide **89b**, but alteration of the carbonyl

species to a methyl ketone (**72**), results in a drastically reduced yield of the desired product **89c**.

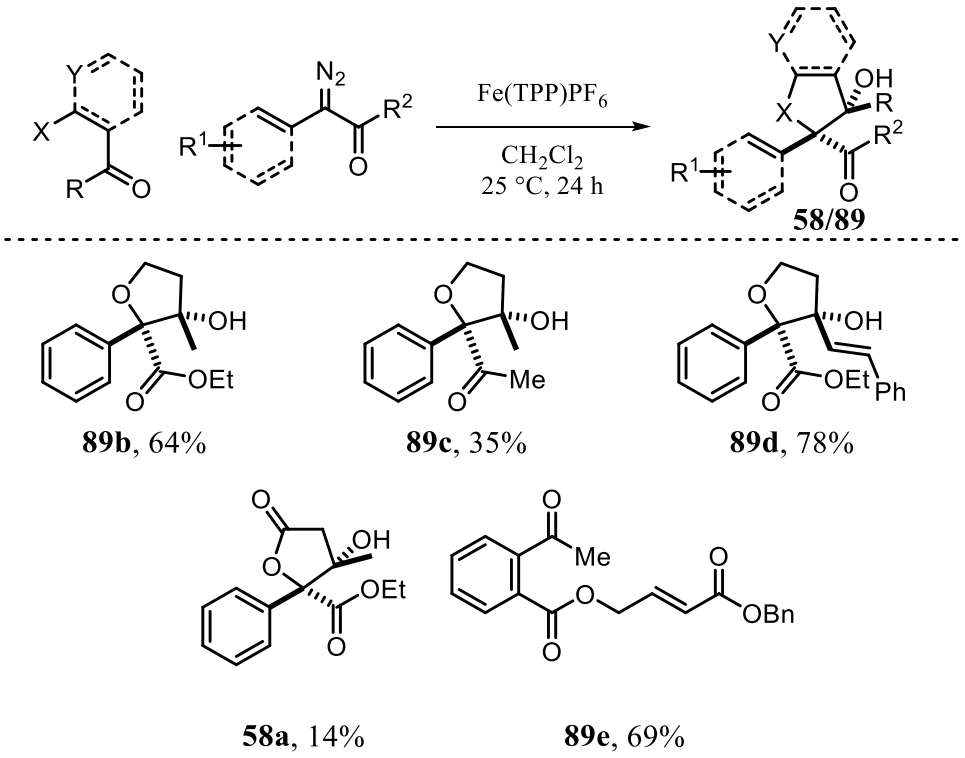

Scheme 44. Iron catalyzed insertion/aldol cascade substrate scope

To our delight, the reaction tolerates a vinyl keto-alcohol to yield **89d** in good yield. Thus, we envisioned we could extend this work for the synthesis of 9-membered rings. Unfortunately, this vinyl keto-alcohol utilized to prepare **89d** did not react with the iron vinylcarbenoid. Thus, we then tested this iron cascade with ketoacids. The O–H carboxylic acid insertion/aldol cascade was achieved with some success, but in much lower yield compared to similar entries with $Rh_2(TFA)_4$ (Scheme 44, **58a**). Interestingly, the rate of reaction increased drastically when ketoacid precursors were utilized. Full conversion and product formation occurred within minutes with ketoacid starting materials; this rate enhancement has not been fully studied to effectively provide reasoning for this observation. Regardless, with these acid insertion aldol results, we once again attempted to

extend this cascade for the synthesis of medium-sized lactones by performing an acid insertion/aldol cascade with benzyl 2-diazobut-3-enoate **48**. To our surprise, we did not observe O-H insertion at the iron carbenoid center, but instead at the vinylogous position yielding product **89e**. At this point, we concluded that this Fe(TPP)PF_6 catalyzed cascade was not going to provide access to medium-sized cyclic ethers and lactones.

3.14 Conclusion and Future Directions

In conclusion, the research reported in chapter 3 discusses the development and application of a rhodium carbenoid initiated carboxylic O–H insertion/aldol cascade sequence, which is convergent in nature and uses readily accessible ketoacids and diazo carbonyls as starting materials to access highly functionalized γ and δ lactones. Furthermore, this cascade was complemented with an oxy-Cope ring expansion strategy to efficiently access η lactones as well as highly functionalized spirophthalolactone fused cyclopentanes via a serendipitous rearrangement. An important feature of this transformation is its high chemo-, regio- and stereo-selectivity. This work specifically with the rhodium carbenoid initiated cascade has been published in *Organic Letters*. Furthermore, this research has led to the identification of a hit compound (Scheme 34, **79b**) that targets the Bax and Bak proteins. Currently, these synthesized scaffolds are now being further diversified in collaboration with the Shao research group at the University of Oklahoma.

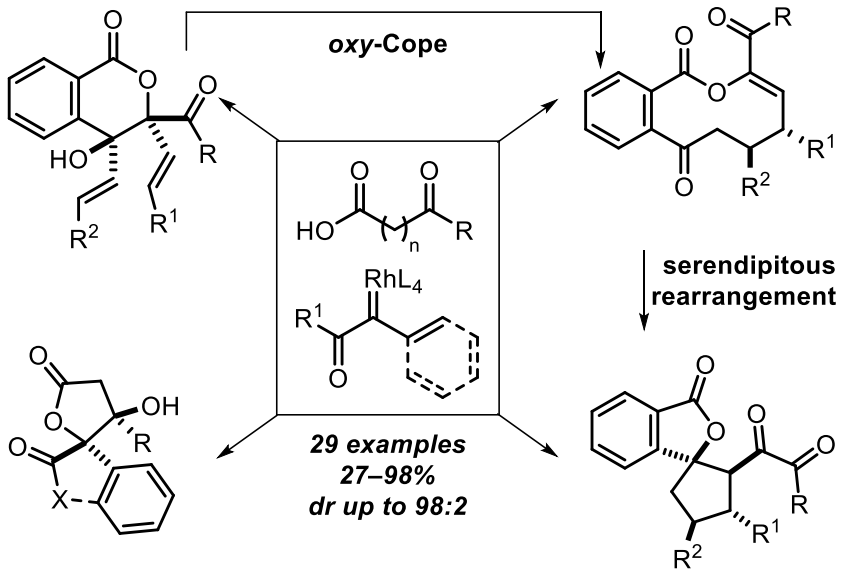

Figure 28. Synthesis of diverse lactones

In addition to the synthesis of medium-sized rings, significant advances have been made in the application of cationic iron (III) porphyrin complexes as suitable earth abundant catalysts for diazo derived carbenoid methodologies. Both O–H and acid insertion/aldol cascade described in chapter 2 and 3 have been successfully performed with $Fe(TPP)PF_6$. This is the first example of an iron catalyzed O–H insertion/aldol cascade, but there is still room for further development due to the limited substrate scope observed by iron in comparison to rhodium catalysts.

Finally, we have demonstrated this ring expansion strategy with two different oxygen nucleophiles. Thus, the next stage of development of our ring expansion cascade strategy is to incorporate nitrogen nucleophiles for the synthesis of diverse azacycles.

Chapter 4: Synthesis of Diverse Tricyclic Quinolines

A serendipitous cascade for the synthesis of functionalized tricyclic quinolines.

4.1 Introduction*

As an extension of our previously developed O–H insertion/aldol/oxy-Cope cascade, we sought to adapt our ring expansion strategy to synthesize medium-sized azacycles. During our initial attempts to identify a model substrate suitable for optimizing this N–H insertion/aldol/oxy-Cope cascade, we did not observe any success with amine starting materials utilized by Moody and coworkers, due to incompatibility with our vinyl diazoacetate precursors.[31] Although, there were reports by Hu and co-workers that 2'-aminochalcone substrates (**90**) efficiently reacted with aryl diazoacetates, such as **87**, to yield **91** (Scheme 45).[144]

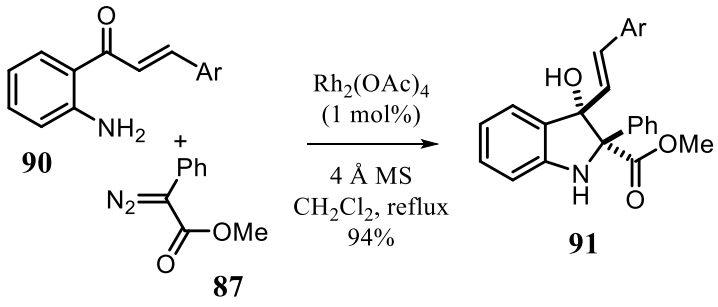

Scheme 45. Benzannulated N-H insertion/aldol cascade by Hu and co-workers[144]

To our delight, these 2'-aminochalcone precursors (**90a**) reacted with the rhodium vinylcarbenoid derived from **48**; the most effective rhodium (II) catalyst identified by Hu and coworkers for benzannulated diverted N–H insertion.[144]

* Reproduced in part from, "A Serendipitous Cascade of Rhodium Vinylcarbenoids with Aminochalcones for the Synthesis of Functionalized Quinolines" Kiran Chinthapally, Nicholas P. Massaro, Haylee L. Padgett and Indrajeet Sharma. *Chem. Commun.*, **2017**, *53*, 12205-12208 with permission from The Royal Society of Chemistry. *Copyright © RSC Publishing.* N.P.M. contributed equally with K.C. concerning the work presented in this chapter. N.P.M. prepared all starting material precursor, prepared multiple products, equally worked with control experiments, grew single crystals for X-ray, and derivatized products.

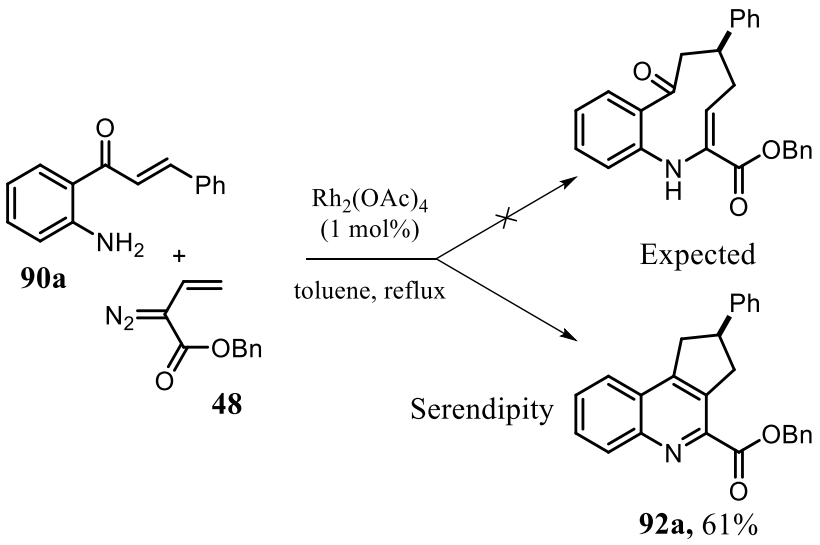

Scheme 46. A serendipitous discovery leading to a biologically relevant scaffold

We expected the formation of a 9-membered azacycle but instead observed a different major product (Scheme 46). After TLC analysis, we determined that the product possessed significant UV activity and was a solid upon purification. The NMR spectral analyses indicated a single product, but the characteristic azacycle enamine proton in ^{1}H-NMR and ketone peak in ^{13}C-NMR spectrum were missing. Further structural analyses suggested the formation of an unexpected quinoline scaffold **92a** (Scheme 46).

Since the discovery of quinoline in 1842 by Gerhardt, the bicyclic ring system has been observed in a myriad of natural products and medicinally relevant compounds.[145] Often quinoline based structures possess a broad range of biological activity, such as antimalarial, anti-bacterial, antifungal, anthelmintic, cardiotonic, anticonvulsant, anti-inflammatory, and analgesic activity.[146-147] In addition, quinoline containing compounds have found significant application in anti-cancer therapeutics, establishing the quinoline ring system as a privileged scaffold. Quinine and Topotecan are key examples of this structural family that have had a profound impact on human health (Figure 29).[148-150]

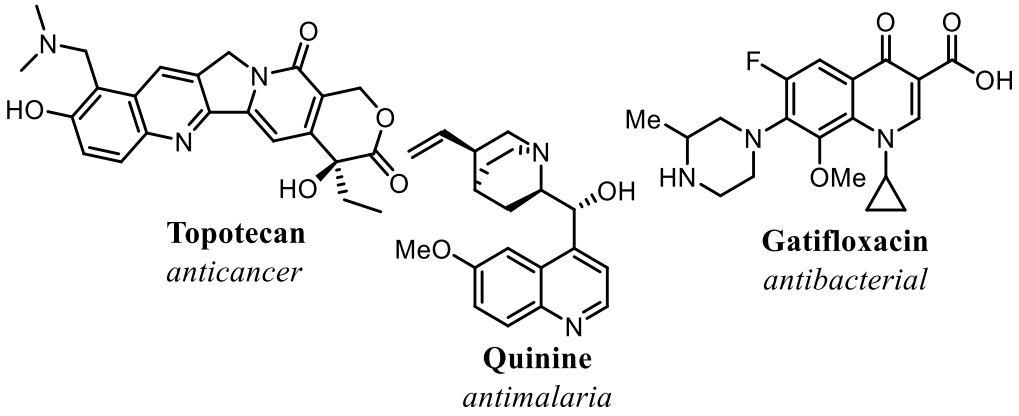

Figure 29. Examples of bioactive quinoline compounds

Due to the bioactive relevance of quinolines and our interests in rhodium vinylcarbenoid initiated tandem reactions, we pursued this unexpected reactivity to develop a new approach to functionalized quinolines that leverages a distinct retrosynthetic disconnection.

4.3 Optimization of Quinoline Synthesis

Encouraged by the preliminary result, we examined different dirhodium carboxylates to increase the yield of quinoline **92a** (Table 7, entries 2–5). Among them, $Rh_2(esp)_2$ was found to be the most efficient, which was consistent with previous literature reports for the corresponding N–H insertion reactions (entry 2).[151-152] With hope to achieve the cascade sequence with earth abundant transition metal catalysts, we screened Fe(TPP)Cl and two copper salts. Both copper catalysts resulted in a complex mixture of different products without any trace of desired quinoline (entries 6, 7).[153-154] To our delight, Fe(TPP)Cl (2 mol %) provided the desired quinoline, albeit in very low yield (entry 8). We thought that increasing the catalyst loading of Fe(TPP)Cl (10 mol%) would improve the yield although this was not observed. We also attempted to synthesize quinoline **92a** without the use of any metal catalyst, but we did not observe any desired product.[155] As expected, benzyl 2-diazobut-3-enoate **48** fully decomposed but did not react with 2'-

aminochalcone **90a**, which was recovered from the reaction in quantitative yield; suggesting the cascade will only proceed with a metal carbenoid.

Table 7 Optimization of the reaction conditions for the formation of the quinoline scaffold **92a**.

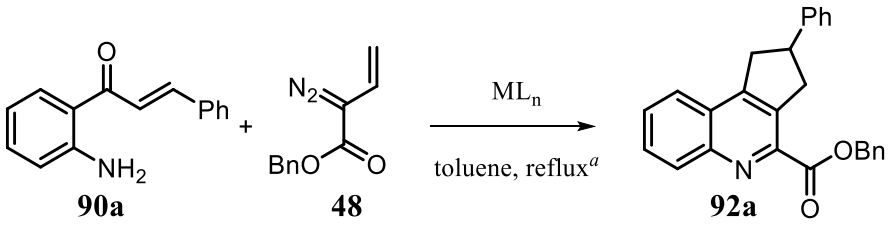

entry	Catalyst	mol (%), t	yield (%)[b]
1	$Rh_2(OAc)_4$	1.0, 3 h	61
2	**$Rh_2(esp)_2$**	**1.0, 3 h**	**77**
3	$Rh_2(TPA)_4$	1.0, 3 h	42
4	$Rh_2(TFA)_4$	1.0, 3 h	12
5	$Rh_2(HFB)_4$	1.0, 3 h	15
6	$(CuOTf)_2$•benzene	5.0, 3 h	CM
7	$Cu(acac)_2$	5.0, 3 h	CM
8	Fe(TPP)Cl	2.0, 3 h	13
9	–	3 h	NR
10	$Rh_2(esp)_2$	0.1, 4 h	67

[a]All optimization reactions were performed by adding a 0.45 M solution of **48** (2.0 equiv) into a 0.1 M solution of **90a** (1 equiv) with catalysts *via* a syringe pump over 2.5 h, after the addition of diazo, all reaction were refluxed for an additional 30 min.

[b]Isolated yields after column chromatography.

Finally, the cascade also functioned with lower catalyst loading of $Rh_2(esp)_2$ (0.1 mol %), obtaining the desired quinoline **92a** in comparable yield (entry 10).

4.2 Preparation of Model Substrates and Other Precursors

Similar to chapter 3, 2'-aminochalcone precursors were easily derivatized to efficiently access a diverse substrate scope. 2'-aminochalcone **90a** and other precursors were prepared via a Claisen-Schmidt condensation with 2'-aminoacetophenones **93** and various aryl aldehydes **68** (Scheme 47).

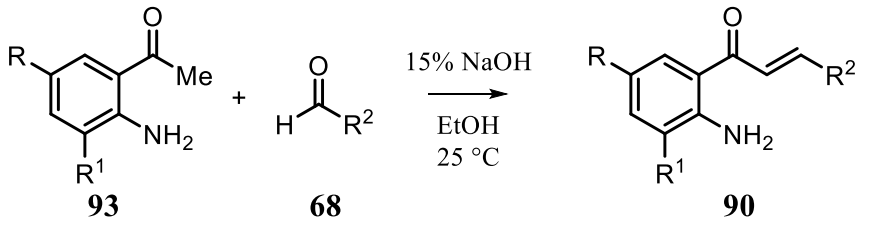

90a; R = H, R^1= H, R^2 = Ph
90b; R = H, R^1= H, R^2 = *p*-Cl-C_6H_4
90c; R = H, R^1= H, R^2 = *o*-OMe-C_6H_4
90d; R = H, R^1= H, R^2 = *p*-OMe-C_6H_4
90e; R = H, R^1= H, R^2 = *p*-OMe-C_6H_4
90f; R = Br, R^1= H, R^2 = Ph
90g; R = Br, R^1= Br, R^2 = Ph
90h; R = CN, R^1= H, R^2 = Ph
90i; R = Ph, R^1= H, R^2 = 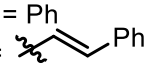
90j; R = H, R^1= H, R^2 = 2-furyl

Scheme 47. Synthesis of 2'-aminochalcones **90**

In terms of the diazo fragment, benzyl 2-diazobut-3-enoate **48** was utilized most often, but two other vinyl diazoacetates were prepared. Prop-2-yn-1-yl 2-diazobut-3-enoate **96** was synthesized similarly to benzyl 2-diazobut-3-enoate **48** (Scheme 48).

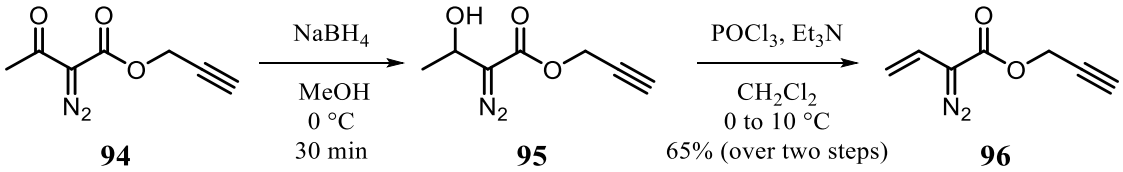

Scheme 48. Synthesis of prop-2-yn-1-yl 2-diazobut-3-enoate **96**

The synthesis of ethyl (*E*)-5-((TBS)oxy)-2-diazopent-3-enoate **100** began first with the selective monoprotection of 1,3-propanediol **97** with TBS-Cl to provide 3-((TBS)oxy)propan-1-ol **98** (Scheme 49).

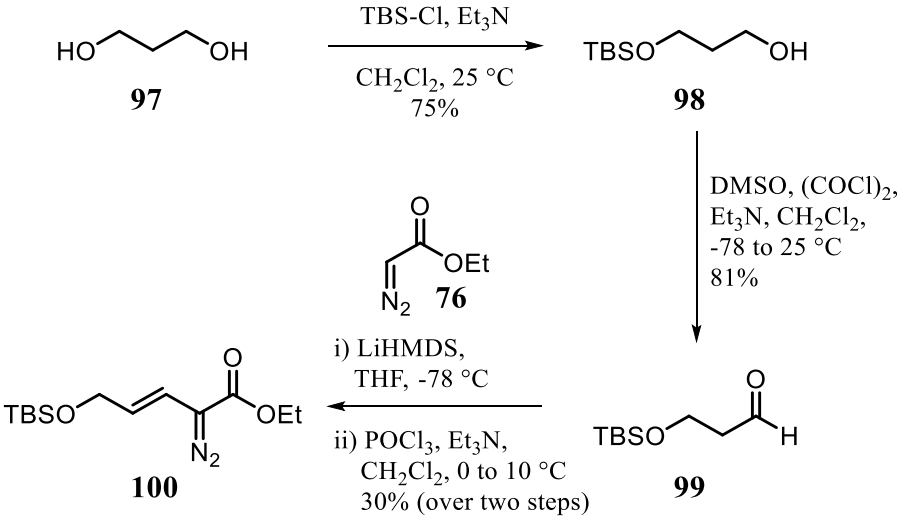

Scheme 49. Synthesis of ethyl (*E*)-5-((TBS)oxy)-2-diazopent-3-enoate **100**

This alcohol was then oxidized to aldehyde **99** via a Swern oxidation. The final transformation incorporated an aldol reaction with ethyl diazoacetate **76** and 3-((TBS)oxy)propanal **99**, furnishing an aldol product that was immediately dehydrated to yield ethyl (*E*)-5-((TBS)oxy)-2-diazopent-3-enoate **100** (Scheme 49).

4.4 Substrate Scope of Quinolines

With starting materials and optimized conditions in hand, we investigated the scope of this cascade sequence using $Rh_2(esp)_2$ as a catalyst (Scheme 50). Both the electron-donating and -withdrawing groups were tolerated on the aromatic side chain of aminochalcones (Scheme 50, **92b**–**92e**). Interestingly, we did not observe expected fluctuation in the yields for compounds **92a** through **92e**. Unexpectedly, the yield decreased with the presence of electron-withdrawing groups on the chalcone **90e** and increased with

the presence of electron-donating groups **90d** which was opposite the trend witnessed during the carboxylic acid insertion/aldol cascade shown in chapter 3.

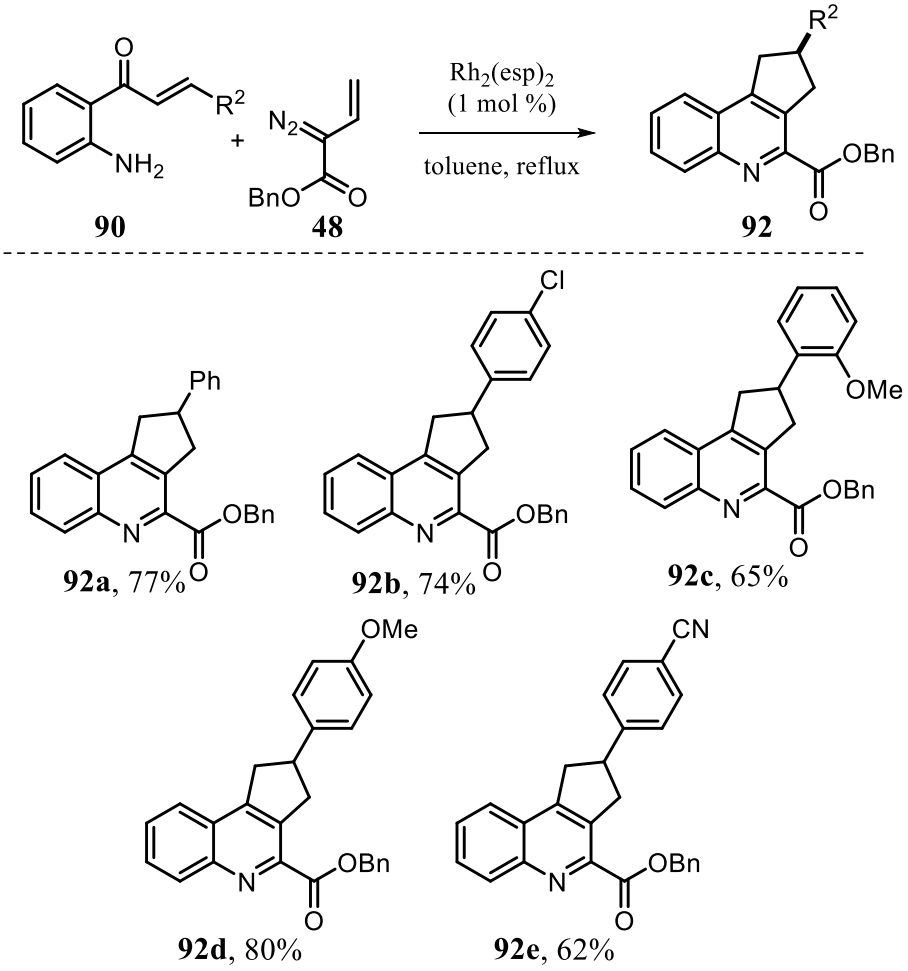

Scheme 50. Scope of $Rh_2(esp)_2$-catalyzed serendipitous cascade

Fortunately, during this initial probing of the substrate scope, we were also able to confirm the structure of **92b** by single crystal X-ray diffraction (Figure 30). We were pleased to find that the cascade sequence equally tolerated substitution at the aniline ring of 2'-aminochalcones (Scheme 51, **92f**–**92i**). It was shown that multiple halogens could be tolerated (**92f**–**92g**) and that electron-withdrawing groups known to slow down carbene-

heteroatom insertion reactions,[151] did not have any strong influence in the efficiency of the cascade process; but did decrease the yield slightly (Scheme 51, **92h**).

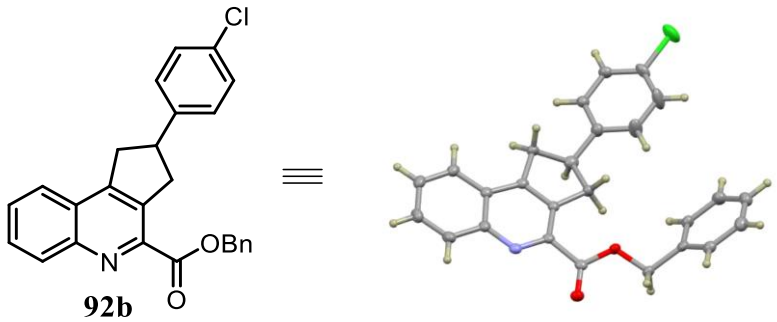

Figure 30. X-ray structure of **92b**

What is also very impressive about this serendipitous cascade is its high chemoselectivity in the presence of additional olefin functionalities present in the aminochalcone **92j** (Scheme 51, **92j**).

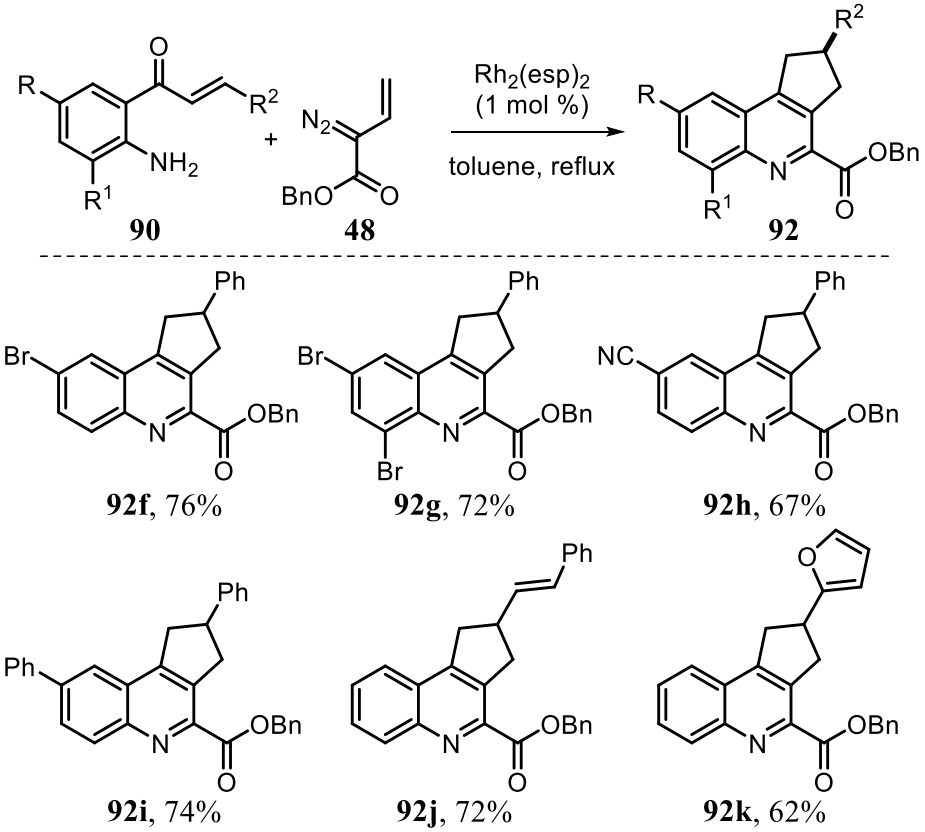

Scheme 51. Continued scope of $Rh_2(esp)_2$-catalyzed serendipitous cascade

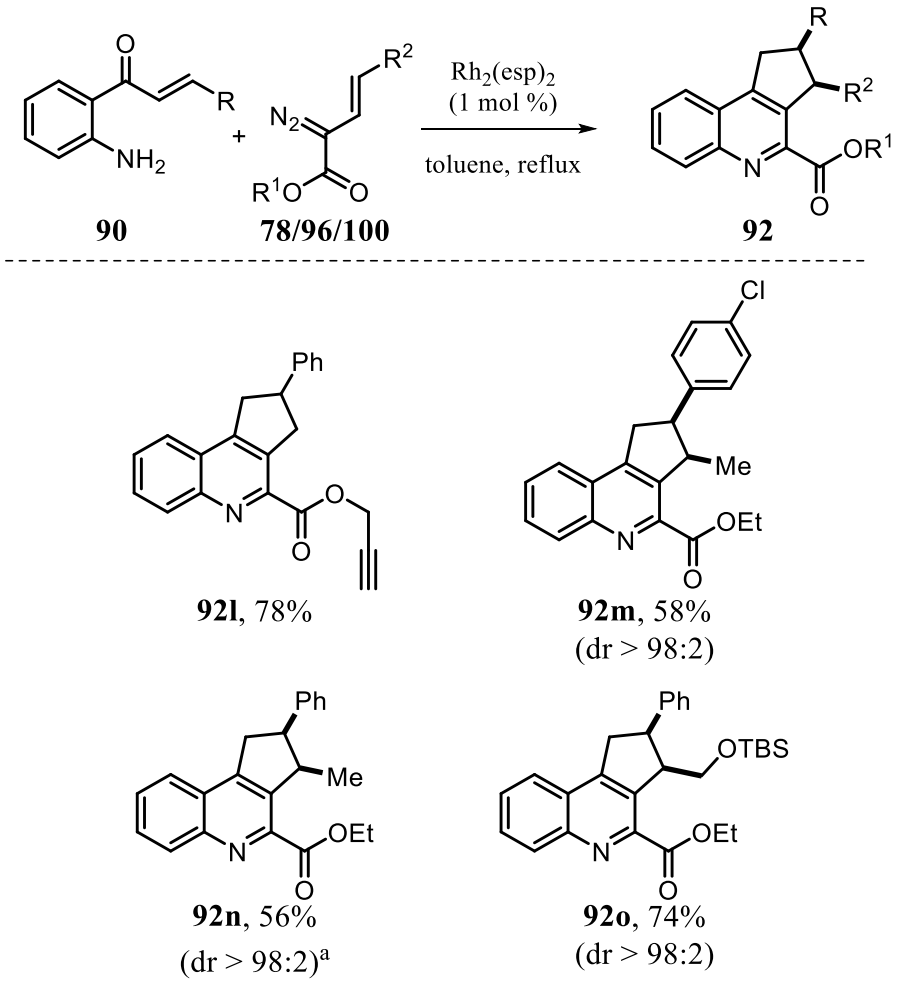

Scheme 52. Scope of $Rh_2(esp)_2$-catalyzed serendipitous cascade with different vinyl diazoacetate precursors

This chemoselectivity was further demonstrated with aminochalcone **92k** bearing a reactive furan functionality performing the cascade successfully (Scheme 51, **92k**).[156-158] To further explore the generality of this transformation, substituted vinyl diazoacetates were also examined with 2'-aminochalcones. Remarkably, prop-2-yn-1-yl 2-diazobut-3-enoate **96** on treatment with 2'-aminochalcone **90a** underwent the desired cascade sequence smoothly to obtain the corresponding quinoline in high yield (Scheme 52, **92l**) without any evidence of side reactions from the alkyne functionality, which has the propensity to undergo cyclopropenation,[159-160] as well as carbene-alkyne metathesis[161-163]

with rhodium carbenoids. We then probed the diastereoselectivity of the cascade reaction. First, ethyl (*E*)-2-diazopent-3-enoate **78** was reacted with **90a** and **90b** both providing the desired quinoline scaffold in good yield with complete *syn* stereoselectivity (Scheme 52, **92m**, **92n**). The stereochemical arrangement of substituents was determined based on the nOe correlations, and was further confirmed by single crystal X-ray diffraction of **92m** (Figure 33).[164] Finally, the cascade was performed with ethyl(*E*)-5-((TBS)oxy)-2-diazopent-3-enoate **100** bearing a TBS-ether side chain as an additional diversification handle.

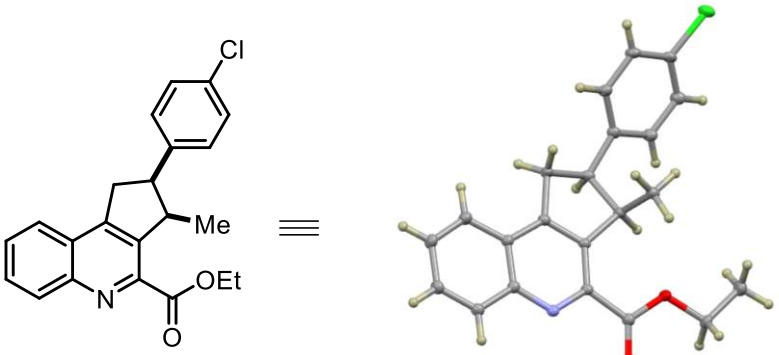

92m
CCDC 1553212

Figure 31. X-ray structure of **92m**

To our delight, the cascade proceeded in high yield to provide quinoline scaffold **92o** with complete stereoselectivity. Subsequent deprotection of the TBS-ether with TBAF triggered lactonization to provide the tetracyclic quinoline scaffold (Scheme 53, **101**).[165]

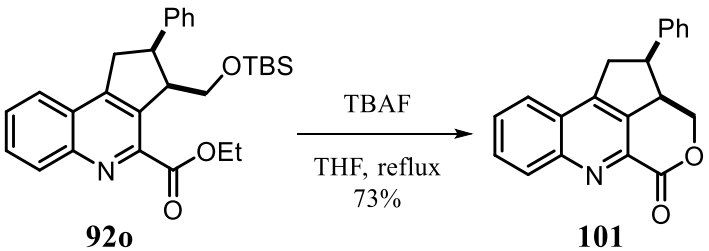

92o **101**

Scheme 53. Further diversification to yield **101**

4.5 Probing the Mechanism of Tricyclic Quinoline Formation

We had suspicion that the cascade was proceeding via a N–H insertion/aldol/oxy-Cope followed by a ring contraction aromatization sequence. To probe for all aspects of this mechanism, we wanted to effectively isolate each possible intermediate to confirm the pathway. First, we synthesized the intermediate aldol cyclization product **91a** as a single diastereomer. This was achieved by treating 2'-aminochalcone **90a** with benzyl 2-diazobut-3-enoate **48** in the presence of $Rh_2(esp)_2$ at 25 °C; surprisingly at dichloromethane refluxing temperatures, quinoline formation still proceeded.[166]

Table 8. Rearrangement of indoline **91a** into quinoline **92a** under thermal, basic and acidic conditions

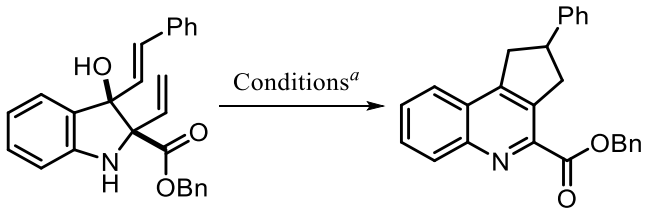

91 **92a**

entry	reagent	solvent, temp (ºC), *t*	yield (%)[b]
1	$Rh_2(esp)_2$	toluene, reflux, 1 h	93
2	–	toluene, reflux, 1 h	95
3	KH, 18-crown-6	THF, 0 ºC, 5 min	CM
4	LiHMDS	THF, 0 ºC, 15 min	CM
5	CSA	toluene, rt to reflux, 1 h	CM

[a]All optimization reactions were performed with 0.1 M solution of **91**

[b]Isolated yields after column chromatography.

We then exposed **91a** to $Rh_2(esp)_2$ in refluxing toluene. As expected, we observed a clean formation of quinoline **92a** in excellent yield (Table 8, entry 1). Next, **91a** was refluxed in toluene without $Rh_2(esp)_2$ to rule out the involvement of Rh-metal in the oxy–Cope rearrangement. As expected, the reaction took the same time to afford **92a** suggesting a thermally driven rearrangement (Table 8, entry 2).[167] As the oxy-Cope rearrangement could be catalyzed under basic conditions,[168-171] aldol product **91a** was subjected to different bases known to promote anionic oxy-Cope rearrangement. As from our previous reports, we observed a complex mixture without any trace of desired quinoline **92a** (Table 8, entry 3, 4). This was suspected to be due to the propensity for retro-aldol of substrate **91a** which had been identified with similar products.[30] We also attempted acidic condition to catalyze oxy-Cope rearrangement, but did not meet any success (Table 8, entry 5).

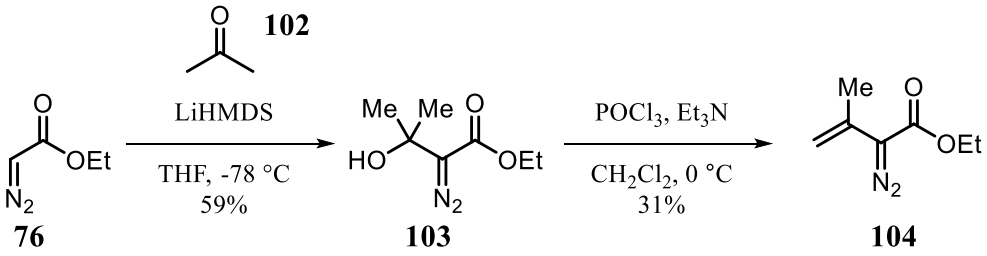

Scheme 54. Synthesis of ethyl 2-diazo-3-methylbut-3-enoate **104**

To further probe the mechanism, we wanted to isolate the intermediate prior to aromatization. To accomplish this, we installed a group methyl group on the vinyl diazoacetate fragment subsequently causing the generation of an all carbon quaternary center incapable of aromatization. First, we prepared ethyl 2-diazo-3-methylbut-3-enoate **104** from a two-step sequence by performing an aldol reaction with ethyl diazo acetate **76** and acetone **102** which provided tertiary alcohol **103**. This tertiary alcohol was then eliminated to provide desired vinyl diazoacetate **104** (Scheme 54). The cascade was then

performed with ethyl 2-diazo-3-methylbut-3-enoate **104** and 2'-aminochalcone **90a**. To our delight, the cascade did proceed and stopped exclusively prior to the aromatization stage of the cascade sequence providing tertiary alcohol **105** (Scheme 55).

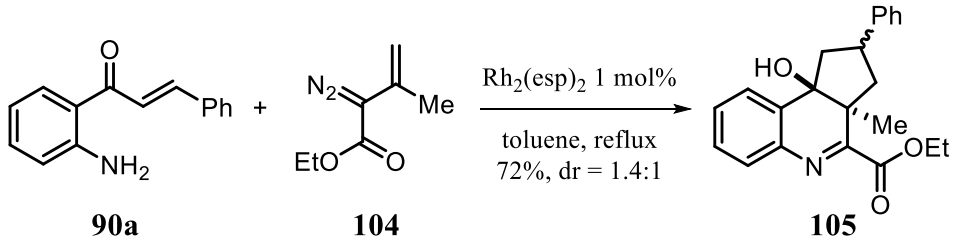

90a **104** **105**

Scheme 55. Synthesis of cascade intermediate **105**

4.6 Proposed Mechanism of the Serendipitous Cascade and New Hypothesis

These findings allow us to propose a reaction mechanism (Scheme 56). First, vinyl diazoacetate is decomposed by the dirhodium carboxylate $Rh_2(esp)_2$ to form a rhodium vinylcarbenoid that undergoes a chemoselective N–H insertion/aldol cyclization to provide indoline **91** with high diastereoselectivity.[166] The intermediate indoline **91** then sets the stage for a thermally driven, concerted oxy-Cope rearrangement to provide an intermediate azacycles having both the substituents *syn* to each other.[167] The azacycle then rearranges to the functionalized quinolines **92** through an intramolecular aldol/dehydration sequence.[172]

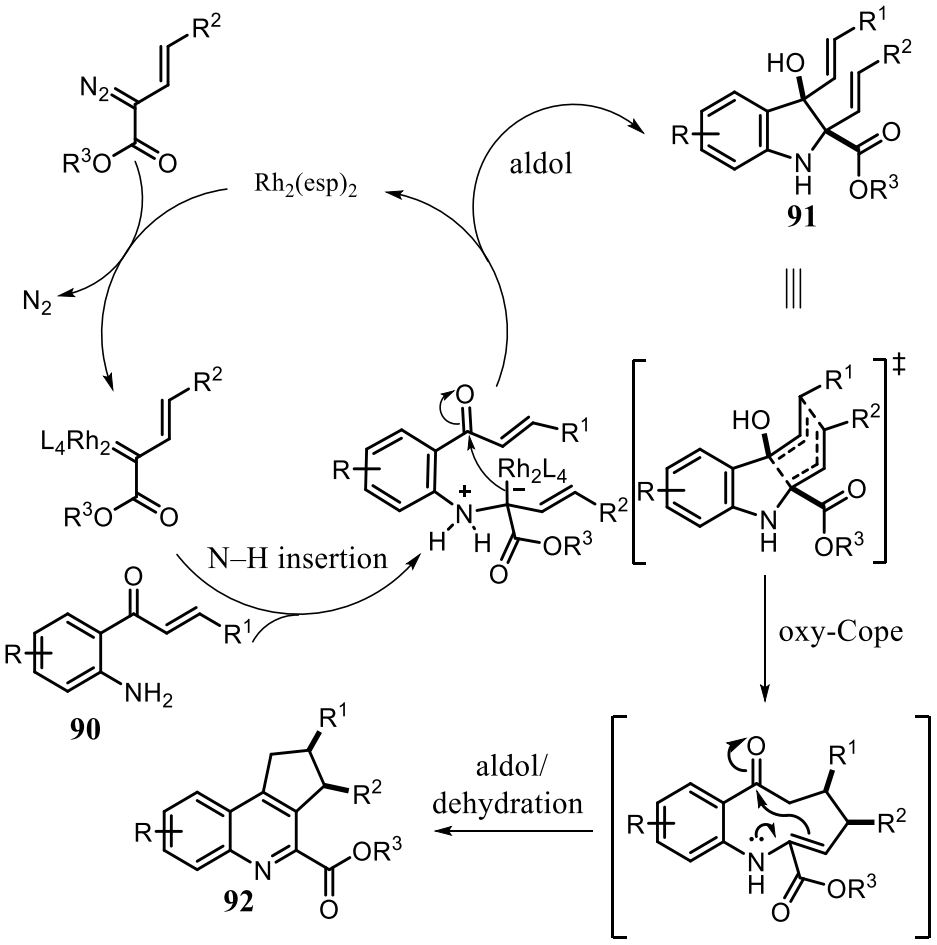

Scheme 56. Proposed reaction mechanism for the rhodium vinylcarbenoid initiated serendipitous cascade for the synthesis of functionalized quinolines

4.7 Conclusion and Future Directions

In summary, the reported rhodium vinylcarbenoid initiated serendipitous five-step cascade is convergent in nature and uses readily accessible starting materials to provide highly functionalized tri- and tetra-cyclic quinolines. An important feature of this transformation is its complete chemo-/regio- and stereo-selectivity. Furthermore, this work was then published in chemical communication[47] and then subsequently highlighted in *Synfacts* by Victor Snieckus and Paul Richardson (Pfizer)[173] (Scheme 57).

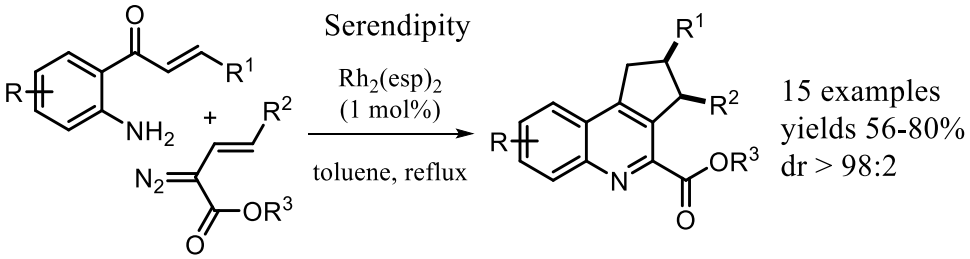

Chem. Commun. **2017**, *53*, 12205-12208

Highlighted in: *Synfacts* **2018**, 14, 0234.
DOI: 10.1055/s-0037-1609309

Scheme 57. A serendipitous discovery leading to a synthetically relevant scaffold

Furthermore, the products synthesized in this methodology were submitted for *In silico* high-through-put screening for a variety of biological targets, but no hits have currently been identified. After this achievement, we turned our attention to our original goal to synthesize medium-sized azacycles. We were sure that an intermediate azacycle was forming through the mechanism of preparing these tricyclic quinolines. Thus, we had to devise a way to stop the intramolecular aldol ring contraction step of this intermediate azacycle.

Trapping Rhodium Vinylcarbenoids with Aminochalcones for the Synthesis of Medium-Sized Azacycles

5.1 Introduction*

Compared to alternative nitrogenous medium-sized circumferences, 9-membered azacycles and lactams in particular are commonly present within indole alkaloid natural products; such as (-)-indolactam V, (-)-rhazinicine,[174] vinblastine[175] and quebrachamine.[176]

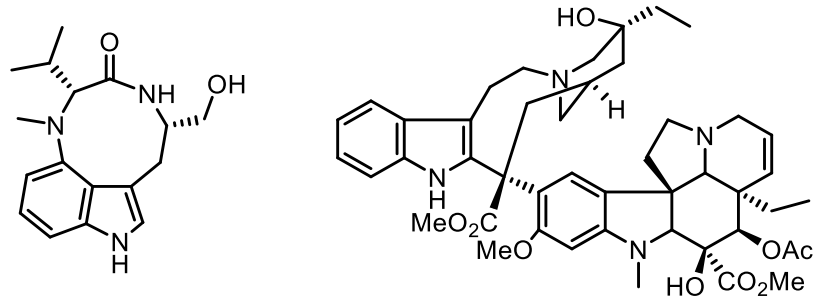

(-)-indolactam V
PKC activator

vinblastine
anticancer

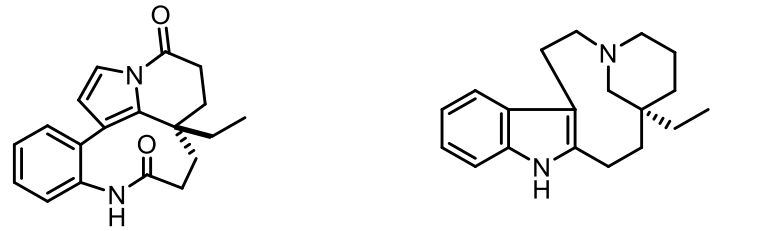

(-)-rhazinicine
anticancer

quebrachamine
adrenergic blocking activity

Figure 32. 9-membered lactam and azacycle natural products

This list provides biologically relevant examples of compounds that contain 9-membered azacycles. Some of these examples have found use as potent anticancer drugs; for example,

* The work presented within this chapter was performed by Chinthapally, K.; Massaro, N. P.; Ton, S.; Gardner, E.; Sharma, I. N.P.M. contributed to optimization of the reaction, all precursor synthesis, some product synthesis, X-ray structures, characterization of products and manuscript preparation.

vinblastine, a current chemotherapy drug, as well as (-)-rhazinicine, which has also shown potent antitumor properties. Their importance and intricate structures have inspired the development of a variety of beautiful methods to construct 9-membered azacycles. The most common method is the head-to-tail cyclization which is seen prominently in alkene metathesis as demonstrated by Aubé and co-workers where they constructed 9-membered cyclic amines (Scheme 63a).[177]

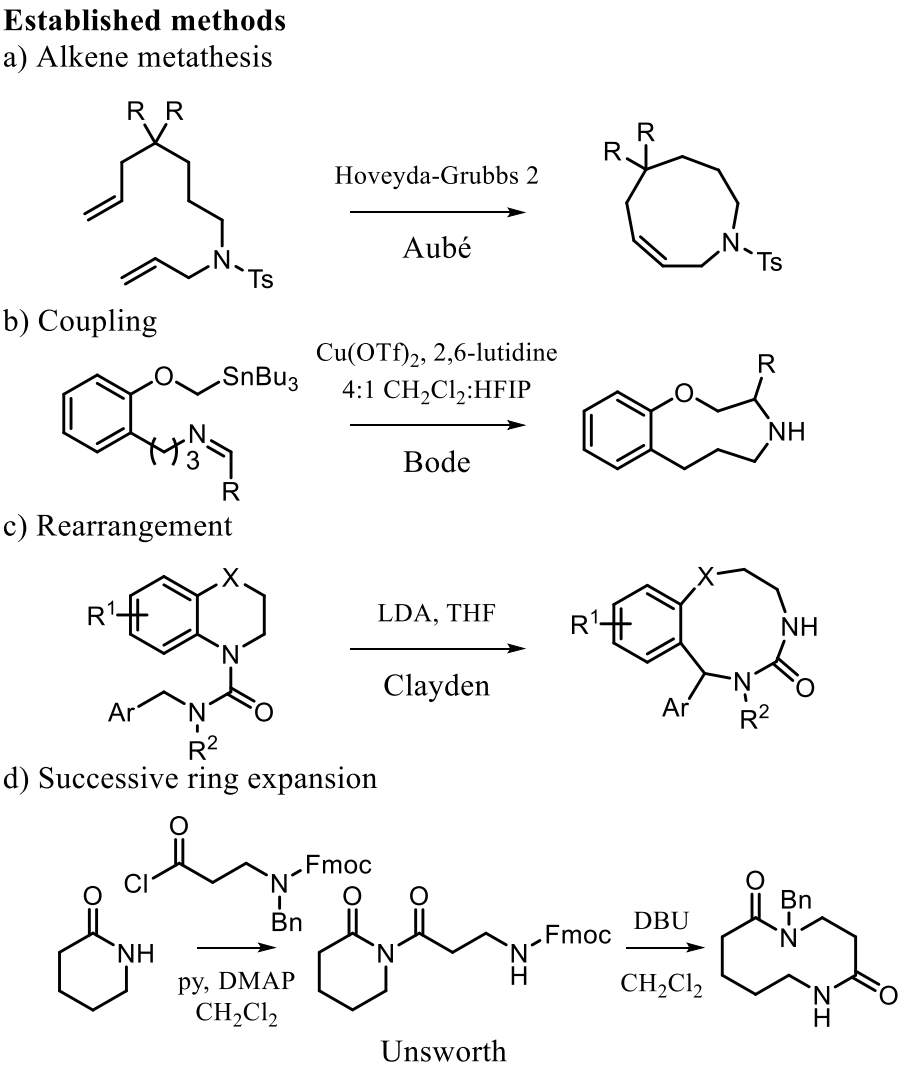

Scheme 58. Common methods to access medium-sized azacycles and lactams

Another very popular method that has been recently developed by Jeffery Bode incorporates his patented SnAP reagent that requires an end-to-end coupling with an alkyl tin reagent (Scheme 63b).[11] Aside from the more prevelent linear approaches, there have also been clever examples of ring rearrangments such as the base induced ring expansion by Clayden[178-179] (Scheme 63c) or the successive ring expansion devised by Unsworth et al. (Scheme 63d).[27]

From the work developed in chapter 4, we had hypothesized that alkylation of the nitrogen atom of 2‘-aminochalcone **105** may provide access to 9-membered azacycles by inhibiting the formation of **107** (Scheme 64). To test this hypothesis, *N*-benzyl protected aminochalcone **121a** was synthesized and exposed to the same reaction conditions with benzyl 2-diazobut-3-enoate **64**.

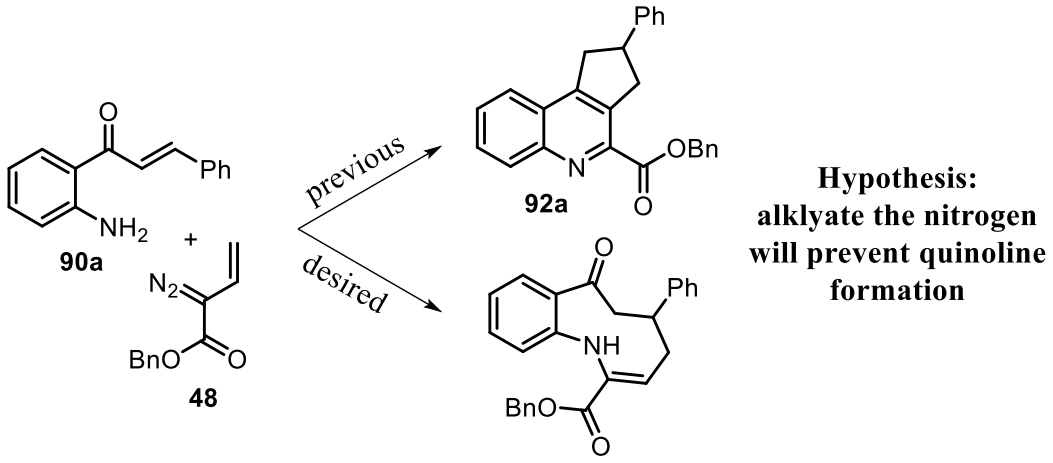

Scheme 59. Finding a solution to synthesize 9-membered azacycles

To our delight, the Rh(II)-catalyzed cascade reaction underwent the carbene N–H insertion/aldol/oxy-Cope sequence to provide azacycle **122a** without any trace of quinoline **107a** (Scheme 65). Unfortunately, the azacycle synthesis was low yielding which is attributed to the corresponding N–H insertion/aldol sequence where the cascade stops at

the first step, favoring the competing 1,2-proton transfer over the desired aldol cyclization. Furthermore, secondary anilines were reported by Hu and co-workers to be less reactive towards diverted N–H insertion cascades.[144] Regardless of the reduced yield, the absence of quinoline formation suggesting that benzyl protection did in-fact provide a solution to the transannular ring contraction aromatization sequence reported in chapter four. [172]

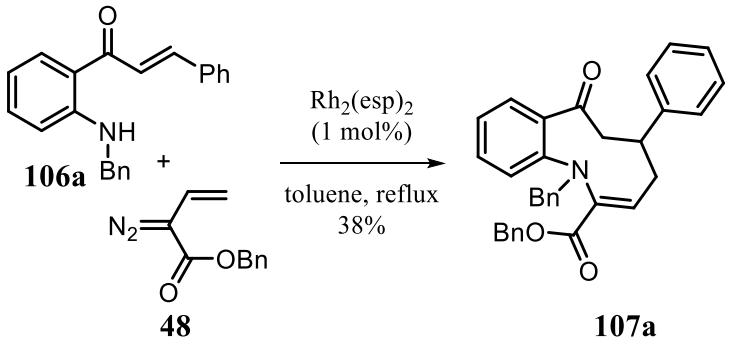

Scheme 60. Rhodium-carbenoid initiated N–H insertion/aldol/oxy–Cope cascade for the synthesis of functionalized azacycles

5.2 Optimization of Azacycle Synthesis

For the initial optimization, (*E*)-1-(2-(benzylamino)phenyl)-3-phenylprop-2-en-1-one **106a** and benzyl 2-diazobut-3-enoate **48** were selected as model substrates. As shown from our initial attempt to achieve the cascade with $Rh_2(esp)_2$ in toluene (boiling point 110 °C) at reflux, we obtained the desired 9-membered azacycle **107a**, albeit in low conversion (entry 1).[47] Encouraged by this interesting result, we screened other Rh(II)-salts to improve the yield of the transformation (Table 9, entries 2−5). Among them, $Rh_2(OAc)_4$ was found to be the most efficient catalyst for the cascade sequence and provided the corresponding 9-membered azacycle **107a** (entry 2). As was consistently seen with bulkier catalysts such as $Rh_2(TPA)_4$, we witnessed no conversion of our **106a**, but full conversion of **48**.With

optimized conditions in hand, we decided to prepare our starting material to test the substrate scope of this transformation.

Table 9. Optimization of azacycle formation

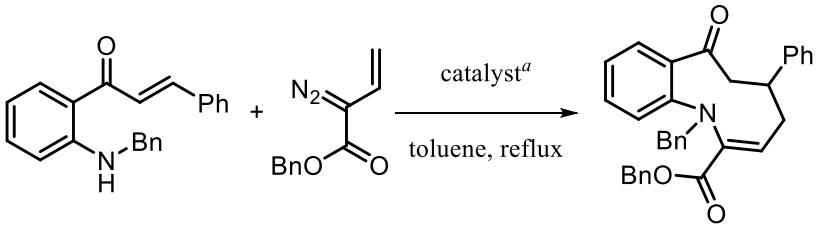

106a **48** **107a**

Entry	Catalyst	Mol (%), t	Yield (%)[b]
1	$Rh_2(esp)_2$	1.0, 3 h	38
2	**$Rh_2(OAc)_4$**	**1.0, 3 h**	**67**
3	$Rh_2(TPA)_4$	1.0, 3 h	NR
4	$Rh_2(TFA)_4$	1.0, 3 h	10

[a]All optimization reactions were performed by adding a 0.45 M solution of **48** (2.0 equiv) into a 0.1 M solution of **106a** (1.0 equiv) with catalysts *via* a syringe pump over 2.5 h, after the addition of diazo, all reactions were refluxed for an additional 30 min.

[b]Isolated yields after column chromatography.

5.1 Preparation of Model Substrates and Precursors for Azacycle Synthesis

Conveniently, many of the starting material for this synthesis were prepared by a one-step benzyl protection of the previously synthesized 2'-aminochalcones utilized for the cascade reported in chapter 4. This benzylation was accomplished by reacting our 2'-aminochalcone starting materials **90** with benzyl bromide and potassium carbonate in DMF at 25 °C. The yields of these protected 2'-aminochalcones **106** ranged from 50% to 60% for most compounds, although purification tended to be a challenge due to the similar Rf values of these starting materials and products (Scheme 61).

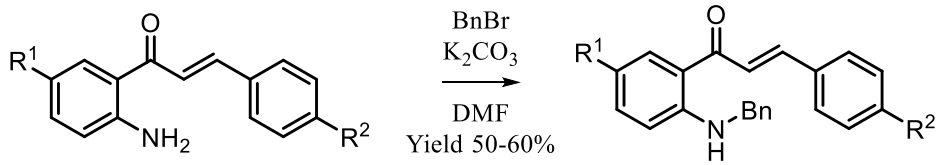

90a: R^1 = H, R^2 = H
90b: R^1 = H, R^2 =Cl
90c: R^1 = H, R^2 = OMe
90d: R^1 = H, R^2 = CN
90e: R^1 = Ph, R^2 = H
90f: R^1 = Br, R^2 = H

106a: R^1 = H, R^2 = H
106b: R^1 = H, R^2 =Cl
106c: R^1 = H, R^2 = OMe
106d: R^1 = H, R^2 = CN
106e: R^1 = Ph, R^2 = H
106f: R^1 = Br, R^2 = H

Scheme 61. Protection of 2'-aminochalcones

For the synthesis of **106g**, a similar 2-step process was followed, although the intermediate chalcone was taken forward at the crude stage, benzyl protected and then purified (Scheme 62).

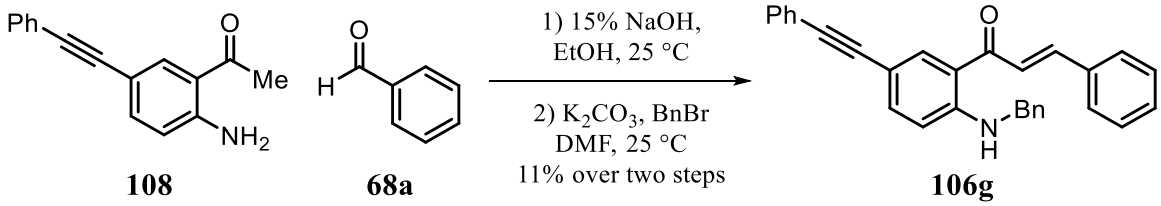

108 **68a** **106g**

Scheme 62. Synthesis of protected 2'-aminochalcone **121g**

Regarding the diazo fragment utilized in this cascade, the vinyl diazobenzoate **48** and propargyl vinyl diazo **96** from our previous reports were utilized.

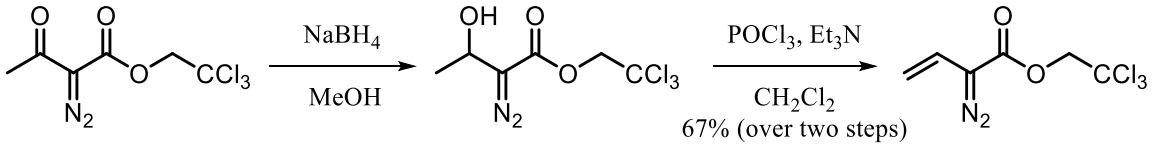

109 **110** **111**

Scheme 63. Synthesis of 2,2,2-trichloroethyl 2-diazobut-3-enoate **126**

Although 2,2,2-trichloroethyl 2-diazobut-3-enoate **111** was prepared via a similar method as **48** starting from literature known **109** followed by selective reduction of the ketone and

elimination of the subsequent secondary alcohol **110** to yield vinyl diazoacetate **111** in 67% yield over two steps (Scheme 63).

5.3 Substrate Scope of Azacycle Synthesis

With optimized conditions in hand, we then investigated the scope of this cascade sequence using $Rh_2(OAc)_4$ as a catalyst. The cascade tolerated a variety of *N*-benzyl protected 2‘-aminochalcones derivatives. The cascade tolerated the presence of halogens (**106b**) by provided azacycle **107b** in good yield.

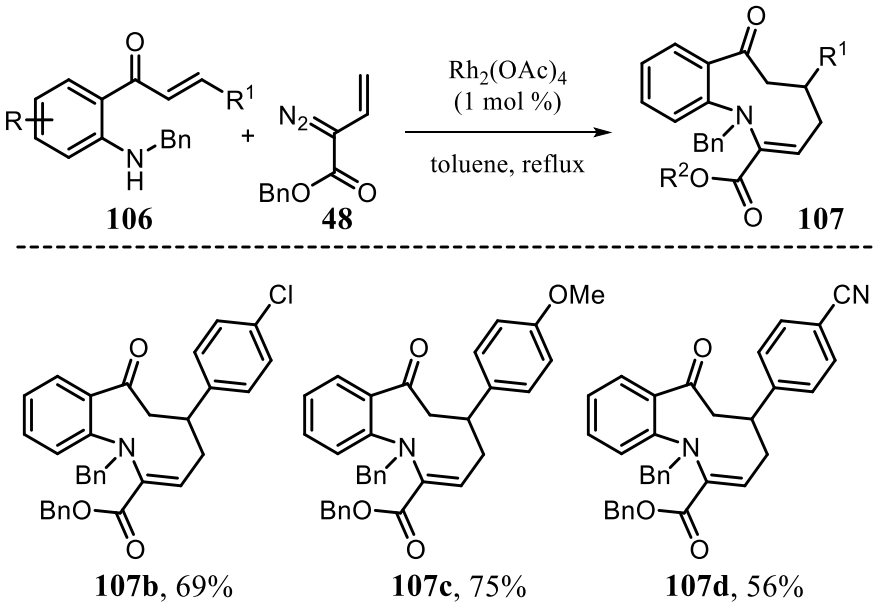

Scheme 64. Substrate Scope, modification of electronics

We screened both electron-withdrawing and electron-donating groups on the aromatic side chain of the protected 2’-aminochalcone observing similar yield trends as the aforementioned quinoline cascade in chapter 4 (Scheme 64, **107c**, **107d**). We were pleased to find that the cascade sequence tolerated substitution at the aniline ring of *N*-benzyl protected 2‘-aminochalcones equally well (Scheme 65, **107e**–**107g**). We did not observe any major byproducts resulting from alkyne functionality (**107g** & **107h**), which have the

propensity to undergo cyclopropenation,[159] as well as carbene-alkyne metathesis[16] with rhodium carbenoids. Finally, the cascade was attempted with vinyl diazoacetate **111** bearing a trichloroethyl ester chain. To our delight, the cascade proceeded in high yield to provide azacycle scaffold **107i** (Scheme 65).

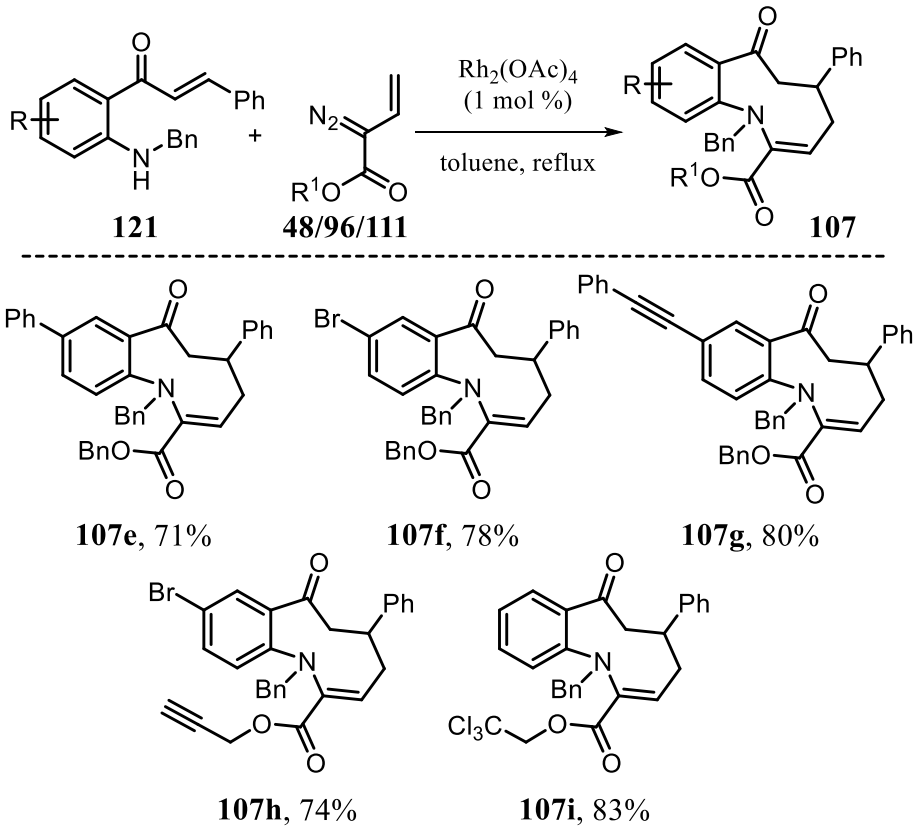

Scheme 65. Substrate Scope, substitution of aniline ring and ester

5.4 Proposed Mechanism of Aza-cycle Cascade

To our delight, while testing the substrate scope of this transformation we were able to confirm the structure of both **107g** and **107i** by X-ray analysis. As expected from our previous reports, the geometry of the double bond is found to be the *Z*-isomer (Figure 33). From our previous knowledge obtained from the cascades developed throughout this thesis and with this crystal structure data, we were able to propose a mechanism for this cascade.

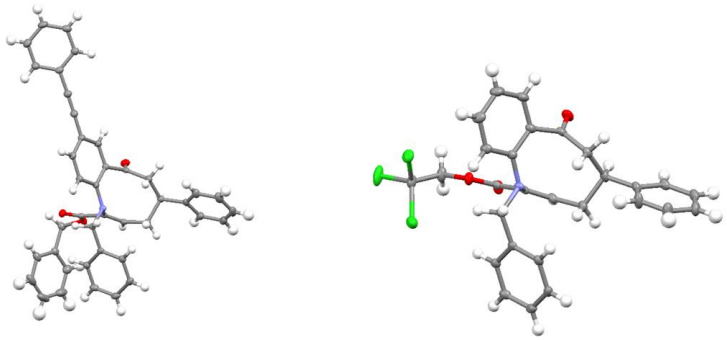

107g **107i**

Figure 33. X-ray structure of **107g** and **107i**

The reaction is initiated by decomposition of the vinyl diazoacetate precursor to the ambiphilic rhodium vinylcarbenoid that undergoes a chemoselective N–H insertion to generate a reactive zwitterionic intermediate that can perform a subsequent intramolecular 5-*exo*-trig cyclization to yield an indoline intermediate primed for oxy-Cope ring expansion under these toluene reflux conditions.

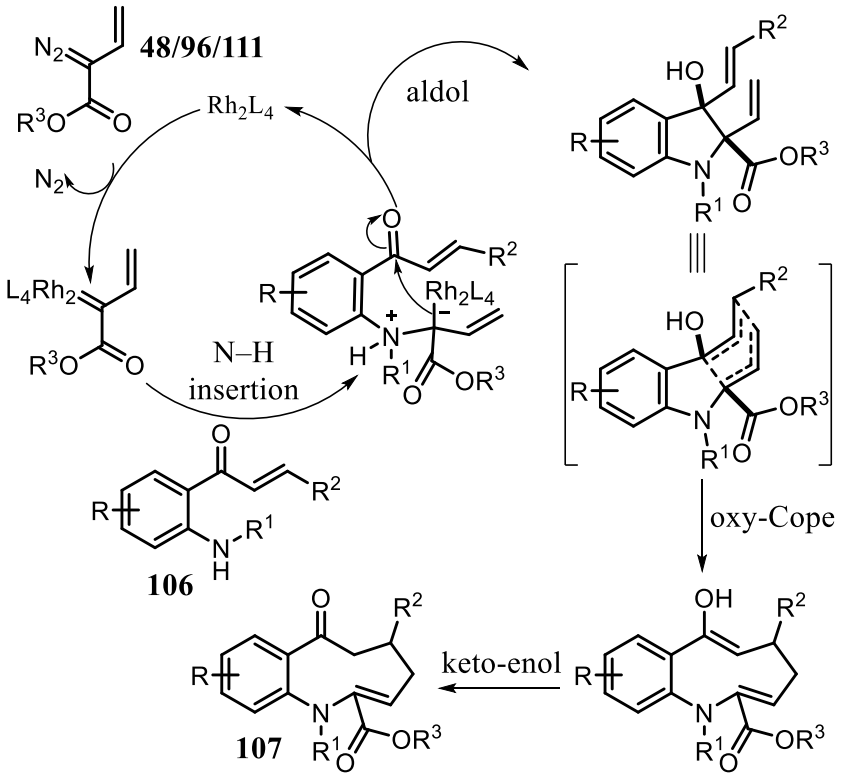

Scheme 66. Proposed mechanism of azacycle cascade

Upon ring expansion, the enol tautomer of the azacycle is formed followed by keto-enol tautomerization yielding the final highly functionalized 9-membered azacycle **107** (Scheme 66).

5.5 Conclusion and Future Directions

In conclusion, this cascade is highly convergent in nature taking readily available diazo precursors and protected 2-aminochalcones to synthesize a variety of highly functionalized 9-membered azacycles in good yield. This research also validates the progression of the cascade in chapter 4 and is a simple solution to an undesired transannular ring contraction. As a final note, the role of the benzyl group may not be to reduce nucleophility but may be due to conformation restriction to prevent the undesired quinoline formation. Currently, this work is being prepared for publication. Future extension of this work will be the transition to possible earth abundant alternatives. Furthermore, many of the compounds synthesized in this cascade will be submitted for high-through-put screening to identify hit compounds that may be elaborated more by future members of the Sharma Research Group.

Chapter 6: Conclusion

Medium-sized rings (8–12 membered) represent a unique class of cyclic molecules present within numerous natural products often exhibiting enhanced pharmacokinetics. Although this motif is currently underrepresented with respect to drug design. This scarcity is linked to the challenges associated with their construction limiting the synthesis of analogues for structure-activity relationships (SAR). Thus, more efficient methods to access these diverse scaffolds will provide a better foundation for medium-sized ring library generation with the goal of drug discovery.

In this thesis, a highly convergent cascade approach to access diverse highly functionalized medium-sized rings was developed. The cascade was based on the ambiphilic reactivity of rhodium vinylcarbenoids and the compatibility of pericyclic reactions such as oxy-Cope being implemented into cascades flawlessly.

With this approach, we first prepared functionalized 9-membered cyclic ethers. Proving not only that our method easily accessed these scaffolds in a one-pot procedure, but that rhodium vinylcarbenoids could perform an O-H insertion aldol reaction. We also proposed a mechanism of this reaction supported by X-ray crystallographic data. During this time, we had identified from our own experiences that previous O-H insertion aldol cascade reactions conditions did not tolerate carboxylic acids due to the lower pKa value.

Thus, we strived to extend this cascade to tolerate carboxylic acids, which was achieved by identifying an electron deficient catalyst capable of the performing the transformation, providing direct access to diverse lactones. The cascade was further modified to promote a 6-*exo*-trig cyclization enabled by aromatic constraint. With this method, a variety of lactones ranging in sizes (5, 6, and 10) were produced. In addition to

these efforts, earth abundant alternatives for O-H insertion aldol cascades was also briefly explored providing some insight into this zwitterionic cascade. Furthermore, a hit compound was identified that is active towards the Bax Bak proteins, and this method now provides direct access to library synthesis

Finally, the strategy was then extended to N-H nucleophiles which provided azacycles, but also highly functionalized tricyclic quinolines during the journey. This serendipitous event to produce quinolines was explored thoroughly identifying and isolating each intermediate in the reaction mechanism to eventually develop a solution to produce 9-membered azacycles exclusively.

Chapter 7: Experimentals

Chapter 7.1. Experimentals for Chapter 2

General Procedure 1 for the synthesis of keto-alcohol. Method A

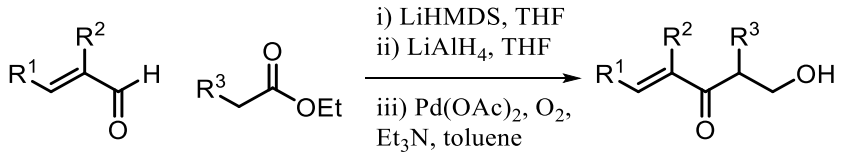

To a stirred solution of ethyl ester (1.0 equiv, commercially available) in THF (0.55 M) was added LiHMDS (1.1 equiv, 1.0 M) at −78 °C. The resulting mixture was stirred for 1 h at −78 °C. Corresponding aldehyde (1.0 equiv, commercially available) was then added *via* syringe and the temperature was maintained for 3 h at −78 °C. Reaction was then quenched at –78 °C with saturated aqueous NH_4Cl solution. The aqueous layer was separated and extracted with ethyl acetate (3x). The combined extracts were dried over Na_2SO_4. The crude reaction extract was filtered through a silica gel plug, evaporated under reduced pressure and the residue was taken forward without further purification.

To a stirred suspension of $LiAlH_4$ (1.2 equiv, 0.25 M) in dry THF at 0 °C was added a solution of crude aldol product (1.0 equiv, 0.4 M) in freshly distilled THF (0.4 M). Reaction was monitored by TLC until completion (1-2 h). Reaction was quenched by adding copious amounts of ethyl acetate followed by 15% aqueous NaOH solution at 0 °C. The crude mixture was filtered through a celite pad and extracted with ethyl acetate (3x). The combined organic layers were then dried over sodium sulfate, filtered through a silica gel plug and concentrated by rotary evaporation to afford the crude diol that was taken forward without further purification.

$Pd(OAc)_2$ (0.01 equiv) and Et_3N (0.03 equiv) were dissolved in THF–toluene (15%; 3.4 mL). Crude diol (1.0 mmol) was added and the reaction mixture was heated to 45 °C

under 1 atm of O_2 (balloon) for 20 h. After completion of reaction, solvent was evaporated under reduced pressure. Purification by silica gel flash chromatography using hexanes-ethyl acetate (30-40%, gradient elution) afforded β-hydroxy vinyl ketone.

General Procedure 2 for the synthesis of keto-alcohol. Method B

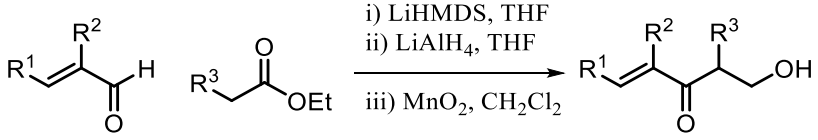

To a stirred solution of ethyl ester (1.0 equiv, commercially available) in THF (0.55 M) was added LiHMDS (1.1 equiv, 1.0 M) at −78 °C. The resulting mixture was stirred for 1 h at −78 °C. Corresponding aldehyde (1.0 equiv, commercially available) was then added *via* syringe and the temperature was maintained for 3 h at −78 °C. Reaction was then quenched at –78 °C with saturated aqueous NH_4Cl solution. The aqueous layer was separated and extracted with ethyl acetate (3x). The combined extracts were dried over Na_2SO_4. The crude reaction extract was filtered through a silica gel plug, evaporated under reduced pressure and the residue was taken forward without further purification.

To a stirred suspension of $LiAlH_4$ (1.2 equiv, 0.25 M) in dry THF at 0 °C was added a solution of crude aldol product (1.0 equiv, 0.4 M) in freshly distilled THF (0.4 M). Reaction was monitored by TLC until completion (1-2 h). Reaction was quenched by adding copious amounts of ethyl acetate followed by 15% aqueous NaOH solution at 0 °C. The crude mixture was filtered through a celite pad and extracted with ethyl acetate (3x). The combined organic layers were then dried over sodium sulfate, filtered through a silica gel plug and concentrated by rotary evaporation to afford the crude diol that was taken forward without further purification.

To a stirred solution of crude diol (1.0 equiv) in CH_2Cl_2 (0.1 M) was added MnO_2 (20.0 equiv) all at once. The reaction was stirred 12–24 hours. Then the mixture was filtered over a celite pad and concentrated by rotary evaporation to afford the crude product. Purification by silica gel flash chromatography using hexanes-ethyl acetate (30-40%, gradient elution) afforded β-hydroxy vinyl ketone.

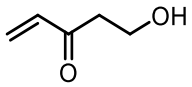

5-hydroxypent-1-en-3-one (39a). Prepared from acrolein and ethyl acetate using general procedure **1**. Pale yellow oil (392 mg, 80%). **TLC**: R_f 0.28 (1:1 hexanes/EtOAc). **IR** (NaCl): 3410, 3394, 2947, 2893, 1672, 1614, 1406, 1197, 1049, 972, 621. **^{1}H NMR** (500 MHz) δ 6.33 (dd, J = 17.7, 10.5 Hz, 1H), 6.23 (dd, J = 17.7, 1.1 Hz, 1H), 5.88 (dd, J = 10.4, 1.1 Hz, 1H), 3.87 (t, J = 5.5 Hz, 2H), 2.84 (t, J = 5.0 Hz, 2H), 2.78 (s, 1H). **^{13}C NMR** (126 MHz) δ 200.9, 136.5, 129.1, 57.6, 41.1.

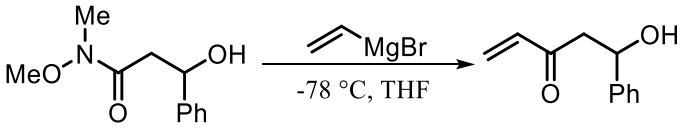

5-hydroxy-5-phenylpent-1-en-3-one (39b). To a solution of Weinreb amide (600 mg, 2.87 mmol 1.0 equiv, prepared from known literature protocol[180]) in THF (48 mL) was added vinyl magnesium bromide solution (6.9 mL, 6.90 mmol, 2.4 equiv, 1.0 M) at –78 °C over the course of 10 minutes. The temperature was maintained at –78 °C for six hours prior to quenching with ammonium chloride at –78 °C. The aqueous layer was separated and extracted with ethyl acetate (3x). The combined extracts were dried over Na_2SO_4 and concentrated by rotary evaporation to afford crude product. Purification by silica gel flash chromatography using hexanes-ethyl acetate (25-30%, gradient elution) afforded pure **2f**

as a pale yellow oil (121 mg, 24%). **TLC**: R_f 0.40 (7:3 hexanes/EtOAc). **IR** (NaCl): 3458, 1682, 1614, 1402, 760, 702. **^{1}H NMR** (400 MHz) δ 7.41–7.31 (m, 4H), 7.31–7.23 (m, 1H), 6.35 (dd, J = 17.7, 10.4 Hz, 1H), 6.22 (dd, J = 17.8, 1.1 Hz, 1H), 5.89 (dd, J = 10.5, 1.1 Hz, 1H), 5.19 (dt, J = 8.8, 2.6 Hz, 1H), 3.51 (d, J = 2.9 Hz, 1H), 3.09–2.89 (m, 2H). **^{13}C NMR** (101 MHz) δ 200.4, 142.8, 136.5, 129.4, 128.4 (2C), 127.5, 125.6 (2C), 69.7, 47.8. Data matches known literature values.[181]

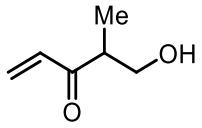

5-hydroxy-4-methylpent-1-en-3-one (39c). Prepared from acrolein and ethyl propionate using general procedure **1**. Pale yellow oil (127 mg, 16% isolated over three steps). **TLC**: R_f 0.30 (2:3 hexanes/EtOAc). **IR** (NaCl): 3491, 2972, 2935, 2882, 1738, 1686, 1516, 1462, 1406, 1030, 980. **^{1}H NMR** (400 MHz) δ 6.39 (dd, J = 17.5, 10.5 Hz, 1H), 6.24 (dd, J = 17.6, 1.3 Hz, 1H), 5.78 (dd, J = 10.5, 1.3 Hz, 1H), 3.77–3.57 (m, 2H), 3.00 (pd, J = 7.2, 4.5 Hz, 1H), 1.07 (d, J = 7.2 Hz, 3H). **^{13}C NMR** (101 MHz) δ 203.8, 135.1, 128.9, 64.0, 45.2, 13.4. Data matches known literature values.[182]

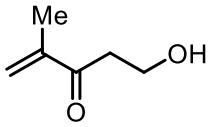

5-hydroxy-2-methylpent-1-en-3-one (39d). Prepared from methacrolein and ethyl acetate using general procedure **2**. Pale yellow oil (347 mg, 27% isolated over three steps). **TLC**: R_f 0.20 (3:2 hexanes/EtOAc). **IR** (NaCl): 3445, 2957, 2928, 2889, 2357, 2326, 1672, 1373, 1053, 939, 737. **^{1}H NMR** (400 MHz) δ 6.00 (s, 1H), 5.85–5.83 (m, 1H), 3.91 (q, J = 5.3 Hz, 2H), 2.95 (t, J = 5.4 Hz, 2H), 2.53 (s, 1H), 1.92–1.86 (m, 3H). **^{13}C NMR** (101 MHz) δ 201.4, 144.1, 125.3, 57.6, 39.3, 16.9.

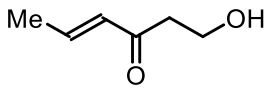

(*E*)-1-hydroxyhex-4-en-3-one (39e). Prepared from predominately trans crotonaldehyde and ethyl acetate using general procedure **2**. Pale yellow oil (726 mg, 61% isolated over three steps). **TLC**: R_f 0.48 (1:1 hexanes/EtOAc). **IR** (NaCl): 3443, 3422, 3398, 2965, 2945, 2889, 1661, 1632, 1443, 1373, 1055, 972, 737. **^{1}H NMR** (400 MHz) δ 6.89 (dq, J = 15.8, 6.8 Hz, 1H), 6.13 (dq, J = 15.8, 1.7 Hz, 1H), 3.88 (t, J = 5.4 Hz, 2H), 2.79 (t, J = 5.4 Hz, 2H), 2.61 (s, 1H), 1.92 (dd, J = 6.8, 1.7 Hz, 3H). **^{13}C NMR** (101 MHz) δ 200.6, 143.9, 132.1, 58.1, 41.2, 18.3. Data matches known literature values.[183]

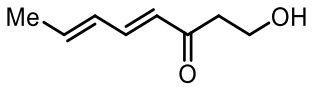

(4*E*,6*E*)-1-hydroxyocta-4,6-dien-3-one (39f). Prepared from sorbaldehyde and ethyl acetate using general procedure **2**. Pale yellow oil (412 mg, 35% isolated over three steps). **TLC**: R_f 0.2 (3:2 hexanes/EtOAc). **IR** (NaCl): 3441, 3416, 2963, 2938, 2913, 2886, 2359, 1678, 1636, 1591, 1377, 1190, 1055, 999. **^{1}H NMR** (500 MHz) δ 7.19–7.12 (m, 1H), 6.29–6.13 (m, 2H), 6.07 (d, J = 15.7 Hz, 1H), 3.89 (t, J = 5.4 Hz, 2H), 2.82 (t, J = 5.4 Hz, 2H), 2.65 (s, 1H), 1.88 (d, J = 5.1 Hz, 3H). **^{13}C NMR** (126 MHz) δ 201.0, 143.9, 141.2, 130.1, 127.6, 58.2, 41.7, 18.8.

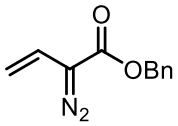

Benzyl 2-diazobut-3-enoate (**48).** Compound was prepared using known literature procedure.[92]

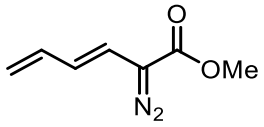

Methyl (*E*)-2-diazohexa-3,5-dienoate (52). To a stirred solution of diisopropylamine (1.1 mL, 8.09 mmol, 1.2 equiv) in dry THF (10 mL) at –78 °C was added *n*-BuLi (4.6 mL, 7.44 mmol, 1.1 equiv, 1.6 M) and stirred for 30 minutes at –78 ºC. Then HMPA (2.3 mL, 13.5 mmol, 2.0 equiv) was added and allowed to stir for an additional 5 minutes. Methyl (*E*)-hexa-3,5-dienoate, prepared from known literature procedures[93] was then added (850 mg, 6.70 mmol, 1.0 equiv) in 10 mL THF and allowed to stir for 30 minutes at −78 °C. Once enolate formation was complete, a solution of 4-Acetamidobenzenesulfonyl azide (*p*-ABSA) (1.94 g, 8.09 mmol) in 8 mL THF was added and the reaction was allowed to stir for an additional 30 minutes at −78 °C. The reaction was then allowed to slowly reach −20 °C over 1.5 h before it was quenched with saturated solution of NH_4Cl (10 mL). The reaction mixture was then extracted with EtOAc (3 × 30 mL), and the combined EtOAc layers were washed with water (20 mL), dried over anhydrous Na_2SO_4 and concentrated under reduced pressure to give crude compound. Column chromatographic purification of the crude compound over silica gel (9:1 hexanes/EtOAc) afforded the compound **1b** (622 mg, 65%) as a red oil. **TLC**: R_f 0.50 (9:1 hexanes/EtOAc). **IR** (NaCl): 3005, 2085, 1710, 1627, 1436, 1327, 1168, 1103, 999, 742. **^{1}H NMR** (400 MHz) δ 6.57–6.30 (m, 1H), 5.93 (m, J = 1.6 Hz, 2H), 5.14–5.07 (dd, 1H), 4.99 (dd, J = 10.1, 1.6 Hz, 1H), 3.80 (s, 3H). **^{13}C NMR** (101 MHz) δ 165.3, 136.0, 124.2, 115.1, 114.9, 52.2.

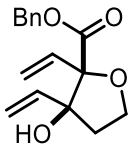

Benzyl 3-hydroxy-2,3-divinyltetrahydrofuran-2-carboxylate (53). To a flame dried 15 mL pear shaped round bottom with stir bar was added $Rh_2(esp)_2$ (1 mol%). A solution of *β*-hydroxy vinyl ketone (25 mg, 0.25 mmol) in 1.5 mL CH_2Cl_2 was then added, the flask was equipped with a reflux condenser, and set to stirring while at reflux. While at reflux, a solution of vinyl diazo (76 mg, 0.37 mmol) in 1 mL CH_2Cl_2 was added over 3 h *via* syringe pump at this temperature. After the addition was completed, the reaction was left to reflux for an additional 1 hour. After reaction was completed, the crude reaction mixture was concentrated using rotary evaporation and then purified using flash column chromatography eluting with 1:3 ethyl acetate: hexanes to afford aldol product **3a** as a colorless liquid (49 mg, 72%). **TLC**: R_f 0.21 (7:3 hexanes/EtOAc). **IR** (NaCl): 3522, 3496, 3481, 3466, 2981, 2951, 2893, 1734, 1718, 1639, 1456, 1375, 1267, 1151, 1056, 991, 929, 742. **^{1}H NMR** (400 MHz) δ 7.36–7.31 (m, 5H), 6.09–5.98 (m, 2H), 5.51 (dd, J = 17.0, 1.4 Hz, 1H), 5.33 (dd, J = 17.3, 1.1 Hz, 1H), 5.29–5.15 (m, 4H), 4.33–4.25 (m, 1H), 4.20–4.15 (m, 1H), 2.43 (d, J = 2.8 Hz, 1H), 2.25–2.16 (m, 1H), 1.90 (ddd, J = 12.8, 6.1, 1.7 Hz, 1H). **^{13}C NMR** (101 MHz): δ 170.2, 137.4, 135.5, 135.3, 128.5 (2C), 128.2, 128.1 (2C), 116.5, 115.8, 91.9, 84.3, 67.0, 66.9, 37.2. **ESI-MS** *m/z* calcd for $C_{16}H_{18}O_4Na$ ($[M+Na]^+$) 297.1102; found 296.5. Relative stereochemistry was assigned based on previous literature reports.[184]

General Procedure 3 for the Synthesis of Oxacycles 54a–54k

To a flame dried 15 mL pear shaped round bottom with stir bar was added $Rh_2(OAc)_4$ (1 mol%). A solution of *β*-hydroxy vinyl ketone (0.25 mmol) in 1.5 mL toluene was then added, the flask was equipped with a reflux condenser, and set to stirring while at reflux. While at reflux a solution of vinyl diazo (0.37 mmol) in 1 mL toluene was added over 3 h

via syringe pump at this temperature. After the addition was completed, the reaction was left to reflux for an additional 1 hour. After reaction was completed, the crude reaction mixture was purified using flash column chromatography eluting with 1:3 ethyl acetate: hexanes to afford oxacycle **54a–54k**.

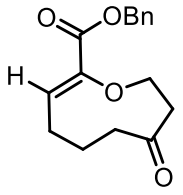

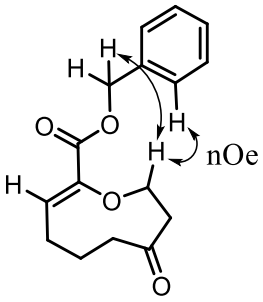

Benzyl (*Z*)-7-oxo-4,5,6,7,8,9-hexahydrooxonine-2-carboxylate (54a). Synthesized using general procedure 3. Colorless liquid (47 mg, 68%). **TLC**: R_f 0.34 (7:3 hexanes/EtOAc). **IR** (NaCl): 3496, 2953, 2937, 1726, 1712, 1647, 1498, 1454, 1269, 1170, 1101, 769, 752, 738, 698. **^{1}H NMR** (400 MHz) δ 7.40–7.34 (m, 5H), 6.39 (t, J = 8.4 Hz, 1H), 5.23 (s, 2H), 4.34 (t, J = 6.0 Hz, 2H), 2.67 (t, J = 6.0 Hz, 2H), 2.47–2.44 (m, 2H), 2.26–2.20 (m, 2H), 1.94–1.88 (m, 2H). **^{13}C NMR** (101 MHz): δ 212.6, 163.4, 146.8, 135.6, 128.7, 128.6 (2C), 128.3, 128.2 (2C), 127.4, 69.8, 66.8, 44.6, 37.6, 23.0. **HRMS** (ESI) *m/z* calcd for $C_{16}H_{18}O_4Na$ ($[M+Na]^+$) 297.1102; found 297.1105.

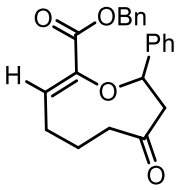

Benzyl (*Z*)-7-oxo-9-phenyl-4,5,6,7,8,9-hexahydrooxonine-2-carboxylate (54b). Synthesized using general procedure 3. Colorless liquid (34.6 mg, 58%). **TLC**: R_f 0.46 (7:3 hexanes/EtOAc). **IR** (NaCl): 3061, 3032, 2947, 1712, 1649, 1498, 1452, 1379, 1263, 975, 916, 744, 698. **^{1}H NMR** (400 MHz) δ 7.40–7.26 (m, 8H), 7.17–7.15 (m, 2H), 6.37 (t, J =

7.9 Hz, 1H), 5.27 (dd, *J* = 11.2, 3.5 Hz, 1H), 5.06 (q, *J* = 12.3 Hz, 2H), 3.18 (dd, *J* = 14.3, 11.3 Hz, 1H), 2.66–2.57 (m, 3H), 2.55–2.49 (m, 1H), 2.39 (dt, *J* = 17.0, 6.5 Hz, 1H), 2.13 (dtd, *J* = 14.8, 7.6, 2.8 Hz, 1H), 1.80–1.71 (m, 1H). **^{13}C NMR** (101 MHz): *δ* 211.7, 163.3, 146.5, 141.4, 135.4, 128.4 (2C), 128.4 (2C), 128.2 (2C), 128.1, 127.6, 127.0, 125.5 (2C), 82.4, 66.7, 52.5, 41.4, 24.6, 22.9. **HRMS** (ESI) *m/z* calcd for $C_{22}H_{22}O_4Na$ ($[M+Na]^+$) 373.1415; found 373.1419.

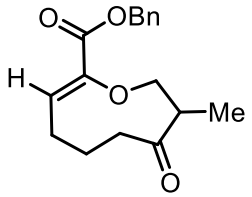

Benzyl (*Z*)-8-methyl-7-oxo-4,5,6,7,8,9-hexahydrooxonine-2-carboxylate (54c). Synthesized using general procedure 3. Colorless liquid (35 mg, 60%). **TLC**: R_f 0.44 (7:3 hexanes/EtOAc). **IR** (NaCl): 3977, 2960, 2933, 1743, 1718, 1647, 1456, 1269, 1170, 1103, 752, 738, 698. **^{1}H NMR** (400 MHz) *δ* 7.39–7.33 (m, 5H), 6.36 (t, *J* = 8.5 Hz, 1H), 5.22 (s, 2H), 4.33 (dd, *J* = 11.7, 5.4 Hz, 1H), 3.94 (dd, *J* = 11.6, 8.6 Hz, 1H), 2.87 (ddd, *J* = 8.4, 7.0, 5.4 Hz, 1H), 2.44–2.40 (m, 2H), 2.19 (dtd, *J* = 12.7, 8.5, 4.3 Hz, 2H), 1.93 (td, *J* = 7.7, 3.9 Hz, 1H), 1.89–1.78 (m, 1H), 1.04 (d, *J* = 7.0 Hz, 3H). **^{13}C NMR** (101 MHz): *δ* 214.6, 163.4, 147.4, 135.6, 128.6 (2C), 128.3, 128.2 (2C), 126.7, 76.0, 66.8, 48.0, 35.5, 22.8, 22.4, 12.6. **HRMS** (ESI) *m/z* calcd for $C_{17}H_{20}O_4Na$ ($[M+Na]^+$) 311.1259; found 311.1263.

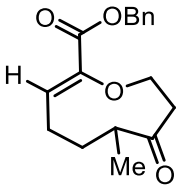

Benzyl (*Z*)-6-methyl-7-oxo-4,5,6,7,8,9-hexahydrooxonine-2-carboxylate (54d). Synthesized using general procedure 3. Colorless liquid (45 mg, 71%). **TLC**: R_f 0.43 (7:3

hexanes/EtOAc). **IR** (NaCl): 3859, 3741, 3647, 1737, 1712, 1647, 1543, 1512, 1456, 1265, 1165, 1095, 893, 842, 740. **^{1}H NMR** (400 MHz) δ 7.38–7.32 (m, 5H), 6.40 (dd, J = 9.2, 7.7 Hz, 1H), 5.26–5.18 (m, 2H), 4.46 (dt, J = 12.0, 5.2 Hz, 1H), 4.18 (ddd, J = 12.0, 8.9, 4.3 Hz, 1H), 2.88 (ddt, J = 9.9, 7.4, 3.7 Hz, 1H), 2.73 (ddd, J = 15.2, 5.5, 4.3 Hz, 1H), 2.62 (ddd, J = 15.0, 8.9, 5.0 Hz, 1H), 2.43–2.33 (m, 1H), 2.11–2.04 (m, 1H), 1.87 (tdd, J = 10.9, 5.8, 3.6 Hz, 1H), 1.68–1.60 (m, 1H), 1.03 (d, J = 6.7 Hz, 3H). **^{13}C NMR** (101 MHz): δ 215.7, 163.4, 146.3, 135.6, 128.6 (2C), 128.3, 128.2 (3C), 69.4, 66.8, 43.2, 42.5, 31.9, 22.7, 17.7. **HRMS** (ESI) *m/z* calcd for $C_{17}H_{20}O_4Na$ ($[M+Na]^+$) 311.1259; found 311.1263.

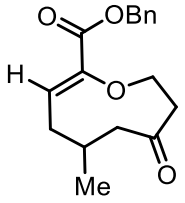

Benzyl (*Z*)-5-methyl-7-oxo-4,5,6,7,8,9-hexahydrooxonine-2-carboxylate (54e). Synthesized using general procedure 3. Colorless liquid (48.5 mg, 64%). **TLC**: R_f 0.45 (7:3 hexanes/EtOAc). **IR** (NaCl): 2956, 2929, 1726, 1716, 1456, 1267, 1093, 750, 738, 698. **^{1}H NMR** (400 MHz) δ 7.38–7.33 (m, 5H), 6.44 (t, J = 8.5 Hz, 1H), 5.27–5.18 (m, 2H), 4.47 (dt, J = 11.8, 5.0 Hz, 1H), 4.20 (ddd, J = 11.8, 9.6, 4.3 Hz, 1H), 2.70 (ddd, J = 14.9, 9.6, 5.1 Hz, 1H), 2.58 (dt, J = 15.5, 4.6 Hz, 1H), 2.52–2.45 (m, 1H), 2.45–2.36 (m, 2H), 2.22–2.18 (m, 1H), 2.02 (ddd, J = 13.5, 8.3, 6.0 Hz, 1H), 1.05 (d, J = 6.5 Hz, 3H). **^{13}C NMR** (101 MHz): δ 211.9, 163.3, 146.5, 135.6, 128.6 (2C), 128.3, 128.2 (2C), 126.5, 69.7, 66.8, 45.7, 44.8, 31.3, 30.1, 21.4. **HRMS** (ESI) *m/z* calcd for $C_{17}H_{20}O_4Na$ ($[M+Na]^+$) 311.1259; found 311.1263.

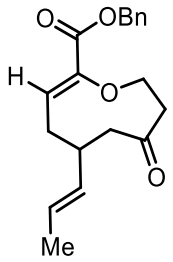

Benzyl (*Z*)-7-oxo-5-((E)-prop-1-en-1-yl)-4,5,6,7,8,9-hexahydrooxonine-2-carboxylate (54f). Synthesized using general procedure 3. Colorless liquid (34 mg, 61%). **TLC**: R_f 0.57 (7:3 hexanes/EtOAc). **IR** (NaCl): 3747, 3736, 3469, 2960, 1747, 1710, 1649, 1558, 1541, 1521, 1506, 1454, 1265, 1101, 752, 738, 698. **^{1}H NMR** (400 MHz) δ 7.39–7.32 (m, 5H), 6.42 (dd, *J* = 9.3, 8.0 Hz, 1H), 5.49–5.45 (m, 1H), 5.29–5.18 (m, 2H), 4.49 (dt, *J* = 11.8, 4.9 Hz, 1H), 4.20 (ddd, *J* = 11.8, 9.6, 4.5 Hz, 1H), 2.95 (ddd, *J* = 12.2, 8.0, 4.2 Hz, 1H), 2.74–2.66 (m, 1H), 2.65–2.61 (m, 1H), 2.58 (t, *J* = 4.6 Hz, 1H), 2.47 (ddd, *J* = 13.1, 9.3, 4.0 Hz, 1H), 2.22 (dd, *J* = 13.5, 4.5 Hz, 1H), 2.10 (ddd, *J* = 13.4, 8.0, 5.7 Hz, 1H), 1.89–1.86 (m, 1H), 1.66 (d, *J* = 8.0, 3H). **^{13}C NMR** (101 MHz): δ 211.5, 163.3, 146.7, 135.6, 133.5, 128.6 (2C), 128.3, 128.2 (2C), 126.4, 124.8, 69.7, 66.8, 44.8, 43.4, 38.8, 28.9, 17.9. **HRMS** (ESI) *m/z* calcd for $C_{19}H_{22}O_4Na$ ($[M+Na]^+$) 337.1415; found 337.1417.

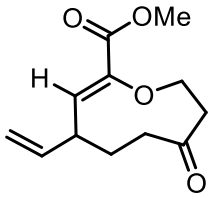

Methyl (*Z*)-7-oxo-4-vinyl-4,5,6,7,8,9-hexahydrooxonine-2-carboxylate (54g). Synthesized using general procedure 3. Colorless liquid (34.5 mg, 64%). **TLC**: R_f 0.44 (7:3 hexanes/EtOAc). **IR** (NaCl): 3745, 2954, 1722, 1647, 1541, 1512, 1433, 1340, 1309, 1292, 1246, 1097, 1001, 918, 775. **^{1}H NMR** (400 MHz) δ 6.17 (dd, *J* = 9.4, 0.9 Hz, 1H), 5.79–5.70 (m, 1H), 5.09–5.00 (m, 2H), 4.54–4.49 (m, 1H), 4.21–4.14 (m, 1H), 3.80 (s, 3H),

3.33–3.24 (m, 1H), 2.78–2.69 (m, 2H), 2.64–2.58 (m, 1H), 2.25–2.14 (m, 2H), 1.62–1.50 (m, 1H). **^{13}C NMR** (101 MHz): δ 212.2, 163.9, 145.5, 139.5, 129.4, 115.1, 69.5, 52.1, 44.5, 37.9, 37.1, 30.0. **HRMS** (ESI) ***m/z*** calcd for $C_{12}H_{16}O_4Na$ ($[M+Na]^+$) 247.0946; found 247.0948.

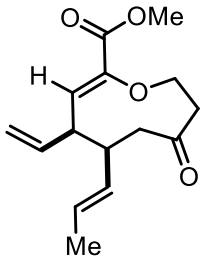

Methyl (*Z*)-7-oxo-5-((*E*)-prop-1-en-1-yl)-4-vinyl-4,5,6,7,8,9-hexahydrooxonine-2-carboxylate (54h). Synthesized using general procedure 3. Colorless liquid (32 mg, 59%, (dr > 98:2)). **TLC**: R_f 0.53 (7:3 hexanes/EtOAc). **IR** (NaCl): 2954, 2927, 2872, 1714, 1639, 1456, 1435, 1315, 1271, 1238, 1195, 1087, 974, 777, 732. **^{1}H NMR** (400 MHz) δ 6.72 (d, J = 10.8 Hz, 1H), 6.09–6.02 (m, 1H), 5.86 (ddd, J = 15.4, 8.3, 6.3 Hz, 1H), 5.38–5.21 (m, 2H), 4.29 (ddd, J = 12.4, 8.1, 2.0 Hz, 1H), 4.20 (ddd, J = 12.4, 6.4, 2.2 Hz, 1H), 3.77 (s, 3H), 3.01 (d, J = 7.4 Hz, 2H), 2.70 (ddd, J = 19.0, 8.2, 2.2 Hz, 1H), 2.57 (ddd, J = 18.9, 6.4, 2.0 Hz, 1H), 2.22–2.11 (m, 2H), 1.91–1.82 (m, 1H), 1.06 (d, J = 6.7 Hz, 3H). **^{13}C NMR** (101 MHz): δ 204.4, 164.4, 141.4, 140.0, 136.9, 127.9, 127.7, 122.0, 64.1, 51.9, 47.1, 40.3, 39.0, 37.0, 20.6. **HRMS** (ESI) *m/z* calcd for $C_{15}H_{20}O_4Na$ ($[M+Na]^+$) 287.1259; found 287.1261.

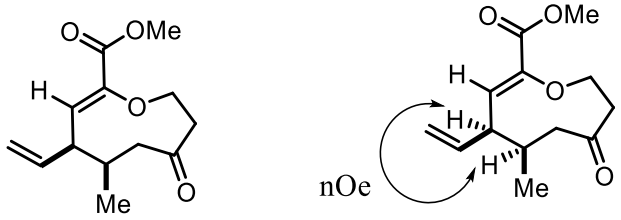

Methyl (*Z*)-5-methyl-7-oxo-4-vinyl-4,5,6,7,8,9-hexahydrooxonine-2-carboxylate (54i). Synthesized using general procedure 3. (36 mg, 60%, (dr > 98:2)). Recrystallization from hexanes (slow evaporation method) yielded monoclinic colorless crystal (mp 72–74 °C). **TLC**: R_f 0.40 (7:3 hexanes/EtOAc). **IR** (NaCl): 2962, 1720, 1641, 1442, 1429, 1300, 1238, 1161, 1095, 1004, 767, 723, 671, 644. **^{1}H NMR** (400 MHz) δ 6.31 (d, J = 10.0 Hz, 1H), 5.81 (ddd, J = 17.2, 10.5, 5.7 Hz, 1H), 5.13–4.98 (m, 2H), 4.57 (ddd, J = 11.9, 5.8, 3.1 Hz, 1H), 4.11 (td, J = 11.6, 4.2 Hz, 1H), 3.82 (s, 3H), 3.43 (dtt, J = 9.5, 3.6, 1.8 Hz, 1H), 2.83–2.75 (m, 1H), 2.64–2.43 (m, 3H), 2.10 (dd, J = 13.7, 4.5 Hz, 1H), 0.88 (d, J = 6.9 Hz, 3H). **^{13}C NMR** (101 MHz): δ 211.6, 163.8, 146.5, 138.8, 126.7, 115.9, 77.3, 77.0, 76.7, 69.8, 52.2, 45.1, 44.5, 40.7, 36.1, 15.2. **HRMS** (ESI) *m/z* calcd for $C_{13}H_{18}O_4Na$ ($[M+Na]^+$) 261.1102; found 261.1100. CCDC 1510906.

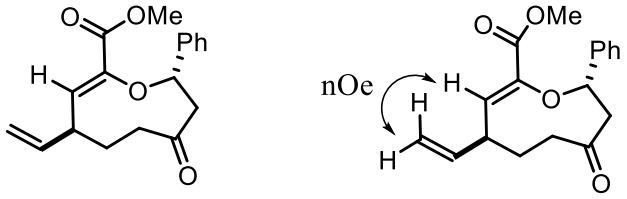

Methyl (*Z*)-7-oxo-9-phenyl-4-vinyl-4,5,6,7,8,9-hexahydrooxonine-2-carboxylate (54j). Synthesized using general procedure 3. Colorless liquid (33 mg, 67%, (dr > 98:2)). **TLC**: R_f 0.41 (7:3 hexanes/EtOAc). **IR** (NaCl): 3734, 2312, 1722, 1647, 1541, 1508, 1436, 1352, 1300, 1247, 1203, 1143, 1097, 1001, 925, 877, 761, 694, 671. **^{1}H NMR** (400 MHz) δ 7.44–7.34 (m, 4H), 7.33–7.27 (m, 1H), 6.17 (d, J = 9.3 Hz, 1H), 5.80 (ddd, J = 17.1, 10.3, 6.7 Hz, 1H), 5.25 (dd, J = 11.2, 3.8 Hz, 1H), 5.16–5.02 (m, 2H), 3.58 (s, 3H), 3.49–3.38 (m, 1H), 3.08 (dd, J = 15.3, 11.2 Hz, 1H), 2.82–2.70 (m, 2H), 2.44 (ddd, J = 13.9, 6.5, 4.4 Hz, 1H), 2.28–2.20 (m, 1H), 1.69–1.57 (m, 1H). **^{13}C NMR** (101 MHz): δ 210.9, 163.8, 145.6,

141.5, 139.8, 129.2, 128.3 (2C), 127.6, 125.4 (2C), 115.1, 81.9, 53.1, 51.8, 38.4, 38.2, 30.0. **HRMS** (ESI) *m/z* calcd for $C_{18}H_{20}O_4Na$ ($[M+Na]^+$) 323.1259; found 323.1255.

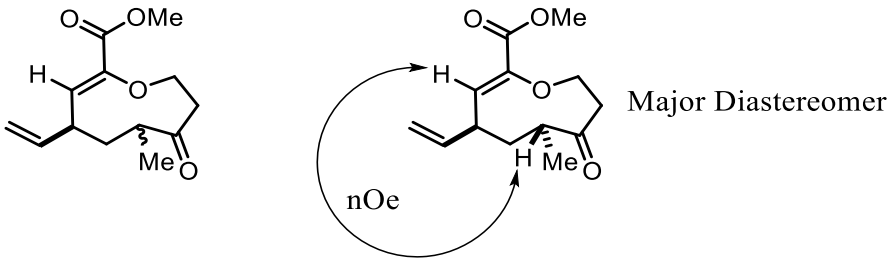

Methyl (*Z*)-6-methyl-7-oxo-4-vinyl-4,5,6,7,8,9-hexahydrooxonine-2-carboxylate (54k). Synthesized using general procedure 3. (41 mg, 68%, (dr = 3:1); **70k (Major diastereomer):** White solid mp 49–50 °C). **TLC**: R_f 0.50 (7:3 hexanes/EtOAc). **IR** (NaCl): 2962, 1722, 1645, 1460, 1294, 1246, 1093, 999, 923, 775, 675, 624. **^{1}H NMR** (400 MHz) δ 6.20 (d, J = 9.7 Hz, 1H), 5.77–5.63 (m, 1H), 5.08–4.94 (m, 2H), 4.55–4.48 (m, 1H), 4.21–4.11 (m, 1H), 3.78 (s, 3H), 3.32–3.23 (m, 1H), 2.94–2.86 (m, 1H), 2.74–2.62 (m, 2H), 1.99–1.90 (m, 1H), 1.49–1.39 (m, 1H), 1.03 (d, J = 6.8 Hz, 3H). **^{13}C NMR** (101 MHz): δ 215.4, 163.9, 145.4, 139.5, 129.9, 114.9, 69.2, 52.1, 43.3, 40.9, 38.7, 37.3, 17.8. **HRMS** (ESI) *m/z* calcd for $C_{13}H_{18}O_4Na$ ($[M+Na]^+$) 261.1102; found 261.1107. **54k (Minor diastereomer):** isolated as pale yellow liquid along with major diastereomer (dr = 1:1); **^{1}H NMR** (400 MHz) δ 6.21 (d, J = 9.6 Hz, 1H), 6.11 (d, J = 9.5 Hz, 1H), 5.72 (dddd, J = 17.1, 10.4, 6.8, 5.1 Hz, 2H), 5.06–4.98 (m, 4H), 4.52 (dd, J = 11.2, 5.8 Hz, 1H), 4.35–4.23 (m, 2H), 4.17 (ddd, J = 11.9, 9.1, 4.9 Hz, 1H), 3.80 (s, 3H), 3.76 (s, 3H), 3.41–3.25 (m, 2H), 2.96–2.83 (m, 2H), 2.75–2.64 (m, 2H), 1.99–1.86 (m, 3H), 1.79 (ddd, J = 14.0, 4.8, 2.5 Hz, 1H), 1.46 (td, J = 12.8, 4.0 Hz, 1H), 1.05 (s, 3H), 1.04 (s, 3H). **^{13}C NMR** (101 MHz): δ 215.6, 215.4, 163.9, 145.4, 143.4, 139.9, 139.5, 130.7, 123.0, 115.0, 114.7, 69.2, 68.7, 52.1, 52.1, 46.6, 43.3, 42.7, 41.0, 41.0, 39.5, 38.8, 37.4, 17.9, 17.8.

Chapter 7.2. Experimentals for Chapter 3

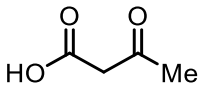

3-oxobutanoic acid (55). Starting material was synthesized using known literature protocol.[117]

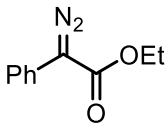

Ethyl 2-diazo-2-phenylacetate (56a). Compound was prepared using known literature procedure.[118]

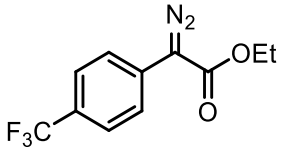

Ethyl 2-diazo-2-(4-(trifluoromethyl)phenyl)acetate (56b). Compound was prepared using known literature procedure.[120]

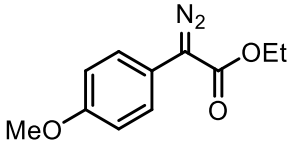

Ethyl 2-diazo-2-(4-methoxyphenyl)acetate (56c). Compound was prepared using known literature procedure.[119]

General Procedure 4 for the Synthesis of γ-Lactones 58a–58e

To a stirred solution of keto-acid **55/67** (0.10 mmol) and $Rh_2(TFA)_4$ (1 mol%) in 0.5 mL dichloromethane was added a solution of corresponding diazo compound **56/75** (0.20 mmol) in 0.5 mL dichloromethane over 1.5 h via syringe pump at reflux. After the addition was completed, the reaction was refluxed for an additional 30 minutes. The crude reaction

mixture was concentrated using rotary evaporation and then purified using flash column chromatography eluting with 1:10 ethyl acetate:hexanes gradient to 3:7 ethyl acetate:hexanes affording 3-hydroxybutyrolactone **58a**–**58e**.

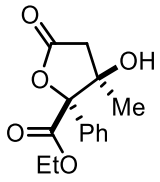

Ethyl-3-hydroxy-3-methyl-5-oxo-2-phenyltetrahydrofuran-2-carboxylate (58a). Synthesized using general procedure 4. Pale yellow oil (16.0 mg, 52%). **TLC**: R_f 0.20 (7:3 hexanes/EtOAc). **IR** (NaCl): 3480, 3061, 2984, 2938, 2907, 1800, 1778, 1755, 1734, 1491, 1449, 1383, 1369, 1296, 1267, 1231, 1215, 1099, 1055, 1032, 758, 702. **^{1}H NMR** (600 MHz) δ 7.51 (dd, J = 7.9, 1.8 Hz, 2H), 7.42–7.39 (m, 3H), 4.29 (qq, J = 10.7, 7.1 Hz, 2H), 3.43 (d, J = 1.6 Hz, 1H), 2.75 (d, J = 17.1 Hz, 1H), 2.57 (dd, J = 17.1, 1.7 Hz, 1H), 1.27 (s, 3H), 1.26 (t, J = 7.2 Hz, 3H). **^{13}C NMR** (151 MHz) δ 172.9, 169.8, 134.2, 129.0, 128.7 (2C), 125.0 (2C), 91.4, 79.3, 62.8, 42.2, 24.2, 13.8. **HRMS** (ESI) *m/z* calcd for $C_{14}H_{16}O_5Na$ ($[M+Na]^+$) 287.0895; found 287.0899.

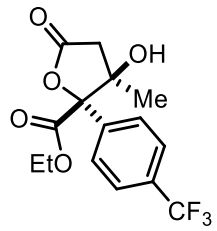

Ethyl-3-hydroxy-3-methyl-5-oxo-2-(4-(trifluoromethyl)phenyl)tetrahydrofuran-2-carboxylate (58b). Synthesized using general procedure 4. Pale yellow oil (12.7 mg, 35%). **TLC**: R_f 0.30 (7:3 hexanes/EtOAc). **IR** (NaCl): 3480, 2986, 2940, 1805, 1778, 1736, 1620, 1456, 1414, 1385, 1369, 1329, 1302, 1281, 1267, 1233, 1169, 1126, 1072, 1018, 847. **^{1}H NMR** (600 MHz) δ 7.70–7.67 (m, 4H), 4.30 (qq, J = 10.9, 7.2 Hz, 2H), 3.44 (s, 1H), 2.87

(d, J = 17.1 Hz, 1H), 2.59 (dd, J = 17.2, 1.3 Hz, 1H), 1.27 (t, J = 7.1 Hz, 3H), 1.23 (s, 3H). **^{13}C NMR** (151 MHz) δ 172.1, 169.5, 138.0, 131.3 (q, $J_{C\text{-}F}$ = 32.6 Hz, 1C), 125.8 (2C), 125.6 (q, $J_{C\text{-}F}$ = 3.9 Hz, 2C), 90.4, 79.3, 63.2, 42.5, 24.4, 13.8 [Note: While peaks corresponding to the CF_3 were observed, some portion of the peaks were lost in signal noise]. **^{19}F NMR** (376 MHz) δ –62.86. **HRMS** (ESI) *m/z* calcd for $C_{15}H_{15}F_3O_5Na$ ($[M+Na]^+$) 355.0769; found 355.0775.

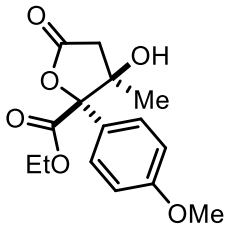

Ethyl-3-hydroxy-2-(4-methoxyphenyl)-3-methyl-5-oxotetrahydrofuran-2-carboxylate (58c). Synthesized using general procedure 4. Pale yellow oil (15.5 mg, 49%). **TLC**: R_f 0.20 (7:3 hexanes/EtOAc). **IR** (NaCl): 3480, 2980, 2959, 2934, 2849, 1780, 1778, 1755, 1732, 1611, 1514, 1456, 1369, 1302, 1256, 1233, 1182, 1099, 1059, 1030, 839. **^{1}H NMR** (600 MHz) δ 7.42 (d, J = 8.9 Hz, 2H), 6.92 (d, J = 8.9 Hz, 2H), 4.32–4.25 (m, 2H), 3.82 (s, 3H), 3.30 (d, J = 1.7 Hz, 1H), 2.71 (d, J = 17.2 Hz, 1H), 2.56 (dd, J = 17.1, 1.8 Hz, 1H), 1.29 (s, 3H), 1.27 (t, J = 7.2 Hz, 3H). **^{13}C NMR** (151 MHz) δ 173.0, 170.0, 160.1, 126.4 (2C), 126.1, 114.0 (2C), 91.4, 79.4, 62.7, 55.3, 42.1, 24.1, 13.9. **HRMS** (ESI) *m/z* calcd for $C_{15}H_{18}O_6Na$ ($[M+Na]^+$) 317.1001; found 317.1007.

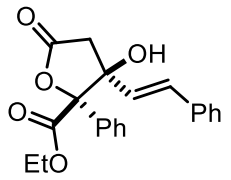

Ethyl-3-hydroxy-5-oxo-2-phenyl-3-((*E*)-styryl)tetrahydrofuran-2-carboxylate (58e). Synthesized using general procedure 4. Pale yellow oil (9.7 mg, 27%). **TLC**: R_f 0.30 (7:3

hexanes/EtOAc). **IR** (NaCl): 3468, 3059, 3026, 2982, 2936, 1802, 1776, 1753, 1734, 1493, 1449, 1369, 1298, 1277, 1252, 1213, 1179, 1096, 1053, 972, 893, 854, 748, 694. **^{1}H NMR** (600 MHz) δ 7.50–7.48 (m, 2H), 7.42–7.39 (m, 3H), 7.30–7.24 (m, 3H), 7.21 (dd, J = 7.0, 1.6 Hz, 2H), 6.64 (d, J = 16.0 Hz, 1H), 5.95 (d, J = 16.0 Hz, 1H), 4.34–4.26 (m, 2H), 3.65 (s, 1H), 2.79 (dd, J = 17.2, 1.8 Hz, 1H), 2.74 (d, J = 17.2 Hz, 1H), 1.27 (t, J = 7.2 Hz, 3H). **^{13}C NMR** (151 MHz) δ 172.8, 169.1, 135.7, 133.9, 131.2, 129.3, 128.7 (2C), 128.6 (2C), 128.3, 127.2, 126.6 (2C), 125.4 (2C), 92.1, 81.3, 62.9, 41.1, 13.9. **HRMS** (ESI) *m/z* calcd for $C_{21}H_{20}O_5Na$ ([M+Na]$^+$) 375.1208; found 375.1207.

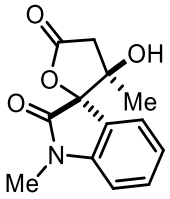

3-hydroxy-1',3-dimethyl-3,4-dihydro-5*H*-spiro[furan-2,3'-indoline]-2',5-dione (58d). Synthesized using general procedure 4. Pale yellow/orange oil (15.8 mg, 54%, mp 178–180 °C). **TLC**: R_f 0.40 (2:3 hexanes/EtOAc). **IR** (NaCl): 3406, 3065, 2984, 2938, 2887, 1803, 1715, 1612, 1493, 1470, 1418, 1377, 1356, 1267, 1204, 1157, 1098, 1024, 972, 922, 883, 760, 696. **^{1}H NMR** (600 MHz) δ 7.43 (t, J = 7.8 Hz, 1H), 7.30 (d, J = 7.5 Hz, 1H), 7.14 (t, J = 7.2 Hz, 1H), 6.92 (d, J = 7.9 Hz, 1H), 3.46 (s, 1H), 3.39 (d, J = 17.0 Hz, 1H), 3.23 (s, 3H), 2.81 (dd, J = 17.0, 1.3 Hz, 1H), 1.40 (s, 3H). **^{13}C NMR** (151 MHz) δ 173.3, 173.2, 144.6, 131.4, 125.7, 123.3, 123.0, 109.4, 87.0, 78.0, 42.6, 26.5, 24.4. **HRMS** (ESI) *m/z* calcd for $C_{13}H_{13}NO_4Na$ ([M+Na]$^+$) 270.0742; found 270.0747. CCDC 1844116.

General Procedure 5 for the Synthesis of Ketoacids 59b–59h

According to literature known protocol[1], to a solution of 2-Acetylbenzoic acid **59a** (1.0 equiv) and corresponding aldehyde (1.2 equiv) in ethanol (0.3 M) was added an aqueous

solution of NaOH (4.0 M, 2.0 equiv) at 0 °C. The ice-bath was removed, and the reaction stirred at 25 °C until complete consumption of starting material. The reaction was then acidified with 1 M HCl aqueous solution at 0 °C. Then the EtOH was removed completely by rotoevaporation and the remaining aqueous layer was extracted with EtOAc, the combined organic layers were dried over anhydrous Na_2SO_4 and concentrated under reduced pressure. The crude solids were further purified by trituration using dichloromethane and hexanes to provide pure ketoacids **59b**–**59f**.

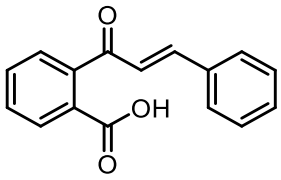

2-cinnamoylbenzoic acid (59b). Starting Material was prepared using general procedure 5 and matched literature known values. [148]

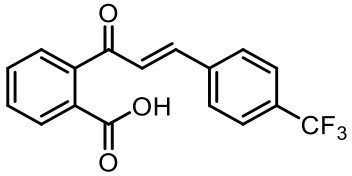

(*E*)-2-(3-(4-(trifluoromethyl)phenyl)acryloyl)benzoic acid (**59c).** Synthesized using general procedure 5. White solid (109.5 mg, 38%, mp 195–196 °C). **TLC**: R_f 0.50 (EtOAc). **IR** (neat): 3051, 3033, 2983, 2836, 2664, 2541, 1686, 1647, 1630, 1595, 1577, 1491, 1416, 1326, 1298, 1287, 1280, 1268, 1253, 1207, 1192, 1172, 1152, 1113, 1069, 1060, 1041, 1016, 981, 959, 926, 890, 853, 830, 803, 771, 744, 708, 661, 649, 611, 592, 578, 567, 555, 549, 542, 529, 521. **^{1}H NMR** (600 MHz) δ 8.09 (d, J = 7.7 Hz, 1H), 7.69 (t, J = 7.3 Hz, 1H), 7.63–7.57 (m, 5H), 7.43 (d, J = 7.6 Hz, 1H), 7.20 (d, J = 16.1 Hz, 1H), 7.08 (d, J = 16.1 Hz, 1H). **^{13}C NMR** (151 MHz) δ 196.3, 170.3, 143.3, 142.2, 137.7, 133.3, 131.1,

130.0, 129.5, 128.5 (2C), 127.7, 127.6, 125.8 (q, $J_{C\text{-}F}$ = 3.4 Hz, 2C) [Note: While peaks corresponding to the CF_3 were observed, some portion of the peaks were lost in signal noise]. **^{19}F NMR** (376 MHz) δ –62.94. **HRMS** (ESI) *m/z* calcd for $C_{17}H_{11}F_3O_3Na$ ($[M+Na]^+$) 343.0558; found 343.0559.

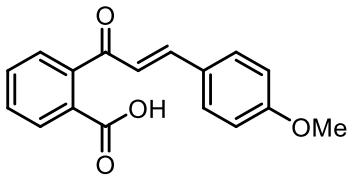

(*E*)-2-(3-(4-methoxyphenyl)acryloyl)benzoic acid (59d). Starting Material was prepared using general procedure 5 and matched literature known values.[148]

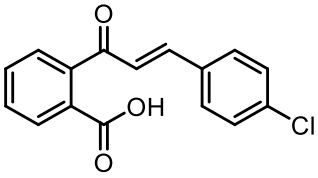

(*E*)-2-(3-(4-chlorophenyl)acryloyl)benzoic acid (59e). Starting Material was prepared using general procedure 5 and matched literature known values.[148]

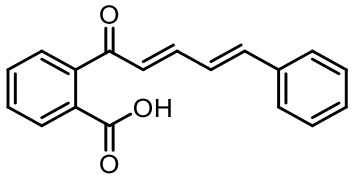

2-((2*E*,4*E*)-5-phenylpenta-2,4-dienoyl)benzoic acid (**59f).** Synthesized using general procedure 5. Pale yellow solid (697.9 mg, 83%, mp 163–165 °C). **TLC**: R_f 0.50 (EtOAc). **IR** (neat): 3016, 2827, 2657, 2533, 1686, 1640, 1617, 1592, 1575, 1488, 1448, 1416, 1285, 1147, 1060, 994, 947, 885, 771, 754, 711, 695, 684, 658, 615, 552, 542, 529. **^{1}H NMR** (600 MHz) δ 8.08 (d, *J* = 7.9 Hz, 1H), 7.65 (t, *J* = 7.5 Hz, 1H), 7.55 (t, *J* = 7.7 Hz, 1H), 7.43 (d, *J* = 7.4 Hz, 2H), 7.40 (d, *J* = 7.5 Hz, 1H), 7.36–7.29 (m, 3H), 7.00–6.92 (m, 2H), 6.83 (d, *J* = 14.3 Hz, 1H), 6.59 (d, *J* = 14.4 Hz, 1H). **^{13}C NMR** (151 MHz) δ 196.8, 170.6,

146.0, 142.5, 141.9, 135.9, 133.0, 131.1, 130.6, 129.6, 129.3, 128.8 (2C), 127.9, 127.7, 127.3 (2C), 126.7. **HRMS** (ESI) *m/z* calcd for $C_{18}H_{14}O_3Na$ ($[M+Na]^+$) 301.0841; found 301.0841.

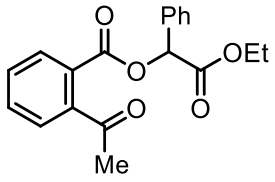

2-ethoxy-2-oxo-1-phenylethyl 2-acetylbenzoate (60a). Isolated from optimization table experiments as a pale yellow oil. **TLC**: R_f 0.30 (4:1 hexanes/EtOAc). **IR** (NaCl): 3065, 3035, 2982, 2923, 2852, 1722, 1703, 1597, 1575, 1497, 1456, 1446, 1354, 1282, 1258, 1211, 1181, 1137, 1100, 1063, 1031, 1004, 958, 908, 856, 761, 732, 697, 661, 648, 592. **^{1}H NMR** (600 MHz) δ 8.00 (dd, J = 7.8, 1.2 Hz, 1H), 7.58 (td, J = 7.5, 1.3 Hz, 1H), 7.53–7.50 (m, 3H), 7.43–7.39 (m, 4H), 6.12 (s, 1H), 4.22 (ddq, J = 43.0, 10.8, 7.1 Hz, 2H), 2.50 (s, 3H), 1.23 (t, J = 7.1 Hz, 3H). **^{13}C NMR** (151 MHz) δ 202.8, 168.5, 166.1, 143.2, 133.5, 132.5, 130.1, 123.0, 129.3, 128.8 (2C), 127.8, 127.7 (2C), 126.5, 75.6, 61.8, 30.1, 13.9. **LRMS** (ESI) *m/z* calcd for $C_{19}H_{18}O_5Na$ ($[M+Na]^+$) 349.1; found 348.9.

General Procedure 6 for the Synthesis of δ-Lactones 61a–61o

To a stirred solution of ketoacid **1** (0.06 mmol) and $Rh_2(TFA)_4$ (1 mol%) in 0.5 mL dichloromethane was added a solution of corresponding diazo carbonyl **2** (0.12 mmol) in 0.5 mL dichloromethane over 1.5 h via syringe pump at reflux. After the addition was completed, the reaction was refluxed for an additional 30 minutes. The crude reaction mixture was concentrated and then purified using flash column chromatography eluting with 1:10 ethyl acetate:hexanes gradient to 3:7 ethyl acetate:hexanes affording lactones **61a**–**61o**.

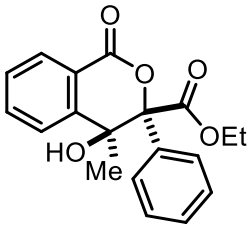

Ethyl-4-hydroxy-4-methyl-1-oxo-3-phenylisochromane-3-carboxylate (61a). Synthesized using general procedure 6. Pale yellow oil (11.9 mg, 60%). **TLC**: R_f 0.80 (7:3 hexanes/EtOAc). **IR** (NaCl): 3480, 3067, 2986, 2936, 1746, 1603, 1495, 1452, 1369, 1290, 1260, 1101, 1057, 1028, 766, 739, 704, 571, 500. **^{1}H NMR** (600 MHz) δ 8.06 (dd, J = 7.9, 1.4 Hz, 1H), 7.86 (d, J = 8.4 Hz, 2H), 7.82 (d, J = 7.8 Hz, 1H), 7.70 (td, J = 7.6, 1.4 Hz, 1H), 7.47–7.41 (m, 4H), 4.83 (s, 1H), 4.10 (dq, J = 10.8, 7.2 Hz, 1H), 3.96 (dtd, J = 10.8, 7.2 Hz, 1H), 1.25 (s, 3H), 0.97 (td, J = 7.1, 1.3 Hz, 3H). **^{13}C NMR** (151 MHz) δ 172.4, 163.1, 148.0, 135.2, 132.3, 129.8, 129.0, 128.4, 128.2 (2C), 126.5 (2C), 124.1, 122.2, 86.9, 74.3, 62.9, 24.6, 13.5. **HRMS** (ESI) *m/z* calcd for $C_{19}H_{19}O_5$ ($[M+H]^+$) 327.1232; found 327.1239.

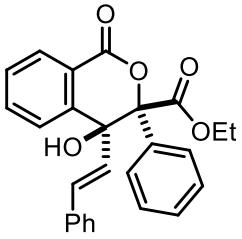

Ethyl-4-hydroxy-1-oxo-3-phenyl-4-((*E*)-styryl)isochromane-3-carboxylate (61b). When synthesized using general procedure 6. Pale yellow oil (23.1 mg, 94%). When reaction was performed at a 1.07 mmol scale. To a stirred solution of ketoacid **59b** (1.07 mmol) and $Rh_2(TFA)_4$ (1 mol%) in 8.9 mL dichloromethane was added a solution of diazo carbonyl **56a** (2.14 mmol) in 8.9 mL dichloromethane over 1.5 h via syringe pump at reflux. After the addition was completed, the reaction was refluxed for an additional 30

minutes. The crude reaction mixture was concentrated and then purified using flash column chromatography eluting with 1:10 ethyl acetate:hexanes gradient to 3:7 ethyl acetate:hexanes affording lactone **61b** as a pale yellow oil (369.6 mg, 83%).**TLC**: R_f 0.60 (7:3 hexanes/EtOAc). **IR** (NaCl): 3458, 3063, 3028, 2982, 1746, 1713, 1647, 1603, 1495, 1450, 1389, 1369, 1287, 1260, 1248, 1088, 1053, 1030, 1011, 968, 748, 710, 694, 559, 428. **^{1}H NMR** (600 MHz) δ 8.11 (d, J = 7.8 Hz, 1H), 7.81 (d, J = 7.7 Hz, 1H), 7.80–7.78 (m, 2H), 7.72 (td, J = 7.6, 1.2 Hz, 1H), 7.51 (td, J = 7.6, 1.2 Hz, 1H), 7.42–7.38 (m, 3H), 7.21–7.15 (m, 3H), 7.12 (d, J = 7.6 Hz, 2H), 6.19 (d, J = 15.9 Hz, 1H), 6.07 (d, J = 15.9, 1H), 5.23 (s, 1H), 4.15 (dq, J = 10.8, 7.2 Hz, 1H), 4.01 (dq, J = 10.8, 7.2 Hz, 1H), 1.01 (t, J = 7.1 Hz, 3H). **^{13}C NMR** (151 MHz) δ 172.3, 163.2, 145.2, 136.0, 135.3, 132.9, 132.1, 129.8, 129.1, 128.8, 128.4 (2C), 128.0 (2C), 128.0, 126.9, 126.7 (2C), 126.7 (2C), 125.1, 122.9, 87.1, 76.6, 63.1, 13.6. **HRMS** (ESI) *m/z* calcd for $C_{26}H_{23}O_5$ ($[M+H]^+$) 415.1545; found 415.1548.

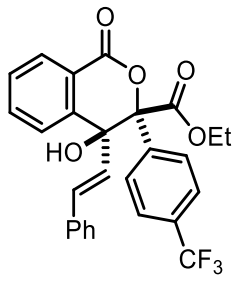

Ethyl-4-hydroxy-1-oxo-4-((*E*)-styryl)-3-(4-(trifluoromethyl)phenyl)isochromane-3-carboxylate (61c). Synthesized using general procedure 6. Pale yellow oil (20.6 mg, 72%). **TLC**: R_f 0.70 (7:3 hexanes/EtOAc). **IR** (NaCl): 3472, 3063, 3028, 2984, 2936, 2909, 2874, 2320, 1950, 1749, 1717, 1603, 1454, 1412, 1371, 1327, 1287, 1250, 1169, 1126, 1074, 1018, 970, 849, 743, 696. **^{1}H NMR** (600 MHz) δ 8.12 (d, J = 7.9 Hz, 1H), 7.95 (d, J = 8.3 Hz, 2H), 7.81 (d, J = 7.8 Hz, 1H), 7.74 (t, J = 8.4 Hz, 1H), 7.66 (d, J = 8.3 Hz, 2H), 7.53

(td, *J* = 7.5, 1.2 Hz, 1H), 7.23–7.17 (m, 3H), 7.11 (d, *J* = 7.8 Hz, 2H), 6.23 (d, *J* = 15.8 Hz, 1H), 6.03 (dd, *J* = 15.9, 1.3 Hz, 1H), 5.18 (s, 1H), 4.15 (dq, *J* = 10.7, 7.1 Hz, 1H), 4.02 (dq, *J* = 10.8, 7.1 Hz, 1H), 1.01 (t, *J* = 7.2 Hz, 3H). **^{13}C NMR** (151 MHz) δ 171.9, 162.7, 144.9, 136.1, 135.7, 135.5, 133.3, 131.19 (q, $J_{C\text{-}F}$ = 32.8 Hz, 1C), 129.9, 129.0, 128.5 (2C), 128.2, 127.3 (2C), 126.7 (2C), 126.1, 125.1, 125.0 (q, $J_{C\text{-}F}$ = 3.9 Hz, 2C), 123.9 (q, $J_{C\text{-}F}$ = 272.1 Hz, 1C), 122.7, 86.6, 76.6, 63.5, 13.5 [Note: While peaks corresponding to the CF_3 were observed, some portion of the peaks were lost in signal noise]. **^{19}F NMR** (376 MHz) δ –62.77. **HRMS** (ESI) *m/z* calcd for $C_{27}H_{22}F_3O_5$ ($[M+H]^+$) 483.1419; found 483.1428.

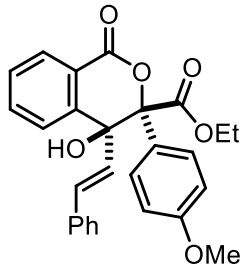

Ethyl-4-hydroxy-3-(4-methoxyphenyl)-1-oxo-4-((*E*)-styryl)isochromane-3-carboxylate (61d). Synthesized using general procedure 6. Pale yellow oil (24.2 mg, 92%). **TLC**: R_f 0.60 (7:3 hexanes/EtOAc). **IR** (NaCl): 3466, 3061, 3026, 2982, 2936, 2907, 2837, 1744, 1709, 1607, 1512, 1458, 1369, 1285, 1250, 1184, 1086, 1032, 968, 839, 741, 696. **^{1}H NMR** (600 MHz) δ 8.11 (dd, *J* = 7.8, 1.3 Hz, 1H), 7.81 (dd, *J* = 7.8, 1.1 Hz, 1H), 7.73–7.70 (m, 3H), 7.50 (td, *J* = 7.6, 1.1 Hz, 1H), 7.22–7.13 (m, 5H), 6.93–6.90 (m, 2H), 6.22 (d, *J* = 15.9 Hz, 1H), 6.09 (dd, *J* = 15.9, 1.1 Hz, 1H), 5.22 (s, 1H), 4.13 (dq, *J* = 10.7, 7.1 Hz, 1H), 4.01 (dq, *J* = 10.7, 7.1 Hz, 1H), 3.82 (s, 3H), 1.00 (t, *J* = 7.1 Hz, 3H). **^{13}C NMR** (151 MHz) δ 172.4, 163.3, 160.0, 145.3, 136.0, 135.2, 132.8, 129.7, 128.7, 128.4 (2C), 128.1 (2C), 128.0, 127.0, 126.7 (2C), 125.1, 124.2, 123.0, 113.4 (2C), 86.9, 76.7, 63.0, 55.3, 13.6. **HRMS** (ESI) *m/z* calcd for $C_{27}H_{25}O_6$ ($[M+H]^+$) 445.1651; found 445.1655.

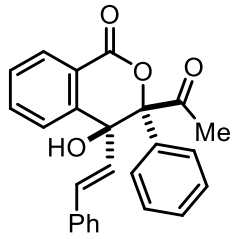

3-acetyl-4-hydroxy-3-phenyl-4-((*E*)-styryl)isochroman-1-one (61e). Synthesized using general procedure 6. Pale yellow oil (15.1 mg, 66%). **TLC**: R_f 0.80 (7:3 hexanes/EtOAc). **IR** (NaCl): 3462, 3059, 3026, 2924, 1740, 1705, 1603, 1495, 1450, 1358, 1287, 1248, 1209, 1082, 1045, 1034, 968, 770, 748, 718, 694, 592, 557. **^{1}H NMR** (600 MHz) δ 8.12 (d, J = 7.8 Hz, 1H), 7.81 (d, J = 7.9 Hz, 1H), 7.73 (t, J = 7.6 Hz, 1H), 7.68 (d, J = 7.8 Hz, 2H), 7.49 (t, J = 7.6 Hz, 1H), 7.42 (q, J = 7.8, 7.2 Hz, 3H), 7.18 (qd, J = 7.3, 3.8 Hz, 3H), 7.08 (d, J = 7.8 Hz, 2H), 6.09 (d, J = 16.0 Hz, 1H), 5.97 (d, J = 15.9 Hz, 1H), 5.24 (s, 1H), 2.13 (s, 3H). **^{13}C NMR** (151 MHz) δ 211.2, 163.1, 146.3, 136.0, 135.8, 132.2, 131.4, 130.3, 129.2, 128.6, 128.4 (2C), 128.3 (2C), 128.0, 127.8, 126.7 (2C), 126.6 (2C), 125.2, 122.0, 90.6, 76.8, 27.5. **HRMS** (ESI) *m/z* calcd for $C_{25}H_{20}O_4Na$ ($[M+Na]^+$) 407.1259; found 407.1263.

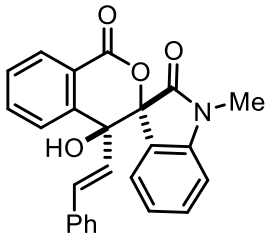

4'-hydroxy-1-methyl-4'-((*E*)-styryl)spiro[indoline-3,3'-isochromane]-1',2-dione (61f). Synthesized using general procedure 6. White solid (14.4 mg, 61%, mp 187–190 °C). **TLC**: R_f 0.60 (2:3 hexanes/EtOAc). **IR** (NaCl): 3337, 3024, 2924, 2853, 1761, 1701, 1612, 1468, 1460, 1371, 1217, 1090, 1016, 972, 750, 718, 691, 428. **^{1}H NMR** (600 MHz) δ 7.66 (d, J = 7.6 Hz, 1H), 7.56 (t, J = 7.2 Hz, 2H), 7.50–7.48 (m, 3H), 7.39 (t, J = 7.5 Hz, 1H), 7.33

(t, *J* = 7.5 Hz, 2H), 7.28 (d, *J* = 7.2 Hz, 1H), 7.19 (t, *J* = 7.2 Hz, 1H), 7.05 (d, *J* = 7.0 Hz, 2H), 7.00 (t, *J* = 7.7 Hz, 1H), 6.57 (d, *J* = 7.8 Hz, 1H), 3.40 (s, 1H), 3.10 (s, 3H). **^{13}C NMR** (151 MHz) δ 174.3, 169.1, 147.3, 143.2, 135.5, 133.8, 133.4, 130.5, 129.8, 128.7 (2C), 128.6, 127.1 (2C), 126.1, 125.7, 125.6, 125.3, 123.4, 121.8, 121.1, 108.3, 89.7, 80.1, 26.0. **HRMS** (ESI) *m/z* calcd for $C_{25}H_{20}NO_4$ ($[M+H]^+$) 398.1392; found 398.1397. CCDC 1844114.

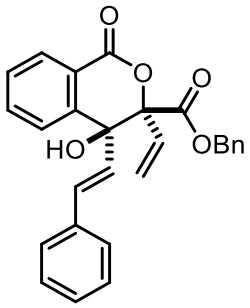

Benzyl-4-hydroxy-1-oxo-4-((*E*)-styryl)-3-vinylisochromane-3-carboxylate (61g). Synthesized using general procedure 6. Pale yellow oil (24.5 mg, 97%). **TLC**: R_f 0.60 (7:3 hexanes/EtOAc). **IR** (NaCl): 3462, 3063, 3032, 2953, 2922, 2851, 1746, 1721, 1602, 1454, 1285, 1250, 1163, 1086, 970, 746, 696. **^{1}H NMR** (600 MHz) δ 7.82 (dd, *J* = 7.2, 0.6 Hz, 1H), 7.66 (dd, *J* = 8.4, 1.2 Hz, 1H), 7.59 (td, *J* = 7.5, 1.3 Hz, 1H), 7.32 (td, *J* = 7.5, 1.2 Hz, 1H), 7.29–7.19 (m, 8H), 7.05–7.03 (m, 2H), 6.54 (d, *J* = 15.8 Hz, 1H), 6.28 (dd, *J* = 15.8, 1.3 Hz, 1H), 6.26 (dd, *J* = 8.4, 6.0 Hz, 1H), 5.81 (dd, *J* = 17.3, 0.6 Hz, 1H), 5.55 (dd, *J* = 11.0, 0.7 Hz, 1H), 5.15 (d, *J* = 12.0 Hz, 1H), 4.95 (d, *J* = 12.0 Hz, 1H), 4.91 (d, *J* = 1.3 Hz, 1H). **^{13}C NMR** (151 MHz) δ 171.7, 162.8, 143.9, 135.9, 134.8, 133.8, 132.5, 129.9, 129.2, 128.7, 128.6, 128.6 (2C), 128.5 (2C), 128.3 (2C), 128.1, 126.8 (2C), 126.6, 124.4, 122.9, 120.6, 86.1, 75.4, 68.4. **HRMS** (ESI) *m/z* calcd for $C_{27}H_{22}O_5Na$ ($[M+Na]^+$) 449.1365; found 449.1376.

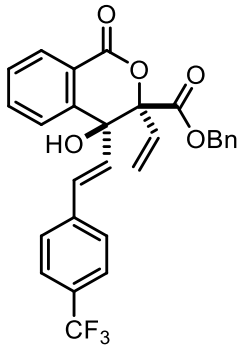

Benzyl-4-hydroxy-1-oxo-4-((*E*)-4-(trifluoromethyl)styryl)-3-vinylisochromane-3-carboxylate (61h). Synthesized using general procedure 6. Pale yellow oil (28.8 mg, 98%). **TLC**: R_f 0.50 (7:3 hexanes/EtOAc). **IR** (NaCl): 3462, 3069, 3036, 2957, 1746, 1722, 1609, 1456, 1325, 1250,1167,1123,1069, 974, 741, 698. **^{1}H NMR** (600 MHz) δ 7.83 (dd, J = 7.7, 1.3 Hz, 1H), 7.65 (d, J = 7.8 Hz, 1H), 7.60 (td, J = 7.6, 1.3 Hz, 1H), 7.50 (d, J = 8.2 Hz, 2H), 7.37 (d, J = 8.1 Hz, 2H), 7.34 (td, J = 7.6, 1.2 Hz, 1H), 7.29–7.27 (m, 1H), 7.24 (t, J = 7.2 Hz, 2H), 7.04 (d, J = 7.8 Hz, 2H), 6.62 (d, J = 15.8 Hz, 1H), 6.36 (dd, J = 15.7, 1.4 Hz, 1H), 6.24 (dd, J = 17.3, 11.0 Hz, 1H), 5.82 (d, J = 17.3 Hz, 1H), 5.55 (d, J = 11.0 Hz, 1H), 5.16 (d, J = 12.0 Hz, 1H), 4.97–4.94 (m, 2H). **^{13}C NMR** (151 MHz) δ 171.5, 162.7, 143.5, 139.4, 135.0, 133.8, 131.1, 130.0, 129.3, 129.0, 128.9, 128.7, 128.6 (2C), 128.3 (2C), 127.0 (2C), 125.5 (q, $J_{C\text{-}F}$ = 4.0 Hz, 2C), 124.4, 122.8, 120.7, 86.0, 75.4, 68.5 [Note: While peaks corresponding to the CF_3 were observed, some portion of the peaks were lost in signal noise]. **^{19}F NMR** (376 MHz) δ –62.7. **HRMS** (ESI) *m/z* calcd for $C_{28}H_{22}F_3O_5$ ($[M+H]^+$) 495.1419; found 495.1429.

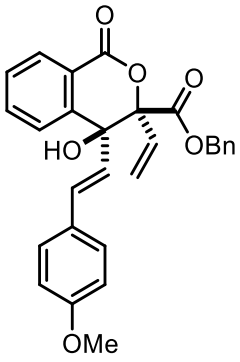

Benzyl-4-hydroxy-4-((*E*)-4-methoxystyryl)-1-oxo-3-vinylisochromane-3-carboxylate (61i). Synthesized using general procedure 6. Pale yellow oil (15.1 mg, 55%). **TLC**: R_f 0.40 (7:3 hexanes/EtOAc). **IR** (NaCl): 3462, 3067, 3034, 3007, 2957, 2934, 2835, 1744, 1605, 1512, 1456, 1287, 1250, 1175, 1086, 1032, 970, 779, 696. **^{1}H NMR** (600 MHz) δ 7.82 (d, J = 7.8 Hz, 1H), 7.65 (d, J = 7.7 Hz, 1H), 7.59 (td, J = 7.6, 1.2 Hz, 1H), 7.32 (t, J = 7.2 Hz, 1H), 7.24–7.22 (m, 3H), 7.21 (d, J = 8.5 Hz, 2H), 7.04 (d, J = 7.4 Hz, 2H), 6.78 (d, J = 8.8 Hz, 2H), 6.43 (d, J = 15.8 Hz, 1H), 6.26 (dd, J = 17.3, 11.0 Hz, 1H), 6.15 (dd, J = 15.8, 1.2 Hz, 1H), 5.80 (d, J = 17.3 Hz, 1H), 5.55 (d, J = 11.0 Hz, 1H), 5.15 (d, J = 11.9 Hz, 1H), 4.95 (d, J = 12.0 Hz, 1H), 4.88 (s, 1H), 3.77 (s, 3H). **^{13}C NMR** (151 MHz) δ 171.7, 162.9, 159.6, 144.1, 134.8, 133.9, 132.1, 129.8, 129.2, 128.7, 128.6, 128.6, 128.6 (2C), 128.3 (2C), 128.1 (2C), 124.4, 124.4, 122.9, 120.5, 113.9 (2C), 86.2, 75.5, 68.4, 55.3. **HRMS** (ESI) *m/z* calcd for $C_{28}H_{25}O_6$ ($[M+H]^+$) 457.1651; found 457.1654.

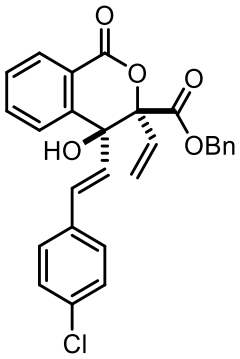

Benzyl-4-((*E*)-4-chlorostyryl)-4-hydroxy-1-oxo-3-vinylisochromane-3-carboxylate (61j). Synthesized using general procedure 6. Pale yellow oil (21.0 mg, 77%). **TLC**: R_f 0.50 (7:3 hexanes/EtOAc). **IR** (NaCl): 3458, 3065, 3034, 2957, 1744, 1719, 1601, 1491, 1454, 1375, 1248, 1155, 1088, 972, 910, 748, 696. **^{1}H NMR** (600 MHz) δ 7.82 (d, J = 7.8 Hz, 1H), 7.64 (d, J = 7.7 Hz, 1H), 7.59 (t, J = 7.6 Hz, 1H), 7.39–7.28 (m, 2H), 7.28–7.19 (m, 6H), 7.04 (d, J = 7.8 Hz, 2H), 6.50 (d, J = 15.8 Hz, 1H), 6.25 (d, J = 9.0 Hz, 1H), 6.23 (d, J = 8.4 Hz, 1H), 5.81 (d, J = 17.3 Hz, 1H), 5.55 (d, J = 11.0 Hz, 1H), 5.15 (d, J = 12.0 Hz, 1H), 4.95 (d, J = 12.0 Hz, 1H), 4.92 (s, 1H). **^{13}C NMR** (151 MHz) δ 171.6, 162.7, 143.7, 134.9, 134.5, 133.8, 133.8 131.3, 129.9, 129.1, 128.8, 128.7 (3C), 128.6 (2C), 128.3 (2C), 128.0 (2C), 127.4, 124.4, 122.9, 120.6, 86.1, 75.4, 68.5. **HRMS** (ESI) *m/z* calcd for $C_{27}H_{22}ClO_5$ ($[M+H]^+$) 461.1156; found 461.1165.

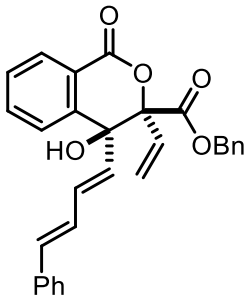

Benzyl-4-hydroxy-1-oxo-4-((1*E*,3*E*)-4-phenylbuta-1,3-dien-1-yl)-3-vinylisochromane-3-carboxylate (61k). Synthesized using general procedure 6. Pale yellow oil (14.9 mg, 54%). **TLC**: R_f 0.70 (7:3 hexanes/EtOAc). **IR** (NaCl): 3460, 3063, 3030, 2959, 1744, 1717, 1601, 1452, 1250, 1084, 989, 748, 696. **^{1}H NMR** (600 MHz) δ 7.82 (d, J = 7.8 Hz, 1H), 7.64 (d, J = 7.7 Hz, 1H), 7.59 (td, J = 7.5, 1.2 Hz, 1H), 7.34–7.31 (m, 4H), 7.28 (d, J = 7.7 Hz, 2H), 7.24–7.19 (m, 3H), 7.03 (d, J = 7.5 Hz, 2H), 6.67 (dd, J = 15.6, 10.6 Hz, 1H), 6.49 (d, J = 15.6 Hz, 1H), 6.31–6.22 (m, 2H), 5.90 (d, J = 15.1 Hz, 1H), 5.81 (d, J = 17.3 Hz, 1H), 5.57 (d, J = 11.0 Hz, 1H), 5.14 (d, J = 12.0 Hz, 1H), 4.94

(d, *J* = 12.0 Hz, 1H), 4.83 (s, 1H). **^{13}C NMR** (151 MHz) *δ* 171.6, 162.8, 143.8, 136.8, 134.8, 134.5, 133.8, 133.0, 130.4, 129.9, 129.1, 128.7, 128.6, 128.6 (2C), 128.6 (2C), 128.3 (2C), 127.8, 127.5, 126.5 (2C), 124.4, 122.9, 120.6, 86.1, 75.4, 68.4. **HRMS** (ESI) *m/z* calcd for $C_{29}H_{25}O_5$ ($[M+H]^+$) 453.1702; found 453.1711.

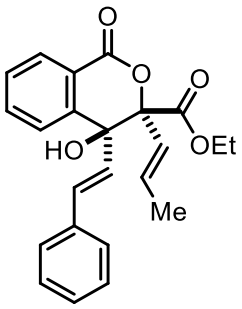

Ethyl-4-hydroxy-1-oxo-3-((*E*)-prop-1-en-1-yl)-4-((*E*)-styryl)isochromane-3-carboxylate (61l). Synthesized using general procedure 6. Pale yellow oil (12.5 mg, 56% dr 5:1). **TLC**: R_f 0.71 (7:3 hexanes/EtOAc). **IR** (NaCl): 3455, 3028, 2978, 2924, 2855, 1744, 1603, 1452, 1369, 1285, 1248, 1084, 1045, 1028, 966, 750, 694. **^{1}H NMR** (600 MHz) δ 8.04 (d, *J* = 7.8 Hz, 1H), 7.73 (d, *J* = 7.8 Hz, 1H), 7.66 (t, *J* = 7.6 Hz, 1H), 7.45 (t, *J* = 7.6 Hz, 1H), 7.29 (t, *J* = 8.2 Hz, 3H), 7.26–7.25 (m, 2H), 7.22 (d, *J* = 7.1 Hz, 1H), 6.55 (d, *J* = 15.8 Hz, 1H), 6.32 (d, *J* = 15.8 Hz, 1H), 6.21 (dq, *J* = 13.6, 6.6 Hz, 1H), 5.90 (d, *J* = 16.8 Hz, 1H), 5.02 (s, 1H), 4.14–4.07 (m, 1H), 4.05–3.99 (m, 1H), 1.80 (d, *J* = 6.6 Hz, 3H), 0.98 (t, *J* = 7.1 Hz, 3H). **^{13}C NMR** (151 MHz) *δ* 172.4, 163.2, 144.5, 136.1, 134.9, 132.5, 132.3, 129.7, 128.7, 128.5 (2C), 128.0, 126.9, 126.8 (2C), 124.6, 123.1, 122.2, 85.9, 75.5, 62.9, 18.1, 13.6. **HRMS** (ESI) *m/z* calcd for $C_{23}H_{22}O_5Na$ ($[M+Na]^+$) 401.1365; found 401.1377.

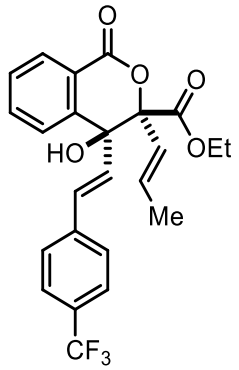

Ethyl-4-hydroxy-1-oxo-3-((*E*)-prop-1-en-1-yl)-4-((*E*)-4-(trifluoromethyl)styryl)isochromane-3-carboxylate (61m). Synthesized using general procedure 6. Pale yellow oil (18.2 mg, 69% dr 14:1). **TLC**: R_f 0.75 (7:3 hexanes/EtOAc). **IR** (neat): 3452, 2982, 2940, 1740, 1712, 1615, 1604, 1456, 1370, 1322, 1298, 1285, 1245, 1162, 1120, 1108, 1082, 1066, 1045, 1015, 966, 864, 825, 809, 762, 731, 702, 650, 596, 564. **^{1}H NMR** (600 MHz) δ 8.06 (dd, J = 7.7, 1.3 Hz, 1H), 7.73 (dd, J = 7.8, 1.2 Hz, 1H), 7.67 (td, J = 7.6, 1.3 Hz, 1H), 7.52 (d, J = 8.2 Hz, 2H), 7.47 (td, J = 7.5, 1.3 Hz, 1H), 7.39 (d, J = 8.1 Hz, 2H), 6.64 (d, J = 15.8 Hz, 1H), 6.40 (dd, J = 15.8, 1.3 Hz, 1H), 6.23 (dq, J = 15.7, 6.7 Hz, 1H), 5.88 (dq, J = 15.6, 1.7 Hz, 1H), 5.07 (d, J = 1.4 Hz, 1H), 4.12 (dq, J = 10.5, 7.0 Hz, 1H), 4.03 (dq, J = 10.7, 7.1 Hz, 1H), 1.80 (dd, J = 6.7, 1.7 Hz, 3H), 0.99 (t, J = 7.1 Hz, 3H).**^{13}C NMR** (151 MHz) δ 172.2, 163.0, 144.1, 139.5, 135.1, 132.4, 131.0, 129.8 (q, $J_{C\text{-}F}$ = 32.7 Hz), 129.8, 129.6, 128.9, 127.0 (2C), 125.5 (q, $J_{C\text{-}F}$ = 3.8 Hz, 2C), 124.6, 124.0 (q, $J_{C\text{-}F}$ = 271.8 Hz) 123.1, 122.0, 85.7, 75.4, 63.0, 18.1, 13.6. **^{19}F NMR** (376 MHz) δ –62.62. **HRMS** (ESI) *m/z* calcd for $C_{24}H_{21}F_3O_5Na$ ($[M+Na]^+$) 469.1239; found 469.1253.

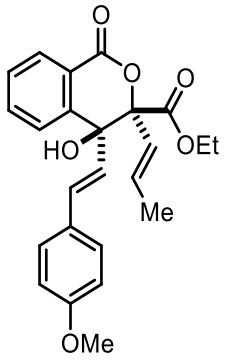

Ethyl-4-hydroxy-4-((*E*)-4-methoxystyryl)-1-oxo-3-((*E*)-prop-1-en-1-yl)isochromane-3-carboxylate (61n). Synthesized using general procedure 6. Pale yellow oil (16.0 mg, 65% dr 22:1). **TLC**: R_f 0.56 (7:3 hexanes/EtOAc). **IR** (neat): 3451, 3035, 2963, 2936, 2917, 2854, 2838, 1739, 1713, 1606, 1456, 1285, 1245, 1174, 1082, 1029, 966, 761, 701. **^{1}H NMR** (600 MHz) δ 8.03 (dd, J = 7.8, 1.4 Hz, 1H), 7.72 (dd, J = 7.9, 1.3 Hz, 1H), 7.65 (td, J = 7.5, 1.4 Hz, 1H), 7.44 (td, J = 7.6, 1.3 Hz, 1H), 7.23 (d, J = 8.8 Hz, 2H), 6.79 (d, J = 8.9 Hz, 1H), 6.45 (d, J = 15.8 Hz, 1H), 6.25–6.15 (m, 2H), 5.90 (dt, J = 15.6, 1.8 Hz, 1H), 4.98 (s, 1H), 4.11 (dq, J = 10.8, 7.0 Hz, 1H), 4.01 (dq, J = 10.8, 7.0 Hz, 1H), 3.77 (s, 2H), 1.80 (dd, J = 6.6, 1.7 Hz, 3H), 0.98 (dd, J = 7.6, 6.7 Hz, 3H). **^{13}C NMR** (151 MHz) δ 172.4, 163.3, 159.5, 144.6, 134.9, 132.2, 132.1, 129.6, 128.9, 128.6, 128.1 (2C), 124.7, 124.7, 123.2, 122.3, 113.9 (2C), 85.9, 75.6, 62.9, 55.3, 18.1, 13.6. **HRMS** (ESI) *m/z* calcd for $C_{24}H_{24}O_6Na$ ($[M+Na]^+$) 431.1471; found 431.1475.

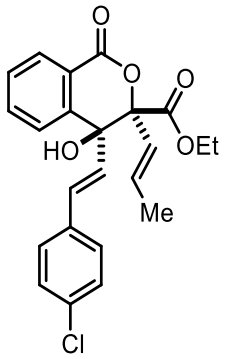

Ethyl-4-((*E*)-4-chlorostyryl)-4-hydroxy-1-oxo-3-((*E*)-prop-1-en-1-yl)isochromane-3-carboxylate (61o). Synthesized using general procedure 6. Pale yellow oil (11.8 mg, 48% dr 8:1). **TLC**: R_f 0.75 (7:3 hexanes/EtOAc). **IR** (NaCl): 3455, 3069, 3038, 2980, 2938, 2918, 2874, 2855, 1744, 1713, 1668, 1603, 1491, 1456, 1369, 1298, 1285, 1246, 1155, 1090, 1045, 1028, 1013, 968, 910, 864, 802, 758, 735, 712, 702, 565. **^{1}H NMR** (600 MHz) δ 8.04 (dd, J = 7.8, 1.3 Hz, 1H), 7.72 (dd, J = 7.7, 1.2 Hz, 1H), 7.66 (td, J = 7.6, 1.4 Hz, 1H), 7.46 (td, J = 7.5, 1.3 Hz, 1H), 7.25–7.21 (m, 4H), 6.52 (d, J = 15.8 Hz, 1H), 6.29 (dd, J = 15.8, 1.3 Hz, 1H), 6.21 (dq, J = 15.6, 6.7 Hz, 1H), 5.88 (dq, J = 15.6, 1.7 Hz, 1H), 5.03 (s, 1H), 4.11 (dq, J = 10.7, 7.1 Hz, 1H), 4.02 (dq, J = 10.7, 7.1 Hz, 1H), 1.80 (dd, J = 6.7, 1.7 Hz, 3H), 0.98 (t, J = 7.1 Hz, 3H). **^{13}C NMR** (151 MHz) δ 172.3, 163.1, 144.3, 135.0, 134.6, 133.7, 132.4, 131.3, 129.8, 128.8, 128.7 (2C), 128.0 (2C), 127.6, 124.6, 123.1, 122.1, 85.8, 75.5, 63.0, 18.1, 13.6. **HRMS** (ESI) *m/z* calcd for $C_{23}H_{21}ClO_5Na$ ([M+Na]$^+$) 435.0975; found 435.0980.

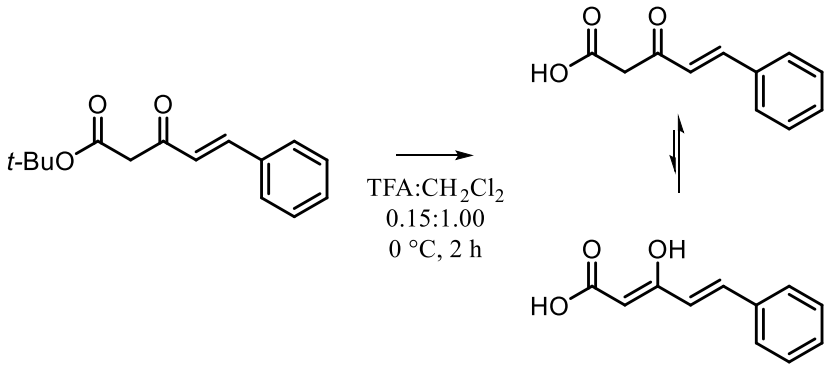

(*E*)-3-oxo-5-phenylpent-4-enoic acid (67). To a solution of (*E*)-3-oxo-5-phenylpent-4-enoic acid (100 mg, 0.40 mmol) in dichloromethane (9.4 mL) prepared from literature protocol[185] was added trifluoroacetic acid (1.4 mL) at 0 °C. The mixture was stirred at 0 °C for 3 h and concentrated in vacuo. The crude residue was then purified by trituration with dichloromethane and hexane followed by filtration to provide **67** as a white solid

existing in a 1.00:0.85 mixture of the keto and enol tautomers respectively (42.5 mg, 55%, mp 108–109 °C, decarboxylation observed). **TLC**: R_f 0.50 (EtOAc). **IR** (neat): 3023, 2638, 1644, 1623, 1587, 1570, 1497, 1481, 1452, 1446, 1319, 1301, 1274, 1235, 1206, 1153, 973, 930, 863, 854, 809, 789, 759, 717, 690, 666, 654, 555. **^{1}H NMR** (600 MHz) Major Ketoacid δ 7.72 (d, J = 16.2 Hz, 1H), 7.60 (d, J = 7.5 Hz, 2H), 7.48–7.43 (m, 1H), 7.38 (dt, J = 12.8, 7.2 Hz, 2H), 6.82 (d, J = 16.1 Hz, 1H), 3.80 (s, 2H). Minor Enolacid δ 11.76 (s, 1H, enol OH), 7.52 (d, J = 8.6 Hz, 2H), 7.48–7.43 (m, 4H), 6.48 (d, J = 15.8 Hz, 1H), 5.23 (s, 1H) **HRMS** (ESI) *m/z* calcd for $C_{11}H_{10}O_3Na$ ($[M+Na]^+$) 213.0528; found 213.0531.

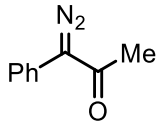

1-diazo-1-phenylpropan-2-one (72). Compound was prepared using known literature procedures.[121]

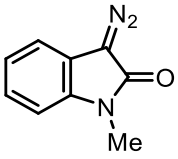

3-diazo-1-methylindolin-2-one (75). Compound was prepared using known literature procedures.[122]

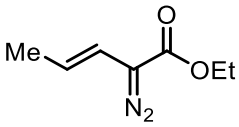

Ethyl (E)-2-diazopent-3-enoate (78). Compound was prepared using known literature procedures.[40]

General Procedure 7 for the Synthesis of Decanolides 79a–79e

A solution of lactone **61g**–**61k** (0.40–0.60 mmol, 0.01 M) in 4–6 mL chlorobenzene was heated to 140 °C for 12–18 h in a sealed tube under N_2 atmosphere. The reaction was cooled to room temperature and purified by flash column chromatography eluting with 1:10 ethyl acetate:hexanes gradient to 3:7 ethyl acetate:hexanes affording decanolides **79a**–**79e**.

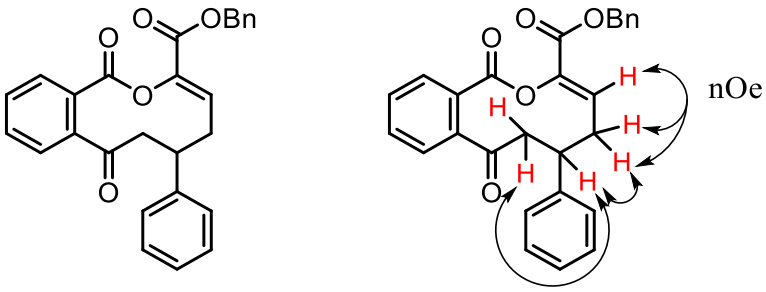

Benzyl (*Z*)-1,8-dioxo-6-phenyl-5,6,7,8-tetrahydro-1*H*-benzo[*c*]oxecine-3-carboxylate (79a). Synthesized using general procedure 7. Pale yellow oil (23.1 mg, 91%). **TLC**: R_f 0.70 (7:3 hexanes/EtOAc). **IR** (NaCl): 3063, 3032, 2949, 2889, 2359, 2336, 1732, 1694, 1599, 1497, 1452, 1377, 1275, 1242, 1098, 1034, 907, 748, 700. **^{1}H NMR** (600 MHz) δ 7.81 (dd, J = 6.9, 1.8 Hz, 1H), 7.66–7.60 (m, 3H), 7.38 (d, J = 4.3 Hz, 4H), 7.36–7.30 (m, 3H), 7.25–7.23 (m, 3H), 6.42 (t, J = 8.1 Hz, 1H), 5.33 (d, J = 12.4 Hz, 1H), 5.24 (d, J = 12.4 Hz, 1H), 3.93 (dq, J = 12.6, 4.3 Hz, 1H), 3.50 (dd, J = 17.4, 11.8 Hz, 1H), 3.04 (ddd, J = 13.8, 7.7, 3.6 Hz, 1H), 2.62 (dd, J = 17.4, 4.1 Hz, 1H), 2.41 (ddd, J = 13.9, 8.5, 5.3 Hz, 1H). **^{13}C NMR** (151 MHz) δ 202.0, 165.7, 161.6, 142.7, 142.0, 141.1, 135.4, 132.7, 131.4, 130.1, 129.2, 128.7 (2C), 128.5 (2C), 128.3, 128.3, 128.2 (2C), 127.9, 127.4 (2C), 127.0, 67.2, 46.4, 40.8, 29.6. **HRMS** (ESI) *m/z* calcd for $C_{27}H_{23}O_5$ ($[M+H]^+$) 427.1545; found 427.1556.

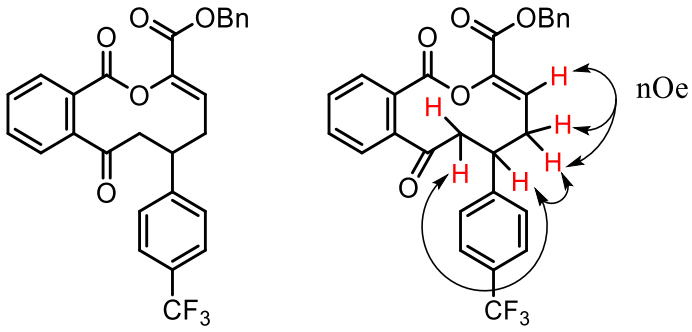

Benzyl (*Z*)-1,8-dioxo-6-(4-(trifluoromethyl)phenyl)-5,6,7,8-tetrahydro-1*H*-benzo[*c*]oxecine-3-carboxylate (79b). Synthesized using general procedure 7. Pale yellow oil (12.5 mg, 57%). **TLC**: R_f 0.70 (7:3 hexanes/EtOAc). **IR** (NaCl): 3067, 3036, 2951, 2893, 2359, 1734, 1694, 1618, 1597, 1452, 1420, 1379, 1325, 1277, 1242, 1165, 1113, 1094, 1072, 1036, 1018, 843, 752, 700. **^{1}H NMR** (600 MHz) δ 7.81 (dt, J = 7.7, 1.2 Hz, 1H), 7.67–7.60 (m, 3H), 7.58 (d, J = 8.0 Hz, 2H), 7.38–7.33(m, 7H), 6.37 (t, J = 8.0 Hz, 1H), 5.34 (d, J = 12.3 Hz, 1H), 5.24 (d, J = 12.4 Hz, 1H), 3.98 (dd, J = 11.5, 4.9 Hz, 1H), 3.48 (dd, J = 17.3, 11.5 Hz, 1H), 3.05 (ddd, J = 14.0, 7.7, 3.5 Hz, 1H), 2.62 (dd, J = 17.3, 4.2 Hz, 1H), 2.41 (ddd, J = 13.9, 8.3, 5.4 Hz, 1H). **^{13}C NMR** (151 MHz) δ 201.5, 165.6, 161.4, 146.7, 142.4, 140.9, 135.3, 132.8, 131.6, 130.0, 129.3, 128.6 (2C), 128.4, 128.3, 128.2 (2C), 127.8 (2C), 126.9, 125.7 (q, $J_{C\text{-}F}$ = 3.8 Hz, 2C), 124.0 (q, $J_{C\text{-}F}$ = 271.6 Hz, 1C), 67.3, 46.0, 40.6, 29.3 [Note: While peaks corresponding to the CF_3 were observed, some portion of the peaks were lost in signal noise]. **^{19}F NMR** (376 MHz) δ –62.55. **HRMS** (ESI) *m/z* calcd for $C_{28}H_{22}F_3O_5$ ($[M+H]^+$) 495.1419; found 495.1428.

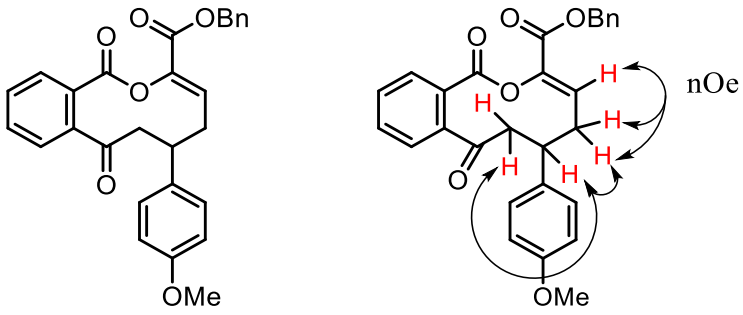

Benzyl (*Z*)-6-(4-methoxyphenyl)-1,8-dioxo-5,6,7,8-tetrahydro-1*H*-benzo[*c*]oxecine-3-carboxylate (79c). Synthesized using general procedure 7. Pale yellow oil (14.4 mg, 65%). **TLC**: R_f 0.70 (7:3 hexanes/EtOAc). **IR** (NaCl): 3063, 3034, 2999, 2955, 2835, 1730, 1694, 1607, 1512, 1454, 1375, 1277, 1242, 1184, 1109, 1090, 1034, 833, 754, 737, 702. **^{1}H NMR** (600 MHz) δ 7.80 (dd, J = 7.0, 1.4 Hz, 1H), 7.65–7.59 (m, 3H), 7.38 (d, J = 4.3 Hz, 4H), 7.36–7.32 (m, 1H), 7.17 (d, J = 8.5 Hz, 2H), 6.85 (d, J = 8.4 Hz, 2H), 6.41 (t, J = 8.1 Hz, 1H), 5.33 (dd, J = 12.3, 1.1 Hz, 1H), 5.24 (d, J = 12.0 Hz, 1H), 3.90–3.86 (m, 1H), 3.79 (s, 3H), 3.45 (dd, J = 17.4, 11.8 Hz, 1H), 3.02 (ddd, J = 13.5, 7.7, 3.6 Hz, 1H), 2.59 (dd, J = 17.4, 4.2 Hz, 1H), 2.37 (ddd, J = 13.8, 8.6, 5.3 Hz, 1H). **^{13}C NMR** (151 MHz) δ 202.0, 165.7, 161.6, 158.5, 142.0, 141.1, 135.4, 134.7, 132.7, 131.4, 130.2, 129.2, 128.5 (2C), 128.3, 128.3 (2C), 128.3, 128.2 (2C), 128.1, 114.0 (2C), 67.1, 55.3, 46.6, 40.0, 29.8. **HRMS** (ESI) *m/z* calcd for $C_{28}H_{25}O_6$ ($[M+H]^+$) 457.1651; found 457.1662.

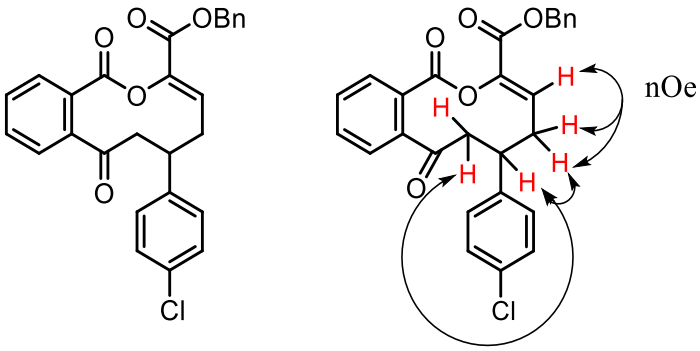

Benzyl (*Z*)-6-(4-chlorophenyl)-1,8-dioxo-5,6,7,8-tetrahydro-1*H*-benzo[*c*]oxecine-3-carboxylate (79d). Synthesized using general procedure 7. Pale yellow oil (25.3 mg, 99%). **TLC**: R_f 0.70 (7:3 hexanes/EtOAc). **IR** (NaCl): 3065, 3034, 2951, 2893, 1732, 1694, 1597, 1493, 1452, 1377, 1275, 1242, 1090, 1036, 1013, 829, 752, 700. **^{1}H NMR** (600 MHz) δ 7.80 (dd, J = 7.7, 1.6 Hz, 1H), 7.66–7.60 (m, 3H), 7.38–7.32 (m, 5H), 7.28 (d, J = 8.4 Hz, 2H), 7.18 (d, J = 8.5 Hz, 2H), 6.37 (t, J = 8.1 Hz, 1H), 5.33 (d, J = 12.3 Hz, 1H), 5.24 (d,

J = 12.3 Hz, 1H), 3.92–3.87 (m, 1H), 3.44 (dd, *J* = 17.4, 11.7 Hz, 1H), 3.02 (ddd, *J* = 13.9, 7.7, 3.6 Hz, 1H), 2.59 (dd, *J* = 17.3, 4.1 Hz, 1H), 2.36 (ddd, *J* = 13.8, 8.4, 5.3 Hz, 1H). **^{13}C NMR** (151 MHz) δ 201.6, 165.6, 161.4, 142.3, 141.1, 140.9, 135.3, 132.8 (2C), 131.5, 130.1, 129.2, 128.9 (2C), 128.7 (2C), 128.6 (2C), 128.4, 128.3, 128.2 (2C), 127.3, 67.2, 46.2, 40.2, 29.5. **HRMS** (ESI) *m/z* calcd for $C_{27}H_{22}ClO_5$ ($[M+H]^+$) 461.1156; found 461.1158.

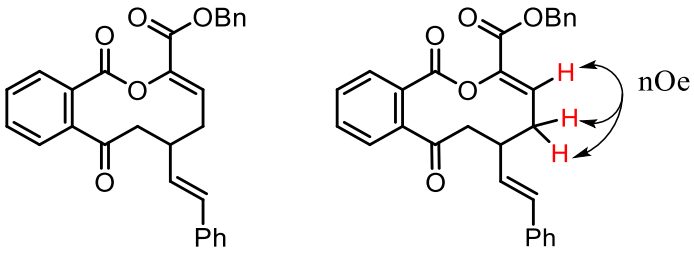

Benzyl (*Z*)-1,8-dioxo-6-((*E*)-styryl)-5,6,7,8-tetrahydro-1*H*-benzo[*c*]oxecine-3-carboxylate (79e). Synthesized using general procedure 7. Pale yellow oil (19.7 mg, 71%). **TLC**: R_f 0.70 (7:3 hexanes/EtOAc). **IR** (NaCl): 3063, 3030, 2955, 2889, 1749, 1732, 1692, 1450, 1279, 1234, 1107, 1088, 966, 752, 696. **^{1}H NMR** (600 MHz) δ 7.78 (d, *J* = 7.4 Hz, 1H), 7.65–7.59 (m, 3H), 7.41–7.35 (m, 7H), 7.31 (t, *J* = 7.5 Hz, 2H), 7.23 (t, *J* = 7.3 Hz, 1H), 6.58 (t, *J* = 8.2 Hz, 1H), 6.49 (d, *J* = 15.9 Hz, 1H), 6.24 (dd, *J* = 15.8, 8.3 Hz, 1H), 5.33 (d, *J* = 12.2 Hz, 1H), 5.25 (d, *J* = 12.2 Hz, 1H), 3.50–3.44 (m, 1H), 3.08 (dd, *J* = 17.4, 11.4 Hz, 1H), 2.88 (t, *J* = 10.7 Hz, 1H), 2.59 (dd, *J* = 17.5, 4.4 Hz, 1H), 2.35 (dt, *J* = 14.1, 7.2 Hz, 1H). **^{13}C NMR** (151 MHz) δ 202.0, 165.5, 161.6, 142.4, 141.1, 136.8, 135.3, 132.7, 131.4, 130.9, 130.6, 130.2, 129.2, 128.6 (4C), 128.4, 128.3 (2C), 128.3, 127.5, 127.4, 126.3 (2C), 67.2, 46.1, 39.2, 28.0. **HRMS** (ESI) *m/z* calcd for $C_{29}H_{25}O_5$ ($[M+H]^+$) 453.1702; found 453.1717.

General Procedure 8 for the Synthesis of Spirophthalolactones 80a–80d

A solution of δ-lactone **61l**–**61o** (0.01–0.03 mmol. 0.01 M) in chlorobenzene was added to a sealed tube under nitrogen atmosphere. Reaction was sealed and heated to 200°C until complete consumption of starting material; 1–3 days. Crude reaction was cooled to room temperature and immediately subjected to flash column chromatography eluting with 1:10 ethyl acetate:hexanes gradient to 3:7 ethyl acetate:hexanes affording spirophthalolactones **80a**–**80d**.

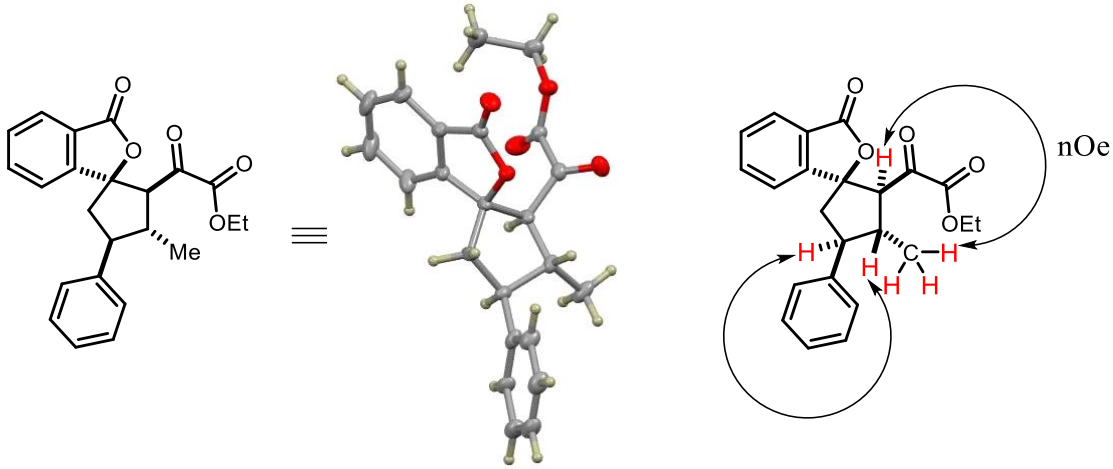

CCDC# 1860137

Ethyl (*Z*)-5-methyl-1,8-dioxo-6-phenyl-5,6,7,8-tetrahydro-1*H*-benzo[*c*]oxecine-3-carboxylate dimer (80a). Synthesized using general procedure 8. White solid (8.8 mg, 73%, mp 104–107 °C). **TLC**: R_f 0.40 (7:3 hexanes/EtOAc). **IR** (NaCl): 3522, 3441, 3059, 3028, 2965, 2934, 2909, 2874, 1778, 1728, 1605, 1495, 1462, 1373, 1339, 1290, 1265, 1231, 1144, 1065, 1036, 1016, 962, 924, 851, 760, 737, 698. **^{1}H NMR** (600 MHz) δ 7.86 (dd, J = 7.7, 1.0 Hz, 1H), 7.79 (t, J = 7.5 Hz, 1H), 7.67 (dd, J = 7.8, 1.0 Hz, 1H), 7.58 (t, J = 7.5 Hz, 1H), 7.37–7.35 (m, 4H), 7.30–7.27 (m, 1H), 3.97 (q, J = 7.1 Hz, 2H), 3.80 (dd, J = 11.1, 0.9 Hz, 1H), 3.08 (td, J = 11.2, 5.9 Hz, 1H), 2.99 (td, J = 10.6, 8.4 Hz, 1H), 2.64 (dd, J = 14.5, 8.5 Hz, 1H), 2.55 (ddd, J = 14.4, 10.3, 1.0 Hz, 1H), 1.15 (t, J = 7.1 Hz, 3H),

1.04 (d, *J* = 6.4 Hz, 3H). **^{13}C NMR** (151 MHz) δ 190.3, 168.5, 161.6, 152.4, 141.2, 134.9, 129.6, 128.8 (2C), 127.7 (2C), 127.1, 125.4, 125.4, 121.1, 91.8, 63.1, 62.7, 51.1, 48.0, 43.1, 16.9, 13.7. **HRMS** (ESI) *m/z* calcd for $C_{23}H_{23}O_5$ ($[M+H]^+$) 379.1545; found 379.1558.

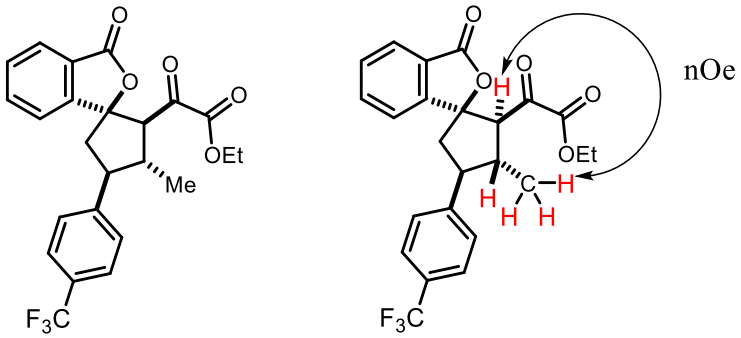

Ethyl 2-3-methyl-3'-oxo-4-(4-(trifluoromethyl)phenyl)-3'*H*-spiro[cyclopentane-1,1'-isobenzofuran]-2-yl)-2-oxoacetate (80b). Synthesized using general procedure 8. White solid (7.2 mg, 53%, mp 164–166 °C). **TLC**: R_f 0.39 (7:3 hexanes/EtOAc). **IR** (neat): 3005, 2958, 2923, 2875, 2853, 1768, 1738, 1618, 1470, 1446, 1327, 1289, 1267, 1228, 1158, 1109, 1066, 1014, 962, 912, 836, 759, 693. **^{1}H NMR** (600 MHz) δ 7.87 (dt, *J* = 7.6, 1.0 Hz, 1H), 7.80 (td, *J* = 7.6, 1.1 Hz, 1H), 7.66 (d, *J* = 7.6 Hz, 1H), 7.62 (d, *J* = 8.1 Hz, 2H), 7.60 (td, *J* = 7.5, 0.9 Hz, 1H), 7.49 (d, *J* = 8.0 Hz, 2H), 3.95 (qd, *J* = 7.2, 0.9 Hz, 2H), 3.84 (d, *J* = 10.6 Hz, 1H), 3.13–3.01 (m, 2H), 2.70 (dd, *J* = 14.6, 8.3 Hz, 1H), 2.52 (dd, *J* = 14.6, 9.4 Hz, 1H), 1.14 (t, *J* = 7.1 Hz, 3H), 1.05 (d, *J* = 6.0 Hz, 3H). **^{13}C NMR** (151 MHz) δ 190.1, 168.2, 161.7, 151.7, 145.7, 134.9, 129.8, 129.6 (q, $J_{C\text{-}F}$ = 32.7 Hz, 2C), 128.1 (2C), 125.8 (q, $J_{C\text{-}F}$ = 3.7 Hz), 125.6, 125.6, 124.1 (q, $J_{C\text{-}F}$ = 271.6 Hz) 121.2, 91.8, 63.1, 62.7, 50.9, 47.9, 43.4, 29.7, 16.8, 13.7. **^{19}F NMR** (376 MHz) δ –62.49. **HRMS** (ESI) *m/z* calcd for $C_{24}H_{22}F_3O_5$ ($[M+H]^+$) 447.1419; found 447.1426.

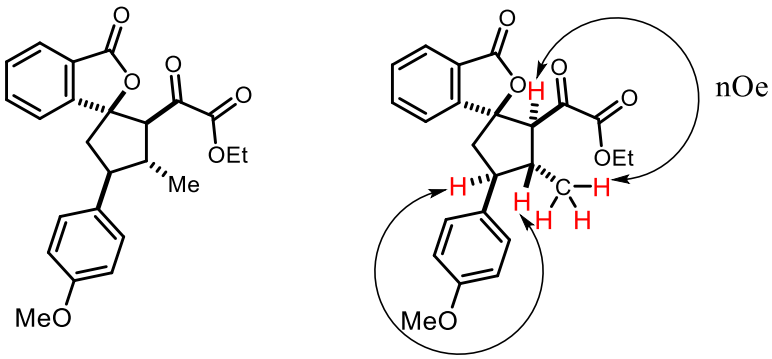

Ethyl 2-3-(4-methoxyphenyl)-4-methyl-3'-oxo-3'*H*-spiro[cyclopentane-1,1'-isobenzofuran]-5-yl)-2-oxoacetate (80c). Synthesized using general procedure 8. Pale yellow oil (9.6 mg, 78%). TLC R_f 0.39 (7:3 hexanes/EtOAc). **IR** (neat): 2958, 2927, 2871, 2853, 1765, 1725, 1611, 1513, 1466, 1288, 1244, 1178, 1059, 1032, 961, 830, 760, 693. **^{1}H NMR** (600 MHz) δ 7.86 (dt, J = 7.7, 0.9 Hz, 1H), 7.79 (td, J = 7.6, 1.1 Hz, 1H), 7.65 (dt, J = 7.8, 0.9 Hz, 1H), 7.58 (td, J = 7.5, 0.9 Hz, 1H), 7.28 (d, J = 8.7 Hz, 2H), 6.90 (d, J = 8.7 Hz, 2H), 3.97 (qd, J = 7.2, 1.1 Hz, 2H), 3.81 (s, 4H), 3.77 (d, J = 11.1 Hz, 1H), 3.02 (td, J = 11.2, 5.9 Hz, 1H), 2.94 (td, J = 10.9, 8.5 Hz, 1H), 2.61 (dd, J = 14.4, 8.4 Hz, 1H), 2.51 (dd, J = 14.4, 10.4 Hz, 1H), 1.15 (t, J = 7.2 Hz, 3H), 1.03 (d, J = 6.4 Hz, 3H). **^{13}C NMR** (151 MHz) δ 190.4, 168.5, 161.7, 158.8, 152.5, 134.8, 133.2, 129.6, 128.6 (2C), 125.5, 125.4, 121.1, 114.2 (2C), 91.8, 63.2, 62.6, 55.3, 50.5, 48.2, 43.1, 16.9, 13.7. **HRMS** (ESI) *m/z* calcd for $C_{24}H_{24}O_6Na$ ([M+Na]$^+$) 431.1471; found 431.1474.

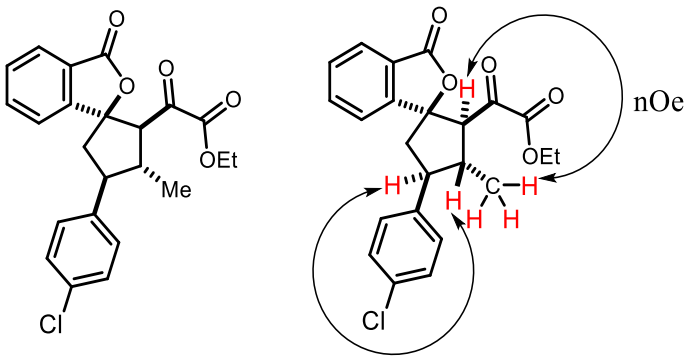

Ethyl 2-(3-(4-chlorophenyl)-4-methyl-3'-oxo-3'*H*-spiro[cyclopentane-1,1'-isobenzofuran]-5-yl)-2-oxoacetate (80d). Synthesized using general procedure 8. White solid (4.8 mg, 90%, mp 131–133 °C). **TLC**: R_f 0.45 (7:3 hexanes/EtOAc). **IR** (neat): 3065, 3033, 2947, 2882, 1762, 1733, 1646, 1612, 1600, 1492, 1471, 1301, 1288, 1261, 1228, 1096, 1067, 1040, 1010. **^{1}H NMR** (600 MHz) δ 7.86 (dt, J = 7.6, 1.0 Hz, 1H), 7.79 (td, J = 7.5, 1.1 Hz, 1H), 7.65 (dt, J = 7.8, 0.9 Hz, 1H), 7.59 (td, J = 7.5, 0.9 Hz, 1H), 7.35–7.28 (m, 4H), 3.95 (q, J = 7.1 Hz, 2H), 3.80 (d, J = 11.0 Hz, 1H), 3.03 (td, J = 11.0, 6.1 Hz, 1H), 2.97 (td, J = 11.0, 10.4, 8.7 Hz, 1H), 2.65 (dd, J = 14.5, 8.6 Hz, 1H), 2.48 (dd, J = 14.5, 9.9 Hz, 1H), 1.14 (t, J = 7.2 Hz, 3H), 1.03 (d, J = 6.3 Hz, 3H). **^{13}C NMR** (151 MHz) δ 190.2, 168.4, 161.6, 152.0, 139.9, 134.9, 132.9, 129.7, 129.0 (2C), 128.9 (2C), 125.5, 125.4, 121.2, 91.7, 62.9, 62.7, 50.5, 47.9, 43.2, 16.8, 13.7. **HRMS** (ESI) *m/z* calcd for $C_{23}H_{22}ClO_5$ ($[M+H]^+$) 413.1156; found 413.1164.

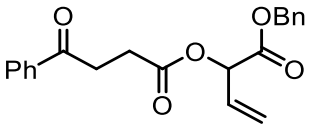

Benzyl 2-((4-oxo-4-phenylbutanoyl)oxy)but-3-enoate (82). To a stirred solution of 3-benzoylpropionic acid (11 mg, 0.06 mmol) and $Rh_2(TFA)_4$ (1 mol%) in 0.5 mL dichloromethane was added a solution of **2a** (25 mg, 0.12 mmol) in 0.5 mL dichloromethane over 1.5 h via syringe pump at reflux. After the addition was completed, the reaction was refluxed for an additional 30 minutes. The crude reaction mixture was concentrated and then purified using flash column chromatography eluting with 1:10 ethyl acetate:hexanes gradient to 3:7 ethyl acetate:hexanes affording **3b** as a clear liquid (13.0 mg, 60%).**TLC**: R_f 0.70 (7:3 hexanes/EtOAc). **IR** (neat): 3064, 3033, 2919, 2849, 1740, 1686, 1449, 1358, 1309, 1268, 1213, 1189, 1126, 1001, 986, 945, 747, 691. **^{1}H NMR** (600

MHz) δ 7.97 (d, J = 7.8 Hz, 2H), 7.57 (t, J = 7.5 Hz, 1H), 7.47 (t, J = 7.2 Hz, 2H), 7.37–7.31 (m, 5H), 5.99–5.93 (m, 1H), 5.58 (dd, J = 6.1, 1.7 Hz, 1H), 5.52 (d, J = 17.2 Hz, 1H), 5.37 (d, J = 10.6 Hz, 1H), 5.20 (q, J = 12.0 Hz, 2H), 3.41–3.28 (m, 2H), 2.99–2.86 (m, 2H). **^{13}C NMR** (151 MHz) δ 197.6, 172.0, 168.3, 136.4, 135.2, 133.3, 129.7, 128.6 (2C), 128.6 (2C), 128.4, 128.1 (2C), 128.0 (2C), 119.9, 73.2, 67.2, 33.2, 28.0. **HRMS** (ESI) *m/z* calcd for $C_{21}H_{21}O_5$ ($[M+H]^+$) 353.1389; found 353.1397.

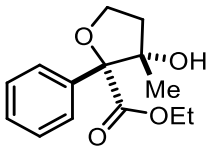

Ethyl 3-hydroxy-3-methyl-2-phenyltetrahydrofuran-2-carboxylate (89b). Isolated product matched literature known values.[184]

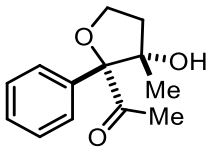

3-hydroxy-3-methyl-2-phenyltetrahydrofuran-2-yl)ethan-1-one (89c). Isolated product matched literature known values.[184]

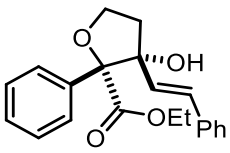

Ethyl 3-hydroxy-2-phenyl-3-((*E*)-styryl)tetrahydrofuran-2-carboxylate (89d). Isolated product matched literature known values.[184]

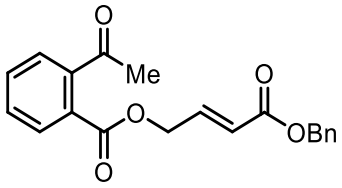

(*E*)-4-(benzyloxy)-4-oxobut-2-en-1-yl 2-acetylbenzoate (89e). 24.5 mg, 69%. ^{1}H NMR (300 MHz, Chloroform-*d*) δ 7.90–7.83 (m, 1H), 7.65–7.42 (m, 3H), 7.42–7.31 (m, 7H), 7.07 (dt, *J* = 15.8, 4.6 Hz, 1H), 6.15 (dt, *J* = 15.8, 2.0 Hz, 1H), 5.20 (s, 2H), 4.98 (dd, *J* = 4.6, 2.0 Hz, 3H), 2.67–2.43 (m, 4H).

Chapter 7.3. Experimentals for Chapter 4

Synthesis of 2'-Aminochalcones 1a–1l

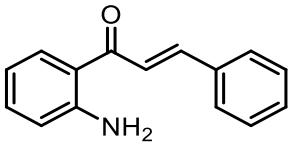

(*E*)-1-(2-aminophenyl)-3-phenylprop-2-en-1-one (90a). Starting material was synthesized using known literature protocol.[186]

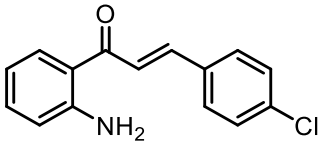

(*E*)-1-(2-aminophenyl)-3-(4-chlorophenyl)prop-2-en-1-one (90b). Starting material was synthesized using known literature protocol.[186]

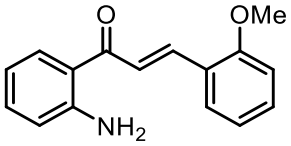

(*E*)-1-(2-aminophenyl)-3-(2-methoxyphenyl)prop-2-en-1-one (90c). Starting material was synthesized using known literature protocol.[187]

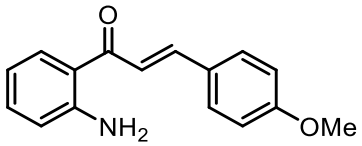

(*E*)-1-(2-aminophenyl)-3-(4-methoxyphenyl)prop-2-en-1-one (90d). Starting material was synthesized using known literature protocol.[186]

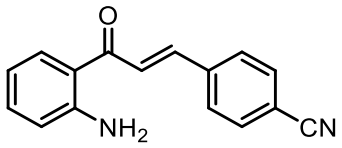

(*E*)-4-(3-(2-aminophenyl)-3-oxoprop-1-en-1-yl)benzonitrile (90e). Starting material was synthesized using known literature protocol.[188]

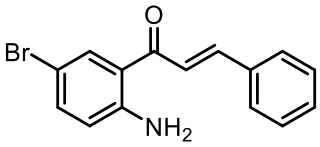

(*E*)-1-(2-amino-5-bromophenyl)-3-phenylprop-2-en-1-one (90f). Starting material was synthesized using known literature protocol.[189]

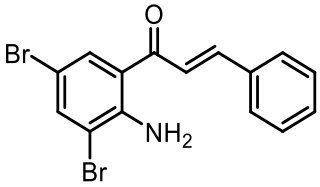

(*E*)-1-(2-amino-3,5-dibromophenyl)-3-phenylprop-2-en-1-one (90g). Starting material was synthesized using known literature protocol.[190]

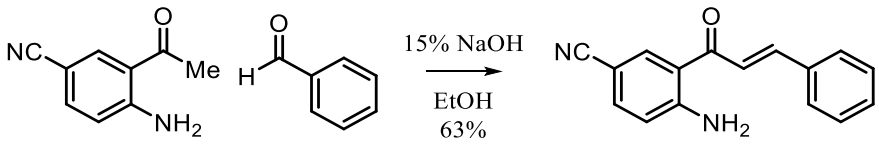

4-amino-3-cinnamoylbenzonitrile (90h). 3-acetyl-4-aminobenzonitrile (3.4 mmol) was added to a solution of benzaldehyde (4.1 mmol) in 15 mL of ethanol containing 15 wt % NaOH and stirred at 25 °C for 7 h then the solvent EtOH was removed completely, diluted with 1 M HCl aqueous solution (10 mL). The aqueous layer was extracted with EtOAc (3 × 10 mL), the combined organic layers were dried over anhydrous Na_2SO_4 and

concentrated under reduced pressure. Chromatographic purification of the crude compound over silica gel (gradient elution with 20–25% EtOAc in Hexane) yielded the compound **90h** as a yellow solid (537 mg, 63%, mp 139–140 °C) **TLC**: R_f 0.25 (4:1 hexanes/EtOAc). **IR** (NaCl): 3435, 3318, 3059, 3028, 2378, 2311, 2218, 1647, 1618, 1570, 1545, 1489, 1449, 1423, 1362, 1335, 1302, 1275, 1227, 1173, 1013, 978, 858, 827, 777, 743, 698, 679, 635. **^{1}H NMR** (400 MHz) δ 8.19 (d, J = 1.9 Hz, 1H), 7.78 (d, J = 12.0 Hz, 1H), 7.69–7.62 (m, 2H), 7.53 (d, J = 12.0 Hz, 1H), 7.50–7.42 (m, 4H), 6.89 (s, 2H), 6.71 (d, J = 8.0 Hz, 1H). **^{13}C NMR** (101 MHz) δ 190.4, 153.5, 144.8, 136.5, 136.2, 134.6, 130.7, 129.0 (2C), 128.5 (2C), 121.5, 119.4, 118.5, 117.8, 98.2.

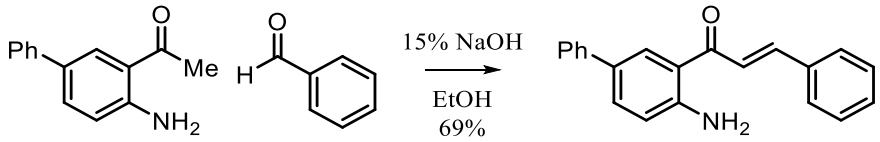

(*E*)-1-(4-amino-[1,1'-biphenyl]-3-yl)-3-phenylprop-2-en-1-one (90i). 1-(4-amino-[1,1'-biphenyl]-3-yl)ethan-1-one (1.7 mmol) was added to a solution of benzaldehyde (1.7 mmol) in 15 mL of ethanol containing 15 wt % NaOH and stirred at 25 °C for 24 h then the solvent EtOH was removed completely, diluted with 1 M HCl aqueous solution (10 mL). The aqueous layer was extracted with EtOAc (3 × 10 mL), the combined organic layers were dried over anhydrous Na_2SO_4 and concentrated under reduced pressure. Chromatographic purification of the crude compound over silica gel (gradient elution with 20–25% EtOAc in Hexane) yielded the compound **90i** as an orange solid (342 mg, 69%, mp 142–143 °C). **TLC**: R_f 0.40 (4:1 hexanes/EtOAc). **IR** (NaCl): 3746, 3470, 3383, 3333, 3059, 3028, 1647, 1620, 1568, 1493, 1479, 1449, 1352, 1331, 1288, 1265, 1202, 1171, 1074, 1007, 974, 854, 827, 764, 734, 696. **^{1}H NMR** (400 MHz) δ 8.08 (d, J = 2.1 Hz, 1H), 7.82 (d, J = 16.0 Hz, 1H), 7.69 (d, J = 16.0 Hz, 1H), 7.67–7.65 (m, 2H), 7.61–7.55 (m,

3H), 7.49–7.41 (m, 5H), 7.37–7.31 (m, 1H), 6.80 (d, *J* = 8.0 Hz, 1H), 6.41 (s, 2H). **^{13}C NMR** (101 MHz) δ 191.7, 150.2, 143.2, 140.5, 135.1, 133.2, 130.1, 129.2, 129.0, 128.8 (2C), 128.8 (2C), 128.3 (2C), 126.5, 126.3 (2C), 123.0, 119.2, 117.8.

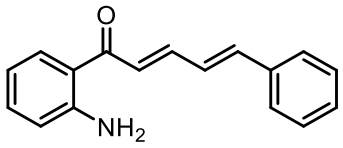

(2*E*,4*E*)-1-(2-aminophenyl)-5-phenylpenta-2,4-dien-1-one (90j). Starting material was synthesized using known literature protocol.[191]

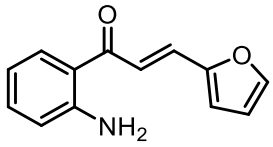

(*E*)-1-(2-aminophenyl)-3-(furan-2-yl)prop-2-en-1-one (90k). Starting material was synthesized using known literature protocol.[192]

Synthesis of aldol cascade intermediate

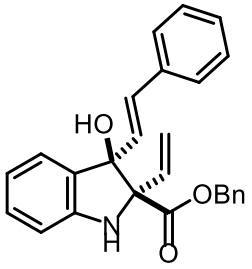

Methyl 2-((*E*)-buta-1,3-dien-1-yl)-3-hydroxy-3-((*E*)-2-oxo-4-phenylbut-3-en-1-yl)tetrahydrofuran-2-carboxylate (91). To a stirred solution of 2'-aminochalcone **90a** (0.11 mmol) and $Rh_2(esp)_2$ (1 mol%) in 1.1 mL CH_2Cl_2 was added a solution of vinyl diazoacetate **48** (0.22 mmol) in 0.5 mL CH_2Cl_2 over 2.5 h *via* syringe pump at room temperature. After the addition was completed, the reaction was left to stir for an additional 30 minutes. The crude reaction mixture was concentrated using rotary evaporation and then

purified using flash column chromatography eluting with 1:3 ethyl acetate: hexanes to afford aldol product **91** as a liquid (29 mg, 65%).**TLC**: R_f 0.24 (7:3 hexanes/EtOAc). **IR** (NaCl): 3375, 3030, 2363, 2338, 1734, 1605, 1476, 1464, 1373, 1275, 1258, 1171, 1128, 1057, 976, 910, 743, 694, 669, 652. **^{1}H NMR** (400 MHz) δ 7.42–7.27 (m, 9H), 7.22 (t, J = 8.1 Hz, 2H), 7.11 (d, J = 7.5 Hz, 1H), 6.90–6.77 (m, 3H), 6.40 (d, J = 16.0 Hz, 1H), 6.18 (dd, J = 17.1, 10.4 Hz, 1H), 5.44–5.29 (m, 2H), 5.18 (dd, J = 11.4, 4.5 Hz, 2H), 4.64 (s, 1H). **^{13}C NMR** (101 MHz) δ 170.9, 149.1, 136.6, 135.8, 135.3, 131.5, 130.5, 130.4, 128.5 (2C), 128.5 (2C), 128.2, 128.1 (3C), 127.7 (2C), 126.7, 124.8, 120.0, 115.8, 110.9, 85.8, 80.4, 67.4. **HRMS** (ESI) *m/z* calcd for $C_{26}H_{23}NO_3Na$ ($[M+Na]^+$) 420.1576; found 420.1581. Relative stereochemistry was assigned based on previous literature reports.[144]

General procedure 9 for the synthesis of quinolines.

To a stirred solution of 2'-aminochalcone **90** (0.11 mmol) and $Rh_2(esp)_2$ (1 mol%) in 1.1 mL toluene was added a solution of corresponding vinyl diazoacetate (0.22 mmol) in 0.5 mL toluene over 2.5 h *via* syringe pump at room temperature. After the addition was completed, the reaction was left to stir for an additional 30 minutes. The crude reaction mixture was concentrated using rotary evaporation and then purified using flash column chromatography eluting with 1:3 ethyl acetate: hexanes to afford quinoline product **92a–92o**.

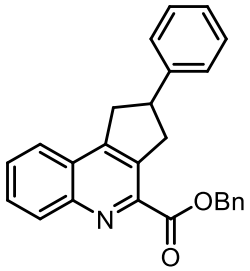

Benzyl 2-phenyl-2,3-dihydro-1*H*-cyclopenta[*c*]quinoline-4-carboxylate (92a). Synthesized using general procedure 9. Pale yellow oil (34.0 mg, 77%). **TLC**: R_f 0.34 (4:1 hexanes/EtOAc). **IR** (NaCl): 3738, 3032, 2943, 1718, 1649, 1568, 1500, 1454, 1390, 1317, 1244, 1192, 1157, 1087, 1012, 754, 698. **^{1}H NMR** (400 MHz) δ 8.32 (d, J = 8.6 Hz, 1H), 7.83 (d, J = 8.2 Hz, 1H), 7.73 (d, J = 7.7 Hz, 1H), 7.65–7.62 (m, 1H), 7.52 (d, J = 6.9 Hz, 2H), 7.40–7.31 (m, 8H), 5.53 (s, 2H), 4.01–3.79 (m, 3H), 3.56 (dd, J = 16.7, 7.0 Hz, 1H), 3.41 (dd, J = 16.6, 7.4 Hz, 1H). **^{13}C NMR** (101 MHz) δ 165.7, 151.6, 146.8, 144.9, 144.8, 136.3, 135.8, 131.1, 129.3, 128.6 (2C), 128.6 (2C), 128.5 (2C), 128.5, 128.3, 126.9 (2C), 126.8, 126.5, 123.9, 67.4, 44.3, 41.7, 39.1. **HRMS** (ESI) *m/z* calcd for $C_{26}H_{22}NO_2$ ($[M+H]^+$) 380.1651; found 380.1656.

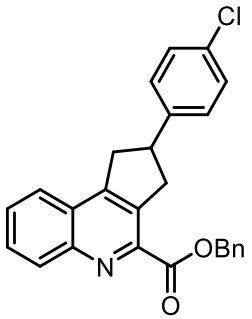

Benzyl 2-(4-chlorophenyl)-2,3-dihydro-1*H*-cyclopenta[*c*]quinoline-4-carboxylate (92b). Synthesized using general procedure 9. Pale yellow solid (35.0 mg, 74%). Recrystallization from ethyl acetate (slow evaporation method) yielded triclinic colorless needles (mp 152–155 °C). **TLC**: R_f 0.18 (4:1 hexanes/EtOAc). **IR** (NaCl): 3062, 3034, 2941, 2370, 1718, 1602, 1579, 1568, 1492, 1454, 1386, 1361, 1317, 1242, 1192, 1157, 1089, 1012, 827, 758, 698. **^{1}H NMR** (400 MHz) δ 8.31 (d, J = 8.5 Hz, 1H), 7.81 (d, J = 8.2 Hz, 1H), 7.73 (ddd, J = 9.0, 7.7, 1.5 Hz, 1H), 7.63 (ddd, J = 8.1, 6.8, 1.3 Hz, 1H), 7.53–7.50 (m, 2H), 7.40–7.33 (m, 3H), 7.29–7.26 (m, 2H), 7.23–7.21 (m, 2H), 5.52 (s, 2H), 3.96 (dd, J = 16.9, 8.3 Hz, 1H), 3.89–3.76 (m, 2H), 3.50 (dd, J = 17.3, 6.7 Hz, 1H), 3.35 (dd, J

= 16.0, 6.6 Hz, 1H). **^{13}C NMR** (101 MHz) δ 165.6, 151.2, 146.9, 144.7, 143.4, 136.1, 135.8, 132.2, 131.1, 129.4, 128.7 (2C), 128.6, 128.5 (2C), 128.5 (2C), 128.3 (2C), 128.3, 126.7, 123.9, 67.4, 43.7, 41.6, 39.0. **HRMS** (ESI) *m/z* calcd for $C_{26}H_{21}ClNO_2$ ($[M+H]^+$) 414.1261; found 414.1270.

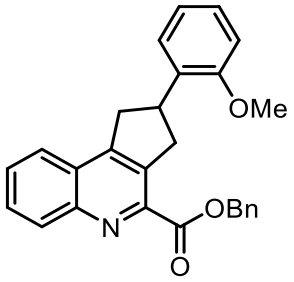

Benzyl 2-(2-methoxyphenyl)-2,3-dihydro-1*H*-cyclopenta[*c*]quinoline-4-carboxylate (92c). Synthesized using general procedure 9. Pale yellow oil (31.0 mg, 65%). **TLC**: R_f 0.39 (7:3 hexanes/EtOAc). **IR** (NaCl): 3062, 3034, 2943, 2837, 1720, 1598, 1581, 1566, 1492, 1458, 1436, 1388, 1317, 1244, 1192, 1157, 1111, 1087, 1053, 1022, 754, 698. **^{1}H NMR** (400 MHz) δ 8.31 (d, *J* = 8.6 Hz, 1H), 7.83 (d, *J* = 8.2 Hz, 1H), 7.71 (d, *J* = 8.4 Hz, 1H), 7.62 (t, *J* = 7.8 Hz, 1H), 7.52 (d, *J* = 7.3 Hz, 1H), 7.39–7.32 (m, 4H), 7.23–7.19 (m, 2H), 6.92–6.87 (m, 2H), 5.52 (s, 2H), 4.20–4.12 (m, 1H), 3.92–3.84 (m, 1H), 3.82 (s, 3H), 3.77–3.70 (m, 1H), 3.60 (dd, *J* = 17.3, 7.7 Hz, 1H), 3.43 (dd, *J* = 17.1, 7.8 Hz, 1H). **^{13}C NMR** (101 MHz) δ 165.8, 157.4, 152.2, 146.7, 144.9, 136.8, 135.9, 132.6, 131.0, 129.1, 128.6, 128.5 (2C), 128.5 (2C), 128.3, 128.2, 127.5, 127.3, 124.1, 120.5, 110.5, 67.3, 55.3, 39.9, 38.7, 37.5. **HRMS** (ESI) *m/z* calcd for $C_{27}H_{24}NO_3$ ($[M+H]^+$) 410.1756; found 410.1768.

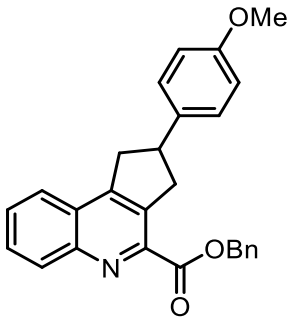

Benzyl 2-(4-methoxyphenyl)-2,3-dihydro-1*H*-cyclopenta[*c*]quinoline-4-carboxylate (92d). Synthesized using general procedure 9. Orange solid (38.3 mg, 80%, mp 108–111 °C). **TLC**: R_f 0.32 (7:3 hexanes/EtOAc). **IR** (NaCl): 3062, 3034, 2939, 2835, 1718, 1610, 1512, 1456, 1382, 1315, 1246, 1188, 1157, 1087, 1031, 1014, 829, 756. **^{1}H NMR** (400 MHz) δ 8.31 (d, J = 8.6 Hz, 1H), 7.82 (dd, J = 8.4, 1.6 Hz, 1H), 7.73 (ddd, J = 8.5, 6.9, 1.6 Hz, 1H), 7.63 (ddd, J = 8.3, 6.9, 1.4 Hz, 1H), 7.54–7.51 (m, 1H), 7.40–7.31 (m, 4H), 7.23–7.21 (m, 2H), 6.86 (d, J = 8.7 Hz, 2H), 5.53 (s, 2H), 3.98–3.91 (m, 1H), 3.88–3.82 (m, 1H), 3.80 (s, 3H), 3.76 (d, J = 8.5 Hz, 1H), 3.51 (dd, J = 17.0, 6.9 Hz, 1H), 3.36 (dd, J = 16.1, 7.1 Hz, 1H). **^{13}C NMR** (101 MHz) δ 165.7, 158.2, 151.7, 146.8, 144.8, 136.9, 136.4, 135.8, 131.1, 129.2, 128.5 (2C), 128.5 (2C), 128.4, 128.3, 127.8 (2C), 126.8, 123.9, 113.9 (2C), 67.4, 55.3, 43.6, 41.8, 39.2. **HRMS** (ESI) *m/z* calcd for $C_{27}H_{24}NO_3$ ($[M+H]^+$) 410.1756; found 410.1762.

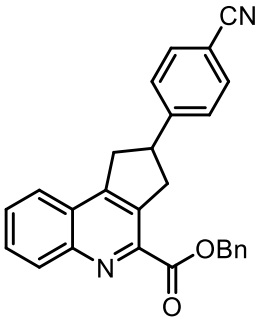

Benzyl 2-(4-cyanophenyl)-2,3-dihydro-1*H*-cyclopenta[*c*]quinoline-4-carboxylate (92e). Synthesized using general procedure 9. Pale yellow solid (30.3 mg, 62%, mp 165–

167 °C). **TLC**: R_f 0.30 (7:3 hexanes/EtOAc). **IR** (NaCl): 3061, 3035, 2926, 2382, 2345, 2225, 1720, 1608, 1502, 1317, 1244, 1192, 1157, 1087, 1012, 839, 756. **^{1}H NMR** (400 MHz) δ 8.32 (d, J = 8.5 Hz, 1H), 7.82 (dd, J = 8.3, 1.4 Hz, 1H), 7.76 (ddd, J = 8.6, 6.8, 1.5 Hz, 1H), 7.66 (ddd, J = 8.2, 6.8, 1.2 Hz, 1H), 7.61 (d, J = 8.3 Hz, 2H), 7.53–7.51 (m, 2H), 7.40–7.33 (m, 5H), 5.52 (s, 2H), 4.04–3.90 (m, 2H), 3.85 (dd, J = 17.0, 8.5 Hz, 1H), 3.54 (dd, J = 16.4, 6.3 Hz, 1H), 3.39 (dd, J = 17.0, 7.1 Hz, 1H). **^{13}C NMR** (101 MHz) δ 165.6, 150.8, 150.6, 146.9, 144.6, 135.7, 132.5 (2C), 131.2, 129.6, 128.8, 128.6 (3C), 128.6 (2C), 128.4, 127.8 (2C), 126.6, 123.8, 118.8, 110.4, 67.5, 44.2, 41.5, 38.8. **HRMS** (ESI) *m/z* calcd for $C_{27}H_{21}N_2O_2$ ($[M+H]^+$) 405.1603; found 405.1601.

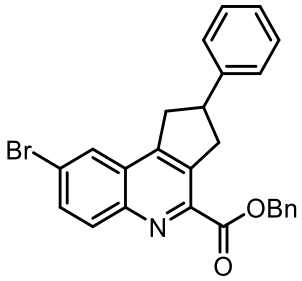

Benzyl 8-bromo-2-phenyl-2,3-dihydro-1*H*-cyclopenta[*c*]quinoline-4-carboxylate (92f). Synthesized using general procedure 9. Pale yellow oil (35.0 mg, 76%). **TLC**: R_f 0.32 (4:1 hexanes/EtOAc). **IR** (NaCl): 3062, 3032, 2922, 1722, 1581, 1490, 1292, 1238, 1182, 1012, 827, 754, 698. **^{1}H NMR** (400 MHz) δ 8.16 (d, J = 9.1 Hz, 1H), 7.99 (s, 1H), 7.79 (d, J = 9.1 Hz, 1H), 7.51 (d, J = 8.0 Hz, 2H), 7.39–7.22 (m, 8H), 5.51 (s, 2H), 4.00–3.85 (m, 2H), 3.76 (dd, J = 17.0, 8.5 Hz, 1H), 3.56 (dd, J = 16.7, 7.0 Hz, 1H), 3.36 (dd, J = 17.1, 7.7 Hz, 1H). **^{13}C NMR** (101 MHz) δ 165.4, 150.8, 145.3, 145.1, 144.6, 137.4, 135.6, 132.9, 132.7, 128.7 (2C), 128.6 (4C), 128.4, 127.9, 126.8 (2C), 126.6, 126.4, 122.9, 67.5, 44.2, 41.6, 38.9. **HRMS** (ESI) *m/z* calcd for $C_{26}H_{20}BrNO_2Na$ ($[M+Na]^+$) 480.0575; found 480.0574.

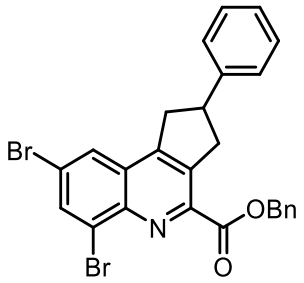

Benzyl 6,8-dibromo-2-phenyl-2,3-dihydro-1*H*-cyclopenta[*c*]quinoline-4-carboxylate (92g). Synthesized using general procedure 9. White needles (30.5 mg, 72%, mp 136–137 °C). **TLC**: R_f 0.62 (7:3 hexanes/EtOAc). **IR** (NaCl): 3062, 3030, 2943, 2895, 1720, 1676, 1597, 1577, 1544, 1496, 1471, 1454, 1425, 1396, 1361, 1330, 1274, 1182, 1116, 1076, 1026, 956, 908, 856, 777. **^{1}H NMR** (500 MHz) δ 8.17 (d, J = 2.0 Hz, 1H), 7.96 (d, J = 2.1 Hz, 1H), 7.58–7.56 (m, 2H), 7.42–7.39 (m, 2H), 7.36–7.32 (m, 3H), 7.29–7.27 (m, 3H), 5.54–5.48 (m, 2H), 4.03–3.90 (m, 2H), 3.77 (dd, J = 17.1, 8.5 Hz, 1H), 3.59 (dd, J = 16.9, 7.0 Hz, 1H), 3.37 (dd, J = 17.2, 7.6 Hz, 1H). **^{13}C NMR** (126 MHz) δ 165.0, 151.6, 145.4, 144.4, 142.8, 138.5, 135.9, 135.7, 128.7 (2C), 128.6 (2C), 128.4, 128.2, 128.1 (2C), 127.8, 126.8 (2C), 126.7, 126.2, 122.1, 67.3, 44.3, 41.2, 39.1. **HRMS** (ESI) *m/z* calcd for $C_{26}H_{19}Br_2NO_2Na$ ($[M+Na]^+$) 557.9680; found 557.9680.

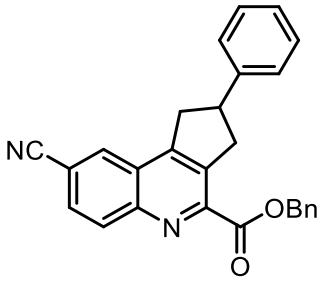

Benzyl 8-cyano-2-phenyl-2,3-dihydro-1*H*-cyclopenta[*c*]quinoline-4-carboxylate (92h). Synthesized using general procedure 9. Pale yellow oil (32.7 mg, 67%). **TLC**: R_f 0.38 (7:3 hexanes/EtOAc). **IR** (NaCl): 3062, 3032, 2949, 2225, 1724, 1647, 1608, 1566, 1498, 1454, 1384, 1348, 1307, 1267, 1246, 1184, 1155, 1095, 1053, 1014, 956, 908, 837,

754. **^{1}H NMR** (400 MHz) δ 8.39 (d, J = 8.8 Hz, 1H), 8.24 (d, J = 1.8 Hz, 1H), 7.86 (dd, J = 8.8, 1.8 Hz, 1H), 7.53–7.50 (m, 2H), 7.39–7.33 (m, 6H), 7.30–7.28 (m, 2H), 5.52 (s, 2H), 4.02–3.92 (m, 2H), 3.87–3.80 (m, 1H), 3.58 (dd, J = 15.8, 5.9 Hz, 1H), 3.47–3.41 (m, 1H). **^{13}C NMR** (101 MHz) δ 165.0, 152.7, 147.6, 147.4, 144.1, 138.2, 135.3, 132.4, 130.6, 129.7, 128.8 (2C), 128.6 (2C), 128.6 (2C), 128.5, 126.8 (2C), 126.8, 126.1, 118.4, 111.9, 67.8, 44.2, 41.5, 38.9. **HRMS** (ESI) *m/z* calcd for $C_{27}H_{21}N_2O_2$ ($[M+H]^+$) 405.1603; found. 405.1603.

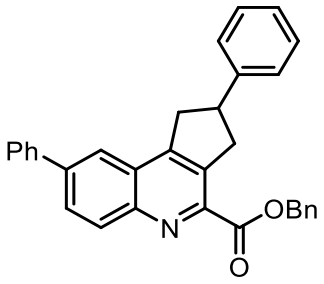

Benzyl 2,8-diphenyl-2,3-dihydro-1*H*-cyclopenta[*c*]quinoline-4-carboxylate (92i). Synthesized using general procedure 9. Pale yellow oil (33.8 mg, 74%). **TLC**: R_f 0.19 (4:1 hexanes/EtOAc). **IR** (NaCl): 3399, 3368, 3341, 3059, 3032, 2947, 2924, 1721, 1493, 1452, 1310, 1252, 1182, 1101, 1013, 908, 837, 754. **^{1}H NMR** (400 MHz) δ 8.38 (d, J = 8.8 Hz, 1H), 8.00 (d, J = 9.8 Hz, 2H), 7.74 (d, J = 7.7 Hz, 2H), 7.52 (q, J = 7.7 Hz, 4H), 7.55–7.32 (m, 9H), 5.54 (s, 2H), 4.03–3.84 (m, 3H), 3.59 (dd, J = 16.9, 6.4 Hz, 1H), 3.46 (dd, J = 15.9, 6.5 Hz, 1H). **^{13}C NMR** (101 MHz) δ 165.7, 151.7, 146.2, 144.9, 144.6, 141.2, 140.1, 136.8, 135.8, 131.5, 129.1, 129.0 (2C), 128.6 (2C), 128.6 (4C), 128.3, 128.1, 127.5 (2C), 127.1, 126.9, 126.5, 121.6, 67.4, 44.3, 41.7, 39.1. **HRMS** (ESI) *m/z* calcd for $C_{32}H_{26}NO_2$ ($[M+H]^+$) 456.1964; found 456.1964.

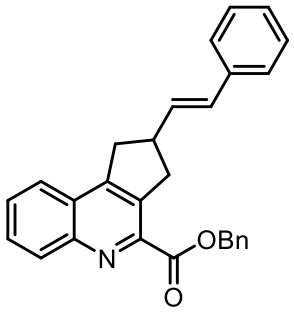

Benzyl (*E*)-2-styryl-2,3-dihydro-1*H*-cyclopenta[*c*]quinoline-4-carboxylate (92j). Synthesized using general procedure 9. Pale yellow oil (35 mg, 72%). **TLC**: R_f 0.45 (7:3 hexanes/EtOAc). **^{1}H NMR** (400 MHz) δ 8.30 (d, J = 8.6 Hz, 1H), 7.83 (d, J = 8.2 Hz, 1H), 7.72 (t, J = 7.6 Hz, 1H), 7.63 (t, J = 7.5 Hz, 1H), 7.53 (d, J = 7.4 Hz, 2H), 7.40–7.29 (m, 7H), 7.26–7.20 (m, 1H), 6.54 (d, J = 15.7 Hz, 1H), 6.39 (dd, J = 15.8, 7.7 Hz, 1H), 5.53 (s, 2H), 3.76 (dd, J = 16.8, 8.0 Hz, 1H), 3.61 (dd, J = 16.6, 8.3 Hz, 1H), 3.52–3.43 (m, 1H), 3.36 (dd, J = 17.0, 7.2 Hz, 1H), 3.21 (dd, J = 16.8, 7.3 Hz, 1H). **^{13}C NMR** (101 MHz) δ 165.7, 151.7, 146.7, 144.9, 137.2, 136.3, 135.8, 133.0, 131.1, 129.8, 129.2, 128.6 (2C), 128.5 (4C), 128.4, 128.3, 127.3, 126.9, 126.1 (2C), 124.0, 67.4, 42.6, 40.1, 37.6. **HRMS** (ESI) *m/z* calcd for $C_{28}H_{24}NO_2$ ($[M+H]^+$) 406.1807; found 406.1806.

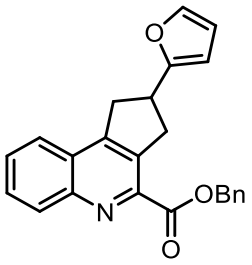

4-((benzyloxy)(l3-oxidaneylidene)methyl)-2-(furan-2-yl)-2,3-dihydro-1*H*-cyclopenta[*c*]quinoline (92k). Synthesized using general procedure 9. Pale yellow oil (30 mg, 62%). **TLC**: R_f 0.33 (4:1 hexanes/EtOAc). **IR** (NaCl): 3743, 3062, 3034, 2947, 1718, 1560, 1504, 1454, 1425, 1388, 1244, 1192, 1157, 1085, 1012, 756, 736, 698. **^{1}H NMR** (400 MHz) δ 8.30 (d, J = 8.5 Hz, 1H), 7.82 (dd, J = 8.2, 1.4 Hz, 1H), 7.72 (ddd, J = 8.5,

6.8, 1.5 Hz, 1H), 7.63 (ddd, *J* = 8.2, 6.8, 1.2 Hz, 1H), 7.54–7.52 (m, 2H), 7.41–7.34 (m, 4H), 6.30 (dd, *J* = 3.2, 1.9 Hz, 1H), 6.11 (d, *J* = 3.2 Hz, 1H), 5.53 (s, 2H), 3.97–3.85 (m, 2H), 3.77–3.70 (m, 1H), 3.65–3.60 (m, 1H), 3.50–3.44 (m, 1H). **^{13}C NMR** (101 MHz) δ 165.6, 157.5, 151.1, 146.7, 144.7, 141.4, 135.9, 135.8, 131.1, 129.3, 128.5 (2C), 128.5 (3C), 128.3, 126.8, 123.9, 110.1, 104.5, 67.4, 39.0, 37.5, 36.5. **HRMS** (ESI) *m/z* calcd for $C_{24}H_{20}NO_3$ ($[M+H]^+$) 370.1443; found 370.1455.

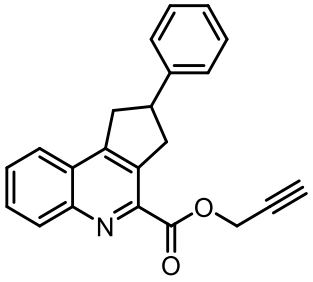

Prop-2-yn-1-yl 2-phenyl-2,3-dihydro-1*H*-cyclopenta[*c*]quinoline-4-carboxylate (92l). Synthesized using general procedure 9. Pale yellow oil (34.2 mg, 78%). **TLC**: R_f 0.28 (4:1 hexanes/EtOAc). **IR** (NaCl): 3286, 3061, 3028, 2937, 2846, 2384, 2345, 2038, 1726, 1570, 1498, 1452, 1429, 1386, 1363, 1317, 1242, 1190, 1157, 1087, 1026, 1004, 758, 702, 636. **^{1}H NMR** (400 MHz) δ 8.32 (d, *J* = 8.5 Hz, 1H), 7.84 (d, *J* = 8.3 Hz, 1H), 7.75 (ddd, *J* = 8.5, 6.8, 1.5 Hz, 1H), 7.65 (ddd, *J* = 8.2, 6.8, 1.2 Hz, 1H), 7.34–7.33 (m, 4H), 7.27–7.23 (m, 1H), 5.06 (d, *J* = 2.5 Hz, 2H), 4.05 (dd, *J* = 17.1, 8.5 Hz, 1H), 3.97–3.87 (m, 1H), 3.83 (dd, *J* = 16.7, 8.8 Hz, 1H), 3.61 (dd, *J* = 17.2, 7.5 Hz, 1H), 3.43 (dd, *J* = 16.8, 7.8 Hz, 1H), 2.53 (t, *J* = 2.5 Hz, 1H). **^{13}C NMR** (101 MHz) δ 165.1, 152.0, 146.9, 145.0, 144.0, 136.8, 131.2, 129.6, 128.8, 128.8 (2C), 127.1 (2C), 127.0, 126.7, 124.2, 77.6, 75.5, 53.3, 44.5, 41.8, 39.3. **HRMS** (ESI) *m/z* calcd for $C_{22}H_{18}NO_2$ ($[M+H]^+$) 328.1338; found 328.1339.

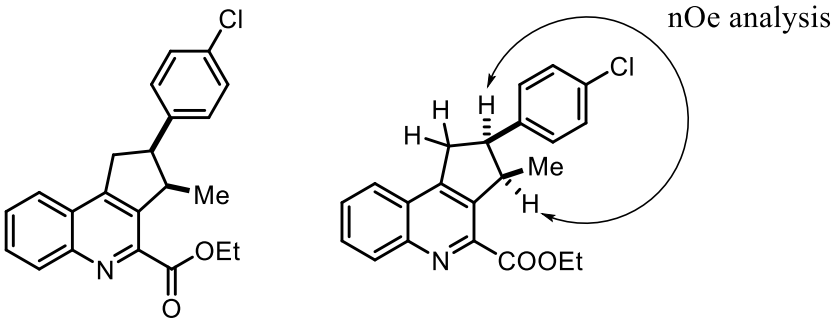

Ethyl 2-(4-chlorophenyl)-3-methyl-2,3-dihydro-1*H*-cyclopenta[*c*]quinoline-4-carboxylate (92m). Synthesized using general procedure 9. Orange solid (24.6 mg, 58%). Recrystallization from ethyl acetate (slow evaporation method) yielded triclinic colorless plates (mp 165–167 °C). **TLC**: R_f 0.50 (7:3 hexanes/EtOAc). **IR** (NaCl): 3061, 2972, 2930, 2868, 1719, 1568, 1493, 1454, 1371, 1317, 1244, 1188, 1159, 1094, 1032, 1022, 829, 760, 733. **^{1}H NMR** (300 MHz) δ 8.32 (d, J = 9.0 Hz, 1H), 7.91 (dt, J = 8.1, 1.0 Hz, 1H), 7.75 (ddd, J = 8.5, 6.8, 1.5 Hz, 1H), 7.66 (ddd, J = 8.1, 6.9, 1.3 Hz, 1H), 7.40–7.32 (m, 4H), 4.56 (q, J = 7.1 Hz, 2H), 4.25 (p, J = 7.1 Hz, 1H), 4.02–3.93 (m, 1H), 3.58 (d, J = 9 Hz, 2H), 1.49 (t, J = 7.1 Hz, 3H), 0.88 (d, J = 7.0 Hz, 3H). **^{13}C NMR** (75 MHz) δ 165.7, 150.6, 146.6, 144.8, 141.9, 138.8, 132.3, 131.1, 129.5 (2C), 129.4, 128.5 (2C), 128.5, 127.0, 124.0, 62.0, 48.8, 43.7, 32.0, 15.4, 14.3. **HRMS** (ESI) *m/z* calcd for $C_{22}H_{21}ClNO_2$ ($[M+H]^+$) 366.1261 ; found 366.1266.

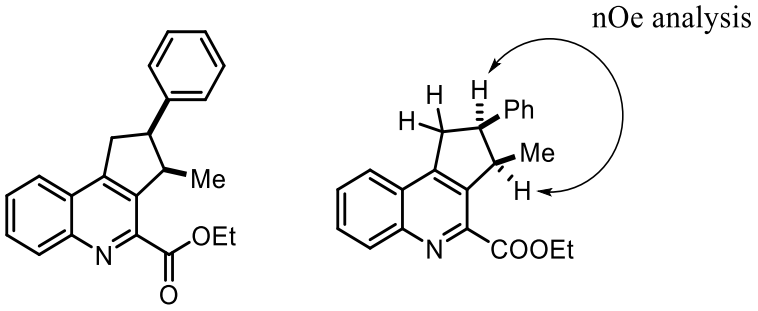

Ethyl 3-methyl-2-phenyl-2,3-dihydro-1*H*-cyclopenta[*c*]quinoline-4-carboxylate (92n). Synthesized using general procedure 9. Pale yellow oil (24.8 mg, 56%). **TLC**: R_f

0.30 (4:1 hexanes/EtOAc). **IR** (NaCl): 3061, 2972, 2934, 2903, 1719, 1603, 1570, 1499, 1452, 1371, 1317, 1242, 1190, 1159, 1099, 1032, 864, 779, 754, 700. **^{1}H NMR** (300 MHz) δ 8.31 (ddd, J = 8.5, 1.4, 0.7 Hz, 1H), 7.92 (ddd, J = 8.1, 1.6, 0.7 Hz, 1H), 7.75 (ddd, J = 8.5, 6.8, 1.6 Hz, 1H), 7.66 (ddd, J = 8.1, 6.8, 1.3 Hz, 1H), 7.42–7.40 (m, 4H), 4.56 (q, J = 6.0 Hz, 2H), 4.27 (p, J = 9.0 Hz, 1H), 4.09–3.94 (dt, J = 12.0, 6.0 Hz, 1H), 3.70–3.53 (m, 3H), 1.49 (t, J = 9.0 Hz, 3H), 0.89 (d, J = 9.0 Hz, 3H). **^{13}C NMR** (75 MHz) δ 165.7, 150.9, 146.6, 144.8, 142.2, 140.2, 131.0, 129.3, 128.3 (2C), 128.2 (2C), 127.0, 126.5, 124.1, 122.4, 62.0, 49.3, 43.8, 31.9, 15.5, 14.3. **HRMS** (ESI) *m/z* calcd for $C_{22}H_{22}NO_2$ ($[M+H]^+$) 332.1651; found 332.1656.

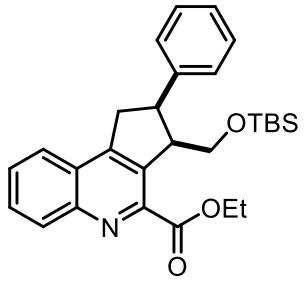

Ethyl 3-(((*tert*-butyldimethylsilyl)oxy)methyl)-2-phenyl-2,3-dihydro-1*H*-cyclopenta[*c*]quinoline-4-carboxylate (92o). Synthesized using general procedure 9. White oil (45.8 mg, 74%). **TLC**: R_f 0.50 (8:2 hexanes/EtOAc). **IR** (NaCl): 3854, 3744, 3618, 2951, 2930, 2887, 2857, 1717, 1647, 1562, 1504, 1464, 1368, 1317, 1248, 1186, 1157, 1119, 1094, 1061, 1030, 837, 777, 698. **^{1}H NMR** (300 MHz) δ 8.30 (d, J = 9 Hz, 1H), 7.89 (ddd, J = 8.1, 1.6, 0.7 Hz, 1H), 7.74 (ddd, J = 8.5, 6.8, 1.5 Hz, 1H), 7.65 (ddd, J = 8.1, 6.8, 1.3 Hz, 1H), 7.54 (ddd, J = 7.6, 1.5, 0.6 Hz, 2H), 7.43–7.36 (m, 2H), 7.33–7.29 (m, 1H), 4.55 (qd, J = 7.1, 1.3 Hz, 2H), 4.18 (dt, J = 9.0, 3.0 Hz, 1H), 4.03 (dt, J = 11.9, 8.0 Hz, 1H), 3.92–3.81 (m, 2H), 3.55–3.46 (m, 2H), 1.48 (t, J = 7.1 Hz, 3H), 0.49 (s, 9H), -0.33 (s, 3H), -0.59 (s, 3H). **^{13}C NMR** (101 MHz) δ 166.1, 154.2, 146.6, 139.9, 137.4,

130.9, 129.3, 128.7 (2C), 128.3, 128.3, 128.2 (2C), 126.8, 126.6, 124.0, 62.8, 61.9, 51.6, 49.1, 35.3, 25.4 (3C), 17.7, 14.4, -6.1, -6.3. **HRMS** (ESI) *m/z* calcd for $C_{28}H_{36}NO_3Si$ ($[M+H]^+$) 462.2464; found 462.2461.

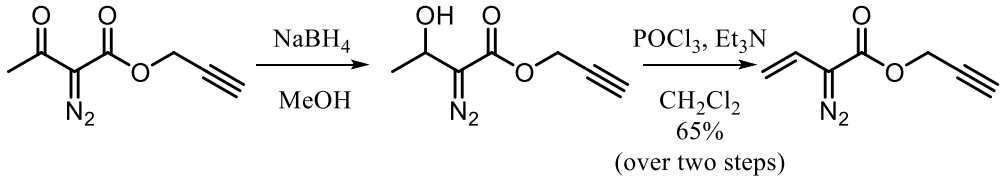

Prop-2-yn-1-yl 2-diazobut-3-enoate (96). The solution of prop-2-yn-1-yl 2-diazo-3-oxobutanoate (3.61 mmol) in 12 mL MeOH at 0 °C was slowly added $NaBH_4$ (137 mg, 3.61 mmol). The resulting solution was warmed to room temperature and stirred for 30 min. The MeOH was evaporated and the residue was diluted with water (15 mL) and extracted with EtOAc (50 mL) and dried over anhydrous Na_2SO_4. After the solvent was evaporated, the crude product was purified by column chromatography (3:1 hexanes/EtOAc) to give alcohol. To a solution of alcohol (3.42 mmol) and Et_3N (4.0 equiv) in 20 mL CH_2Cl_2 at 0 °C was slowly added a solution of $POCl_3$ (0.48 ml, 5.13 mmol, 1.5 equiv) in 5 mL CH_2Cl_2 over 5 minutes. The resulting solution was stirred at 0 °C for 2 h then the reaction mixture was diluted with DCM (10 mL) and water (10 mL). The aqueous layer was extracted with DCM (2 × 20 mL). The combined organic layers were dried over anhydrous Na_2SO_4 and concentrated under reduced pressure. Chromatographic purification of the crude compound over silica gel (gradient elution with 5–10% EtOAc in Hexane) yielded the pure compound **96** (351 mg, 65% over two steps) as a red oil. **IR** (NaCl): 3298, 3951, 2091, 1709, 1616, 1433, 1375, 1306, 1267, 1148, 1099, 1148, 1099, 1032, 978, 920, 880, 743, 681, 644. **^{1}H NMR** (400 MHz) δ 6.15 (ddd, J = 17.3, 11.0, 3.3

Hz, 1H), 5.13 (dd, J = 11.0, 3.3 Hz, 1H), 4.88 (dd, J = 17.6, 3.3 Hz, 1H), 4.80 (s, 2H), 2.49 (s, 1H). **^{13}C NMR** (101 MHz) δ 163.9, 119.9, 107.9, 77.4, 75.2, 52.4 (C=N_2 not observed).

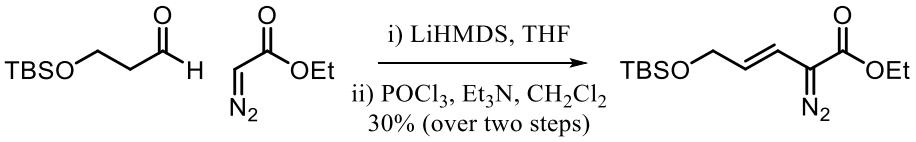

Ethyl (*E*)-5-((*tert*-butyldimethylsilyl)oxy)-2-diazopent-3-enoate (100). To a solution of ethyl diazoacetate (1.0 equiv, 0.2 M) in 7 mL anhydrous THF at –78 °C, was added LiHMDS (1.0 equiv, 1 M) in THF. The resulting mixture was stirred for 15 min at –78 °C. 3-((*tert*-butyldimethylsilyl)oxy)propanal (1.0 equiv, 0.8 M) in THF prepared from known literature protocol was added.[193] The resulting solution was stirred at –78 °C to –20 °C for 2 h. The reaction mixture was quenched by saturated solution of NH_4Cl (10 mL), extracted with EtOAc (30 mL) and the combined layers were dried over Na_2SO_4 and concentrated under reduced pressure to give the crude compound ethyl 5-((*tert*-butyldimethylsilyl)oxy)-2-diazo-3-hydroxypentanoate (0.5 mmol, 1.0 equiv), was redissolved in dry CH_2Cl_2 (3 mL) and Et_3N (2.2 mmol, 4.0 equiv) at 0 °C was slowly added a solution of $POCl_3$ (0.48 mL, 5.3 mmol) in 3 mL CH_2Cl_2 over 5 min. The resulting solution was stirred for 2 h at 0 °C. The reaction mixture was poured into ice water and extracted with DCM (30 mL). The combined layers were dried over Na_2SO_4 and concentrated under reduced pressure. Chromatographic purification of the crude compound over silica gel (1:49 EtOAc:Hex) yielded the pure compound **100** (101 mg, 30% over two steps) as a red liquid **TLC**: R_f 0.60 (9:1 hexanes/EtOAc). **IR** (NaCl): 2955, 2932, 2857, 2083, 1707, 1649, 1468, 1371, 1331, 1128, 1103, 1065, 1011, 955, 837, 777, 739. **^{1}H NMR** (400 MHz) δ 6.02 (dt, J = 16.0, 4.0 Hz, 1H), 5.44 (dt, J = 16.0, 8.0 Hz, 1H), 4.29–4.23 (m, 4H), 1.29 (t, J = 9.0 Hz, 3H), 0.91

(s, 9H), 0.08 (s, 6H). **^{13}C NMR** (101 MHz) δ 165.3, 123.2, 113.2, 63.4, 61.1, 25.9 (3C), 18.4, 14.4, -5.2 (2C).

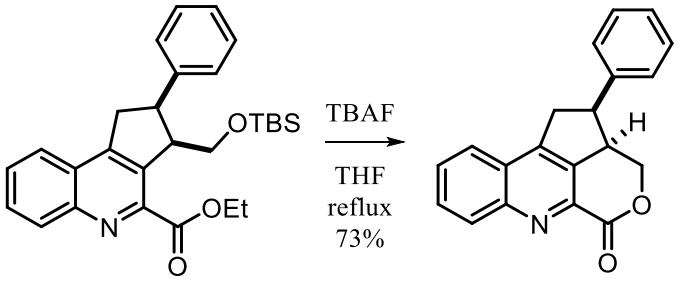

Ethyl 3-(((*tert*-butyldimethylsilyl)oxy)methyl)-2-phenyl-2,3-dihydro-1*H*-cyclopenta[*c*]quinoline-4-carboxylate (101). To a solution of **92o** (0.06 mmol, 0.03 M) in THF was added tetrabutylammonium fluoride solution (4.0 equiv, 1.0 M) in THF at 0 °C. Reaction was then refluxed 4 h and then quenched with water. The aqueous layer was extracted with EtOAc (3 × 5 mL), the combined organic layers were dried over anhydrous Na_2SO_4 and concentrated under reduced pressure. Chromatographic purification of the crude compound over silica gel (gradient elution with 100% EtOAc) yielded the compound **101** as pale yellow oil (13.8 mg, 73%). **TLC**: R_f 0.1 (5% MeOH/EtOAc). **IR** (NaCl): 3408, 3059, 2928, 2880, 1730, 1663, 1589, 1452, 1387, 1240, 1188, 1159, 1074, 1043, 760, 735, 702. **^{1}H NMR** (400 MHz) δ 8.27 (d, J = 8.5 Hz, 1H), 8.04–7.98 (d, J = 9.0 Hz, 1H), 7.85 (t, J = 7.7 Hz, 1H), 7.76 (t, J = 7.6 Hz, 1H), 7.50 (d, J = 6.0 Hz, 2H), 7.43 (t, J = 7.5 Hz, 2H), 7.33 (t, J = 3.0 Hz, 1H), 4.53 (q, J = 6.4 Hz, 1H), 4.12 (dt, J = 12.1, 7.9 Hz, 1H), 3.96–3.86 (m, 2H), 3.62 (dd, J = 16.5, 7.9 Hz, 1H), 3.52 (dd, J = 11.0, 6.6 Hz, 1H). **^{13}C NMR** (101 MHz) δ 164.8, 156.8, 143.8, 142.6, 138.7, 137.7, 131.1, 129.3, 128.7 (2C), 128.0 (2C), 127.5, 127.1, 126.3, 124.6, 62.8, 50.3, 48.8, 33.7. **HRMS** (ESI) *m/z* calcd for $C_{20}H_{16}NO_2$ ($[M+H]^+$) 302.1181; found 302.1178.

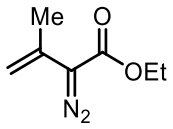

Ethyl 2-diazo-3-methylbut-3-enoate (104). Compound was prepared using known literature procedure.[194]

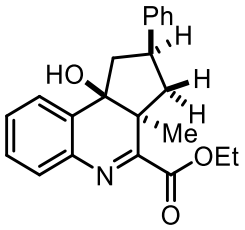

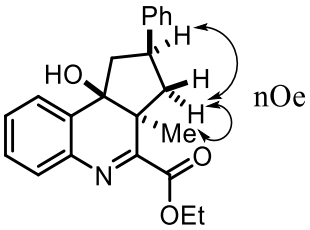

Prepared using general procedure D. Benzyl 9*b*-hydroxy-3*a*-methyl-2-phenyl-2,3,3*a*,9*b*-tetrahydro-1*H*-cyclopenta[*c*]quinoline-4-carboxylate (105, major diastereomer). Yellow oil (34 mg, 72%) as a 1.4:1 mixture of diastereomers 1**05** and **105'**. **TLC**: R_f 0.25 (4:1 hexanes/EtOAc). **IR** (NaCl): 2976, 2938, 2378, 2315, 1722, 1678, 1603, 1514, 1454, 1393, 1369, 1315, 1294, 1265, 1215, 1163, 1128, 1111, 1043, 858, 772, 752, 702. **^{1}H NMR** (400 MHz) δ 7.66–7.64 (m, 1H), 7.56–7.54 (m, 1H), 7.39–7.37 (m, 2H), 7.33–7.28 (m, 4H), 7.22–7.16 (m, 1H), 4.55–4.45 (m, 1H), 4.45–4.35 (m, 1H), 3.22–3.11 (m, 1H), 2.73 (dd, J = 13.4, 7.5 Hz, 1H), 2.42 (dd, J = 15.0, 11.5 Hz, 1H), 2.30–2.26 (m, 1H), 2.13 (dd, J = 15.1, 6.2 Hz, 1H), 1.83–1.77 (m, 1H), 1.44 (t, J = 7.0 Hz, 2H), 1.30 (s, 3H). **^{13}C NMR** (101 MHz) δ 167.3, 165.2, 145.7, 140.1, 133.5, 129.9, 128.8, 128.6, 128.5 (2C), 127.2 (2C), 126.2, 123.8, 80.9, 61.9, 51.6, 49.5, 44.5, 43.1, 15.3, 14.3. **HRMS** (ESI) *m/z* calcd for $C_{22}H_{24}NO_3$ ($[M+H]^+$) 350.1756; found 350.1756.

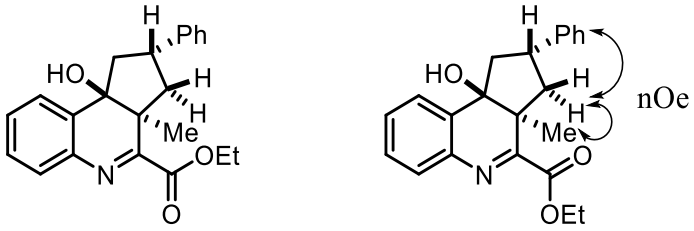

Benzyl 9*b*-hydroxy-3*a*-methyl-2-phenyl-2,3,3*a*,9*b*-tetrahydro-1*H*-cyclopenta[*c*]quinoline-4-carboxylate (105', minor diastereomer). Yellow oil (20.4 mg, 38%). **TLC**: R_f 0.19 (4:1 hexanes/EtOAc). **IR** (NaCl): 2978, 2936, 2361, 2334, 1719, 1649, 1558, 1539, 1508, 1456, 1369, 1290, 1238, 1042, 756, 700. **^{1}H NMR** (400 MHz) δ 7.69–7.67 (m, 1H), 7.60–7.57 (m, 1H), 7.42–7.37 (m, 2H), 7.24 (d, J = 7.4 Hz, 2H), 7.20–7.12 (m, 3H), 4.47–4.39 (m, 1H), 4.36–4.28 (m, 1H), 3.65–3.56 (m, 1H), 2.61 (dd, J = 14.7, 10.5 Hz, 1H), 2.41 (dd, J = 14.8, 7.1 Hz, 1H), 2.27 (dd, J = 13.6, 7.3 Hz, 1H), 2.05 (dd, J = 13.5, 11.5 Hz, 1H), 1.90 (s, 1H), 1.40 (s, 3H), 1.36 (t, J = 7.1 Hz, 2H). **^{13}C NMR** (101 MHz) δ 167.5, 165.3, 144.7, 139.8, 132.9, 130.0, 129.2, 128.8, 128.5 (2C), 127.1 (2C), 126.2, 124.5, 81.7, 61.9, 50.3, 49.0, 45.2, 39.8, 17.6, 14.2. **HRMS** (ESI) *m/z* calcd for $C_{22}H_{24}NO_3$ ([M+H]$^+$) 350.1756; found 350.1759.

Chapter 7.4. Experimentals for Chapter 5.

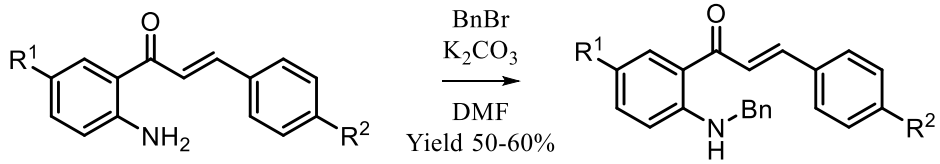

90a: R^1 = H, R^2 = H
90b: R^1 = H, R^2 =Cl
90c: R^1 = H, R^2 = OMe
90d: R^1 = H, R^2 = CN
90e: R^1 = Ph, R^2 = H
90f: R^1 = Br, R^2 = H

106a: R^1 = H, R^2 = H
106b: R^1 = H, R^2 =Cl
106c: R^1 = H, R^2 = OMe
106d: R^1 = H, R^2 = CN
106e: R^1 = Ph, R^2 = H
106f: R^1 = Br, R^2 = H

General Procedure 10: To a solution of corresponding 2'-aminochalcone **90** (1.0 equiv, 0.33 M) in DMF was successively added potassium carbonate (3.0 equiv) and benzyl

bromide (2.0 equiv) at 0 °C. Reaction was then allowed to stir at 25 °C for 12-24 h. Reaction was quenched with water and extracted with diethyl ether (3 x 7 mL). The combined organic layers were dried over anhydrous Na_2SO_4 and concentrated under reduced pressure. Chromatographic purification of the crude compound over silica gel (gradient elution with 5–15% EtOAc in Hexane) yielded pure benzylated product **106**.

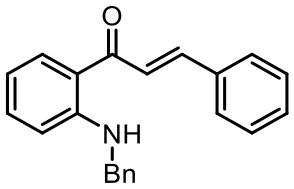

(*E*)-1-(2-(benzylamino)phenyl)-3-phenylprop-2-en-1-one (106a). Starting Material was prepared using general procedure 10 and matched literature known values.[195]

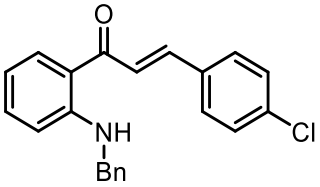

(*E*)-1-(2-(benzylamino)phenyl)-3-(4-chlorophenyl)prop-2-en-1-one (106b). Synthesized using general procedure 10. Orange solid (mp 155–156 °C). **TLC**: R_f 0.57 (4:1 hexanes/EtOAc). **IR** (NaCl): 3289, 3076, 3028, 1638, 1605, 1570, 1514, 1487, 1447, 1406, 1312, 1288, 1269, 1198, 1157, 1086, 1003, 974, 816, 737, 696. **^{1}H NMR** (300 MHz) δ 9.52 (t, J = 5.8 Hz, 1H), 7.92 (dd, J = 8.1, 1.6 Hz, 1H), 7.67 (d, J = 1.6 Hz, 2H), 7.57–7.54 (m, 2H), 7.40–7.26 (m, 8H), 6.72 (d, J = 8.6 Hz, 1H), 6.67 (t, J = 7.5 Hz, 1H), 4.50 (d, J = 5.6 Hz, 2H). **^{13}C NMR** (75 MHz) δ 191.2, 151.7, 141.1, 138.5, 135.8, 135.1, 133.8, 131.5, 129.3 (2C), 129.1 (2C), 128.7 (2C), 127.2, 127.1 (2C), 123.6, 118.3, 114.5, 112.3, 46.9. **HRMS** (ESI) *m/z* calcd for $C_{22}H_{19}ClNO$ ($[M+H]^+$) 348.1155; found 348.1161.

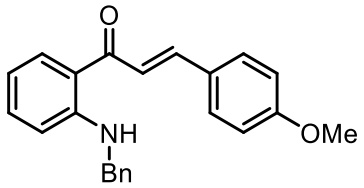

(*E*)-1-(2-(benzylamino)phenyl)-3-(4-methoxyphenyl)prop-2-en-1-one (106c). Starting Material was prepared using general procedure 10 and matched literature known values.[196]

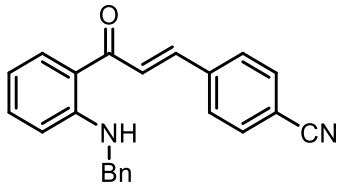

(*E*)-4-(3-(2-(benzylamino)phenyl)-3-oxoprop-1-en-1-yl)benzonitrile (106d). Synthesized using general procedure 10. Orange solid (mp 147–149 °C). **TLC**: R_f 0.80 (4:1 hexanes/EtOAc). **IR** (NaCl): 3319, 3287, 3063, 3032, 2924, 2851, 2224, 1641, 1607, 1572, 1514, 1452, 1414, 1346, 1327, 1296, 1275, 1244, 1207, 1165, 1080, 1053, 1005, 974, 827, 748, 700, 652. **^{1}H NMR** (300 MHz) δ 9.55 (t, J = 5.7 Hz, 1H), 7.90 (dd, J = 8.2, 1.6 Hz, 1H), 7.76 (d, J = 15.6 Hz, 1H), 7.70–7.64 (m, 5H), 7.40–7.26 (m, 6H), 6.73 (dd, J = 8.7, 1.1 Hz, 1H), 6.67 (ddd, J = 8.1, 7.0, 1.1 Hz, 1H), 4.50 (d, J = 5.5 Hz, 2H). **^{13}C NMR** (75 MHz) δ 190.5, 151.8, 139.9, 139.6, 138.3, 135.4, 132.5 (2C), 131.5, 128.7 (2C), 128.4 (2C), 127.2, 127.0 (2C), 126.3, 118.5, 118.0, 114.5, 112.8, 112.3, 46.8. **HRMS** (ESI) *m/z* calcd for $C_{23}H_{19}N_2O$ ($[M+H]^+$) 339.1497; found 339.1498.

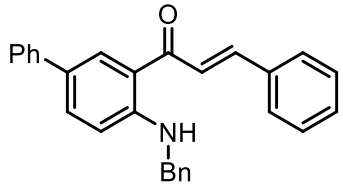

(*E*)-1-(4-(benzylamino)-[1,1'-biphenyl]-3-yl)-3-phenylprop-2-en-1-one (106e). Synthesized using general procedure 10. Orange solid (mp 145–147 °C). **TLC**: R_f 0.77 (4:1 hexanes/EtOAc). **IR** (NaCl): 3300, 3028, 2849, 1641, 1614, 1566, 1524, 1491, 1450, 1425, 1354, 1271, 1186, 1070, 1026, 1001, 974, 853, 818, 766, 737, 696. **^{1}H NMR** (300 MHz) δ 9.58 (t, J = 5.7 Hz, 1H), 8.17 (d, J = 2.3 Hz, 1H), 7.87–7.74 (m, 2H), 7.70–7.58 (m, 5H), 7.50–7.32 (m, 11H), 6.83 (d, J = 8.8 Hz, 1H), 4.57 (d, J = 5.3 Hz, 2H). **^{13}C NMR** (75 MHz) δ 191.7, 150.8, 143.0, 140.6, 138.4, 135.2, 133.8, 130.1, 129.9, 128.8 (2C), 128.8 (2C), 128.7 (2C), 128.3 (2C), 127.6, 127.2, 127.1 (2C), 126.4, 126.3, 123.0, 118.8, 112.8, 46.9. **HRMS** (ESI) *m/z* calcd for $C_{28}H_{24}NO$ ($[M+H]^+$) 390.1858; found 390.1861.

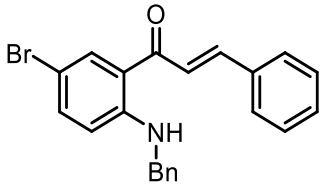

(*E*)-1-(2-(benzylamino)-5-bromophenyl)-3-phenylprop-2-en-1-one (106f). Synthesized using general procedure 10. Orange solid (mp 137–140°C). **TLC**: R_f 0.54 (9:1 hexanes/EtOAc). **IR** (neat): 3285, 3052, 3022, 2933, 2909, 2876,1635, 1597, 1563, 1494, 1474, 1446, 1410, 1348, 1323, 1304, 1276, 1184, 1173, 1096, 988, 854, 805, 769, 734, 687, 643, 576. **^{1}H NMR** (300 MHz) δ 9.48 (t, J = 5.7 Hz, 1H), 8.00 (d, J = 2.4 Hz, 1H), 7.76 (d, J = 15.5 Hz, 1H), 7.68–7.63 (m, 2H), 7.58 (d, J = 15.5 Hz, 1H), 7.46–7.38 (m, 3H), 7.38–7.33 (m, 4H), 7.33–7.27 (m, 1H), 6.60 (dd, J = 9.1, 0.9 Hz, 1H), 4.48 (t, J = 2.9 Hz, 2H). **^{13}C NMR** (75 MHz) δ 190.7, 150.4, 150.2, 143.7, 138.0, 137.4, 135.0, 133.6, 130.3, 128.9, 128.8, 128.4, 127.3, 127.0, 122.4, 122.4, 119.9, 114.2, 114.2, 105.8, 46.9, 46.8. **LRMS** (ESI) *m/z* calcd for $C_{22}H_{21}BrNO_2$ ($[M+H+H_2O]^+$) 410.1; found 410.3.

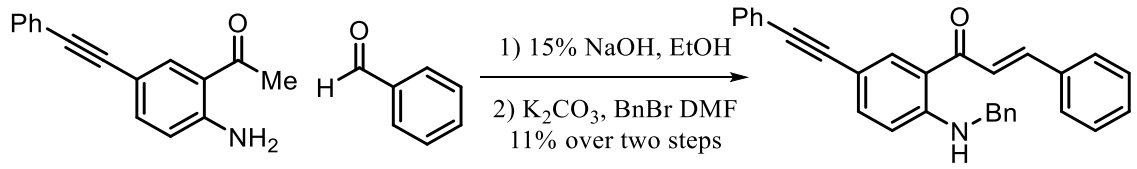

To a solution of 1-(2-amino-5-(phenylethynyl)phenyl)ethan-1-one (2.5 mmol) prepared according to literature known protocol and benzaldehyde (3.0 mmol) in 10 mL of ethanol was added 1.4 mL of 15 wt % NaOH solution at 0 °C. This was allowed to stir to 25 °C for 24 h. A precipitate formed, and this was filtered and washed with water and then hexanes. The isolated solid was taken forward without further purification. Then 550 mg of chalcone was then dissolved in 5 mL anhydrous DMF. Three equivalence of K_2CO_3 was added followed by benzyl bromide at 25 °C. The reaction was allowed to stir for 24 hours upon which it was quenched with ammonium chloride solution and extracted with diethyl ether three times. The combined organic layers were washed twice with water and filtered over sodium sulfate. The filtrate was concentrated to volume and immediately purified by flash column chromatography eluting product with a gradient of hexanes to 30% ethyl acetate:hexanes providing **(*E*)-1-(2-(benzylamino)-5-(phenylethynyl)phenyl)-3-phenylprop-2-en-1-one** (**106g**). 109 mg, 11% yield over two steps. **IR** (neat): 3261, 3056, 3029, 2917, 2848, 2212, 1641, 1611, 1556, 1516, 1427, 1353, 1271, 1186, 1142, 1069, 998, 974, 851, 820, 776, 754, 744, 688, 668, 608, 579. **^{1}H NMR** (400 MHz) δ 9.70 (t, *J* = 5.7 Hz, 1H), 8.14 (d, *J* = 2.0 Hz, 1H), 7.82–7.64 (m, 4H), 7.57–7.51 (m, 2H), 7.49 (dd, *J* = 8.8, 1.9 Hz, 1H), 7.46–7.40 (m, 2H), 7.40–7.28 (m, 5H), 6.71 (d, *J* = 8.8 Hz, 1H), 4.53 (d, *J* = 5.6 Hz, 2H). **^{13}C NMR** (101 MHz) δ 191.2, 151.3, 143.4, 138.0, 137.8, 135.2, 135.1, 131.4 (2C), 130.3, 128.9 (2C), 128.8 (2C), 128.4 (2C), 128.3 (2C), 127.8, 127.4, 127.1 (2C), 123.6, 122.6, 118.4, 112.5, 108.8, 89.5, 87.4, 46.9. **HRMS** (ESI) *m/z* calcd for $C_{30}H_{24}NO$ ($[M+H]^+$) 414.1858; found 414.1866.

General procedure 11 for the synthesis of azacycles 107

To a stirred solution of benzyl protected 2'-aminochalcone (0.11 mmol) and $Rh_2(OAc)_4$ (1 mol%) in 1.1 mL toluene was added a solution of corresponding vinyl diazoacetate **48** (0.22 mmol) in 0.5 mL toluene over 2.5 h *via* syringe pump at reflux. After the addition was completed, the reaction was left to stir at refluxing temperature for an additional 30 minutes. The crude reaction mixture was concentrated using rotary evaporation and then purified using flash column chromatography eluting with 10-15% ethyl acetate: hexanes to afford azacycle product **107a**–**107e.**

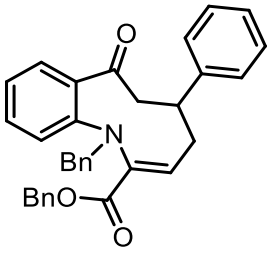

Benzyl (*Z*)-1-benzyl-7-oxo-5-phenyl-4,5,6,7-tetrahydro-1*H*-benzo[*b*]azonine-2-carboxylate (107a). Synthesized using general procedure 11. Pale yellow oil (30 mg, 67%). **TLC**: R_f 0.42 (4:1 hexanes/EtOAc). **IR** (NaCl): 3782, 3030, 2390, 2309, 1721, 1686, 1595, 1485, 1449, 1240, 1163, 1142, 1034, 750, 698. **^{1}H NMR** (500 MHz) δ 7.44 (d, J = 6.9 Hz, 2H), 7.40–7.27 (m, 9H), 7.24–7.15 (m, 6H), 7.12 (d, J = 8.2 Hz, 1H), 7.00–6.92 (m, 2H), 5.10 (d, J = 12.4 Hz, 1H), 5.03–4.92 (m, 2H), 4.40 (d, J = 14.2 Hz, 1H), 3.65–3.56 (m, 1H), 3.46 (t, J = 12.1 Hz, 1H), 2.87 (td, J = 12.1, 9.7 Hz, 1H), 2.44 (d, J = 13.3 Hz, 1H), 2.07–2.00 (m, 1H). **^{13}C NMR** (101 MHz) δ 206.1, 163.9, 146.7, 145.3, 142.5, 140.7, 137.2, 135.6, 134.6, 131.3, 128.7 (2C), 128.7 (2C), 128.6 (2C), 128.4 (2C), 128.1, 128.0 (2C), 127.8, 127.6, 126.6, 126.6 (2C), 121.0, 118.3, 66.7, 55.9, 49.4, 41.7, 34.9. **HRMS** (ESI) *m/z* calcd for $C_{33}H_{29}NO_3Na$ ($[M+Na]^+$) 510.2045; found 510.2061.

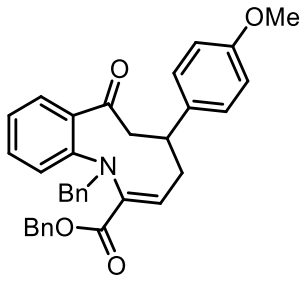

Benzyl (*Z*)-1-benzyl-5-(4-methoxyphenyl)-7-oxo-4,5,6,7-tetrahydro-1*H*-benzo[*b*]azonine-2-carboxylate (107b). Synthesized using general procedure 11. Red oil (32.5 mg, 75%). **TLC**: R_f 0.22 (4:1 hexanes/EtOAc). **IR** (NaCl): 3030, 2932, 2835, 1717, 1682, 1645, 1595, 1512, 1452, 1369, 1288, 1250, 1173, 1142, 1034, 910, 829, 748, 739, 698. **^{1}H NMR** (400 MHz) δ 7.44 (d, J = 7.3 Hz, 2H), 7.39–7.25 (m, 7H), 7.18 (dt, J = 7.5, 2.1 Hz, 3H), 7.12 (dd, J = 8.4, 4.0 Hz, 3H), 7.00–6.92 (m, 2H), 6.85 (d, J = 8.5 Hz, 2H), 5.11 (d, J = 12.4 Hz, 1H), 5.04–4.91 (m, 2H), 4.40 (d, J = 14.3 Hz, 1H), 3.79 (s, 3H), 3.63–3.52 (m, 1H), 3.43 (t, J = 12.2 Hz, 1H), 2.90–2.79 (m, 1H), 2.42 (d, J = 13.3 Hz, 1H), 2.07–1.97 (m, 1H). **^{13}C NMR** (101 MHz) δ 206.3, 163.9, 158.2, 146.7, 142.6, 140.7, 137.4, 137.2, 135.6, 134.6, 131.3, 128.6, 128.5, 128.4, 128.1, 127.9, 127.7, 127.5, 127.5, 120.9, 118.2, 113.9, 66.7, 55.9, 55.2, 49.7, 40.9, 35.2. **HRMS** (ESI) *m/z* calcd for $C_{34}H_{32}NO_4$ ($[M+H]^+$) 518.2331; found 518.2333.

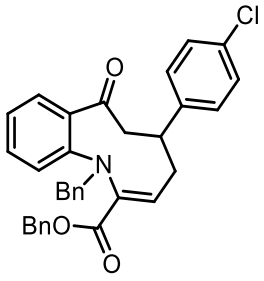

Benzyl (*Z*)-1-benzyl-5-(4-chlorophenyl)-7-oxo-4,5,6,7-tetrahydro-1*H*-benzo[*b*]azonine-2-carboxylate (107c). Synthesized using general procedure 11. Brown oil (25 mg, 69%). **TLC**: R_f 0.40 (4:1 hexanes/EtOAc). **IR** (NaCl): 3063, 3032, 2955, 2932,

2864, 2380, 1717, 1684, 1651, 1595, 1489, 1452, 1371, 1296, 1240, 1165, 1142, 1096, 1042, 1011, 984, 934, 910, 826, 737, 700. **^{1}H NMR** (400 MHz) δ 7.41 (d, J = 7.0 Hz, 2H), 7.38–7.24 (m, 9H), 7.20–7.08 (m, 6H), 6.95 (t, J = 7.4 Hz, 2H), 5.10 (d, J = 12.4 Hz, 1H), 5.00 (d, J = 14.1 Hz, 1H), 4.95 (d, J = 12.4 Hz, 1H), 4.39 (d, J = 14.1 Hz, 1H), 3.56 (t, J = 12.0 Hz, 1H), 3.43 (t, J = 12.1 Hz, 1H), 2.76 (q, J = 12.0 Hz, 1H), 2.39 (d, J = 13.3 Hz, 1H), 1.98–1.93 (m, 1H). **^{13}C NMR** (101 MHz) δ 205.7, 163.9, 146.8, 143.7, 142.1, 140.8, 137.2, 135.6, 134.5, 132.3, 131.4, 128.8 (2C), 128.8 (2C), 128.6 (2C), 128.4 (2C), 128.1, 128.0 (2C), 127.9 (2C), 127.8, 127.6, 121.1, 118.3, 66.8, 55.9, 49.2, 41.1, 34.8. **HRMS** (ESI) *m/z* calcd for $C_{33}H_{29}ClNO_3$ ($[M+H]^+$) 522.1836; found 522.1838.

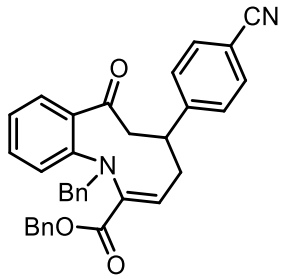

Benzyl (*Z*)-1-benzyl-5-(4-cyanophenyl)-7-oxo-4,5,6,7-tetrahydro-1*H*-benzo[*b*]azonine-2-carboxylate (107d). Synthesized using general procedure 11. Brown oil (24.5 mg, 56%). **TLC**: R_f 0.13 (4:1 hexanes/EtOAc). **IR** (NaCl): 3032, 2432, 2386, 2303, 2228, 1721, 1684, 1595, 1487, 1450, 1375, 1244, 1163, 1043, 910, 735, 700. **^{1}H NMR** (400 MHz) δ 7.60 (d, J = 7.9 Hz, 2H), 7.40 (d, J = 7.5 Hz, 2H), 7.37–7.28 (m, 9H), 7.18 (d, J = 7.5 Hz, 4H), 6.99–6.89 (m, 2H), 5.09 (d, J = 12.5 Hz, 1H), 5.00 (d, J = 14.0 Hz, 1H), 4.95 (d, J = 12.4 Hz, 1H), 4.39 (d, J = 14.1 Hz, 1H), 3.59 (t, J = 12.5 Hz, 1H), 3.48 (t, J = 12.0 Hz, 1H), 2.72 (q, J = 11.3 Hz, 1H), 2.37 (d, J = 13.1 Hz, 1H), 1.93 (t, J = 8.0 Hz, 1H). **^{13}C NMR** (101 MHz) δ 205.1, 163.8, 150.5, 146.9, 141.4, 140.9, 137.2, 135.5, 134.3, 132.6 (2C), 131.6, 128.9 (2C), 128.6 (2C), 128.5, 128.4 (2C), 128.2, 128.0 (2C),

127.9, 127.7, 127.4 (2C), 121.3, 118.4, 110.7, 66.8, 55.8, 48.6, 41.6, 34.3. **HRMS** (ESI) *m/z* calcd for $C_{34}H_{29}N_2O_3$ ($[M+H]^+$) 513.2178; found 513.2182.

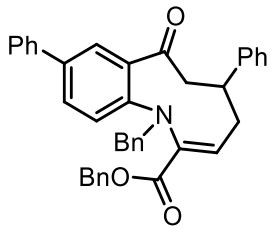

Benzyl (*Z*)-1-benzyl-7-oxo-5,9-diphenyl-4,5,6,7-tetrahydro-1*H*-benzo[*b*]azonine-2-carboxylate (107e). Synthesized using general procedure 11. Brown oil (25 mg, 71%). **TLC**: R_f 0.39 (4:1 hexanes/EtOAc). **IR** (NaCl): 3061, 3030, 2361, 2330, 1717, 1686, 1551, 1603, 1506, 1481, 1452, 1238, 1202, 1153, 1038, 905, 822, 758, 739, 696. **^{1}H NMR** (400 MHz) δ 7.54 (d, *J* = 8.0 Hz, 3H), 7.47 (d, *J* = 7.5 Hz, 3H), 7.43–7.34 (m, 5H), 7.34–7.26 (m, 6H), 7.25–7.15 (m, 6H), 7.01 (t, *J* = 8.4 Hz, 1H), 5.15 (d, *J* = 12.5 Hz, 1H), 5.05 (d, *J* = 14.3 Hz, 1H), 4.96 (d, *J* = 12.4 Hz, 1H), 4.44 (d, *J* = 14.3 Hz, 1H), 3.64 (t, *J* = 12.6 Hz, 1H), 3.49 (t, *J* = 12.1 Hz, 1H), 2.90 (q, *J* = 11.4 Hz, 1H), 2.48 (d, *J* = 13.4 Hz, 1H), 2.06 (dd, *J* = 12.5, 7.0 Hz, 1H). **^{13}C NMR** (101 MHz) δ 206.1, 163.9, 146.1, 145.2, 142.6, 140.7, 139.8, 137.2, 135.6, 134.9, 133.7, 129.6, 128.7 (2C), 128.7 (4C), 128.6 (2C), 128.4 (2C), 128.1, 128.0 (2C), 127.6, 126.9, 126.7, 126.6 (4C), 126.3, 118.7, 66.8, 56.1, 49.5, 41.8, 35.1. **HRMS** (ESI) *m/z* calcd for $C_{39}H_{34}NO_3$ ($[M+H]^+$) 564.2539; found 564.2536.

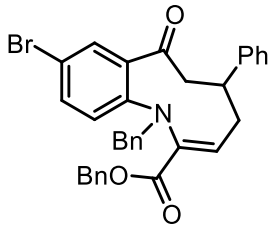

Benzyl (*Z*)-1-benzyl-9-bromo-7-oxo-5-phenyl-4,5,6,7-tetrahydro-1*H*-benzo[*b*]azonine-2-carboxylate (107f). Synthesized using general procedure 11.

Appearance (34.0 mg, 78%). **TLC**: R_f 0.40 (4:1 hexanes/EtOAc). **IR** (neat): 3061, 3029, 2929, 1717, 1687, 1654, 1584, 1474, 1452, 1399, 1232, 1173, 1151, 807, 731, 694. **^{1}H NMR** (300 MHz) δ 7.49–7.11 (m, 18H), 7.04–6.91 (m, 2H), 5.15 (d, *J* = 12.3 Hz, 1H), 4.99–4.85 (m, 2H), 4.38 (d, *J* = 14.3 Hz, 1H), 3.64–3.37 (m, 2H), 2.87 (td, *J* = 11.8, 9.7 Hz, 1H), 2.51–2.37 (m, 1H), 2.06 (ddd, *J* = 11.4, 7.3, 2.2 Hz, 1H). **^{13}C NMR** (101 MHz) δ 204.4, 163.7, 145.8, 144.9, 142.7, 140.5, 136.7, 135.9, 135.4, 133.8, 130.3, 128.8 (2C), 128.7 (2C), 128.6 (2C), 128.5 (2C), 128.2, 128.1 (2C), 127.7, 126.8, 126.5 (2C), 120.2, 113.8, 66.9, 56.1, 49.2, 41.8, 35.0. **HRMS** (ESI) *m/z* calcd for $C_{33}H_{29}BrNO_3$ ($[M+H]^+$) 566.1331; found 566.1300.

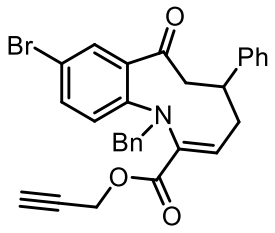

Prop-2-yn-1-yl (*Z*)-1-benzyl-9-bromo-7-oxo-5-phenyl-4,5,6,7-tetrahydro-1*H*-benzo[*b*]azonine-2-carboxylate (107g). Synthesized using general procedure 11. Appearance (29.0 mg, 74%). **TLC**: R_f 0.43 (4:1 hexanes/EtOAc). **IR** (neat): 3285, 3061, 3026, 2129, 1723, 1698, 1597, 1267, 1173, 1074, 933, 731, 697, 632. **^{1}H NMR** (400 MHz) δ 7.49–7.27 (m, 9H), 7.26–7.18 (m, 4H), 7.07 (d, *J* = 8.8 Hz, 1H), 7.04–6.97 (m, 1H), 4.97 (d, *J* = 14.2 Hz, 1H), 4.72–4.63 (m, 1H), 4.52 (dd, *J* = 15.6, 2.5 Hz, 1H), 4.45–4.35 (m, 1H), 3.57 (dd, *J* = 13.3, 11.8 Hz, 1H), 3.51–3.42 (m, 1H), 2.86 (td, *J* = 12.0, 9.7 Hz, 1H), 2.45 (td, *J* = 5.4, 2.1 Hz, 2H), 2.12–2.01 (m, 1H). **^{13}C NMR** (101 MHz) δ 204.5, 163.0, 145.7, 144.9, 143.5, 139.9, 136.7, 135.9, 133.9, 130.3, 128.8 (2C), 128.7 (2C), 128.7 (2C), 127.8, 127.6, 126.8, 126.5 (2C), 120.4, 114.0, 75.1, 56.1, 52.5, 49.2, 41.8, 35.0. **LRMS** (ESI) *m/z* calcd for $C_{29}H_{24}BrNO_3Na$ ($[M+Na]^+$) 536.1; found 537.0.

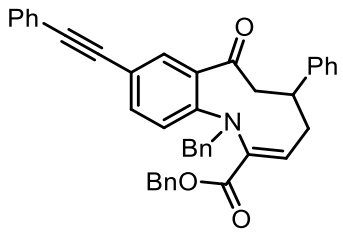

Benzyl (*Z*)-1-benzyl-7-oxo-5-phenyl-9-(phenylethynyl)-4,5,6,7-tetrahydro-1*H*-benzo[*b*]azonine-2-carboxylate (107h). Synthesized using general procedure 11. White solid (28.5 mg, 80%, mp 183–185 °C). **TLC**: R_f 0.38 (4:1 hexanes/EtOAc). **IR** (neat): 3031, 2967, 2949, 2844, 2209, 1703, 1690, 1590, 1494, 1253, 1044, 1033, 1024, 1005, 906, 822, 751, 693, 599. **^{1}H NMR** (500 MHz) δ 7.51–7.47 (m, 2H), 7.43 (ddd, *J* = 8.5, 5.9, 1.8 Hz, 3H), 7.39–7.28 (m, 11H), 7.25–7.15 (m, 5H), 7.08 (d, *J* = 8.6 Hz, 1H), 7.00 (dd, *J* = 9.8, 7.4 Hz, 1H), 5.14 (d, *J* = 12.4 Hz, 1H), 5.03–4.92 (m, 2H), 4.41 (d, *J* = 14.3 Hz, 1H), 3.55 (dd, *J* = 13.3, 11.7 Hz, 1H), 3.47 (tt, *J* = 11.9, 2.0 Hz, 1H), 2.86 (td, *J* = 12.0, 9.8 Hz, 1H), 2.46 (dt, *J* = 13.1, 1.3 Hz, 1H), 2.09–2.01 (m, 1H). **^{13}C NMR** (126 MHz) δ 205.0, 163.8, 146.7, 145.0, 142.9, 140.3, 136.8, 135.5, 134.5, 134.3, 131.5 (2C), 131.1, 128.8 (2C), 128.7 (2C), 128.6 (2C), 128.5 (2C), 128.3 (2C), 128.2, 128.1 (2C), 128.0, 127.7, 126.7, 126.6 (2C), 123.4, 118.2, 115.8, 89.1, 88.7, 66.9, 56.0, 49.4, 41.9, 35.1. **HRMS** (ESI) *m/z* calcd for $C_{41}H_{34}NO_3$ ($[M+H]^+$) 588.2539; found 588.2525. CCDC 1887929.

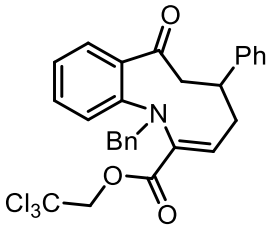

2,2,2-trichloroethyl (*Z*)-1-benzyl-7-oxo-5-phenyl-4,5,6,7-tetrahydro-1*H*-benzo[*b*]azonine-2-carboxylate (107i). Synthesized using general procedure 11. White solid (42 mg, 83%, mp 176-178 °C). **TLC**: R_f 0.35 (4:1 hexanes/EtOAc). **IR** (neat): 3062,

3029, 2949, 2921, 2874, 1719, 1676, 1637, 1593, 1484, 1463, 1225, 1141, 1042, 908, 783, 752, 720, 701, 579. **^{1}H NMR** (500 MHz) δ 7.50–7.46 (m, 2H), 7.40–7.35 (m, 3H), 7.35–7.28 (m, 3H), 7.25–7.19 (m, 4H), 7.15 (dd, *J* = 7.5, 1.6 Hz, 1H), 7.10 (dd, *J* = 9.7, 7.4 Hz, 1H), 6.97–6.91 (m, 1H), 5.06 (d, *J* = 14.0 Hz, 1H), 4.65 (qd, *J* = 12.0, 0.9 Hz, 2H), 4.47 (d, *J* = 14.0 Hz, 1H), 3.60 (dd, *J* = 13.5, 11.7 Hz, 1H), 3.52–3.42 (m, 1H), 2.85 (td, *J* = 12.1, 9.8 Hz, 1H), 2.45 (dt, *J* = 13.5, 1.4 Hz, 1H), 2.10–2.02 (m, 1H). **^{13}C NMR** (101 MHz) δ 206.1, 162.7, 146.4, 145.1, 144.8, 139.4, 137.0, 134.7, 131.4, 128.9 (2C), 128.7 (2C), 128.6 (2C), 127.8, 127.7, 126.7, 126.6 (2C), 121.3, 118.5, 94.8, 74.3, 55.8, 49.4, 41.4, 35.1. **HRMS** (ESI) *m/z* calcd for $C_{28}H_{25}Cl_3NO_3$ ($[M+H]^+$) 528.0900; found 528.0905. CCDC 1887930.

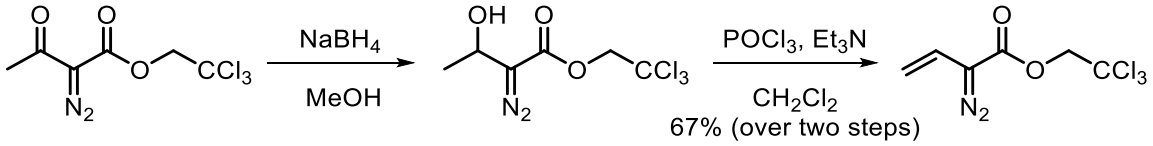

2,2,2-trichloroethyl 2-diazobut-3-enoate (111). Synthesized using the same protocol as diazo compound **48**. (424.1 mg, 67% over two steps) as a red oil. **IR** (neat): 3091, 3071, 3036, 2100, 1713, 1617, 1479, 1373, 1303, 1265, 1113, 1036, 716, 672, 576. **^{1}H NMR** (500 MHz) δ 6.17 (ddd, *J* = 17.5, 11.1, 2.1 Hz, 1H), 5.17 (d, *J* = 11.0 Hz, 1H), 4.95 (d, *J* = 2.2 Hz, 1H), 4.84 (s, 1H). **^{13}C NMR** (126 MHz) δ 163.0, 119.6, 108.4, 94.9, 73.9 (C=N_2 not observed). **HRMS** (ESI) *m/z* calcd for $C_6H_6Cl_3N_2O_2$ ($[M+H]^+$) 242.9495; found 242.9501.

Spectral Data

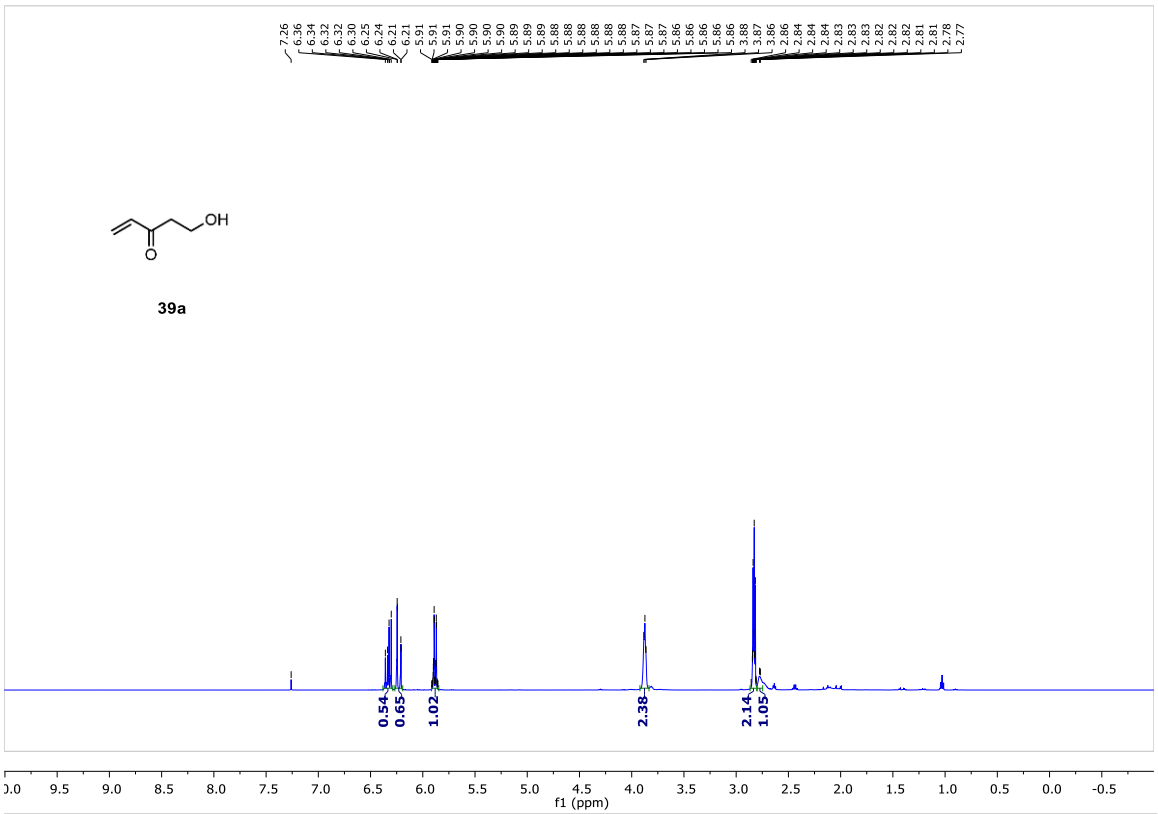
7.26
6.36
6.34
6.32
6.30
6.25
6.24
6.21
5.91
5.90
5.89
5.88
5.87
5.86
3.88
3.87
3.86
2.84
2.83
2.82
2.81
2.78
2.77
OH
O
39a
0.54
0.65
1.02
2.38
2.14
1.05
f1 (ppm)

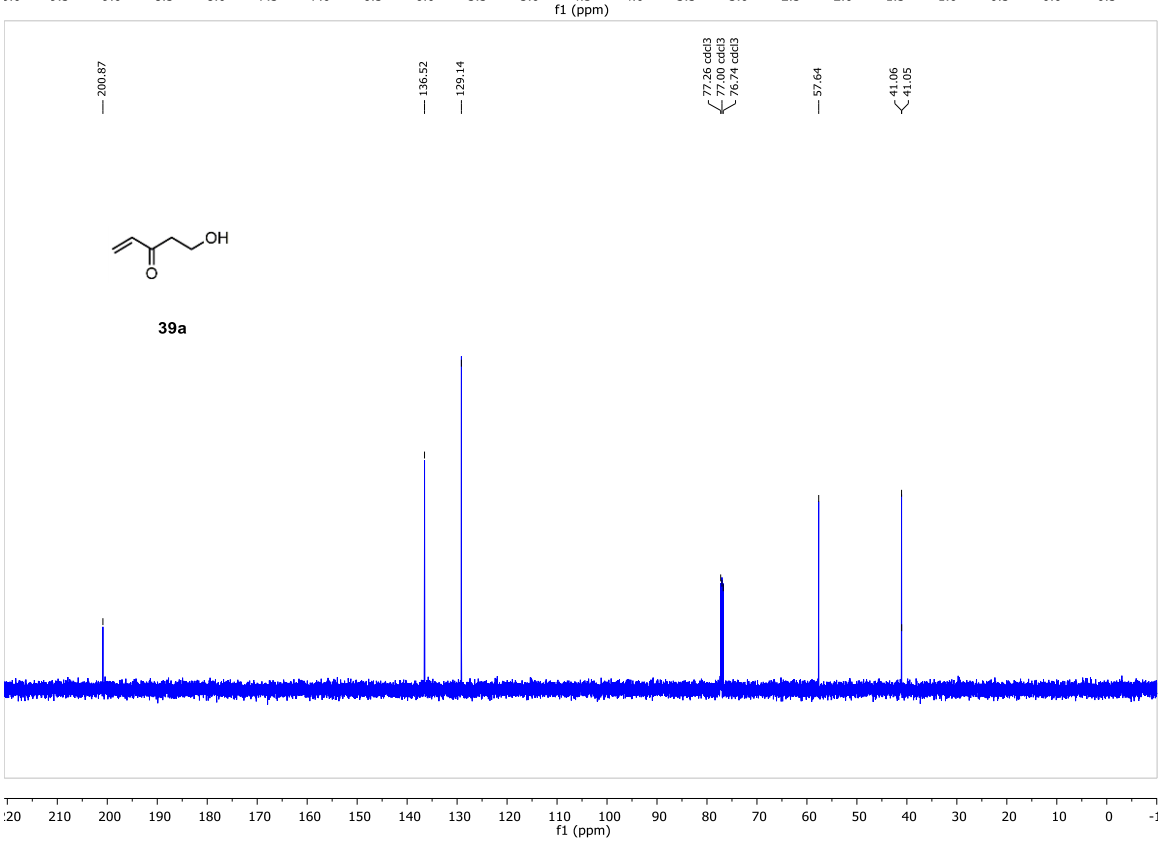
200.87
136.52
129.14
77.26 cdcl3
77.00 cdcl3
76.74 cdcl3
57.64
41.06
41.05
OH
O
39a
f1 (ppm)

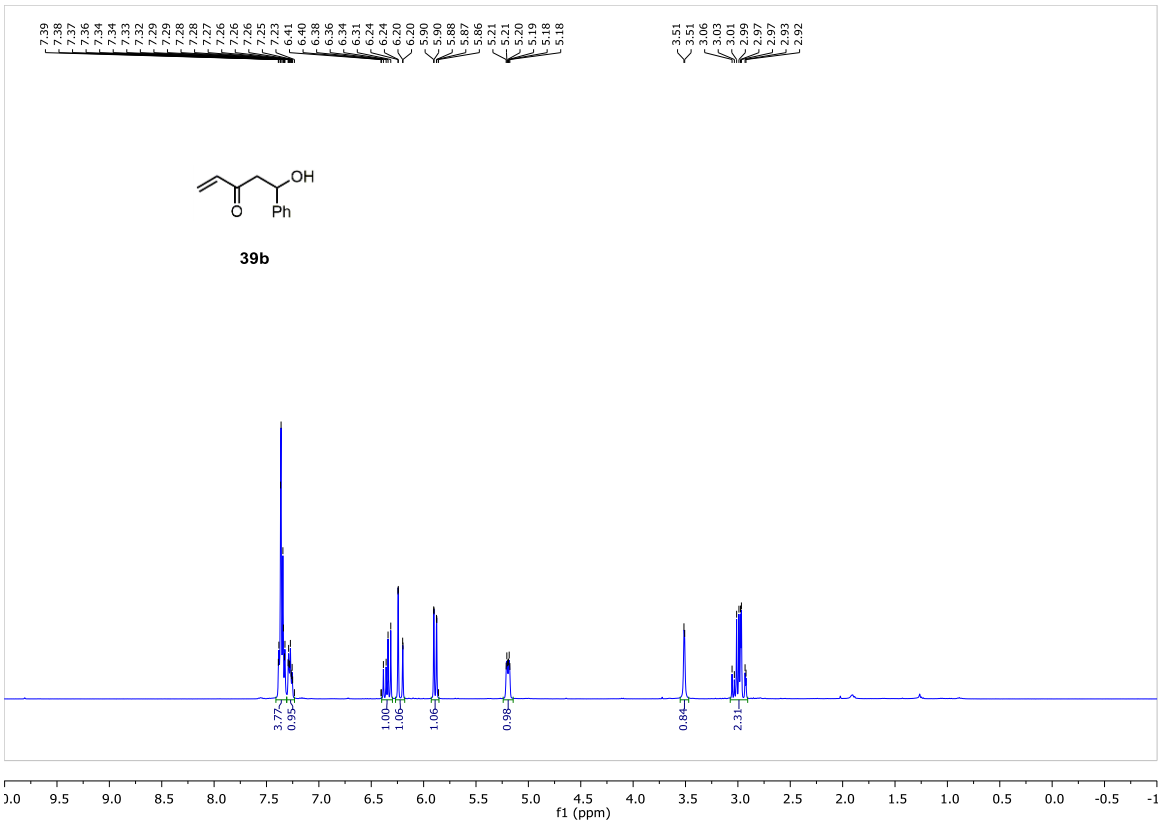
7.39 7.38 7.37 7.36 7.34 7.33 7.32 7.29 7.29 7.28 7.28 7.27 7.26 7.26 7.26 7.25 7.23 6.41 6.40 6.38 6.36 6.34 6.31 6.24 6.24 6.20 6.20 5.90 5.90 5.88 5.87 5.86 5.21 5.20 5.19 5.18 5.18
3.51 3.51 3.06 3.03 3.01 2.99 2.97 2.97 2.93 2.92
OH
O
Ph
39b
3.77 0.95 1.00 1.06 1.06 0.98 0.84 2.31
0.0 9.5 9.0 8.5 8.0 7.5 7.0 6.5 6.0 5.5 5.0 4.5 4.0 3.5 3.0 2.5 2.0 1.5 1.0 0.5 0.0 -0.5 -1
f1 (ppm)

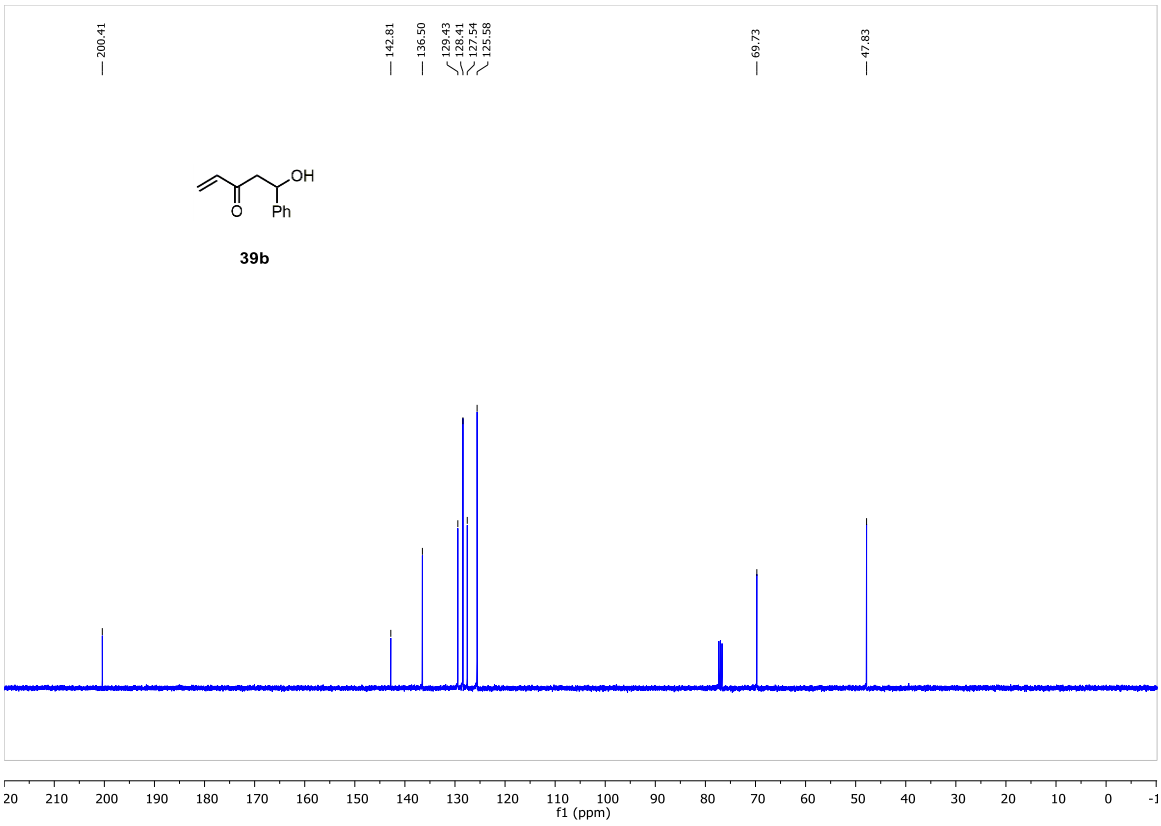
200.41
142.81
136.50
129.43
128.41
127.54
125.58
69.73
47.83
OH
O
Ph
39b
20 210 200 190 180 170 160 150 140 130 120 110 100 90 80 70 60 50 40 30 20 10 0 -1
f1 (ppm)

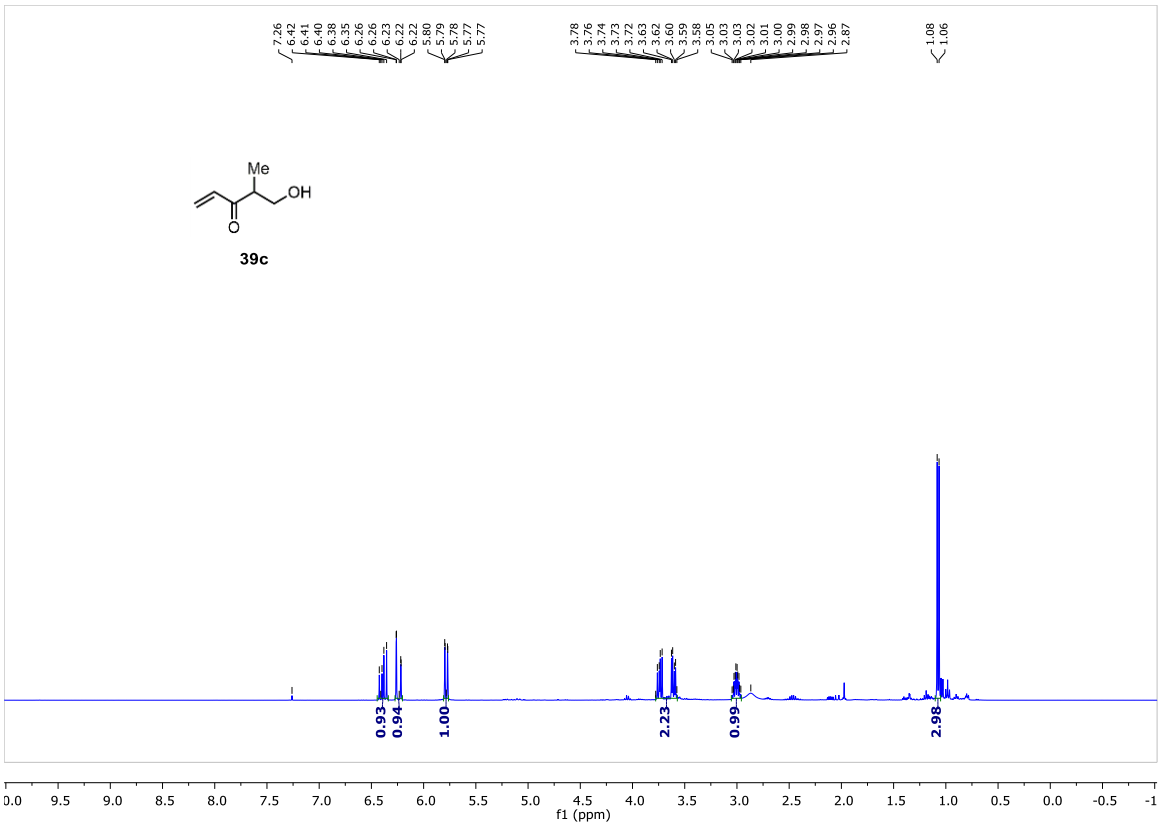
7.26
6.42
6.41
6.40
6.38
6.35
6.26
6.26
6.23
6.22
6.22
5.80
5.79
5.78
5.77
5.77
3.78
3.76
3.74
3.73
3.72
3.63
3.62
3.60
3.59
3.58
3.05
3.03
3.03
3.02
3.01
3.00
2.99
2.98
2.97
2.96
2.87
1.08
1.06
Me
OH
O
39c
0.93
0.94
1.00
2.23
0.99
2.98
f1 (ppm)

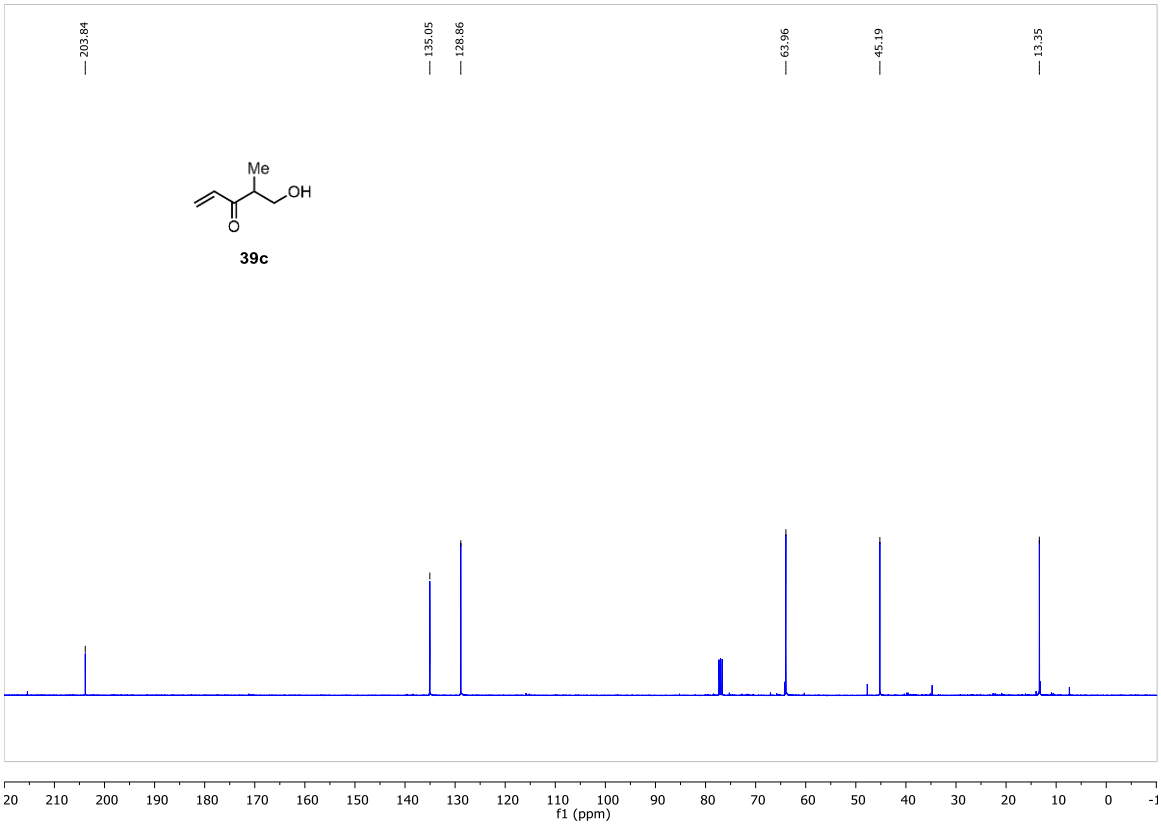
203.84
135.05
128.86
63.96
45.19
13.35
Me
OH
O
39c
f1 (ppm)

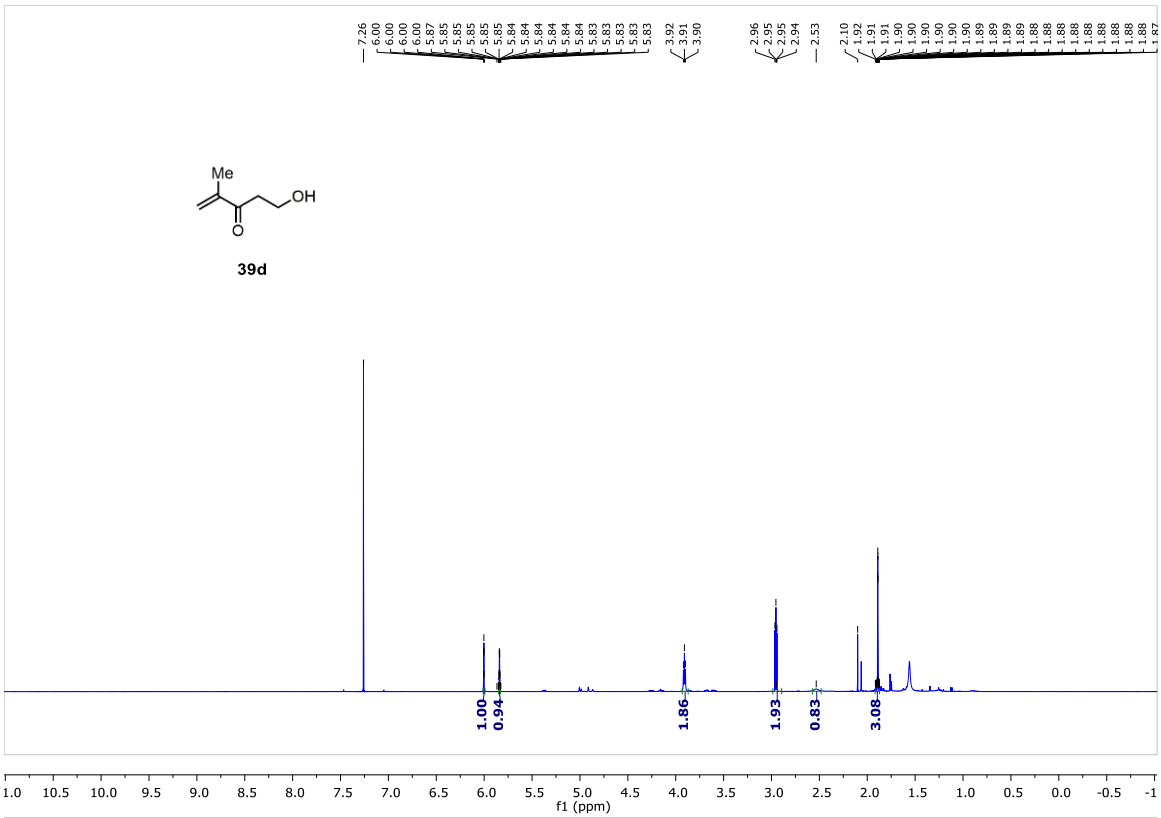
Me
OH
O
39d
1.00
0.94
1.86
1.93
0.83
3.08
f1 (ppm)

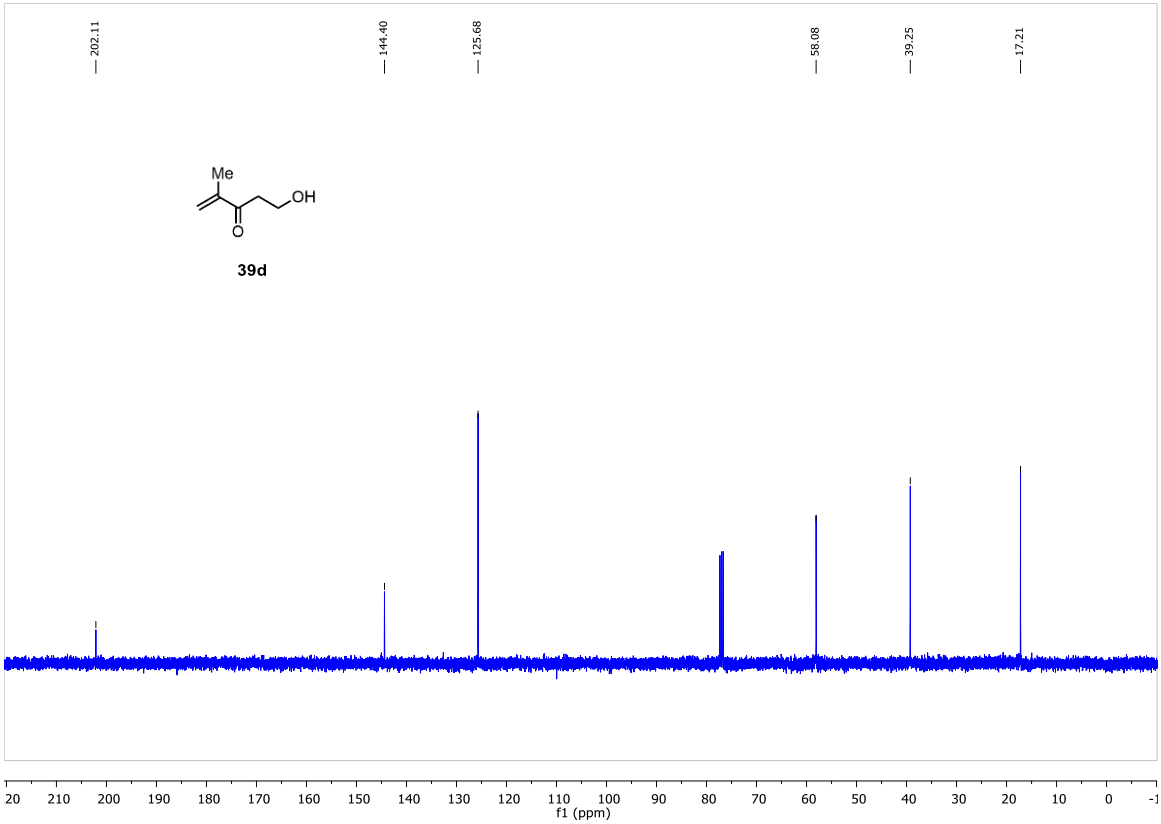
202.11
144.40
125.68
58.08
39.25
17.21
Me
OH
O
39d
f1 (ppm)

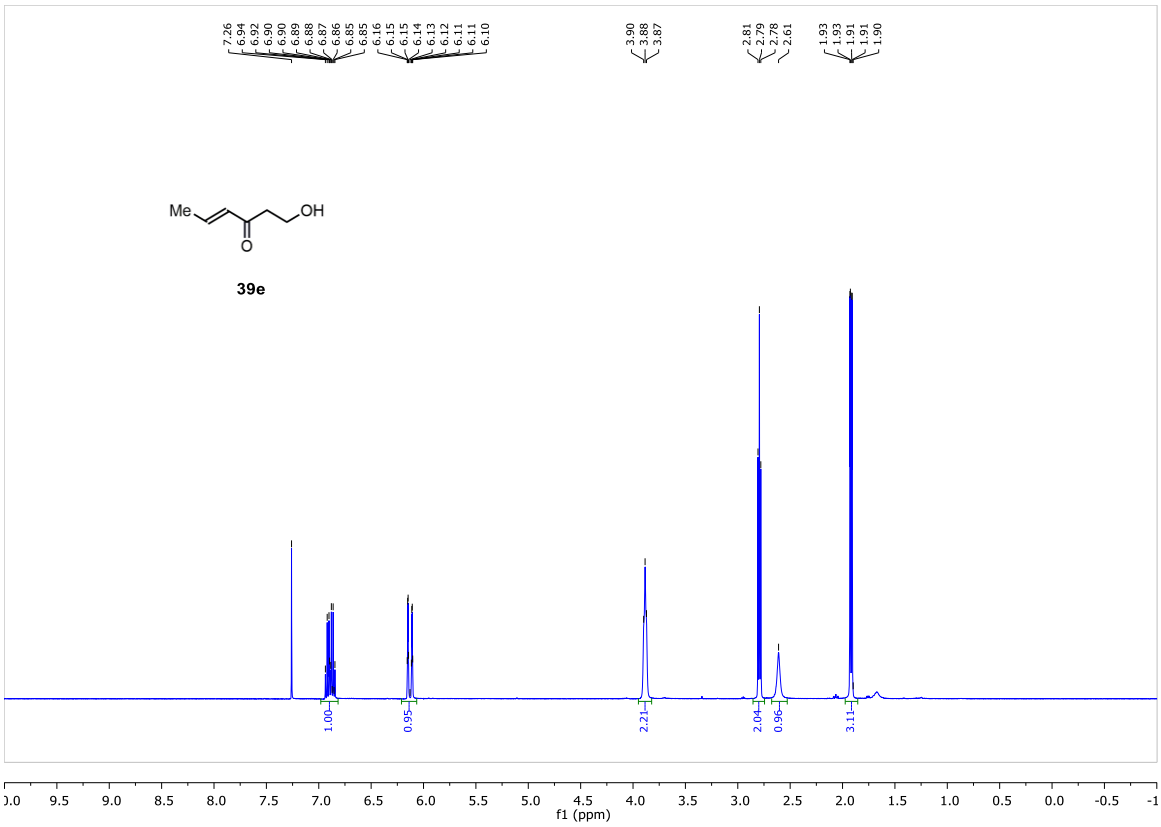
7.26
6.94
6.92
6.90
6.90
6.89
6.88
6.87
6.86
6.85
6.85
6.16
6.15
6.15
6.14
6.13
6.12
6.11
6.11
6.10
3.90
3.88
3.87
2.81
2.79
2.78
2.61
1.93
1.93
1.91
1.91
1.90
Me
OH
O
39e
1.00
0.95
2.21
2.04
0.96
3.11
f1 (ppm)

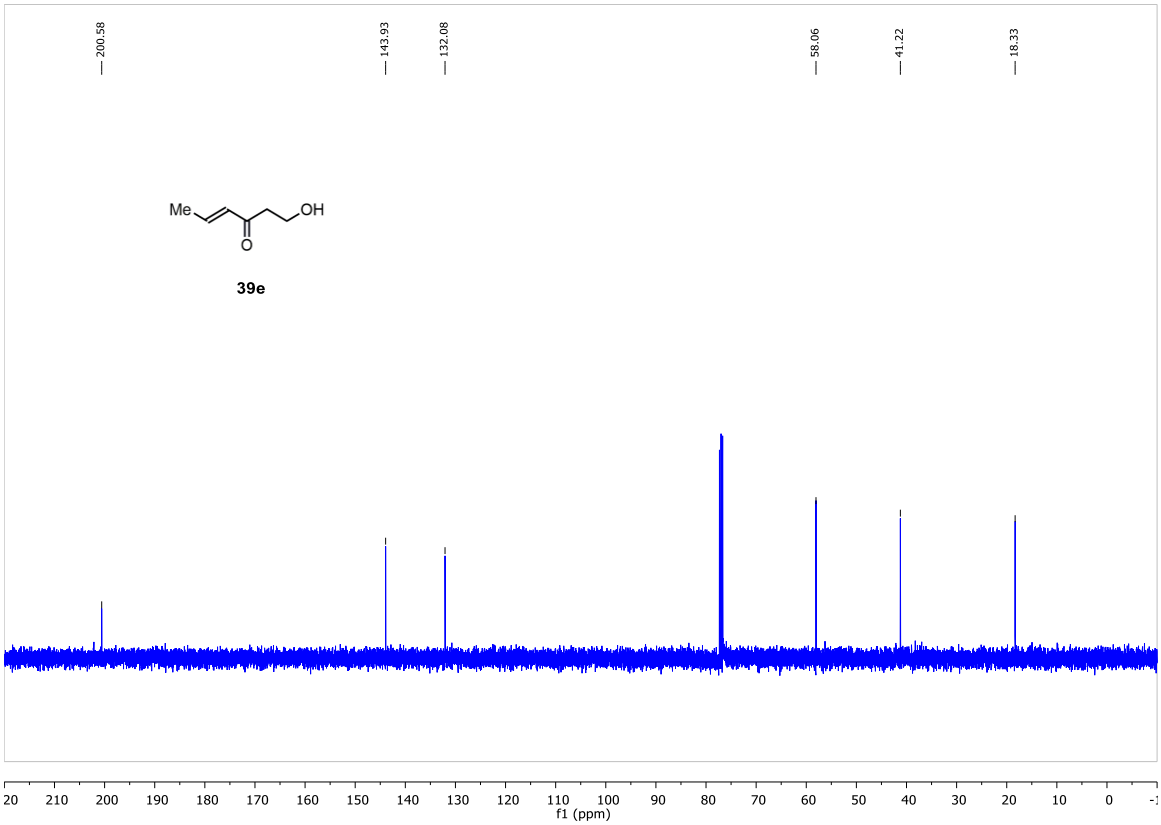
200.58
143.93
132.08
58.06
41.22
18.33
Me
OH
O
39e
f1 (ppm)

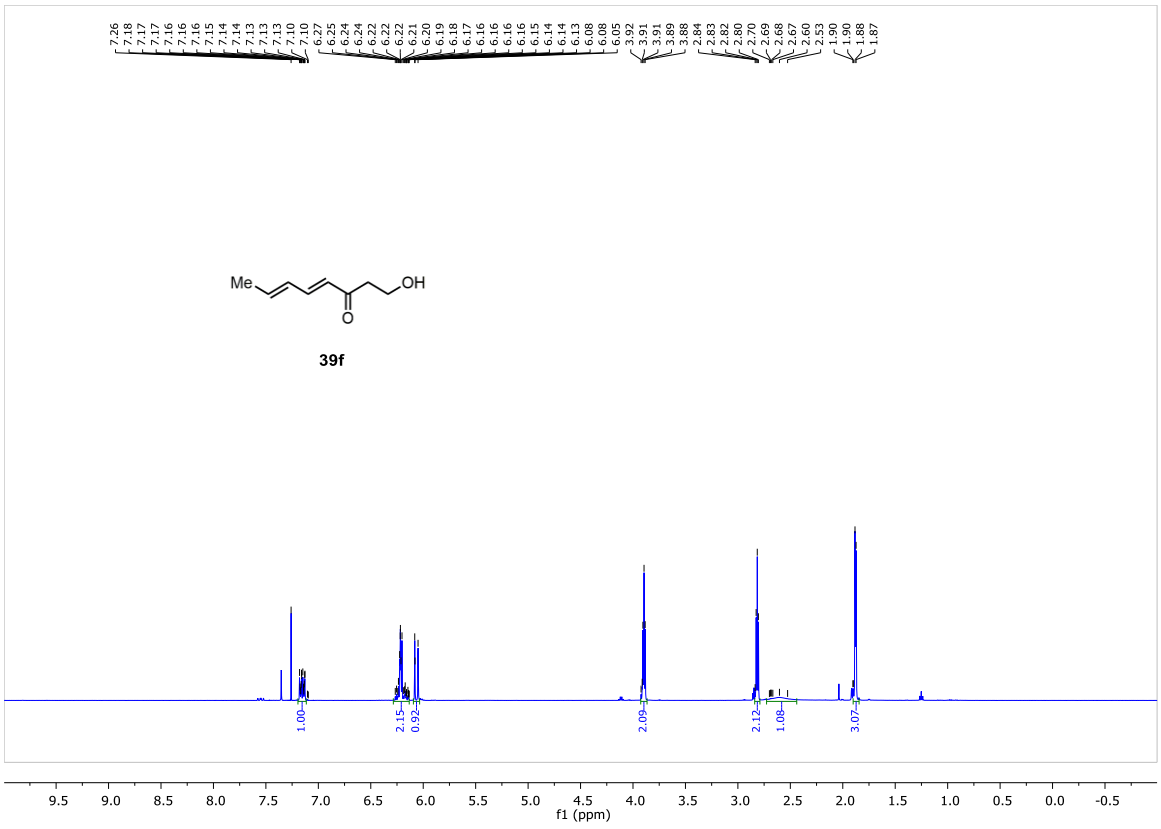
7.26 7.18 7.17 7.17 7.16 7.16 7.15 7.14 7.14 7.13 7.13 7.10 7.10 6.27 6.25 6.24 6.24 6.22 6.22 6.22 6.21 6.20 6.19 6.18 6.17 6.16 6.16 6.16 6.16 6.15 6.14 6.14 6.13 6.08 6.08 6.05 3.92 3.91 3.91 3.89 3.88 2.84 2.83 2.82 2.80 2.70 2.69 2.68 2.67 2.60 2.53 1.90 1.90 1.88 1.87
Me
OH
O
39f
1.00
2.15
0.92
2.09
2.12
1.08
3.07
9.5 9.0 8.5 8.0 7.5 7.0 6.5 6.0 5.5 5.0 4.5 4.0 3.5 3.0 2.5 2.0 1.5 1.0 0.5 0.0 -0.5
f1 (ppm)

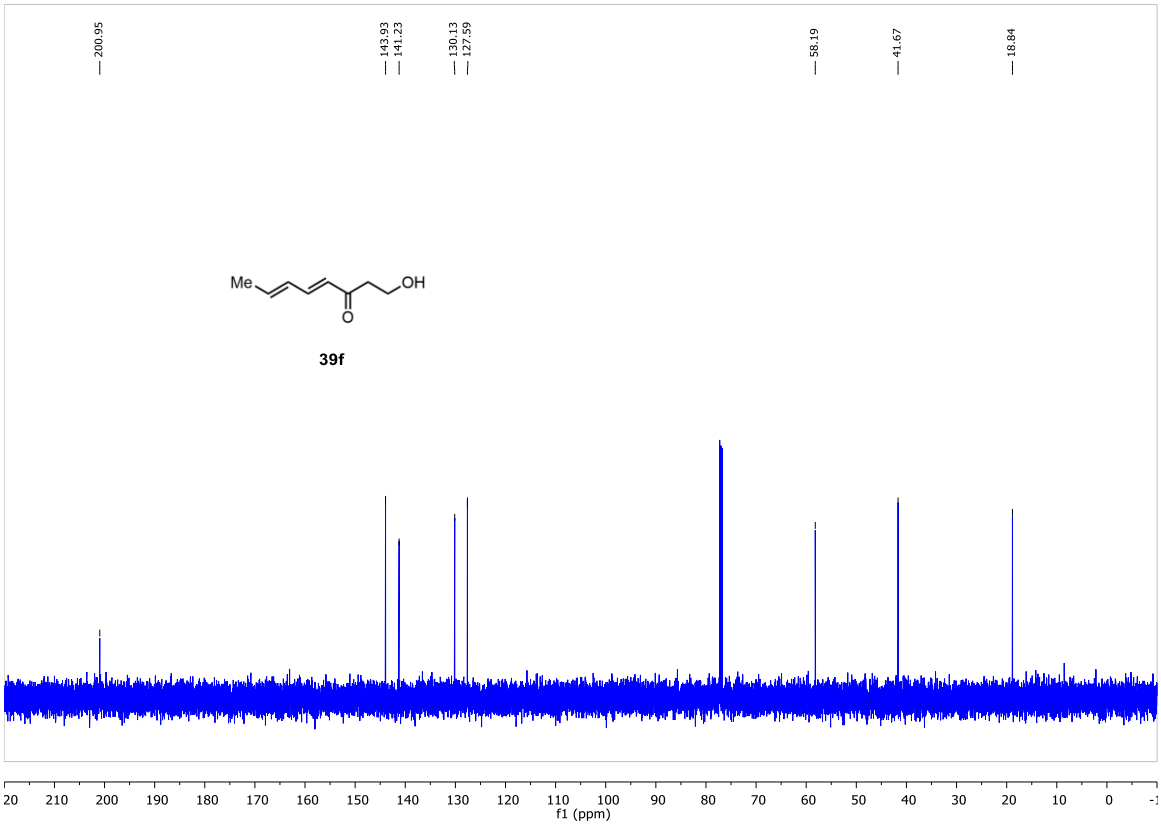
200.95
143.93
141.23
130.13
127.59
58.19
41.67
18.84
Me
OH
O
39f
20 210 200 190 180 170 160 150 140 130 120 110 100 90 80 70 60 50 40 30 20 10 0
f1 (ppm)

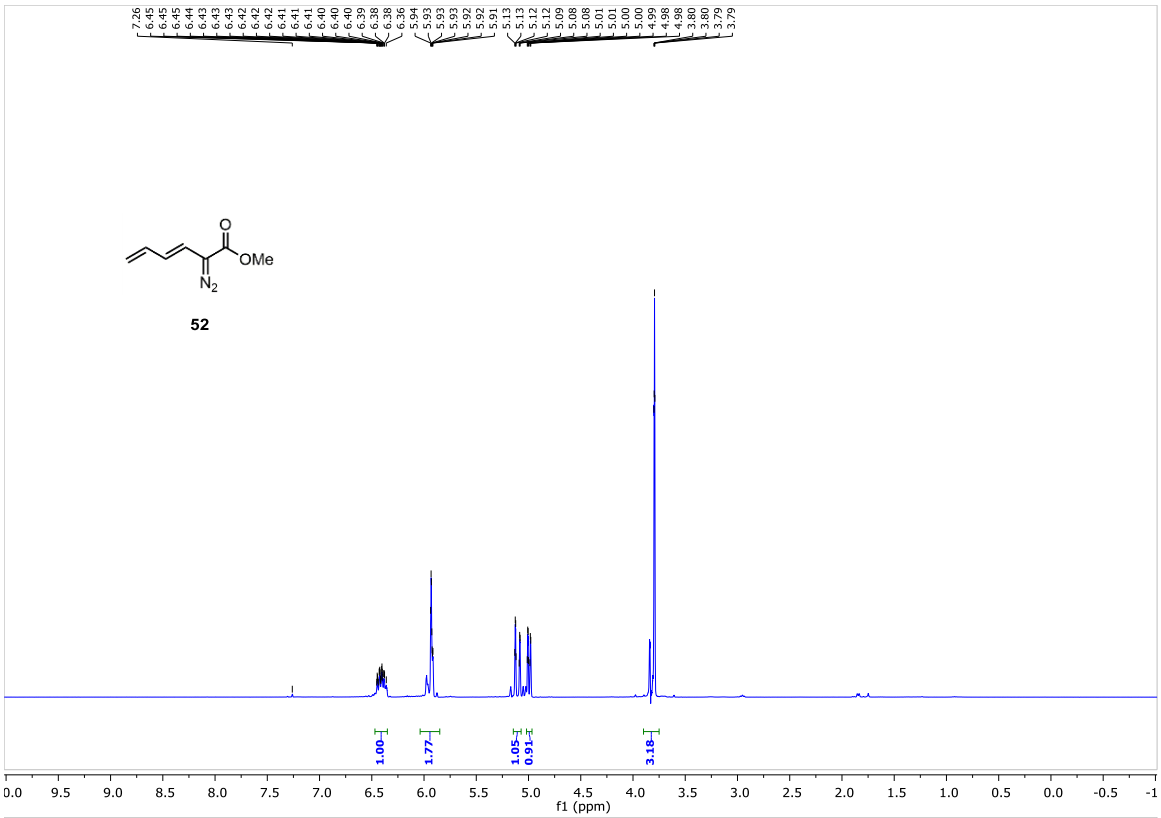
7.26
6.45
6.45
6.45
6.44
6.43
6.43
6.43
6.42
6.42
6.42
6.41
6.41
6.40
6.40
6.40
6.39
6.38
6.38
6.36
5.94
5.93
5.93
5.93
5.92
5.92
5.91
5.13
5.13
5.12
5.12
5.09
5.08
5.08
5.01
5.01
5.00
5.00
4.99
4.98
4.98
3.80
3.80
3.79
3.79
O
OMe
N2
52
1.00
1.77
1.05
0.91
3.18
f1 (ppm)

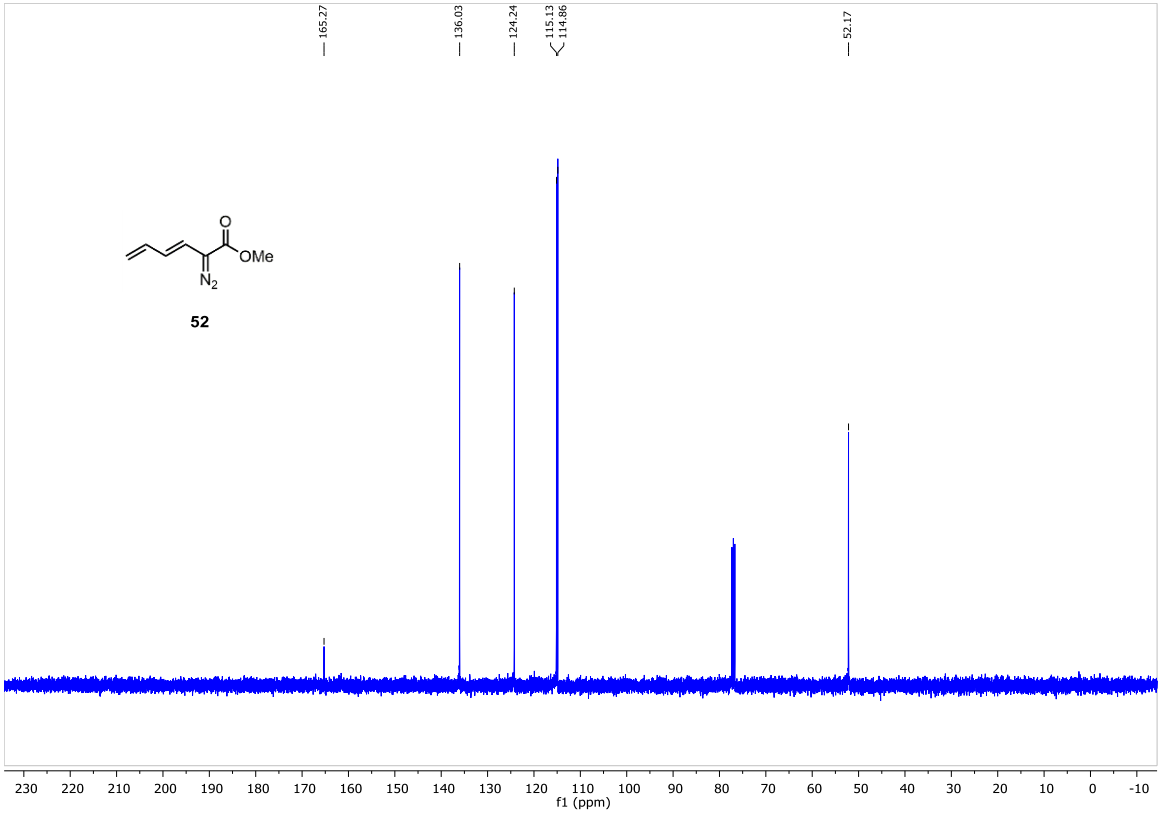
165.27
136.03
124.24
115.13
114.86
52.17
O
OMe
N2
52
f1 (ppm)

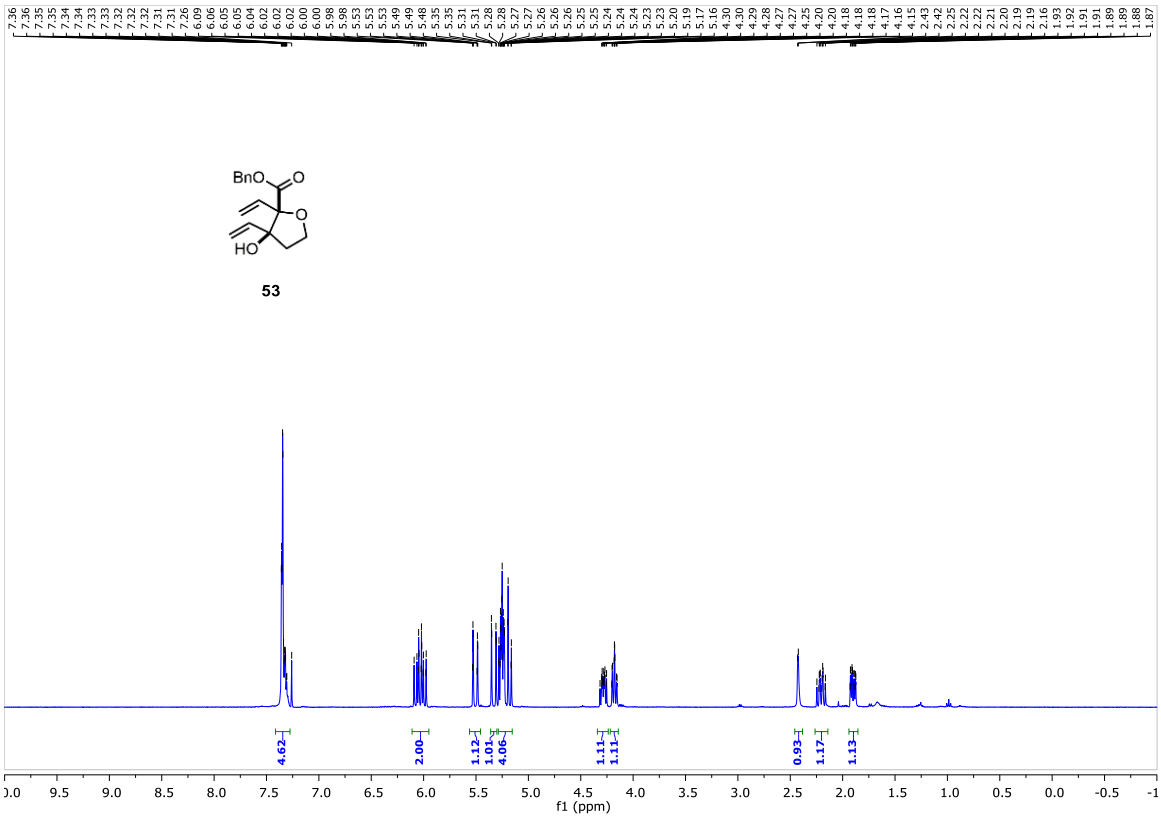
BnO
O
O
HO
53
4.62
2.00
1.12
1.01
4.06
1.11
1.11
0.93
1.17
1.13
f1 (ppm)

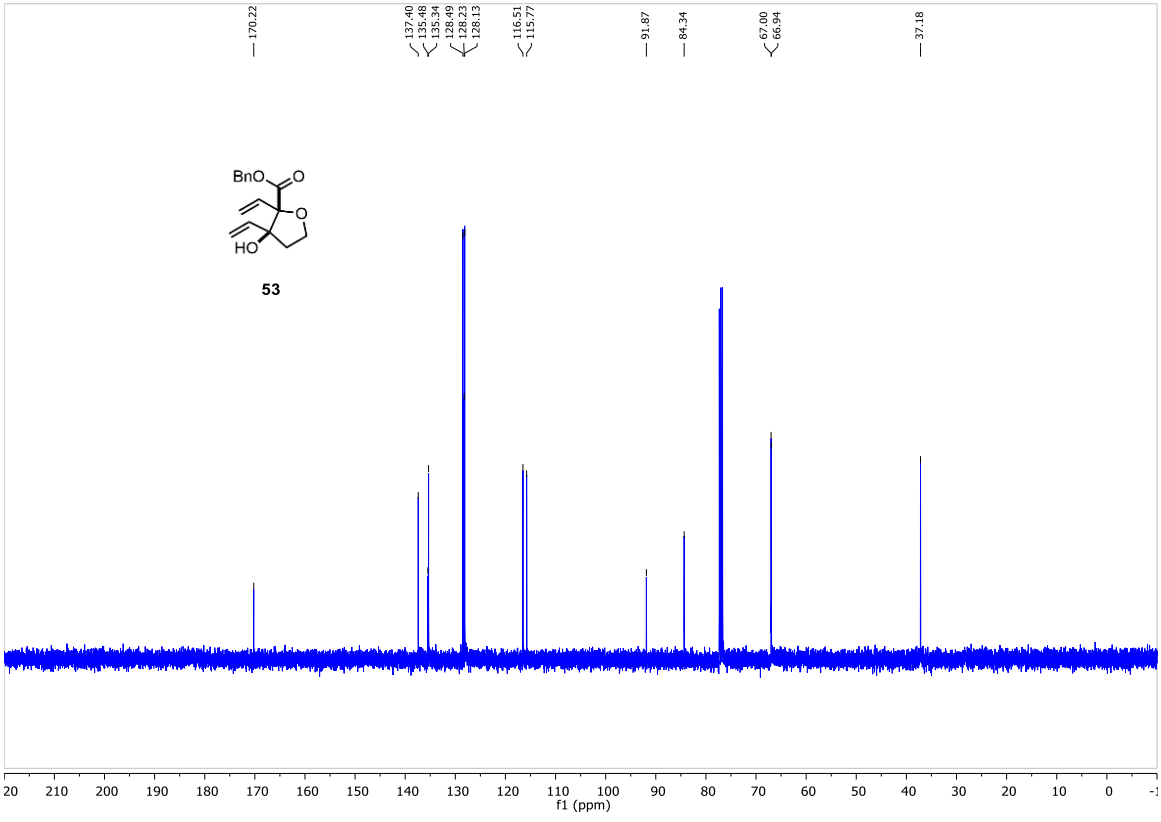
170.22
137.40
135.48
135.34
128.49
128.23
128.13
116.51
115.77
91.87
84.34
67.00
66.94
37.18
BnO
O
O
HO
53
f1 (ppm)

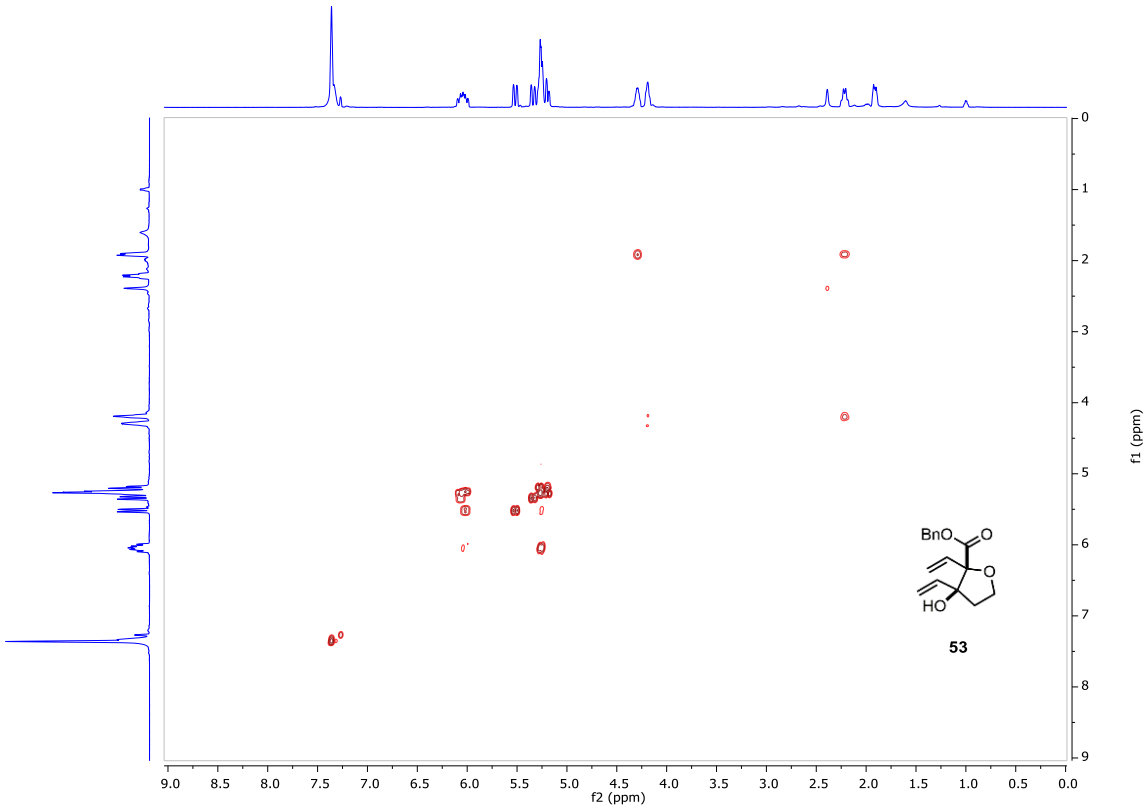
BnO
O
O
HO
53
f2 (ppm)
f1 (ppm)

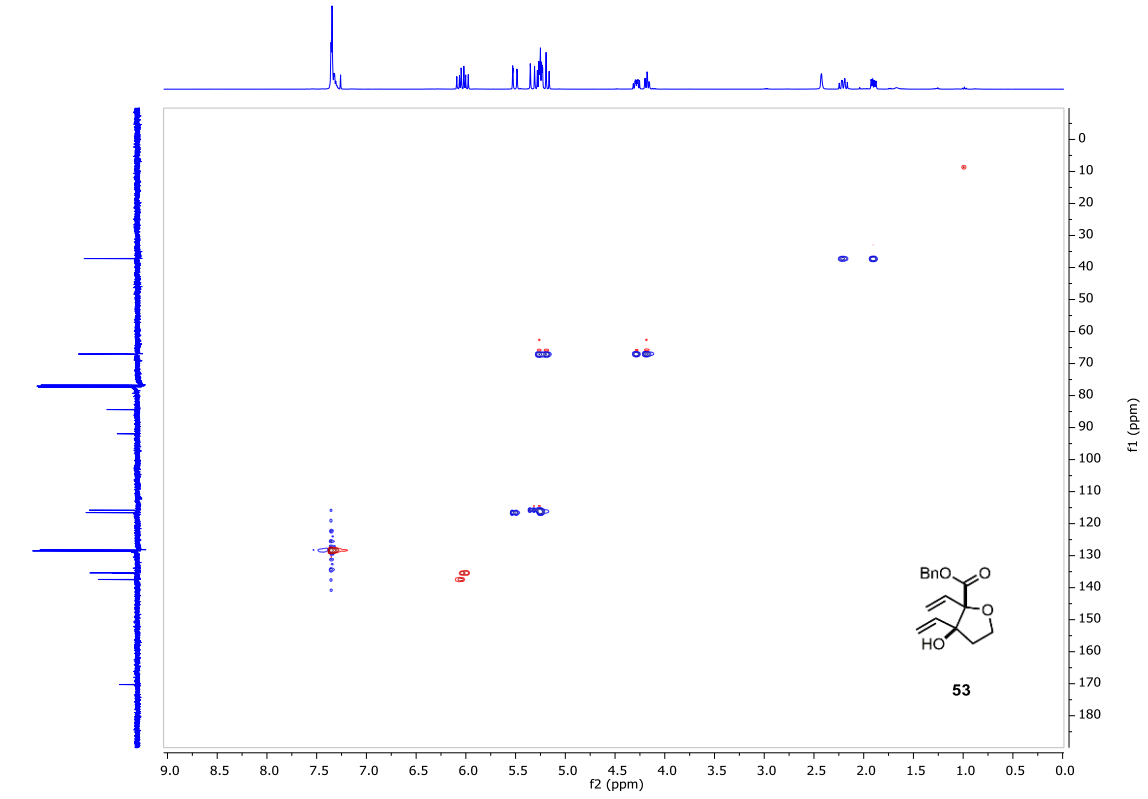
BnO
O
O
HO
53
f2 (ppm)
f1 (ppm)

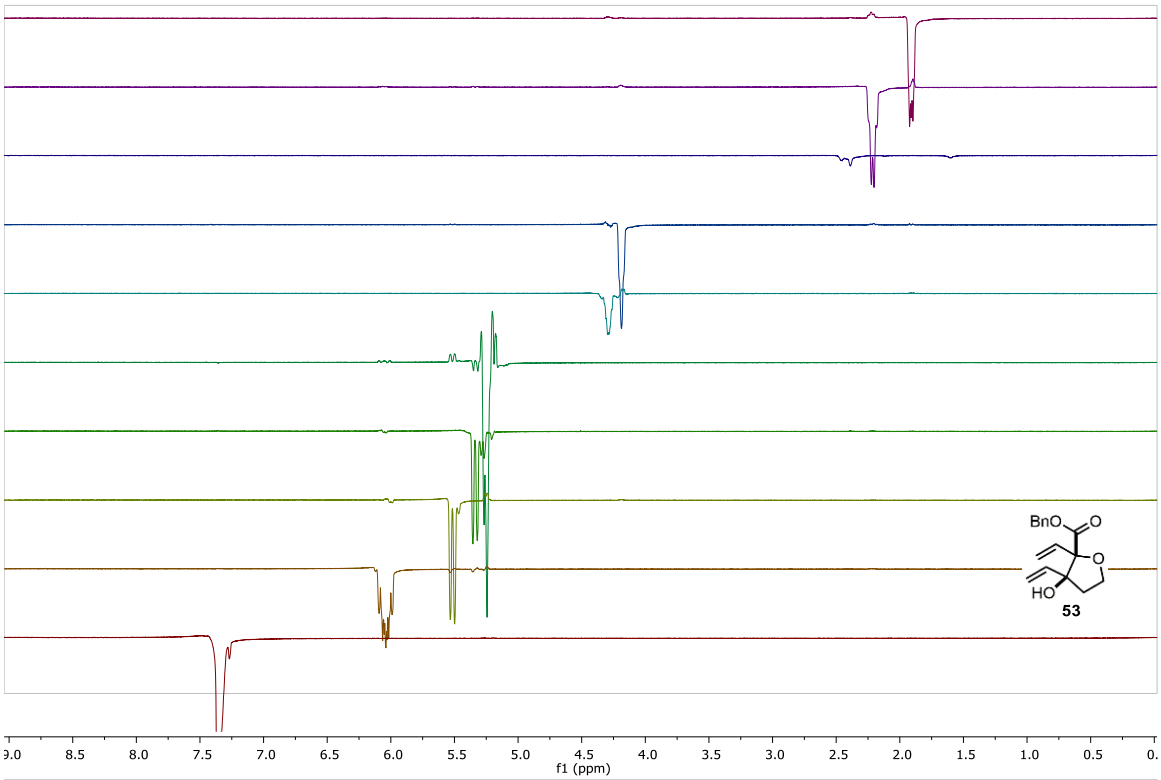
BnO
O
O
HO
53
f1 (ppm)

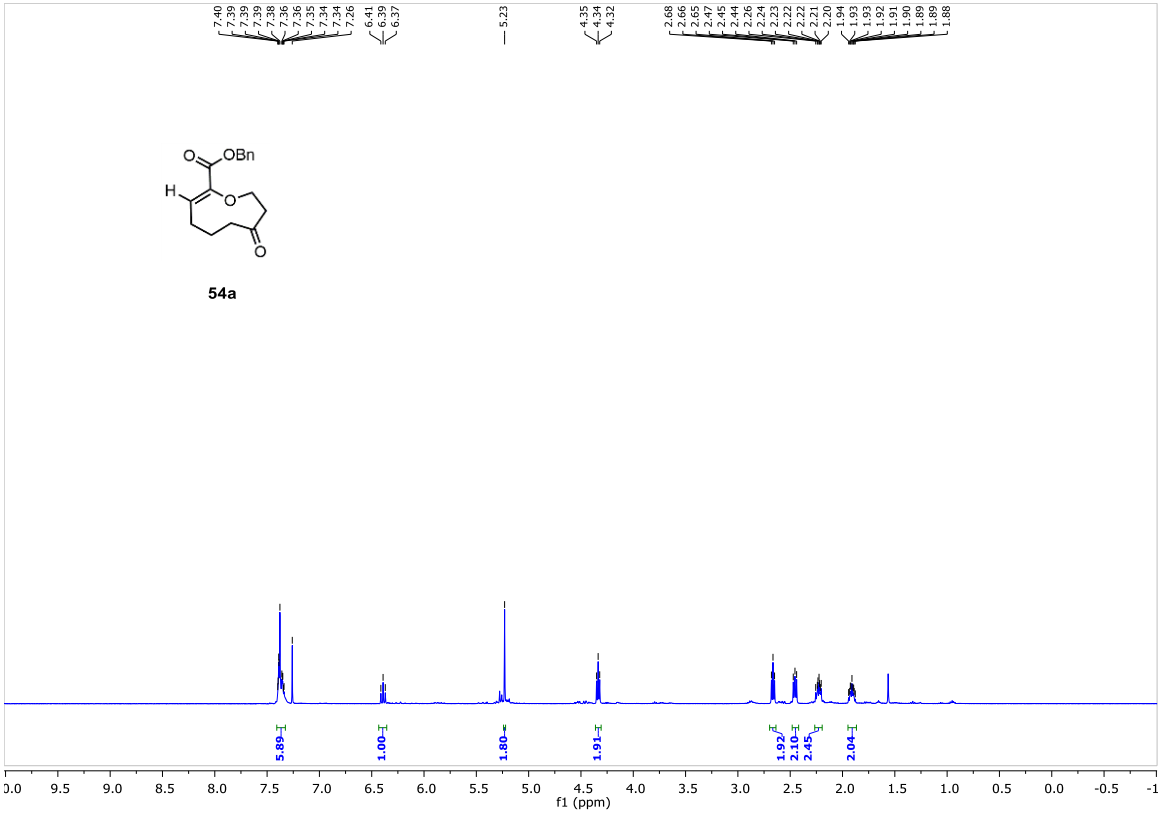
OBn
O
H
O
O
54a
5.89
1.00
1.80
1.91
1.92
2.10
2.45
2.04
f1 (ppm)

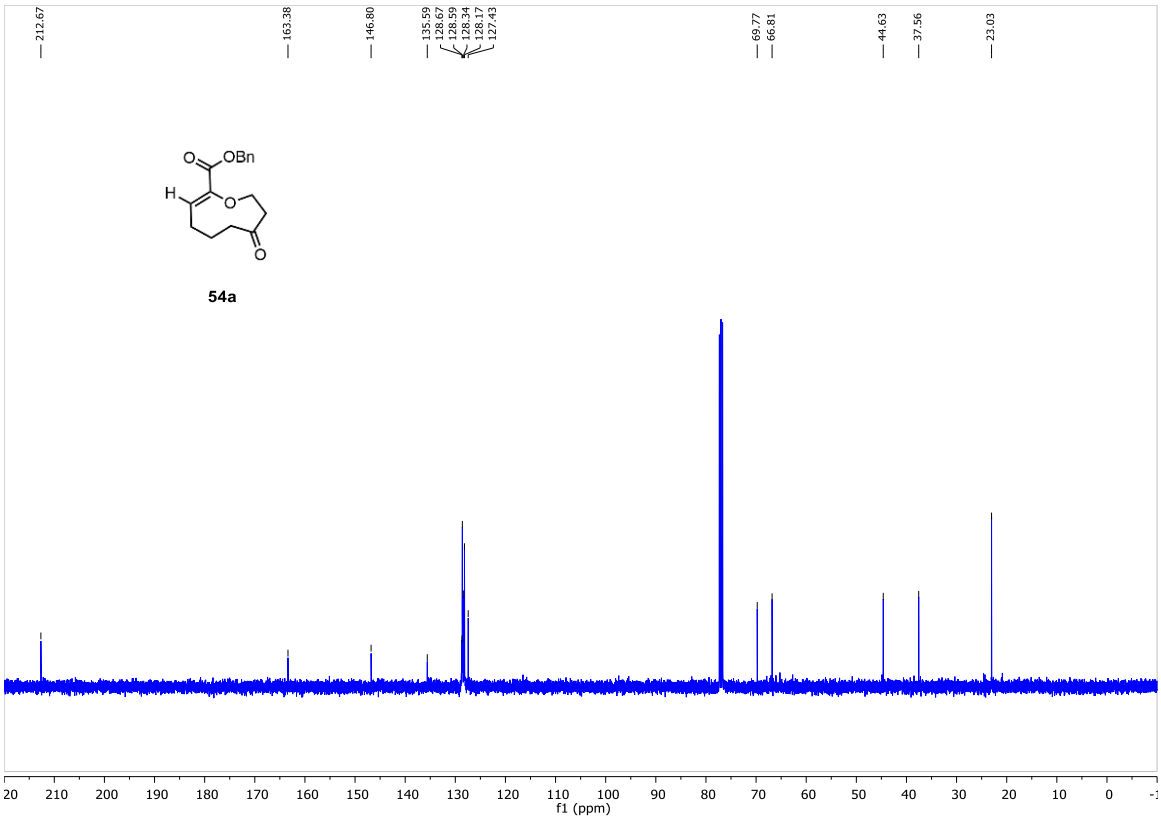
212.67
163.38
146.80
135.59
128.67
128.59
128.34
128.17
127.43
69.77
66.81
44.63
37.56
23.03
OBn
H
O
O
54a
f1 (ppm)

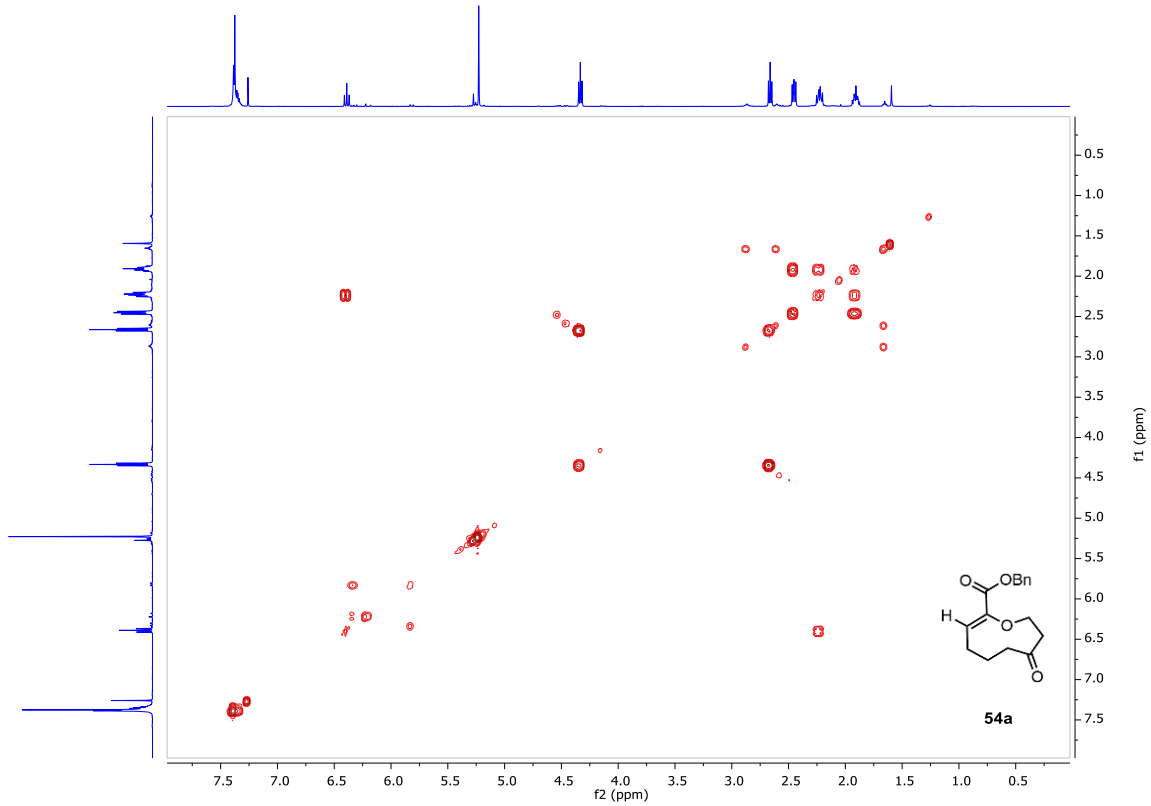
OBn
H
O
O
54a
f2 (ppm)
f1 (ppm)

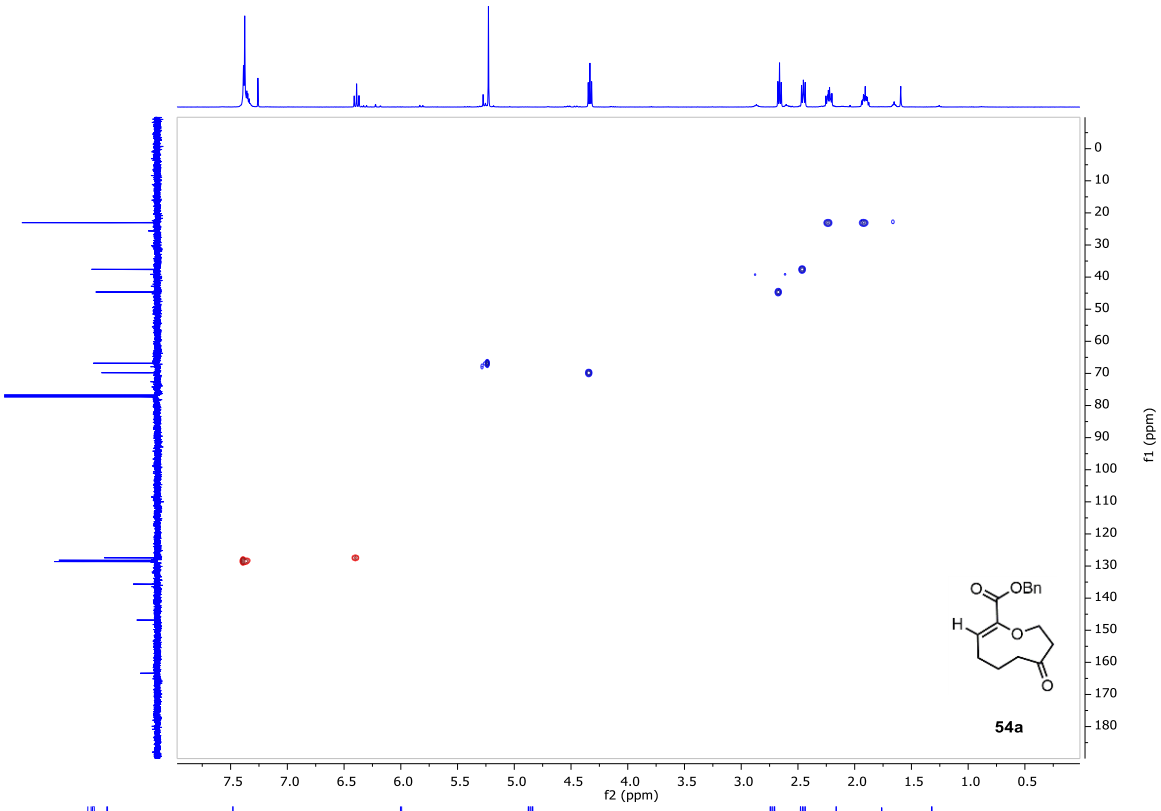
f2 (ppm)
f1 (ppm)
OBn
H
O
O
54a

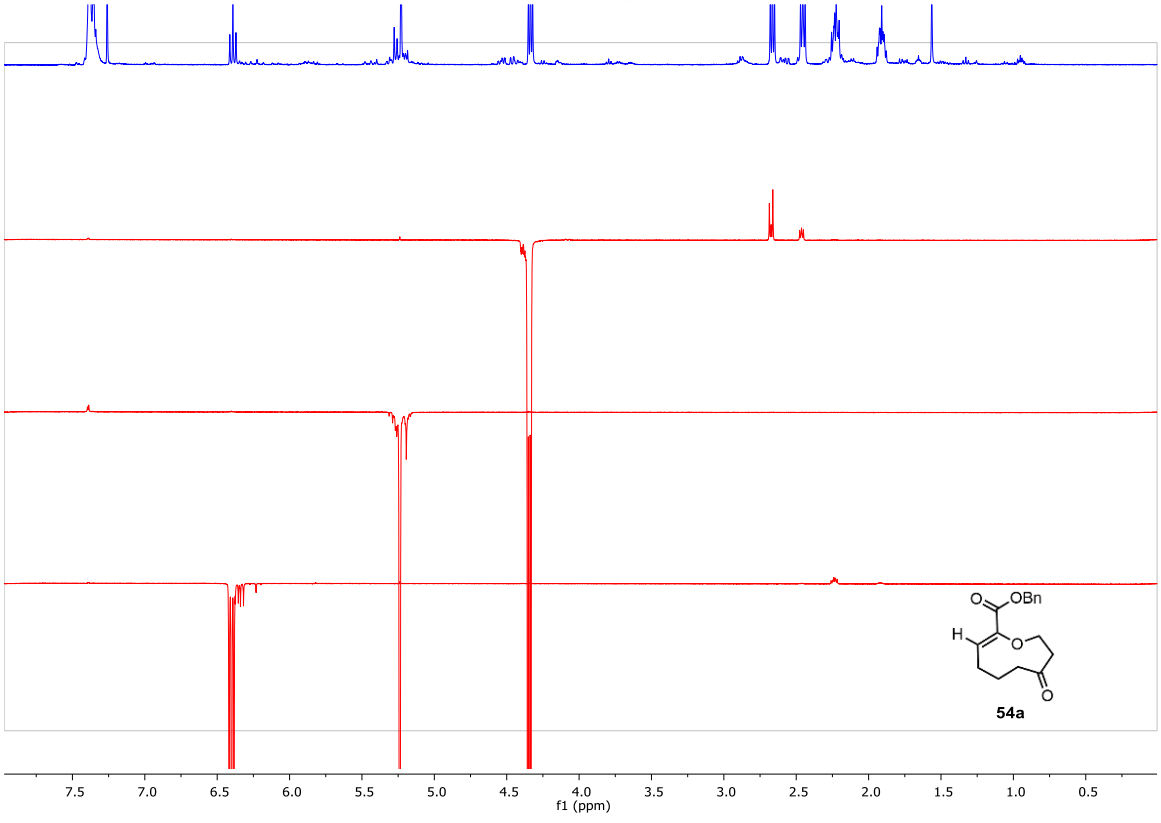
f1 (ppm)
OBn
H
O
O
54a

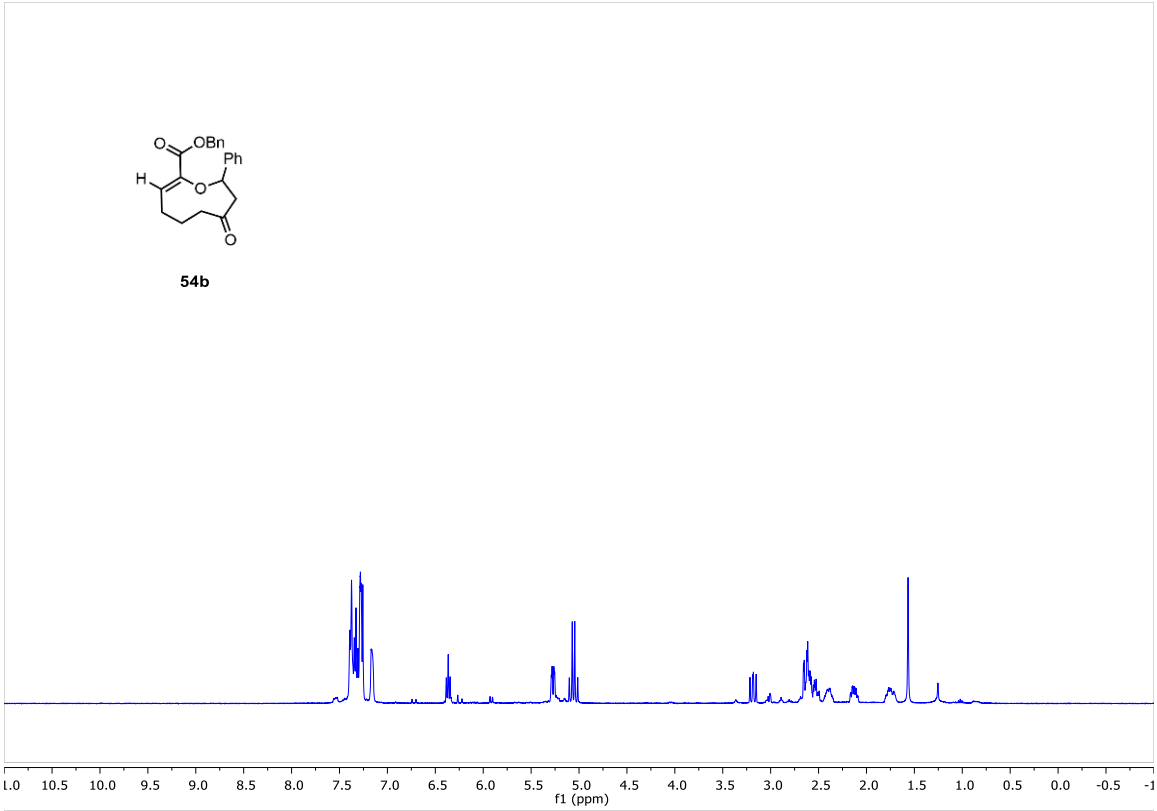
OBn
Ph
H
O
O
54b
f1 (ppm)

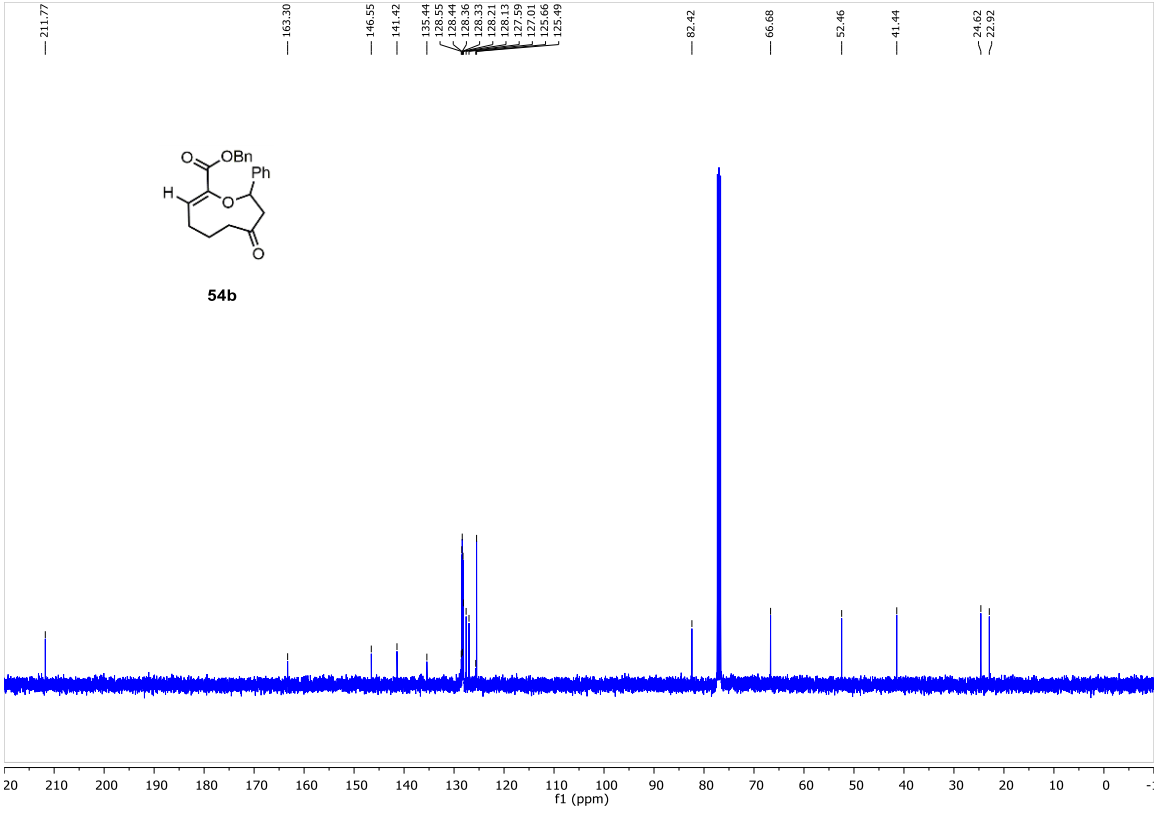
211.77
163.30
146.55
141.42
135.44
128.55
128.44
128.36
128.33
128.21
128.11
127.59
127.01
125.66
125.49
82.42
66.68
52.46
41.44
24.62
22.92
OBn
Ph
H
O
O
54b
f1 (ppm)

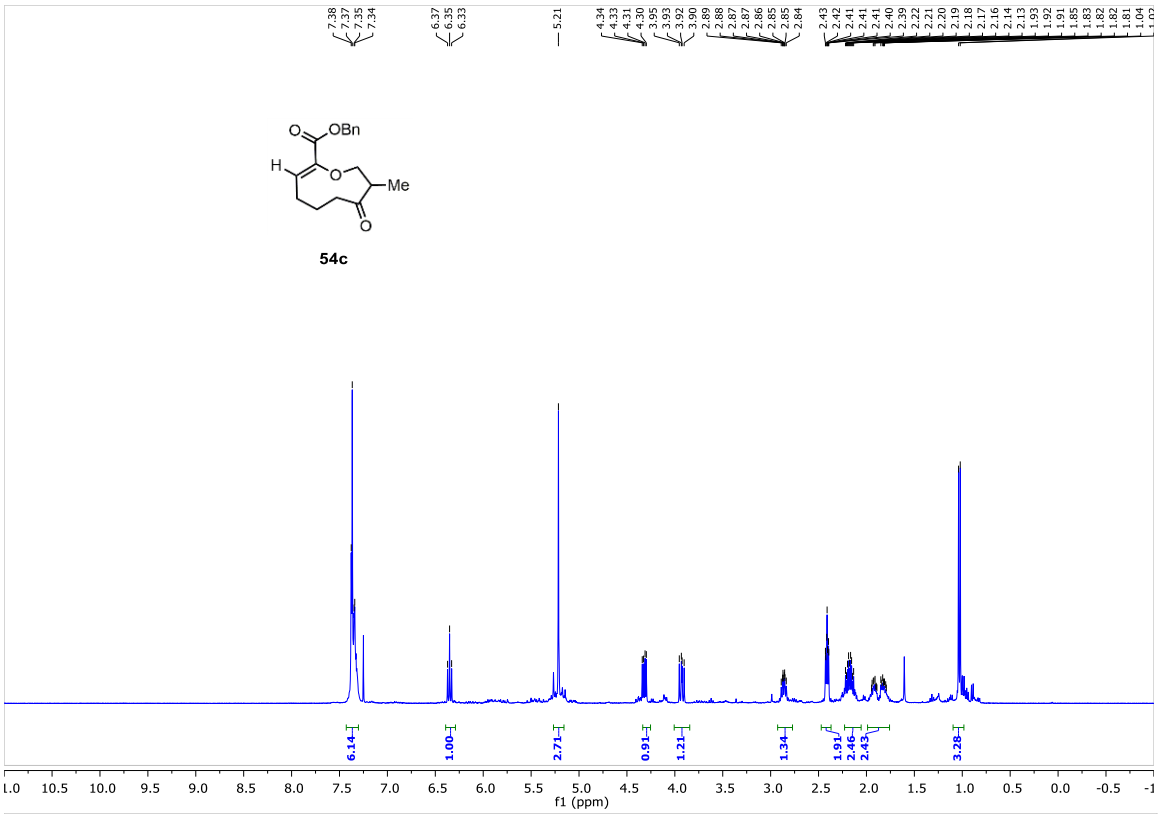
OBn
H
O
Me
O
O
54c
f1 (ppm)

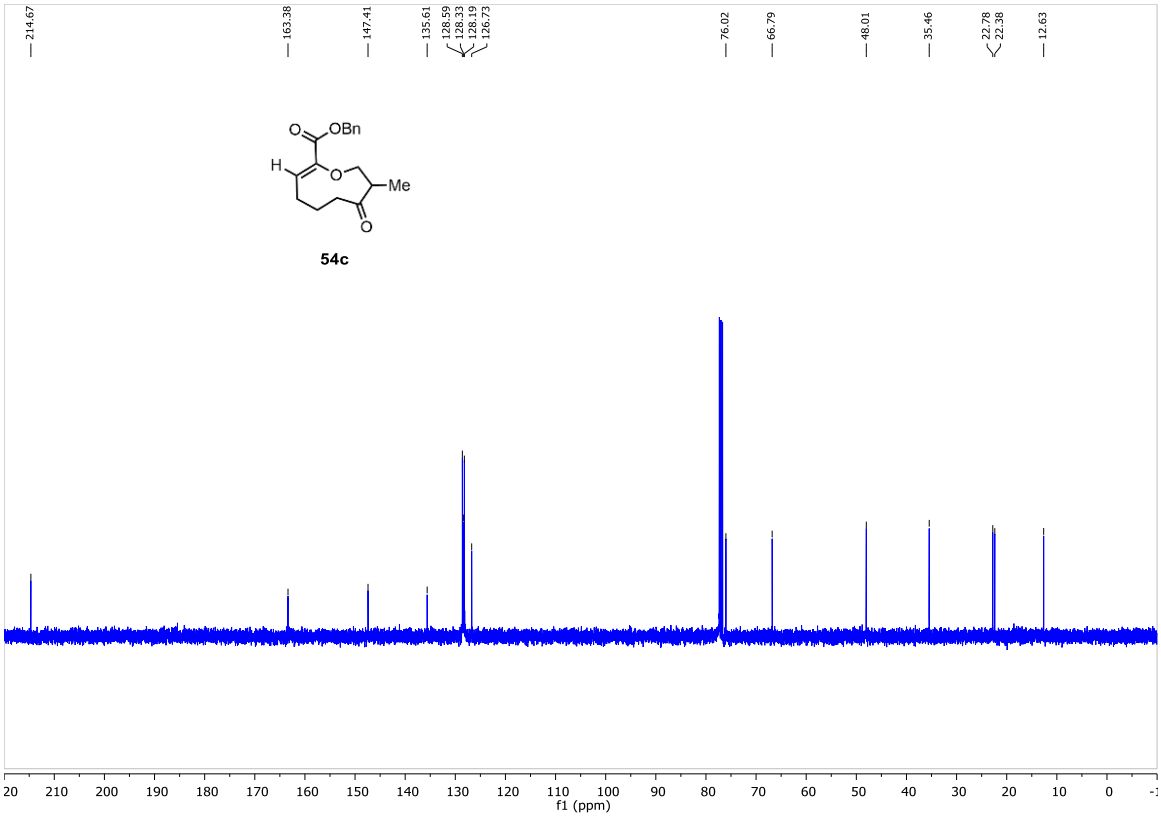
OBn
H
O
Me
O
O
54c
f1 (ppm)

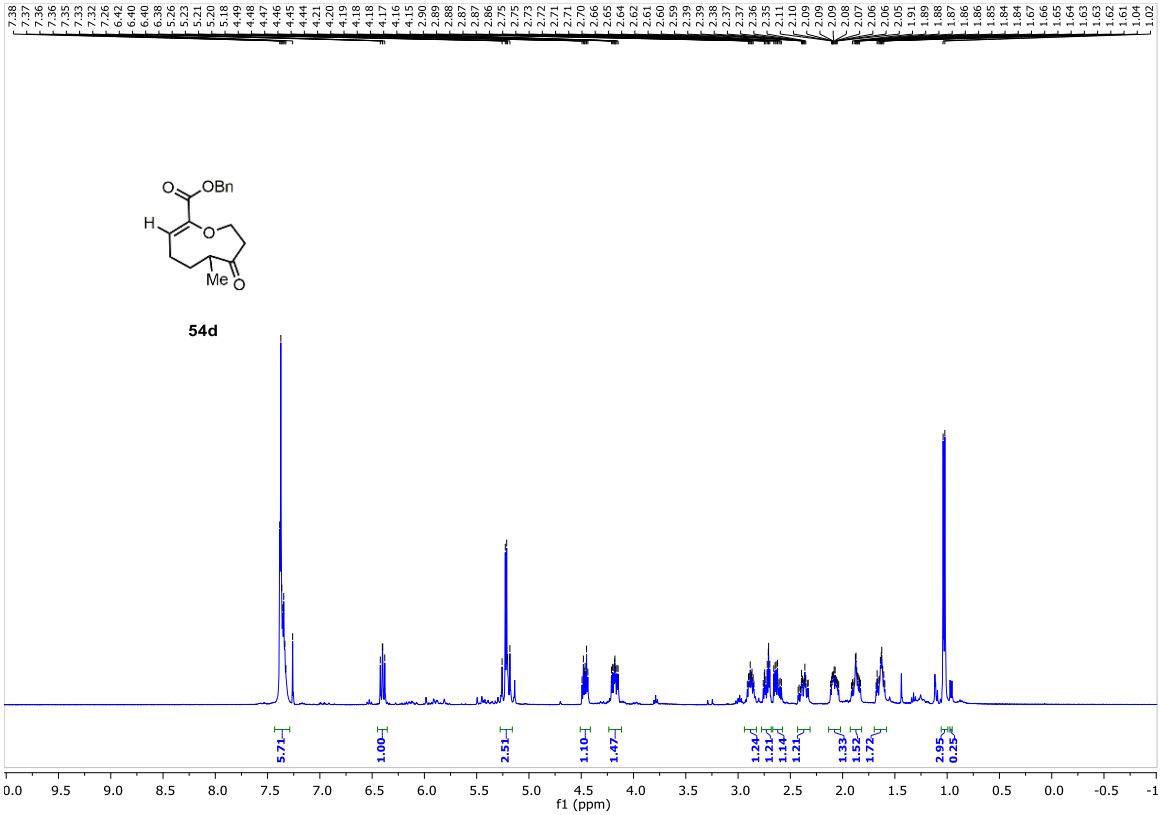
OBn
H
O
Me
O
54d
f1 (ppm)

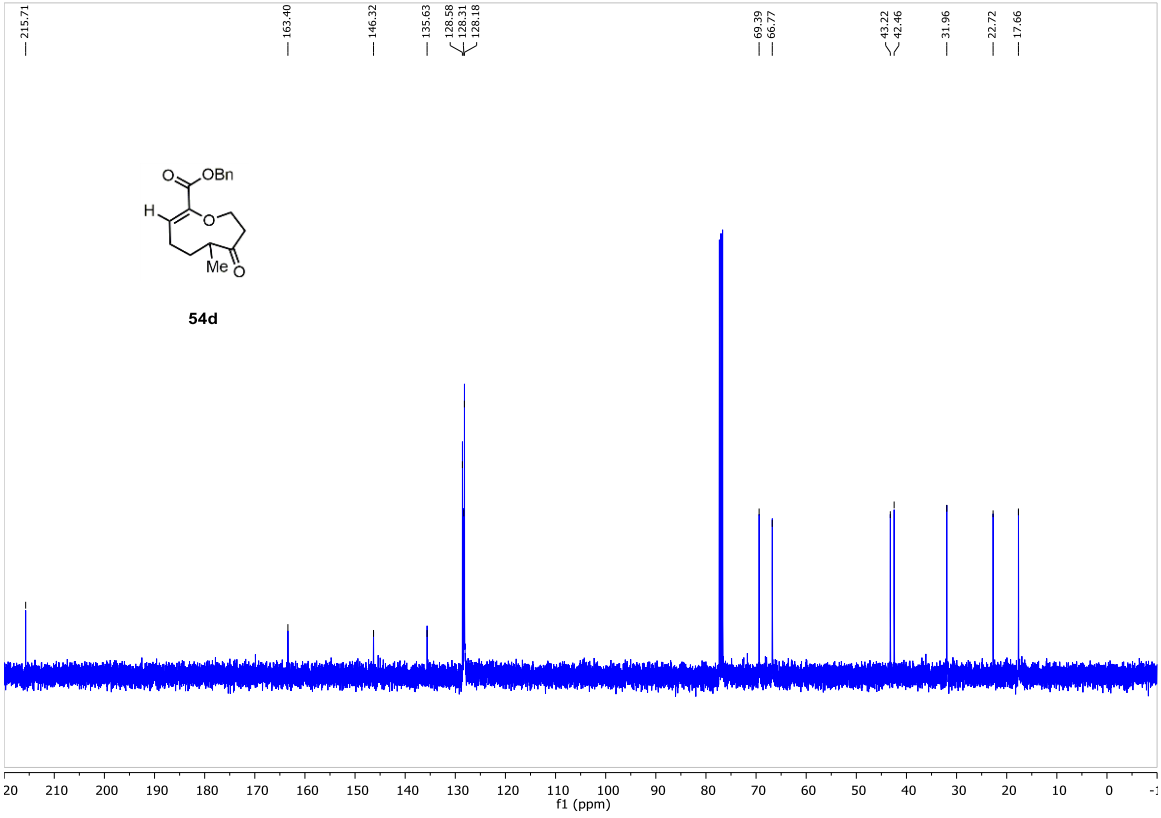
OBn
H
O
Me
O
54d
f1 (ppm)

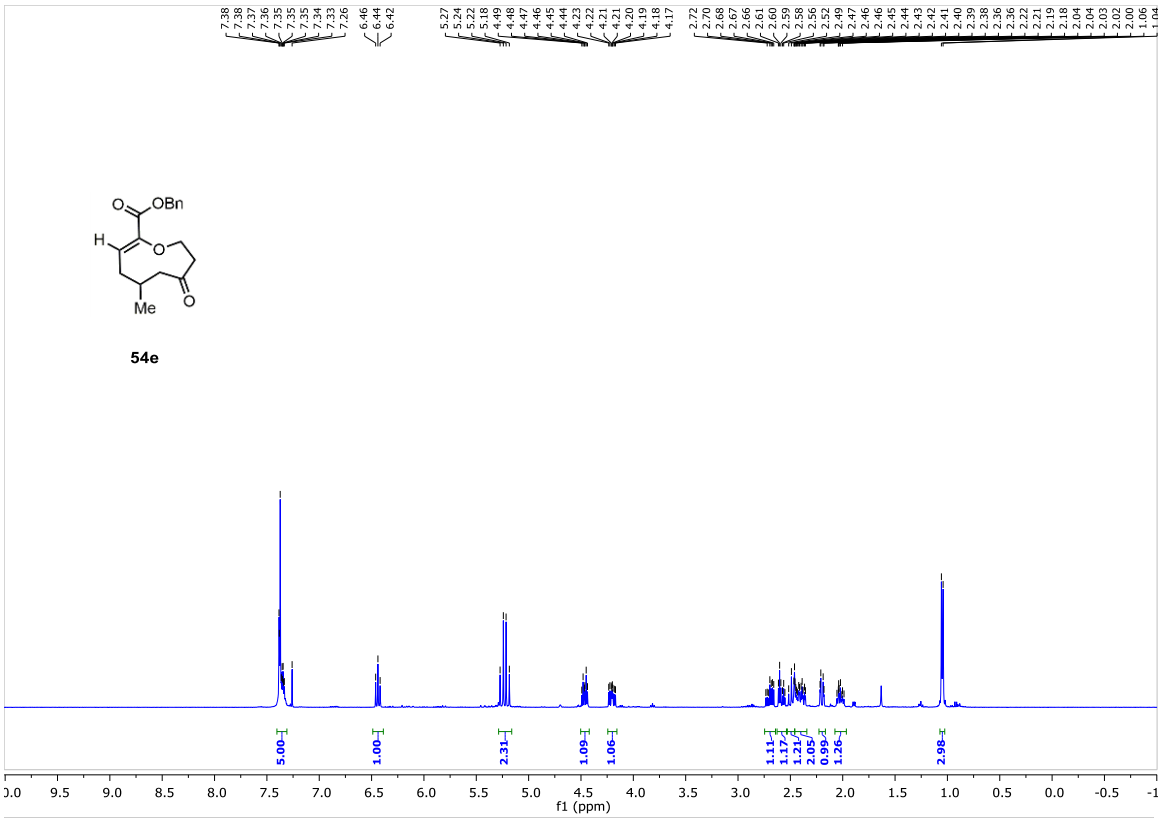
OBn
H
O
Me
O
54e
f1 (ppm)

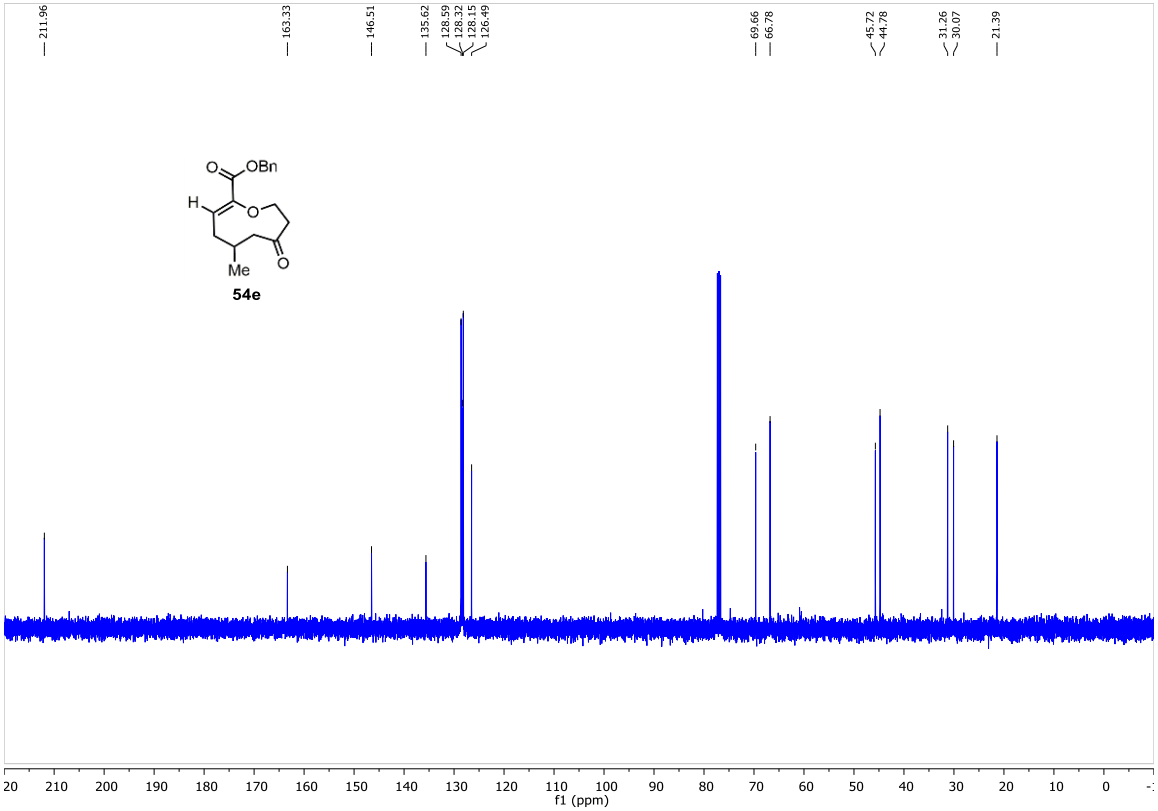
OBn
H
O
Me
O
54e
f1 (ppm)

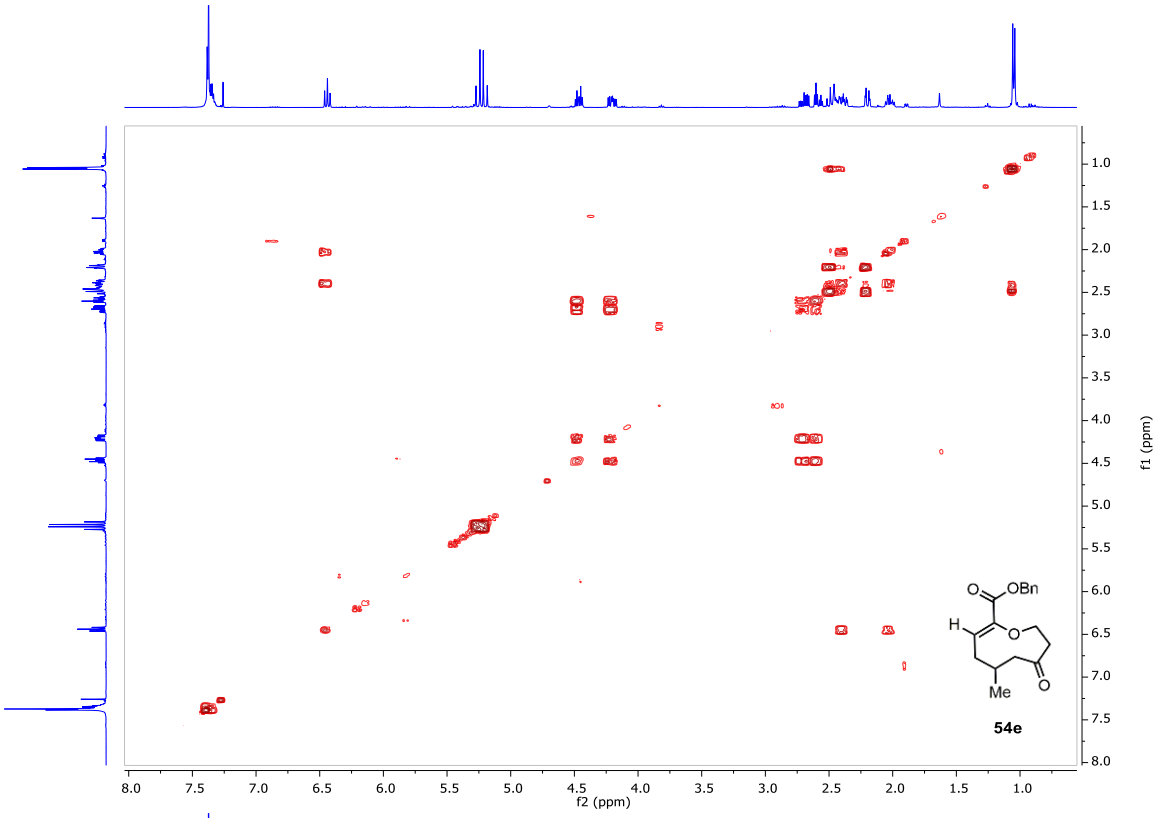
f2 (ppm)
f1 (ppm)
OBn
H
O
Me
54e

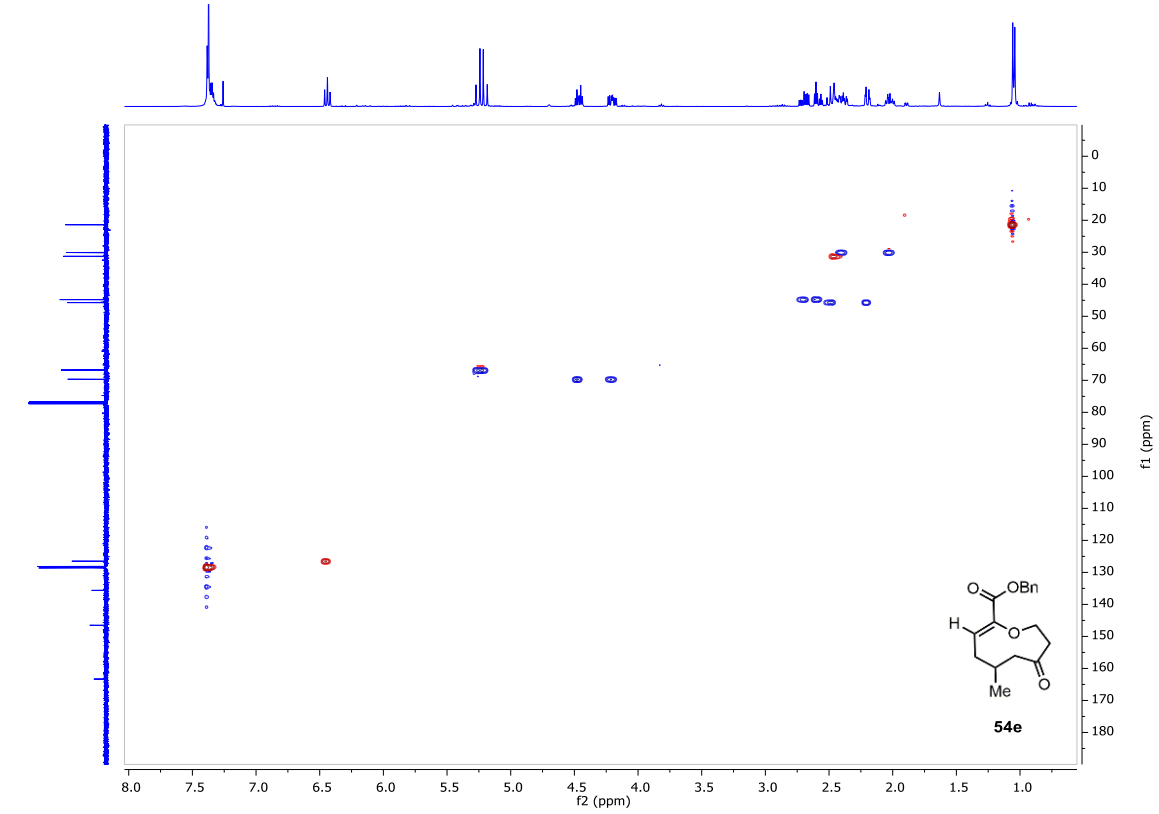
f2 (ppm)
f1 (ppm)
OBn
H
O
Me
54e

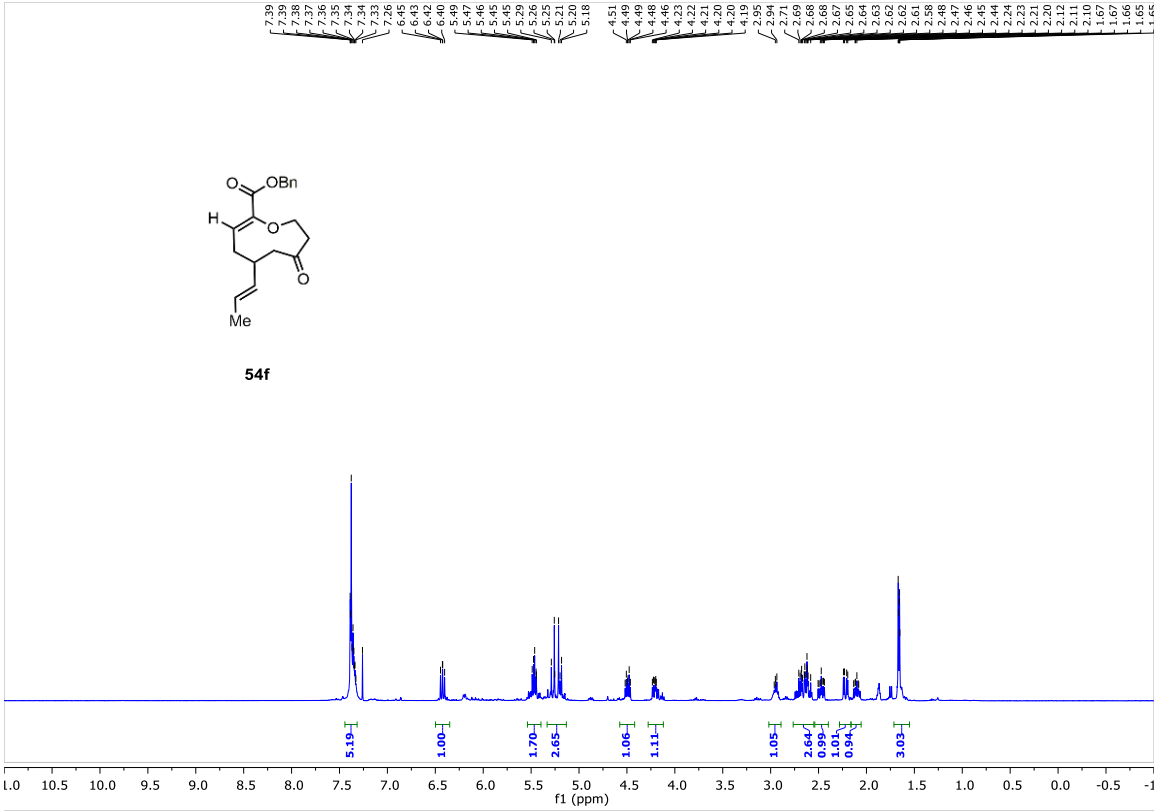
OBn
H
O
O
Me
54f
f1 (ppm)

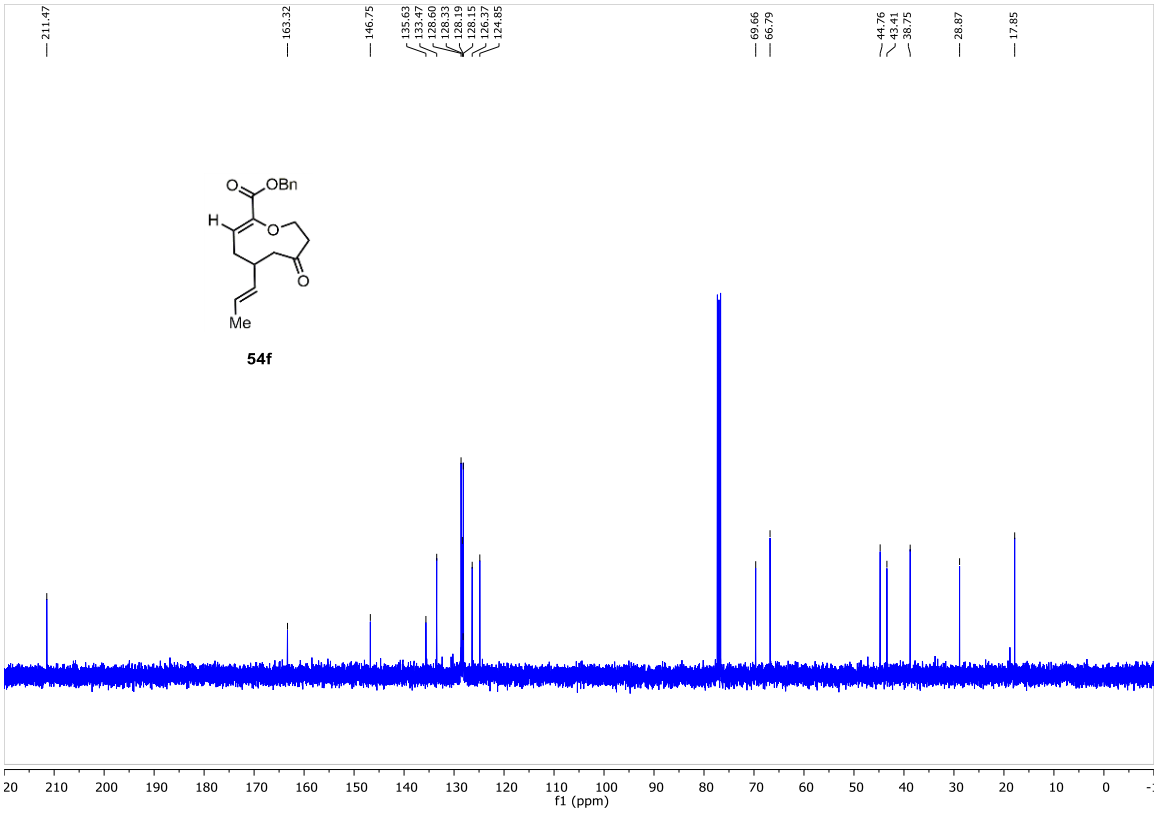
OBn
H
O
O
Me
54f
f1 (ppm)

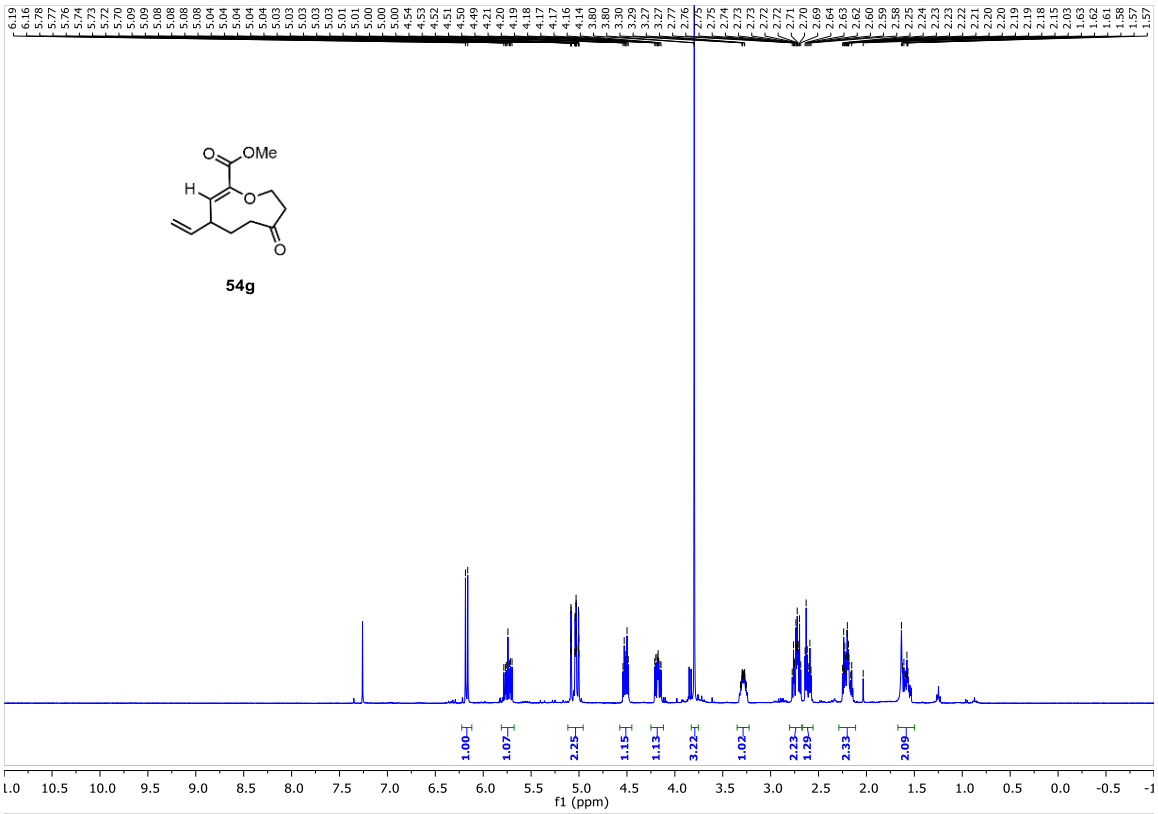
OMe
H
O
O
54g
1.00
1.07
2.25
1.15
1.13
3.22
1.02
2.23
1.29
2.33
2.09
f1 (ppm)

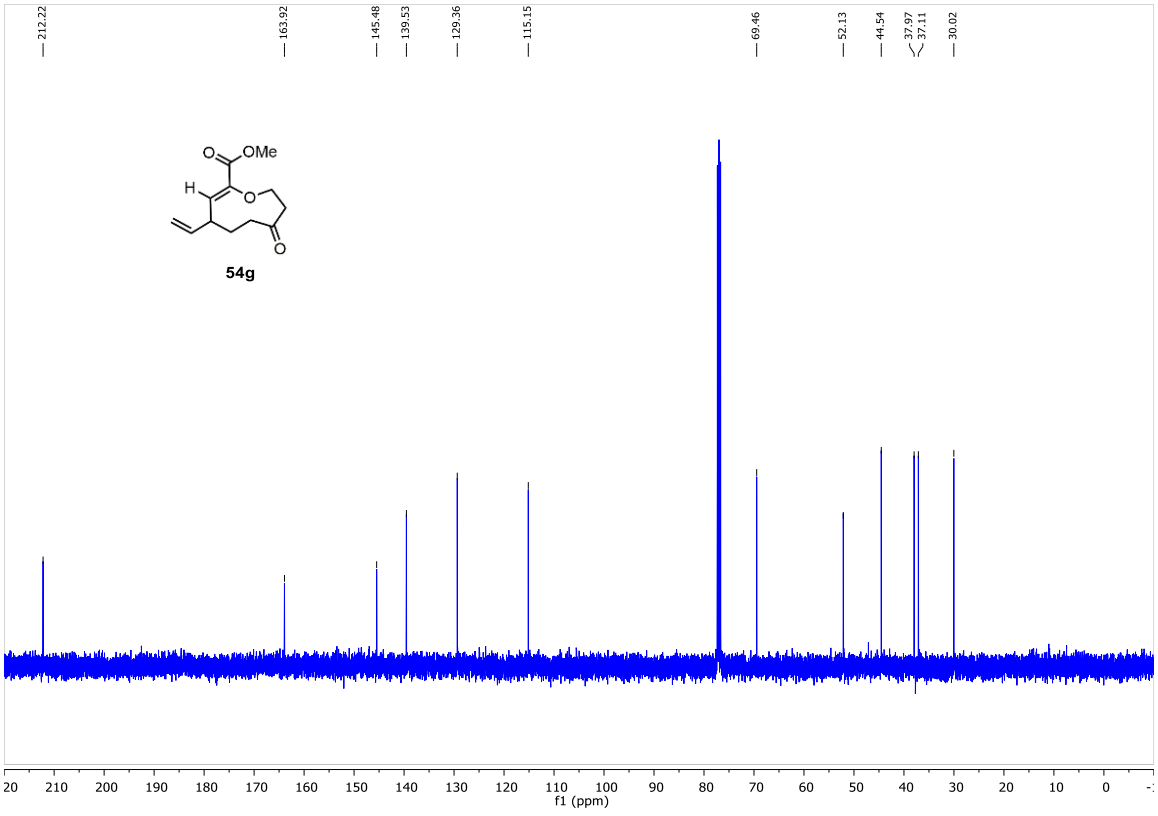
212.22
163.92
145.48
139.53
129.36
115.15
69.46
52.13
44.54
37.97
37.11
30.02
OMe
H
O
O
54g
f1 (ppm)

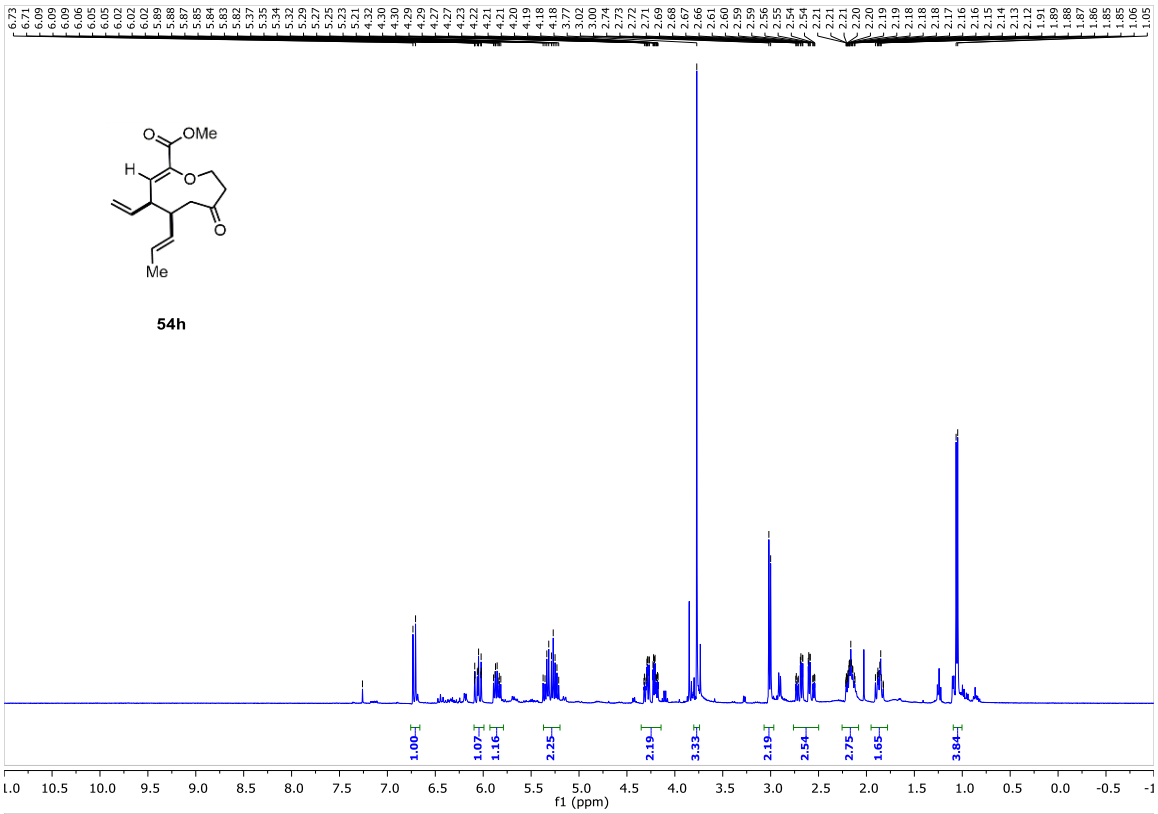
OMe
H
O
O
Me
54h
1.00
1.07
1.16
2.25
2.19
3.33
2.19
2.54
2.75
1.65
3.84
f1 (ppm)

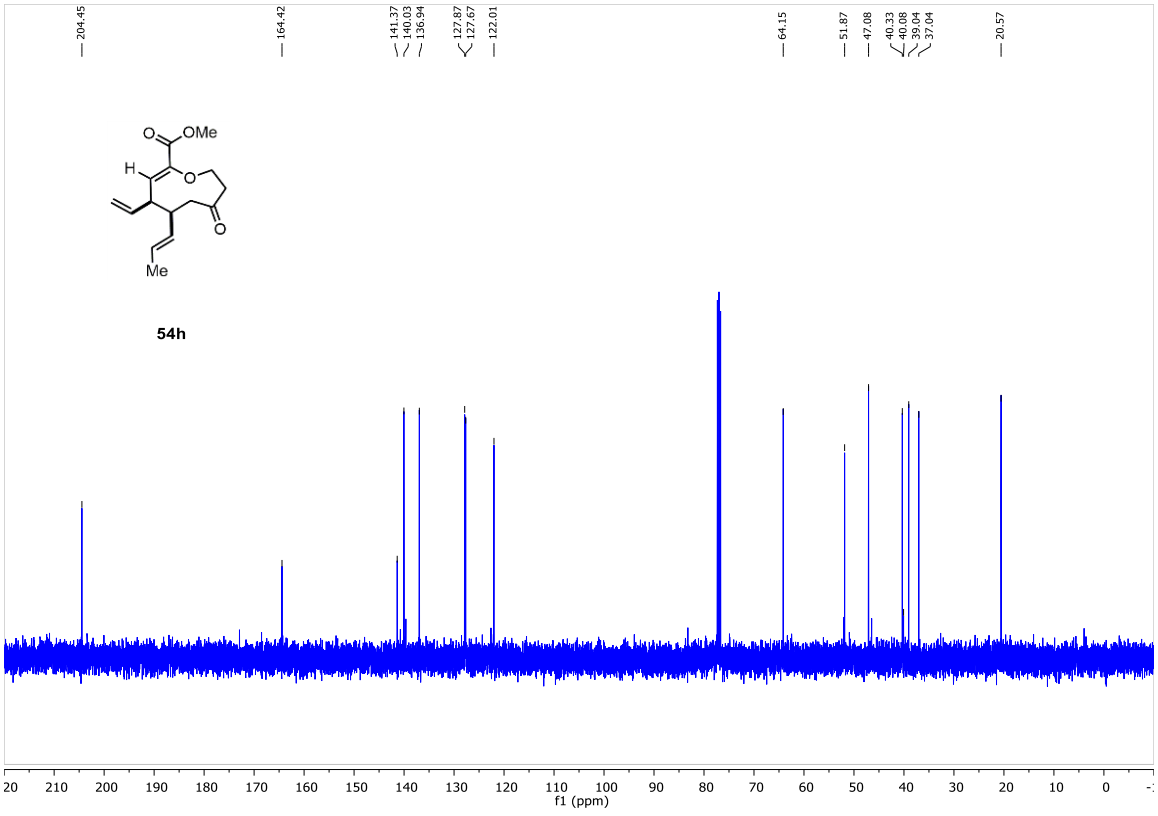
204.45
164.42
141.37
140.03
136.94
127.87
127.67
122.01
64.15
51.87
47.08
40.33
40.08
39.04
37.04
20.57
OMe
H
O
O
Me
54h
f1 (ppm)

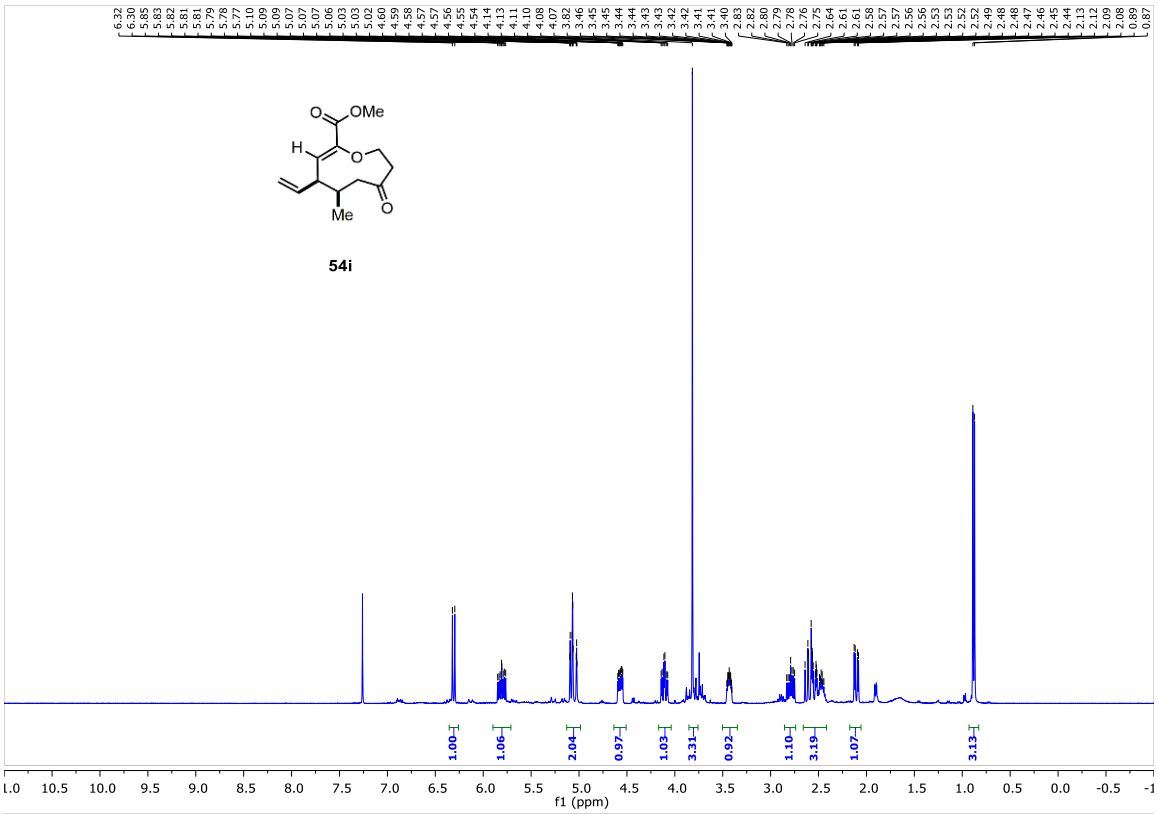
OMe
H
O
Me
O
54i
1.00
1.06
2.04
0.97
1.03
3.31
0.92
1.10
3.19
1.07
3.13
f1 (ppm)

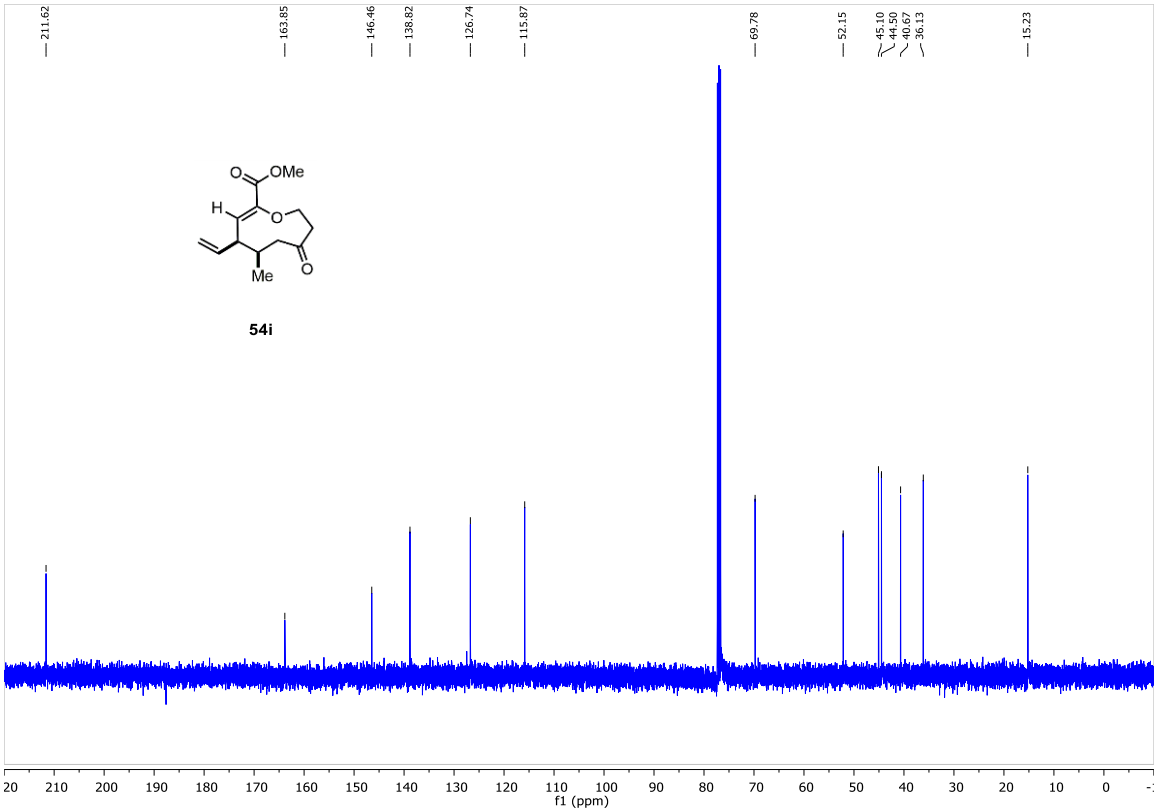
211.62
163.85
146.46
138.82
126.74
115.87
69.78
52.15
45.10
44.50
40.67
36.13
15.23
OMe
H
O
Me
O
54i
f1 (ppm)

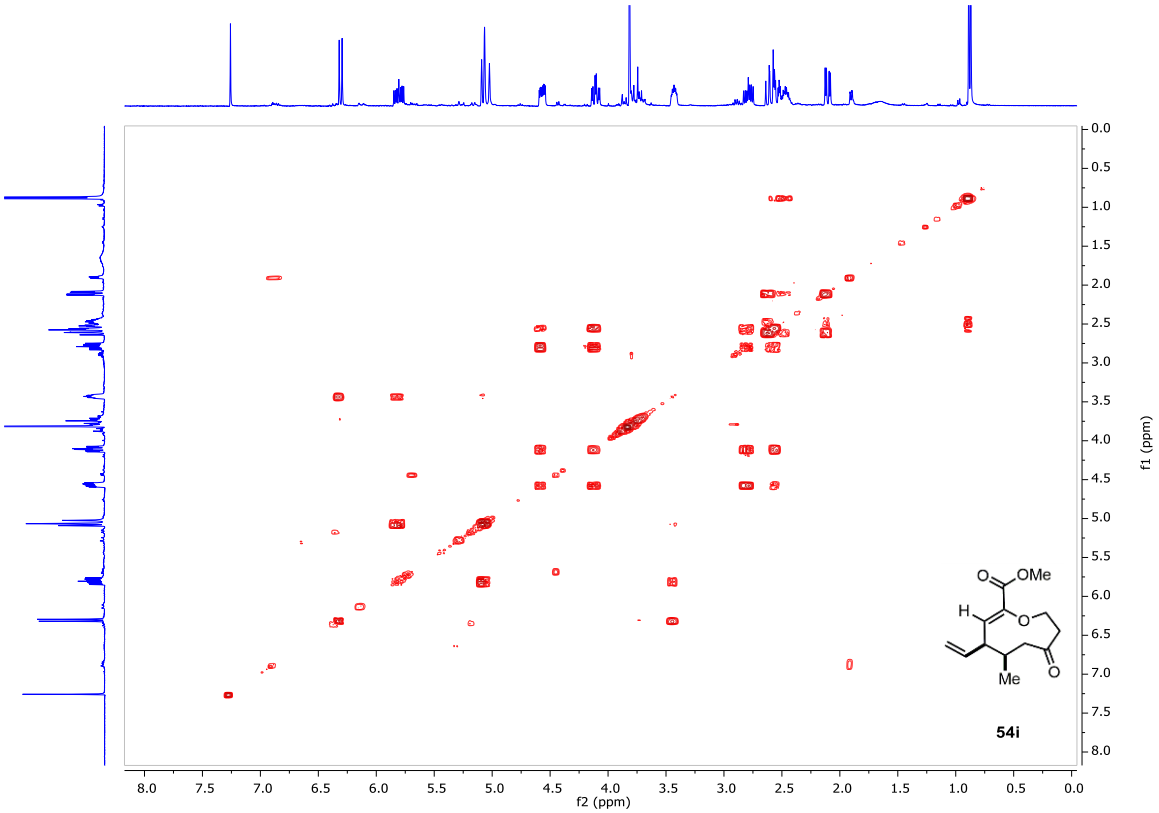
f2 (ppm)
f1 (ppm)
OMe
H
O
Me
O
54i

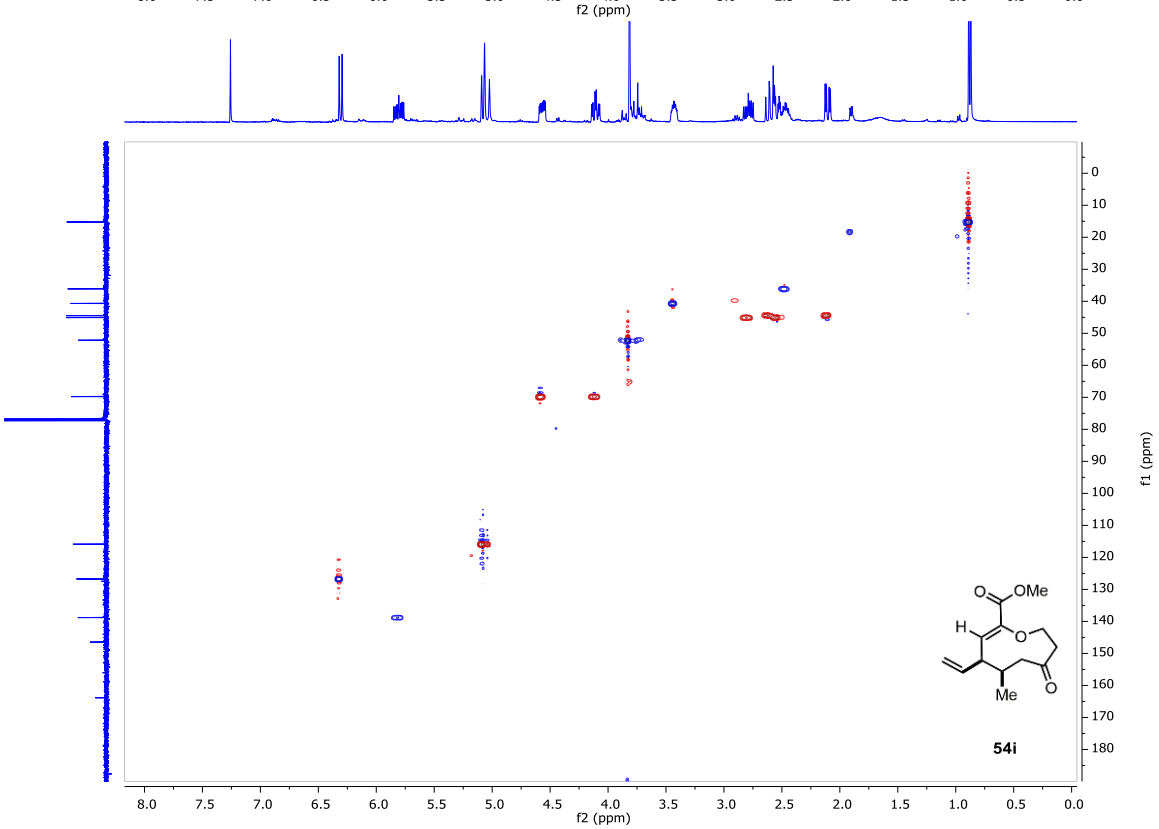
f2 (ppm)
f1 (ppm)
OMe
H
O
Me
O
54i

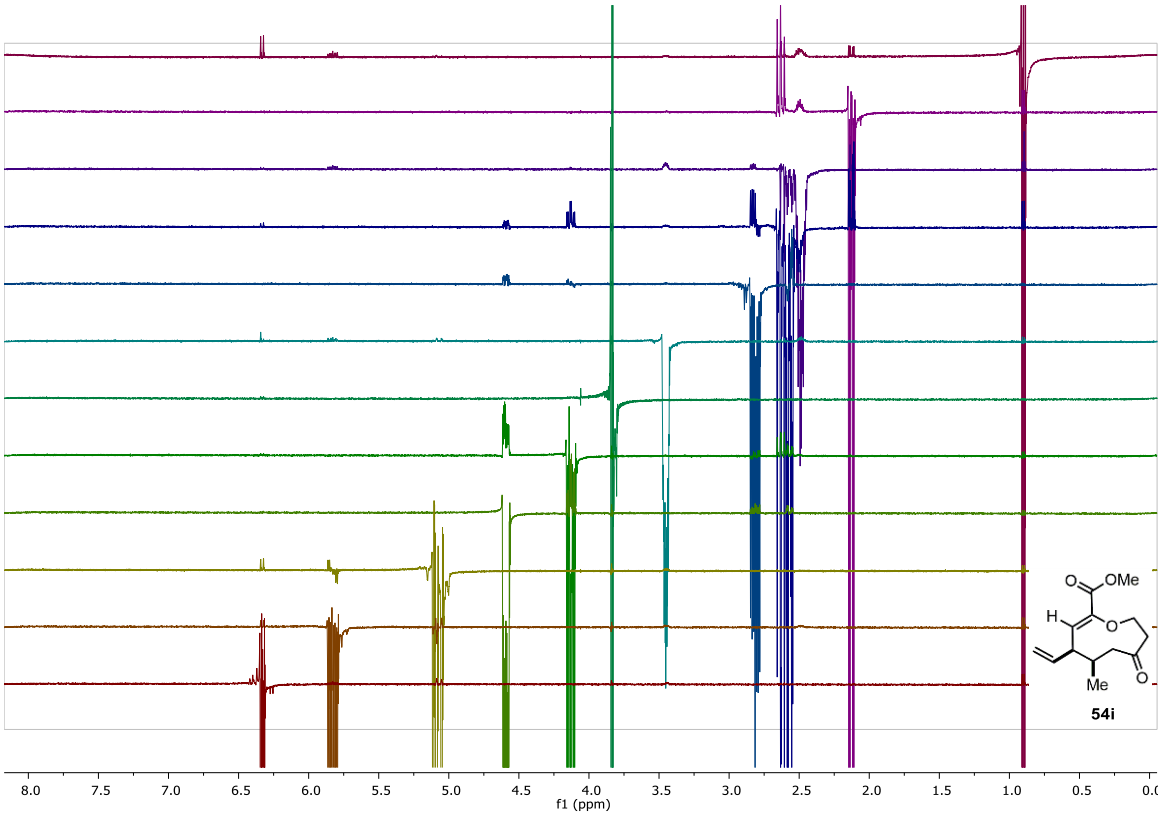
OMe
H
O
Me
54i
f1 (ppm)

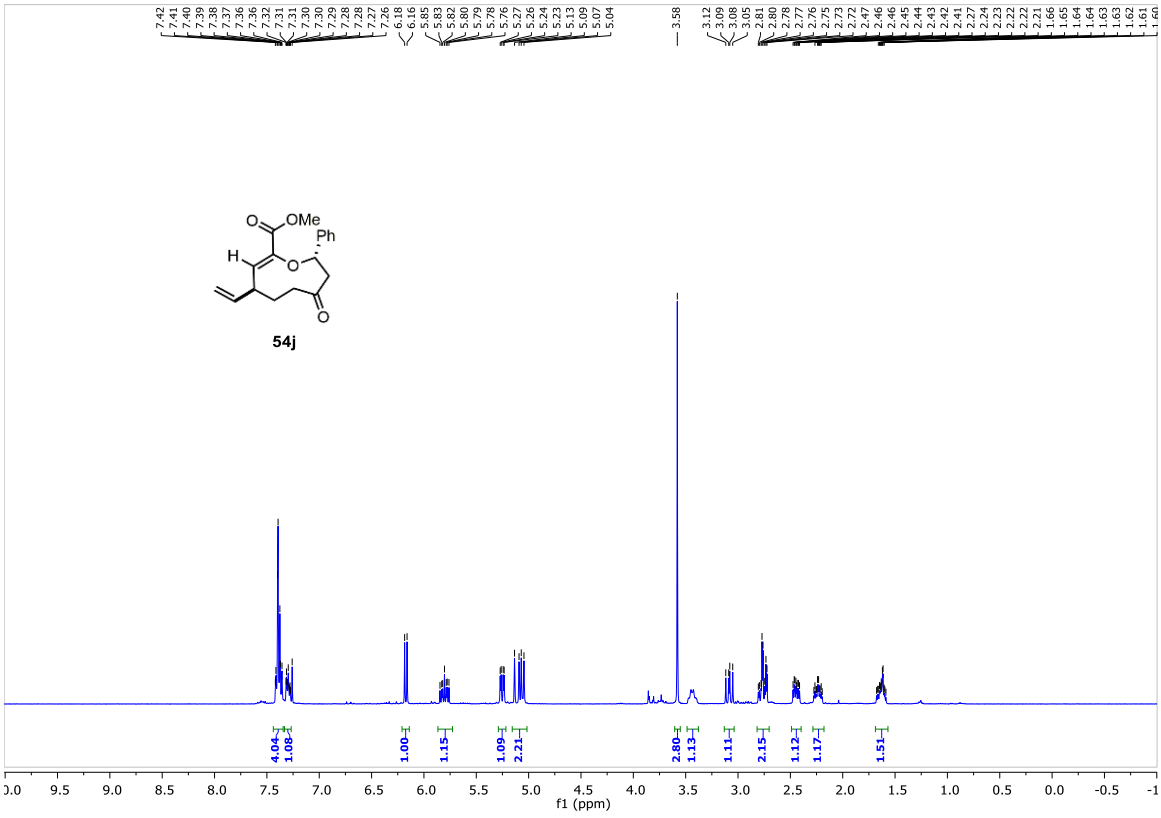
OMe
Ph
H
O
54j
4.04
1.08
1.00
1.15
1.09
2.21
2.80
1.13
1.11
2.15
1.12
1.17
1.51
f1 (ppm)

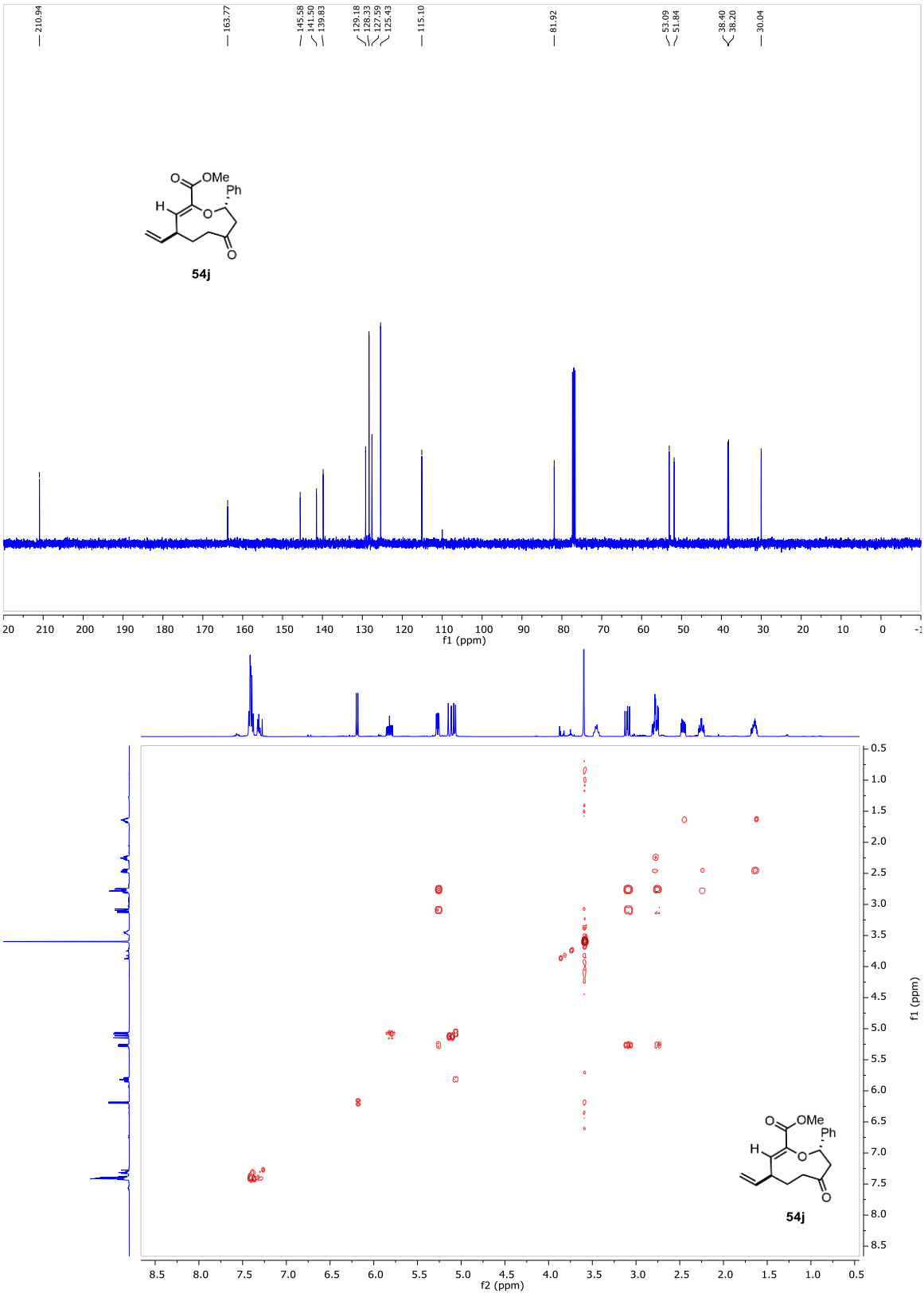
210.94
163.77
145.58
141.50
139.83
129.18
128.33
127.59
125.43
115.10
81.92
53.09
51.84
38.40
38.20
30.04
OMe
Ph
H
O
O
54j
f1 (ppm)
f2 (ppm)

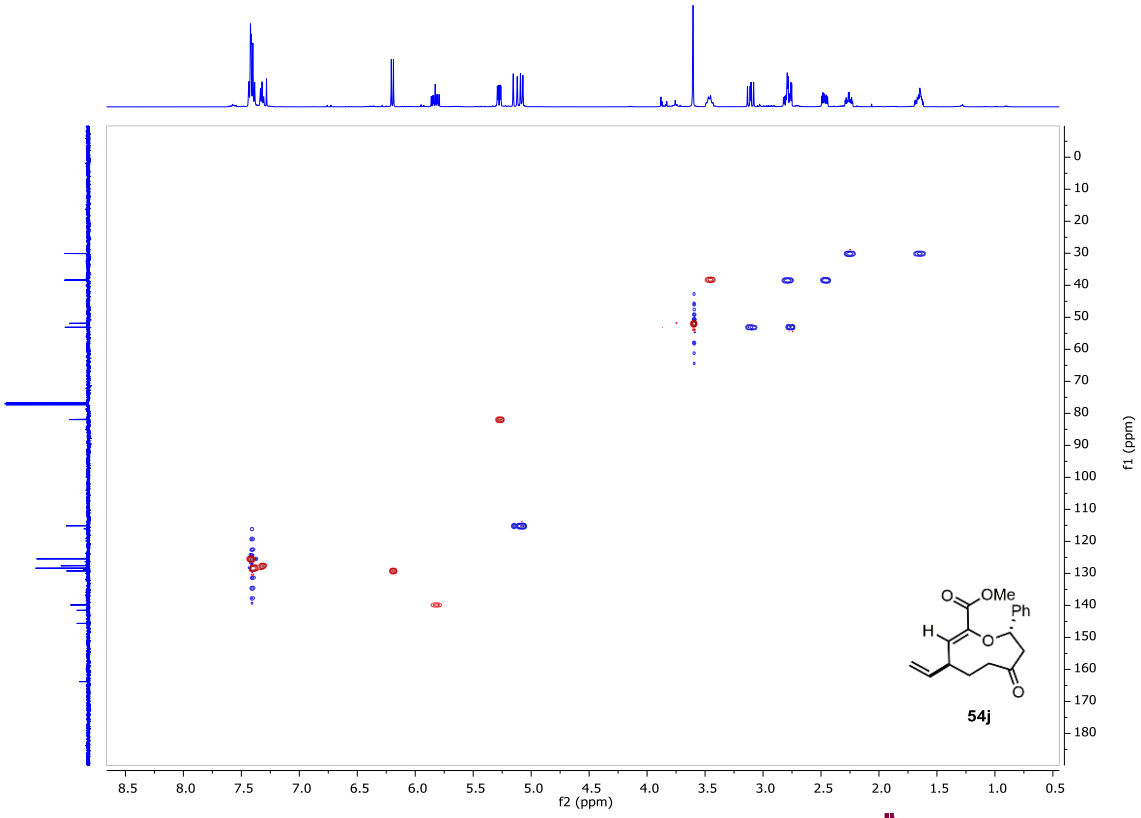
f2 (ppm)
f1 (ppm)
OMe
Ph
H
O
O
54j

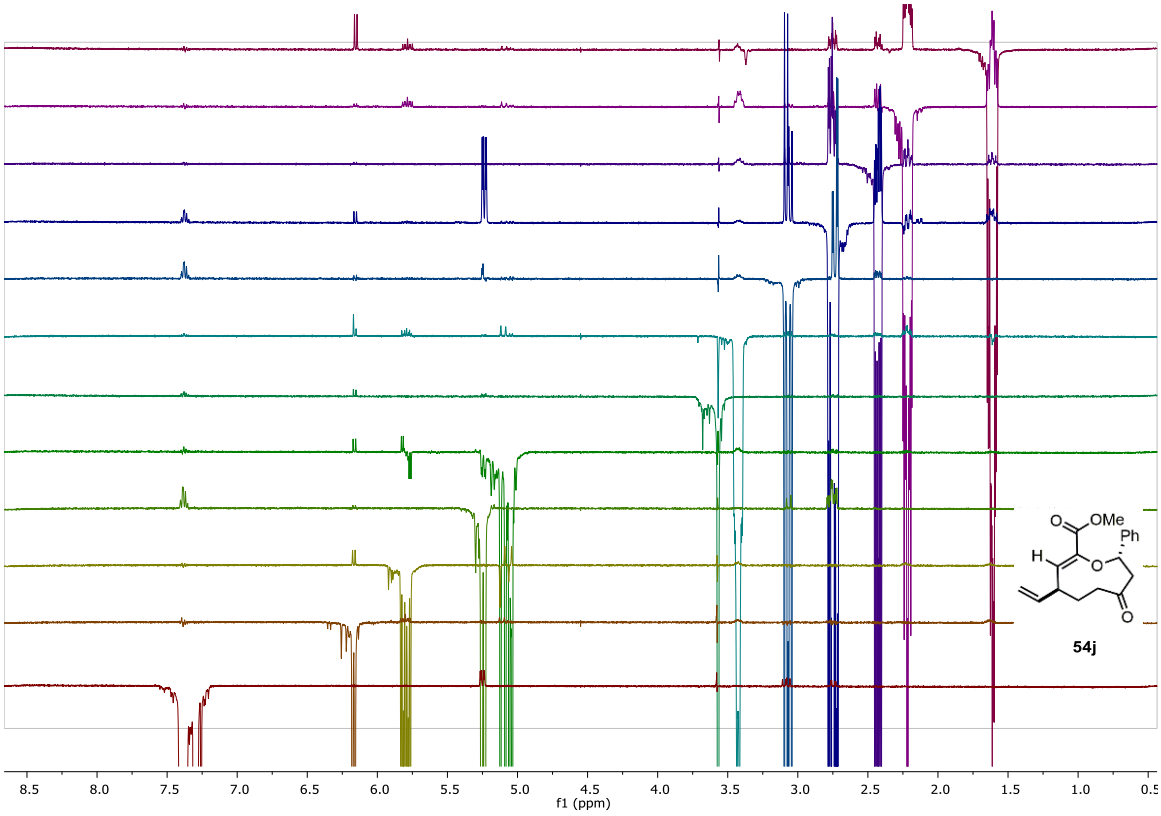
f1 (ppm)
OMe
Ph
H
O
O
54j

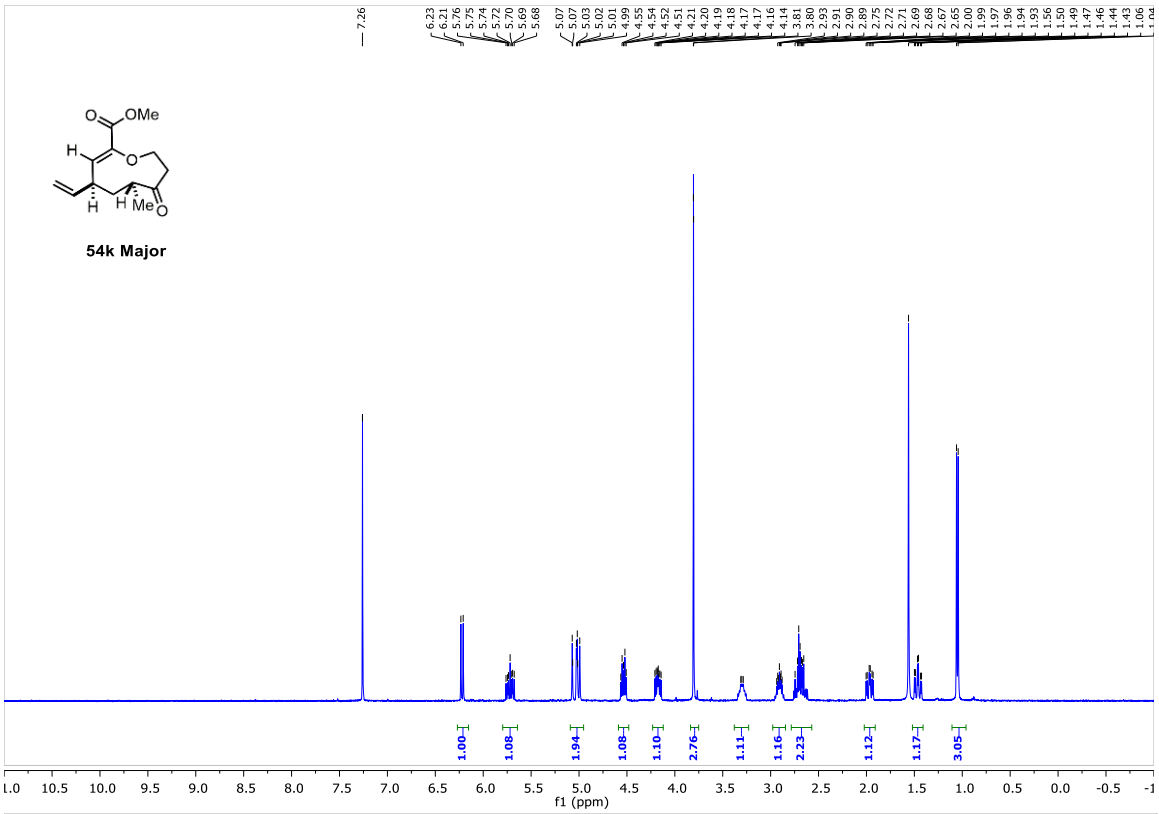
54k Major
f1 (ppm)

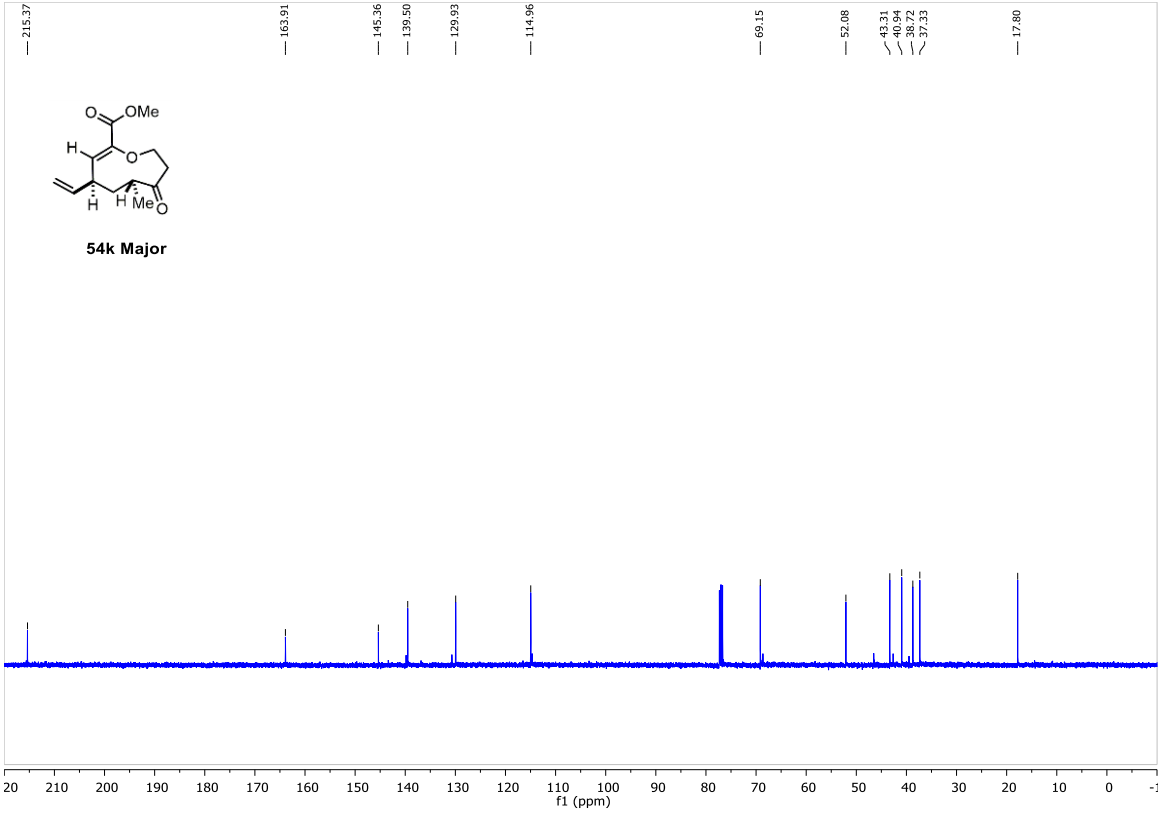
54k Major
f1 (ppm)

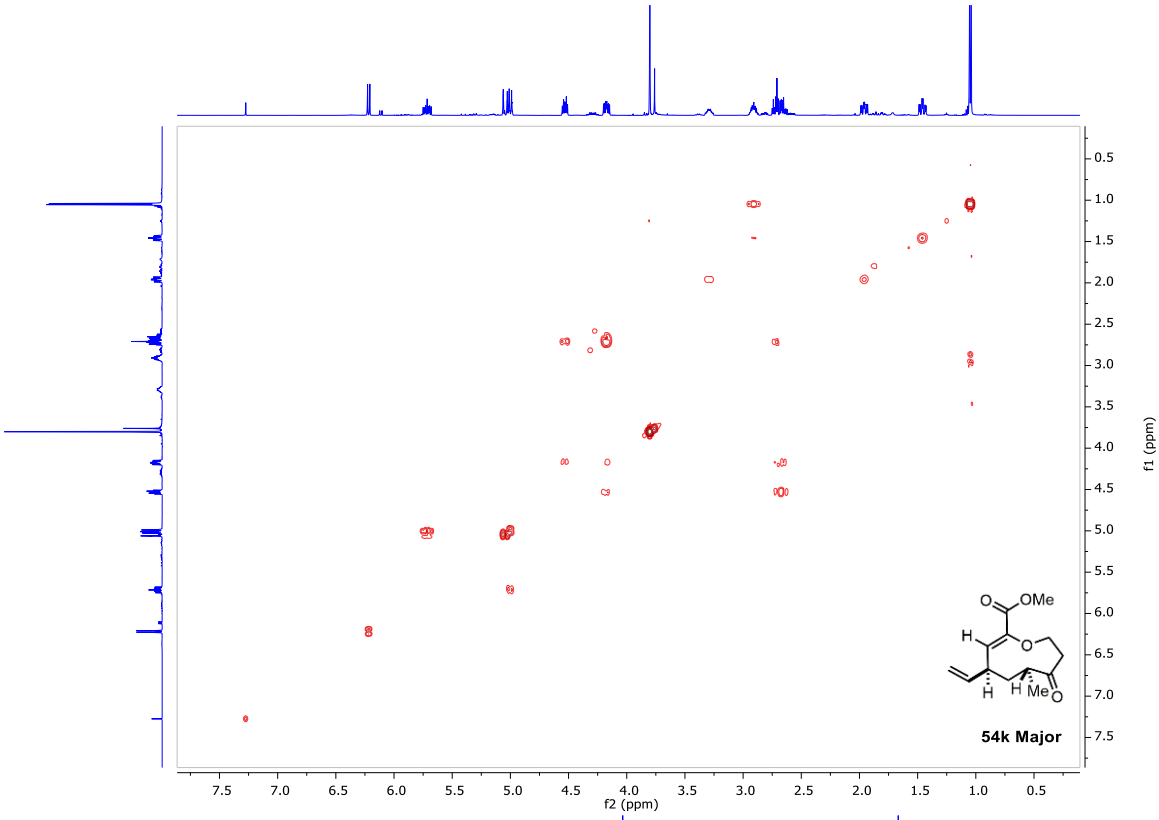
f2 (ppm)
f1 (ppm)
OMe
H
O
H
H
Me
O
54k Major

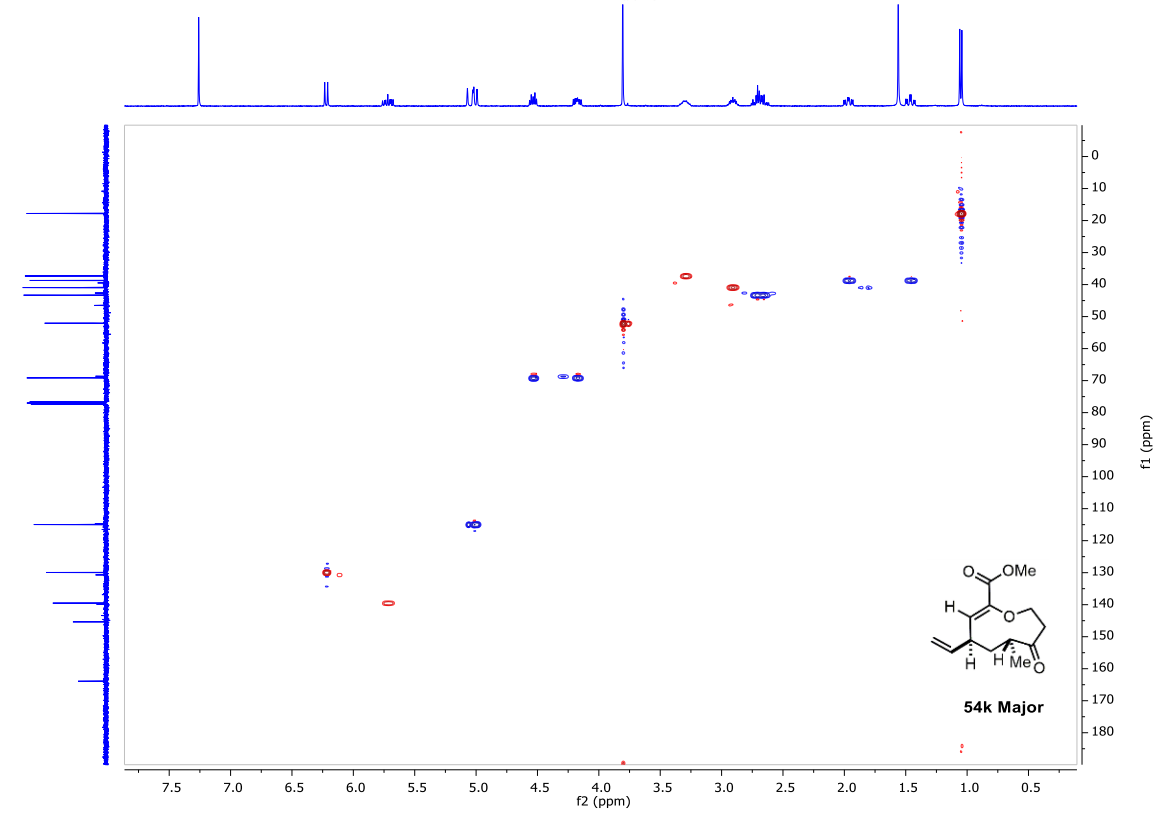
f2 (ppm)
f1 (ppm)
OMe
H
O
H
H
Me
O
54k Major

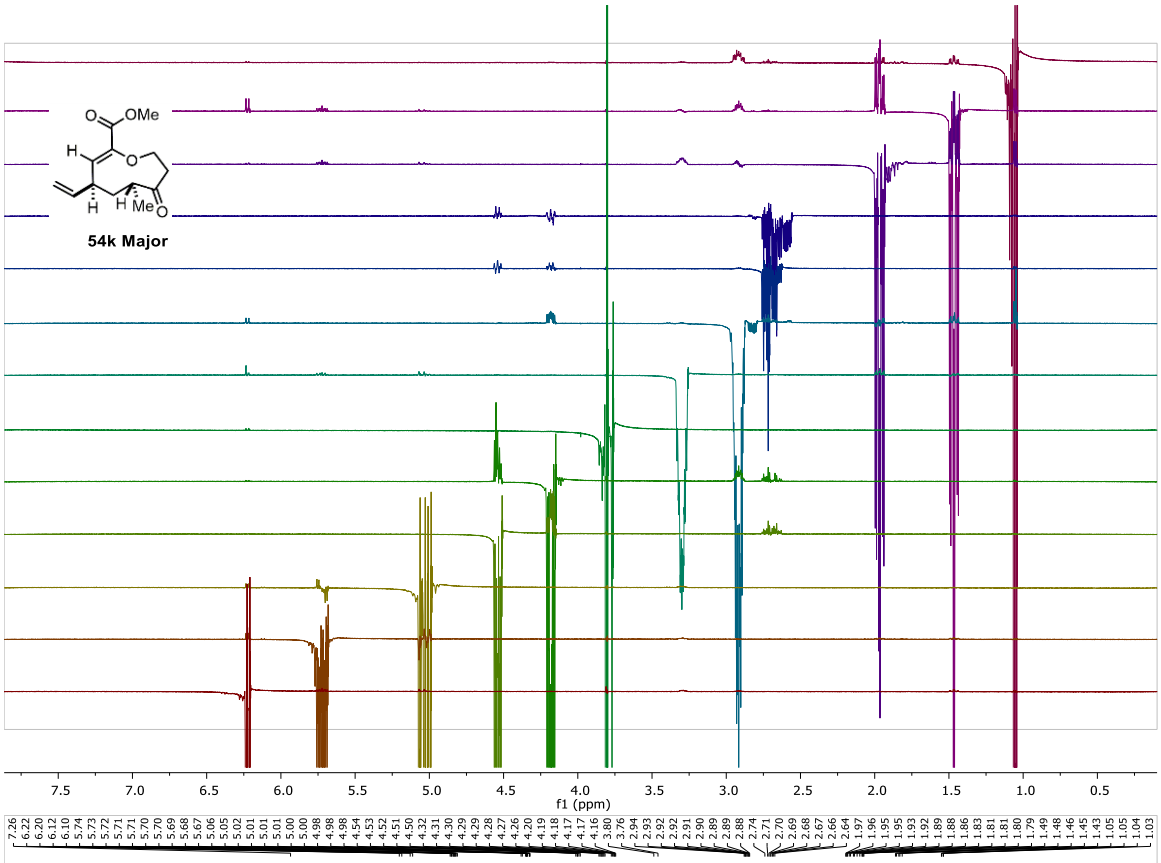
OMe
H
O
H
H
Me
O
54k Major
7.5
7.0
6.5
6.0
5.5
5.0
4.5
4.0
3.5
3.0
2.5
2.0
1.5
1.0
0.5
f1 (ppm)

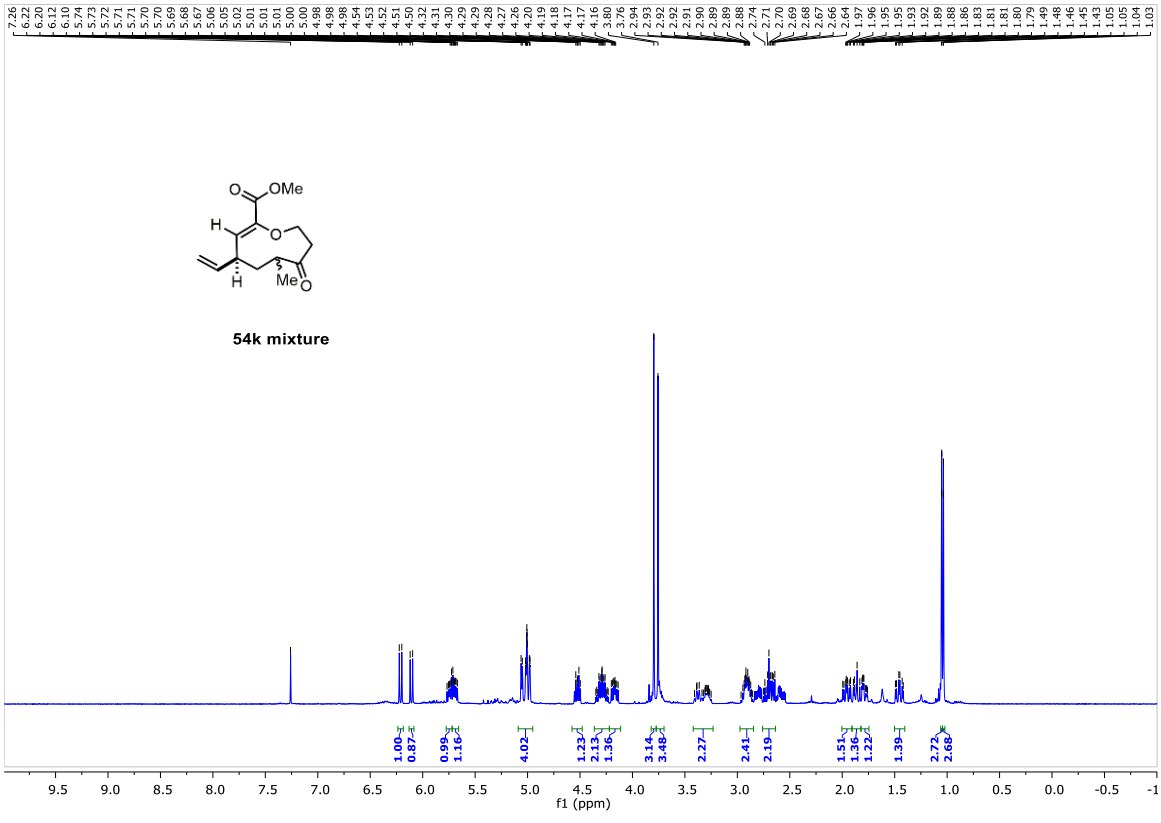
OMe
H
O
H
Me
O
54k mixture
1.00
0.87
0.99
1.16
4.02
1.23
2.13
1.36
3.14
3.48
2.27
2.41
2.19
1.51
1.36
1.22
1.39
2.72
2.68
9.5
9.0
8.5
8.0
7.5
7.0
6.5
6.0
5.5
5.0
4.5
4.0
3.5
3.0
2.5
2.0
1.5
1.0
0.5
0.0
-0.5
-1
f1 (ppm)

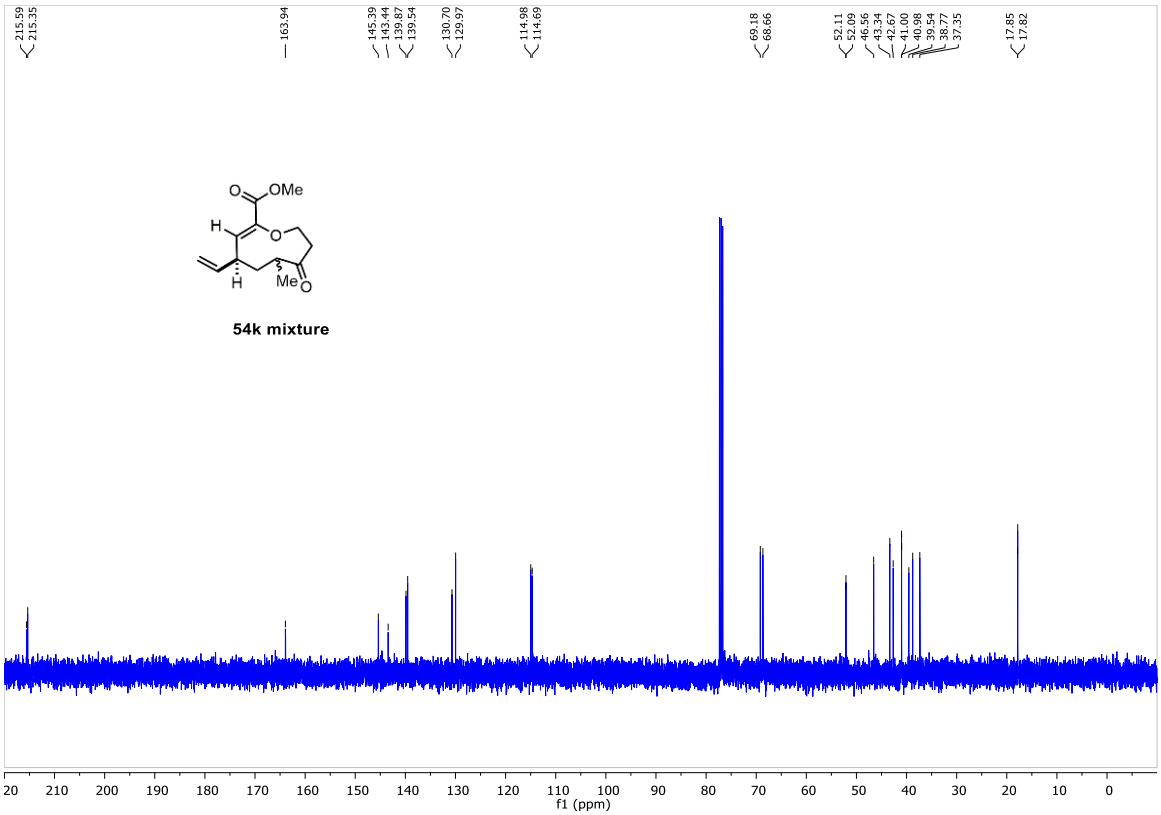
215.59
215.35
163.94
145.39
143.44
139.87
139.54
130.70
129.97
114.98
114.69
69.18
68.66
52.11
52.09
46.56
43.34
42.67
41.00
40.98
39.54
38.77
37.35
17.85
17.82
OMe
O
H
O
H
Me
O
54k mixture
f1 (ppm)

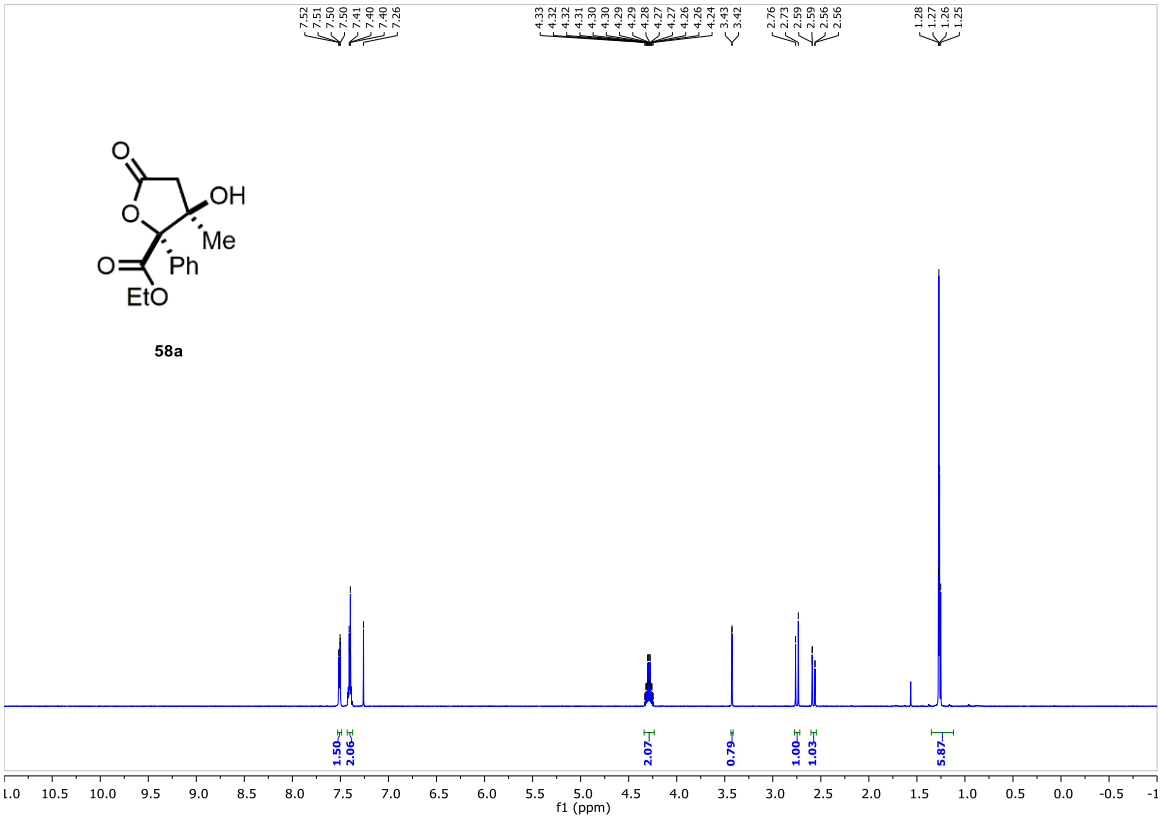
7.52
7.51
7.50
7.50
7.41
7.40
7.40
7.26
4.33
4.32
4.32
4.31
4.30
4.29
4.29
4.28
4.27
4.26
4.26
4.24
3.43
3.42
2.76
2.73
2.59
2.59
2.56
2.56
1.28
1.27
1.26
1.25
O
O
OH
Me
O
Ph
EtO
58a
1.50
2.06
2.07
0.79
1.00
1.03
5.87
f1 (ppm)

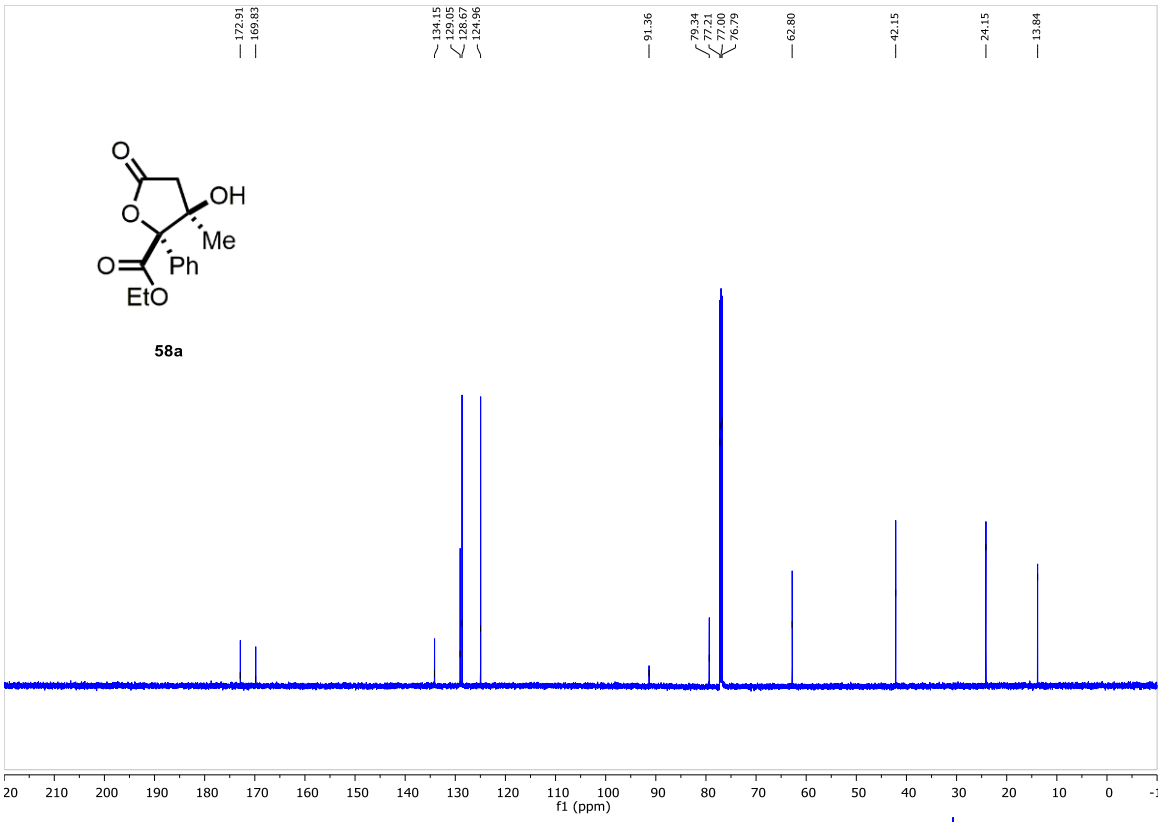
172.91
169.83
134.15
129.05
128.67
124.96
91.36
79.34
77.21
77.00
76.79
62.80
42.15
24.15
13.84
OH
Me
Ph
EtO
58a
f1 (ppm)

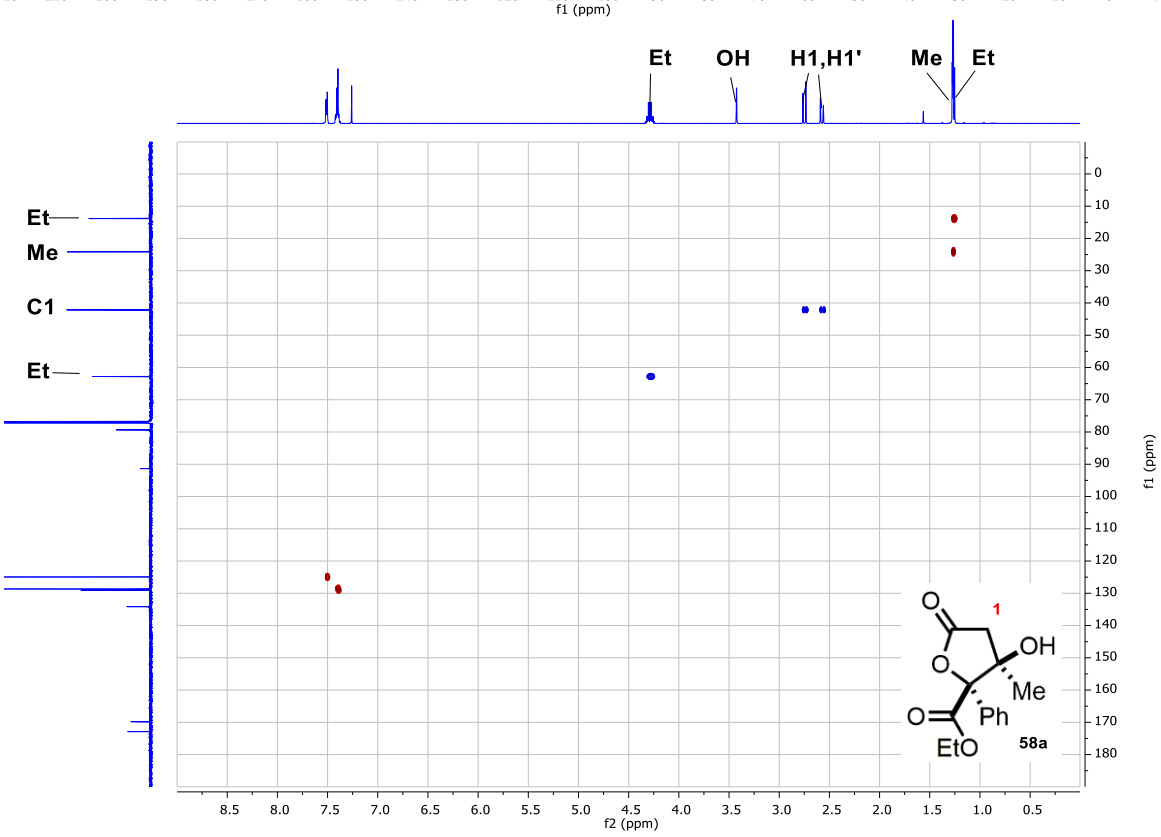
Et
OH
H1,H1'
Me
Et
Et
Me
C1
Et
1
OH
Me
Ph
EtO
58a
f2 (ppm)
f1 (ppm)

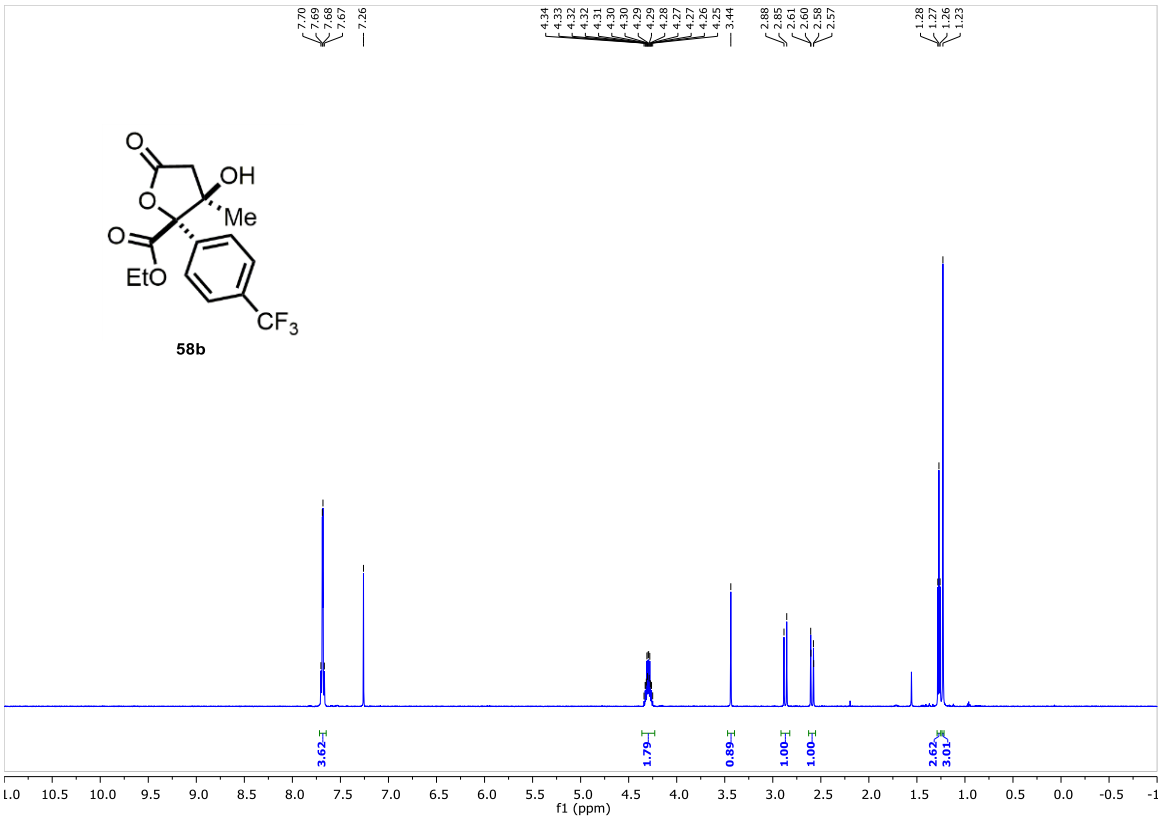
7.70
7.69
7.68
7.67
7.26
4.34
4.33
4.32
4.32
4.31
4.30
4.30
4.29
4.29
4.28
4.27
4.27
4.26
4.25
3.44
2.88
2.85
2.61
2.60
2.58
2.57
1.28
1.27
1.26
1.23
O
OH
O
Me
O
EtO
CF3
58b
3.62
1.79
0.89
1.00
1.00
2.62
3.01
f1 (ppm)

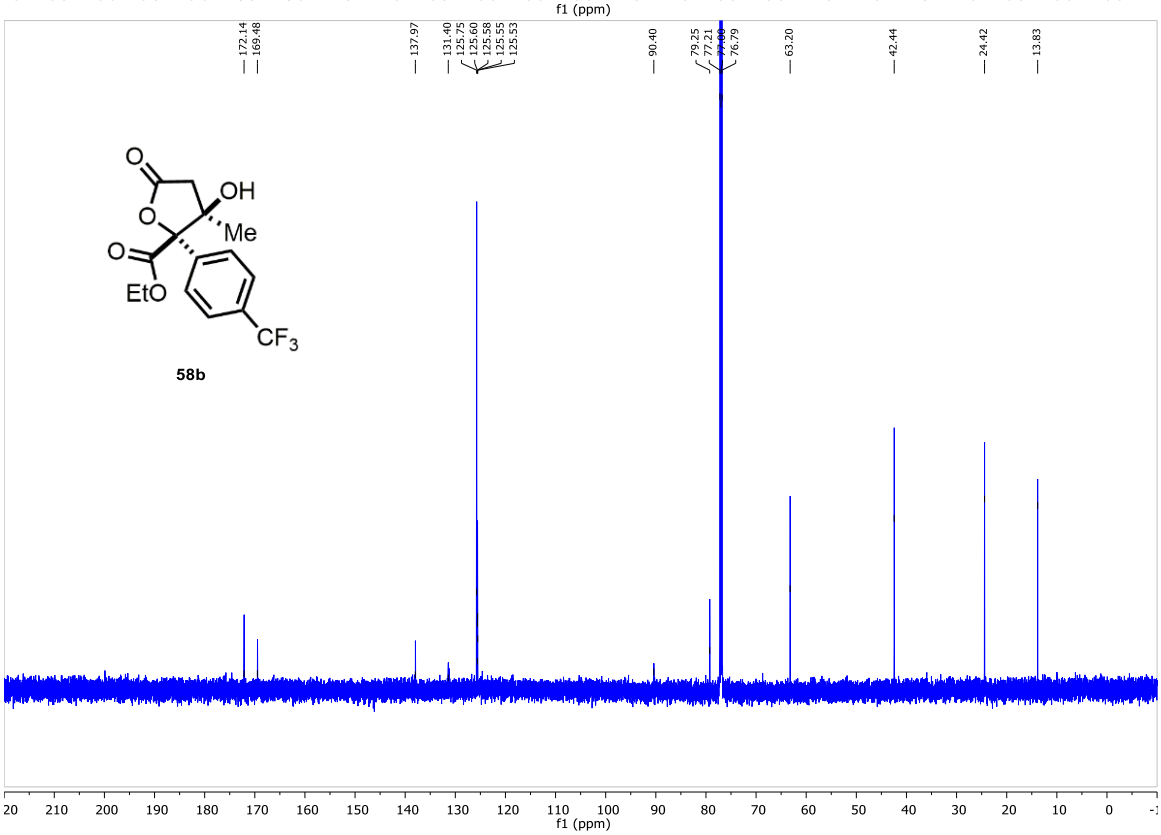
172.14
169.48
137.97
131.40
125.75
125.60
125.58
125.55
125.53
90.40
79.25
77.21
77.00
76.79
63.20
42.44
24.42
13.83
O
OH
O
Me
O
EtO
CF3
58b
f1 (ppm)

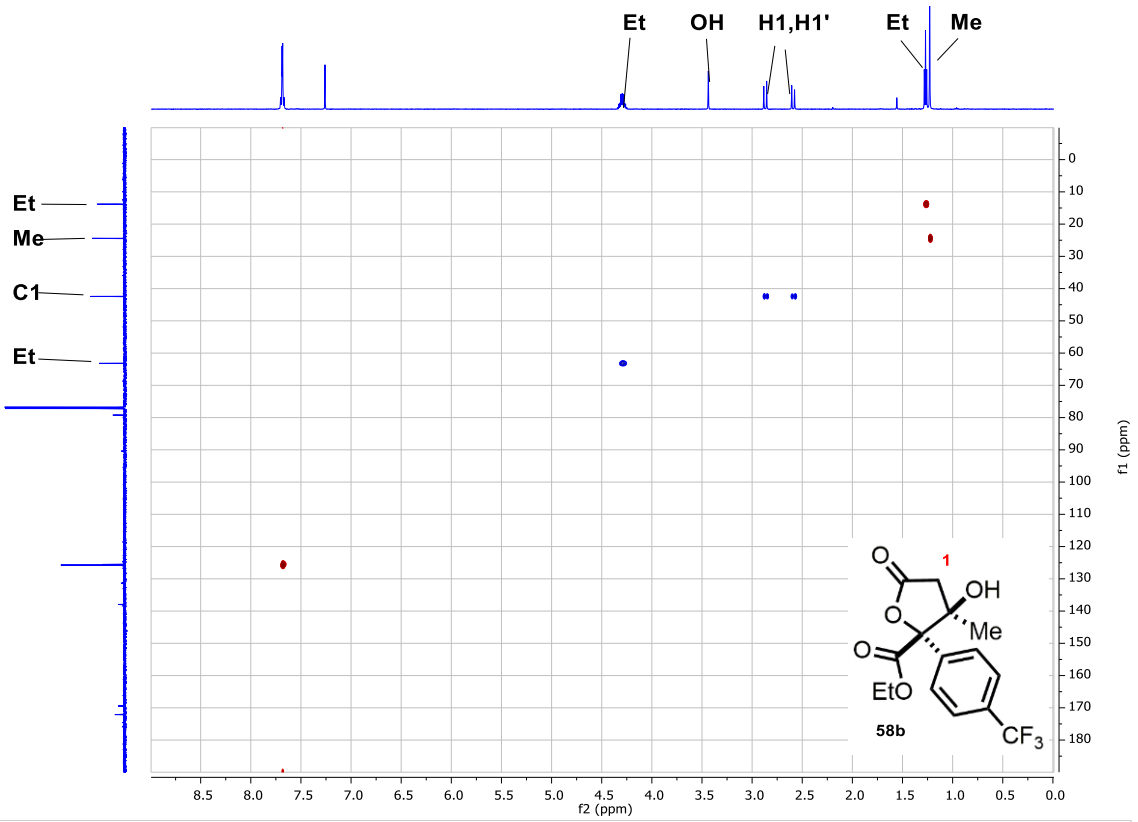
Et
OH
H1,H1'
Et
Me
Et
Me
C1
Et
f1 (ppm)
f2 (ppm)
1
OH
Me
EtO
58b
CF3

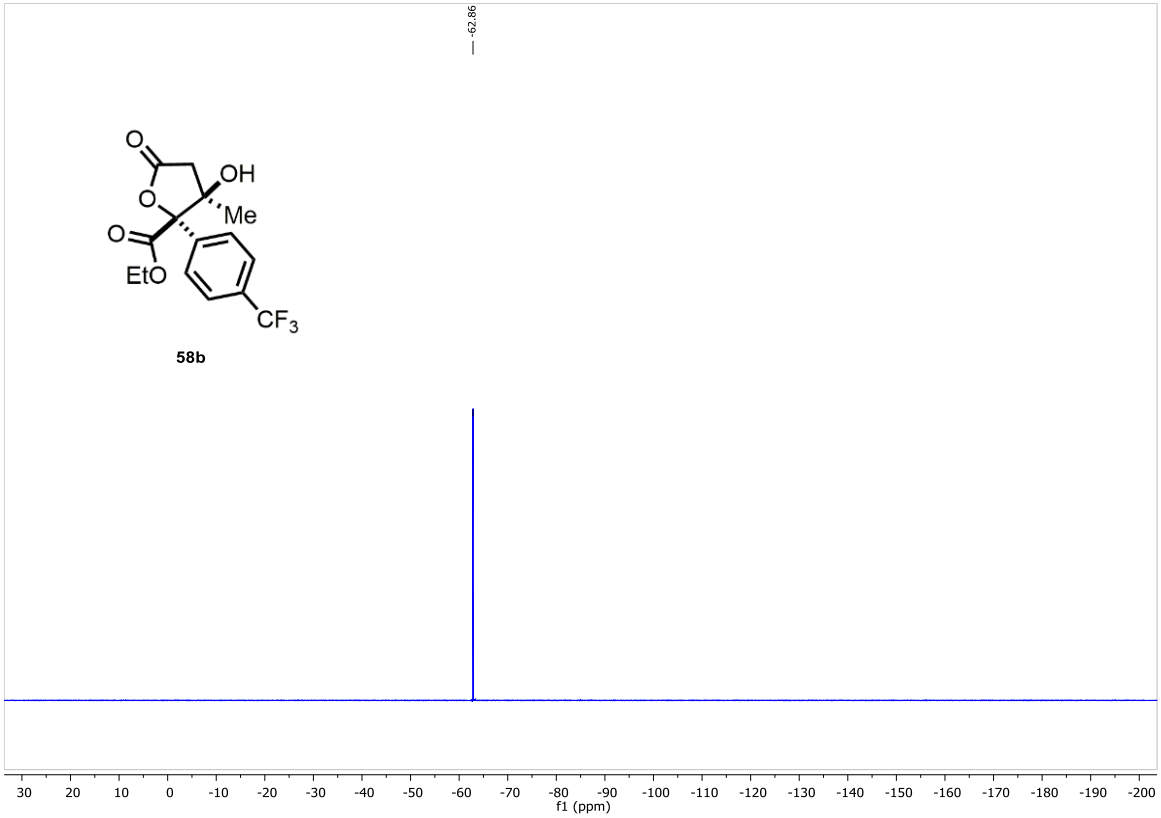
-62.86
OH
Me
EtO
58b
CF3
f1 (ppm)

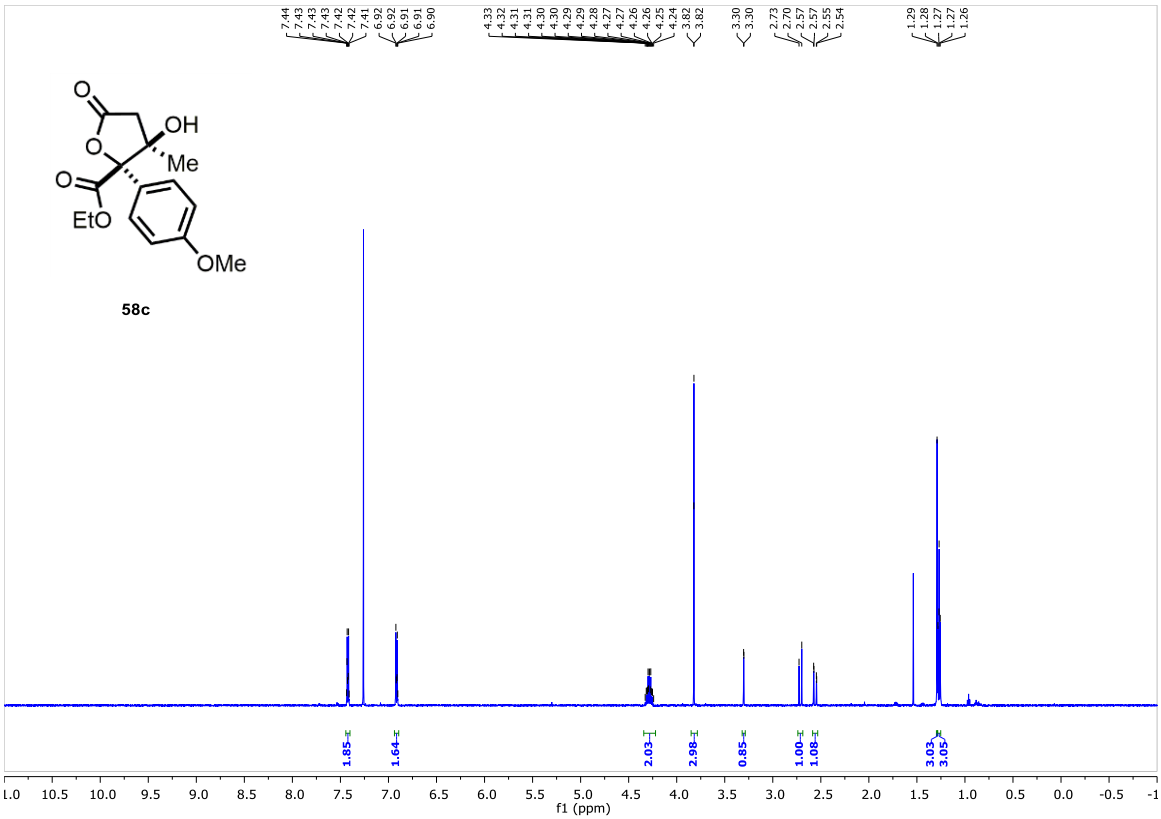
7.44
7.43
7.43
7.43
7.42
7.42
7.41
6.92
6.92
6.91
6.91
6.90
4.33
4.32
4.31
4.31
4.30
4.30
4.29
4.29
4.28
4.27
4.27
4.26
4.26
4.25
4.24
3.82
3.82
3.30
3.30
2.73
2.70
2.57
2.57
2.55
2.54
1.29
1.28
1.27
1.27
1.26
OH
Me
O
O
EtO
OMe
58c
1.85
1.64
2.03
2.98
0.85
1.00
1.08
3.03
3.05
f1 (ppm)

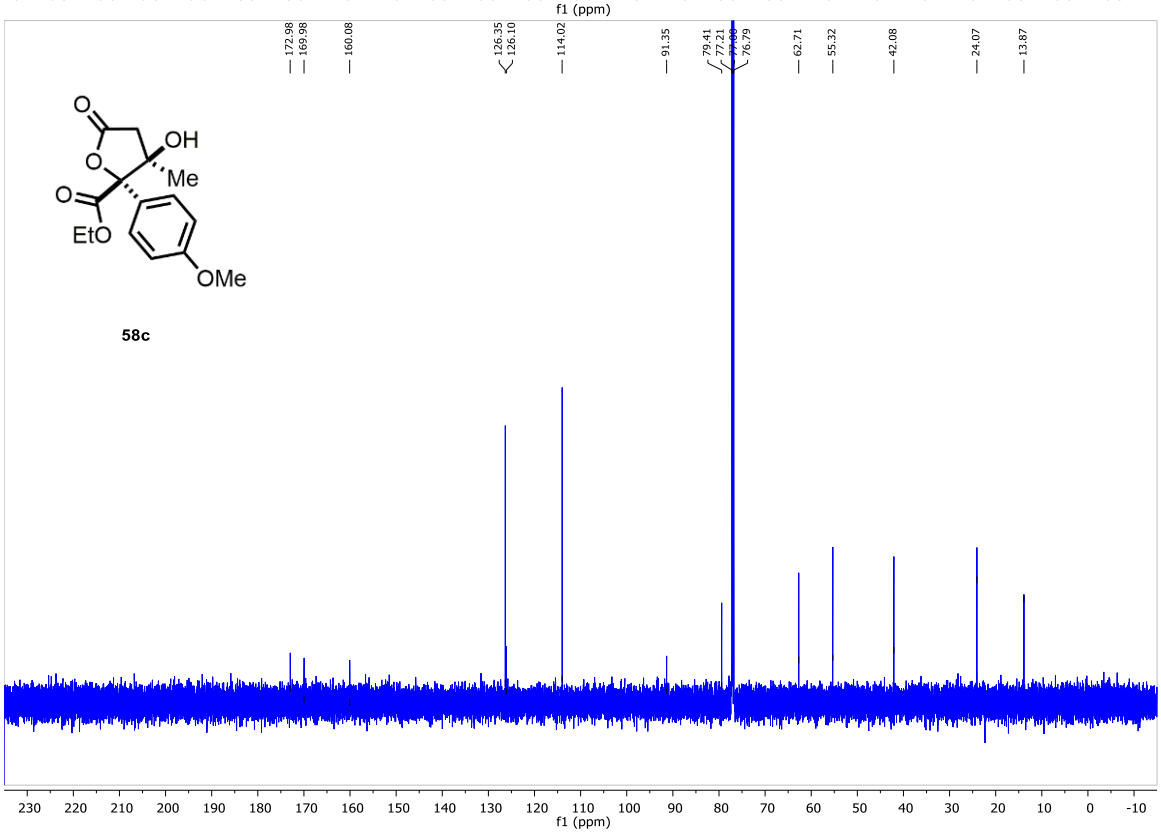
172.98
169.98
160.08
126.35
126.10
114.02
91.35
79.41
77.21
77.00
76.79
62.71
55.32
42.08
24.07
13.87
OH
Me
O
O
EtO
OMe
58c
f1 (ppm)

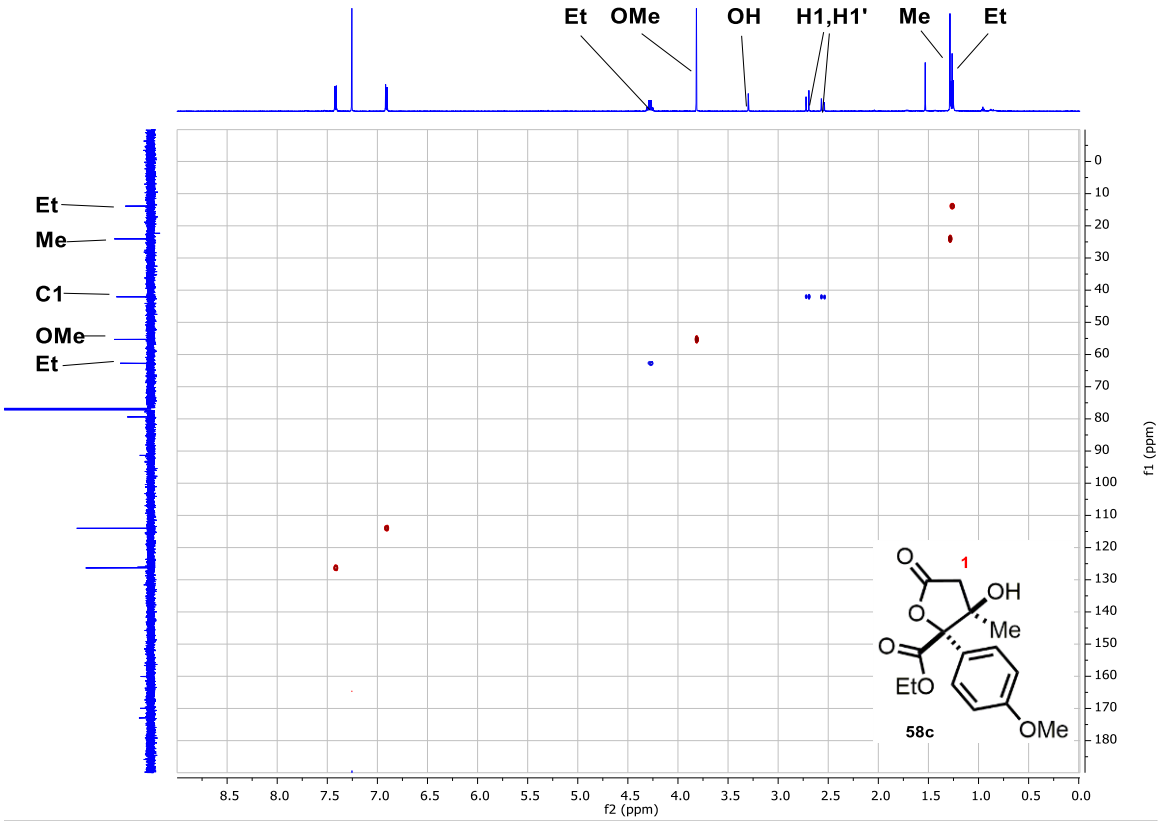
Et
OMe
OH
H1,H1'
Me
Et
Et
Me
C1
OMe
Et
f1 (ppm)
f2 (ppm)
1
OH
Me
EtO
OMe
58c

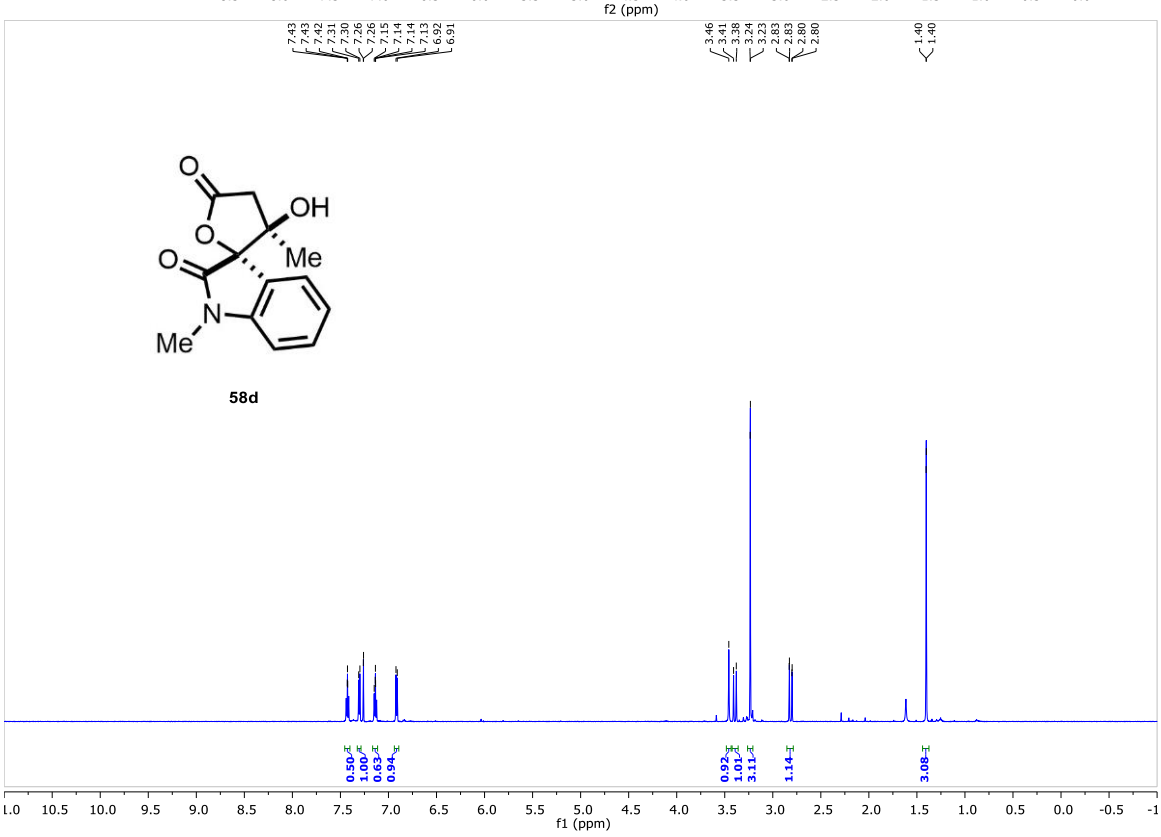
OH
Me
N
Me
58d
f1 (ppm)

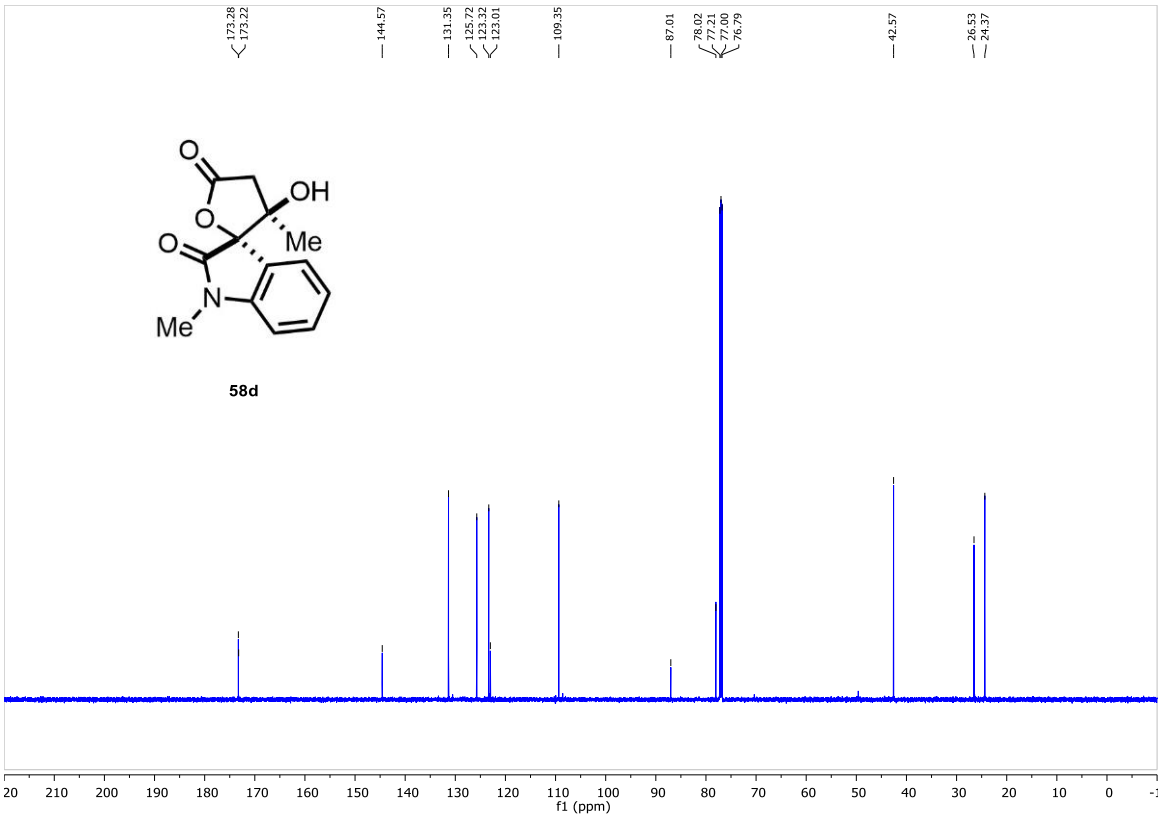
173.28
173.22
144.57
131.35
125.72
123.32
123.01
109.35
87.01
78.02
77.21
77.00
76.79
42.57
26.53
24.37
OH
Me
Me
58d
f1 (ppm)

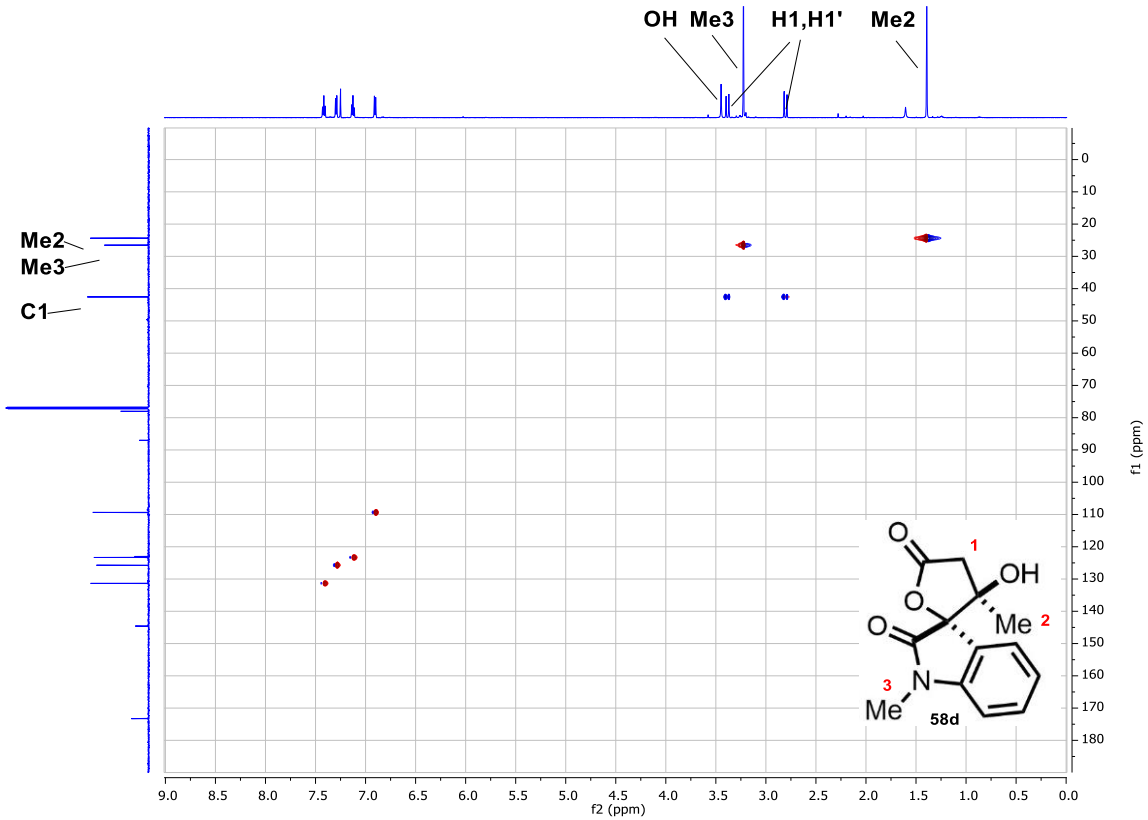
OH
Me3
H1,H1'
Me2
Me2
Me3
C1
1
2
3
58d
f2 (ppm)
f1 (ppm)

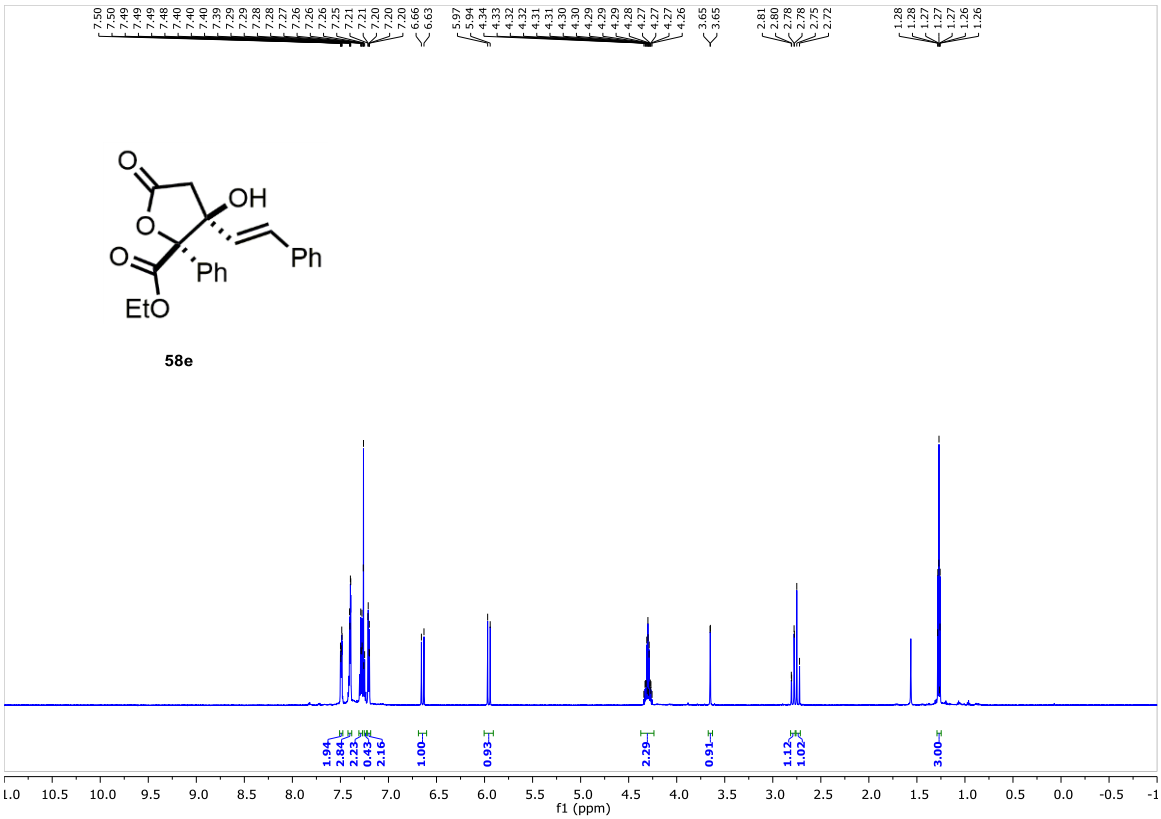
OH
O
O
Ph
Ph
EtO
58e
f1 (ppm)

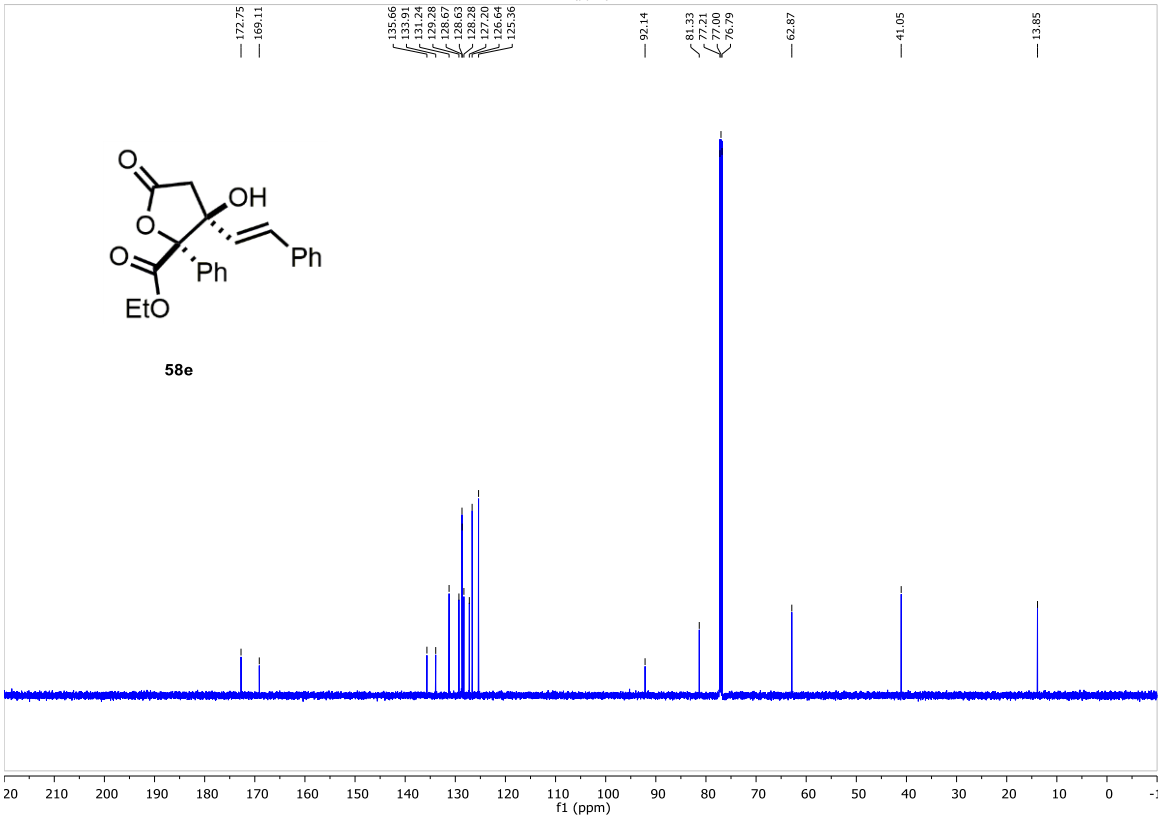
OH
O
O
Ph
Ph
EtO
58e
f1 (ppm)

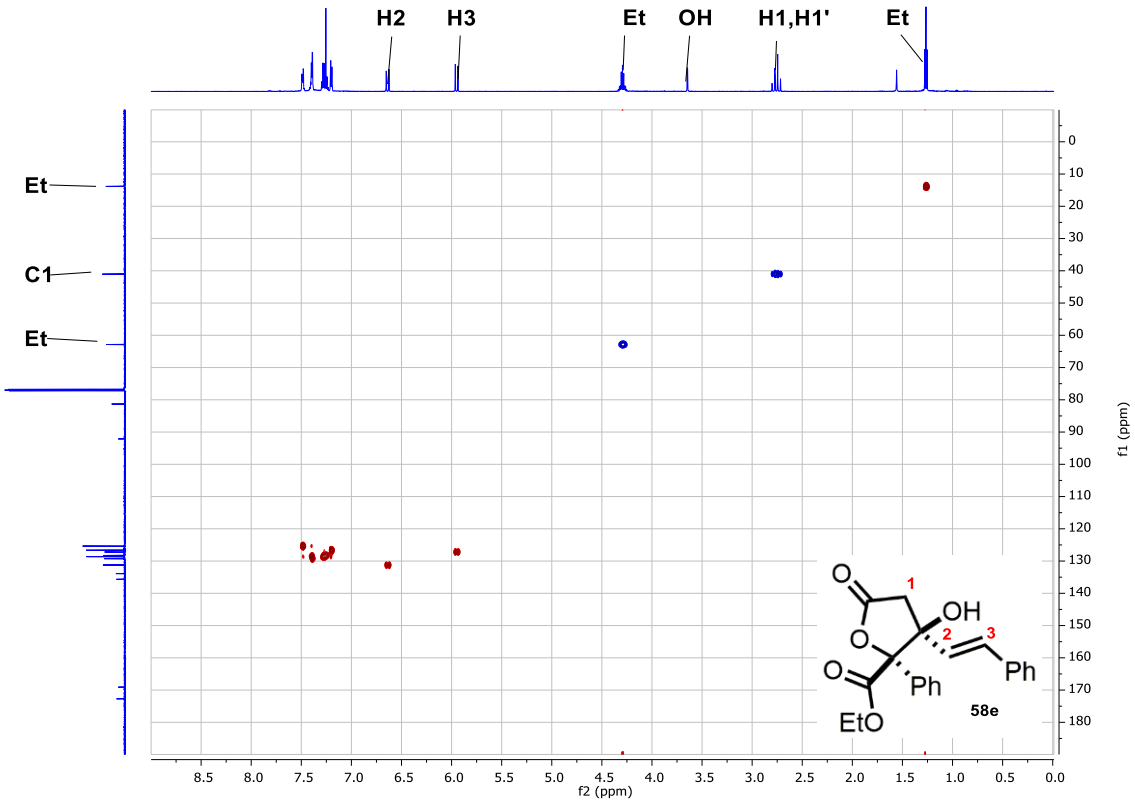
H2
H3
Et
OH
H1,H1'
Et
Et
C1
Et
f2 (ppm)
f1 (ppm)
OH
Ph
Ph
EtO
58e

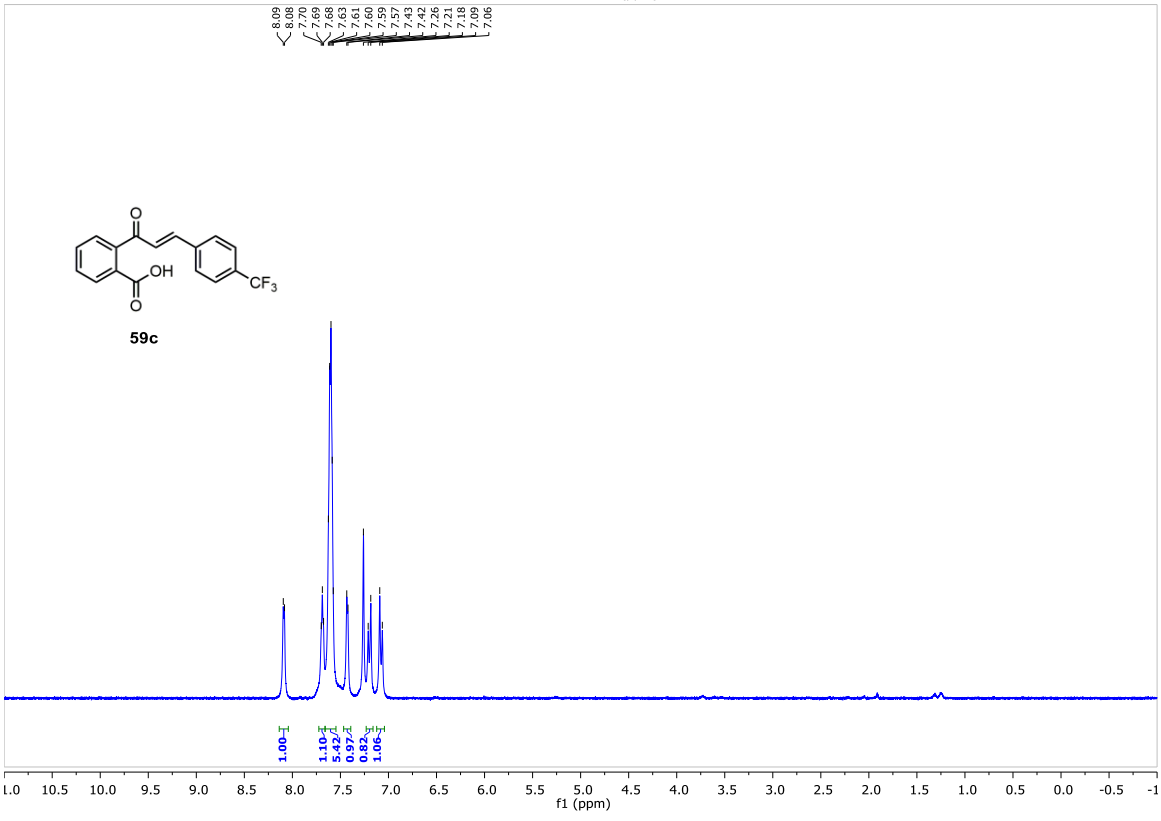
OH
CF3
59c
f1 (ppm)

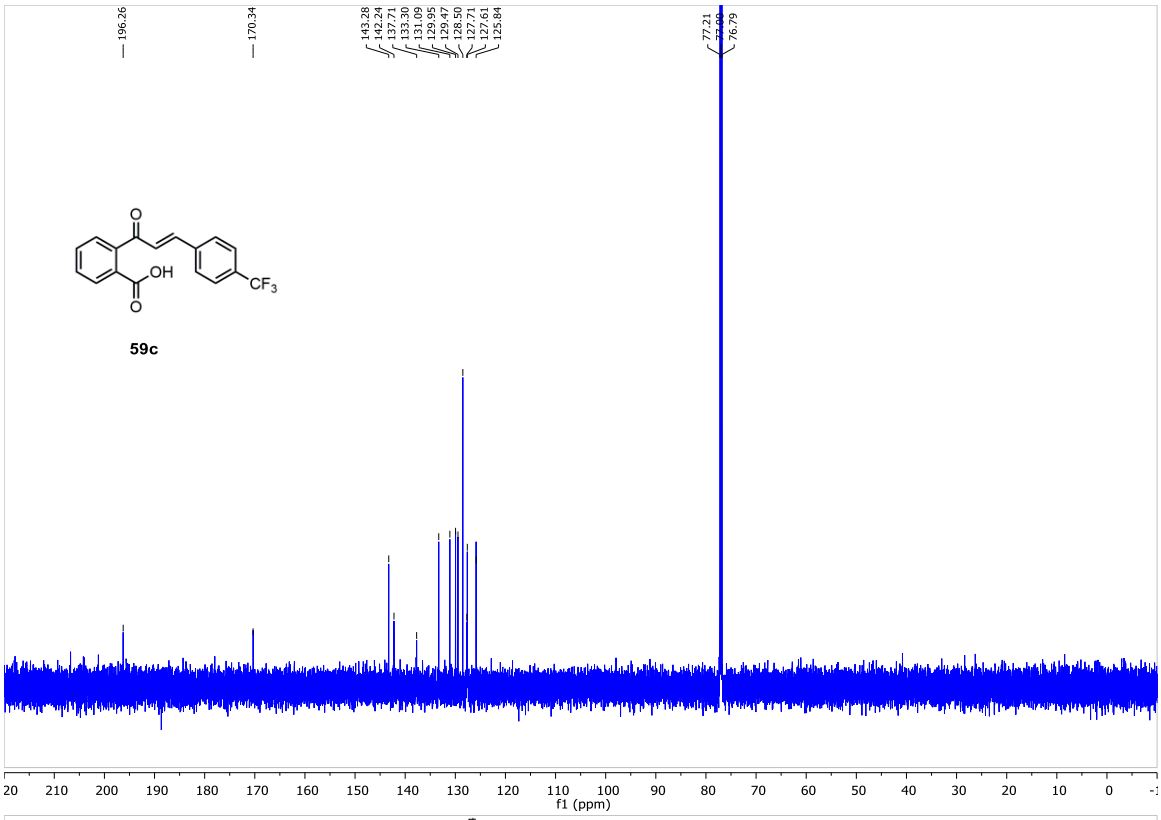
196.26
170.34
143.28
142.24
137.71
133.30
131.09
129.95
129.47
128.50
127.71
127.61
125.84
77.21
77.00
76.79
O
OH
O
CF3
59c
20 210 200 190 180 170 160 150 140 130 120 110 100 90 80 70 60 50 40 30 20 10 0
f1 (ppm)

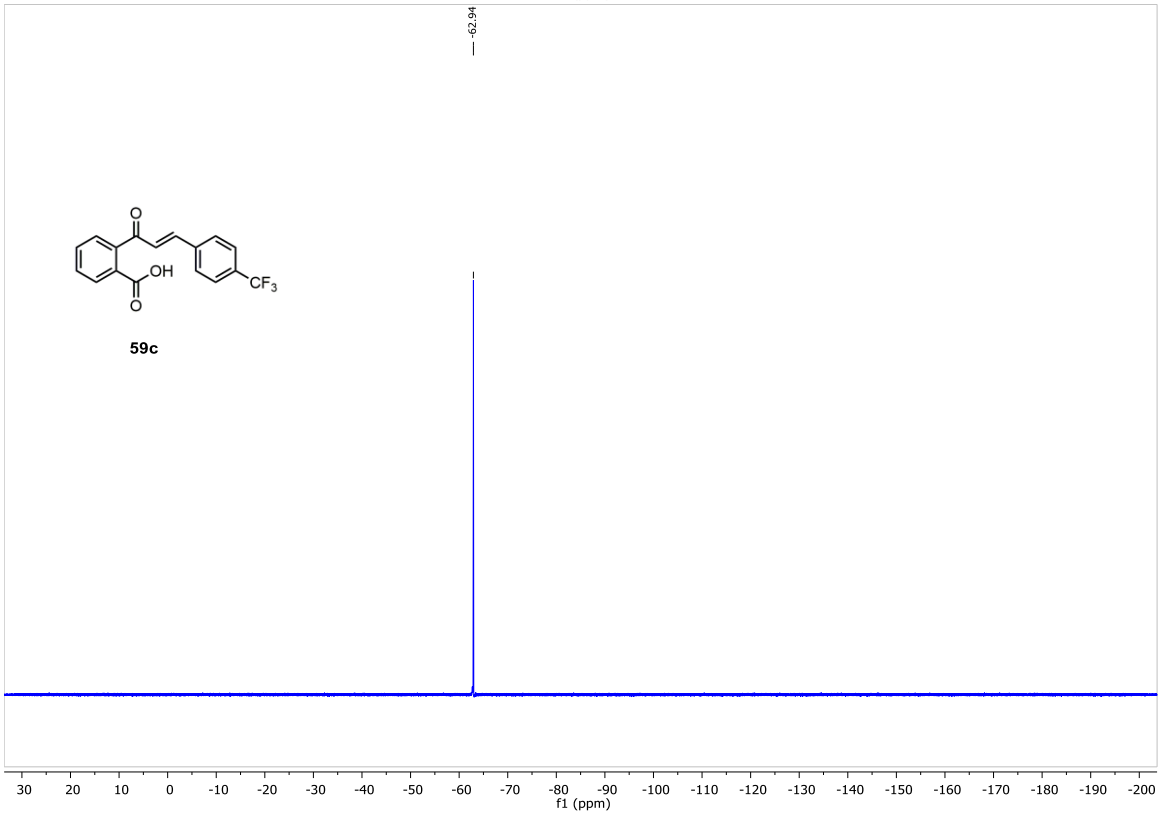
-62.94
O
OH
O
CF3
59c
30 20 10 0 -10 -20 -30 -40 -50 -60 -70 -80 -90 -100 -110 -120 -130 -140 -150 -160 -170 -180 -190 -200
f1 (ppm)

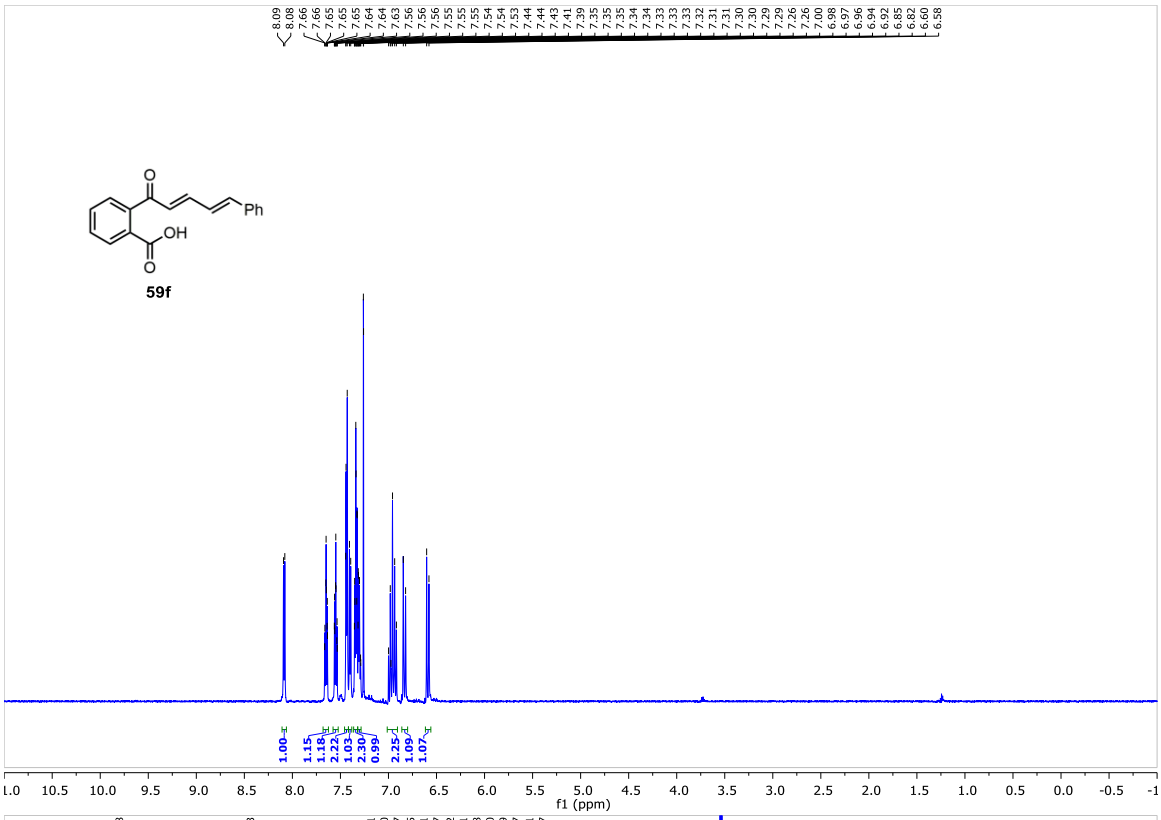
8.09
8.08
7.66
7.66
7.65
7.65
7.65
7.64
7.64
7.63
7.56
7.56
7.56
7.55
7.55
7.55
7.54
7.54
7.53
7.44
7.44
7.43
7.41
7.39
7.35
7.35
7.34
7.34
7.33
7.33
7.32
7.31
7.31
7.30
7.30
7.29
7.29
7.26
7.26
7.00
6.98
6.97
6.96
6.94
6.92
6.85
6.82
6.60
6.58
O
OH
O
Ph
59f
1.00
1.15
1.18
2.22
1.03
2.30
0.99
2.25
1.09
1.07
f1 (ppm)

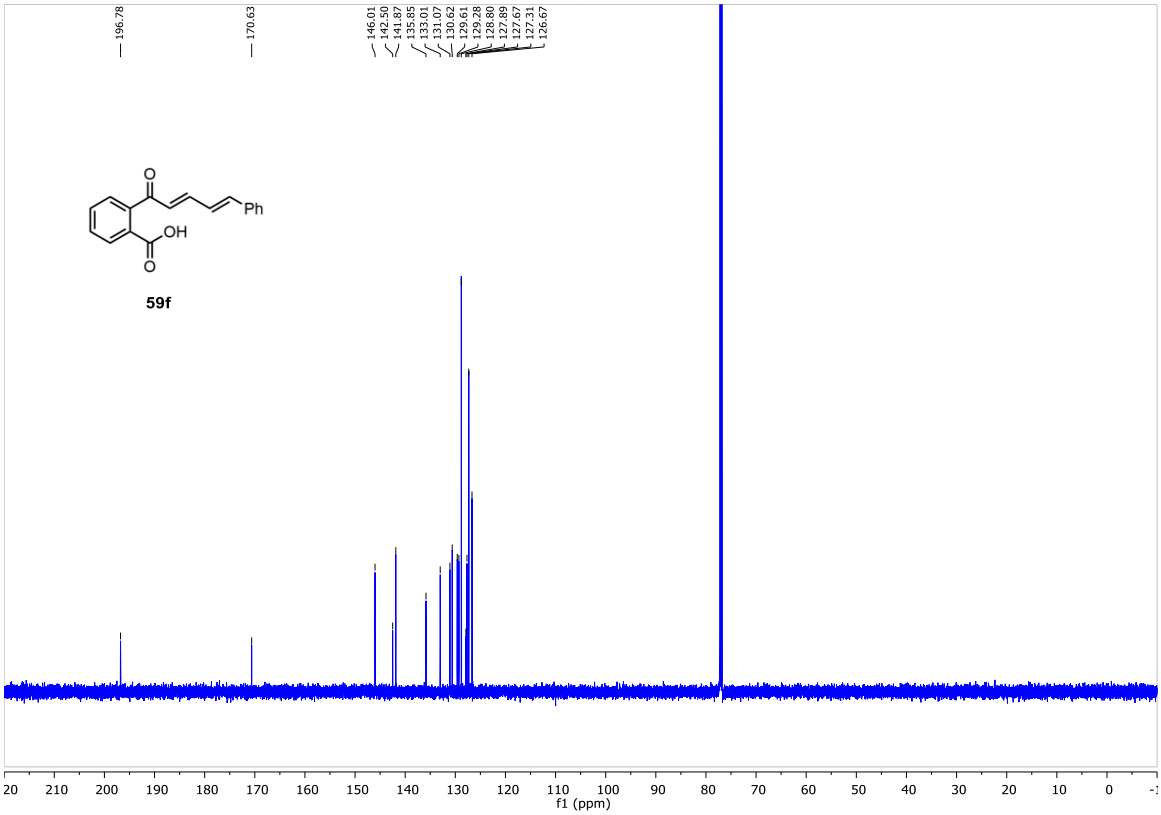
196.78
170.63
146.01
142.50
141.87
135.85
133.01
131.07
130.62
130.61
129.28
128.80
127.89
127.67
127.31
126.67
O
OH
O
Ph
59f
f1 (ppm)

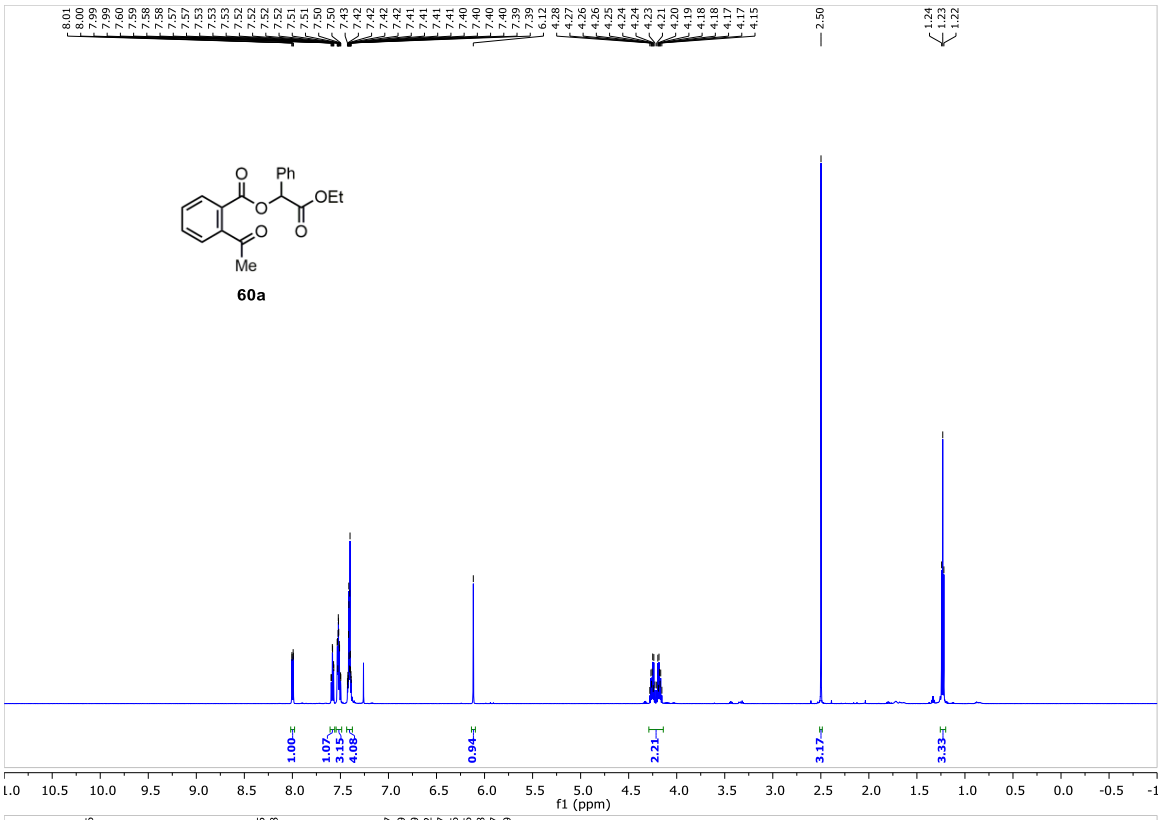
8.01 8.00 7.99 7.99 7.60 7.59 7.58 7.58 7.57 7.57 7.53 7.53 7.52 7.52 7.52 7.51 7.51 7.50 7.50 7.43 7.42 7.42 7.42 7.41 7.41 7.41 7.41 7.40 7.40 7.40 7.40 7.39 6.12 4.28 4.27 4.26 4.26 4.25 4.24 4.24 4.23 4.21 4.20 4.19 4.18 4.18 4.17 4.17 4.15 2.50 1.24 1.23 1.22
O
Ph
OEt
O
O
Me
60a
1.00 1.07 3.15 4.08 0.94 2.21 3.17 3.33
f1 (ppm)

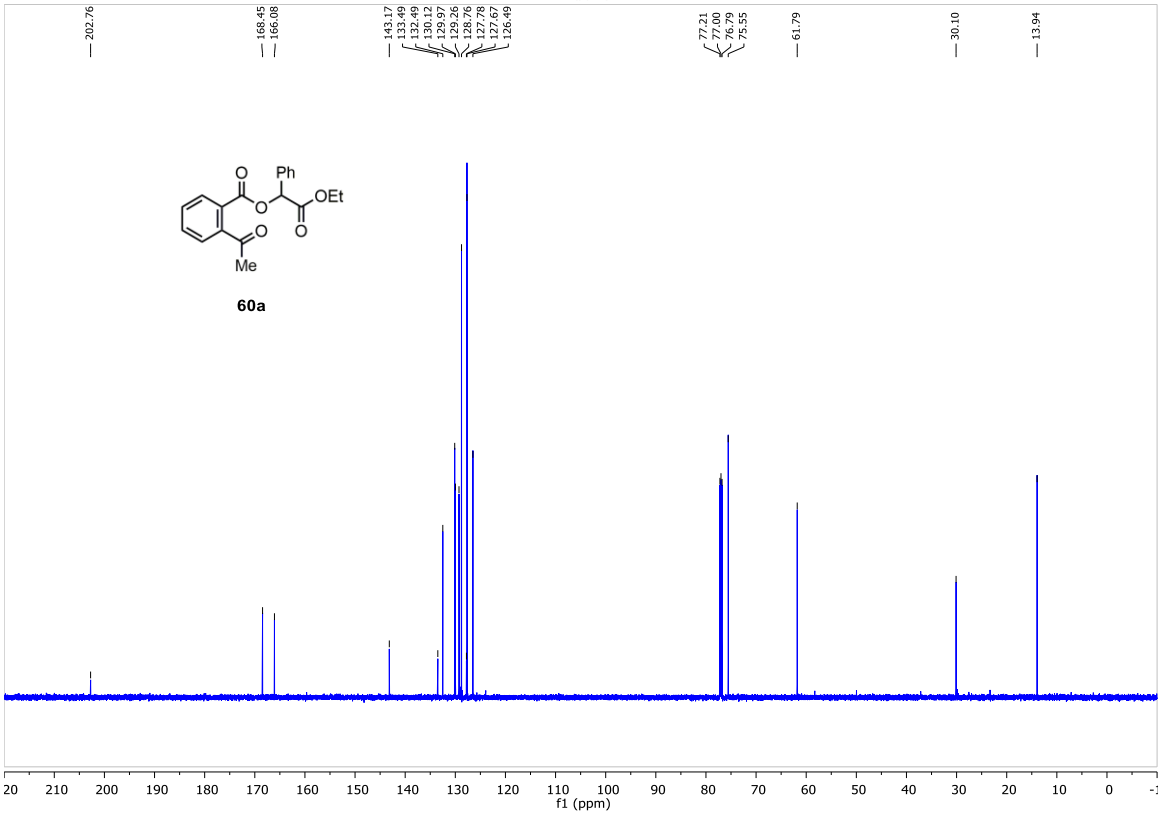
202.76 168.45 166.08 143.17 133.49 132.49 130.12 129.97 129.26 128.76 127.78 127.67 126.49 77.21 77.00 76.79 75.55 61.79 30.10 13.94
O
Ph
OEt
O
O
Me
60a
f1 (ppm)

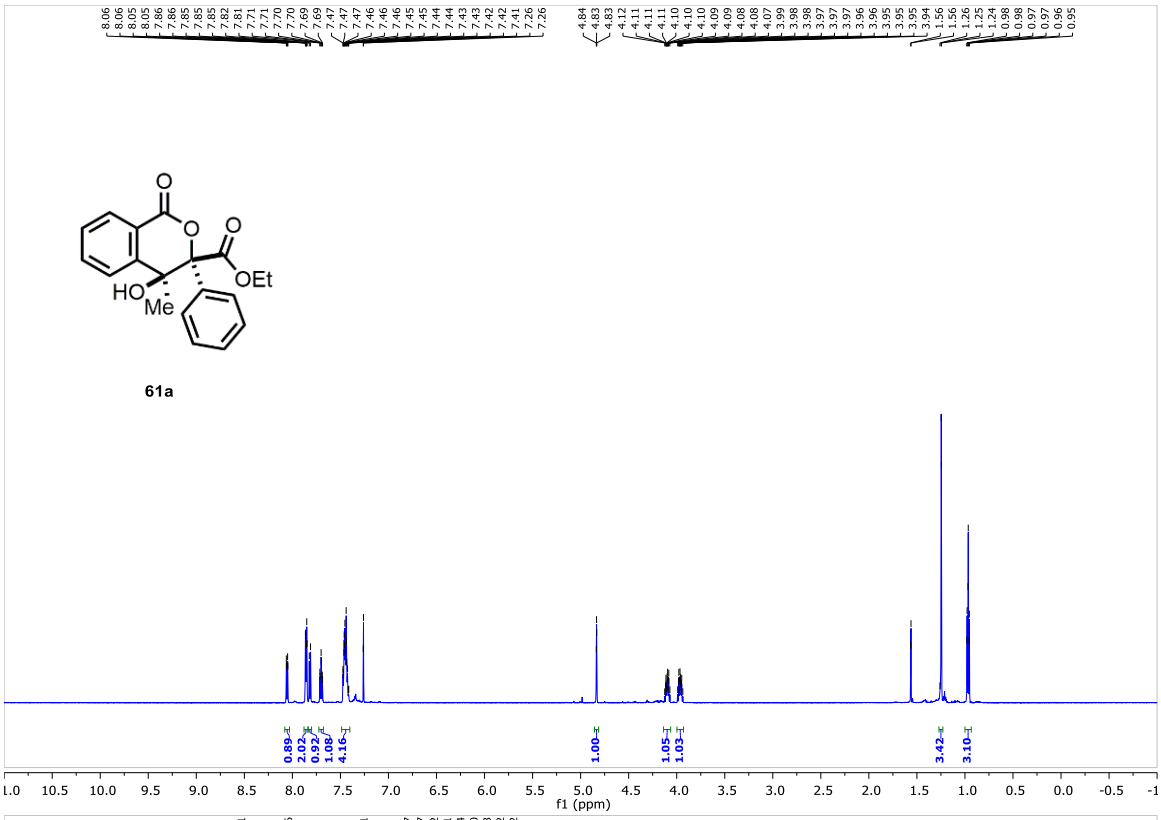
61a
f1 (ppm)

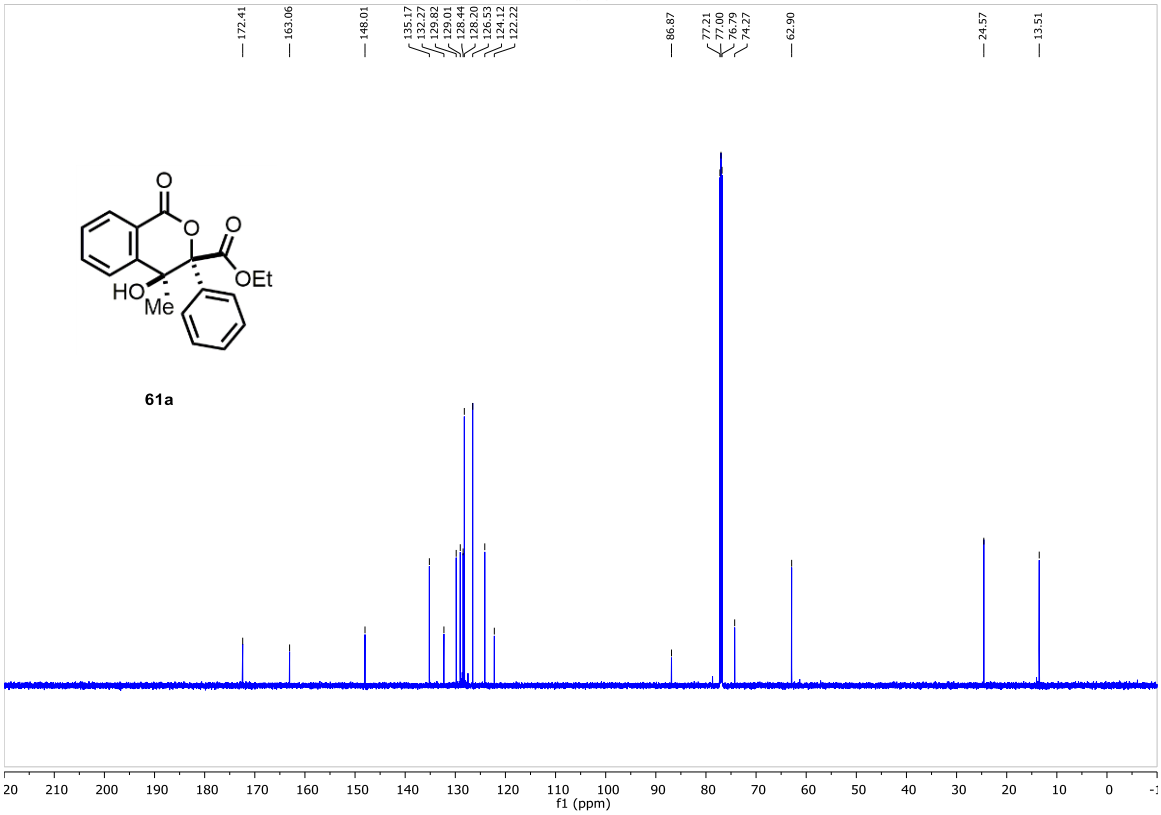
61a
f1 (ppm)

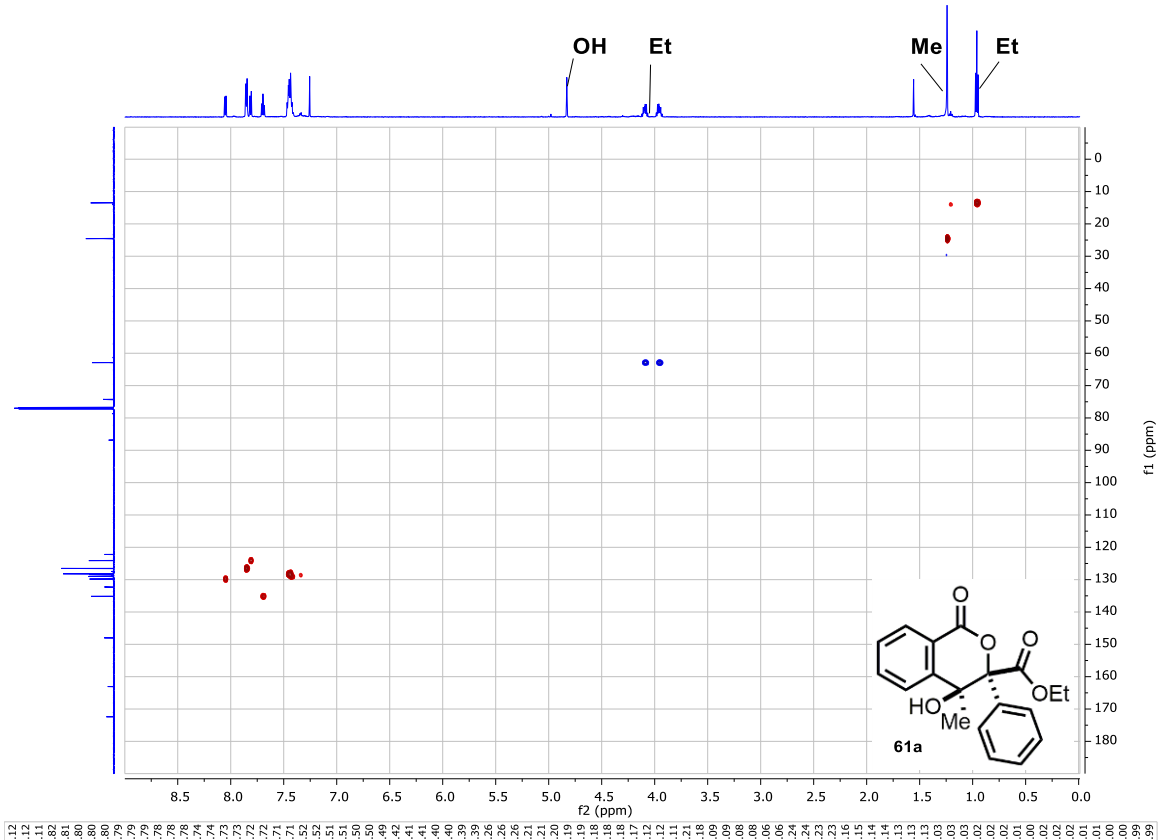
OH
Et
Me
Et
f2 (ppm)
f1 (ppm)
HO
Me
OEt
61a

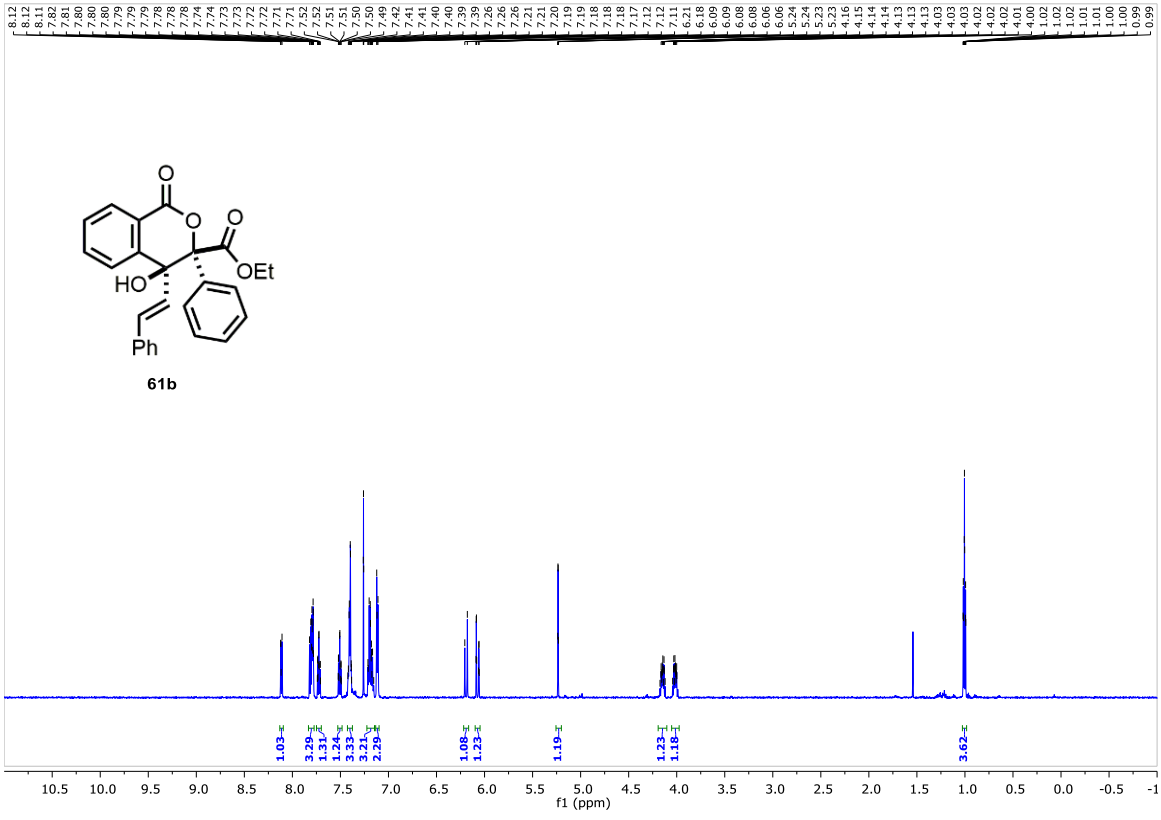
HO
OEt
Ph
61b
f1 (ppm)

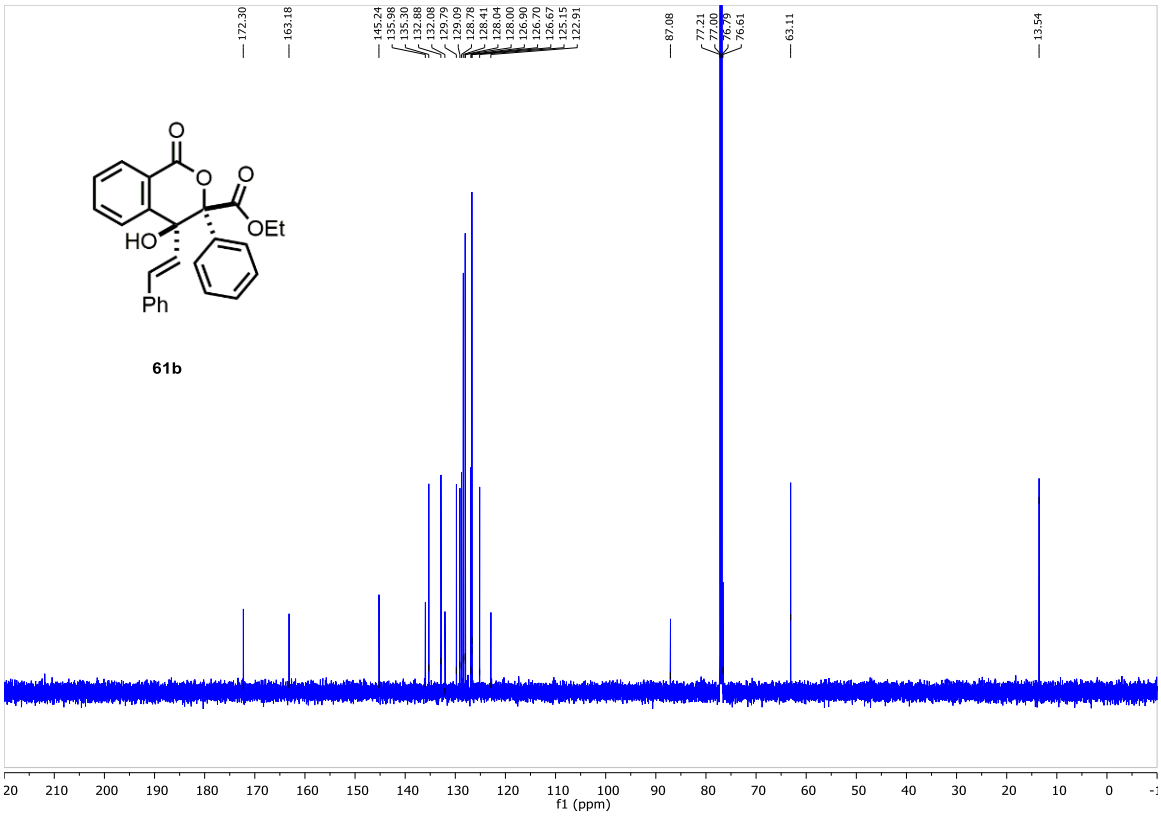
172.30
163.18
145.24
135.98
135.30
132.88
132.08
129.79
129.09
128.78
128.41
128.04
128.00
126.90
126.70
126.67
125.15
122.91
87.08
77.21
77.00
76.79
76.61
63.11
13.54
O
O
O
OEt
HO
Ph
61b
f1 (ppm)

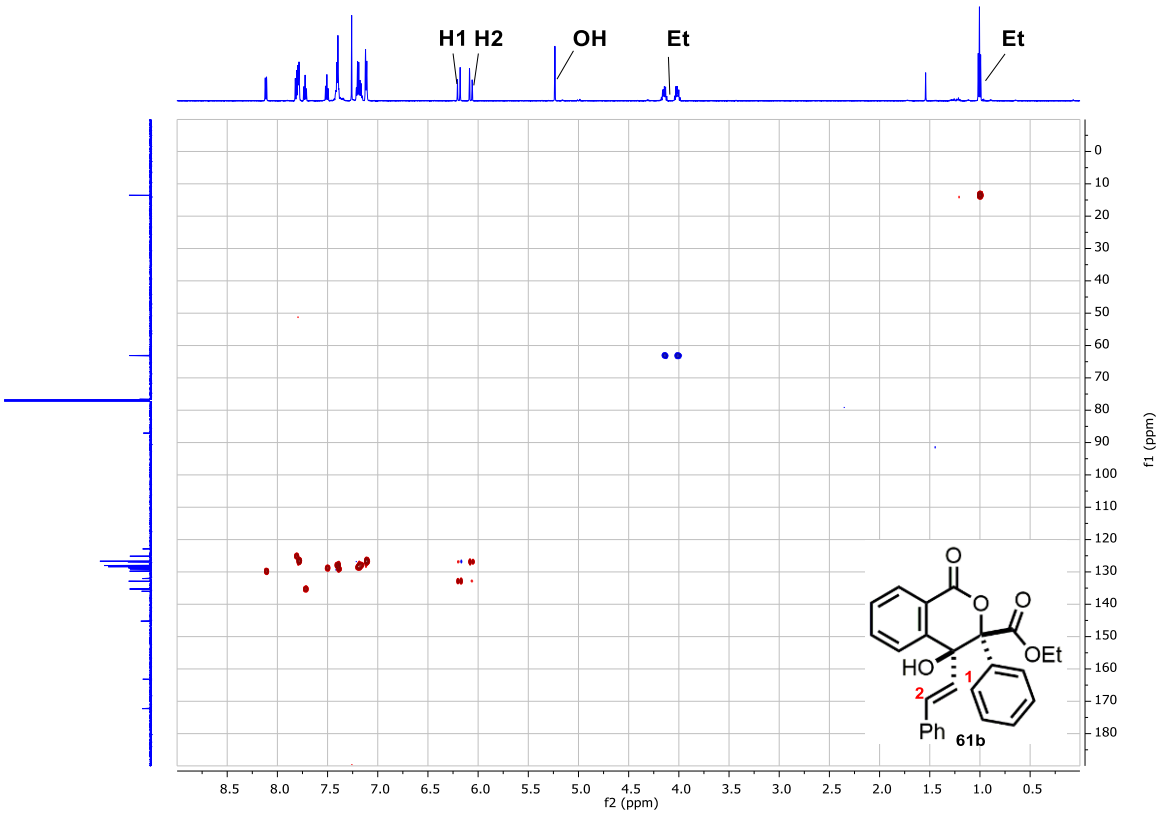
H1 H2
OH
Et
Et
f1 (ppm)
f2 (ppm)
O
O
O
OEt
HO
1
2
Ph
61b

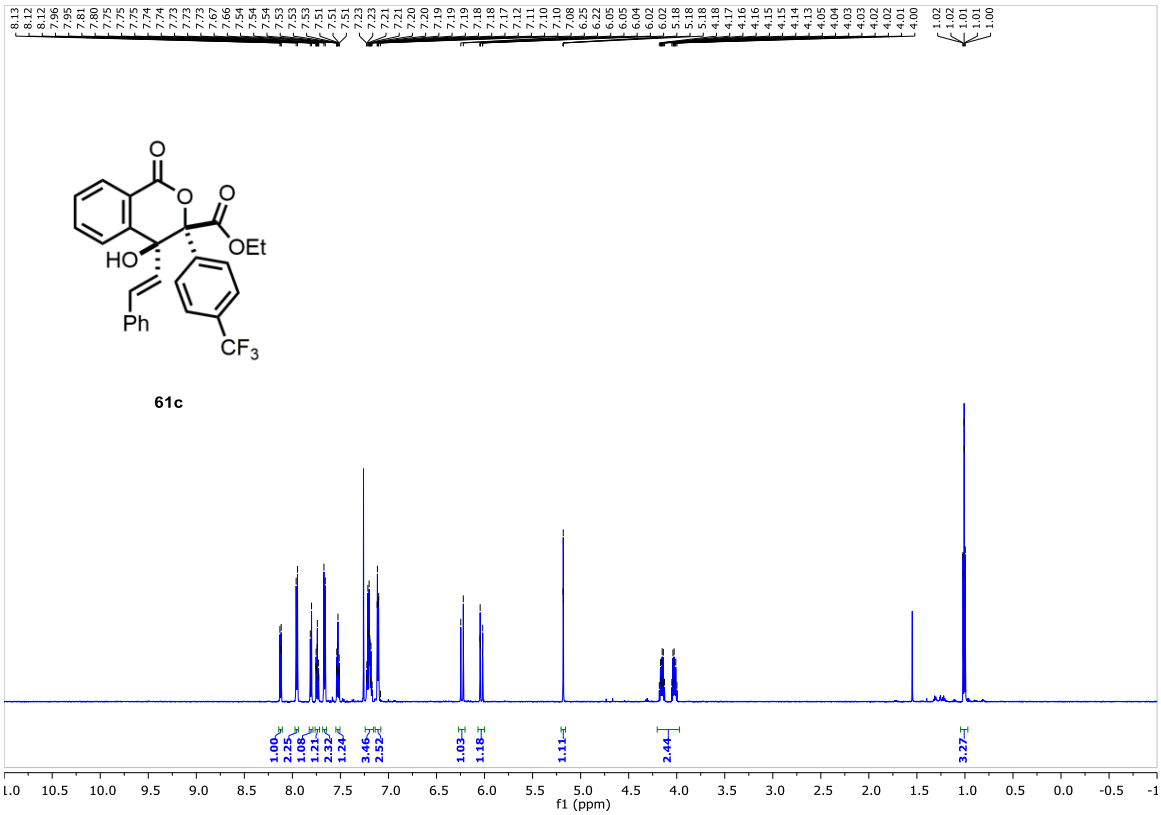
HO
O
O
OEt
Ph
CF3
61c
f1 (ppm)

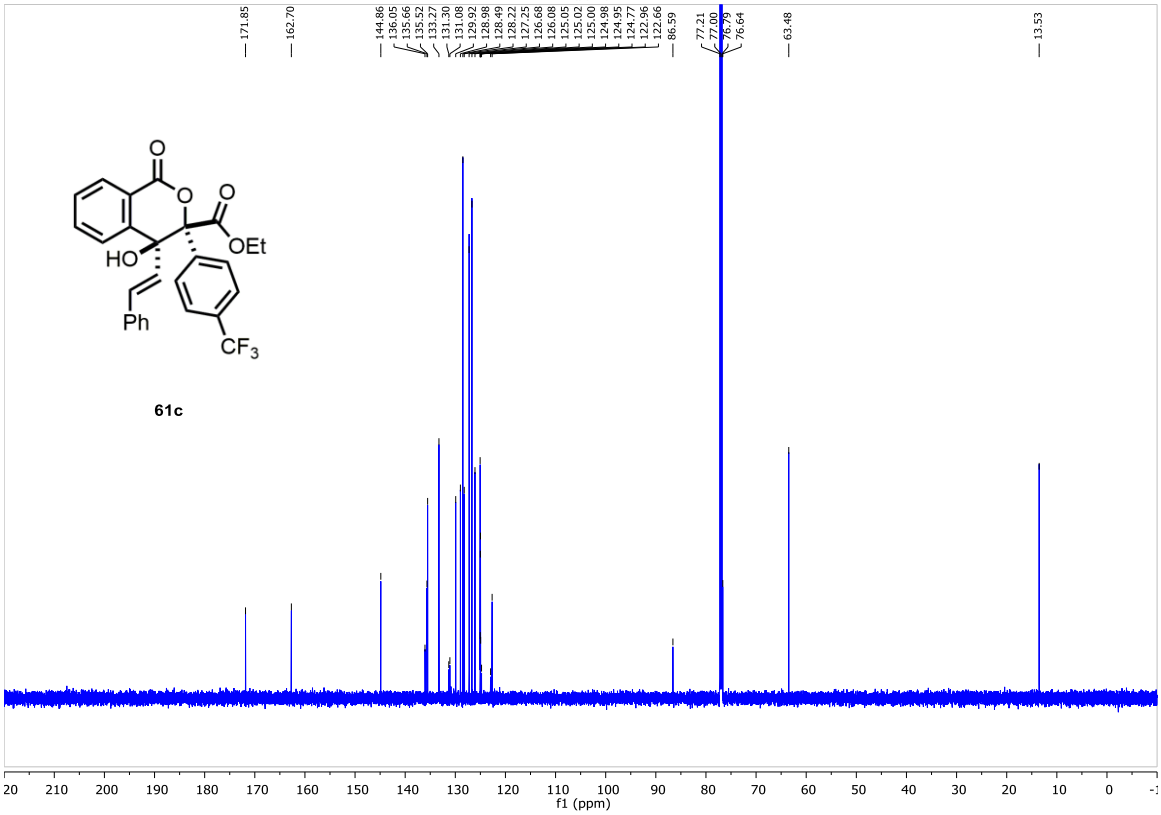
HO
O
O
OEt
Ph
CF3
61c
f1 (ppm)

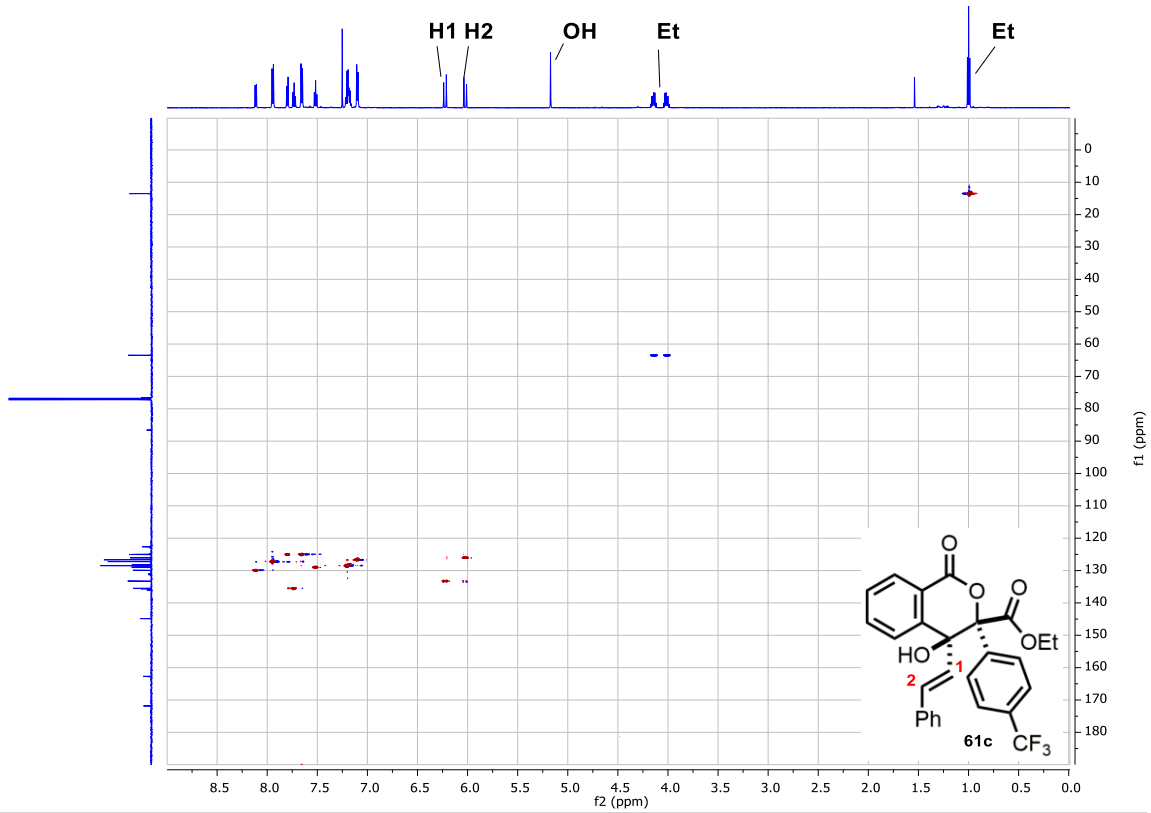
H1 H2
OH
Et
Et
f1 (ppm)
f2 (ppm)
HO
OEt
Ph
CF3
61c

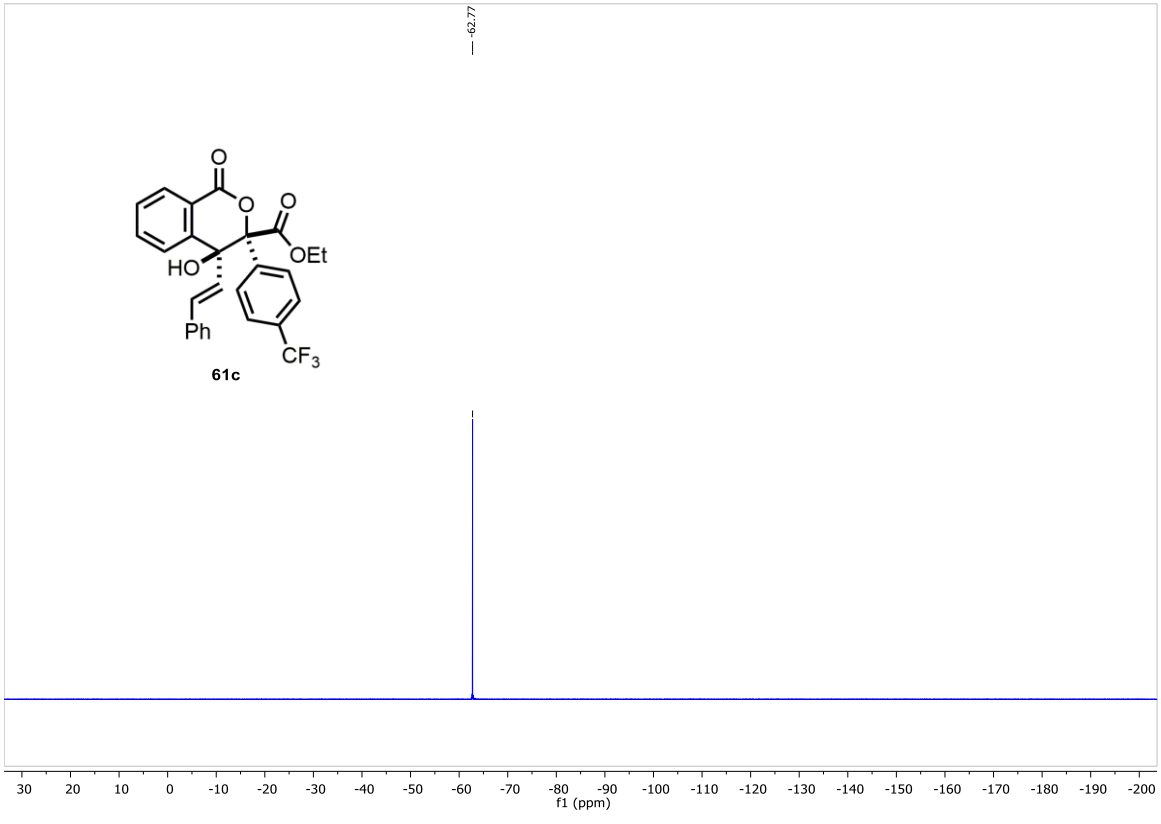
-62.77
HO
OEt
Ph
CF3
61c
f1 (ppm)

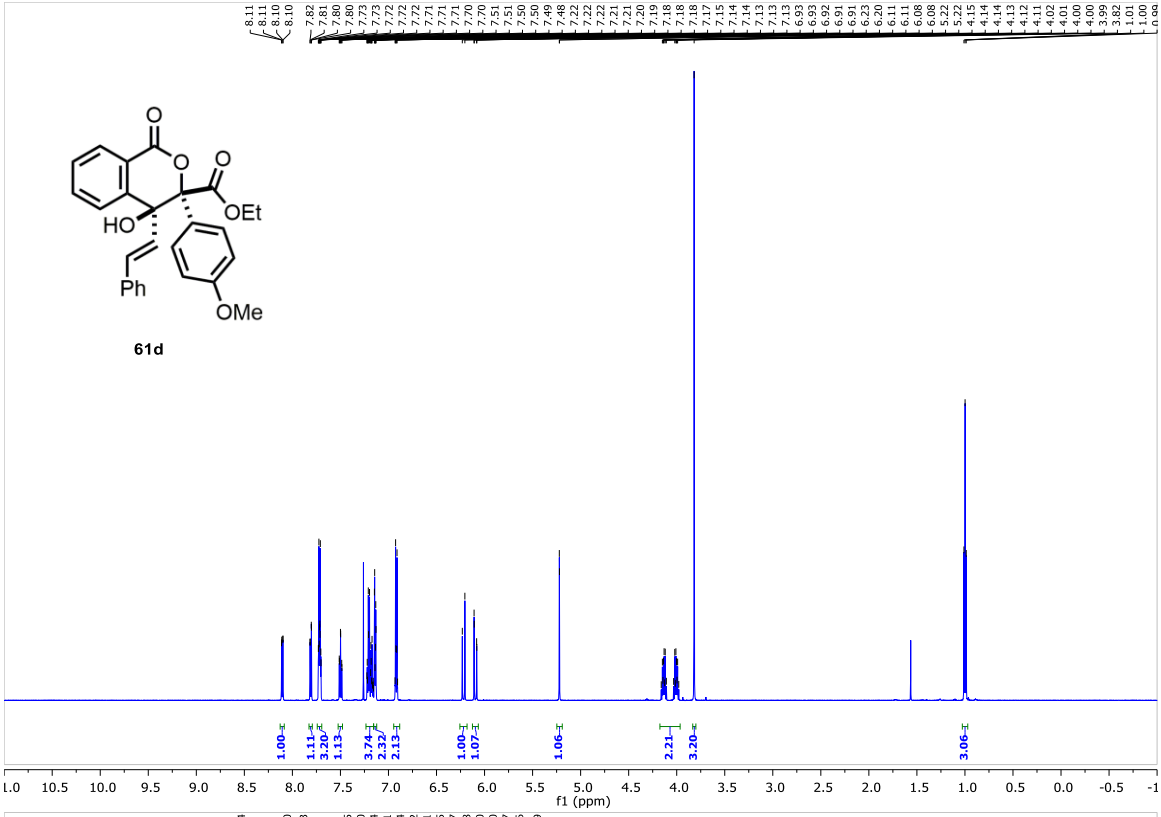
61d
f1 (ppm)

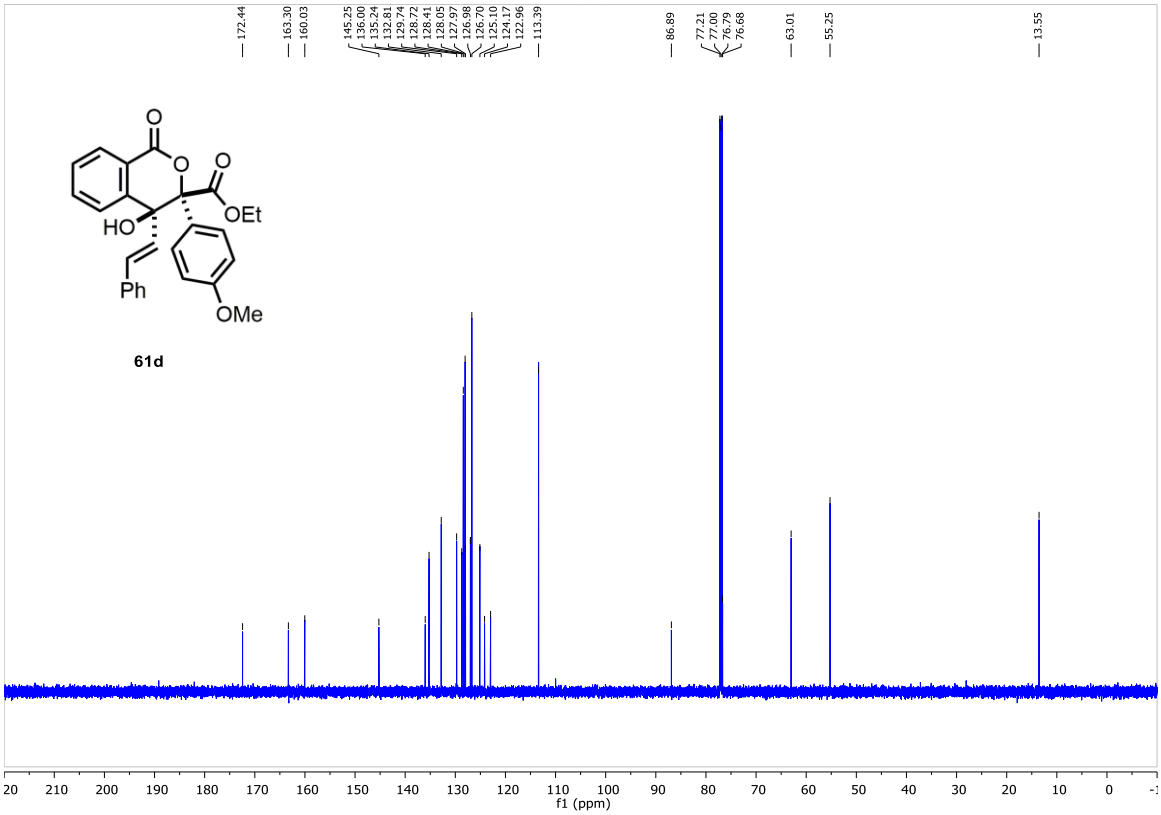
61d
f1 (ppm)

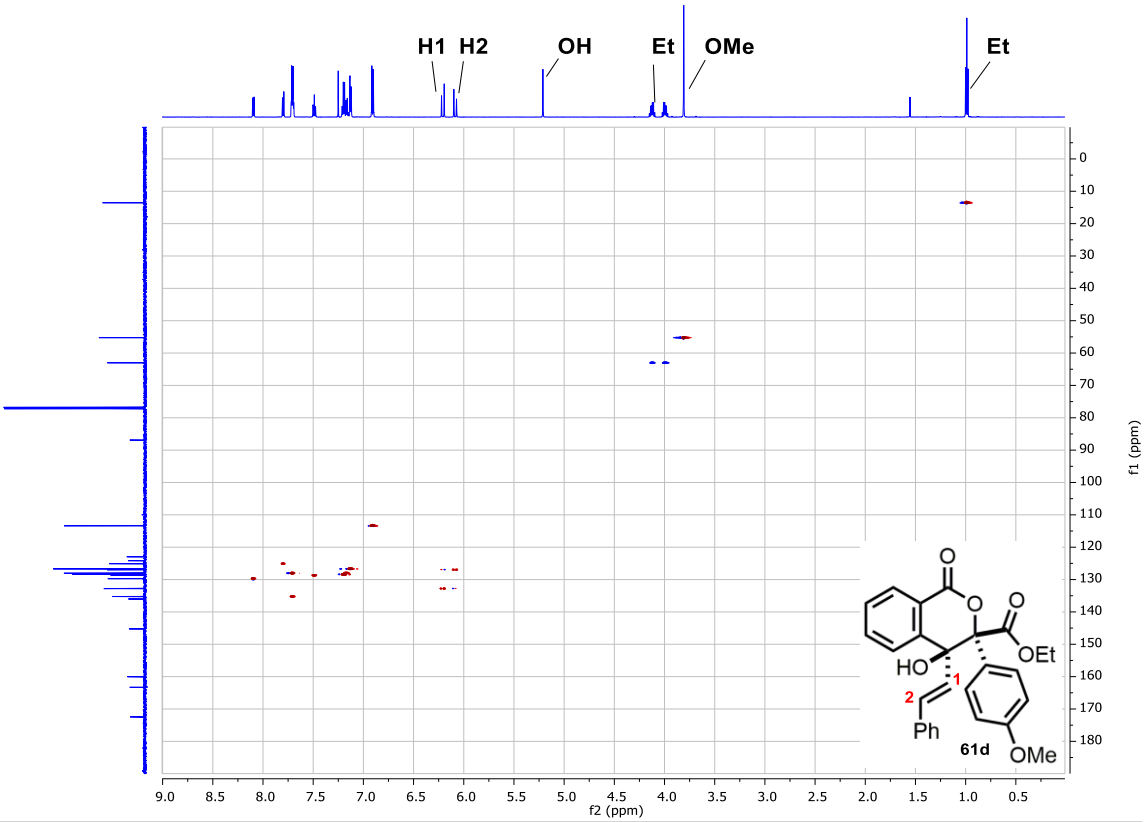
H1
H2
OH
Et
OMe
Et
f2 (ppm)
f1 (ppm)
HO
OEt
Ph
OMe
61d

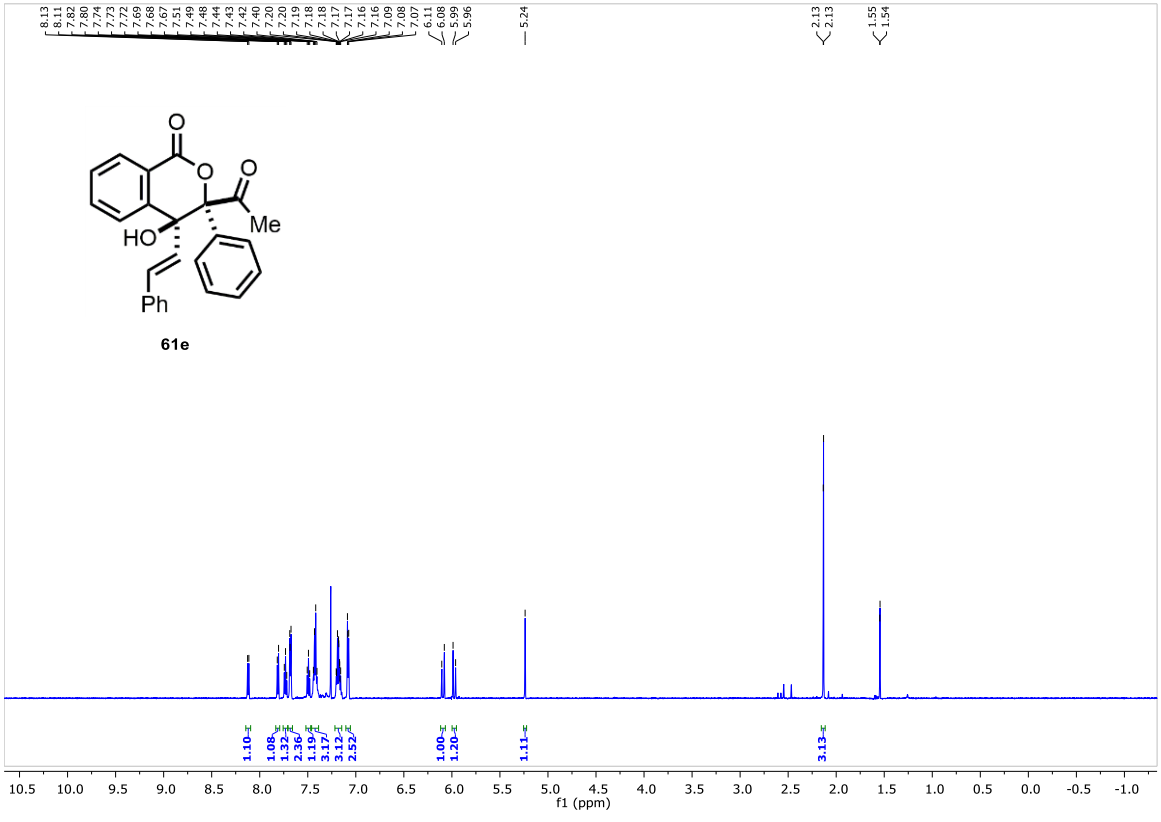
HO
Me
Ph
61e
f1 (ppm)

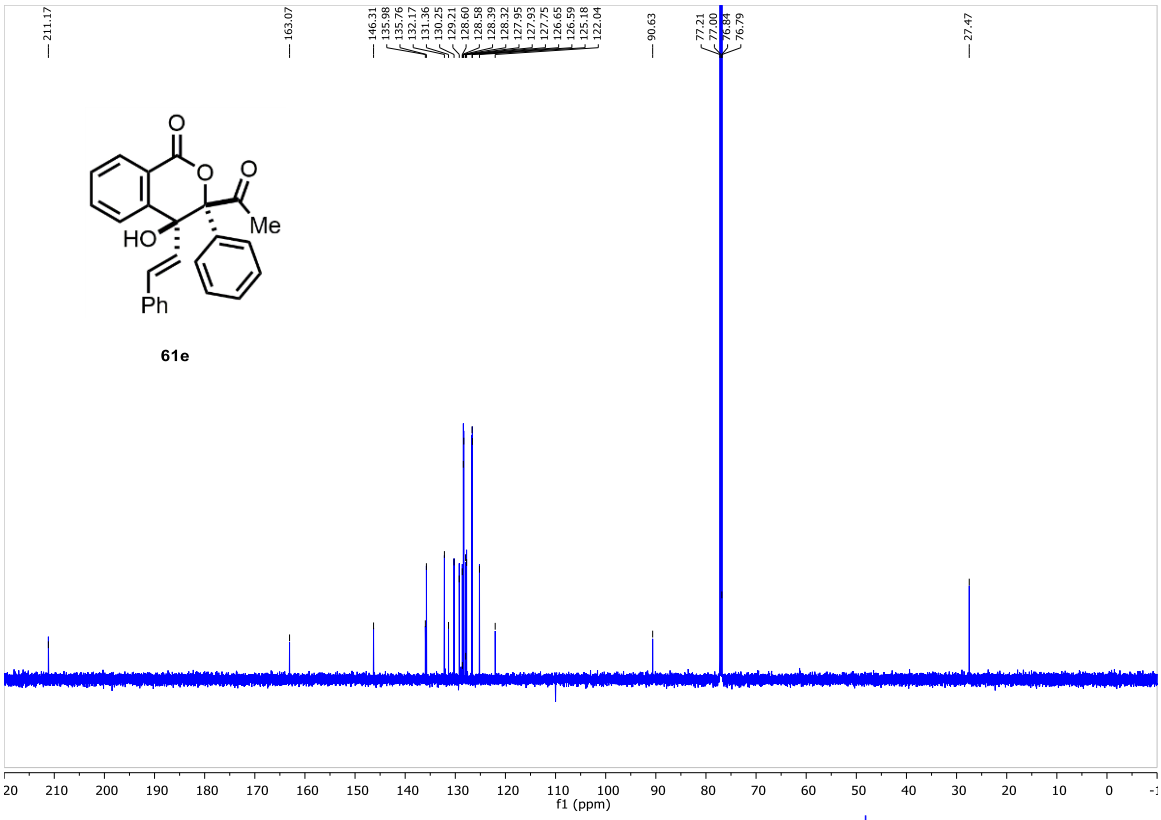
211.17
163.07
146.31
135.98
135.76
132.17
131.36
130.25
129.21
128.60
128.58
128.39
128.32
127.95
127.93
127.75
126.65
126.59
125.18
122.04
90.63
77.21
77.00
76.84
76.79
27.47
O
O
O
Me
HO
Ph
61e
f1 (ppm)

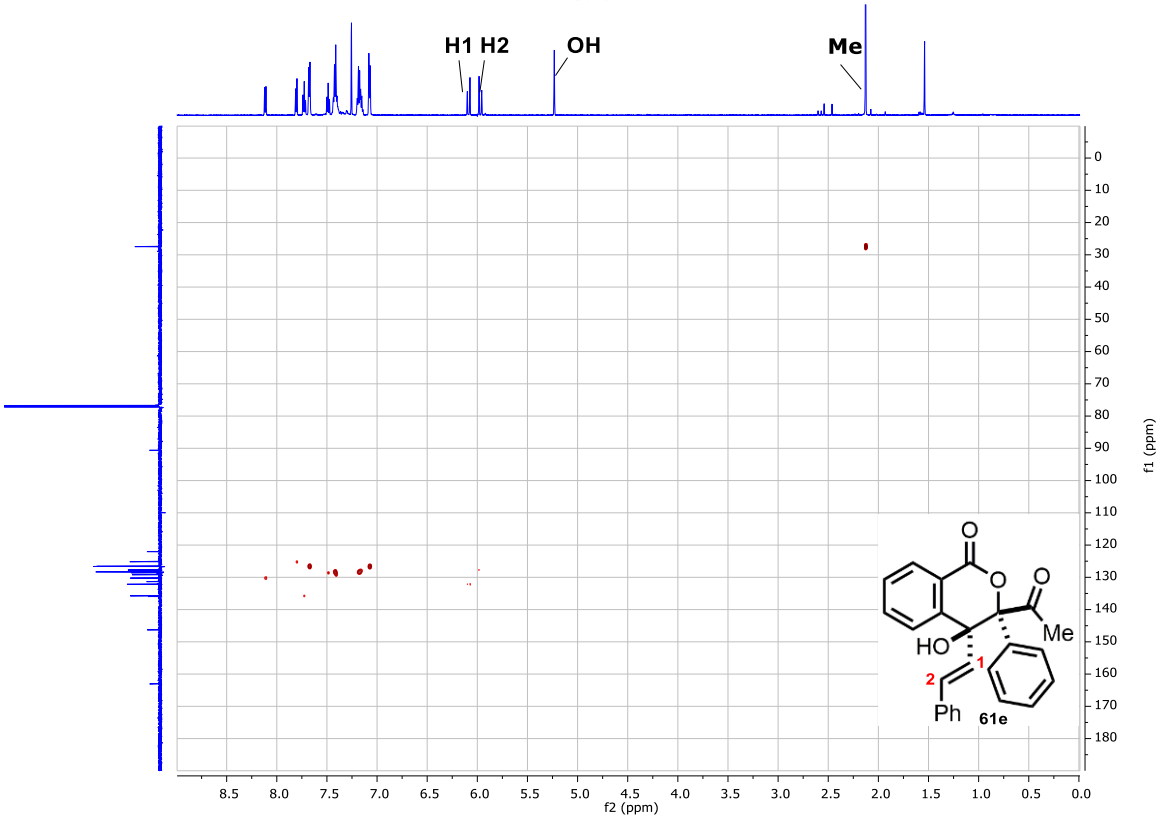
H1 H2
OH
Me
f2 (ppm)
f1 (ppm)
O
O
O
Me
HO
1
2
Ph
61e

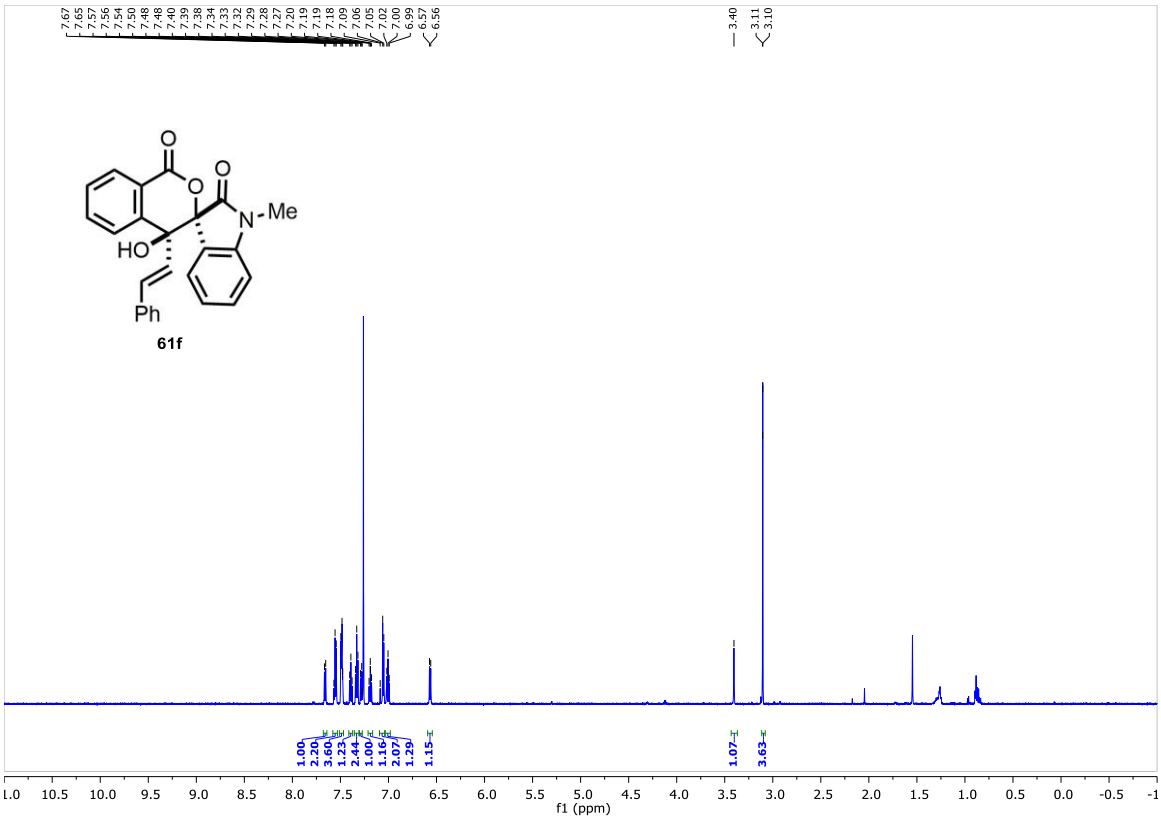
7.67
7.65
7.57
7.56
7.54
7.50
7.48
7.40
7.39
7.38
7.34
7.33
7.32
7.29
7.28
7.27
7.20
7.19
7.19
7.18
7.09
7.06
7.05
7.02
7.00
6.99
6.57
6.56
3.40
3.11
3.10
O
O
O
N-Me
HO
Ph
61f
1.00
2.20
3.60
1.23
2.44
1.00
1.16
2.07
1.29
1.15
1.07
3.63
f1 (ppm)

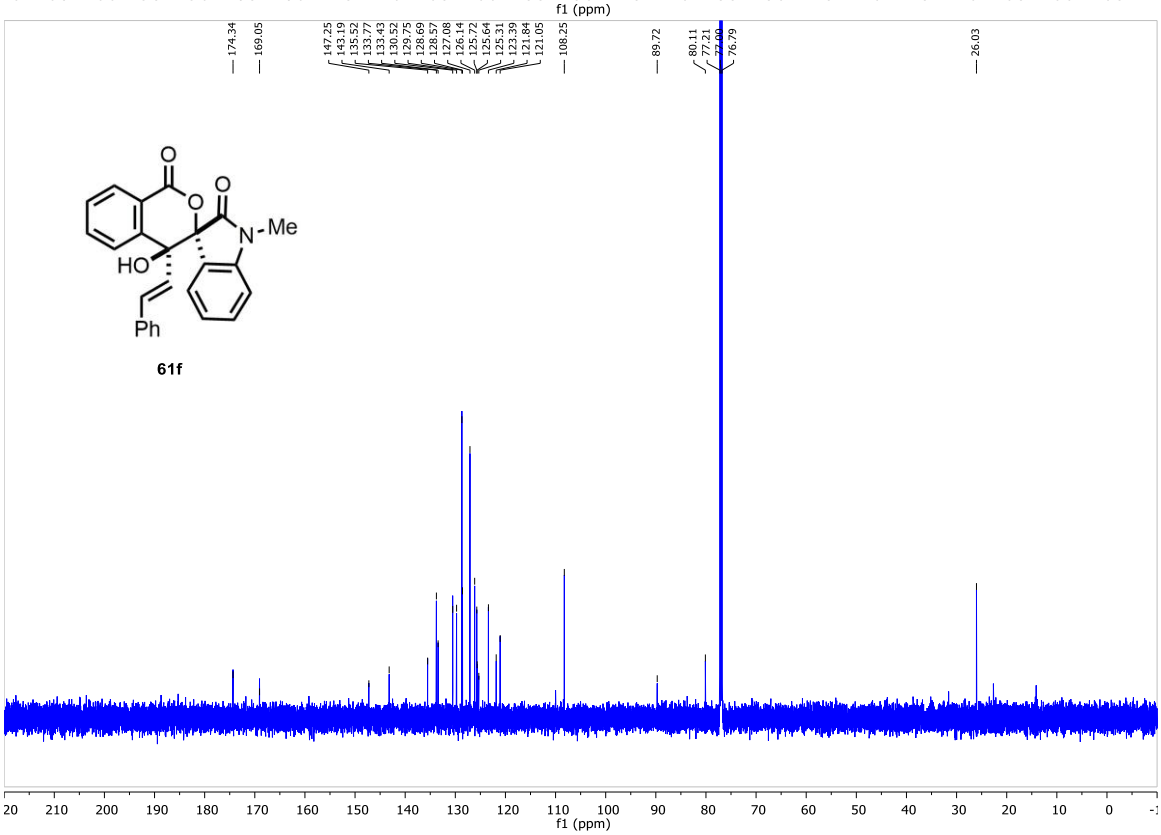
174.34
169.05
147.25
143.19
135.52
133.77
133.43
130.52
129.75
128.69
128.57
127.08
126.14
125.72
125.64
125.31
123.39
121.84
121.05
108.25
89.72
80.11
77.21
77.00
76.79
26.03
O
O
O
N-Me
HO
Ph
61f
f1 (ppm)

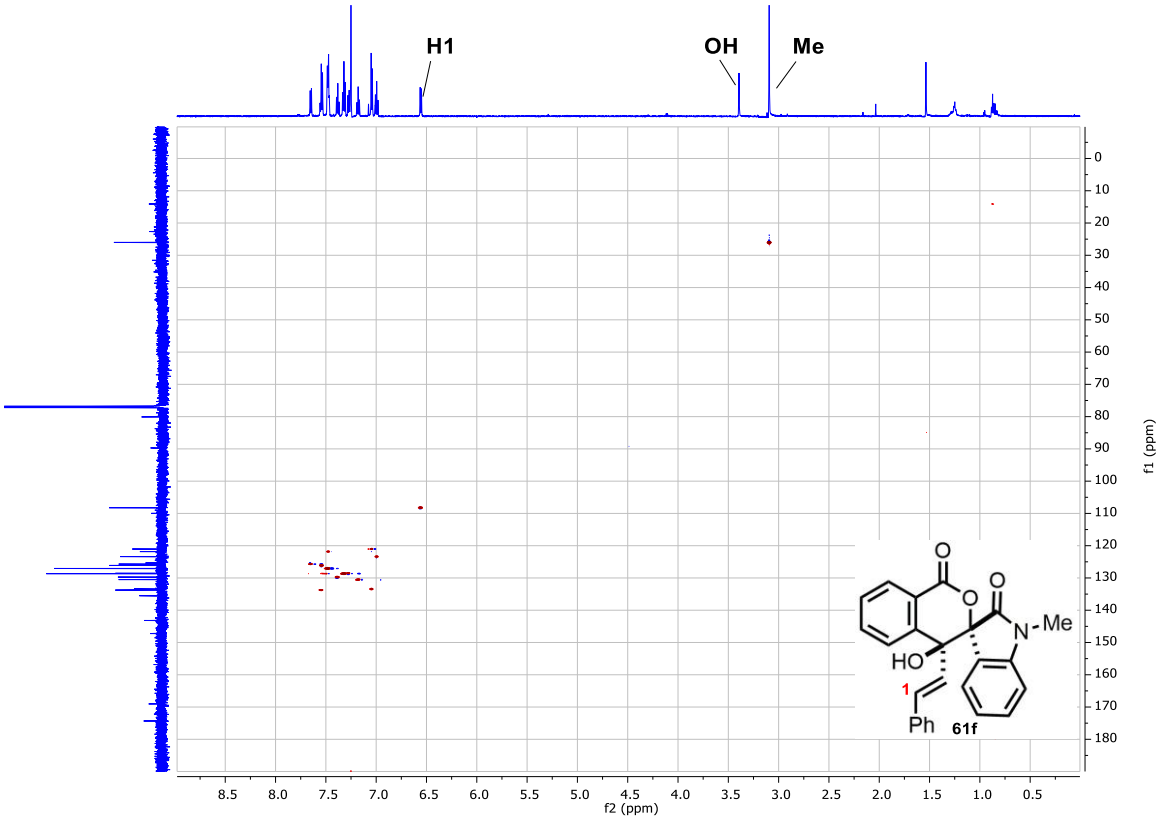
H1
OH
Me
f2 (ppm)
f1 (ppm)
HO
N-Me
Ph
61f

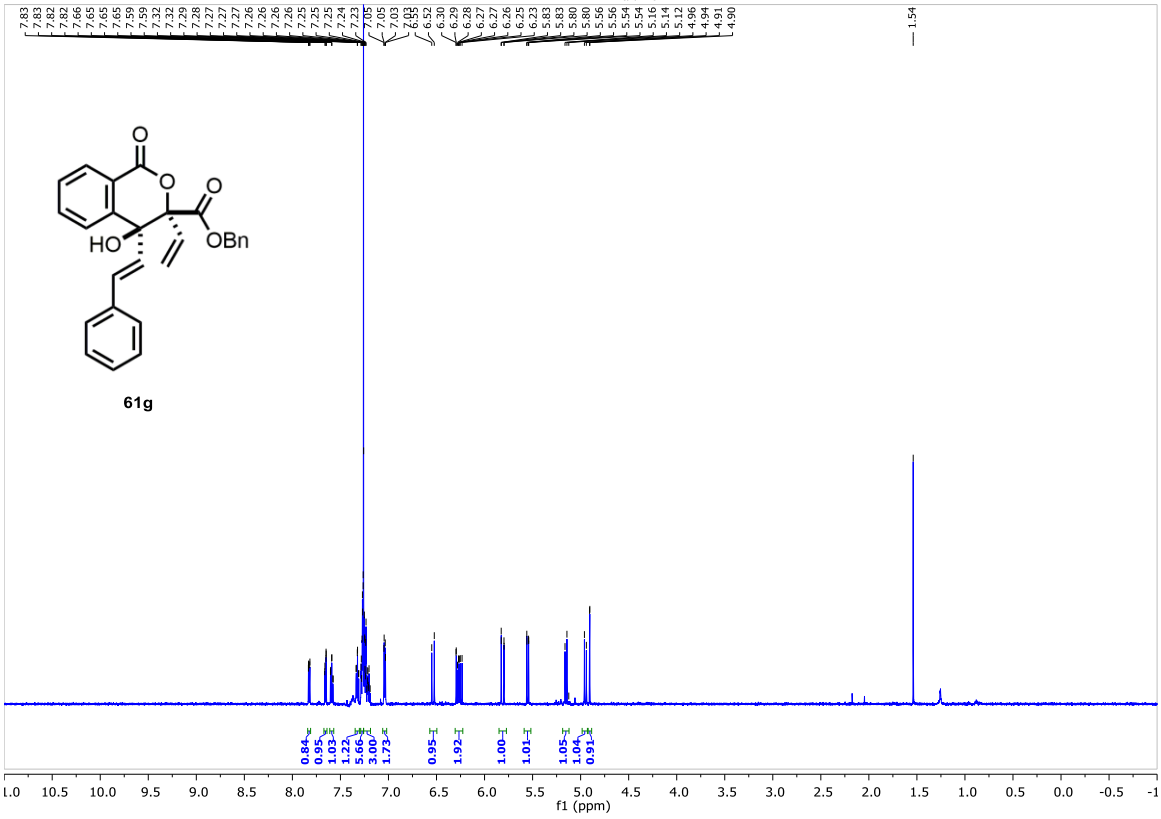
HO
OBn
61g
f1 (ppm)

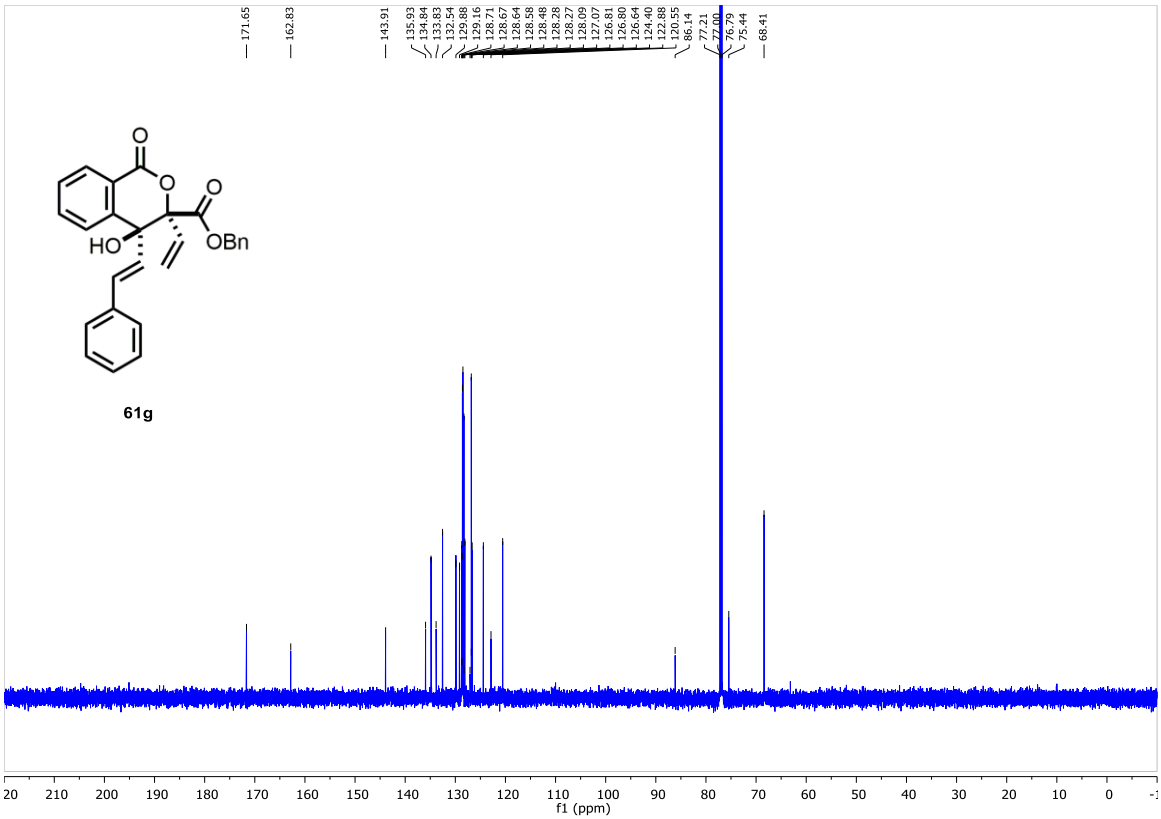
171.65
162.83
143.91
135.93
134.84
133.83
132.54
130.88
129.16
128.71
128.67
128.64
128.58
128.48
128.28
128.27
128.09
127.07
126.81
126.80
126.64
124.40
122.88
120.55
86.14
77.21
76.99
76.79
75.44
68.41
HO
OBn
61g
f1 (ppm)

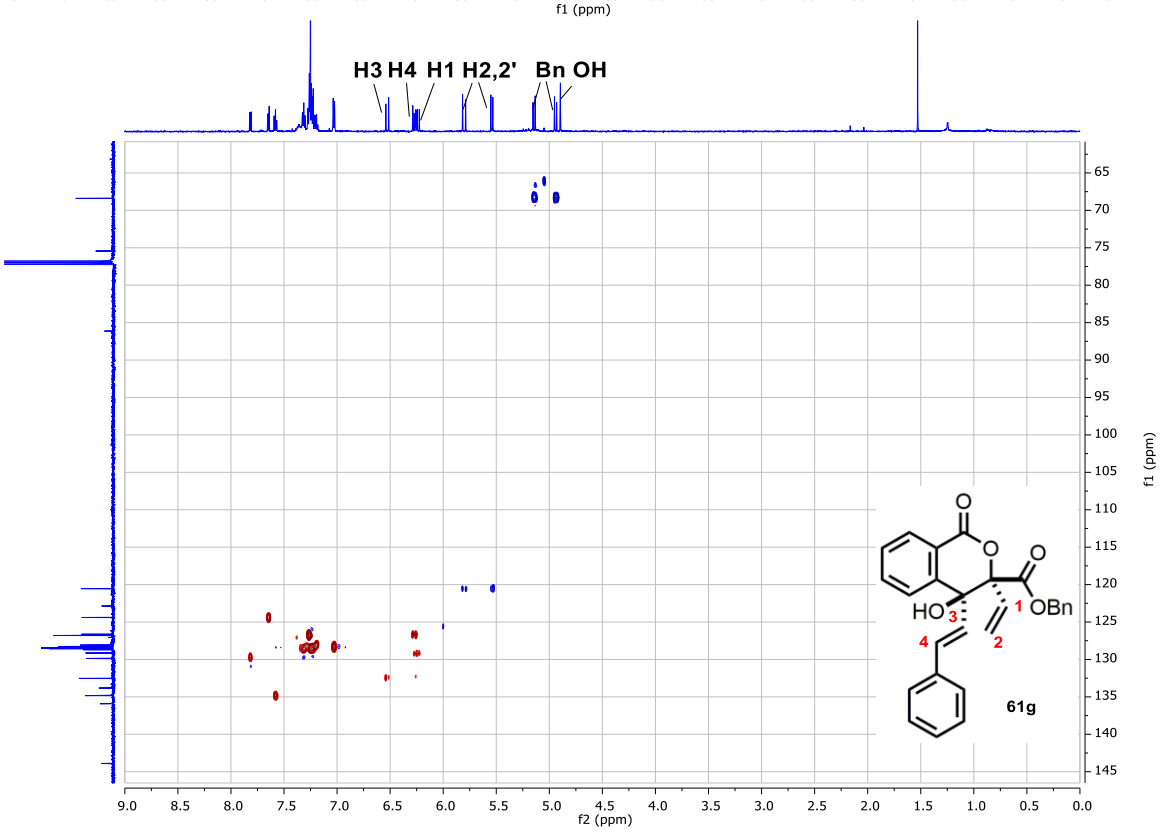
H3 H4 H1 H2,2' Bn OH
HO
OBn
1
2
3
4
61g
f2 (ppm)
f1 (ppm)

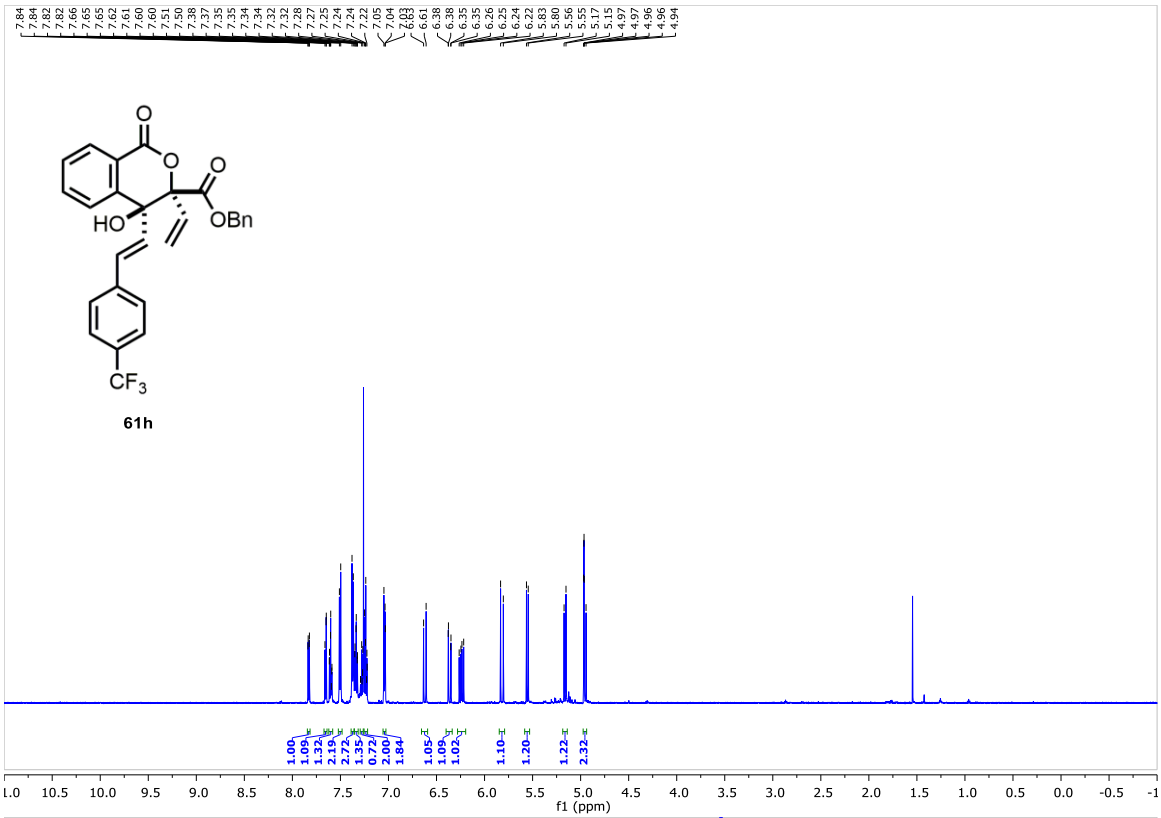
HO
O
O
OBn
CF3
61h
f1 (ppm)

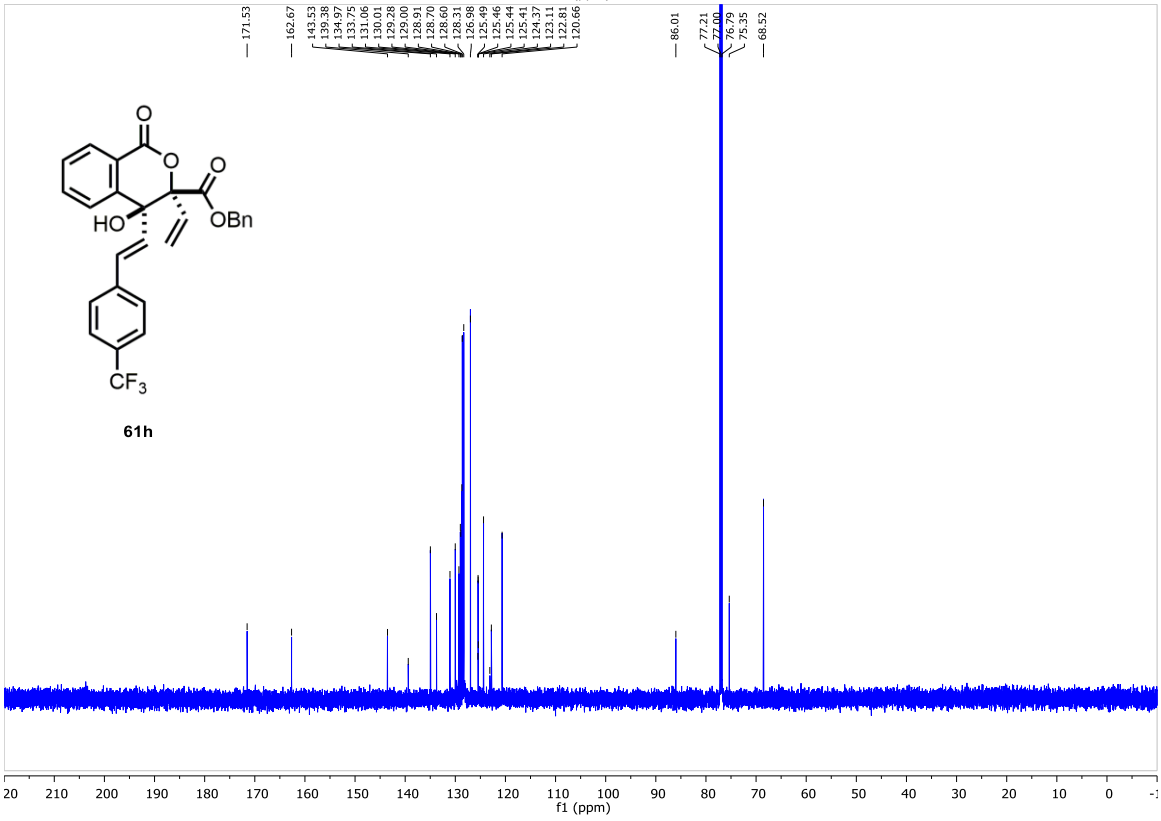
HO
O
O
OBn
CF3
61h
f1 (ppm)

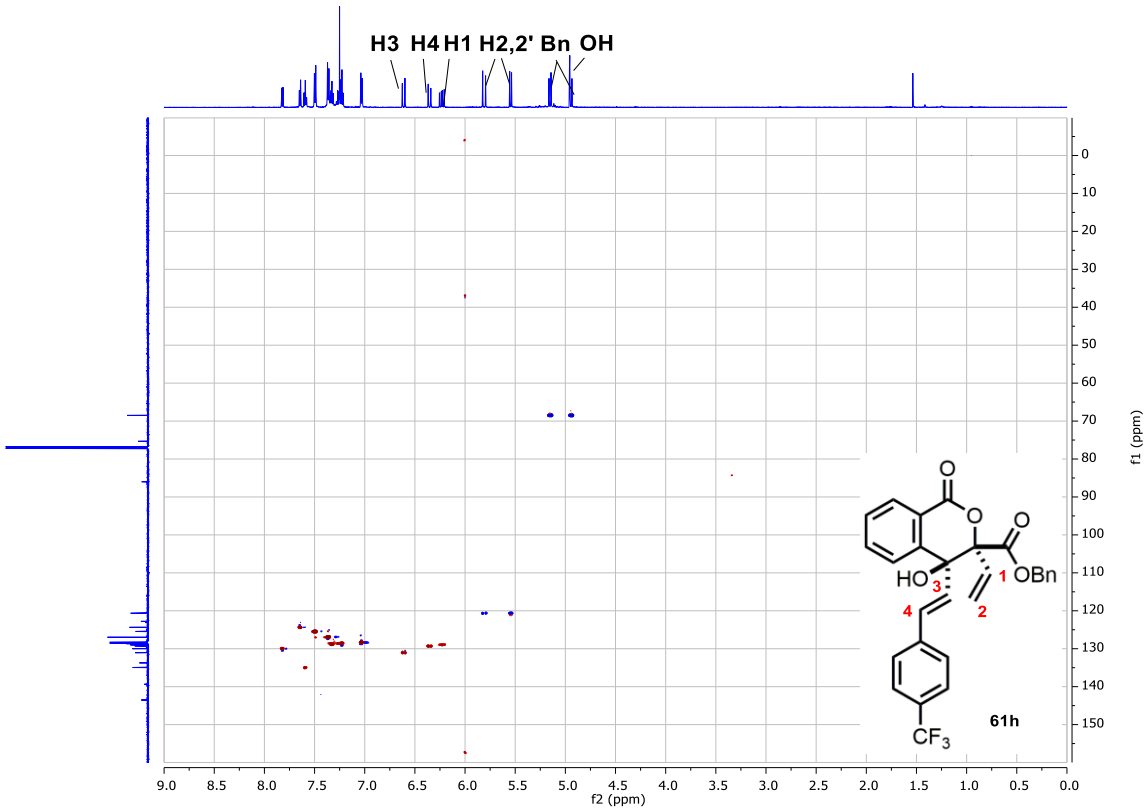
H3
H4
H1
H2,2'
Bn
OH
f2 (ppm)
f1 (ppm)
HO
OBn
CF3
61h

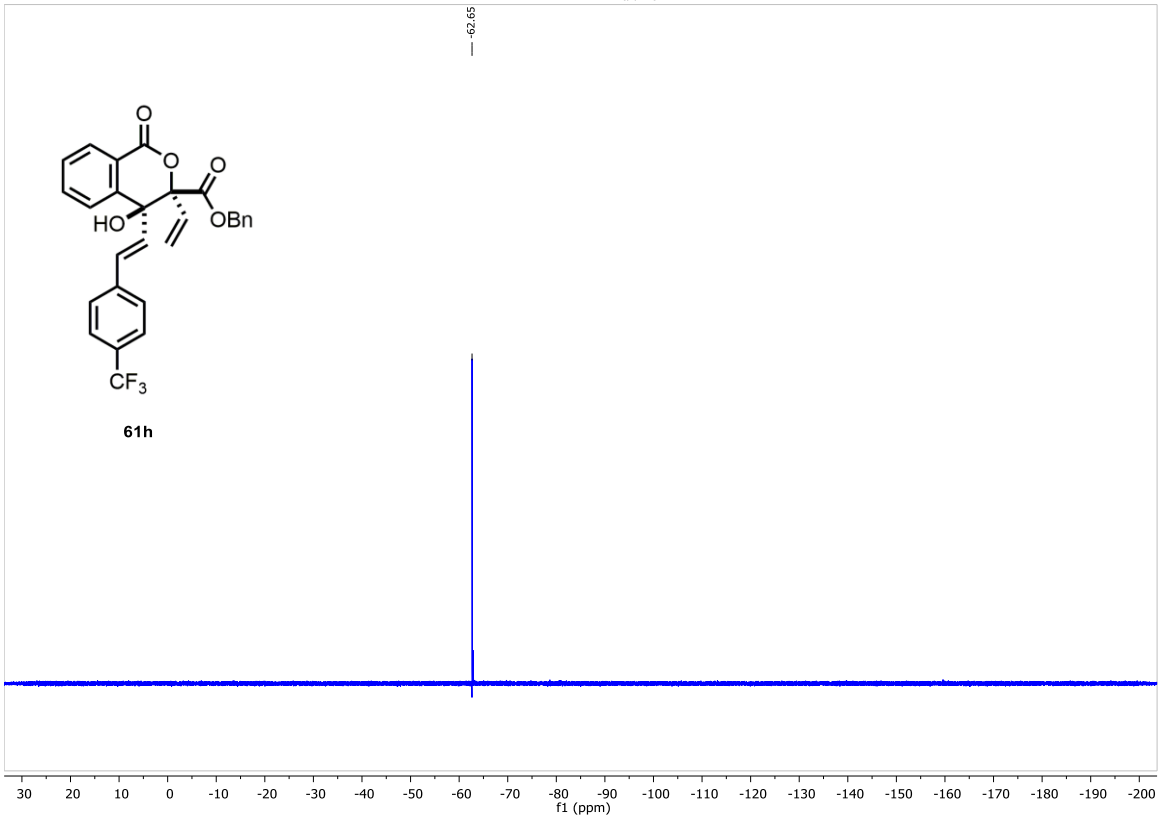
-62.65
HO
OBn
CF3
61h
f1 (ppm)

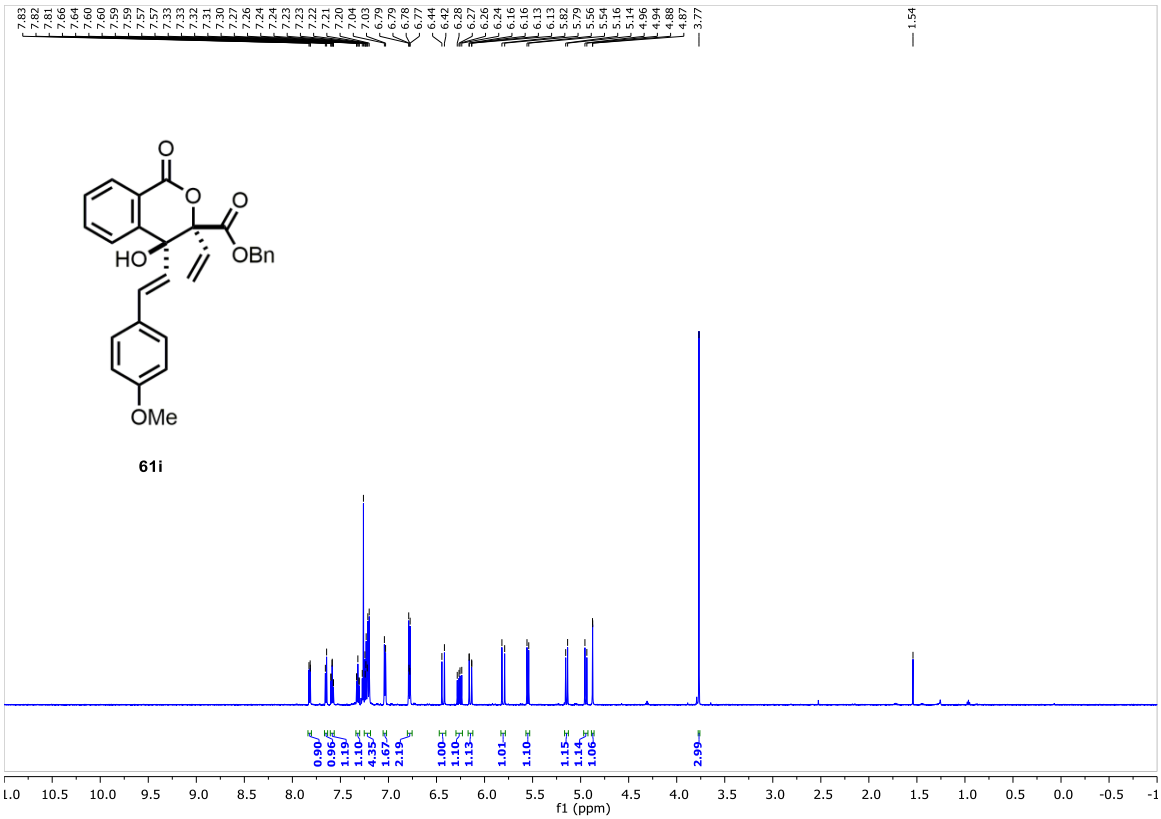
7.83 7.82 7.81 7.66 7.64 7.60 7.60 7.59 7.59 7.57 7.57 7.33 7.32 7.31 7.30 7.27 7.26 7.24 7.24 7.23 7.23 7.22 7.21 7.20 7.04 7.03 6.79 6.78 6.77 6.44 6.42 6.28 6.27 6.26 6.24 6.16 6.16 6.13 6.13 5.82 5.79 5.56 5.54 5.16 5.14 4.96 4.94 4.88 4.87 3.77 1.54
O
O
O
HO
OBn
OMe
61i
0.90 0.96 1.19 1.10 4.35 1.67 2.19 1.00 1.10 1.13 1.01 1.10 1.15 1.14 1.06 2.99
1.0 10.5 10.0 9.5 9.0 8.5 8.0 7.5 7.0 6.5 6.0 5.5 5.0 4.5 4.0 3.5 3.0 2.5 2.0 1.5 1.0 0.5 0.0 -0.5
f1 (ppm)

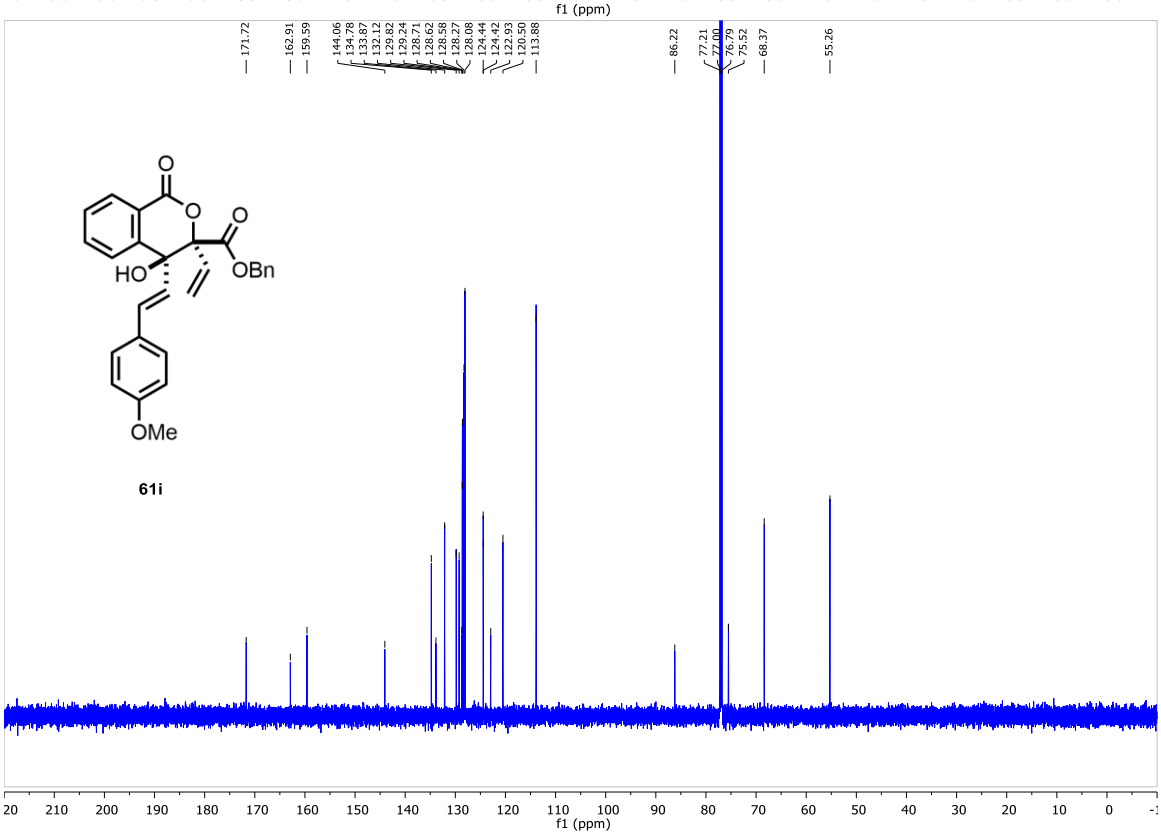
171.72 162.91 159.59 144.06 134.78 133.87 132.12 129.82 129.24 128.71 128.62 128.58 128.27 128.08 124.44 124.42 122.93 120.50 113.88 86.22 77.21 77.00 76.79 75.52 68.37 55.26
O
O
O
HO
OBn
OMe
61i
20 210 200 190 180 170 160 150 140 130 120 110 100 90 80 70 60 50 40 30 20 10 0
f1 (ppm)

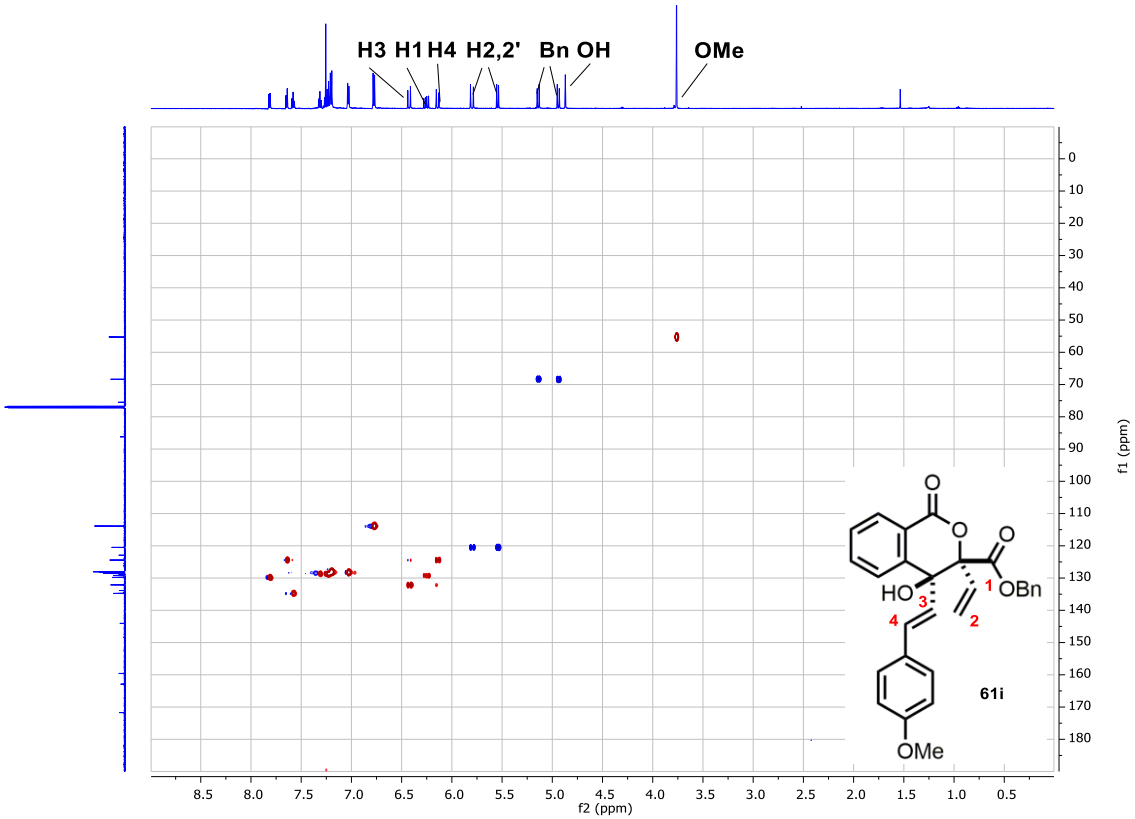
H3 H1 H4 H2,2' Bn OH
OMe
f2 (ppm)
f1 (ppm)
HO
OBn
OMe
61i

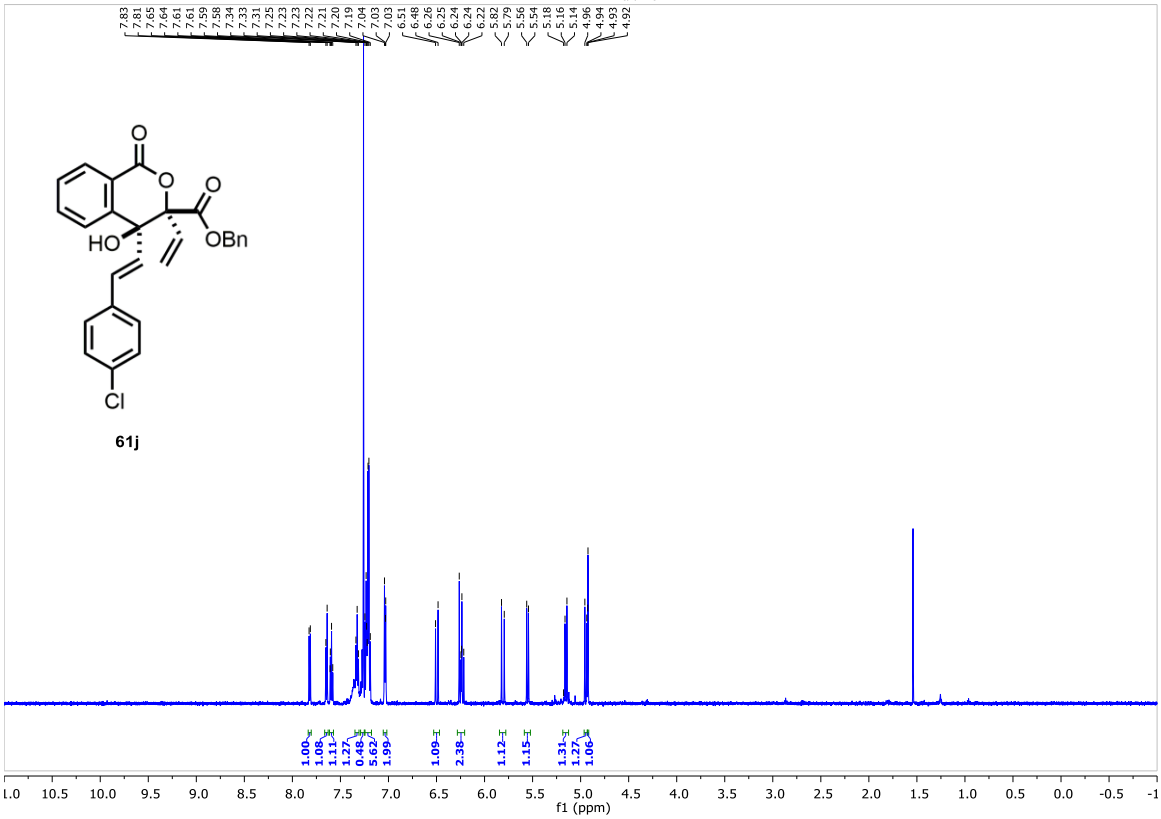
HO
OBn
Cl
61j
f1 (ppm)

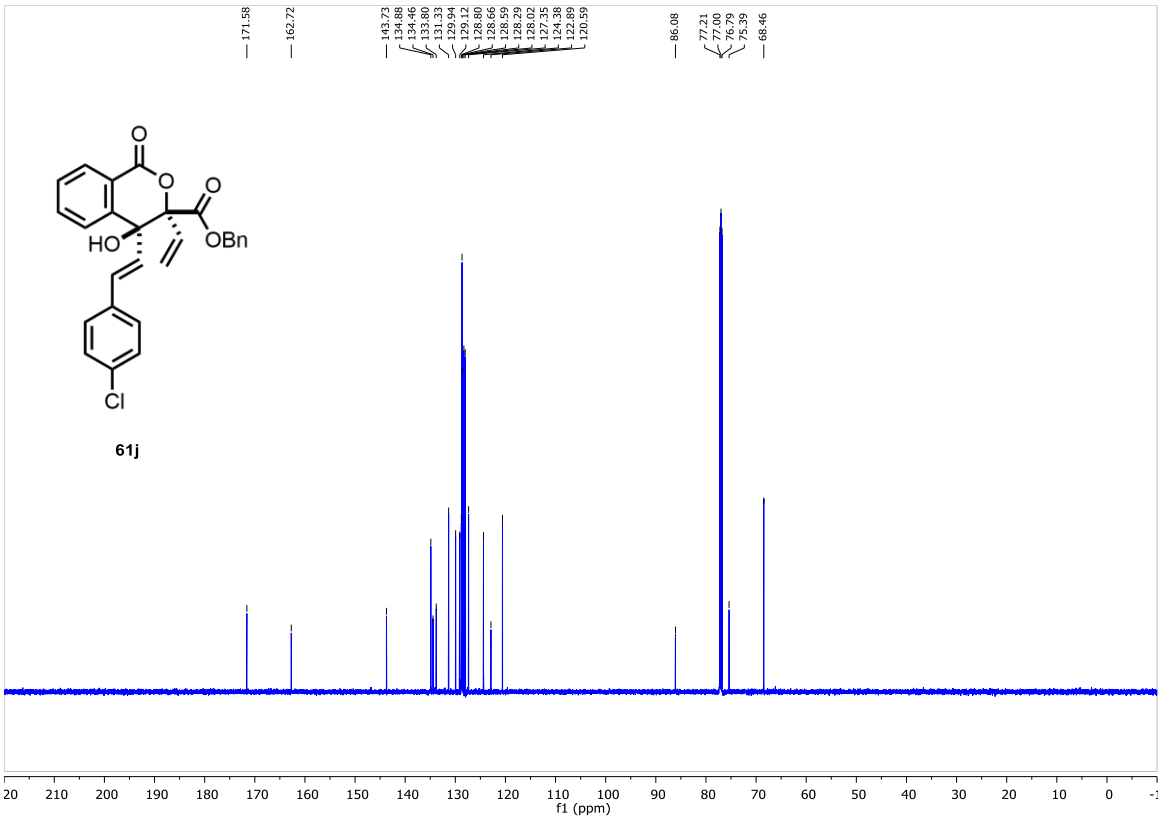
171.58
162.72
143.73
134.88
134.46
133.80
131.33
129.94
129.12
128.80
128.66
128.59
128.29
128.02
127.35
124.38
122.89
120.59
86.08
77.21
77.00
76.79
75.39
68.46
O
O
O
HO
OBn
Cl
61j
f1 (ppm)

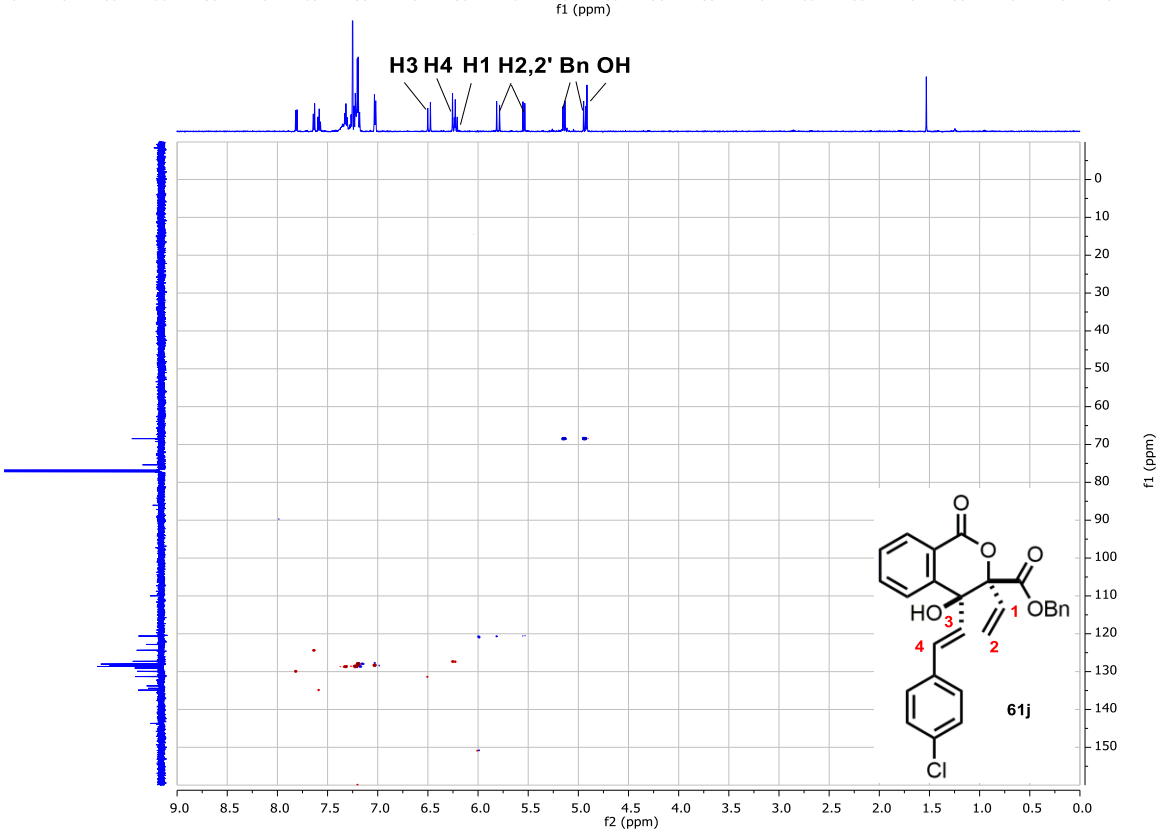
H3 H4 H1 H2,2' Bn OH
f2 (ppm)
f1 (ppm)
O
O
O
HO
3
1
OBn
4
2
61j
Cl

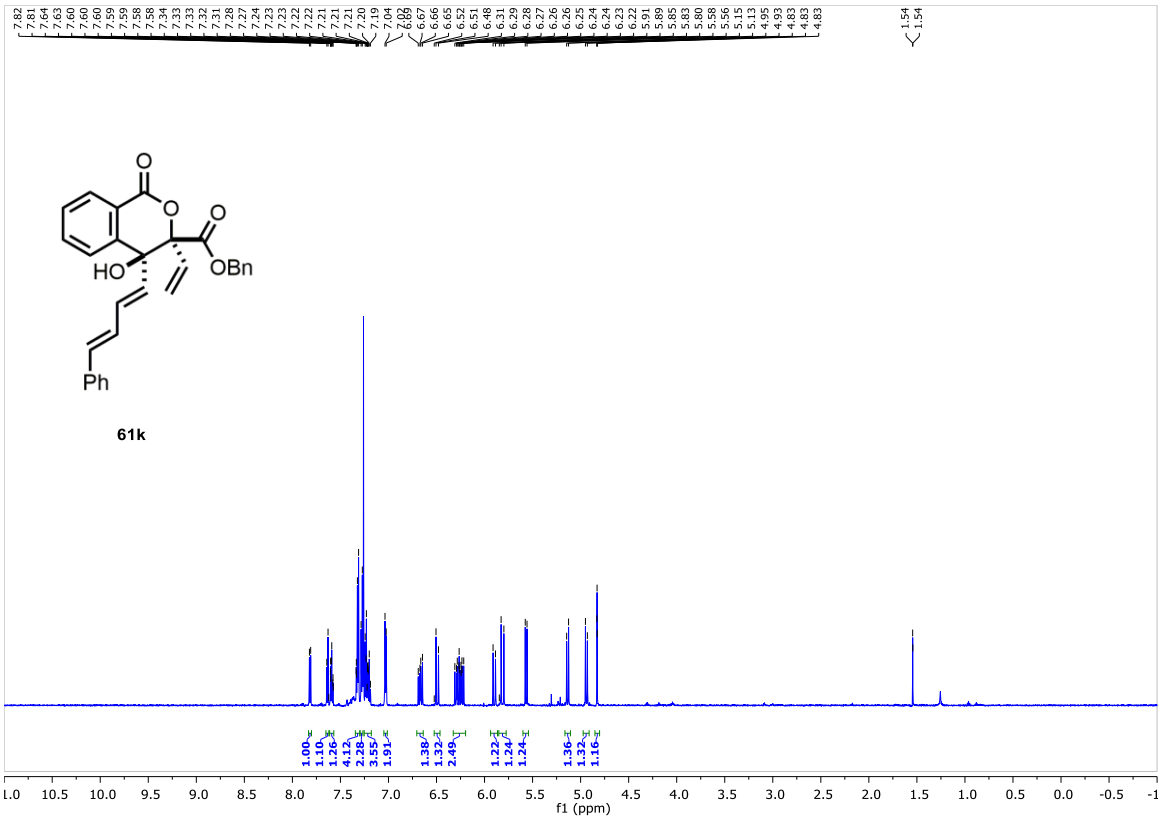
HO
O
O
OBn
Ph
61k
f1 (ppm)

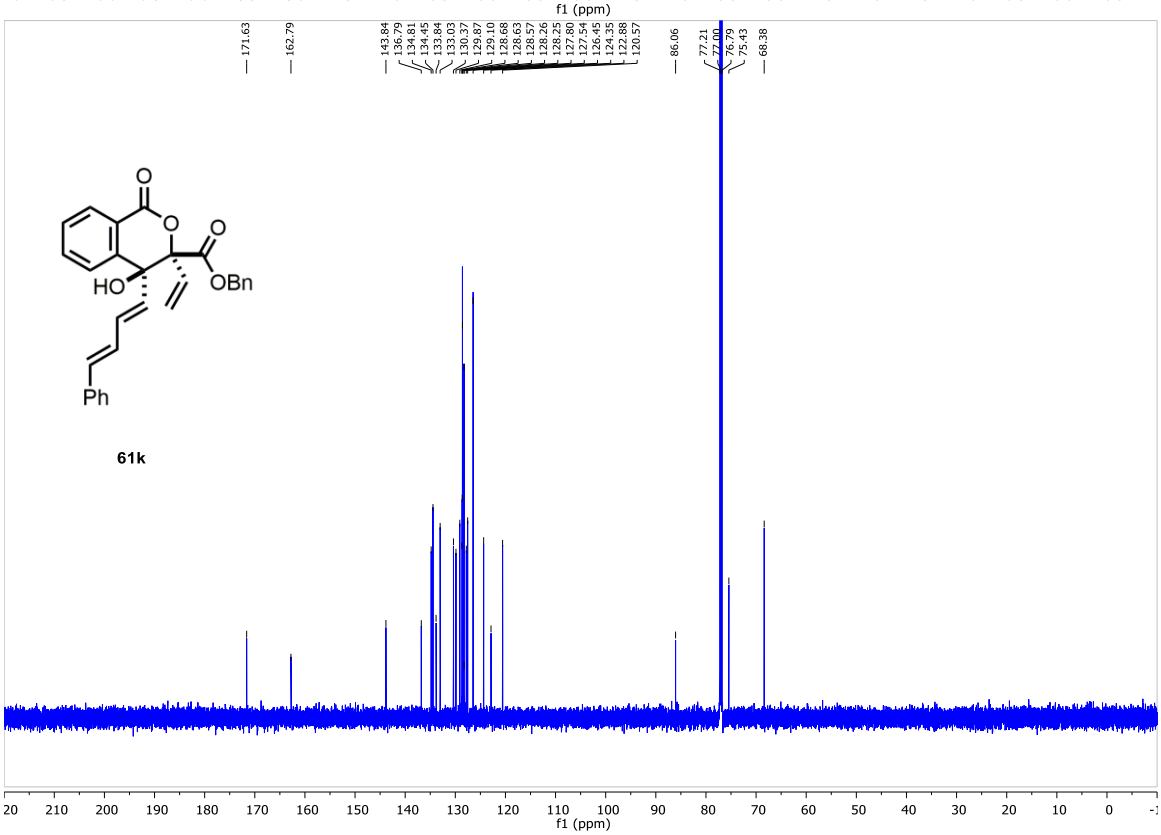
HO
O
O
OBn
Ph
61k
f1 (ppm)

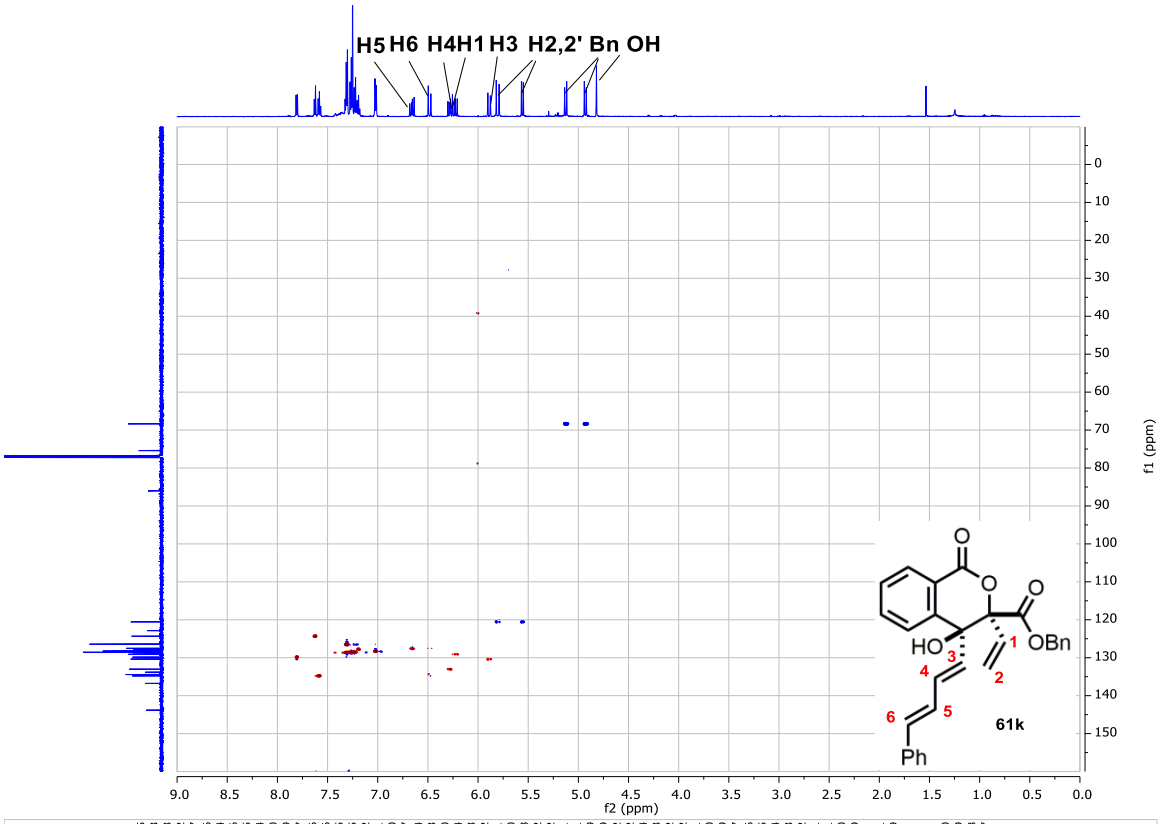
H5 H6 H4 H1 H3 H2,2' Bn OH
f2 (ppm)
f1 (ppm)
HO
OBn
Ph
61k

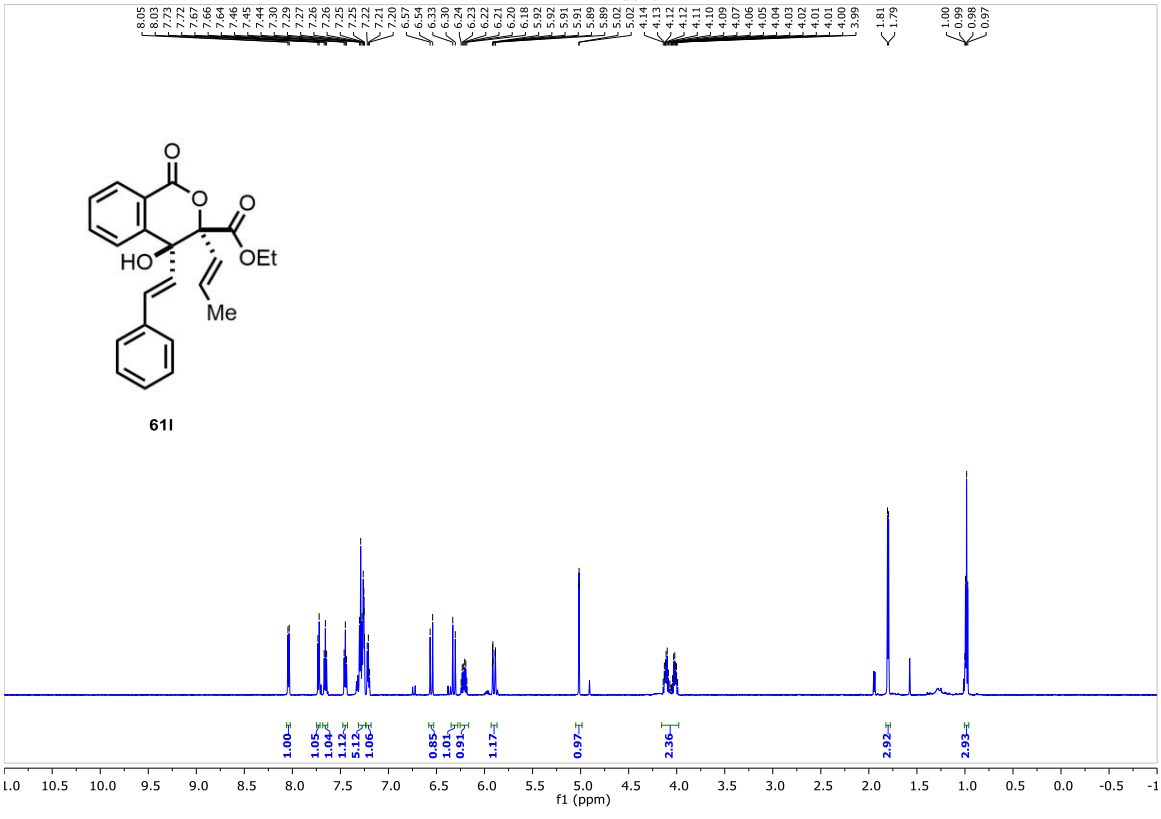
HO
OEt
Me
61l
f1 (ppm)

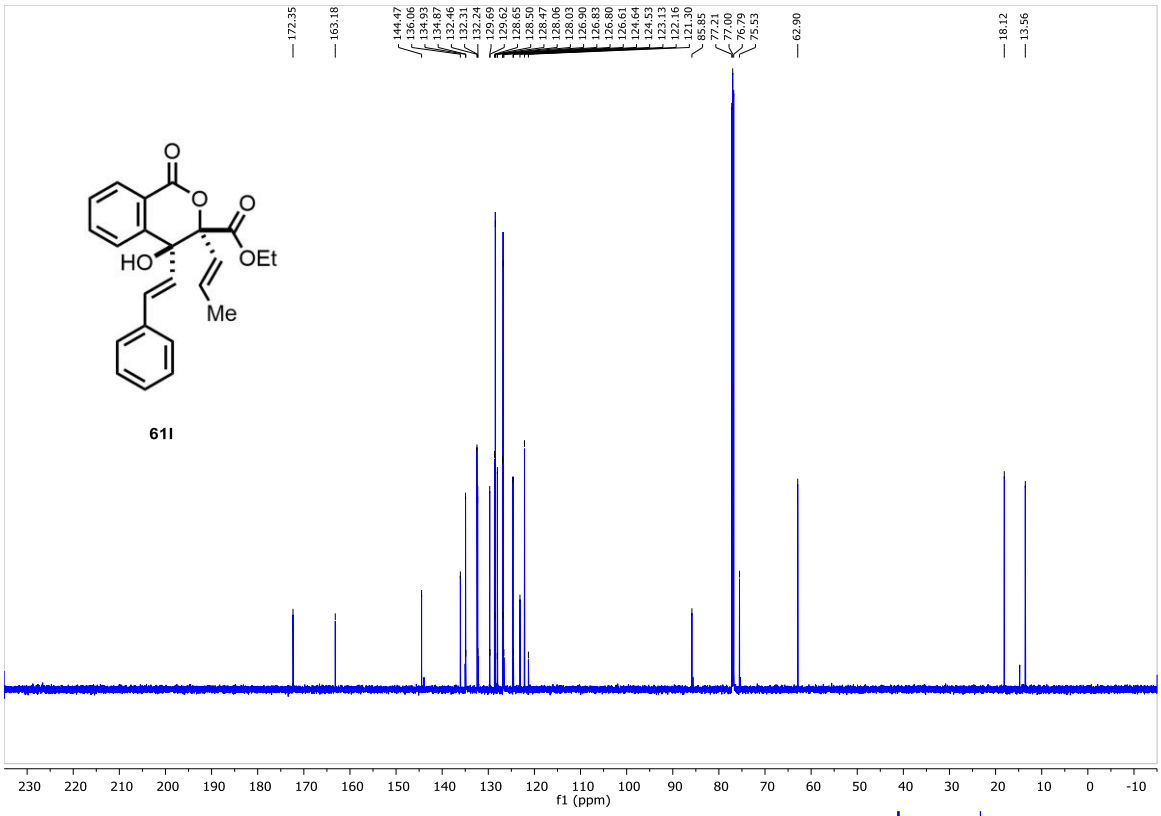
172.35
163.18
144.47
136.06
134.93
134.87
132.46
132.31
132.24
129.69
129.62
128.65
128.50
128.47
128.06
128.03
126.90
126.83
126.80
126.61
124.64
124.53
123.13
122.16
121.30
85.85
77.21
77.00
76.79
75.53
62.90
18.12
13.56
HO
O
OEt
Me
61l
f1 (ppm)

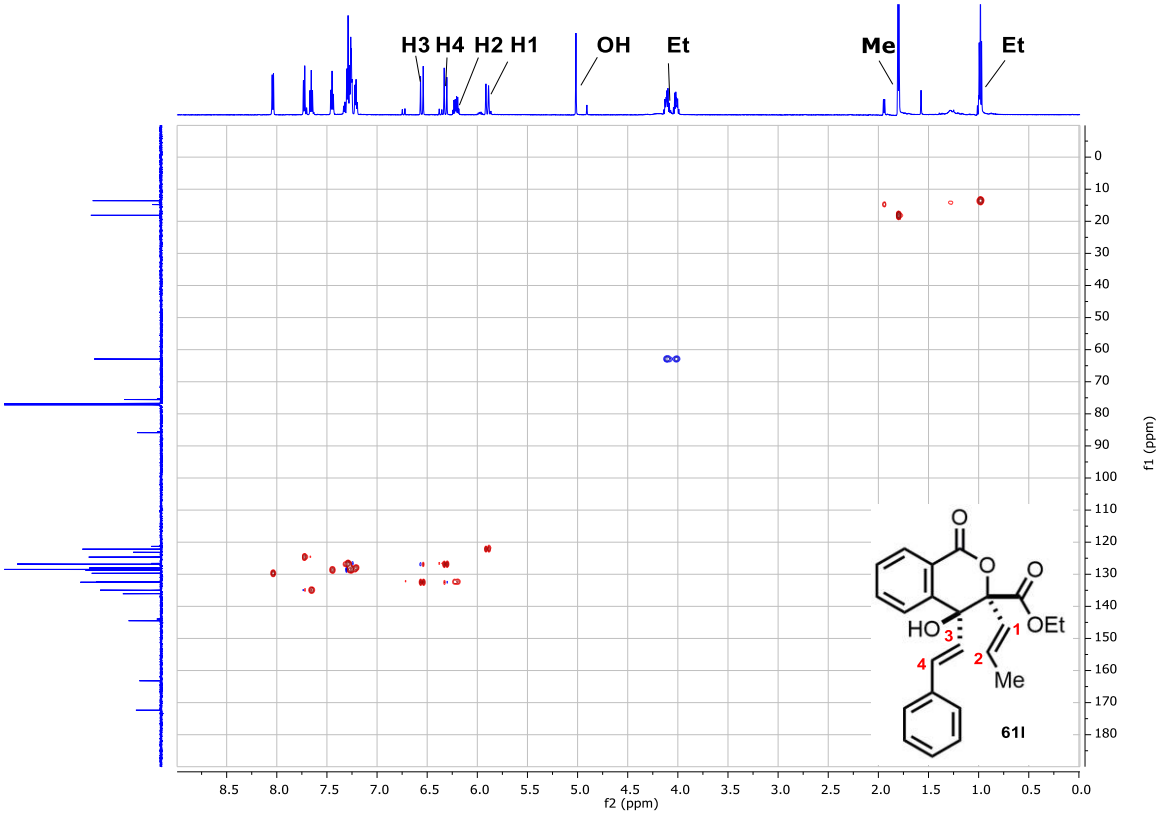
H3 H4 H2 H1
OH
Et
Me
Et
HO
OEt
Me
1
2
3
4
61l
f2 (ppm)
f1 (ppm)

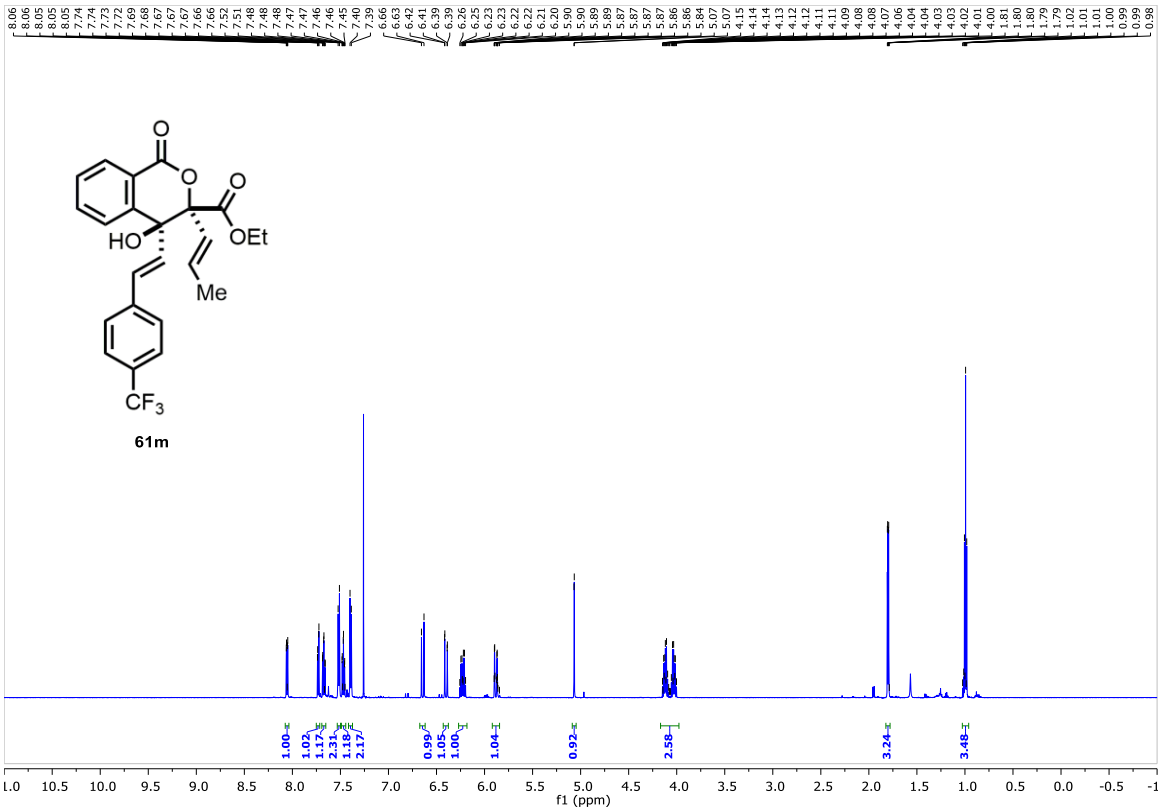
O
O
O
OEt
HO
Me
CF3
61m
1.00
1.02
1.17
2.31
1.18
2.17
0.99
1.05
1.00
1.04
0.92
2.58
3.24
3.48
f1 (ppm)

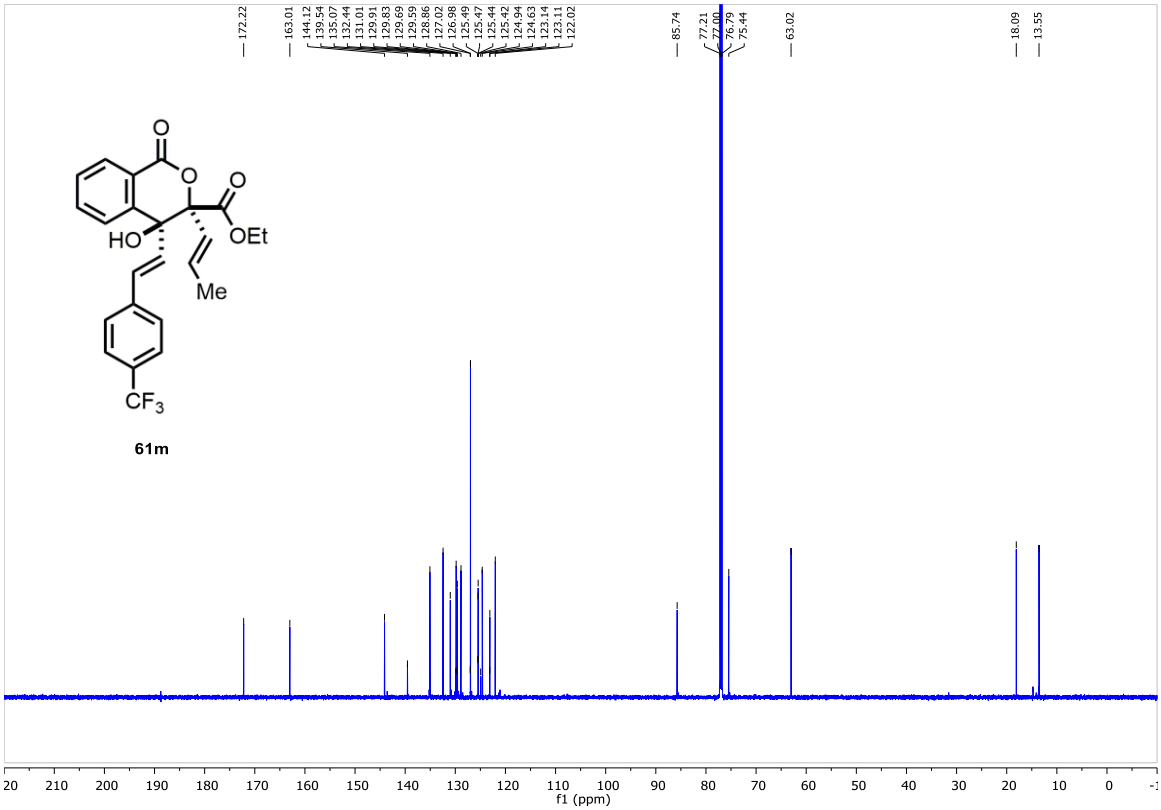
O
O
O
OEt
HO
Me
CF3
61m
172.22
163.01
144.12
139.54
135.07
132.44
131.01
129.91
129.83
129.69
129.59
128.86
127.02
126.98
125.49
125.47
125.44
125.42
124.94
124.63
123.14
123.11
122.02
85.74
77.21
77.00
76.79
75.44
63.02
18.09
13.55
f1 (ppm)

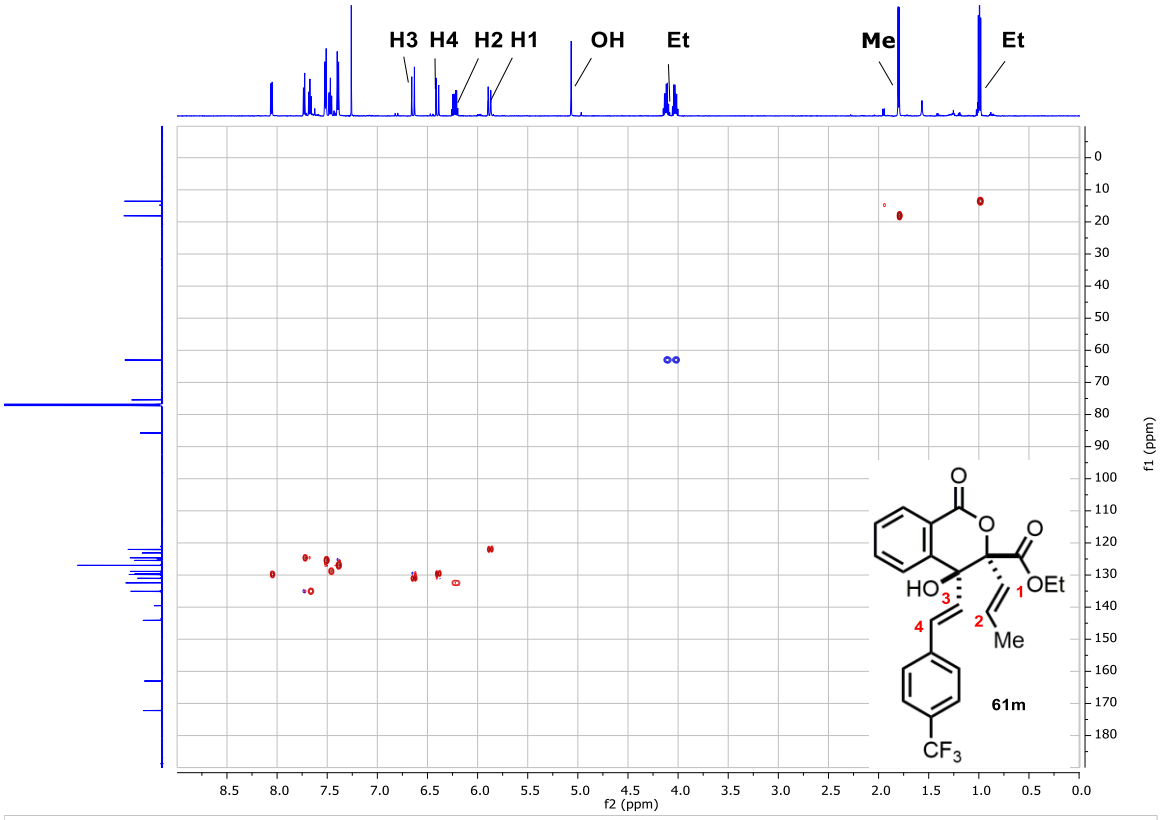
H3
H4
H2
H1
OH
Et
Me
Et
f1 (ppm)
f2 (ppm)
HO
OEt
Me
CF3
61m

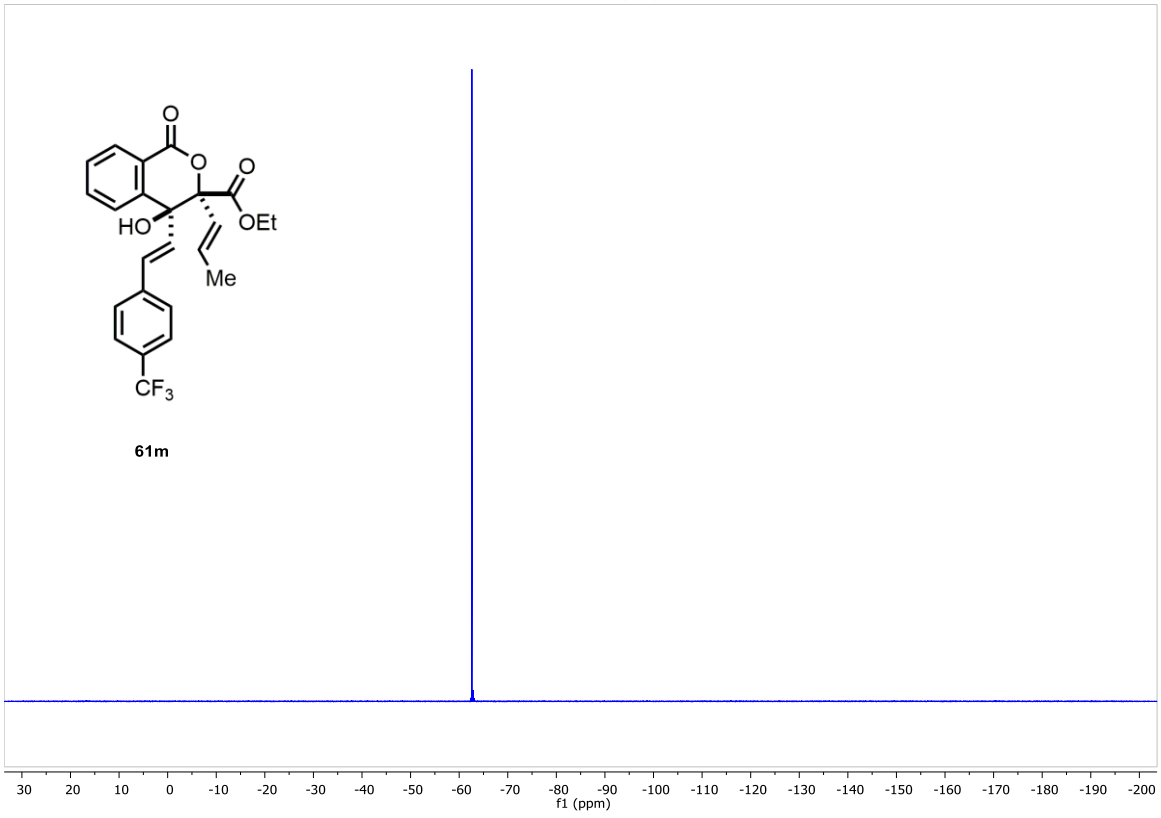
HO
OEt
Me
CF3
61m
f1 (ppm)

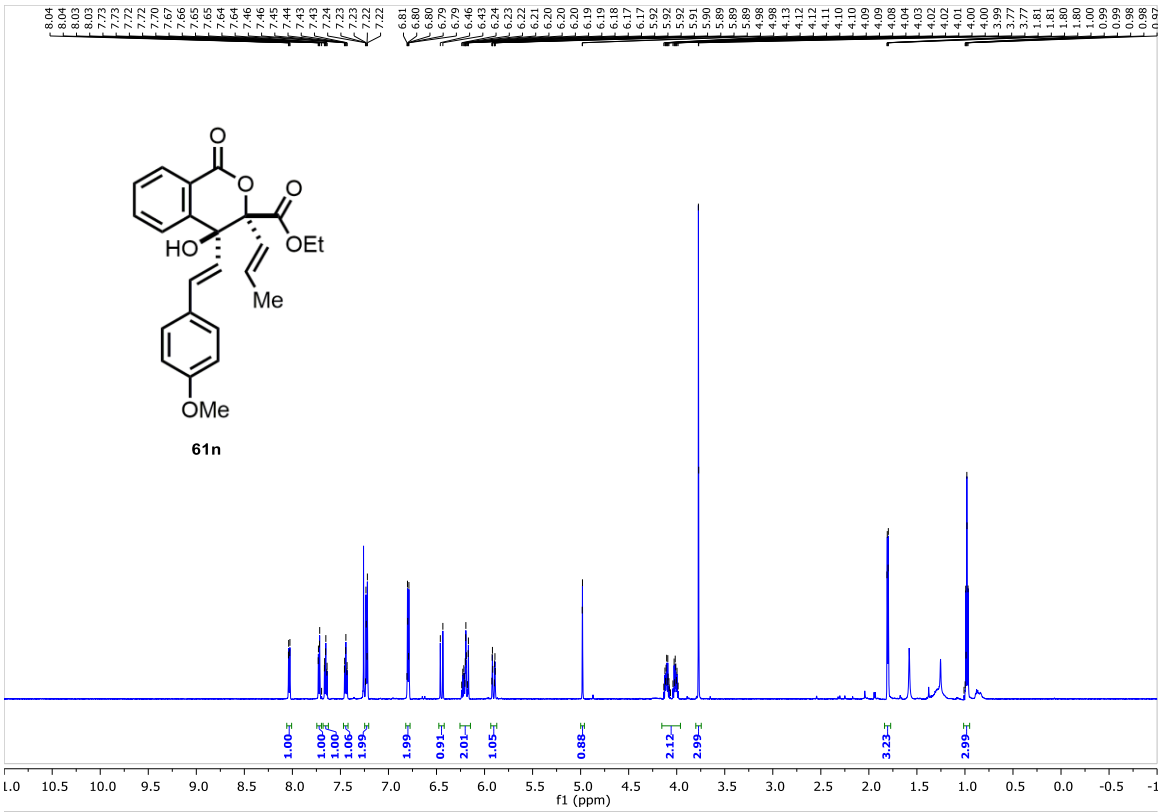
HO
O
O
OEt
Me
OMe
61n
f1 (ppm)

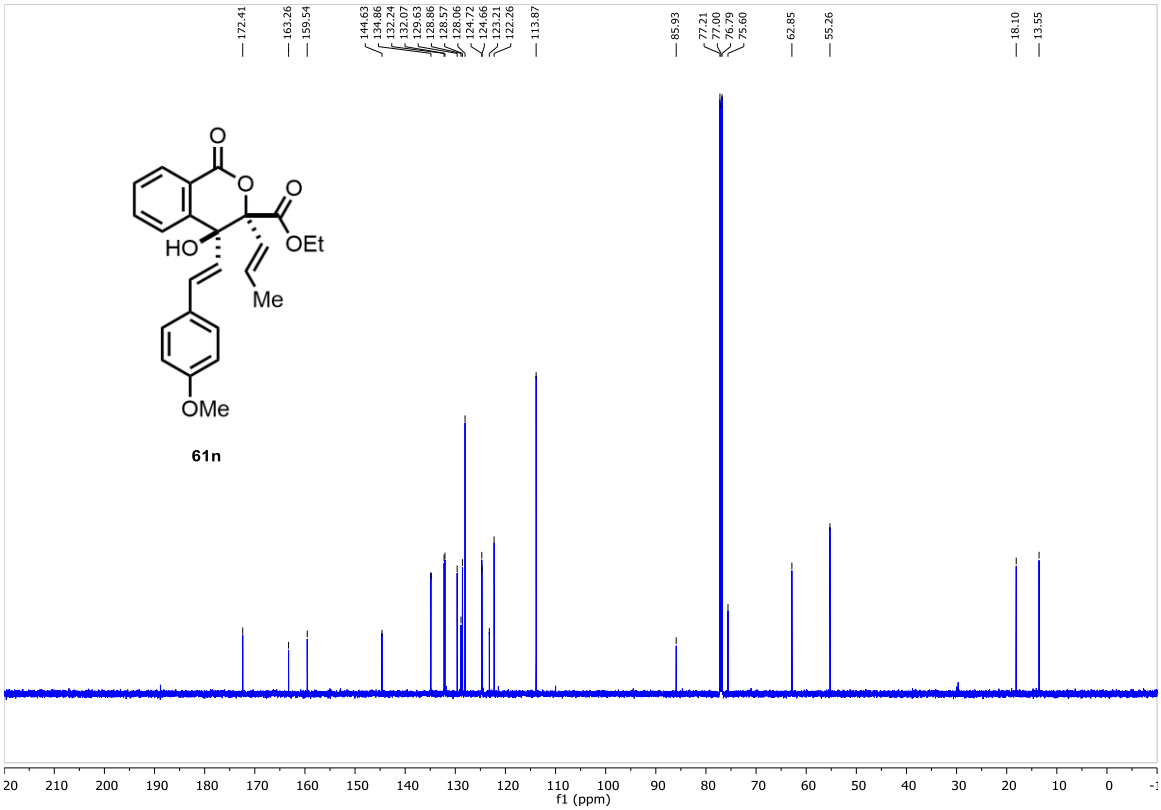
HO
O
O
OEt
Me
OMe
61n
f1 (ppm)

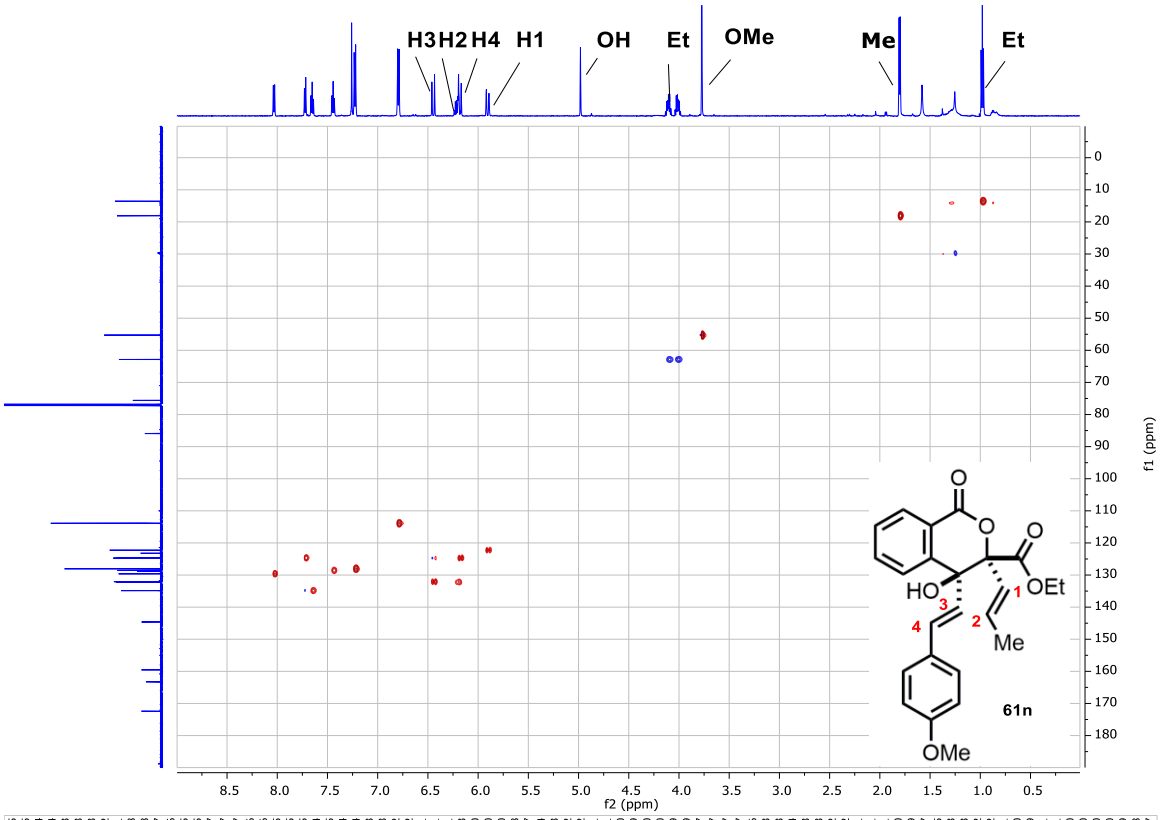
H3
H2
H4
H1
OH
Et
OMe
Me
Et
f2 (ppm)
f1 (ppm)
HO
OEt
Me
OMe
61n

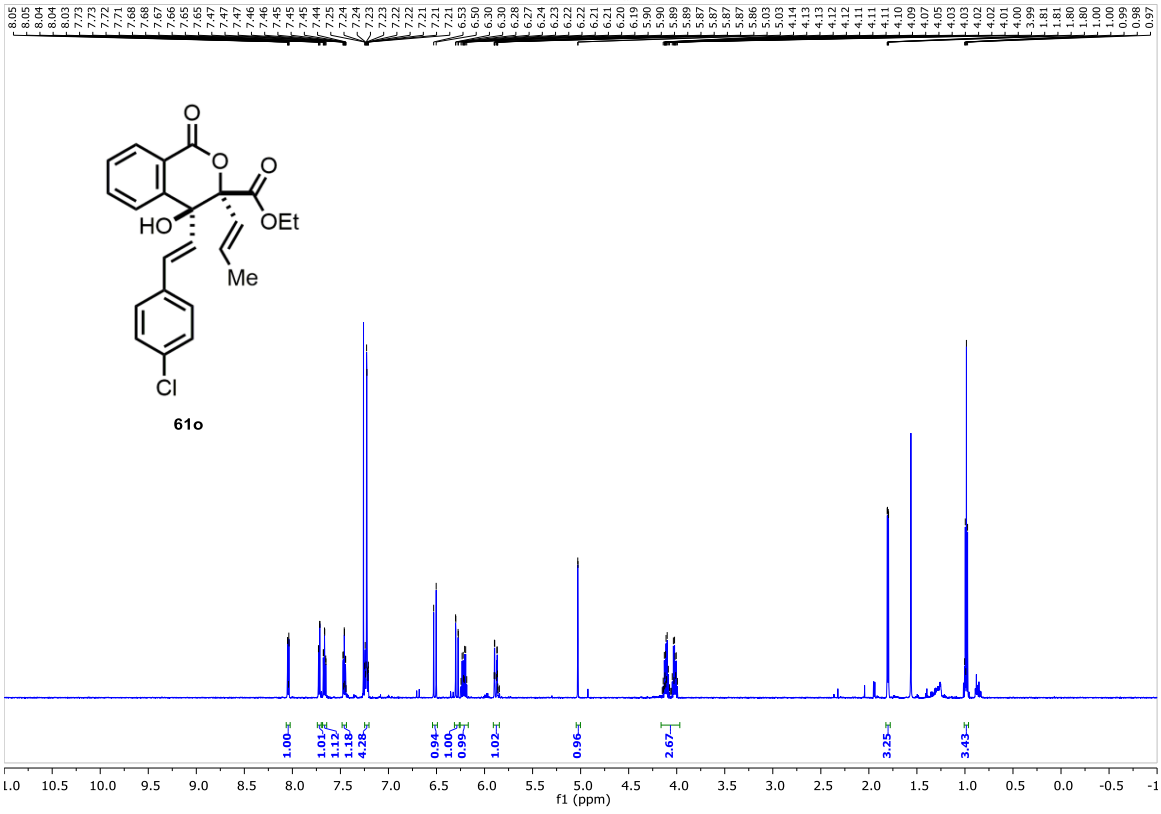
HO
OEt
Me
Cl
61o
f1 (ppm)

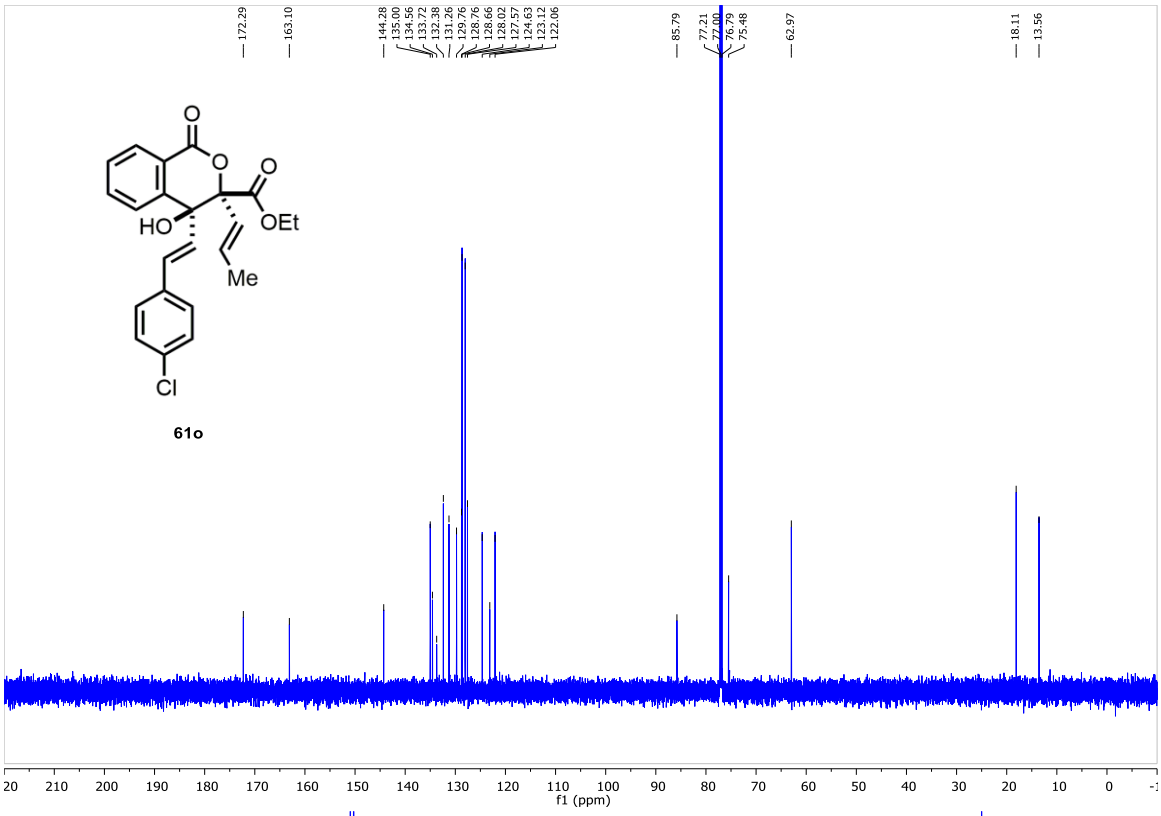
172.29
163.10
144.28
135.00
134.56
133.72
131.38
131.26
129.76
128.76
128.66
128.02
127.57
124.63
123.12
122.06
85.79
77.21
76.79
75.48
62.97
18.11
13.56
O
O
O
HO
OEt
Me
Cl
61o
f1 (ppm)

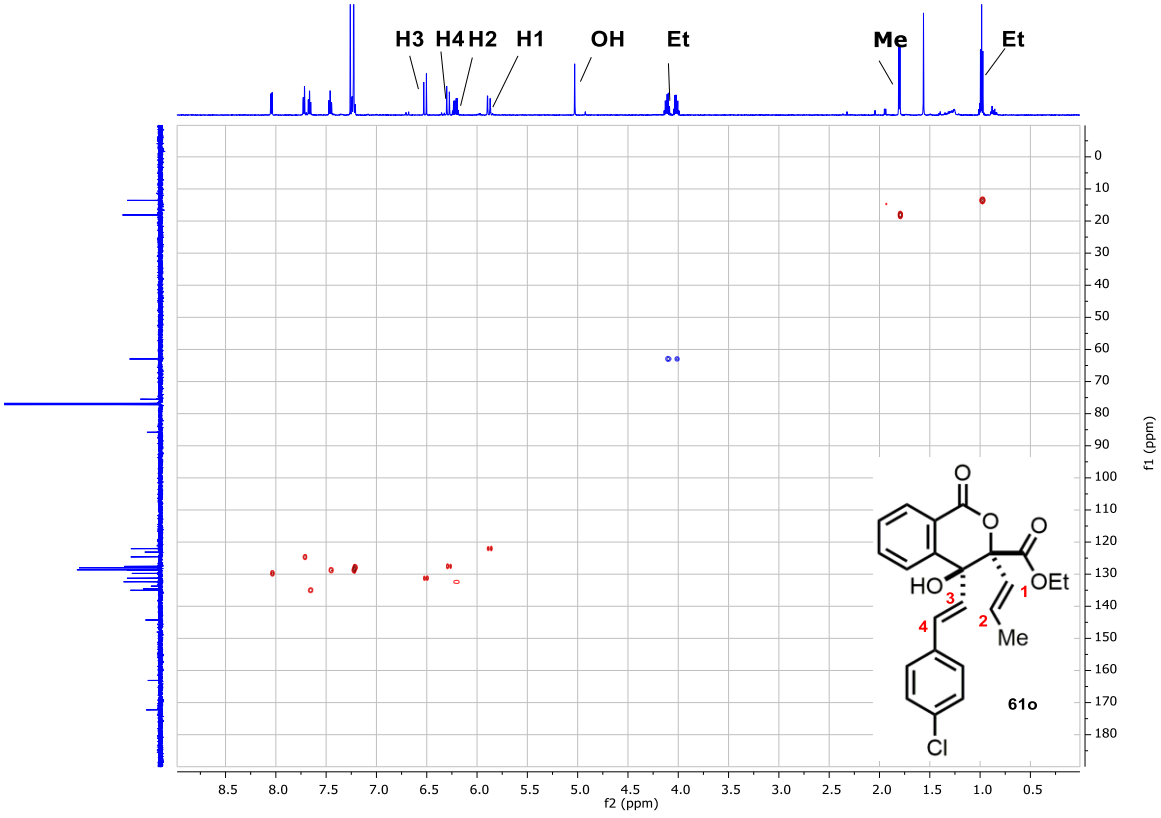
H3
H4
H2
H1
OH
Et
Me
Et
f2 (ppm)
f1 (ppm)
HO
OEt
Me
Cl
61o

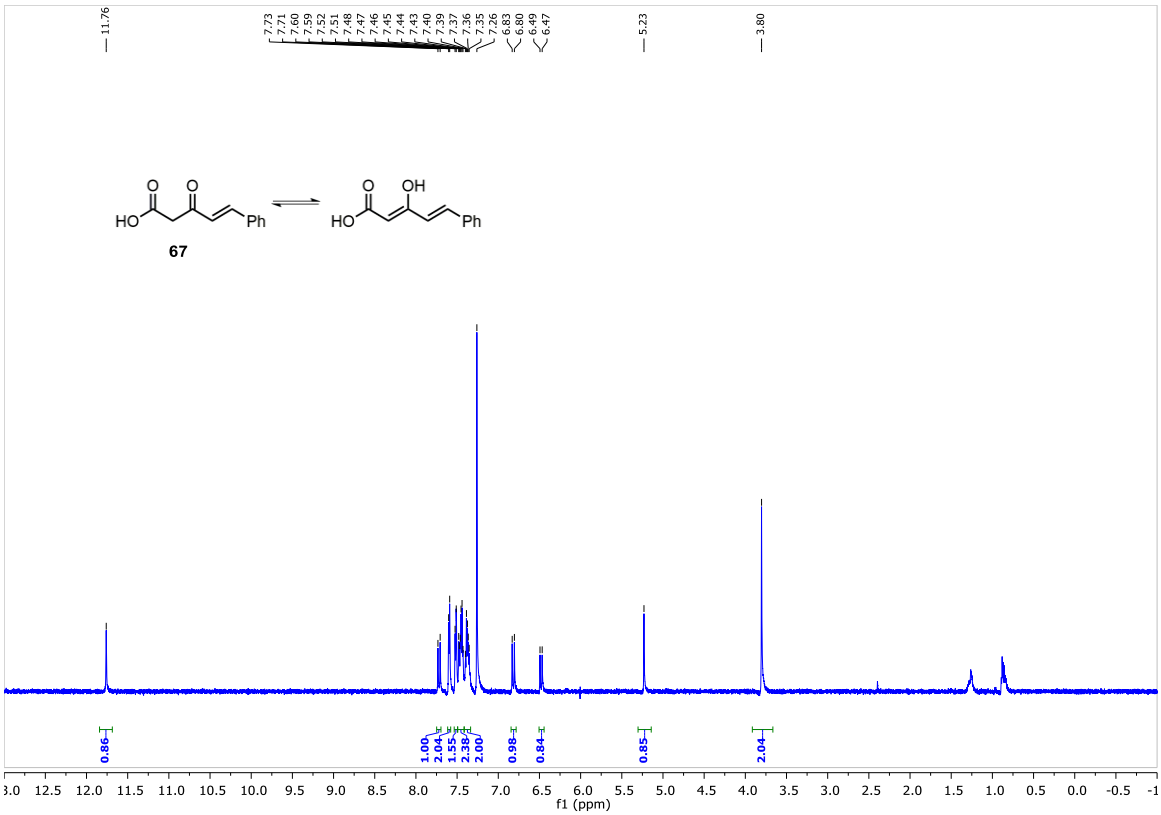
11.76
7.73
7.71
7.60
7.59
7.52
7.51
7.48
7.47
7.46
7.45
7.44
7.43
7.40
7.39
7.37
7.36
7.35
7.26
6.83
6.80
6.49
6.47
5.23
3.80
HO
O
O
Ph
HO
O
OH
Ph
67
0.86
1.00
2.04
1.55
2.38
2.00
0.98
0.84
0.85
2.04
f1 (ppm)

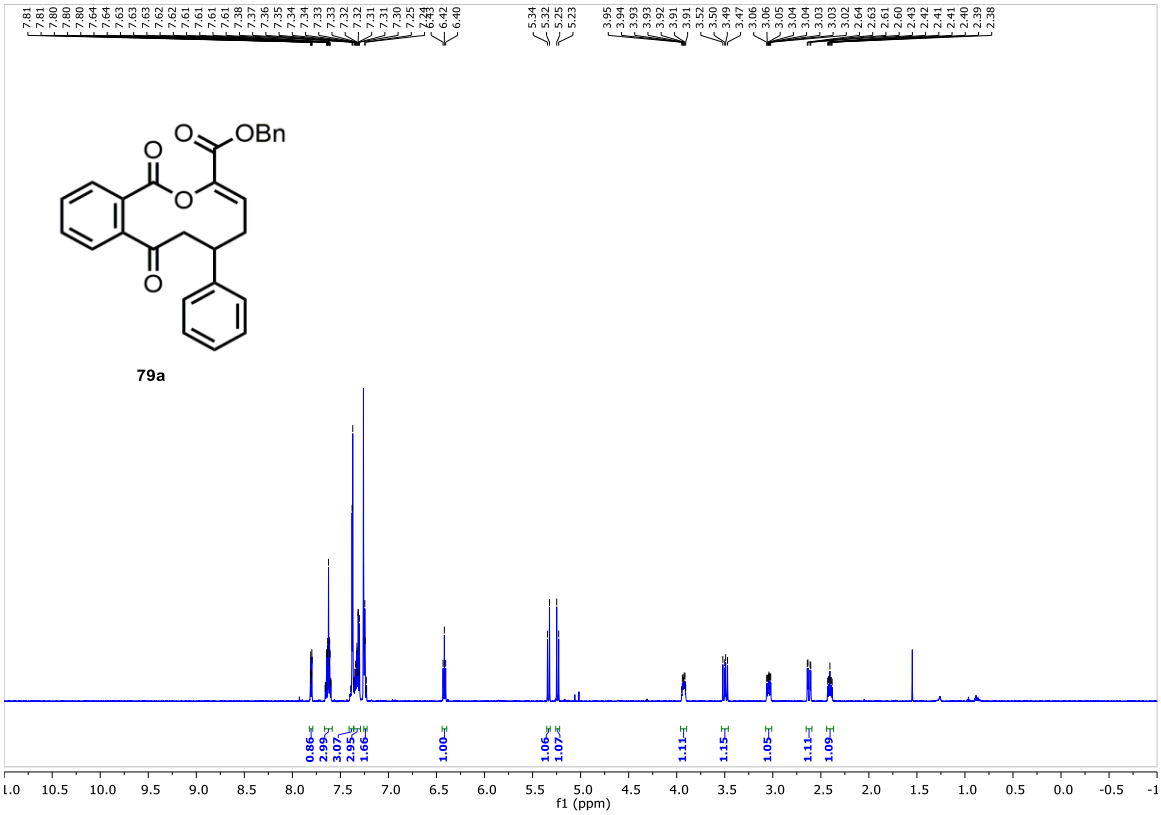
7.81
7.81
7.80
7.80
7.80
7.64
7.64
7.63
7.63
7.63
7.62
7.62
7.61
7.61
7.61
7.61
7.38
7.37
7.36
7.35
7.34
7.34
7.33
7.33
7.32
7.32
7.31
7.31
7.30
7.25
6.43
6.42
6.40
5.34
5.32
5.25
5.23
3.95
3.94
3.93
3.93
3.92
3.91
3.91
3.52
3.50
3.49
3.47
3.06
3.06
3.05
3.04
3.04
3.03
3.03
3.02
2.64
2.63
2.61
2.60
2.45
2.42
2.41
2.41
2.40
2.39
2.38
OBn
O
O
O
O
79a
0.86
2.99
3.07
2.95
1.66
1.00
1.06
1.07
1.11
1.15
1.05
1.11
1.09
f1 (ppm)

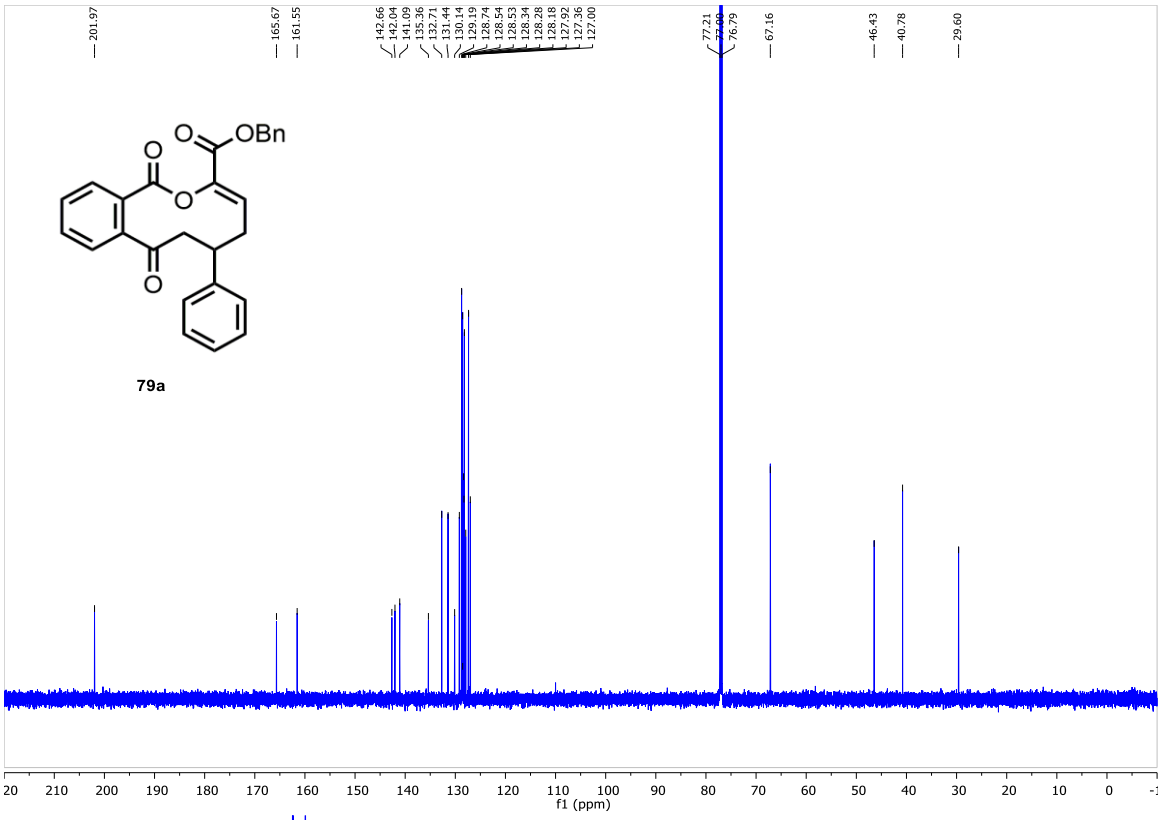
201.97
165.67
161.55
142.66
142.04
141.09
135.36
132.71
131.44
130.14
129.19
128.74
128.54
128.53
128.34
128.28
128.18
127.92
127.36
127.00
77.21
77.00
76.79
67.16
46.43
40.78
29.60
OBn
79a
f1 (ppm)

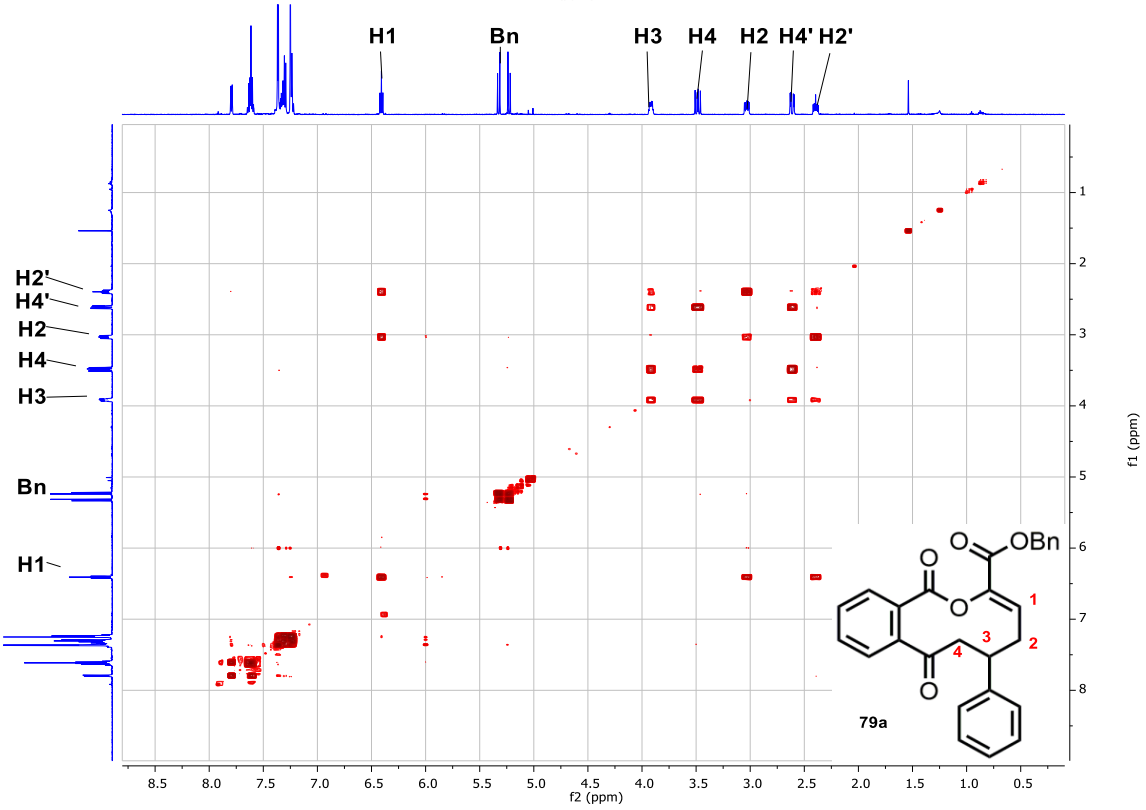
H1
Bn
H3
H4
H2
H4'
H2'
H2'
H4'
H2
H4
H3
Bn
H1
OBn
79a
f2 (ppm)
f1 (ppm)

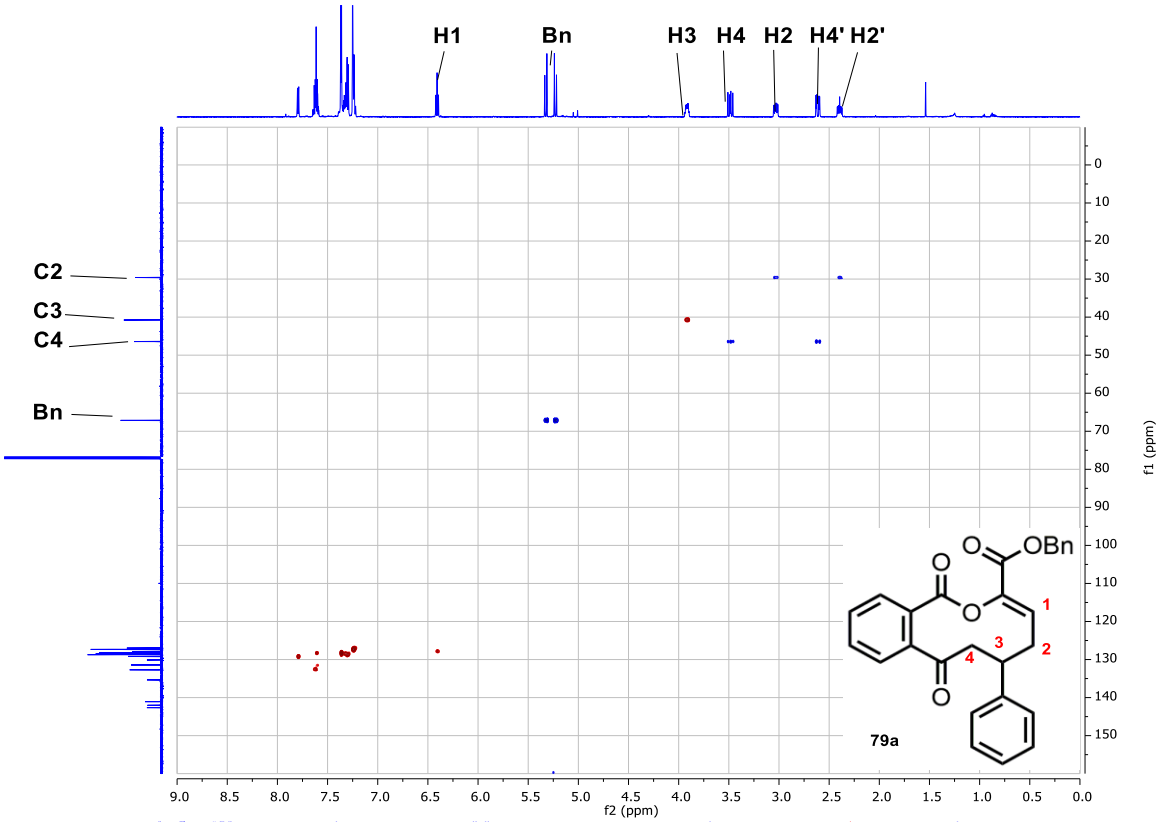
H1
Bn
H3
H4
H2
H4'
H2'
C2
C3
C4
Bn
f1 (ppm)
f2 (ppm)
OBn
79a

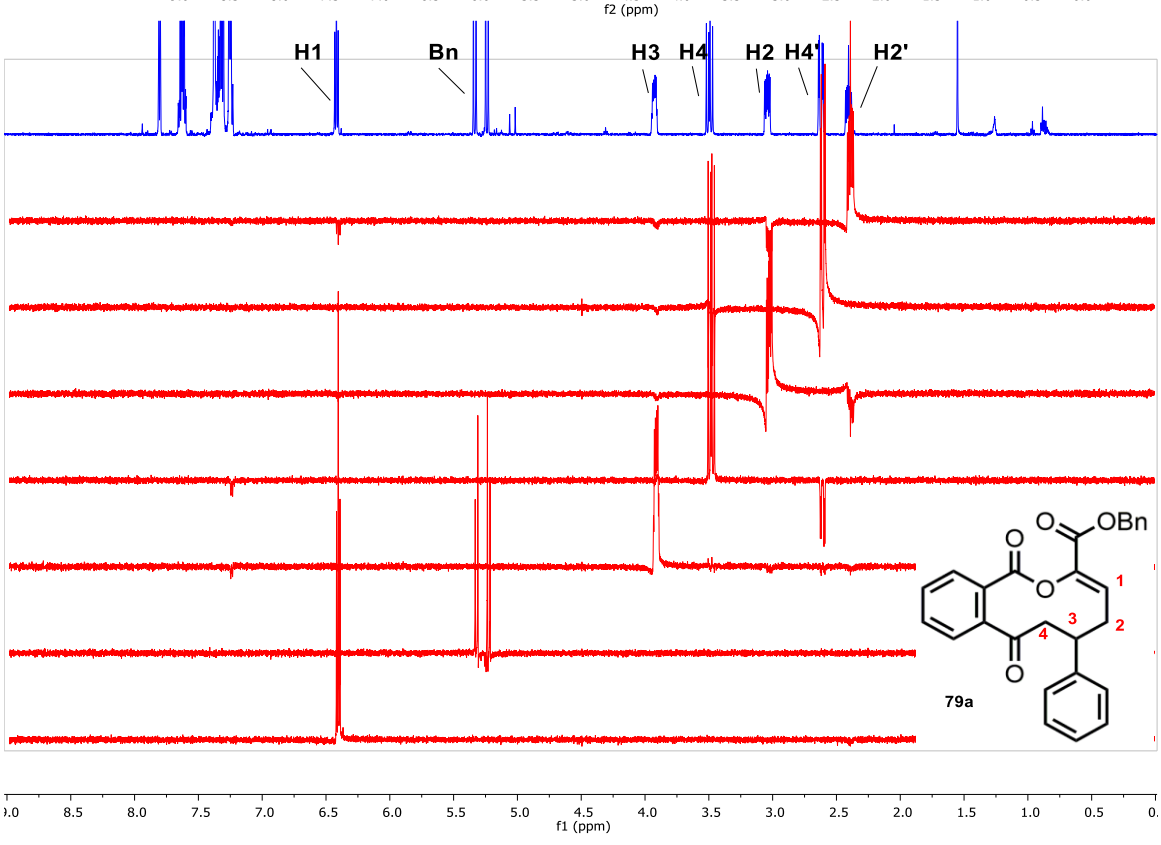
H1
Bn
H3
H4
H2
H4'
H2'
f1 (ppm)
OBn
79a

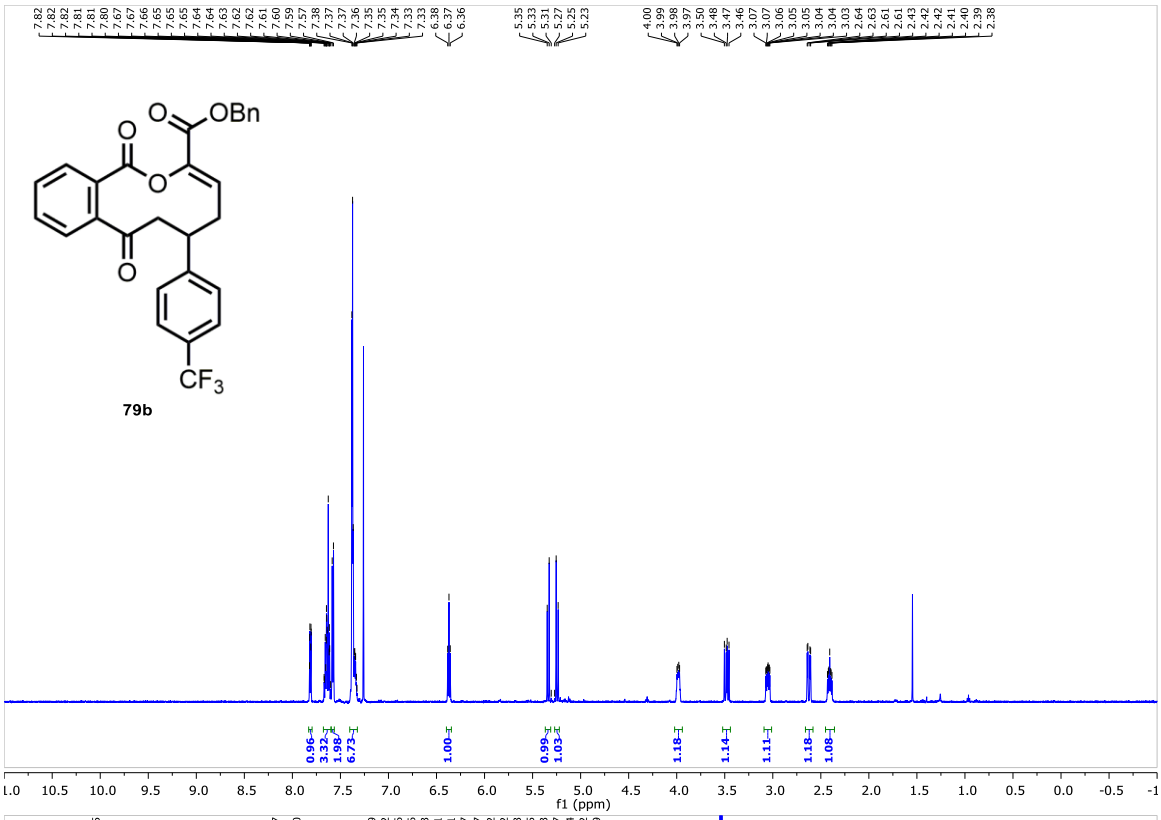
OBn
O
O
O
CF3
79b
f1 (ppm)

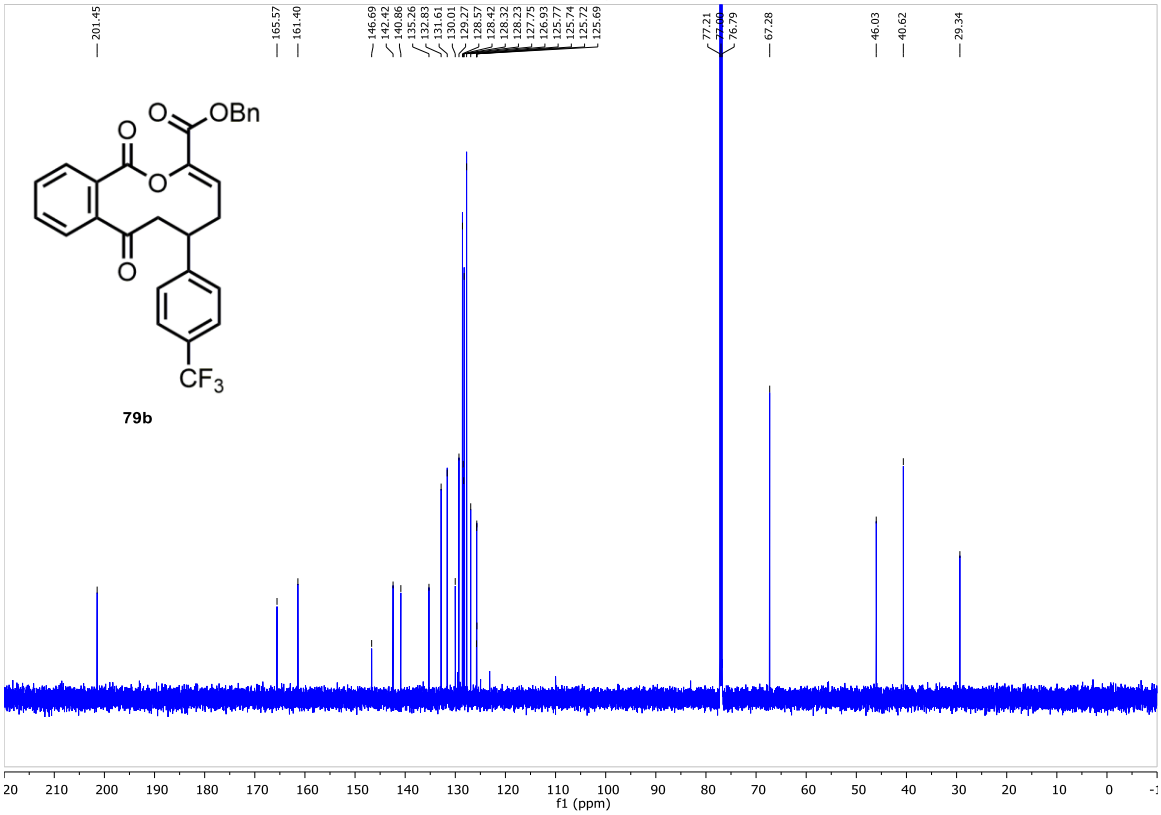
OBn
O
O
O
CF3
79b
f1 (ppm)

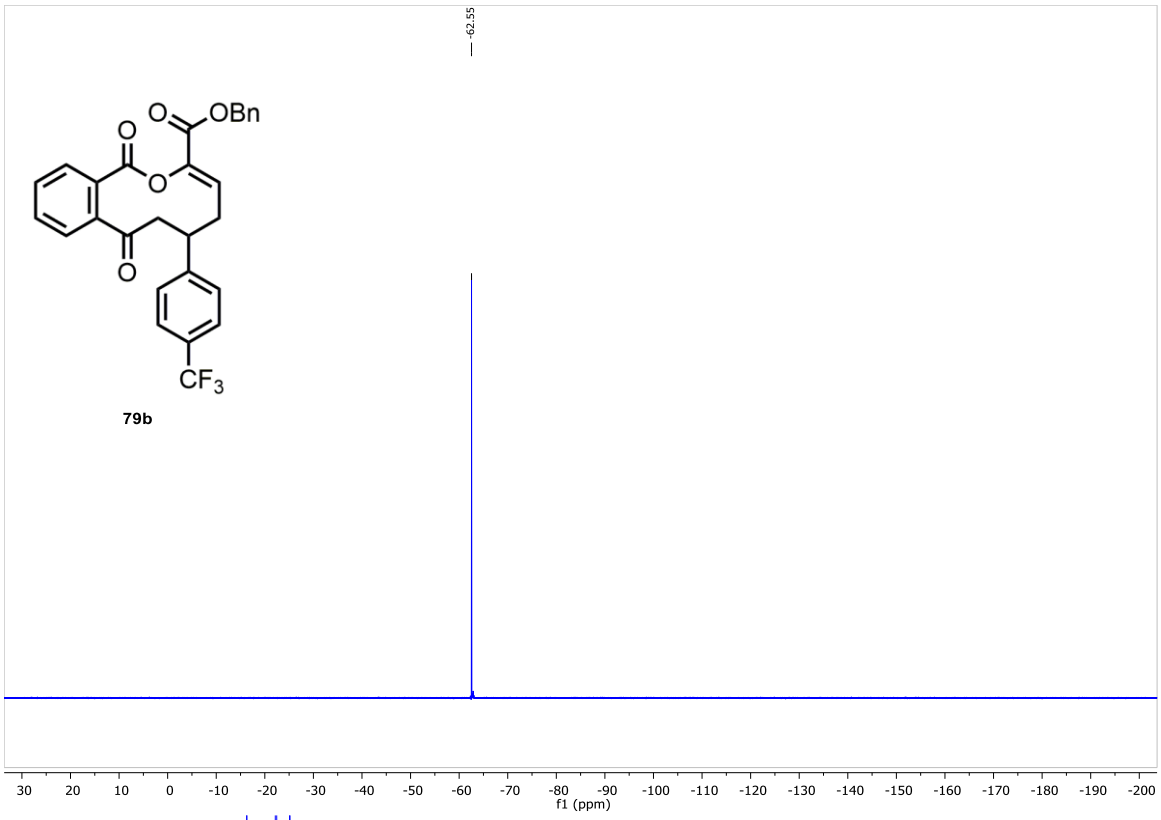
-62.55
OBn
O
O
O
CF3
79b
30 20 10 0 -10 -20 -30 -40 -50 -60 -70 -80 -90 -100 -110 -120 -130 -140 -150 -160 -170 -180 -190 -200
f1 (ppm)

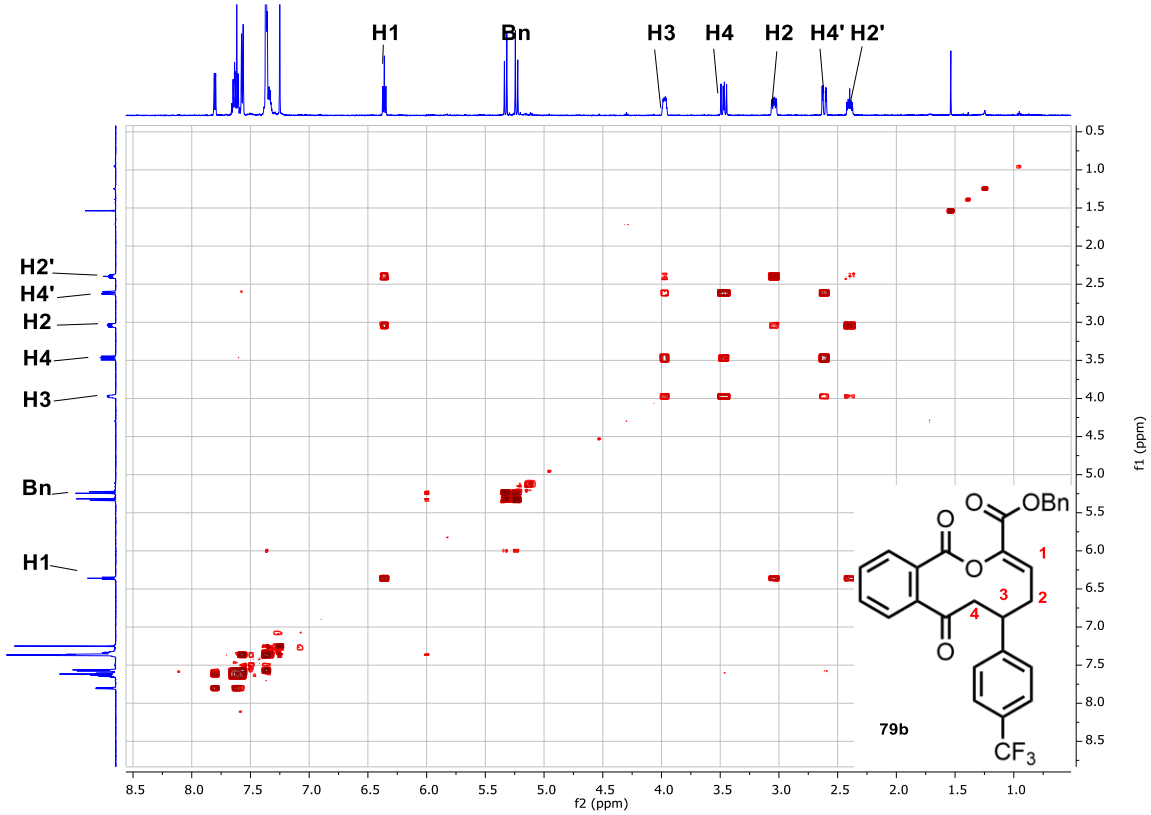
H1
Bn
H3
H4
H2
H4'
H2'
H2'
H4'
H2
H4
H3
Bn
H1
OBn
O
O
O
1
2
3
4
79b
CF3
8.5 8.0 7.5 7.0 6.5 6.0 5.5 5.0 4.5 4.0 3.5 3.0 2.5 2.0 1.5 1.0
f2 (ppm)
0.5 1.0 1.5 2.0 2.5 3.0 3.5 4.0 4.5 5.0 5.5 6.0 6.5 7.0 7.5 8.0 8.5
f1 (ppm)

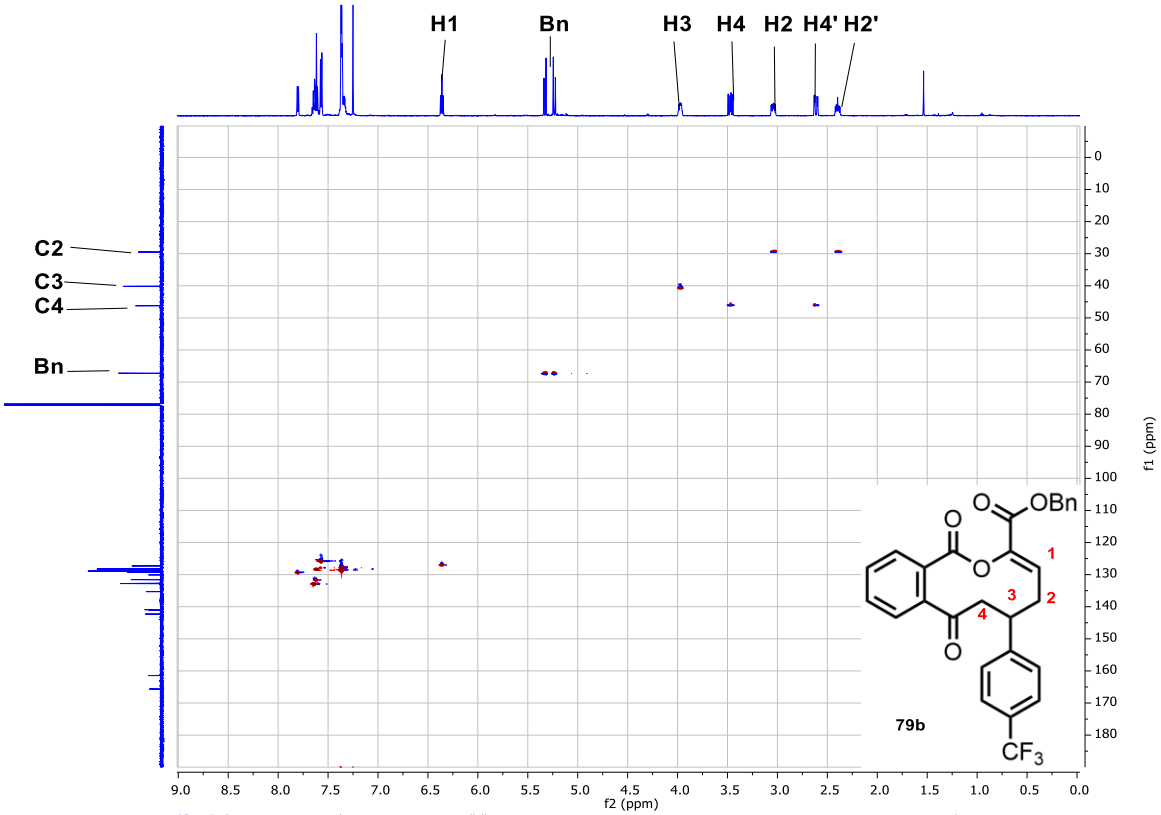
H1
Bn
H3
H4
H2
H4'
H2'
C2
C3
C4
Bn
f2 (ppm)
f1 (ppm)
OBn
79b
CF3

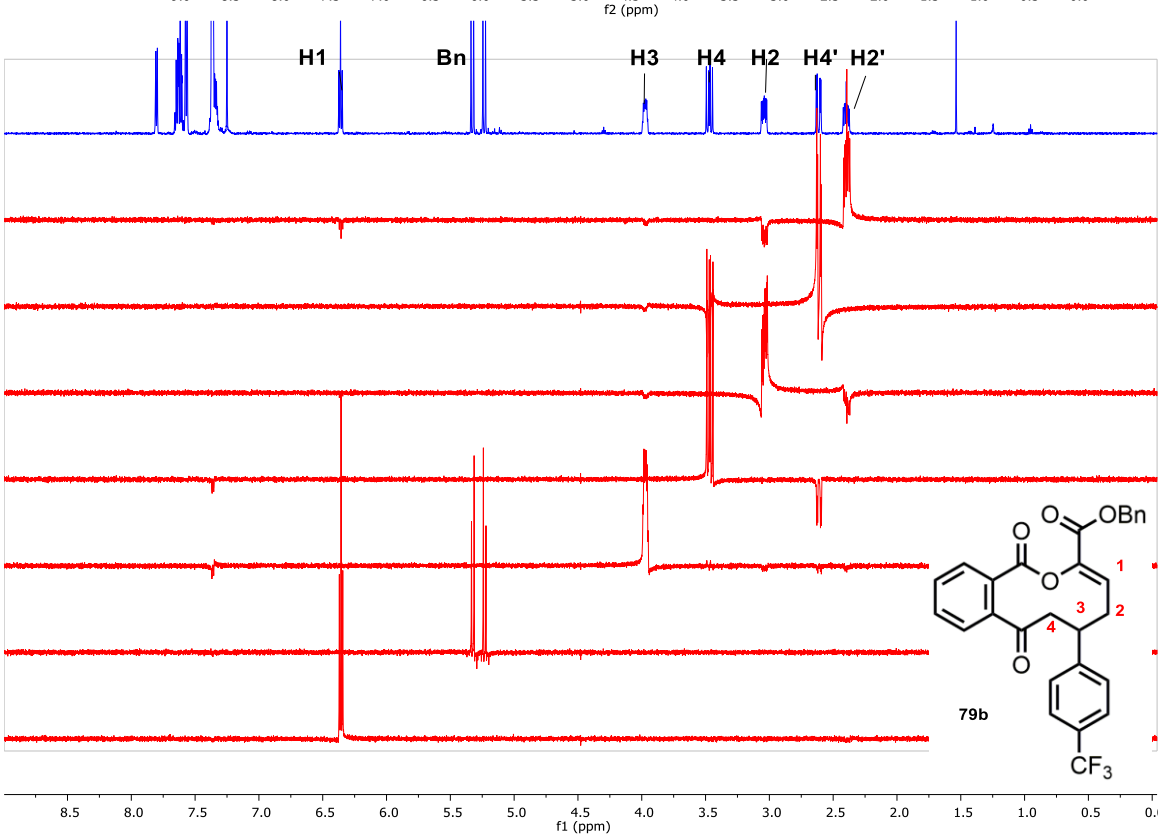
H1
Bn
H3
H4
H2
H4'
H2'
f1 (ppm)
OBn
79b
CF3

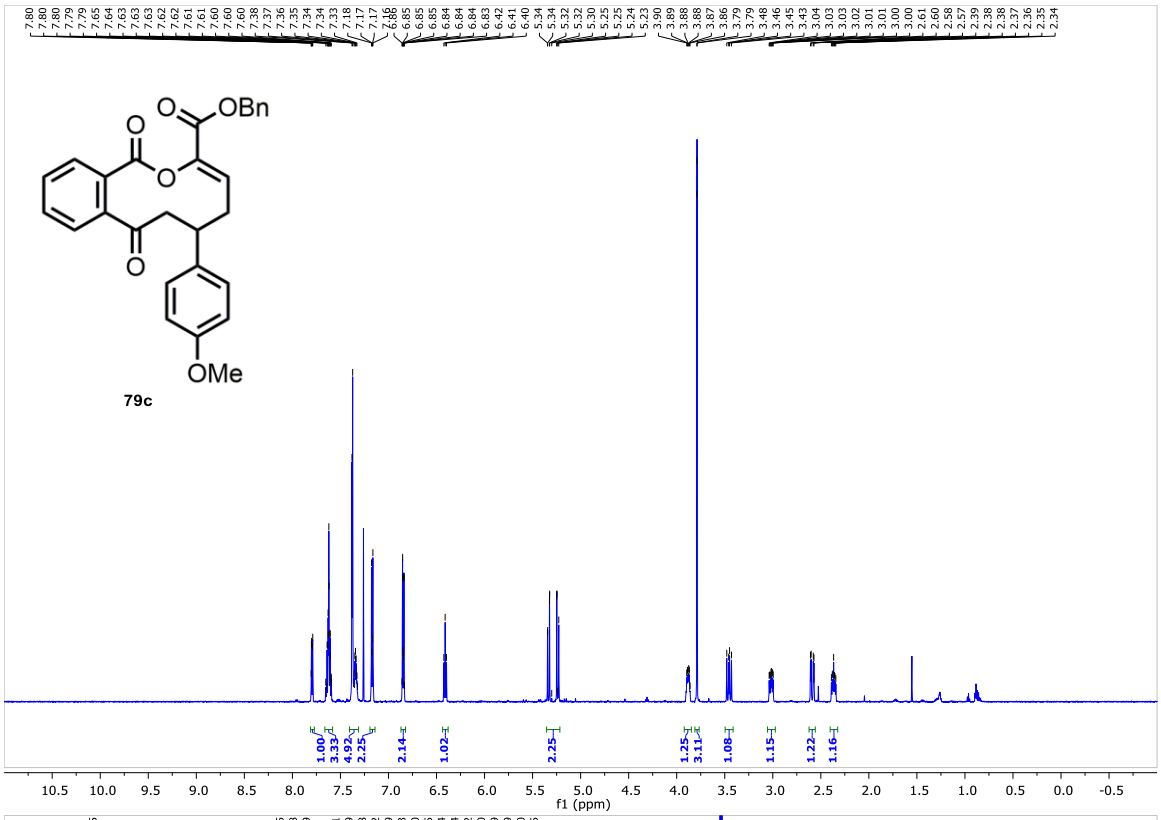
OBn
O
O
O
O
OMe
79c
f1 (ppm)

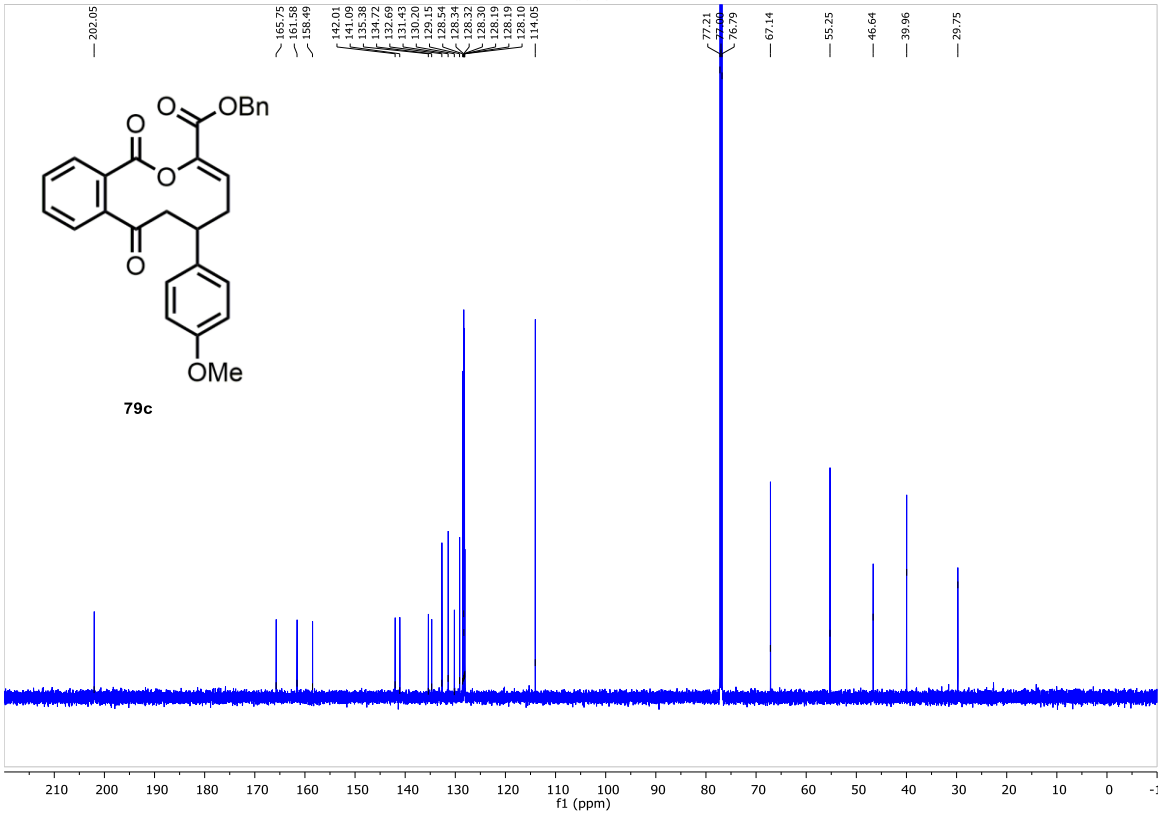
OBn
O
O
O
O
OMe
79c
f1 (ppm)

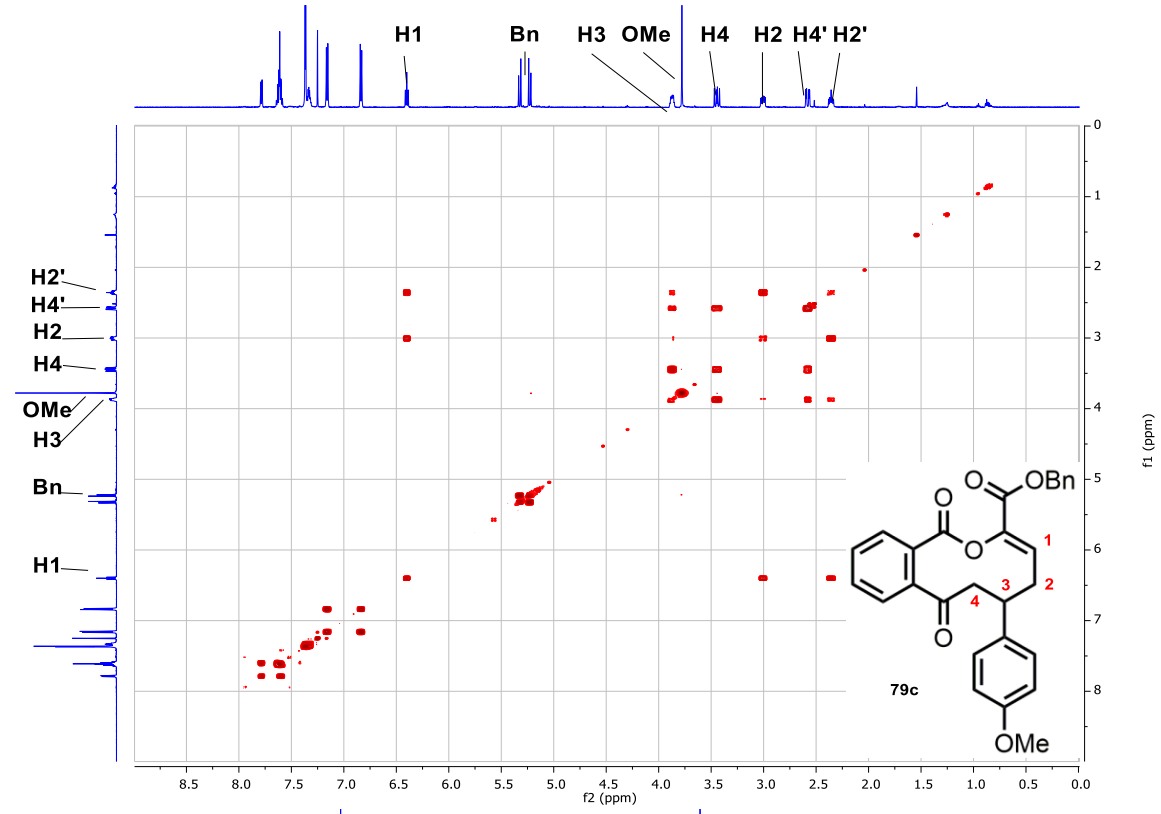
H1
Bn
H3
OMe
H4
H2
H4'
H2'
H2'
H4'
H2
H4
OMe
H3
Bn
H1
OBn
O
O
O
O
1
2
3
4
79c
OMe
f2 (ppm)
f1 (ppm)

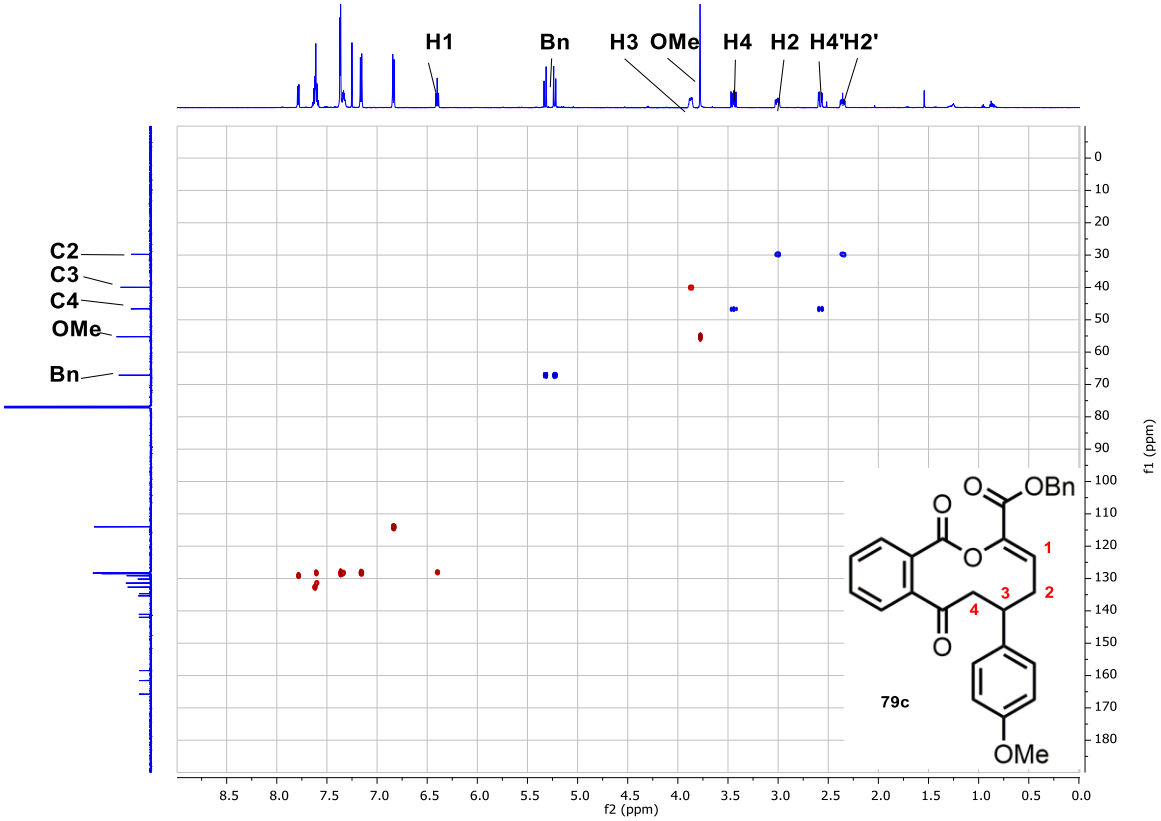
H1
Bn
H3
OMe
H4
H2
H4'
H2'
C2
C3
C4
OMe
Bn
OBn
O
O
O
O
1
2
3
4
79c
OMe
f2 (ppm)
f1 (ppm)

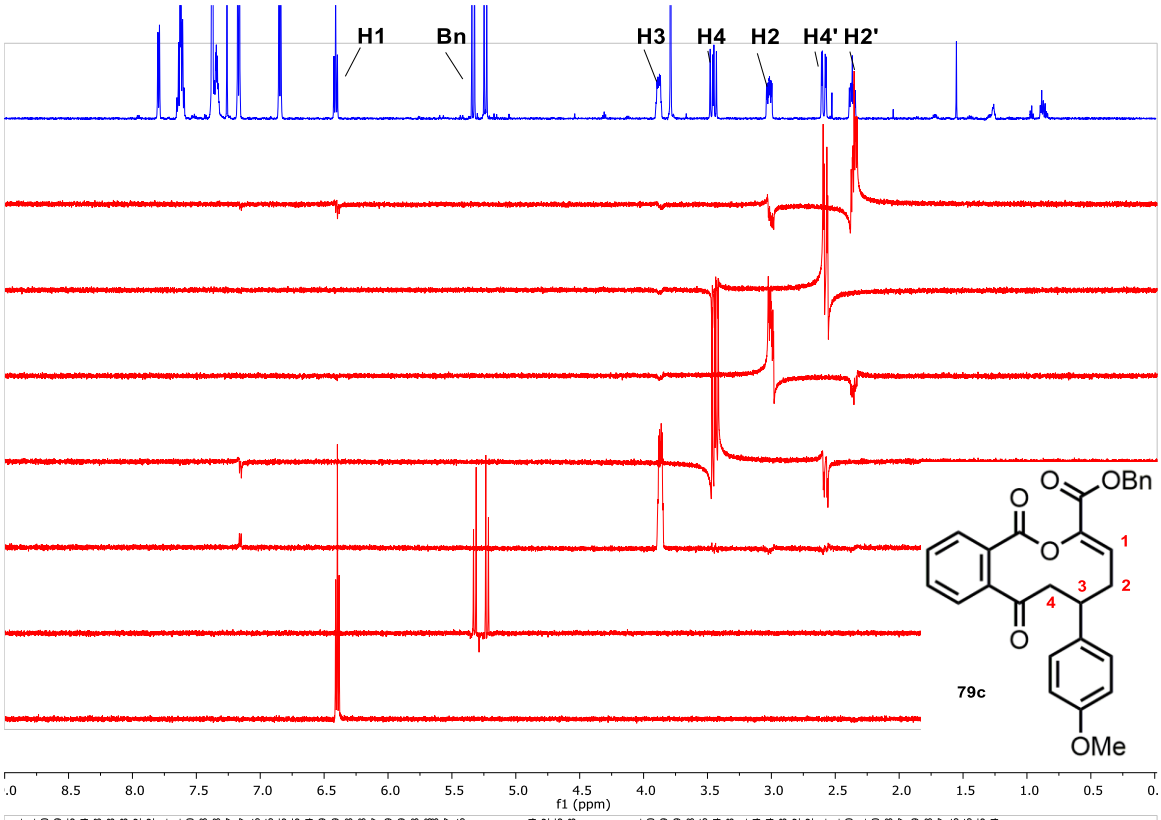
H1
Bn
H3
H4
H2
H4'
H2'
OBn
O
O
O
1
2
3
4
OMe
79c
f1 (ppm)

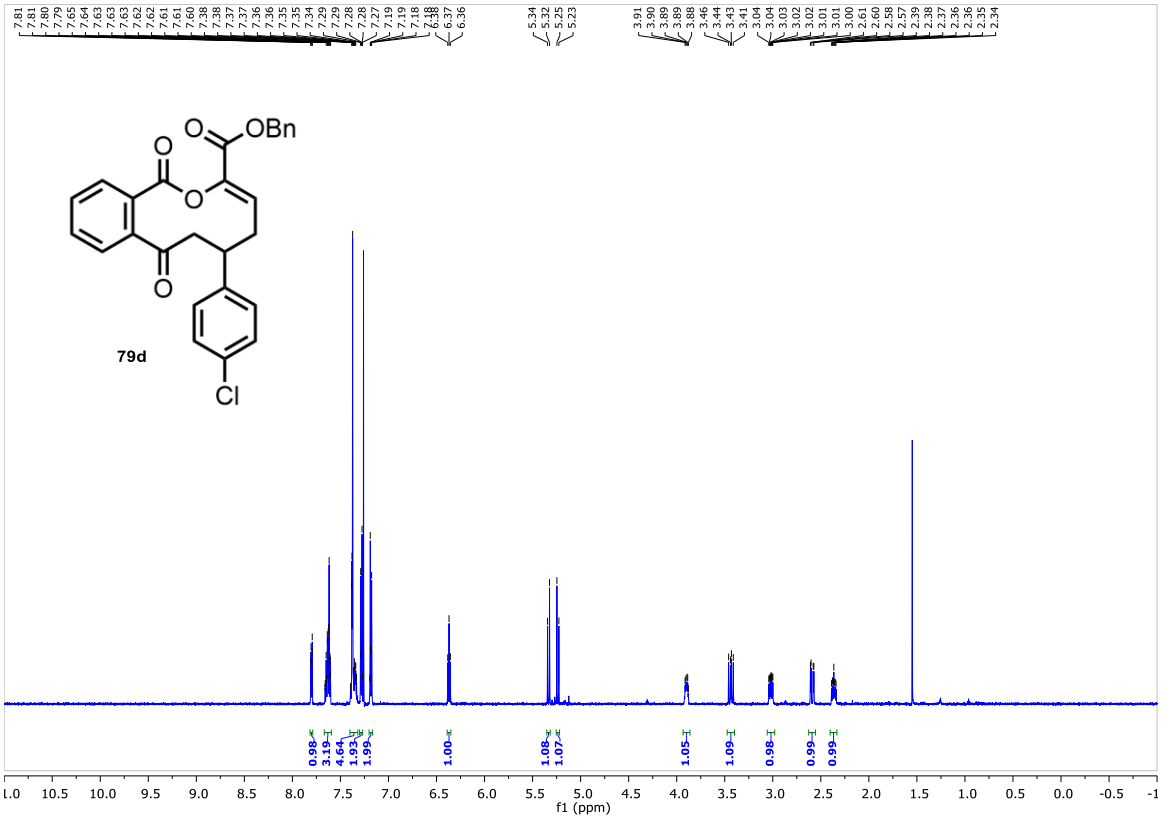
OBn
O
O
O
79d
Cl
0.98
3.19
4.64
1.93
1.99
1.00
1.08
1.07
1.05
1.09
0.98
0.99
0.99
f1 (ppm)

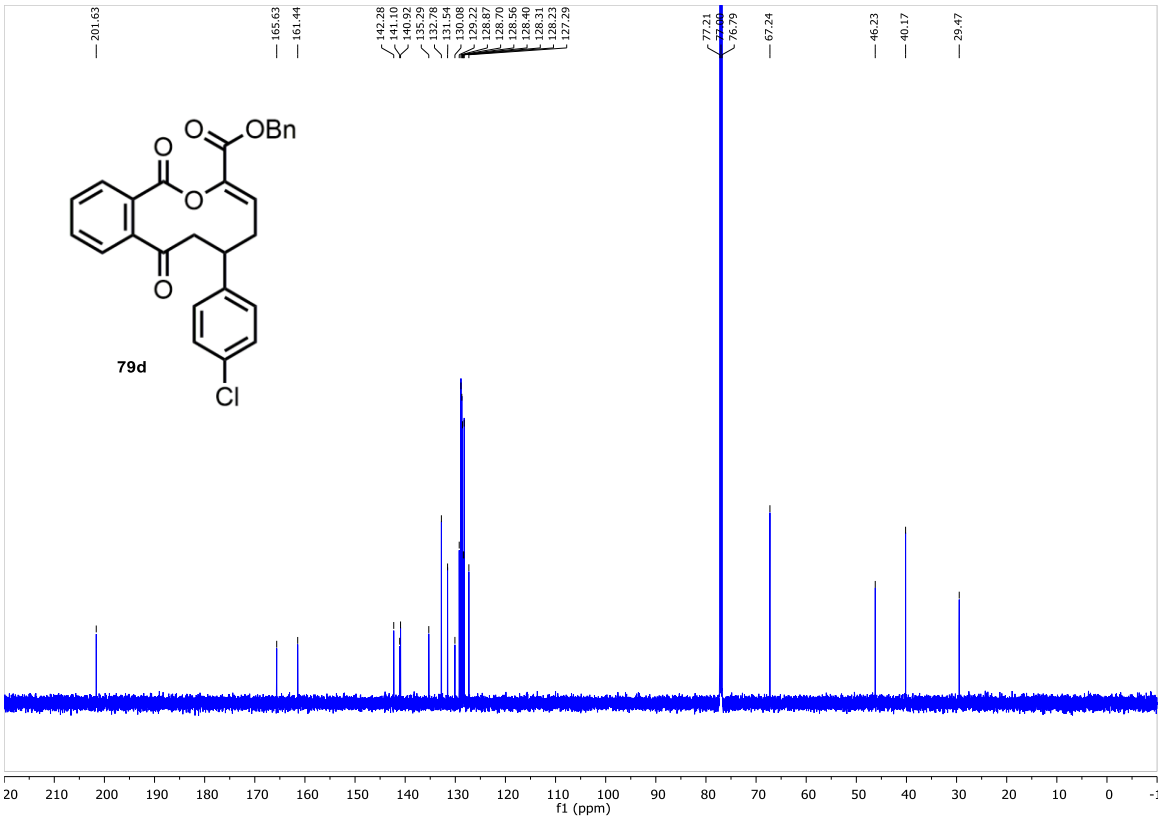
201.63
165.63
161.44
142.28
141.10
140.92
135.29
132.78
131.54
130.08
129.22
128.87
128.70
128.56
128.40
128.31
128.23
127.29
77.21
77.00
76.79
67.24
46.23
40.17
29.47
OBn
O
O
O
O
79d
Cl
f1 (ppm)

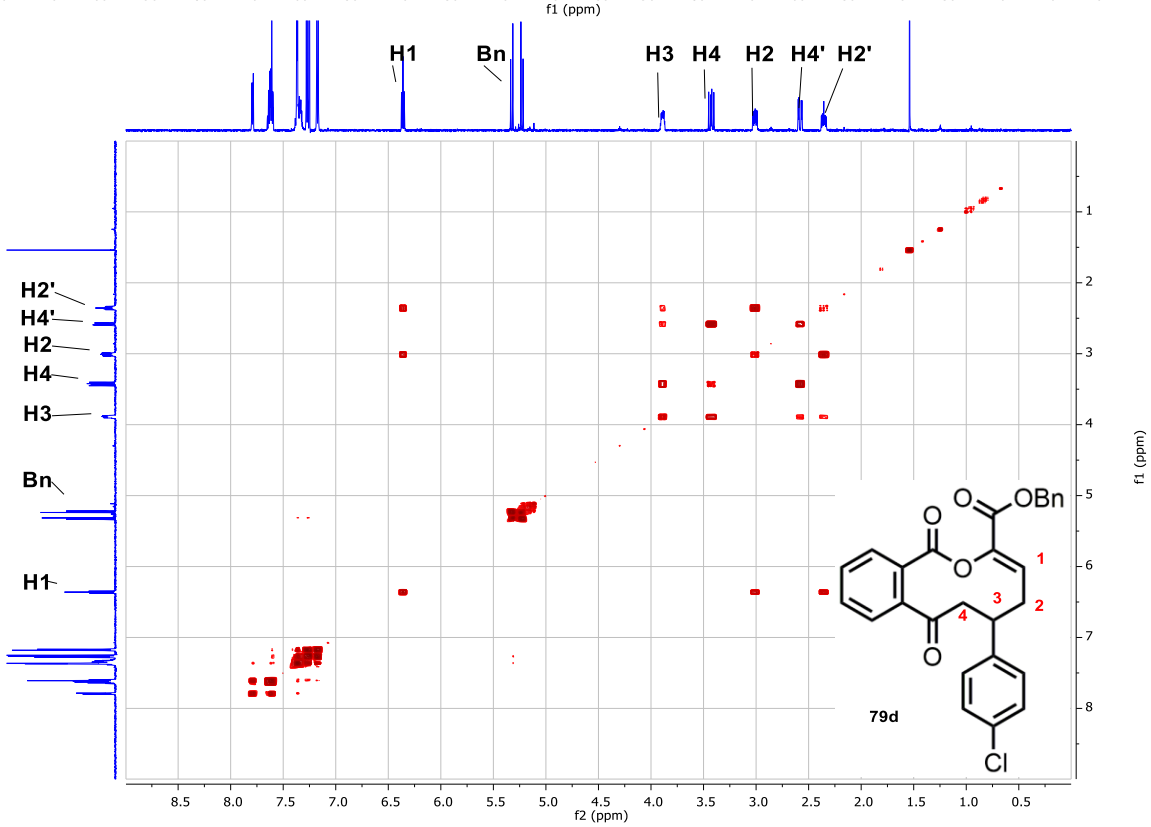
H1
Bn
H3
H4
H2
H4'
H2'
H2'
H4'
H2
H4
H3
Bn
H1
OBn
O
O
O
O
1
2
3
4
79d
Cl
f2 (ppm)
f1 (ppm)

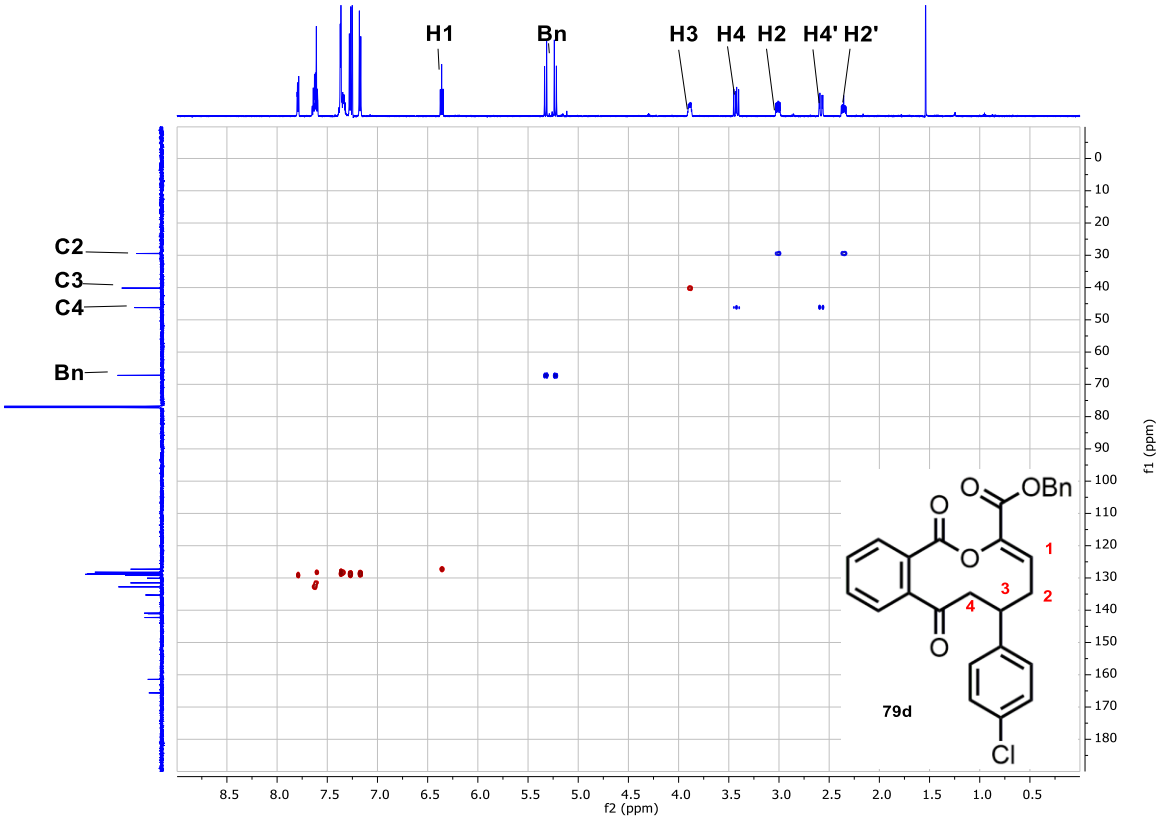
H1
Bn
H3
H4
H2
H4'
H2'
C2
C3
C4
Bn
f2 (ppm)
f1 (ppm)
OBn
79d
Cl

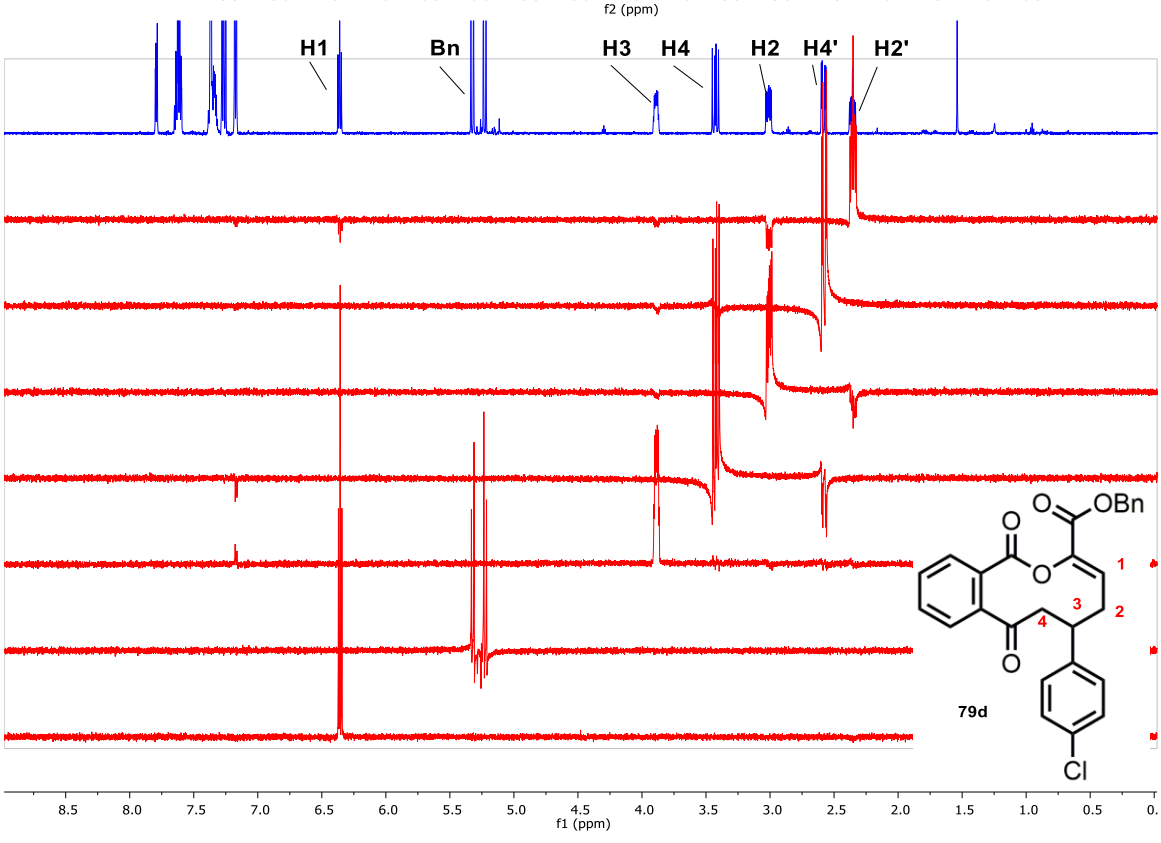
H1
Bn
H3
H4
H2
H4'
H2'
f1 (ppm)
OBn
79d
Cl

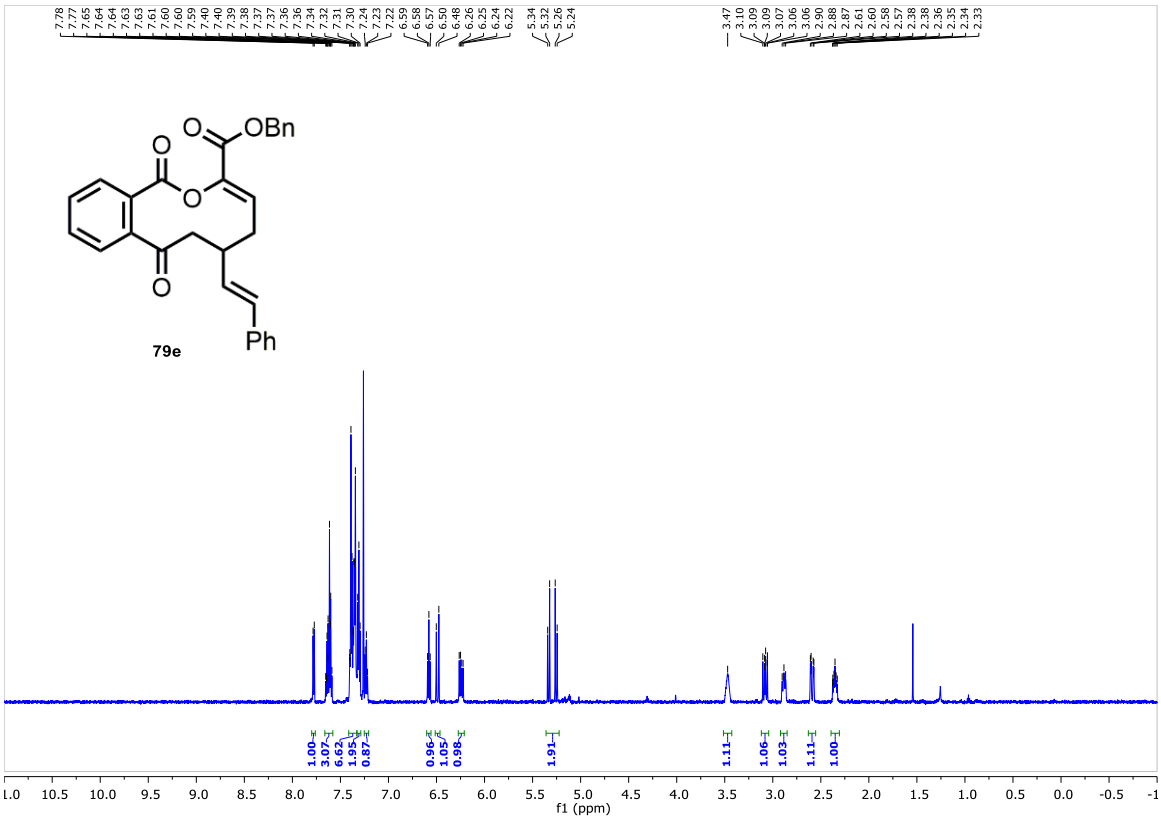
OBn
O
O
O
Ph
79e
f1 (ppm)

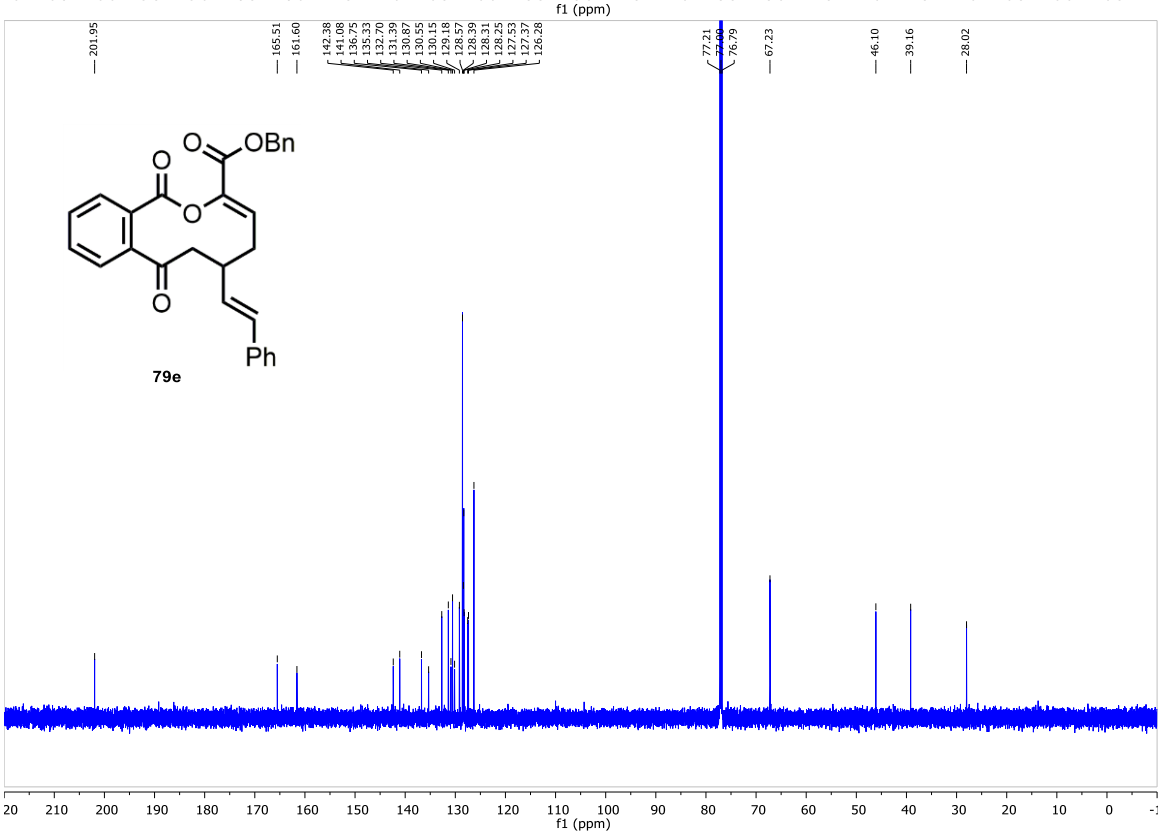
OBn
O
O
O
Ph
79e
f1 (ppm)

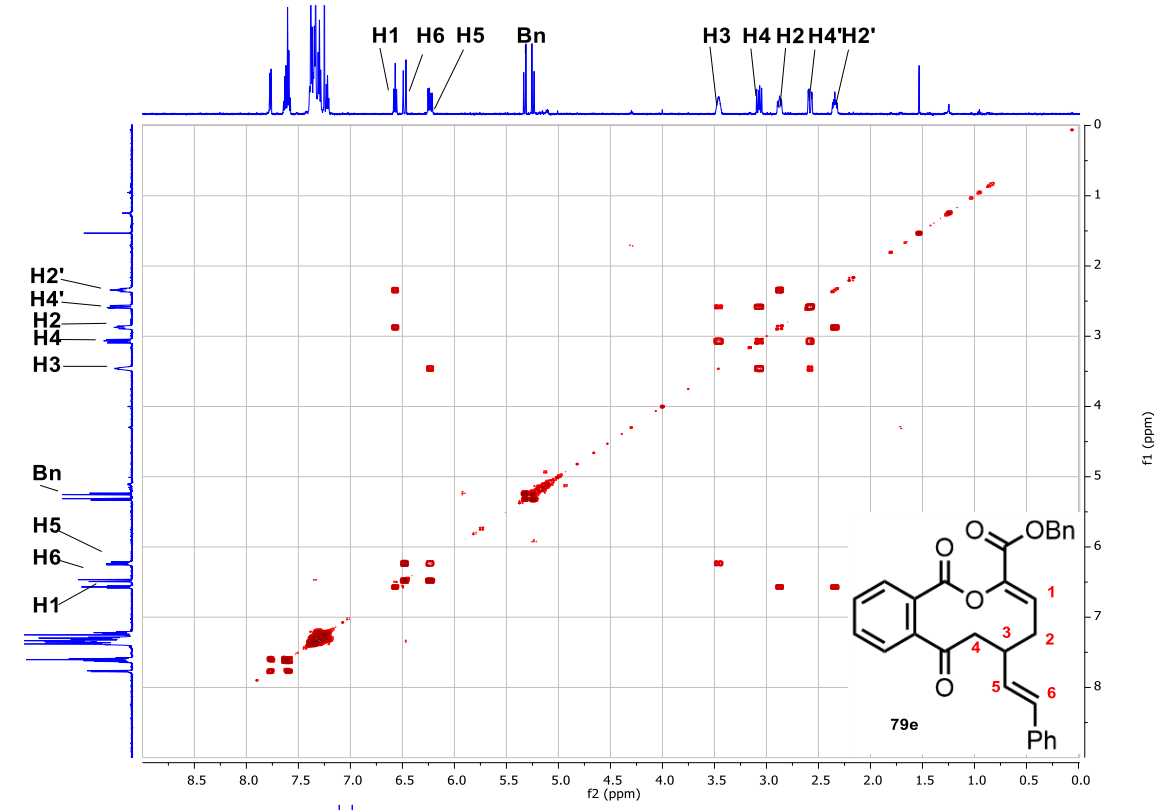
H1
H6
H5
Bn
H3
H4
H2
H4'
H2'
H2'
H4'
H2
H4
H3
Bn
H5
H6
H1
f2 (ppm)
f1 (ppm)
OBn
Ph
79e

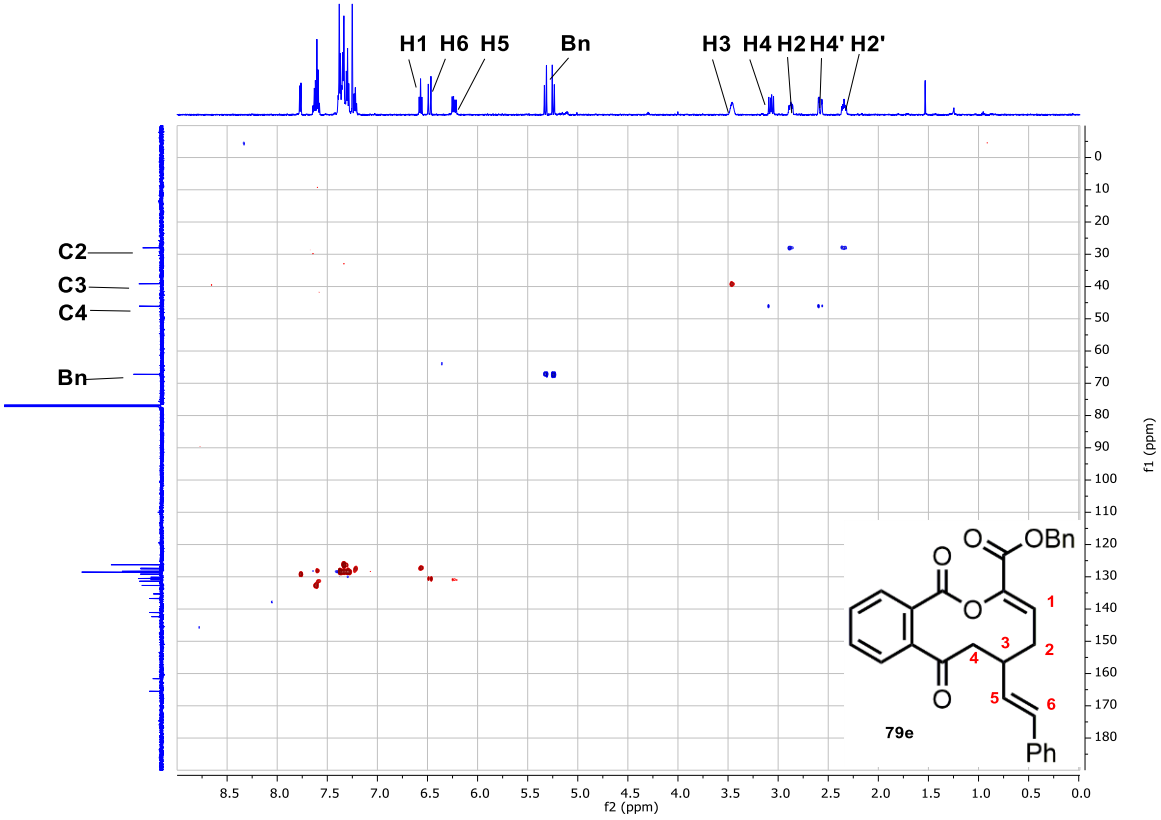
H1
H6
H5
Bn
H3
H4
H2
H4'
H2'
C2
C3
C4
Bn
f2 (ppm)
f1 (ppm)
OBn
Ph
79e

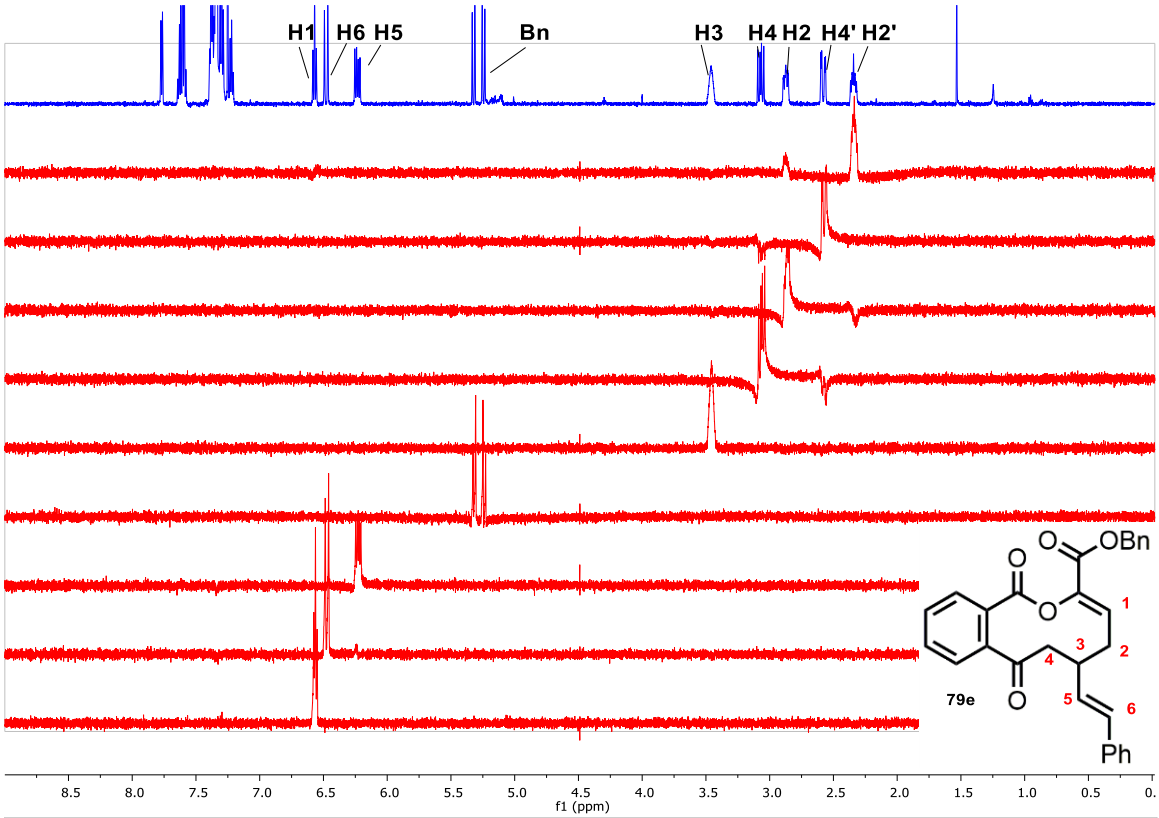
H1
H6
H5
Bn
H3
H4
H2
H4'
H2'
OBn
1
2
3
4
5
6
Ph
79e
f1 (ppm)

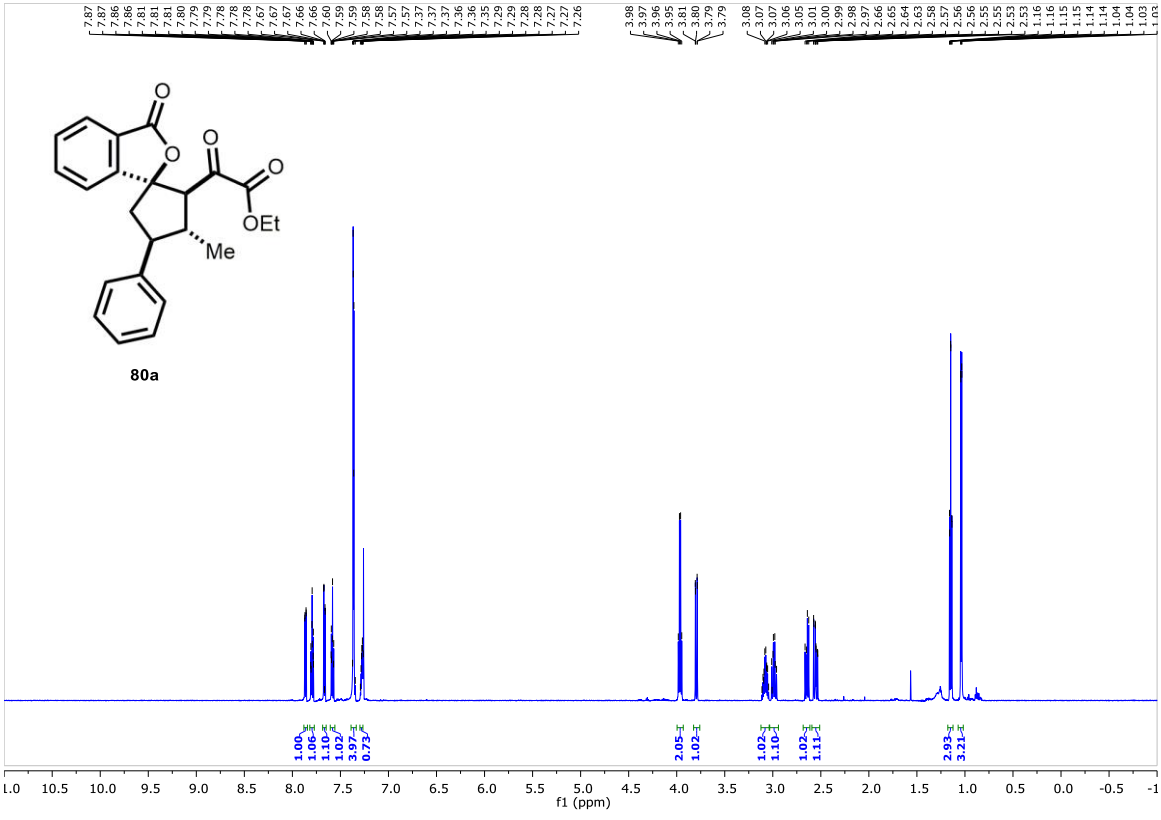
OEt
Me
80a
f1 (ppm)

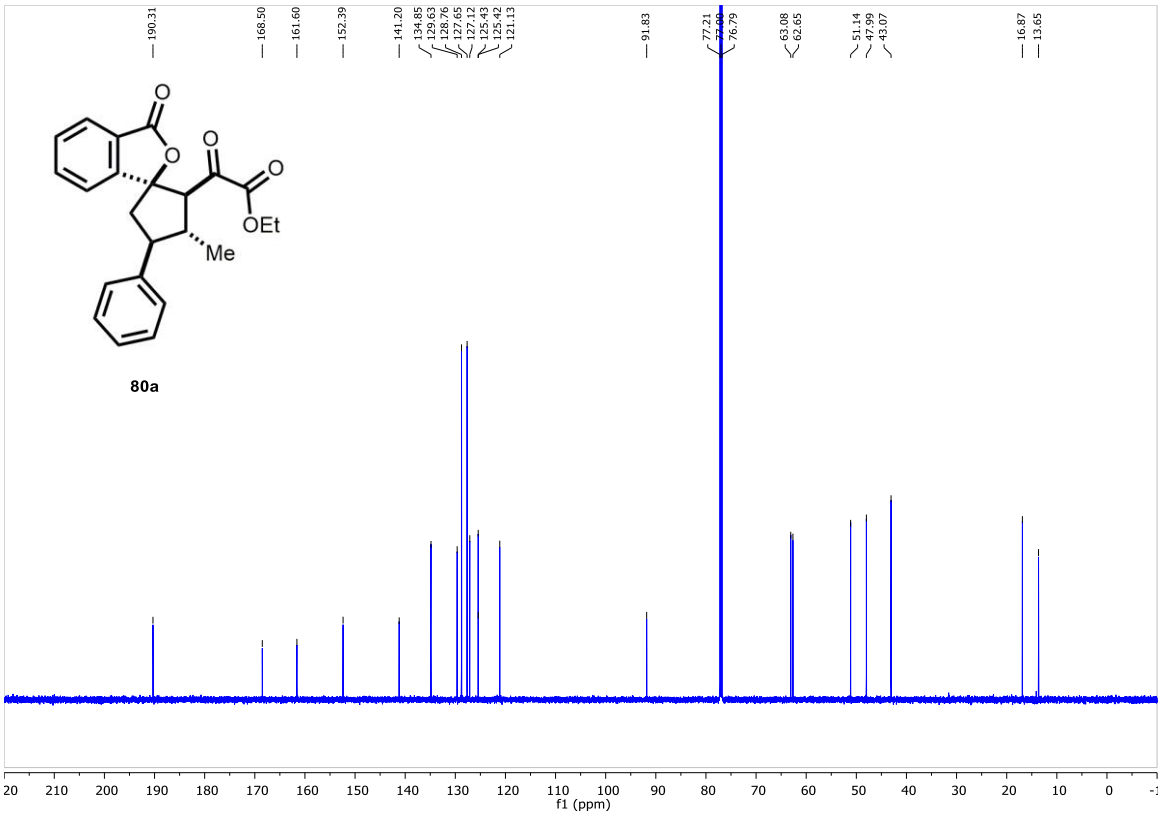
190.31
168.50
161.60
152.39
141.20
134.85
129.63
128.76
127.65
127.12
125.43
125.42
121.13
91.83
77.21
77.00
76.79
63.08
62.65
51.14
47.99
43.07
16.87
13.65
O
O
O
O
OEt
Me
80a
f1 (ppm)

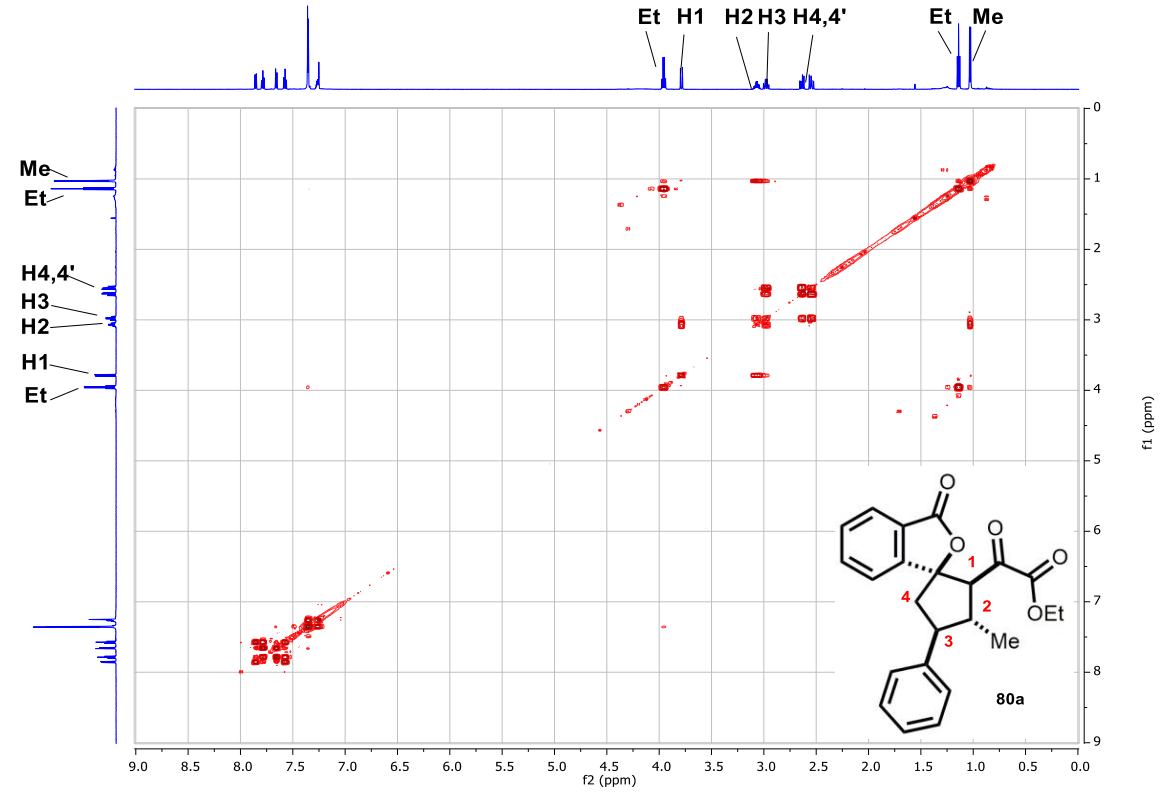
Et
H1
H2
H3
H4,4'
Et
Me
Me
Et
H4,4'
H3
H2
H1
Et
O
O
O
O
OEt
Me
1
2
3
4
80a
f2 (ppm)
f1 (ppm)

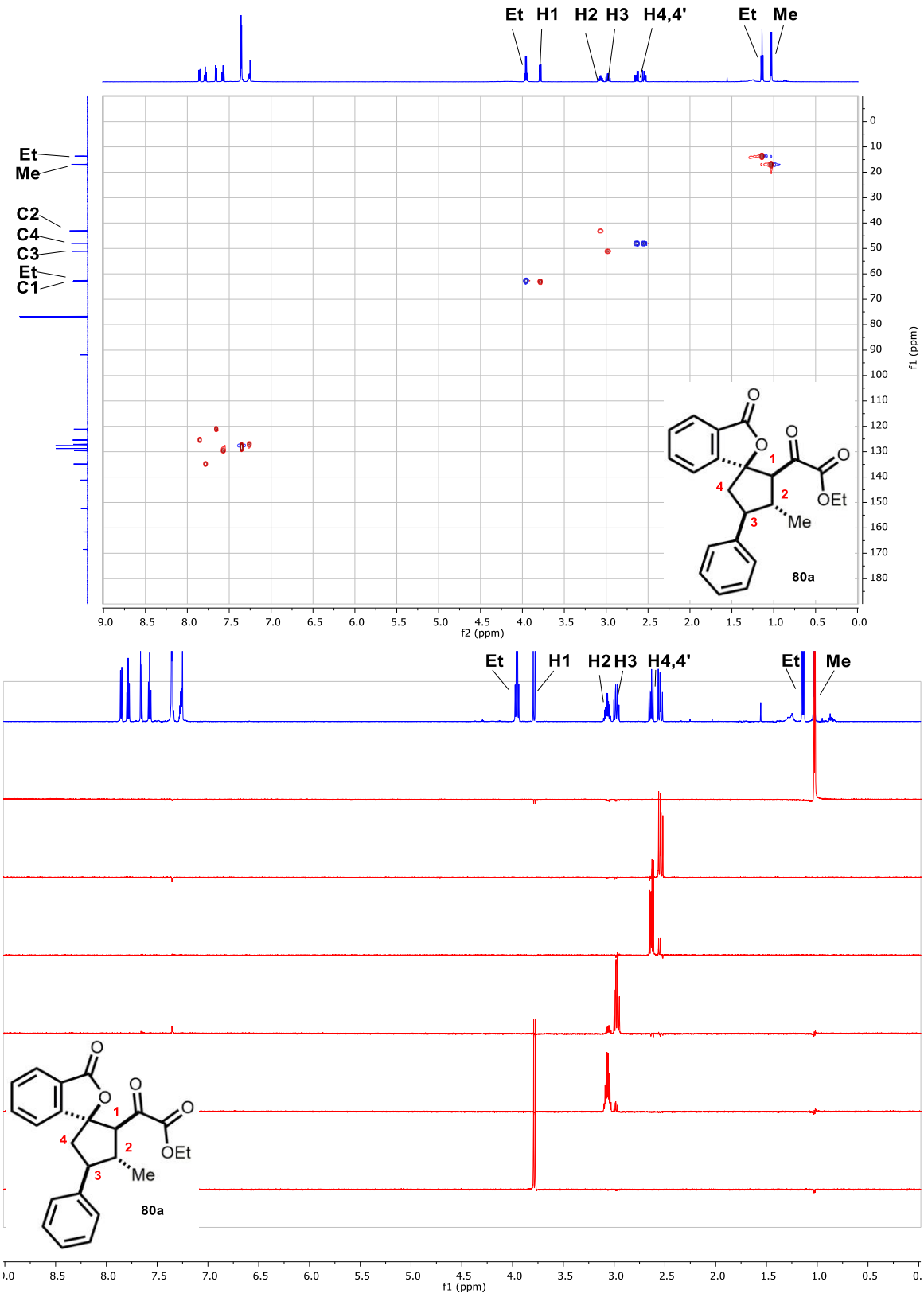
Et H1 H2 H3 H4,4' Et Me
Et
Me
C2
C4
C3
Et
C1
f2 (ppm)
f1 (ppm)
80a
Et H1 H2 H3 H4,4' Et Me
80a
f1 (ppm)

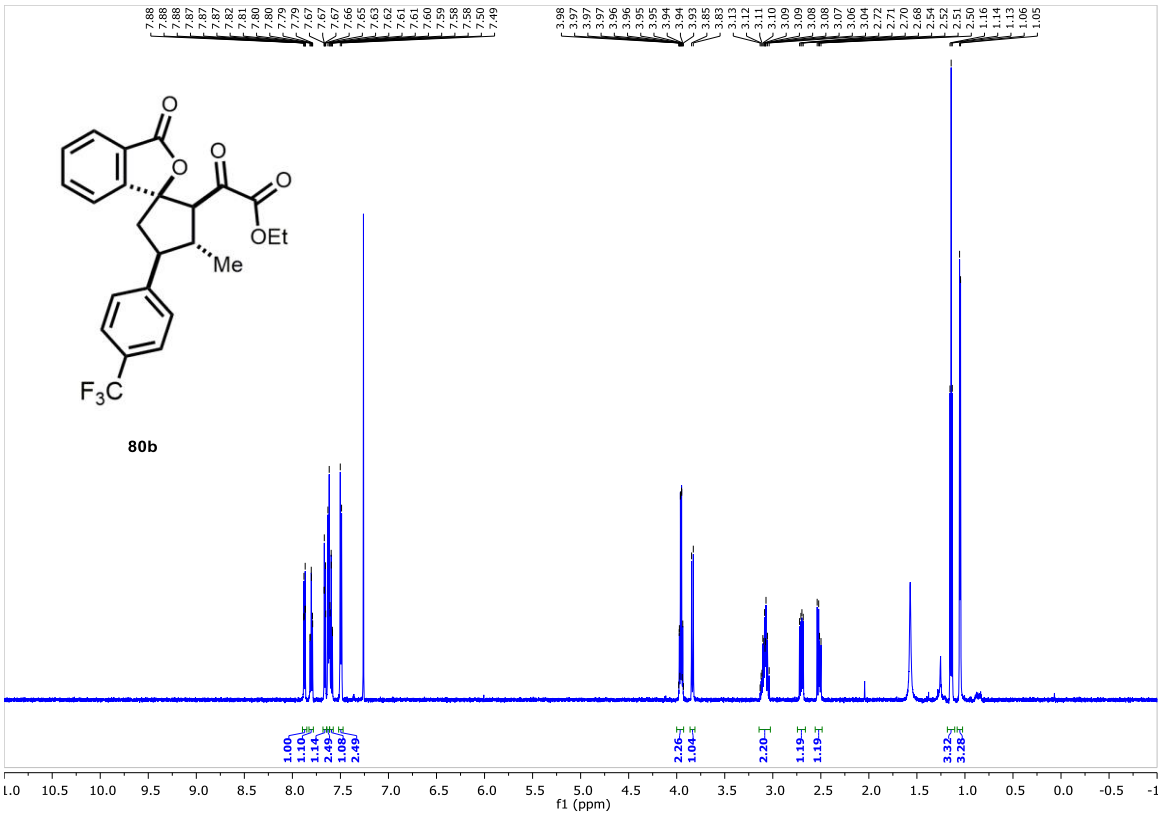
80b
f1 (ppm)

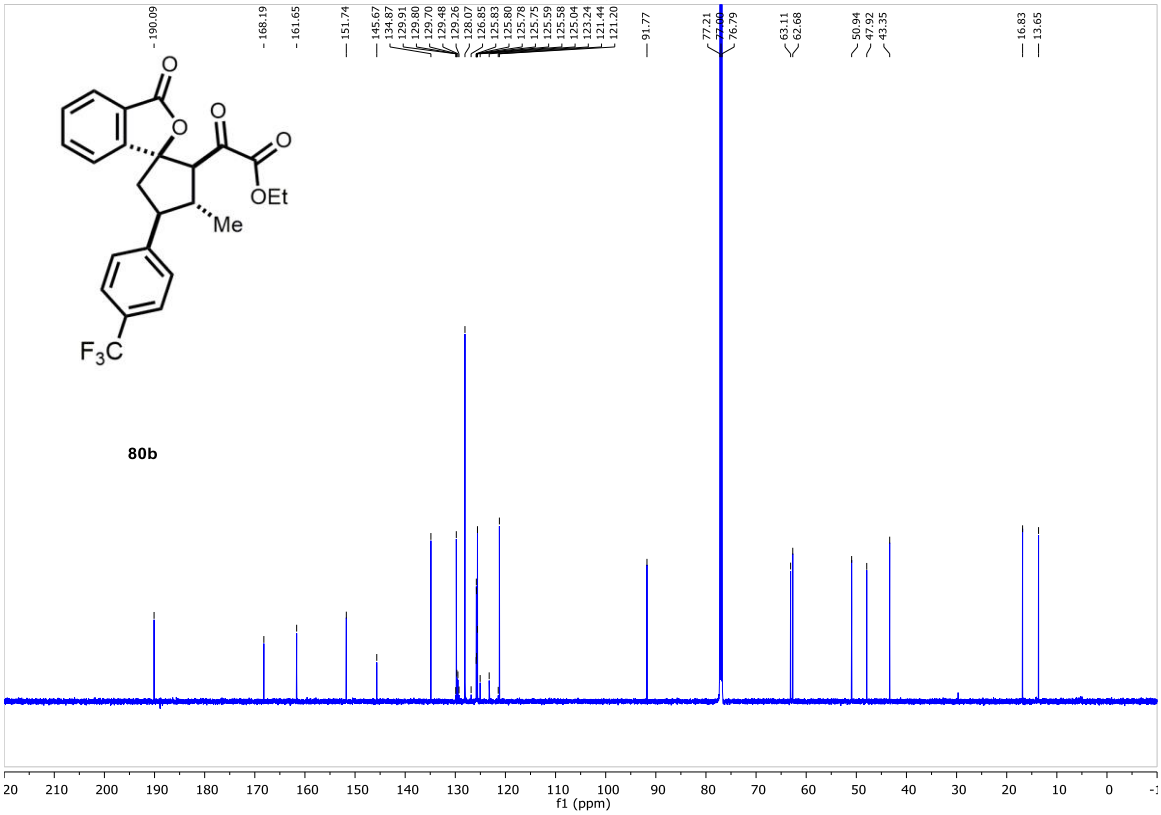
80b
f1 (ppm)

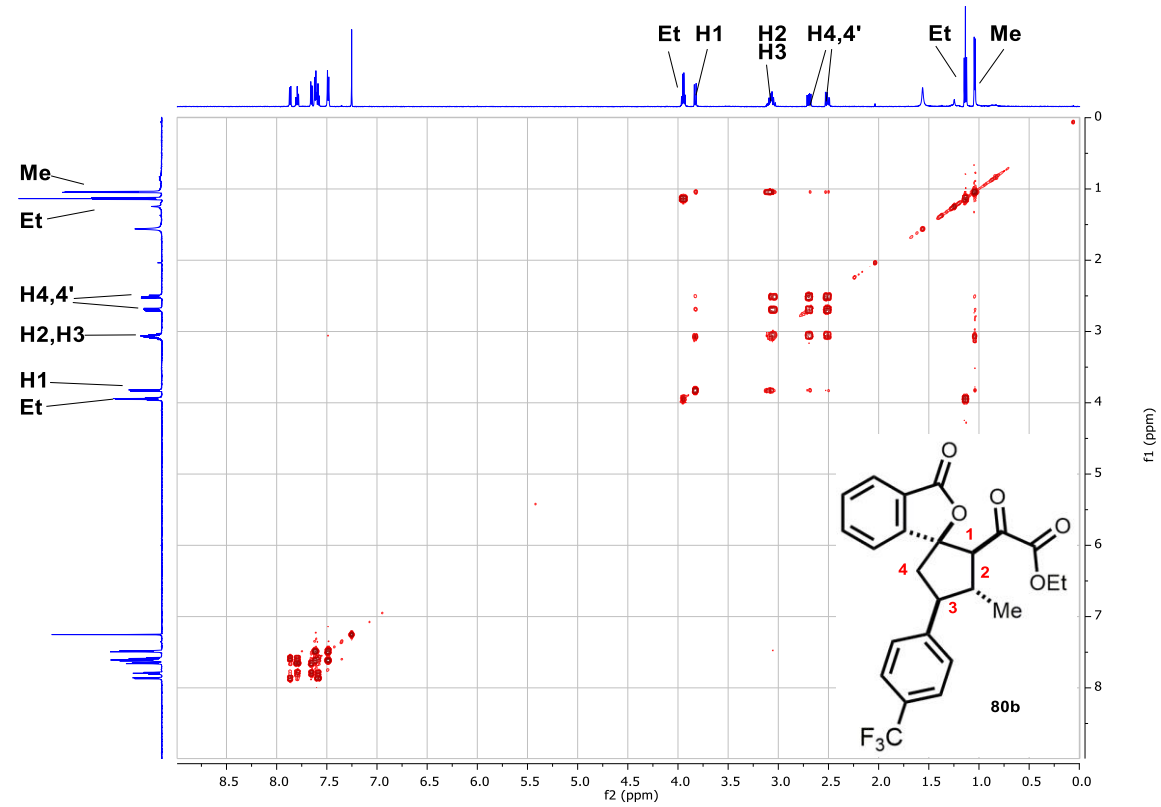
Et
H1
H2
H3
H4,4'
Et
Me
Me
Et
H4,4'
H2,H3
H1
Et
f1 (ppm)
f2 (ppm)
O
O
O
O
1
2
3
4
OEt
Me
F3C
80b

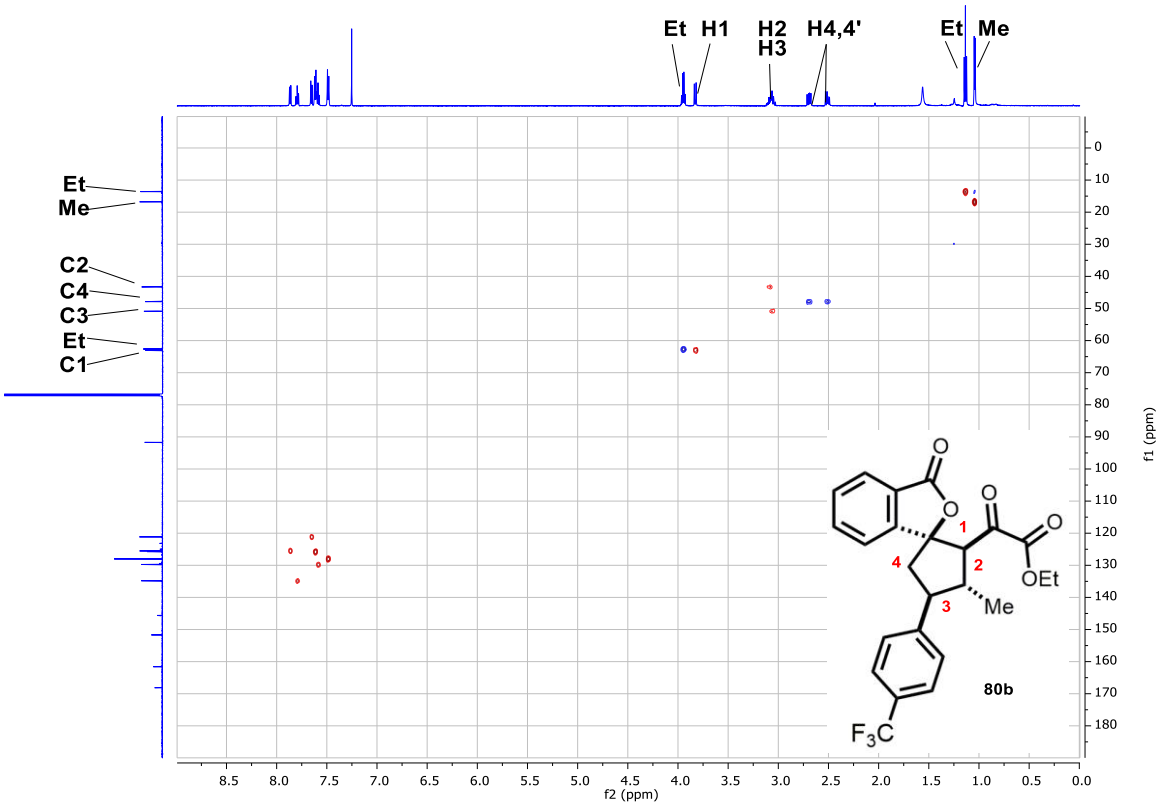
Et
H1
H2
H3
H4,4'
Et
Me
Et
Me
C2
C4
C3
Et
C1
f1 (ppm)
f2 (ppm)
O
O
O
O
1
2
3
4
OEt
Me
F3C
80b

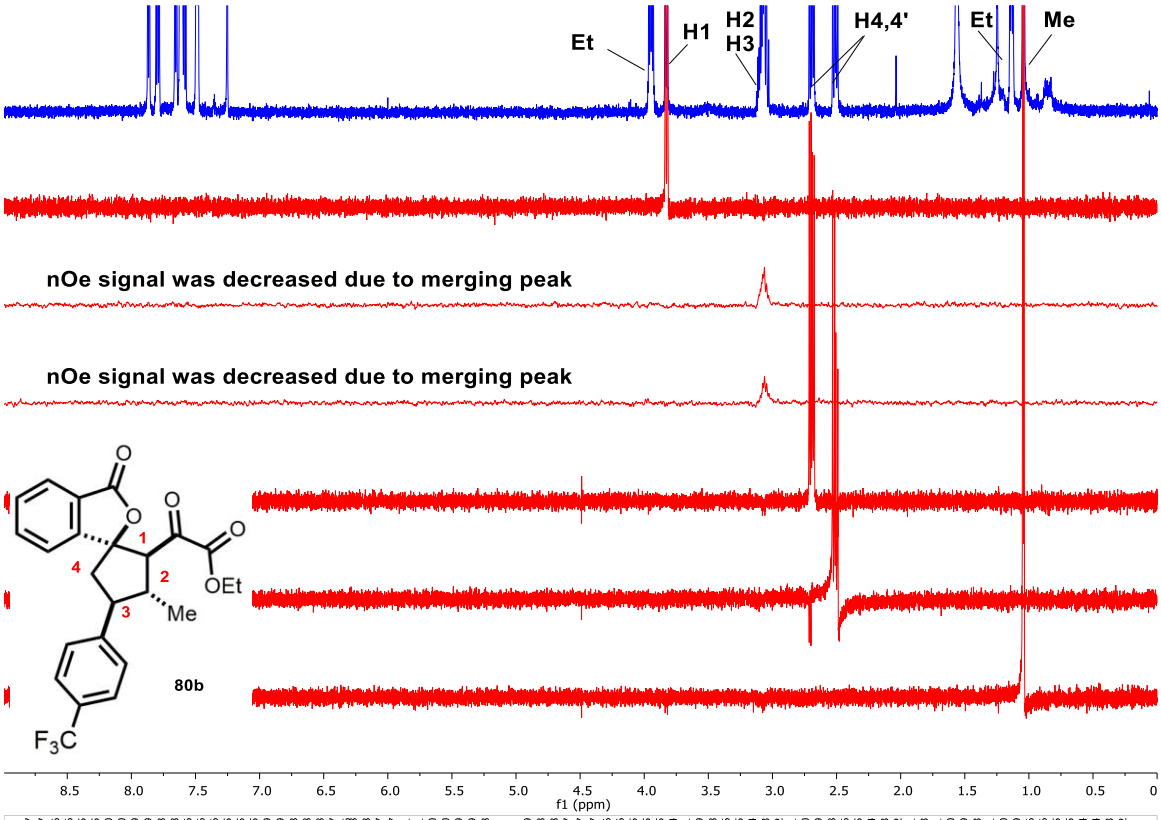
Et
H1
H2
H3
H4,4'
Et
Me
nOe signal was decreased due to merging peak
nOe signal was decreased due to merging peak
O
O
O
O
1
2
3
4
OEt
Me
F3C
80b
8.5
8.0
7.5
7.0
6.5
6.0
5.5
5.0
4.5
4.0
3.5
3.0
2.5
2.0
1.5
1.0
0.5
0
f1 (ppm)

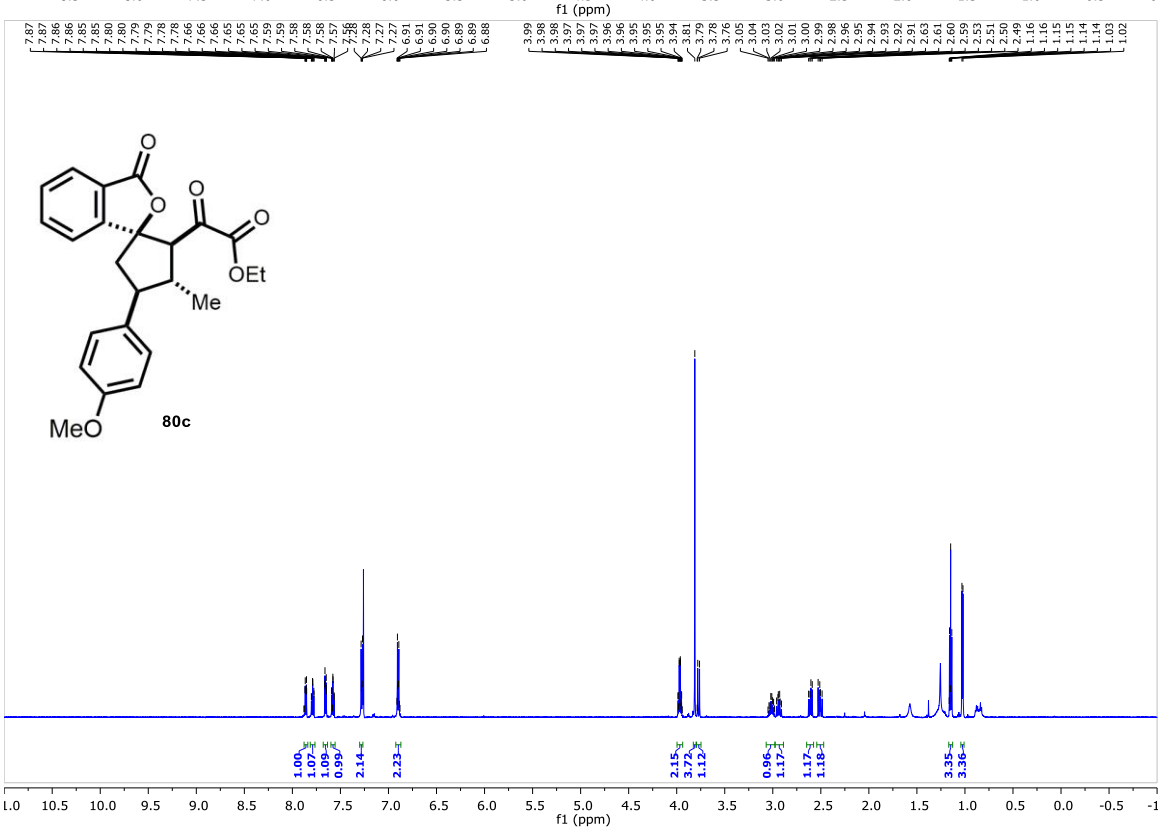
O
O
O
O
OEt
Me
MeO
80c
1.00
1.07
1.09
0.99
2.14
2.23
2.15
3.77
1.12
0.96
1.17
1.18
3.35
3.36
f1 (ppm)

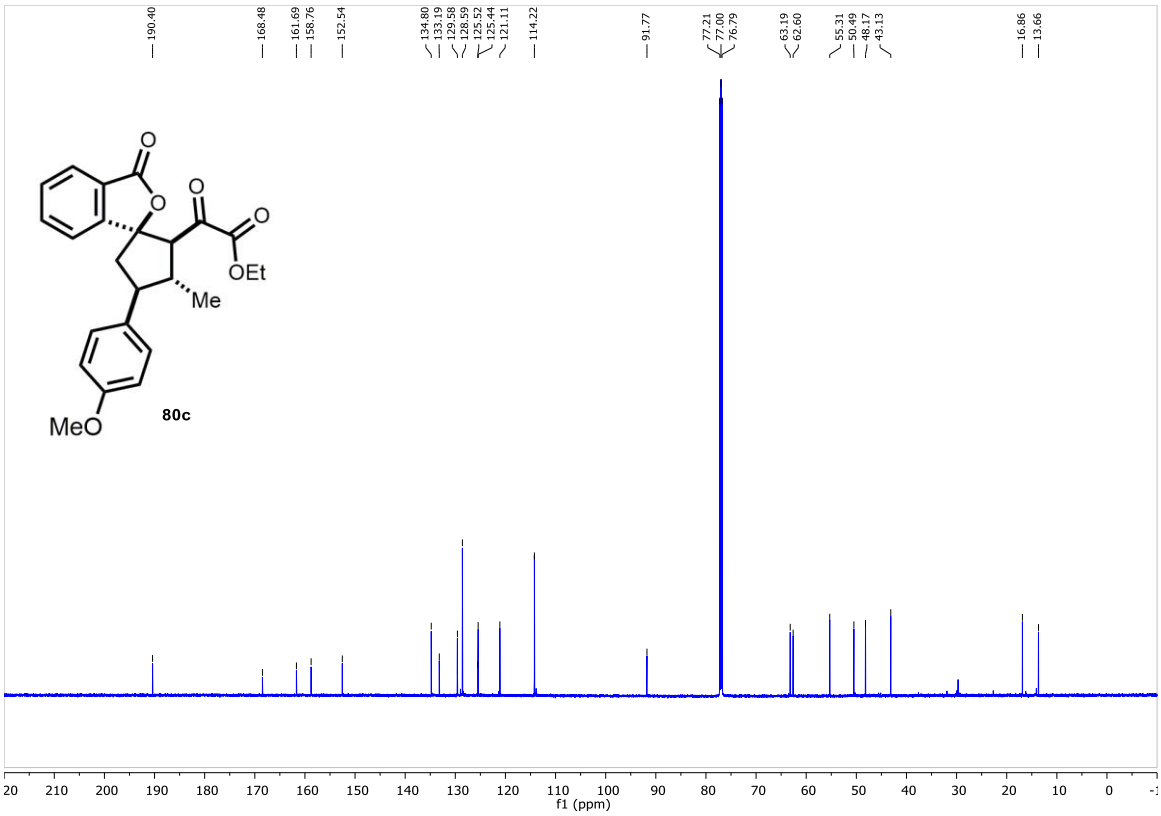
190.40
168.48
161.69
158.76
152.54
134.80
133.19
129.58
128.59
125.52
125.44
121.11
114.22
91.77
77.21
77.00
76.79
63.19
62.60
55.31
50.49
48.17
43.13
16.86
13.66
OEt
Me
MeO
80c
f1 (ppm)

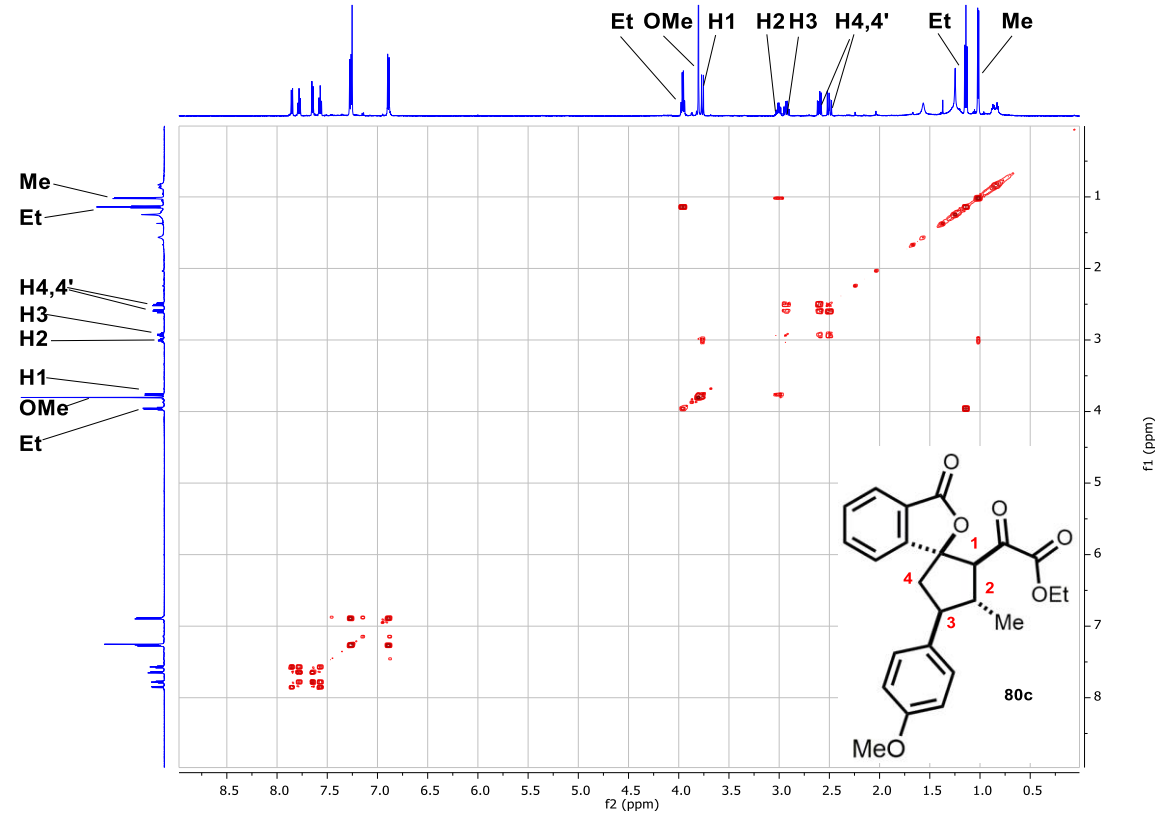
Et
OMe
H1
H2
H3
H4,4'
Et
Me
Me
Et
H4,4'
H3
H2
H1
OMe
Et
OEt
Me
MeO
80c
f2 (ppm)
f1 (ppm)

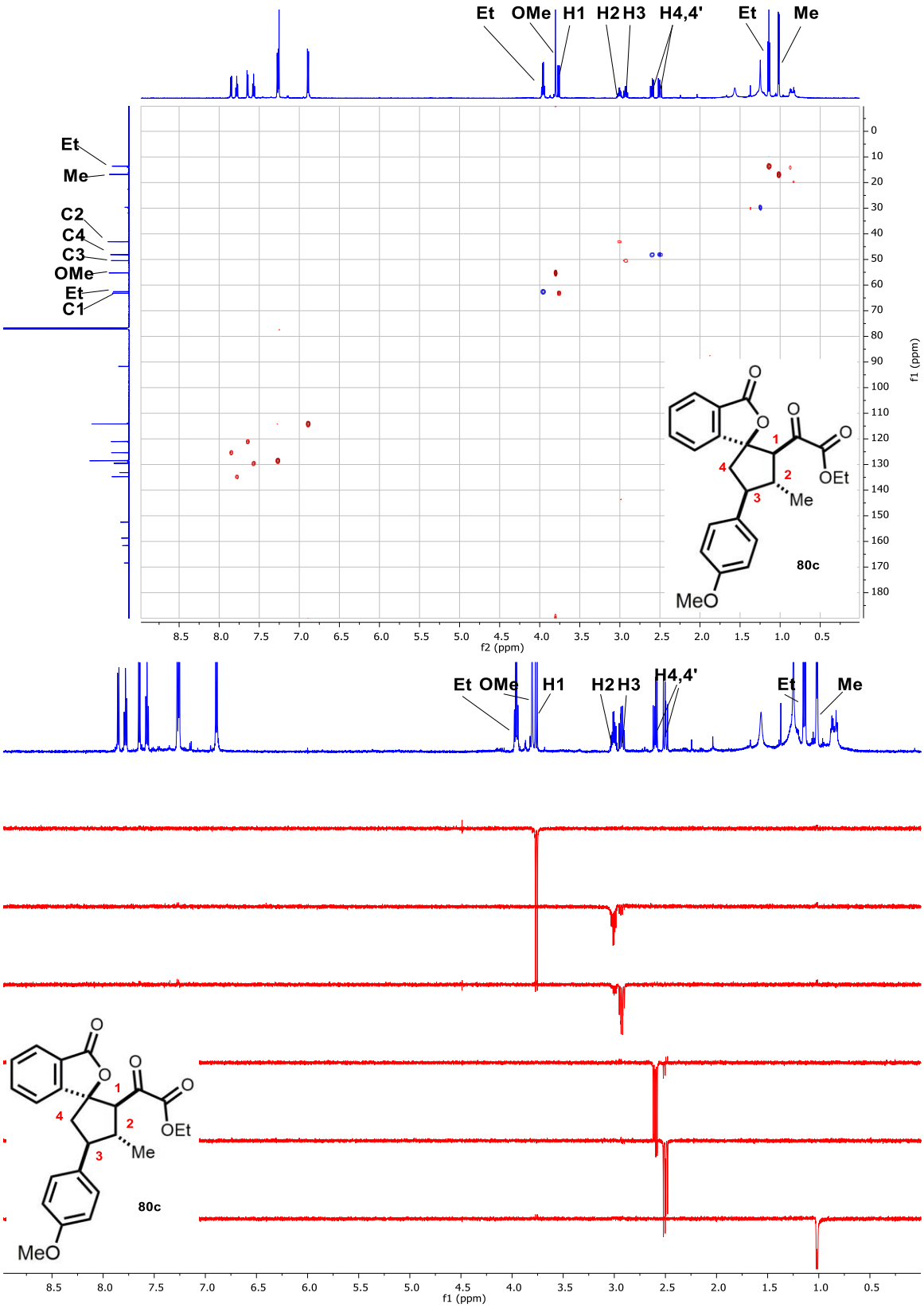
Et
OMe
H1
H2 H3
H4,4'
Et
Me
C2
C4
C3
OMe
Et
C1
f2 (ppm)
f1 (ppm)
80c
MeO
OEt
Me

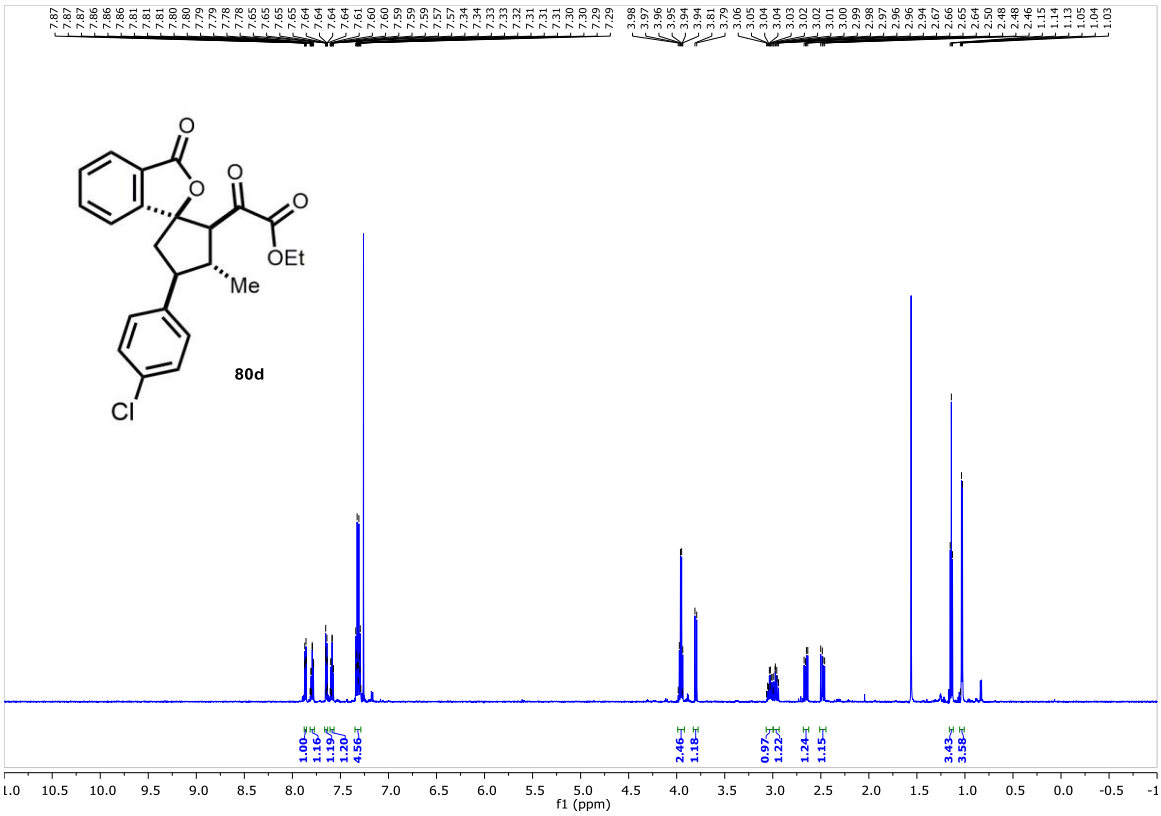

Massaro_N_2018_177pure_CARBON_01 — Massaro_N_2018_177pure —

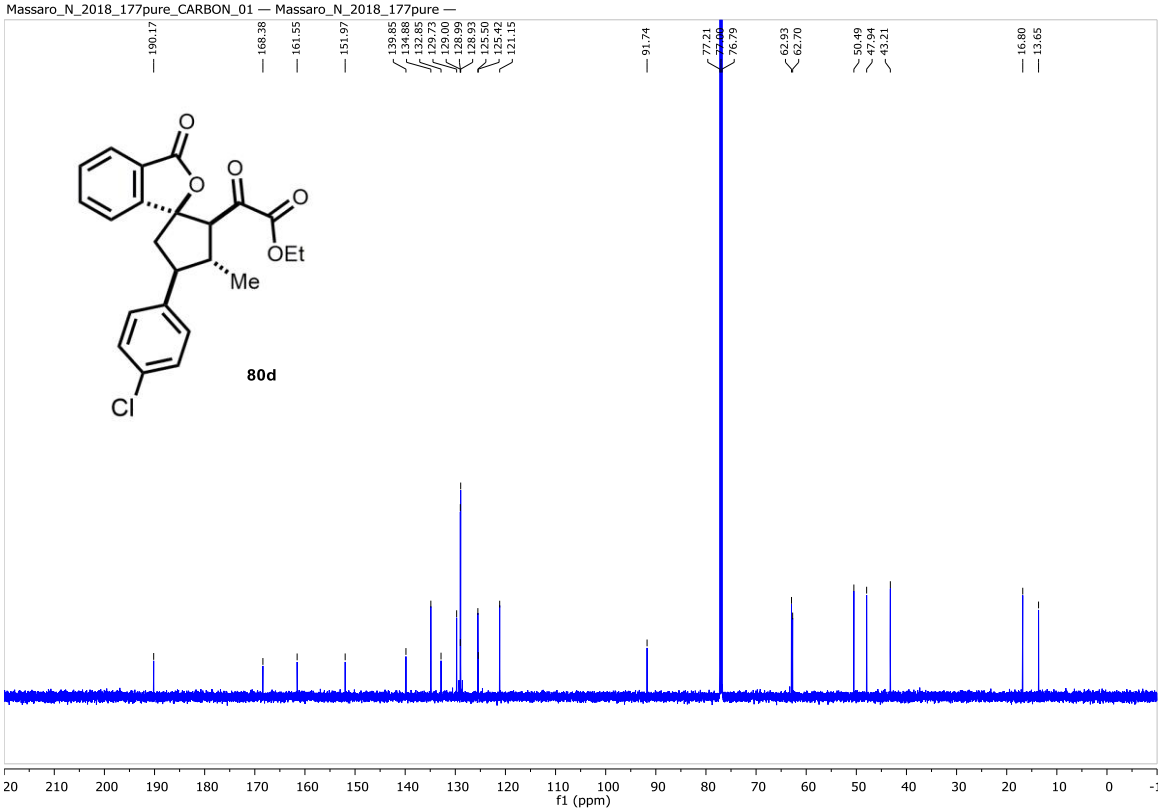

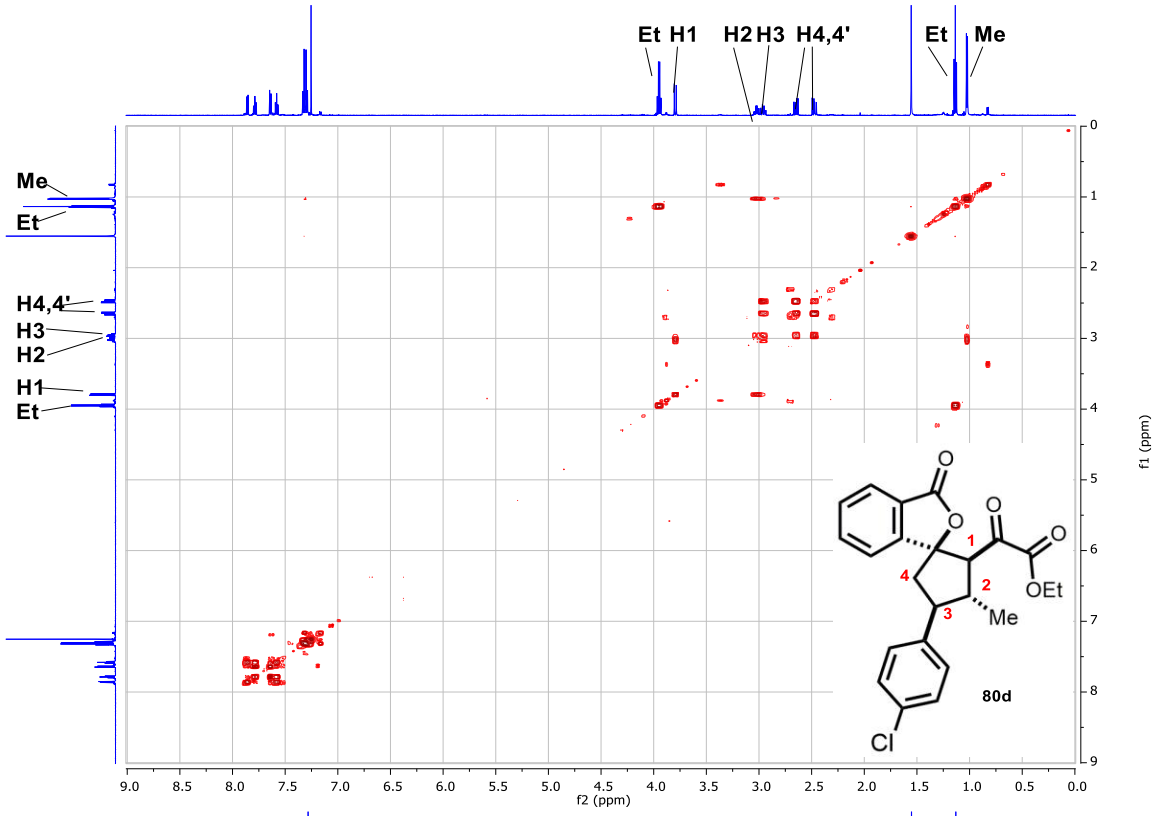
Et H1
H2 H3
H4,4'
Et
Me
Me
Et
H4,4'
H3
H2
H1
Et
O
O
O
O
1
2
3
4
OEt
Me
Cl
80d
f2 (ppm)
f1 (ppm)

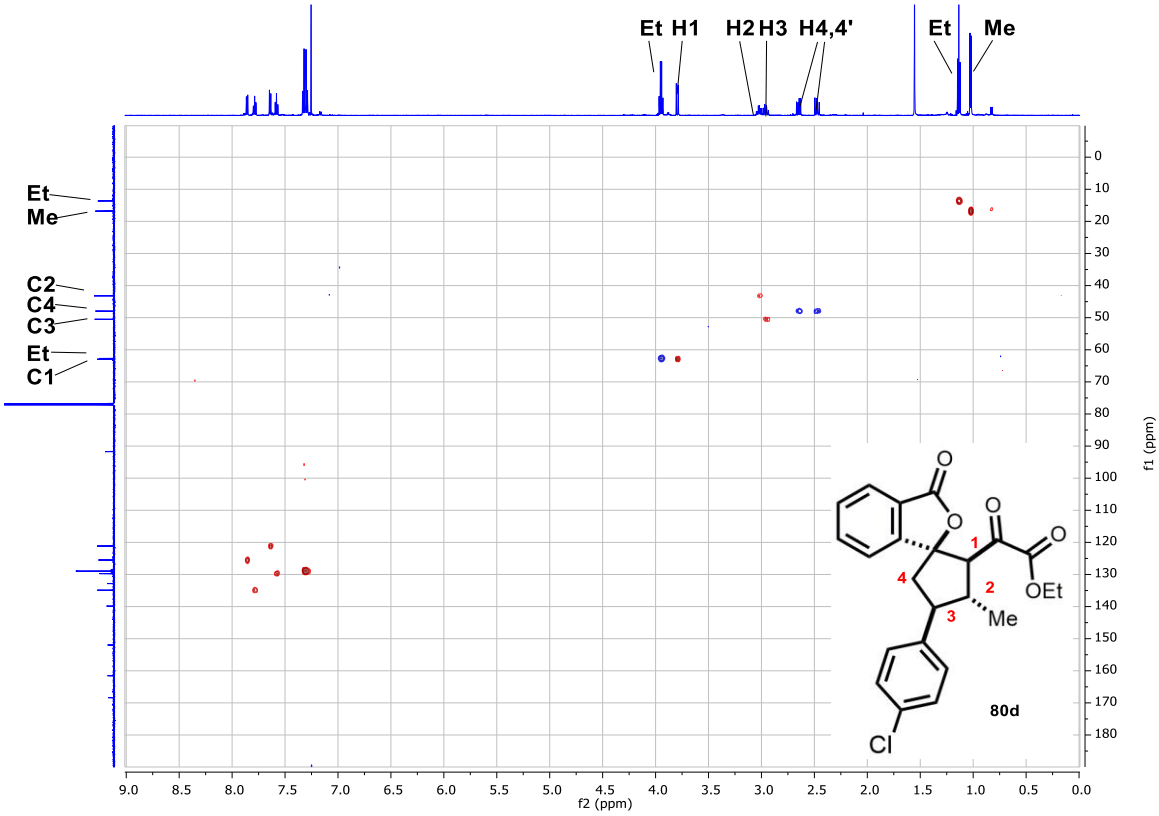
Et H1
H2 H3
H4,4'
Et
Me
Et
Me
C2
C4
C3
Et
C1
O
O
O
O
1
2
3
4
OEt
Me
Cl
80d
f2 (ppm)
f1 (ppm)

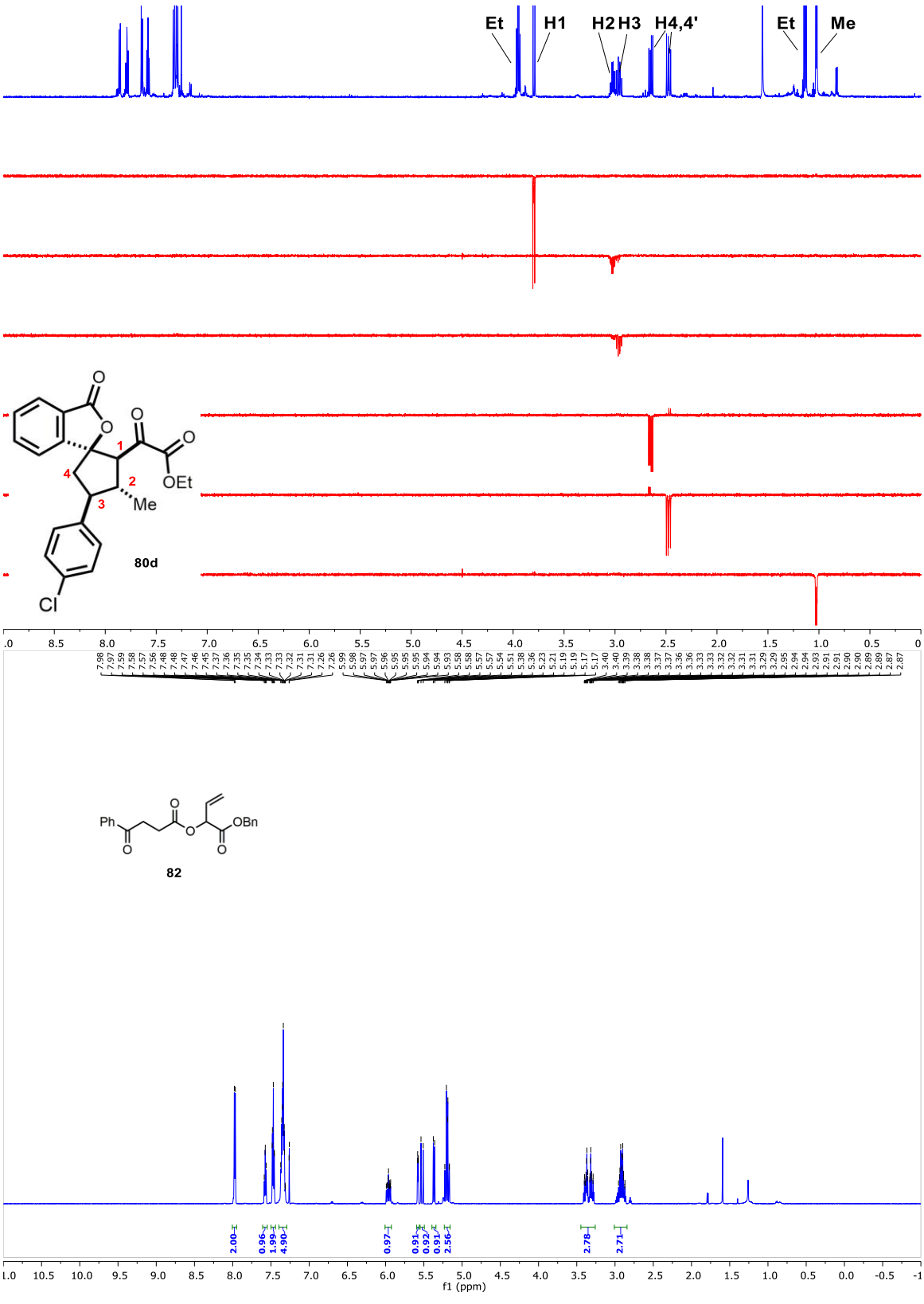
Et
H1
H2 H3
H4,4'
Et
Me
80d
82
Ph
OBn
f1 (ppm)

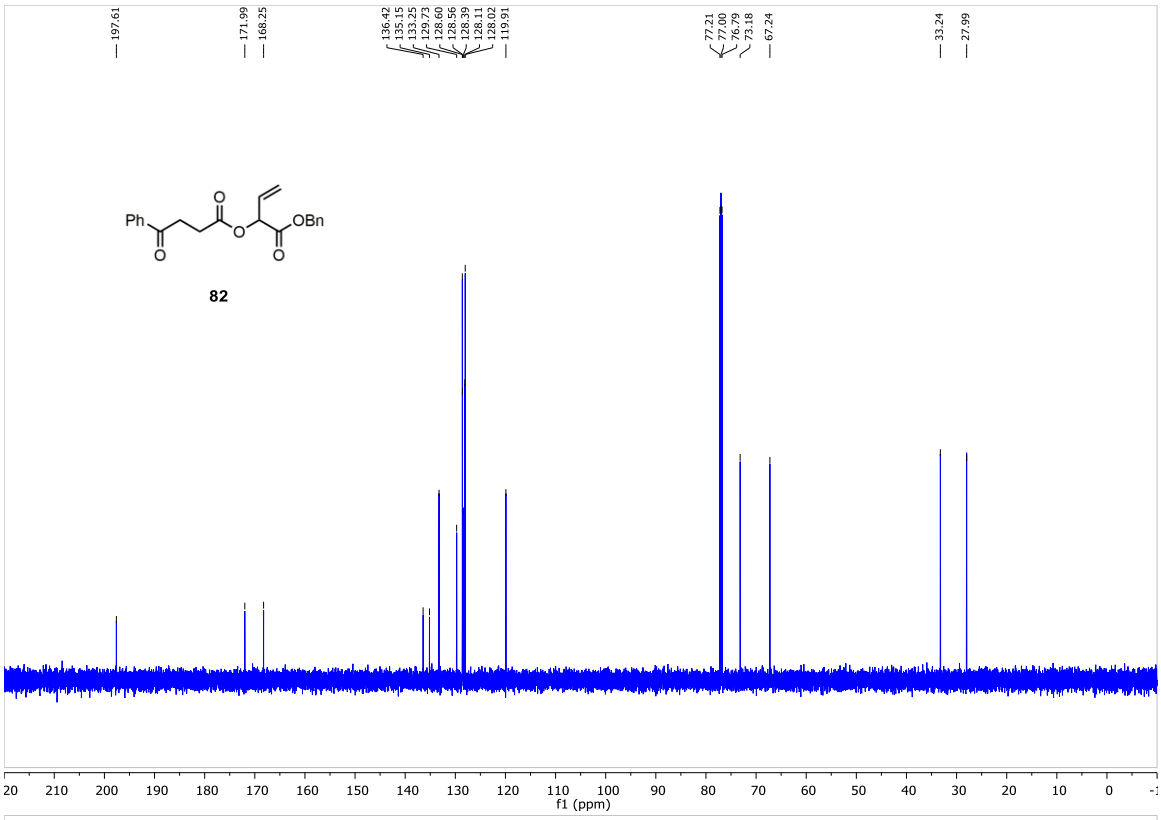
197.61
171.99
168.25
136.42
135.15
133.25
129.73
128.60
128.56
128.39
128.11
119.02
119.91
77.21
77.00
76.79
73.18
67.24
33.24
27.99
Ph
O
O
O
O
OBn
82
f1 (ppm)

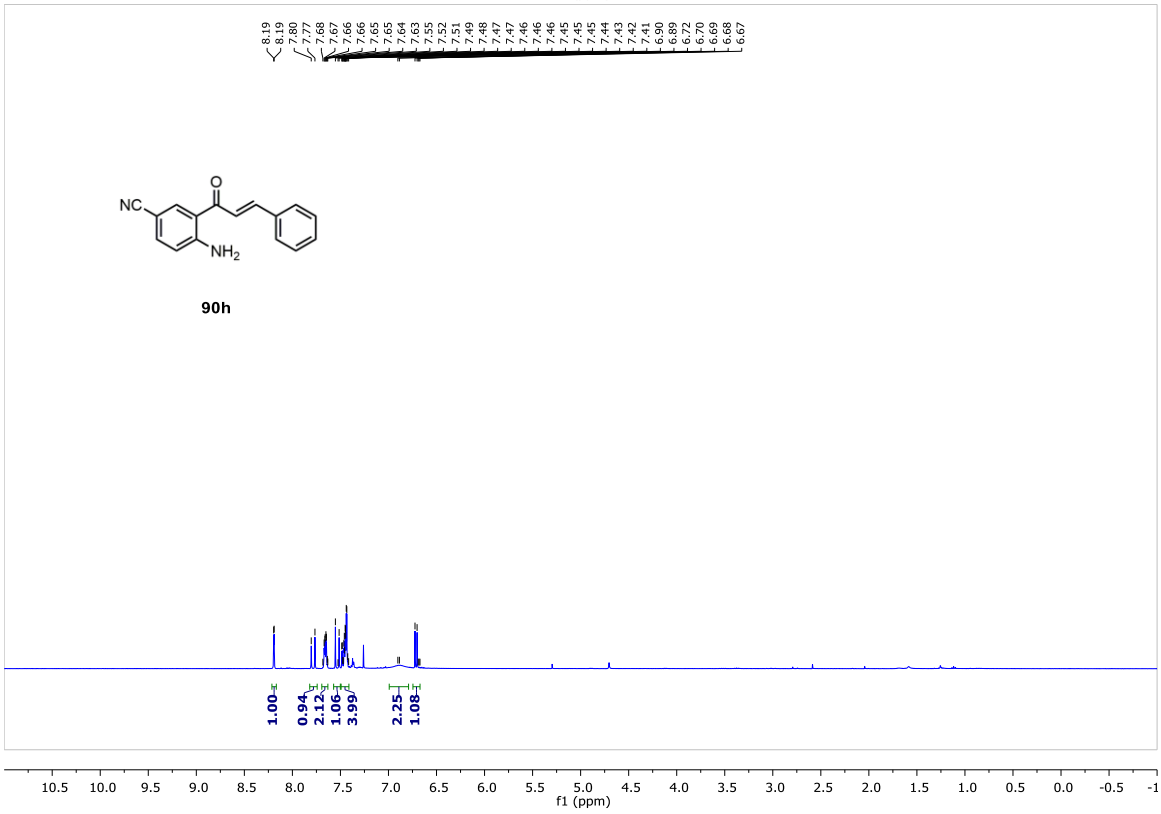
8.19
8.19
7.80
7.77
7.68
7.67
7.66
7.66
7.65
7.65
7.64
7.63
7.55
7.52
7.51
7.49
7.48
7.47
7.47
7.46
7.46
7.46
7.45
7.45
7.45
7.44
7.43
7.42
7.41
6.90
6.89
6.72
6.70
6.69
6.68
6.67
NC
O
NH2
90h
1.00
0.94
2.12
1.06
3.99
2.25
1.08
f1 (ppm)

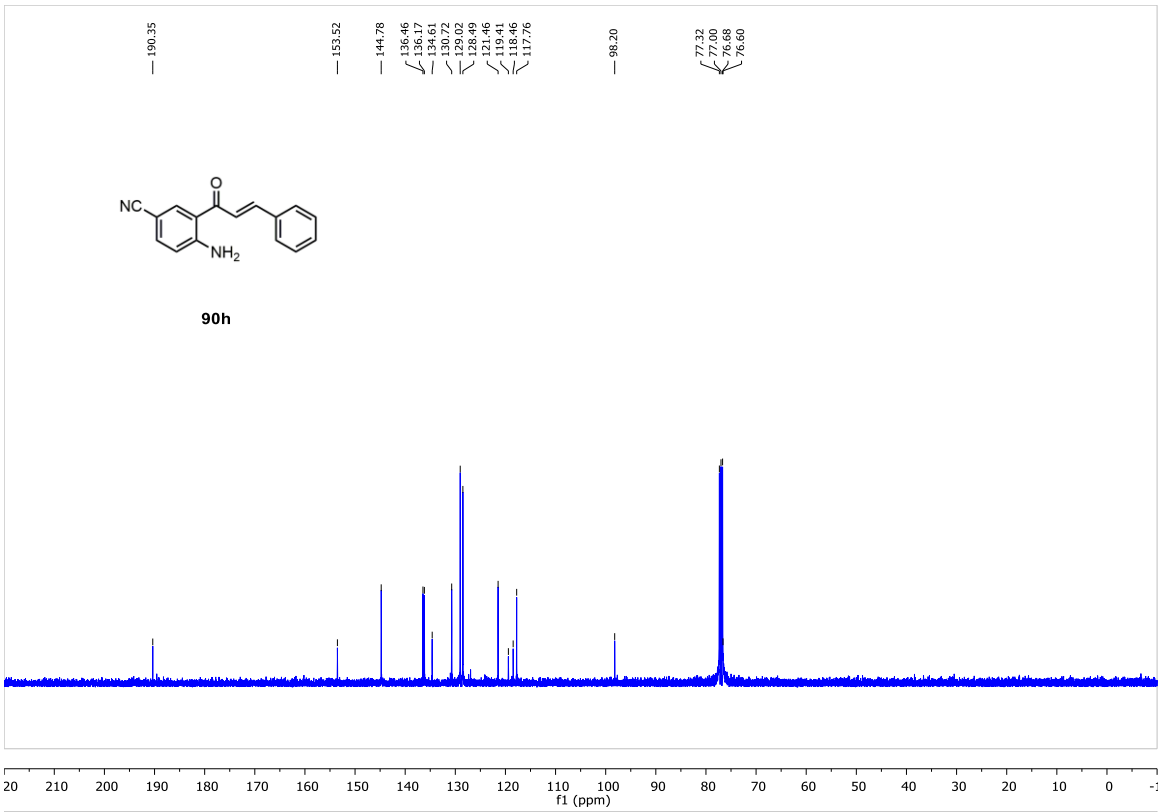
190.35
153.52
144.78
136.46
136.17
134.61
130.72
129.02
128.49
121.46
119.41
118.46
117.76
98.20
77.32
77.00
76.68
76.60
NC
O
NH2
90h
f1 (ppm)

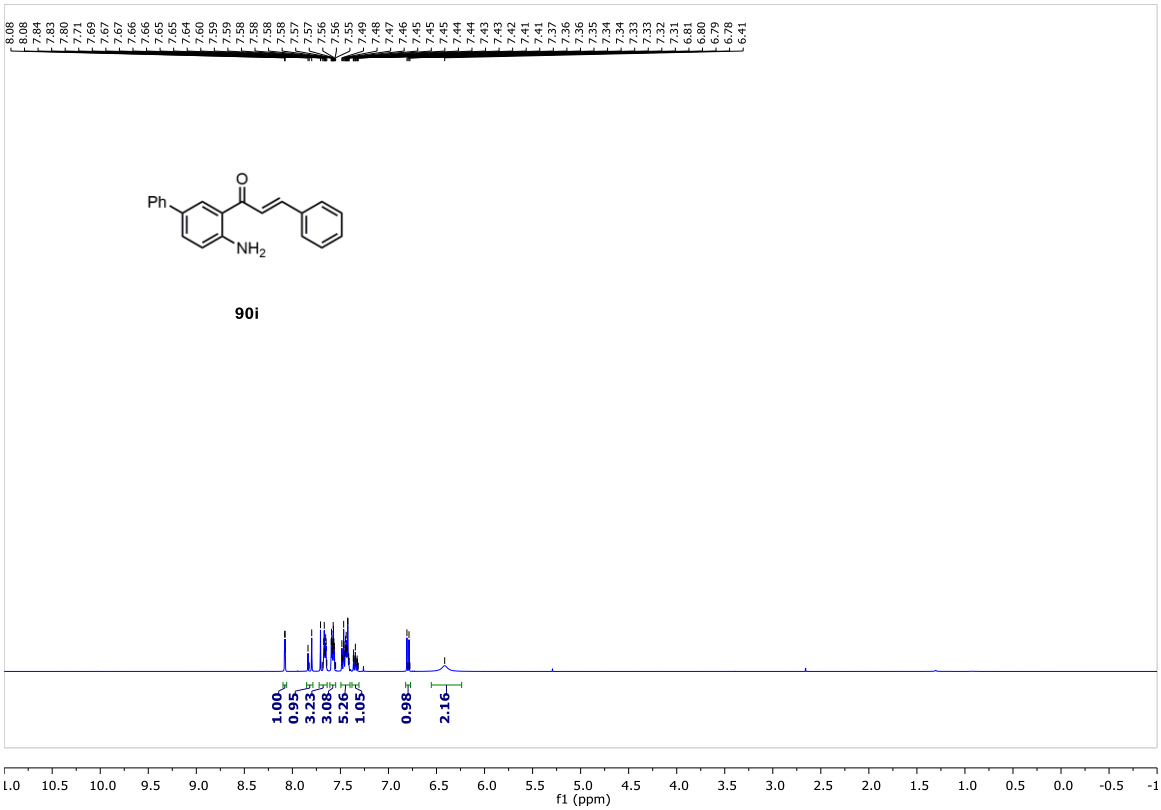
Ph
O
NH2
90i
1.00
0.95
3.23
3.08
5.26
1.05
0.98
2.16
f1 (ppm)

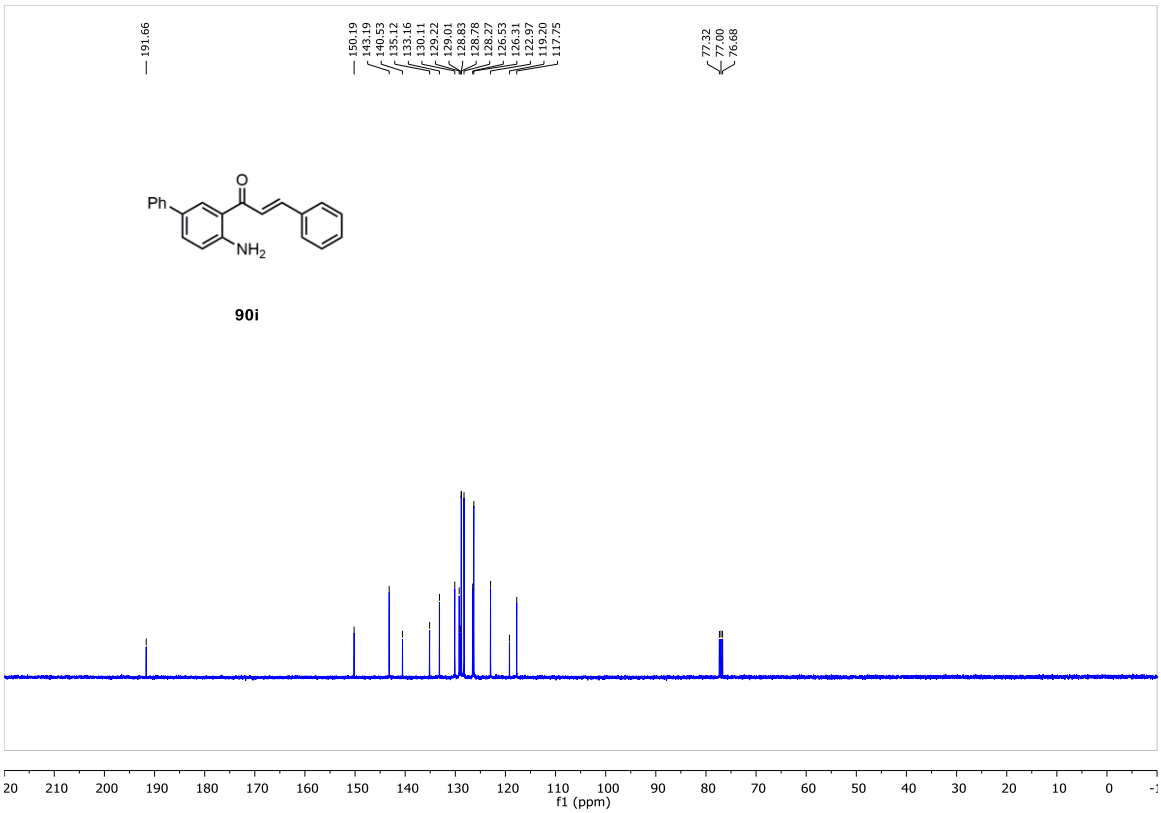
191.66
150.19
143.19
140.53
135.72
133.16
130.11
129.22
129.01
128.83
128.78
128.27
126.53
126.31
122.97
119.20
117.75
77.32
77.00
76.68
O
Ph
NH2
f1 (ppm)

90i

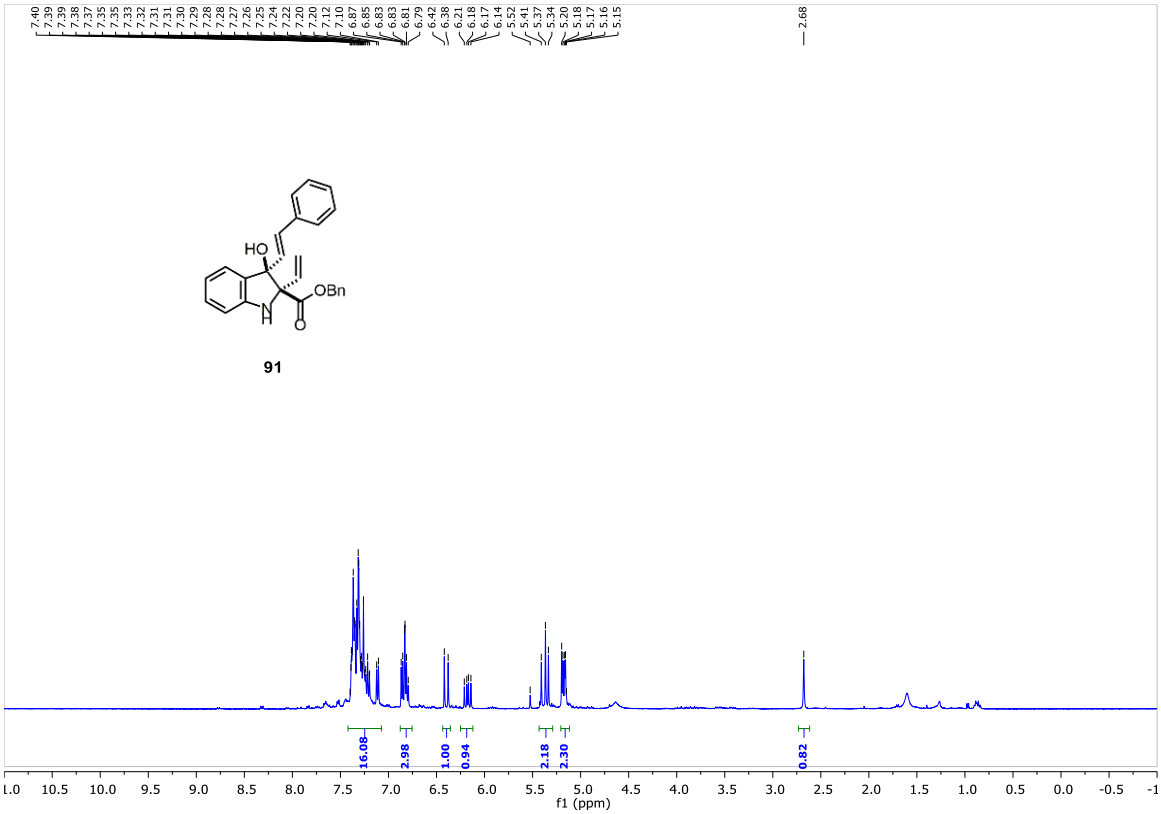
7.40
7.39
7.39
7.38
7.37
7.35
7.35
7.33
7.32
7.31
7.30
7.29
7.28
7.28
7.27
7.26
7.25
7.24
7.22
7.20
7.20
7.12
7.10
6.87
6.85
6.83
6.81
6.79
6.42
6.38
6.21
6.18
6.17
6.14
5.52
5.41
5.37
5.34
5.20
5.18
5.17
5.16
5.15
2.68
HO
OBn
N
H
O
16.08
2.98
1.00
0.94
2.18
2.30
0.82
f1 (ppm)

91

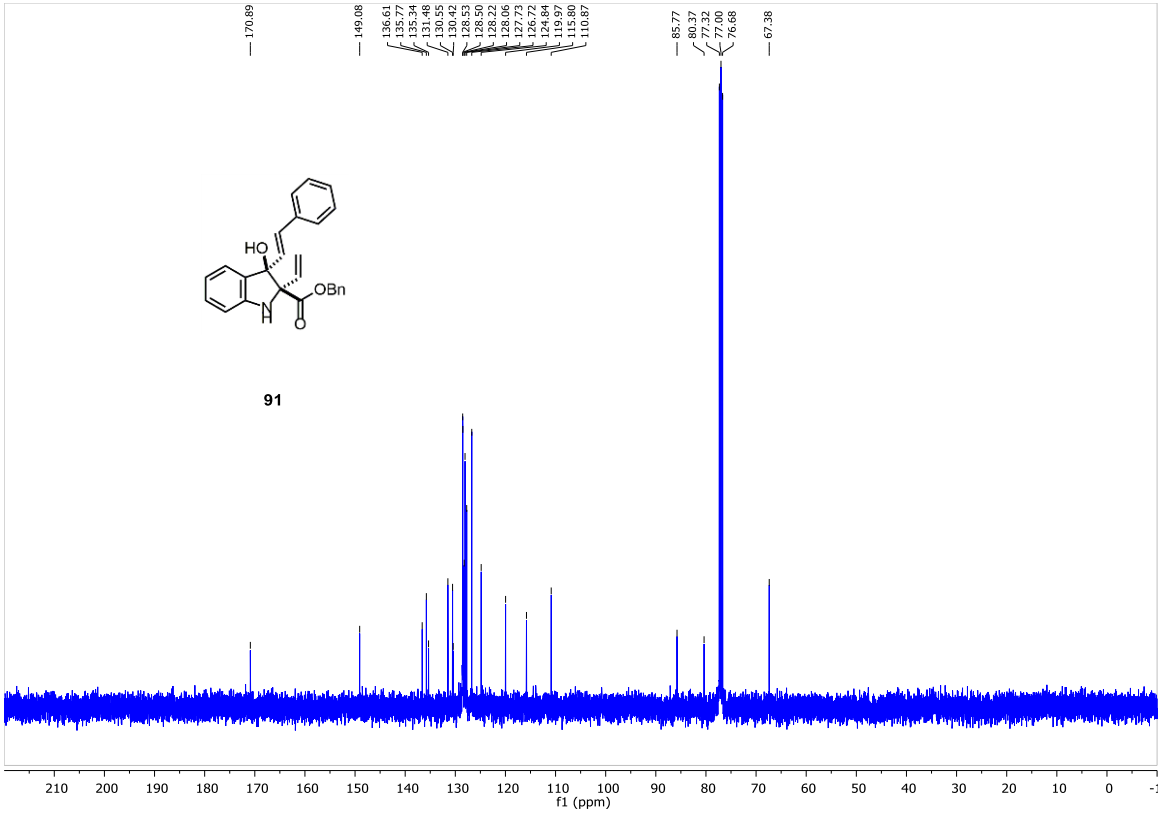
170.89
149.08
136.61
135.77
135.34
131.48
130.55
130.42
128.53
128.50
128.22
128.06
127.73
126.72
124.84
119.97
115.80
110.87
85.77
80.37
77.32
77.00
76.68
67.38
HO
OBn
N
H
O
91
f1 (ppm)

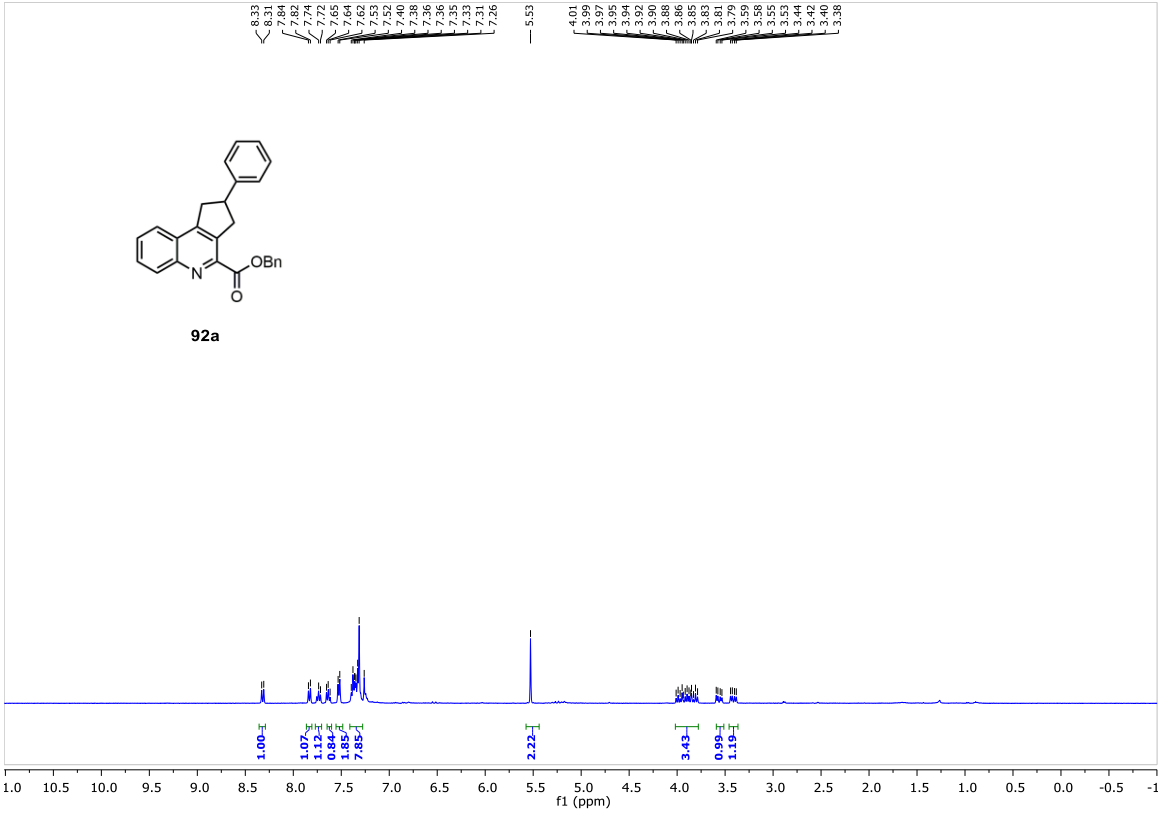
8.33
8.31
7.84
7.82
7.74
7.72
7.65
7.64
7.62
7.53
7.52
7.40
7.38
7.36
7.36
7.35
7.33
7.31
7.26
5.53
4.01
3.99
3.97
3.95
3.94
3.92
3.90
3.88
3.86
3.85
3.83
3.81
3.79
3.59
3.58
3.55
3.53
3.44
3.42
3.40
3.38
N
OBn
O
92a
1.00
1.07
1.12
0.84
1.85
7.85
2.22
3.43
0.99
1.19
f1 (ppm)

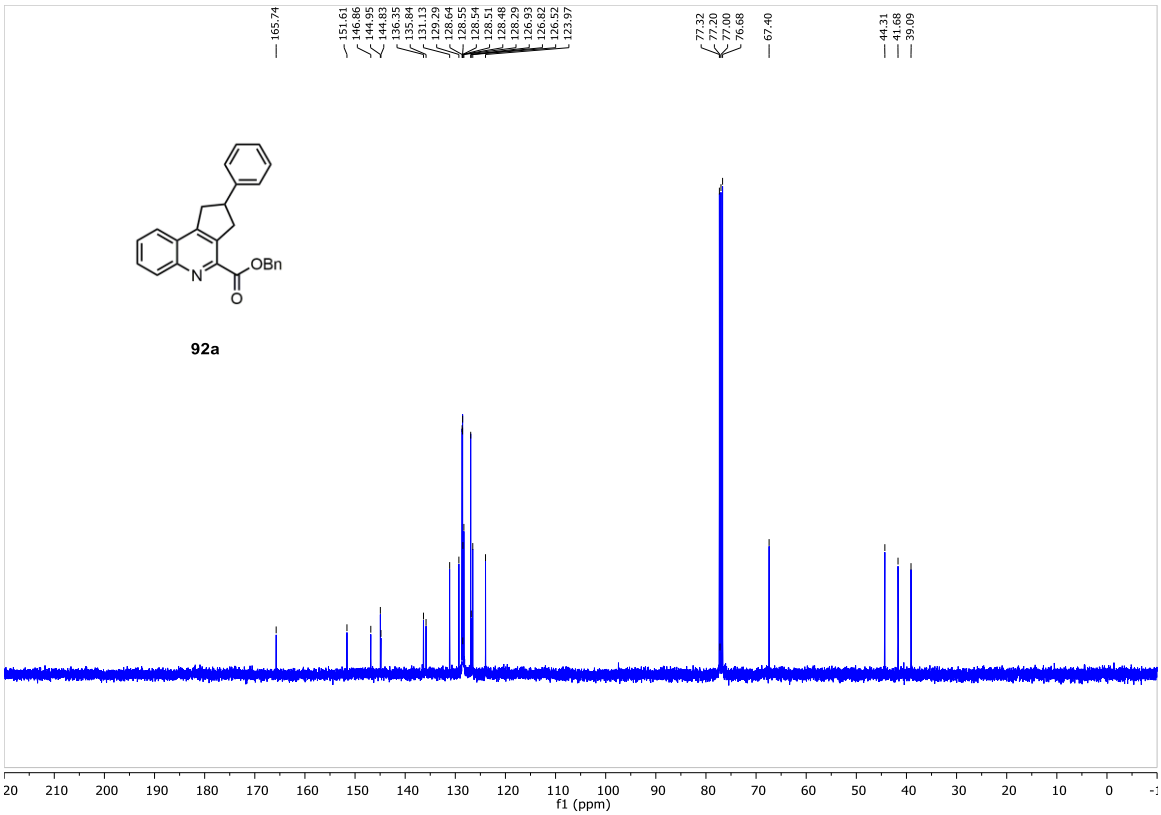
165.74
151.61
146.86
144.95
144.83
136.35
135.84
131.13
130.29
128.64
128.55
128.54
128.51
128.48
128.29
126.93
126.82
126.52
123.97
77.32
77.20
77.00
76.68
67.40
44.31
41.68
39.09
OBn
N
O
92a
f1 (ppm)

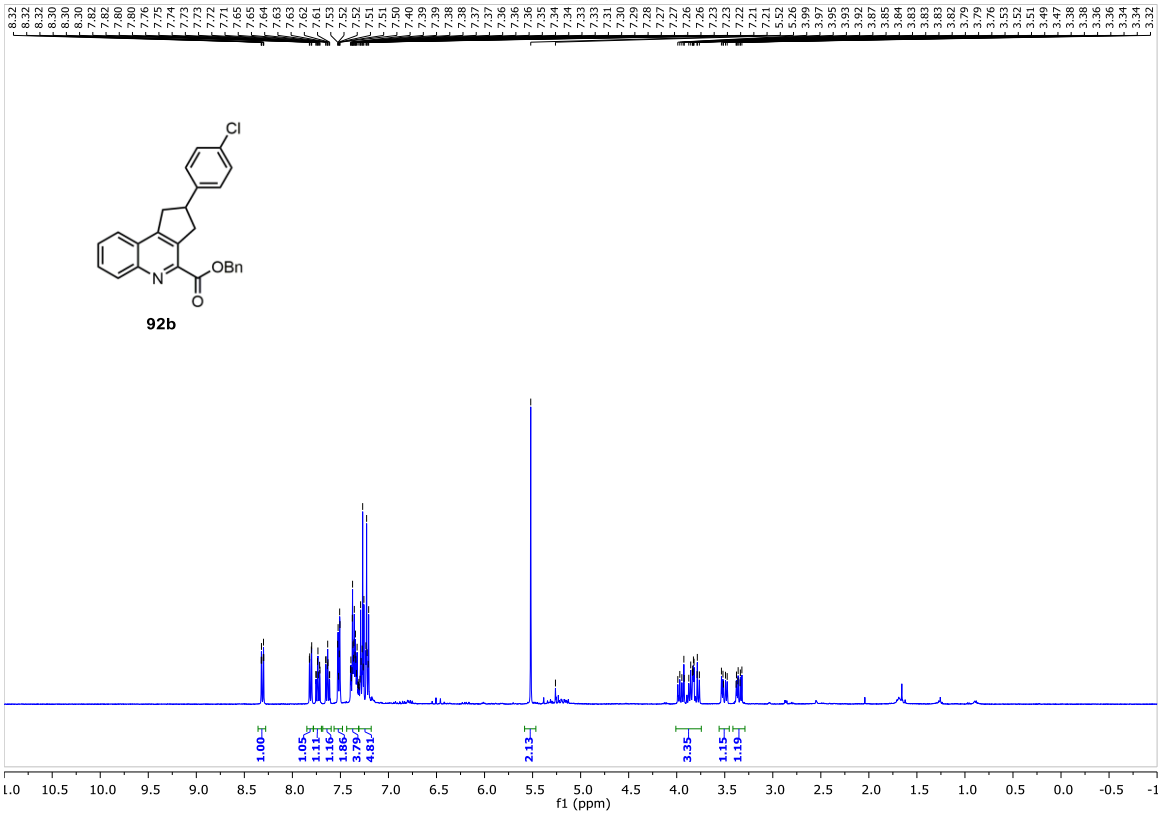
Cl
OBn
N
O
92b
1.00
1.05
1.11
1.16
1.86
3.79
4.81
2.13
3.35
1.15
1.19
f1 (ppm)

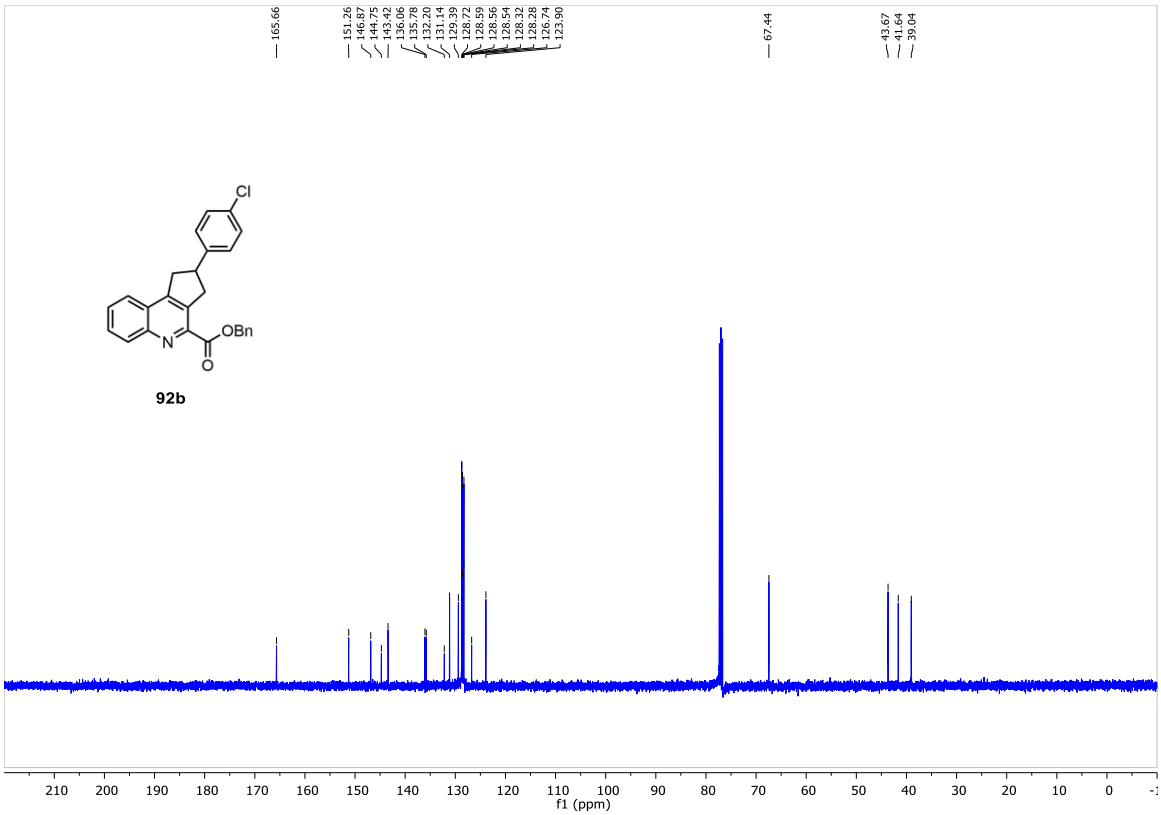
165.66
151.26
146.87
144.75
143.42
136.06
135.78
132.20
131.14
129.39
128.72
128.59
128.56
128.54
128.32
128.28
126.74
123.90
67.44
43.67
41.64
39.04
Cl
OBn
N
O
92b
f1 (ppm)

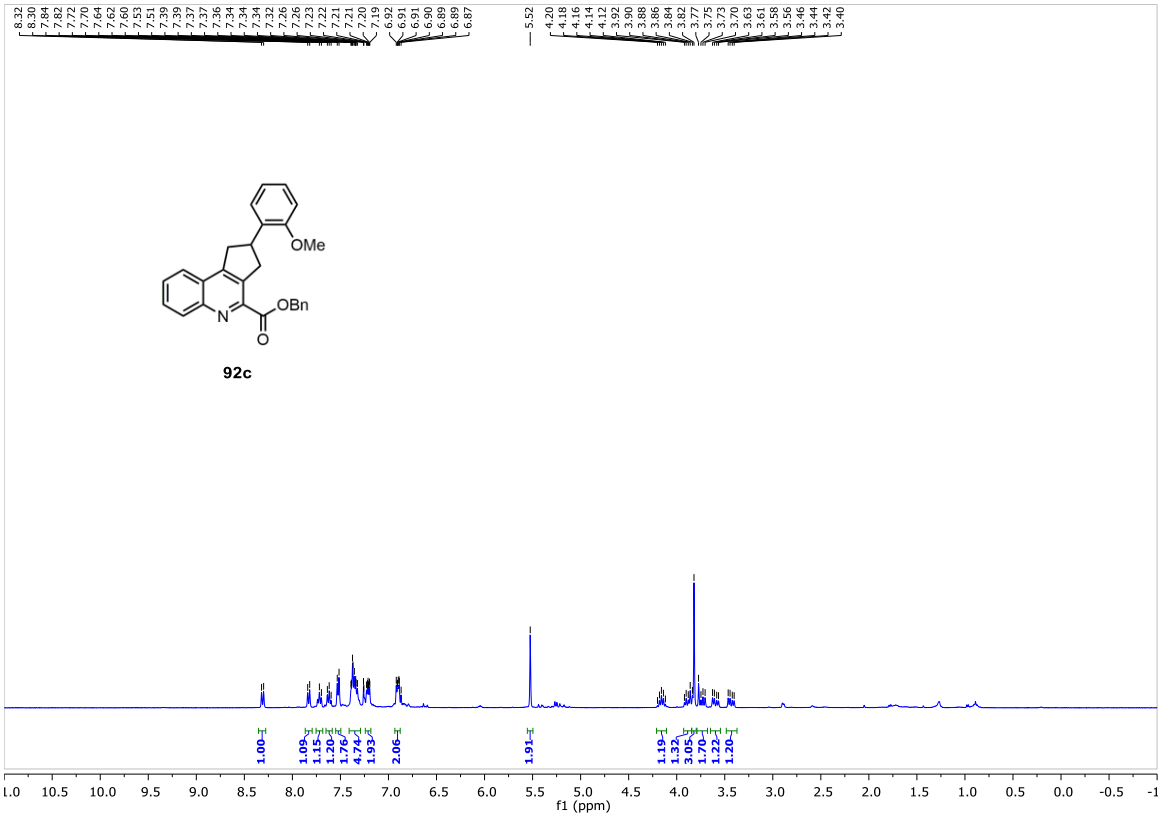
8.32
8.30
7.84
7.82
7.72
7.70
7.64
7.62
7.60
7.53
7.51
7.39
7.39
7.37
7.37
7.36
7.34
7.34
7.34
7.32
7.26
7.26
7.23
7.22
7.21
7.21
7.20
7.19
6.92
6.91
6.91
6.90
6.89
6.89
6.87
5.52
4.20
4.18
4.16
4.14
4.12
3.92
3.90
3.88
3.86
3.84
3.82
3.77
3.75
3.73
3.70
3.63
3.61
3.58
3.56
3.46
3.44
3.42
3.40
OMe
OBn
N
O
92c
1.00
1.09
1.15
1.20
1.76
4.74
1.93
2.06
1.91
1.19
1.32
3.05
1.70
1.20
1.20
f1 (ppm)

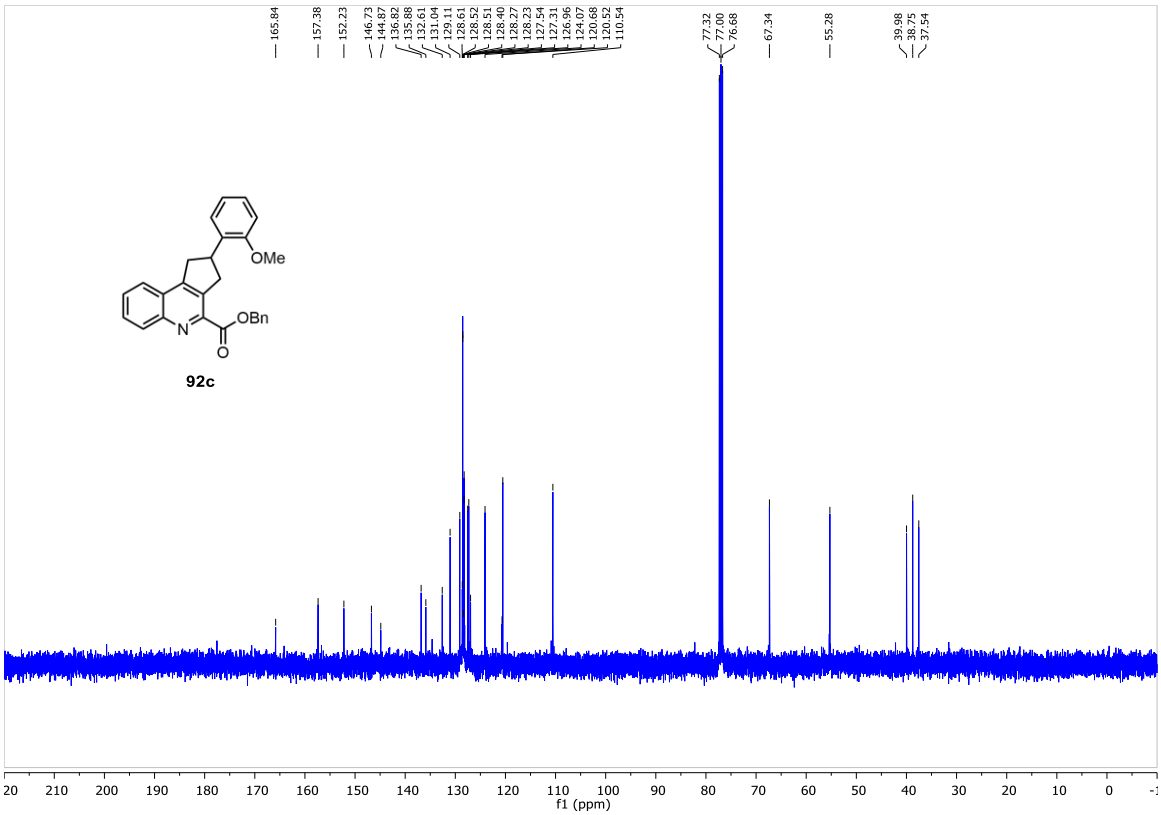
OMe
OBn
N
O
92c
f1 (ppm)

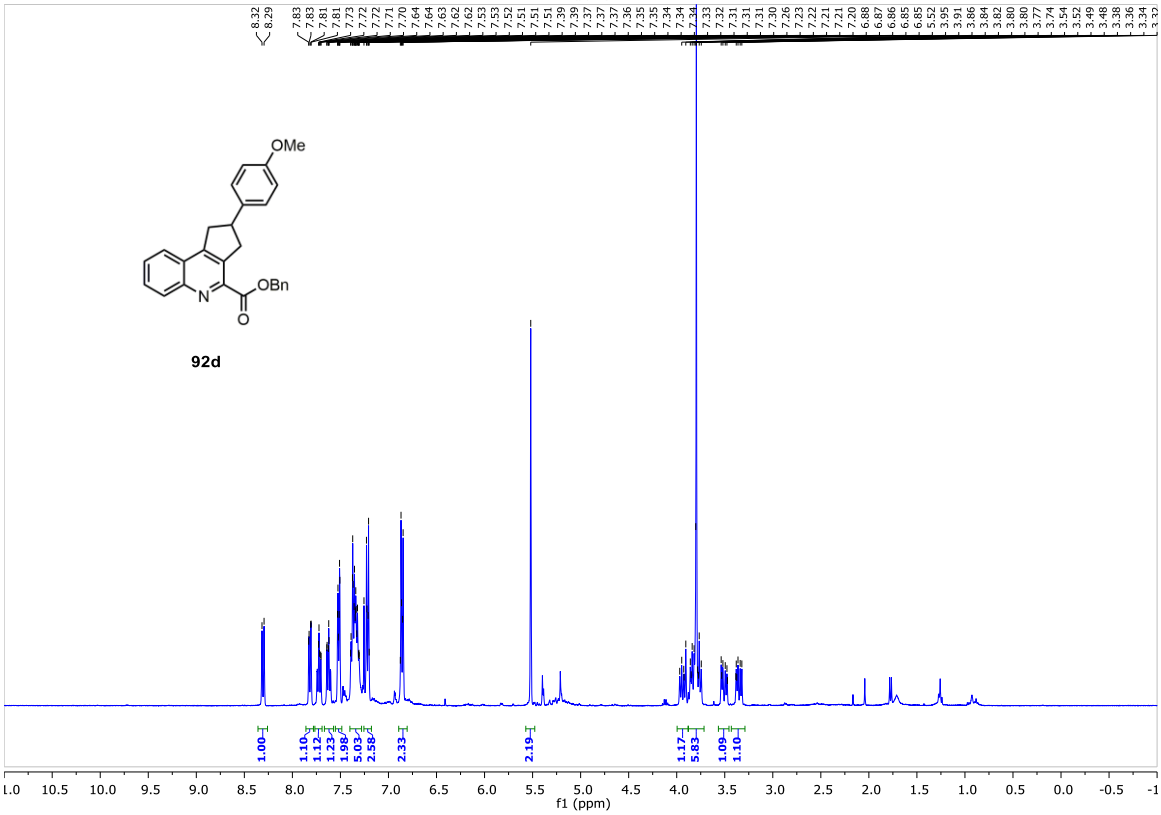
OMe
OBn
N
O
92d
f1 (ppm)

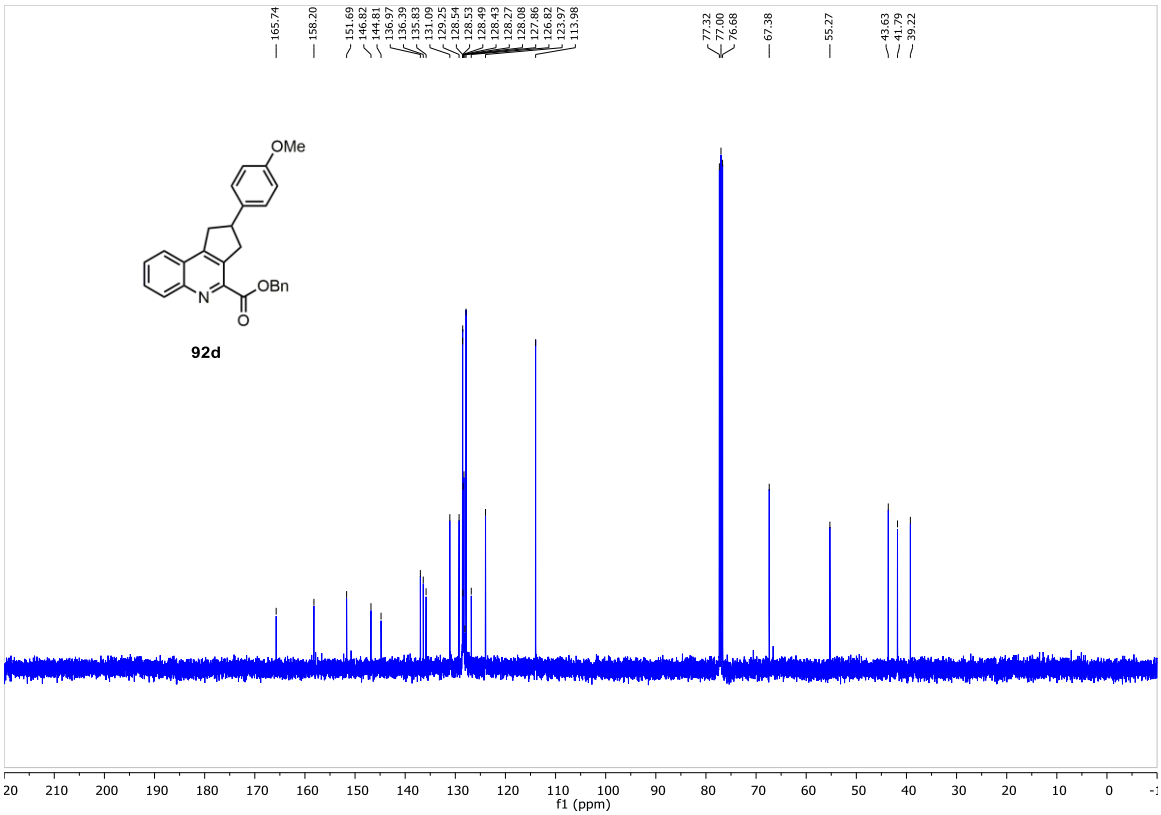
165.74
158.20
151.69
146.82
144.81
136.97
136.39
135.83
131.09
129.25
128.54
128.53
128.49
128.43
128.27
128.08
127.86
126.82
123.97
113.98
77.32
77.00
76.68
67.38
55.27
43.63
41.79
39.22
OMe
OBn
N
O
92d
f1 (ppm)

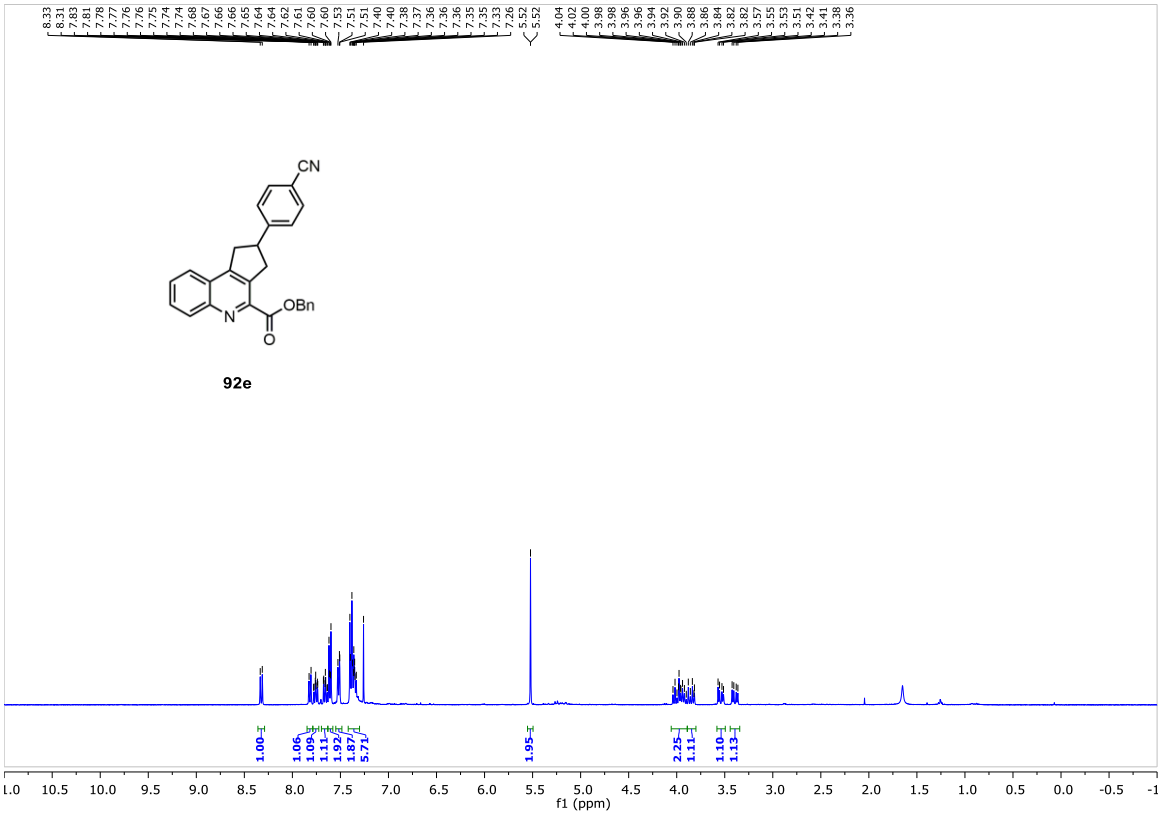
8.33
8.31
7.83
7.81
7.78
7.77
7.76
7.75
7.74
7.68
7.67
7.66
7.65
7.64
7.62
7.61
7.60
7.60
7.53
7.51
7.40
7.38
7.37
7.36
7.36
7.35
7.33
7.26
5.52
5.52
4.04
4.02
4.00
3.98
3.98
3.96
3.96
3.94
3.92
3.90
3.88
3.86
3.84
3.82
3.82
3.57
3.55
3.51
3.42
3.41
3.38
3.36
CN
OBn
N
O
92e
1.00
1.06
1.05
1.11
1.92
1.87
5.71
1.95
2.25
1.11
1.10
1.13
f1 (ppm)

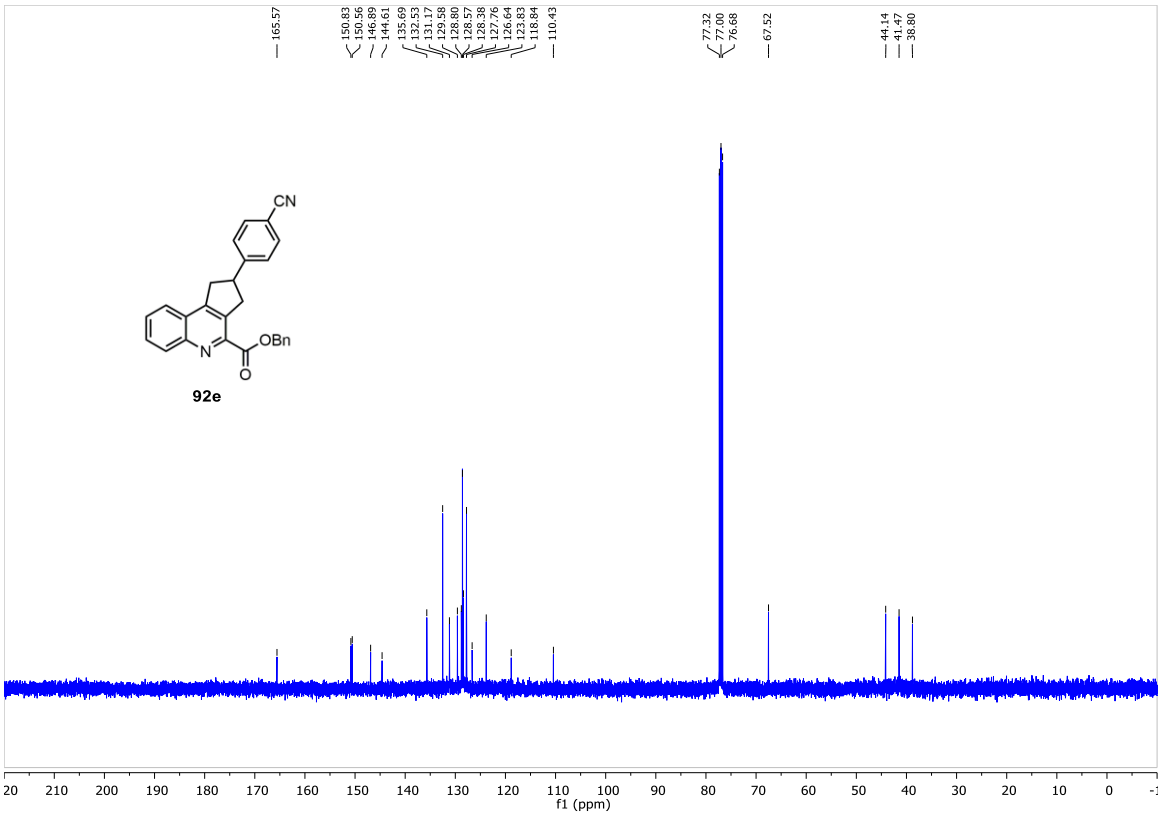
165.57
150.83
150.56
146.89
144.61
135.69
132.53
131.17
129.58
128.80
128.57
128.38
127.76
126.64
123.83
118.84
110.43
77.32
77.00
76.68
67.52
44.14
41.47
38.80
CN
OBn
N
O
92e
f1 (ppm)

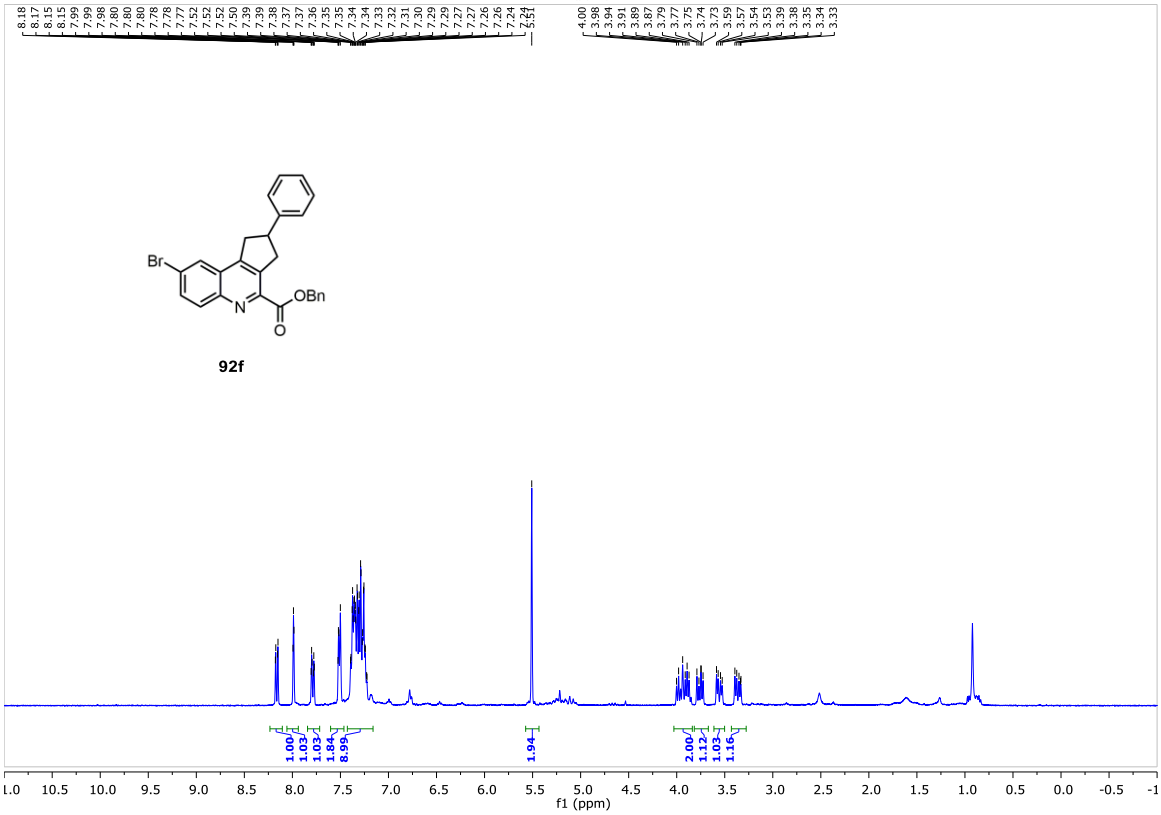
Br
OBn
N
O
92f
1.00
1.03
1.03
1.84
8.99
1.94
2.00
1.12
1.03
1.16
f1 (ppm)

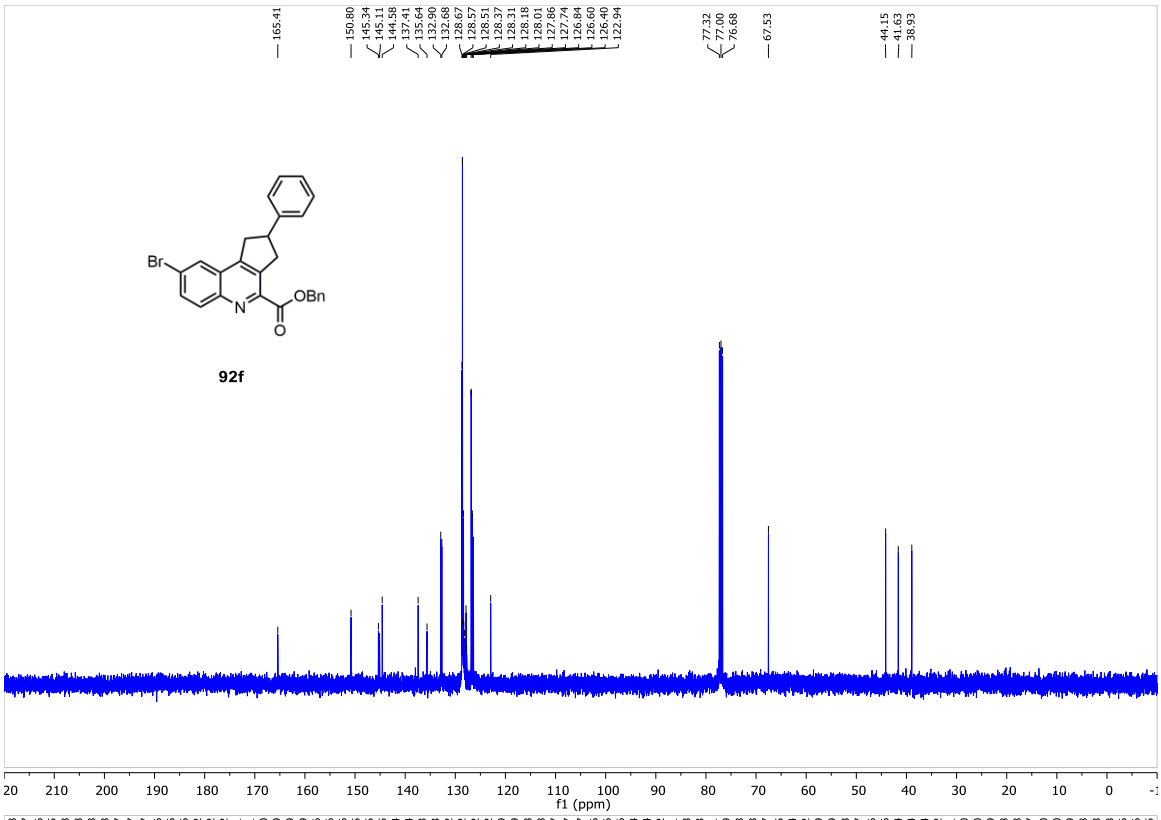
Br
OBn
N
O
92f
f1 (ppm)

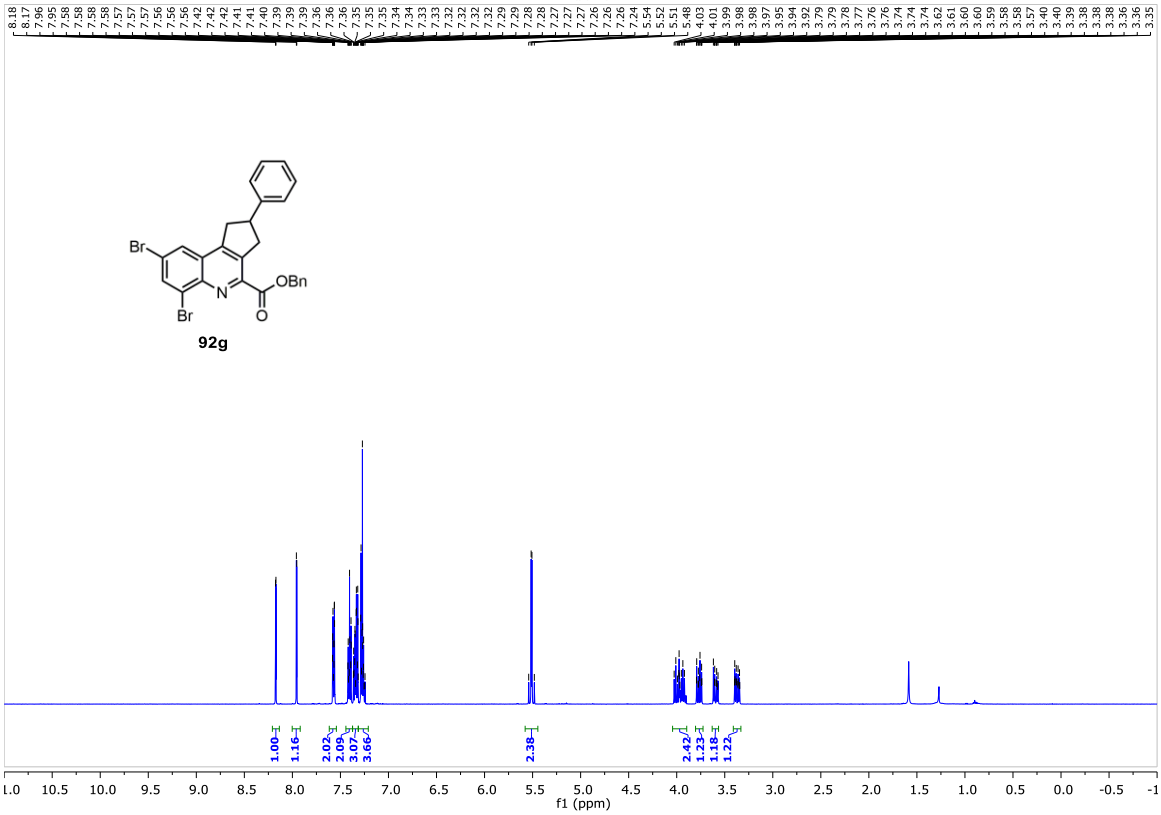
Br
OBn
N
O
Br
92g
1.00
1.16
2.02
2.05
3.07
3.66
2.38
2.42
1.23
1.18
1.22
f1 (ppm)

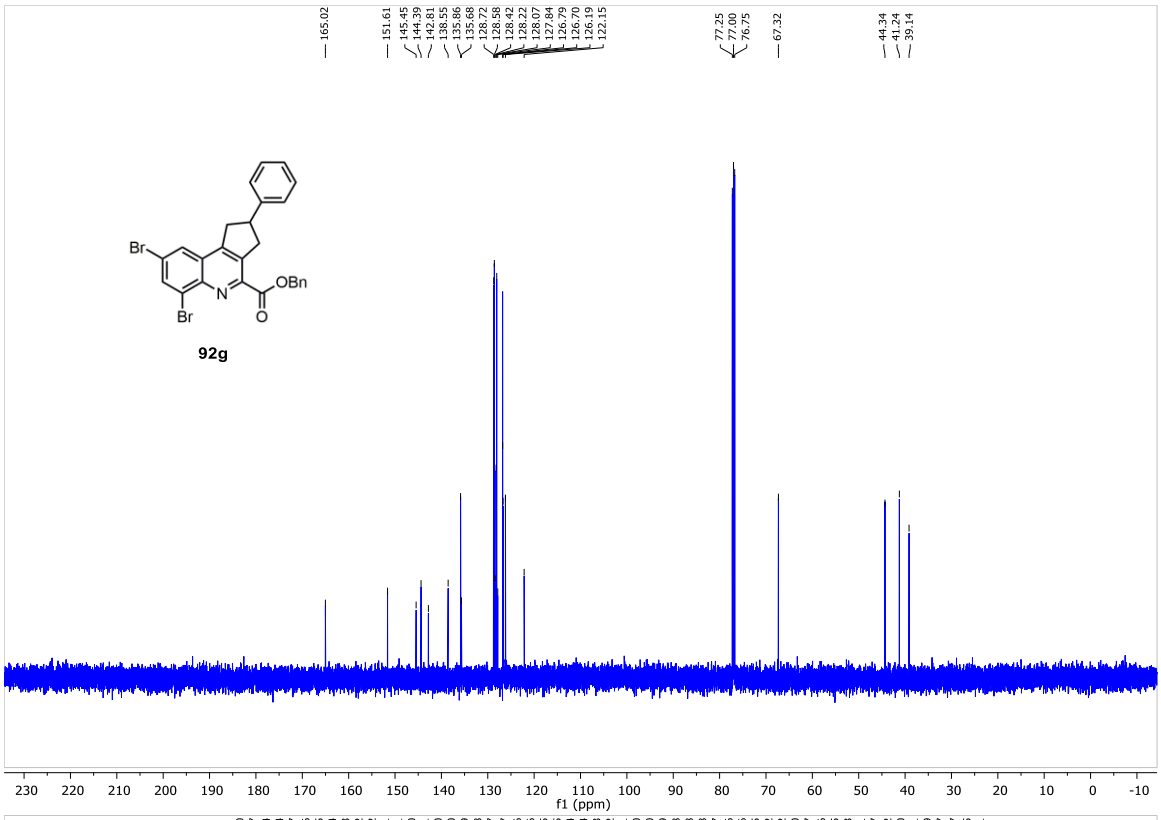
165.02
151.61
145.45
144.39
142.81
138.55
135.86
135.68
128.72
128.58
128.42
128.22
128.07
127.84
126.79
126.70
126.19
122.15
77.25
77.00
76.75
67.32
44.34
41.24
39.14
Br
Br
OBn
N
O
92g
f1 (ppm)

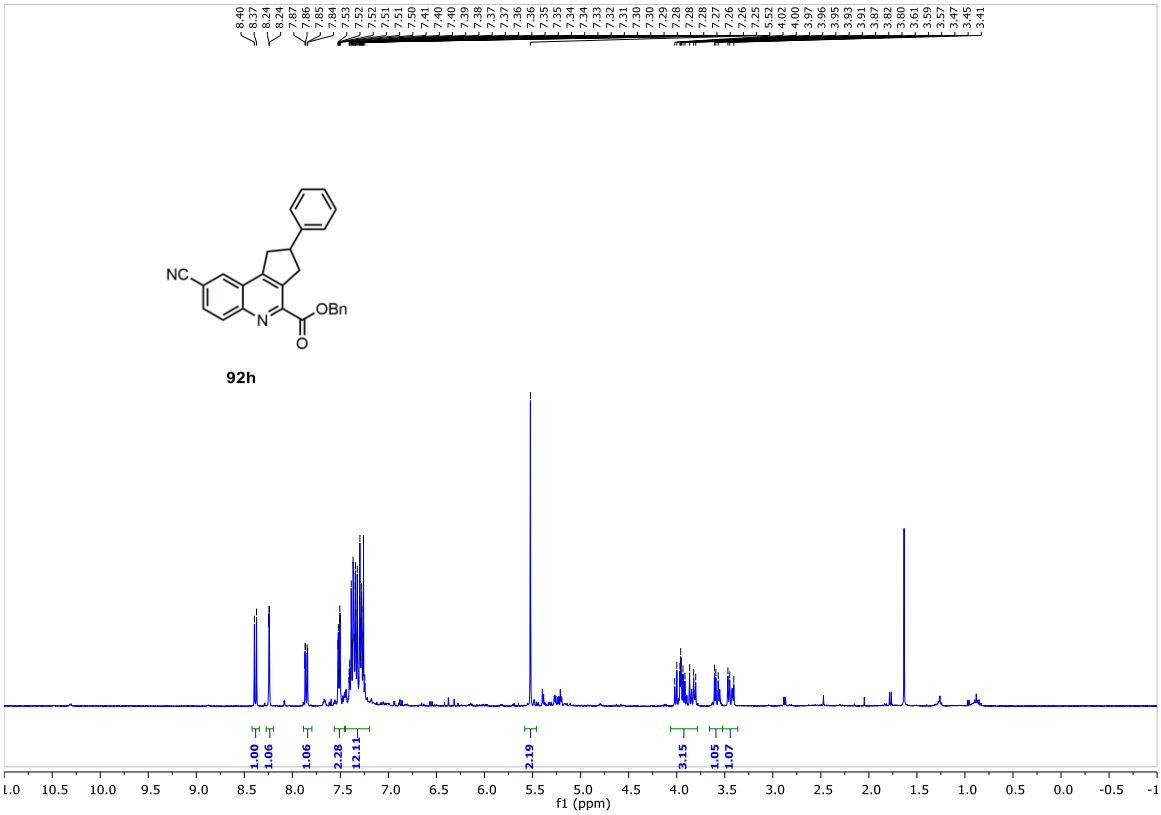
8.40
8.37
8.24
8.24
7.87
7.86
7.85
7.84
7.53
7.52
7.52
7.51
7.51
7.50
7.41
7.40
7.40
7.39
7.38
7.37
7.37
7.36
7.36
7.35
7.35
7.34
7.34
7.33
7.32
7.31
7.30
7.30
7.29
7.28
7.28
7.28
7.27
7.26
7.25
5.52
4.02
4.00
3.97
3.96
3.95
3.93
3.91
3.87
3.82
3.80
3.61
3.59
3.57
3.47
3.45
3.41
NC
OBn
N
O
92h
1.00
1.06
1.06
2.28
12.11
2.19
3.15
1.05
1.07
f1 (ppm)

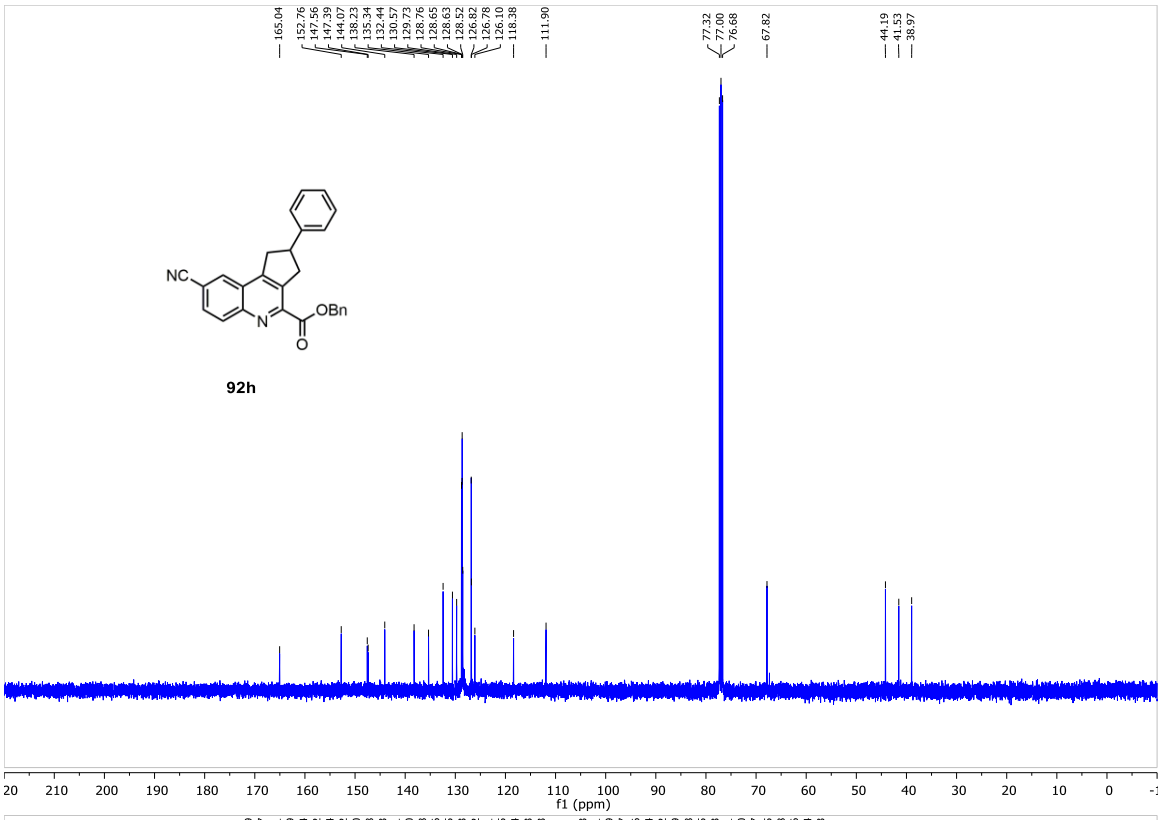
NC
OBn
N
O
92h
165.04
152.76
147.56
147.39
144.07
138.23
135.34
132.44
130.57
129.73
128.76
128.65
128.63
128.52
126.82
126.78
126.10
118.38
111.90
77.32
77.00
76.68
67.82
44.19
41.53
38.97
f1 (ppm)

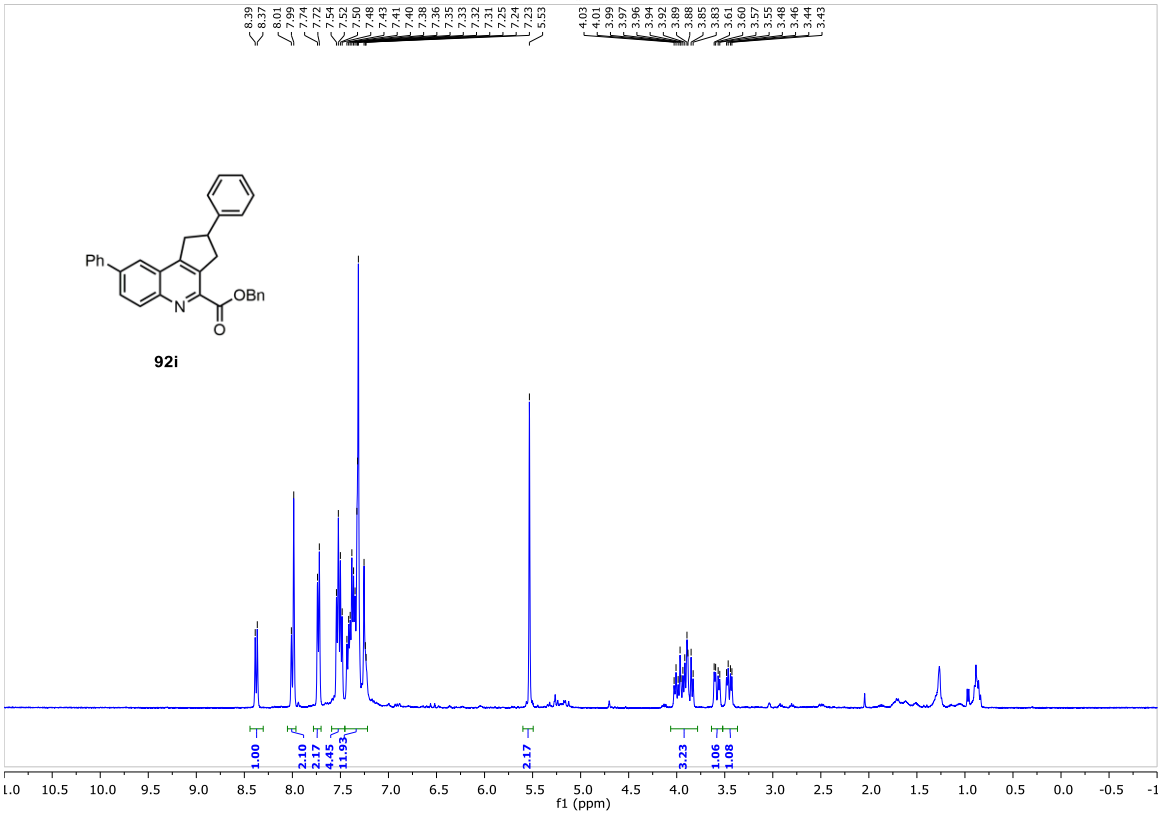
Ph
OBn
N
O
92i
8.39
8.37
8.01
7.99
7.74
7.72
7.54
7.52
7.50
7.48
7.43
7.41
7.40
7.38
7.36
7.33
7.32
7.31
7.25
7.24
7.23
5.53
4.03
4.01
3.99
3.97
3.96
3.94
3.92
3.89
3.88
3.85
3.83
3.61
3.60
3.57
3.55
3.48
3.46
3.44
3.43
1.00
2.10
2.17
4.45
11.93
2.17
3.23
1.06
1.08
f1 (ppm)

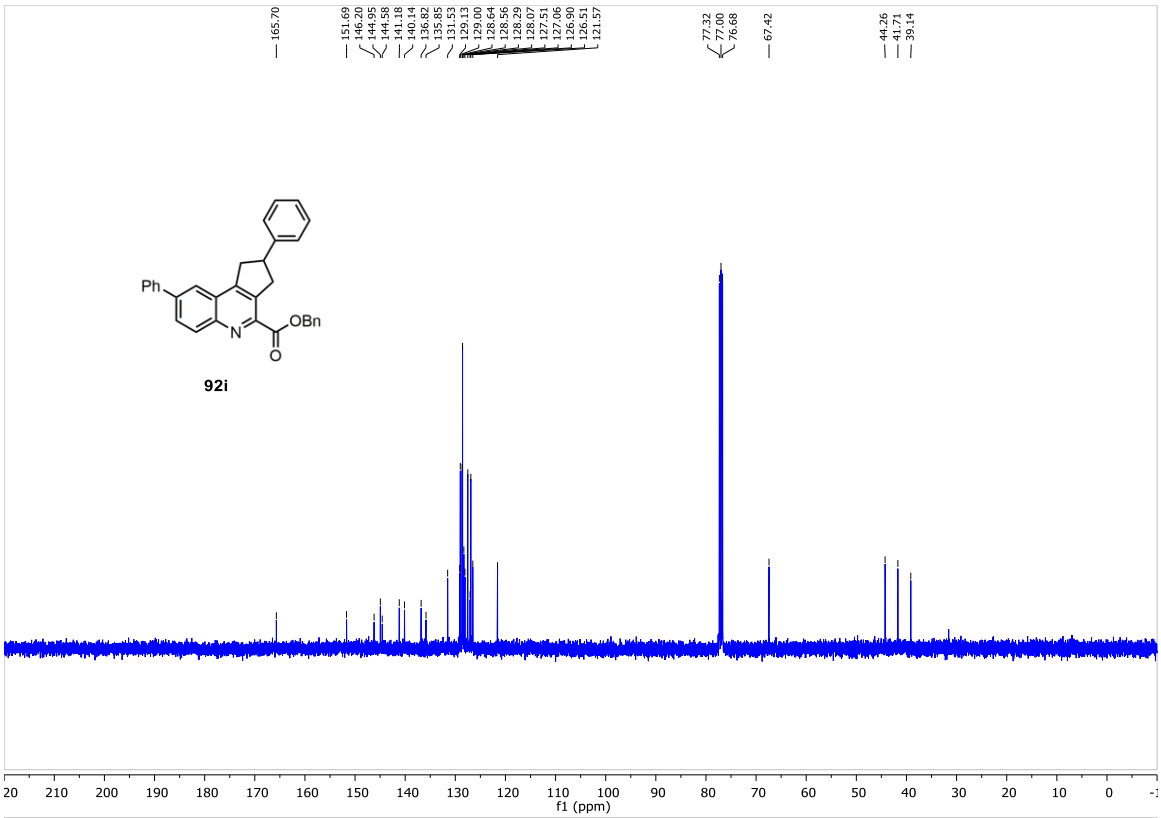
165.70
151.69
146.20
144.95
144.58
141.18
140.14
136.82
135.85
131.53
129.13
129.00
128.64
128.56
128.29
128.07
127.51
127.06
126.90
126.51
121.57
77.32
77.00
76.68
67.42
44.26
41.71
39.14
Ph
N
OBn
O
92i
f1 (ppm)

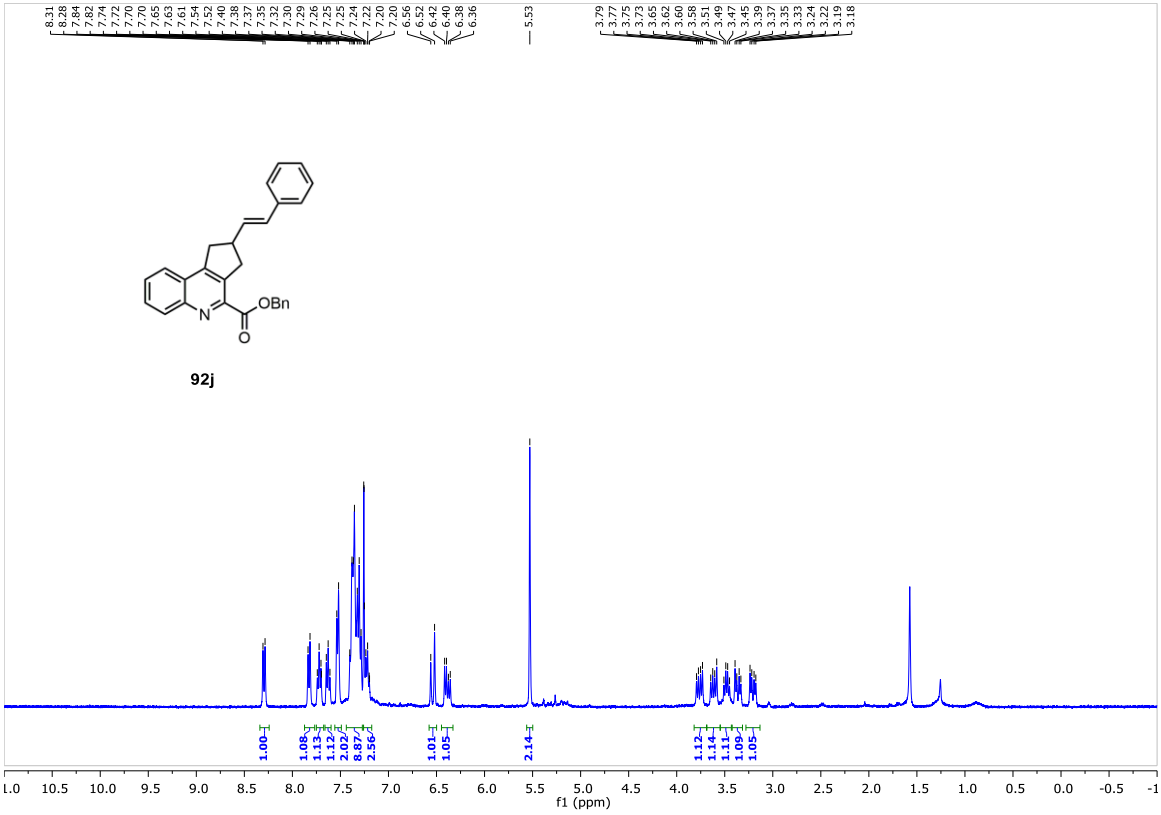
8.31
8.28
7.84
7.82
7.74
7.72
7.70
7.70
7.65
7.63
7.61
7.54
7.52
7.40
7.38
7.37
7.35
7.32
7.30
7.29
7.26
7.25
7.25
7.24
7.22
7.20
7.20
6.56
6.52
6.42
6.40
6.38
6.36
5.53
3.79
3.77
3.75
3.73
3.65
3.62
3.60
3.58
3.51
3.49
3.47
3.45
3.39
3.37
3.35
3.33
3.24
3.22
3.19
3.18
N
OBn
O
92j
1.00
1.08
1.13
1.12
2.02
8.87
2.56
1.01
1.05
2.14
1.12
1.14
1.11
1.09
1.05
f1 (ppm)

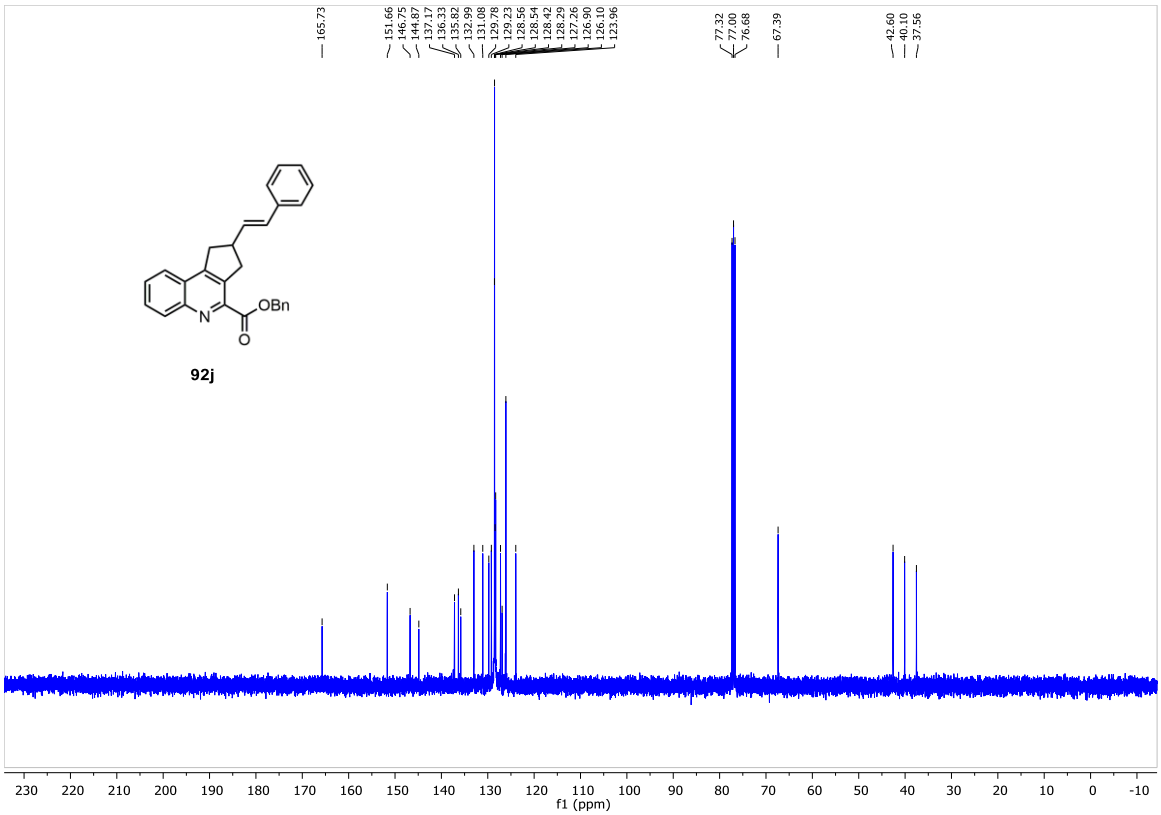
165.73
151.66
146.75
144.87
137.17
136.33
135.82
132.99
131.08
129.78
129.23
128.56
128.54
128.42
128.29
127.26
126.90
126.10
123.96
77.32
77.00
76.68
67.39
42.60
40.10
37.56
OBn
N
O
92j
f1 (ppm)

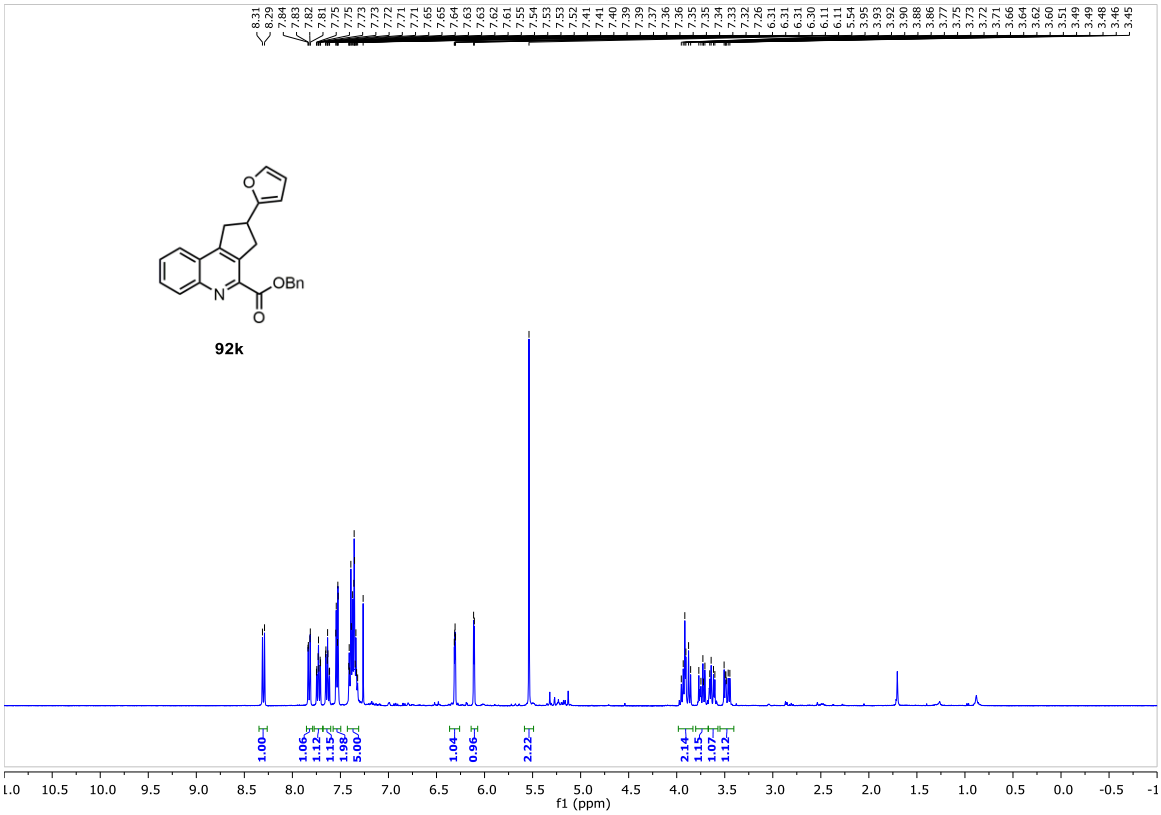
8.31
8.29
7.84
7.83
7.82
7.81
7.75
7.75
7.73
7.73
7.72
7.71
7.71
7.65
7.65
7.64
7.63
7.63
7.62
7.61
7.55
7.54
7.53
7.53
7.52
7.41
7.41
7.40
7.39
7.39
7.37
7.36
7.36
7.35
7.35
7.34
7.33
7.32
7.26
6.31
6.31
6.30
6.11
6.11
5.54
3.95
3.93
3.92
3.90
3.88
3.86
3.77
3.75
3.73
3.72
3.71
3.66
3.64
3.62
3.60
3.51
3.49
3.49
3.48
3.46
3.45
O
OBn
N
O
92k
1.00
1.06
1.12
1.15
1.98
5.00
1.04
0.96
2.22
2.14
1.15
1.07
1.12
f1 (ppm)

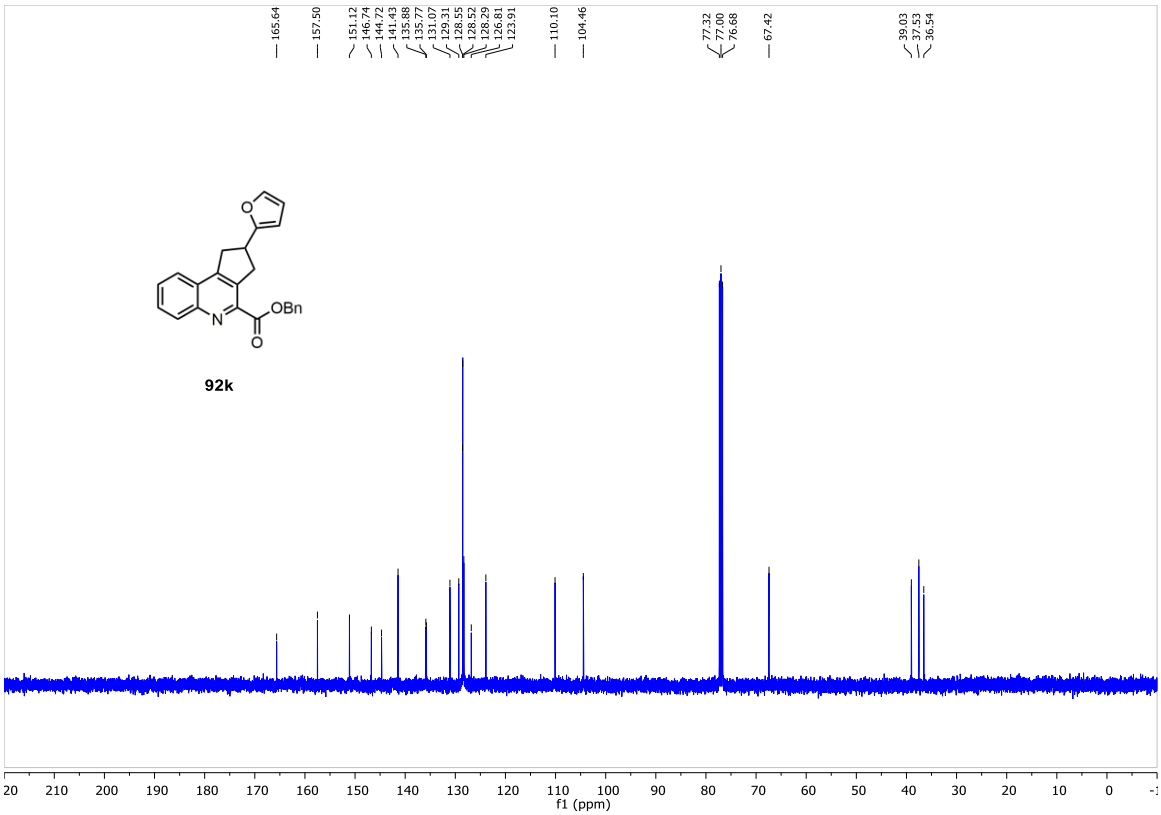
165.64
157.50
151.12
146.74
144.72
141.43
135.88
135.77
131.07
129.31
128.55
128.52
128.29
126.81
123.91
110.10
104.46
77.32
77.00
76.68
67.42
39.03
37.53
36.54
OBn
O
N
O
92k
f1 (ppm)

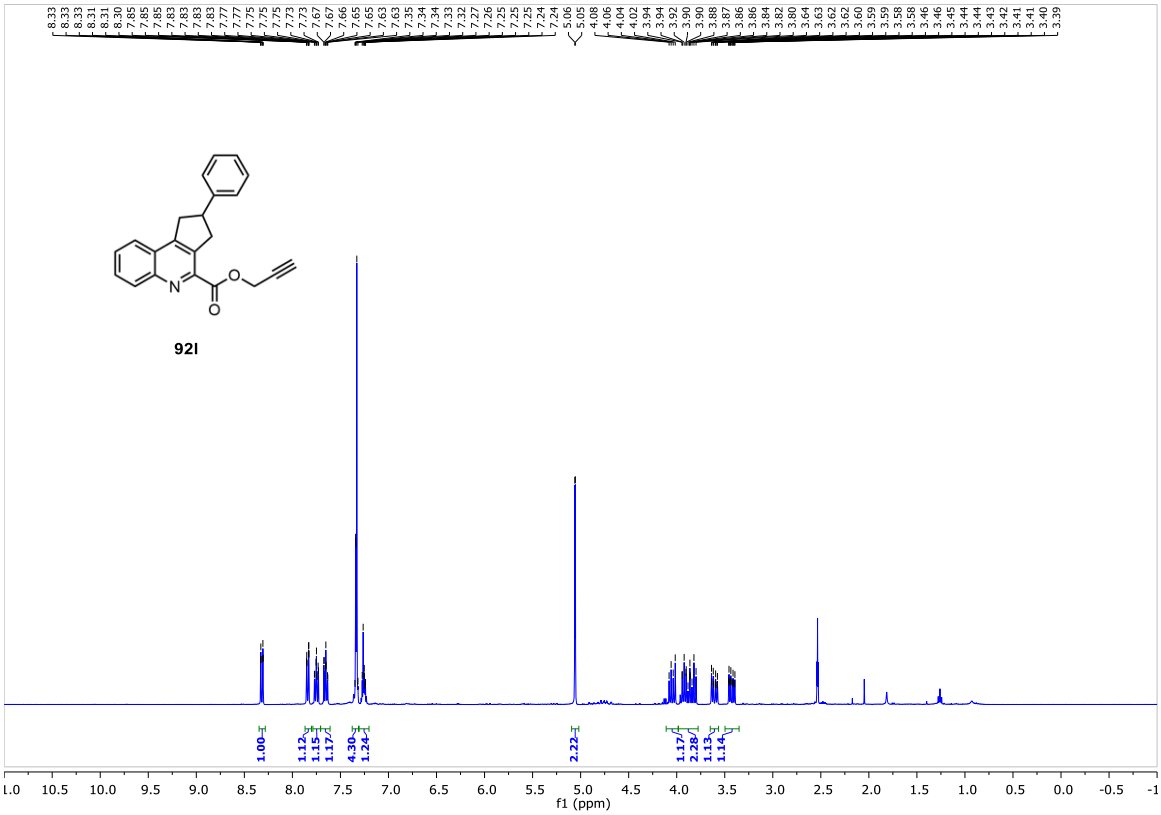
8.33
8.33
8.33
8.31
8.31
8.30
7.85
7.85
7.85
7.83
7.83
7.83
7.83
7.77
7.77
7.75
7.75
7.75
7.73
7.73
7.67
7.67
7.66
7.65
7.65
7.63
7.63
7.35
7.34
7.34
7.33
7.33
7.27
7.26
7.25
7.25
7.25
7.24
7.24
5.06
5.05
4.08
4.06
4.04
4.02
3.94
3.94
3.92
3.90
3.90
3.88
3.87
3.86
3.86
3.84
3.82
3.80
3.64
3.63
3.62
3.62
3.60
3.59
3.59
3.58
3.58
3.46
3.46
3.45
3.44
3.44
3.43
3.42
3.41
3.41
3.40
3.39
N
O
O
92l
1.00
1.12
1.15
1.17
4.30
1.24
2.22
1.17
2.28
1.13
1.14
f1 (ppm)

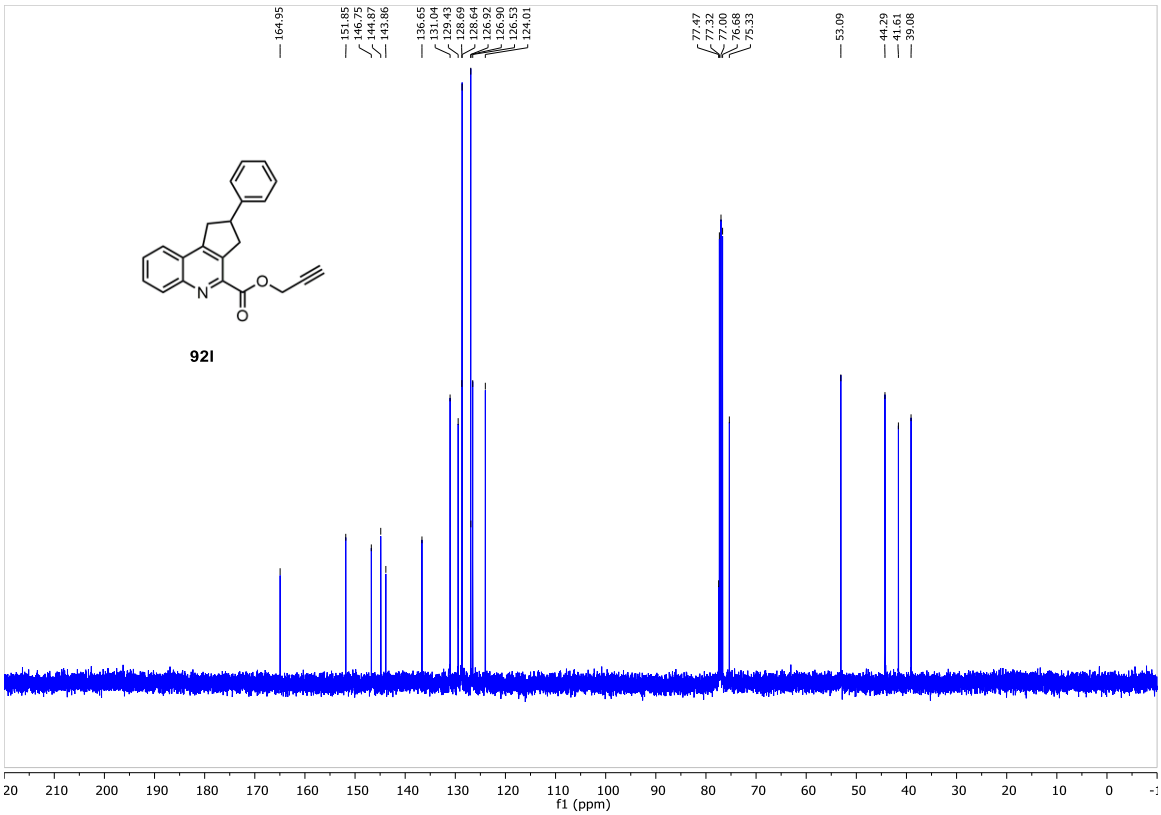
164.95
151.85
146.75
144.87
143.86
136.65
131.04
129.43
128.69
128.64
126.92
126.90
126.53
124.01
77.47
77.32
77.00
76.68
75.33
53.09
44.39
41.61
39.08
N
O
O
f1 (ppm)

92l

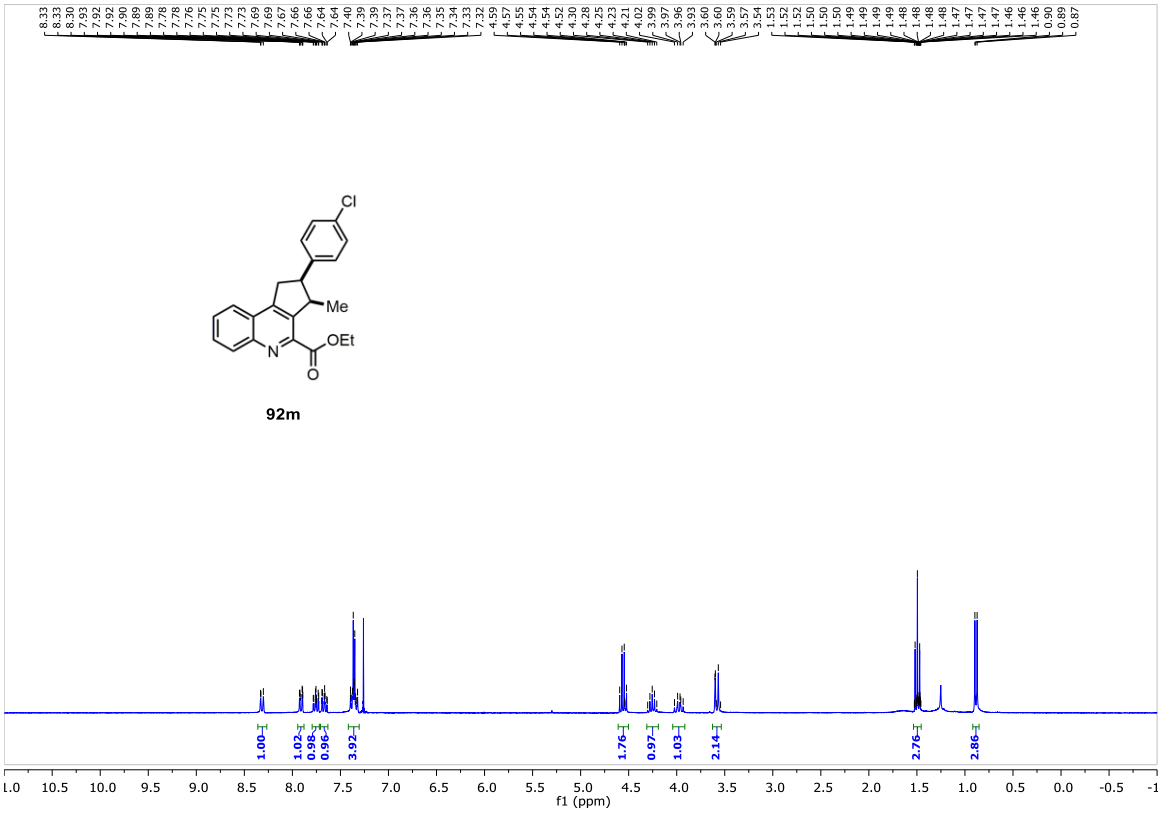
Cl
Me
OEt
N
O
1.00
1.02
0.98
0.96
3.92
1.76
0.97
1.03
2.14
2.76
2.86
f1 (ppm)

92m

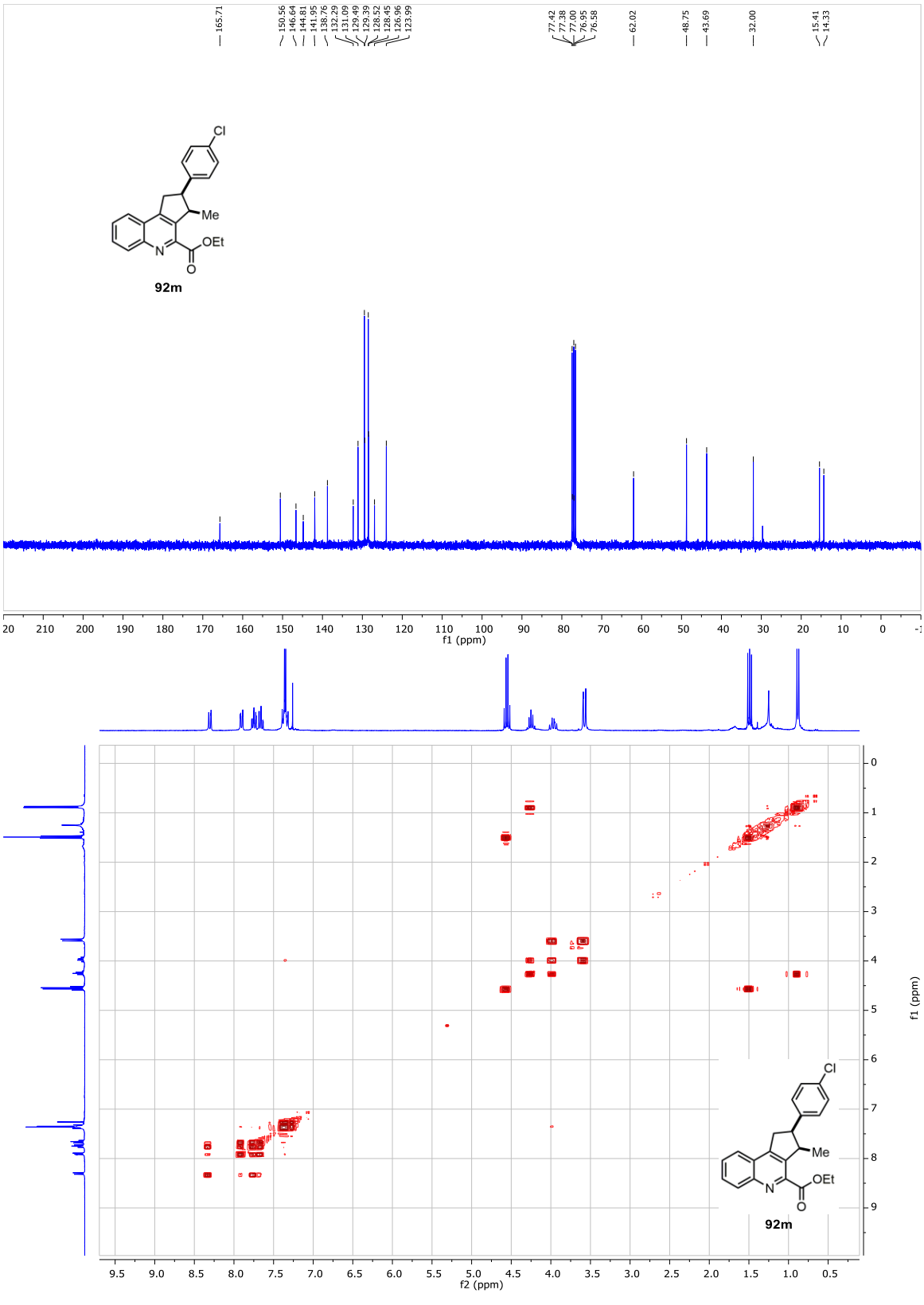
165.71
150.56
146.64
144.81
141.95
138.76
132.29
131.09
129.49
129.39
128.52
128.45
126.96
123.99
77.42
77.38
77.00
76.95
76.58
62.02
48.75
43.69
32.00
15.41
14.33
Cl
Me
OEt
N
O
92m
f1 (ppm)
f2 (ppm)

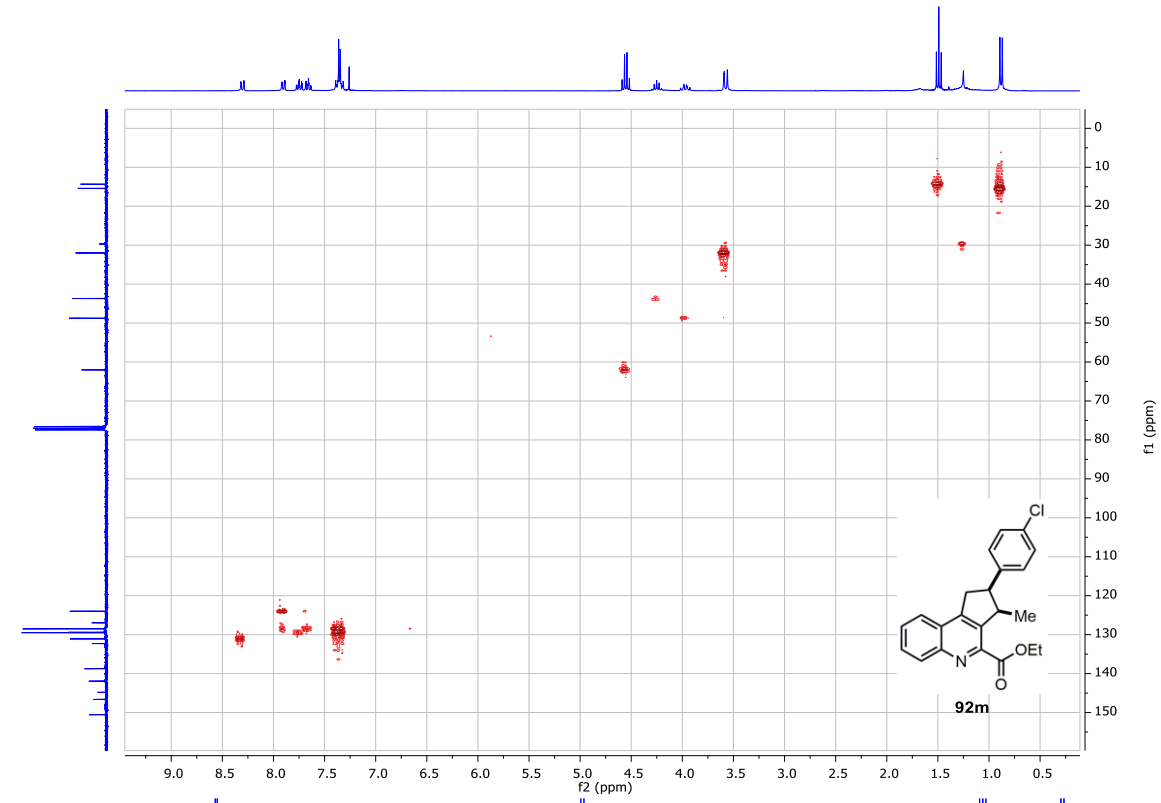
f2 (ppm)
f1 (ppm)
Cl
Me
OEt
N
O
92m

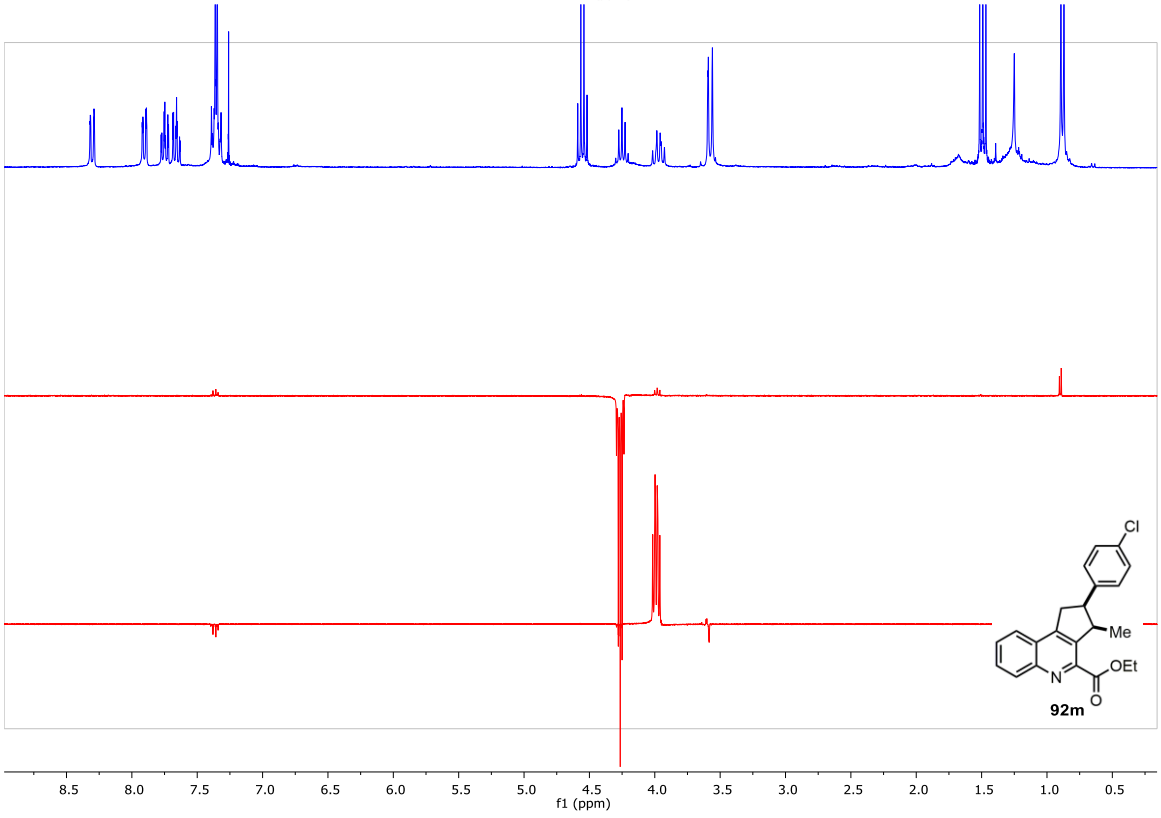
f1 (ppm)
Cl
Me
OEt
N
O
92m

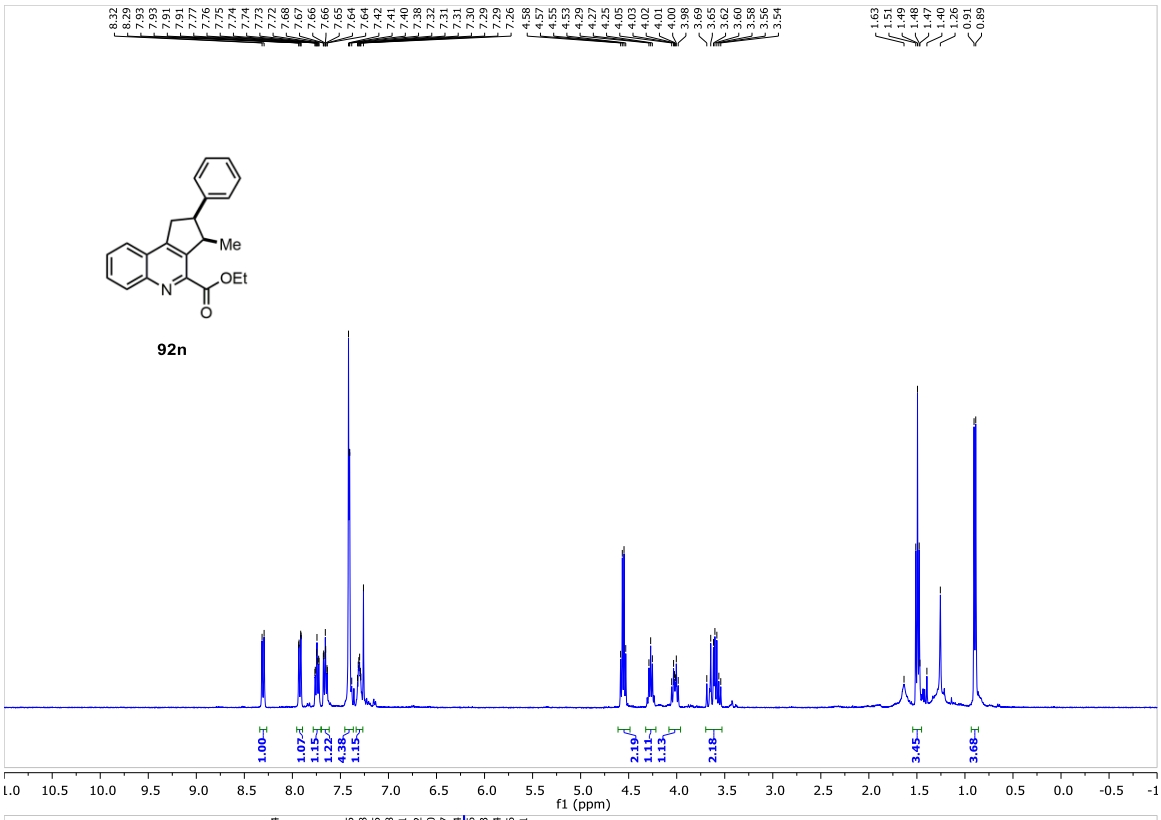
Me
OEt
O
N
92n
f1 (ppm)

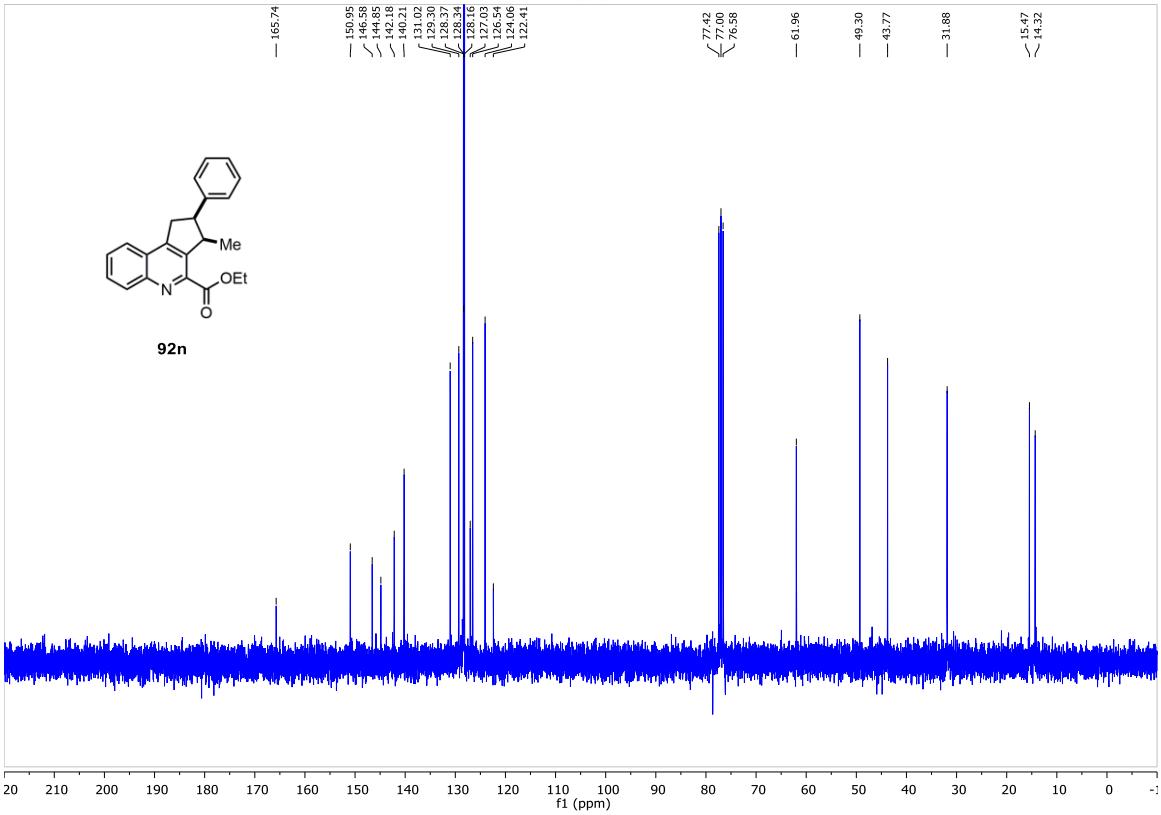
Me
OEt
O
N
92n
f1 (ppm)

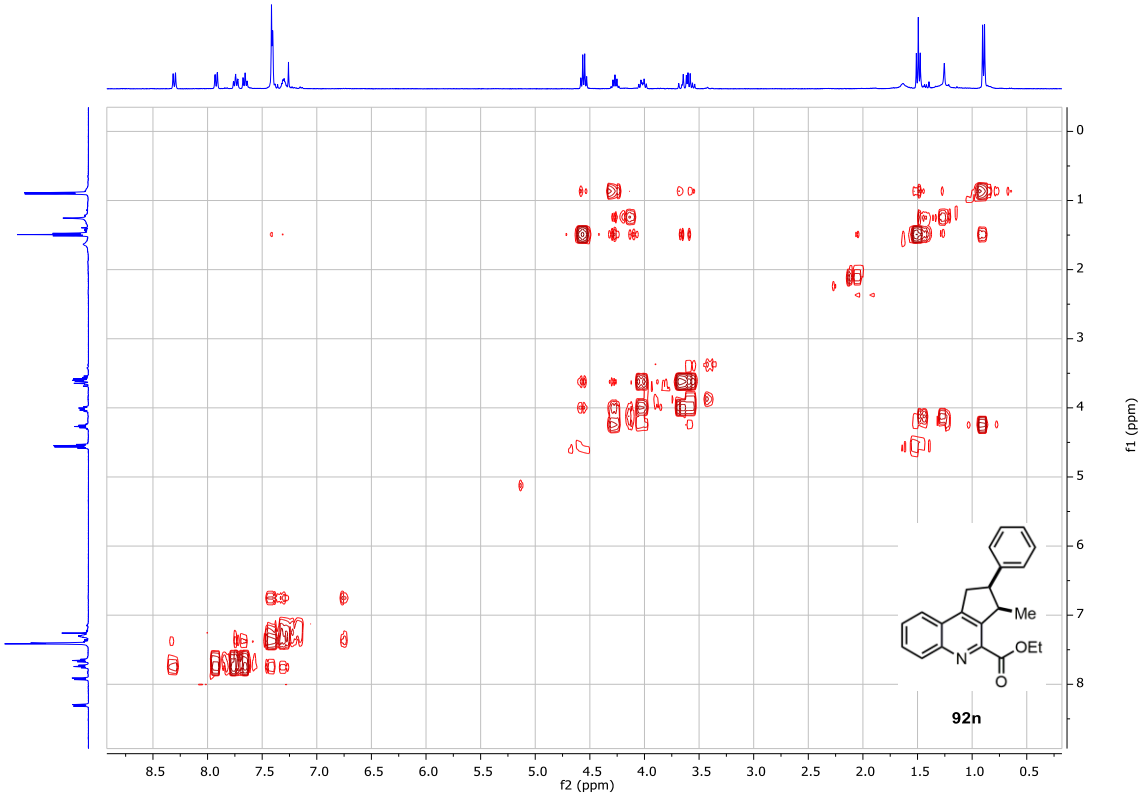
f2 (ppm)
f1 (ppm)
Me
OEt
O
N
92n

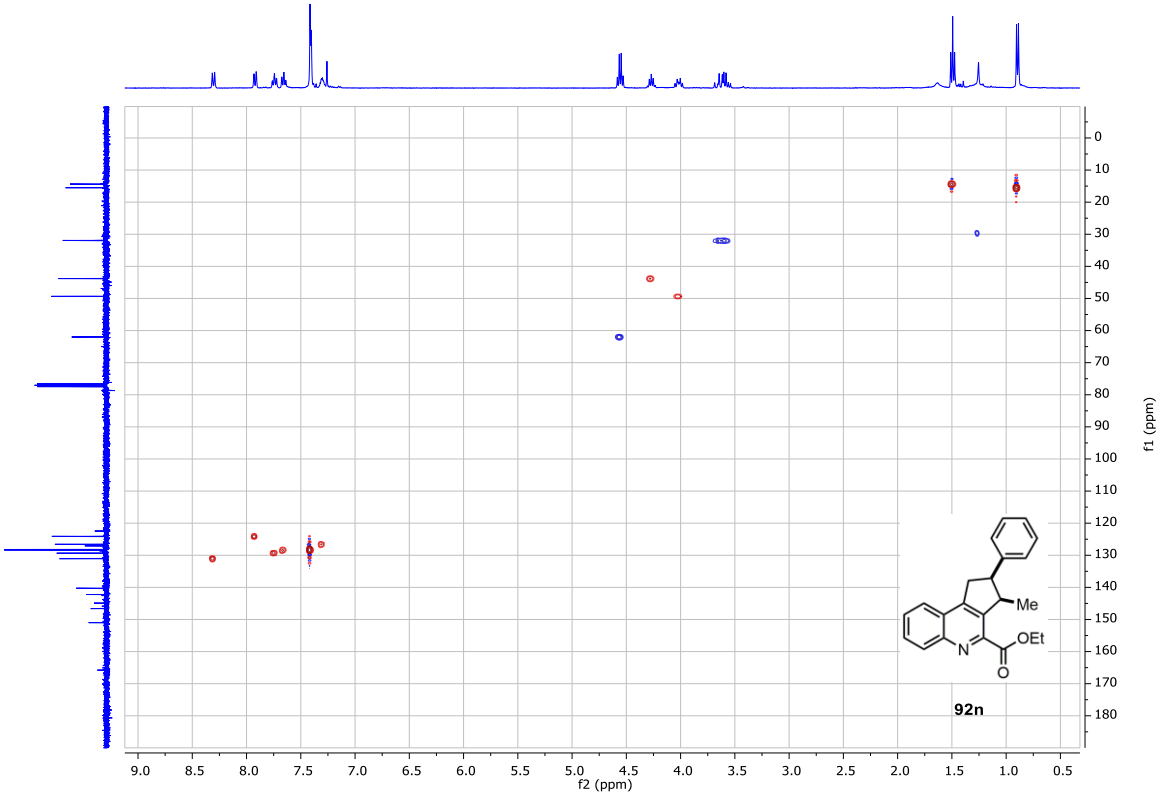
f2 (ppm)
f1 (ppm)
Me
OEt
O
N
92n

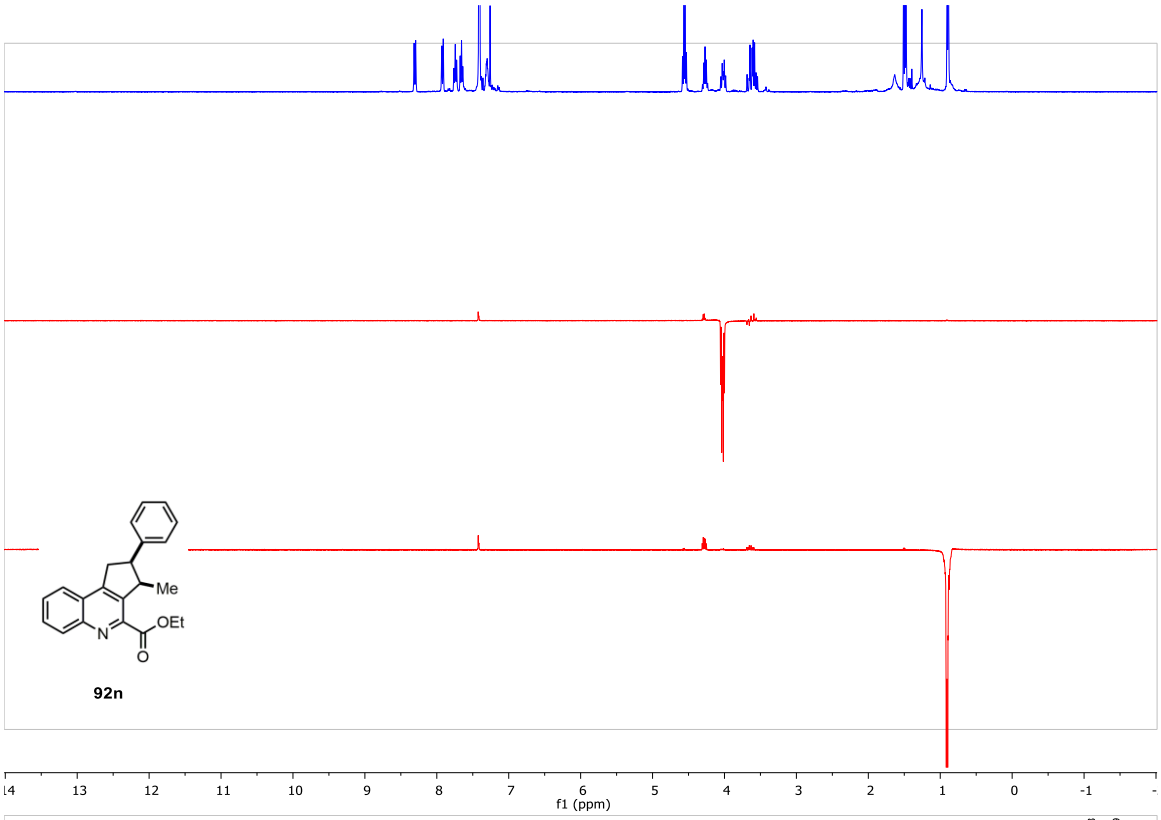
Me
OEt
O
N
92n
f1 (ppm)

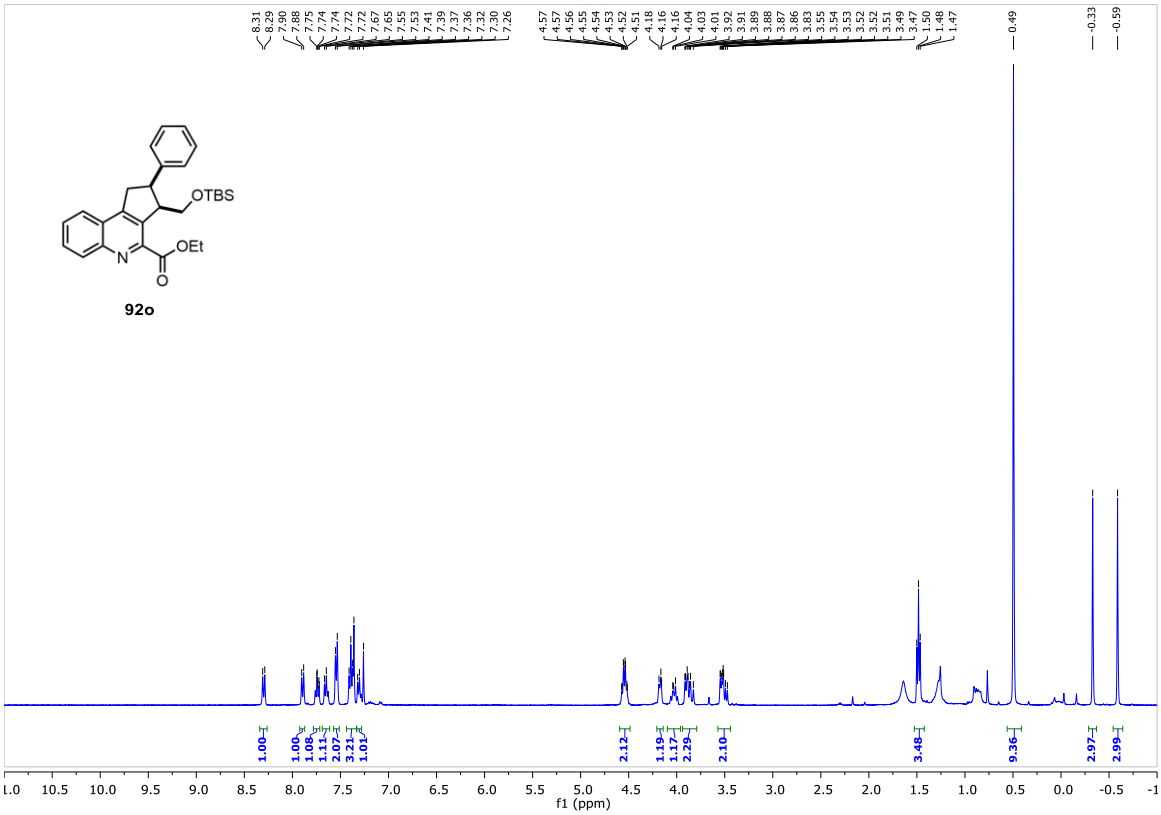
OTBS
OEt
O
N
92o
f1 (ppm)

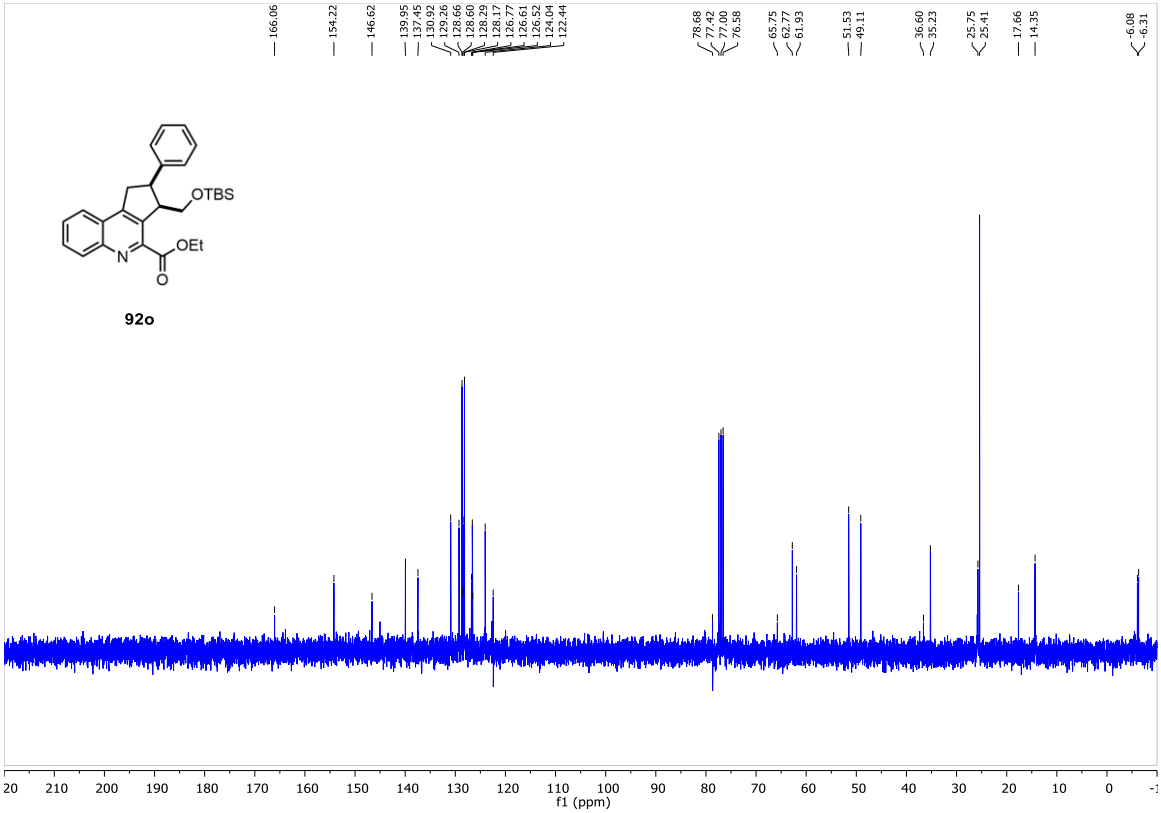
166.06
154.22
146.62
139.95
137.45
130.92
129.26
128.66
128.60
128.29
128.17
126.77
126.61
126.52
124.04
122.44
78.68
77.42
77.00
76.58
65.75
62.77
61.93
51.53
49.11
36.60
35.23
25.75
25.41
17.66
14.35
-6.08
-6.31
OTBS
OEt
N
O
92o
f1 (ppm)

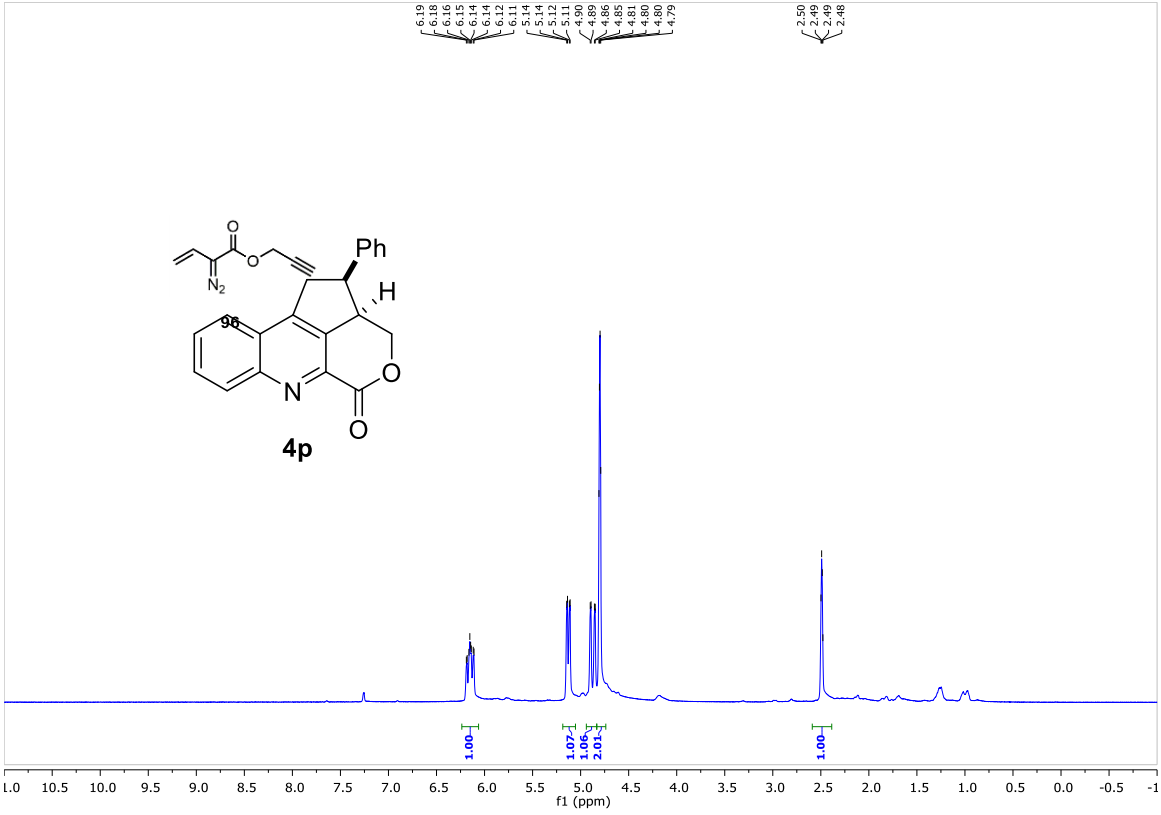
6.19
6.18
6.16
6.15
6.14
6.14
6.12
6.11
5.14
5.14
5.12
5.11
4.90
4.89
4.86
4.85
4.81
4.80
4.80
4.79
2.50
2.49
2.49
2.48
Ph
H
O
N2
N
O
O
4p
1.00
1.07
1.06
2.01
1.00
f1 (ppm)

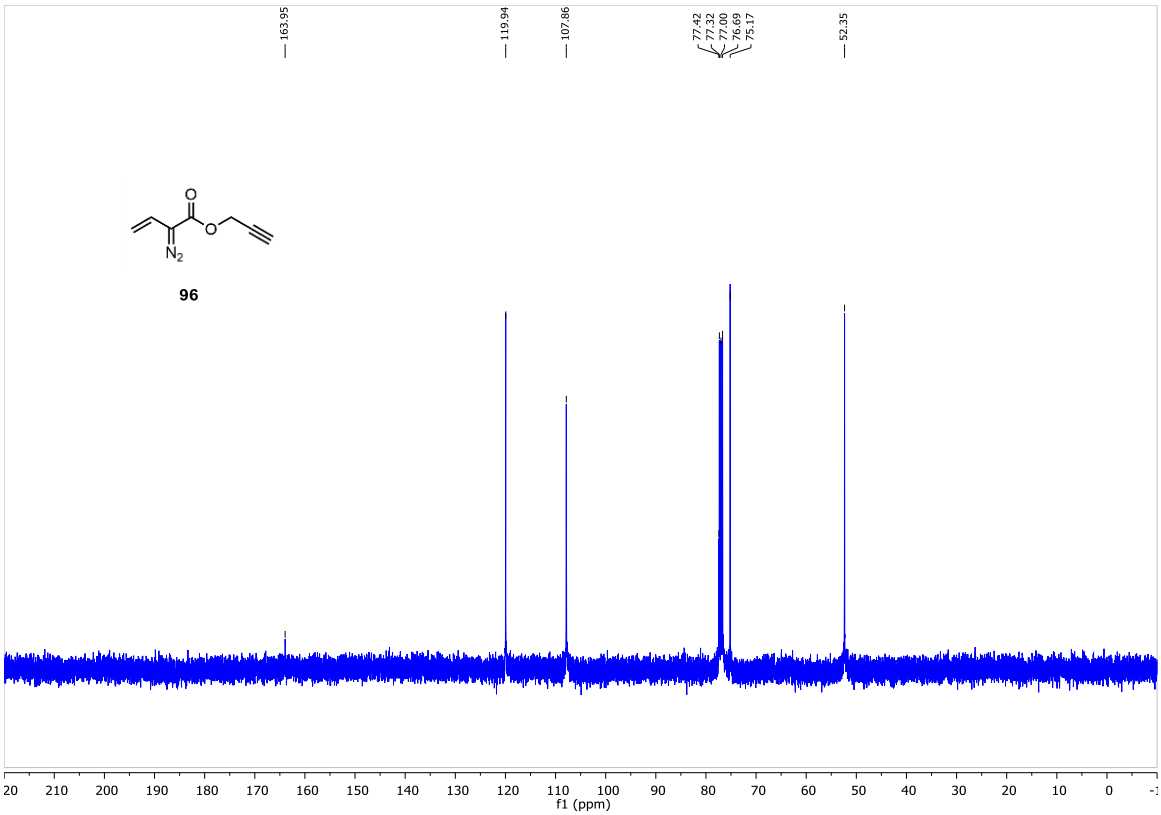
163.95
119.94
107.86
77.42
77.32
77.00
76.69
75.17
52.35
O
O
N2
96
f1 (ppm)

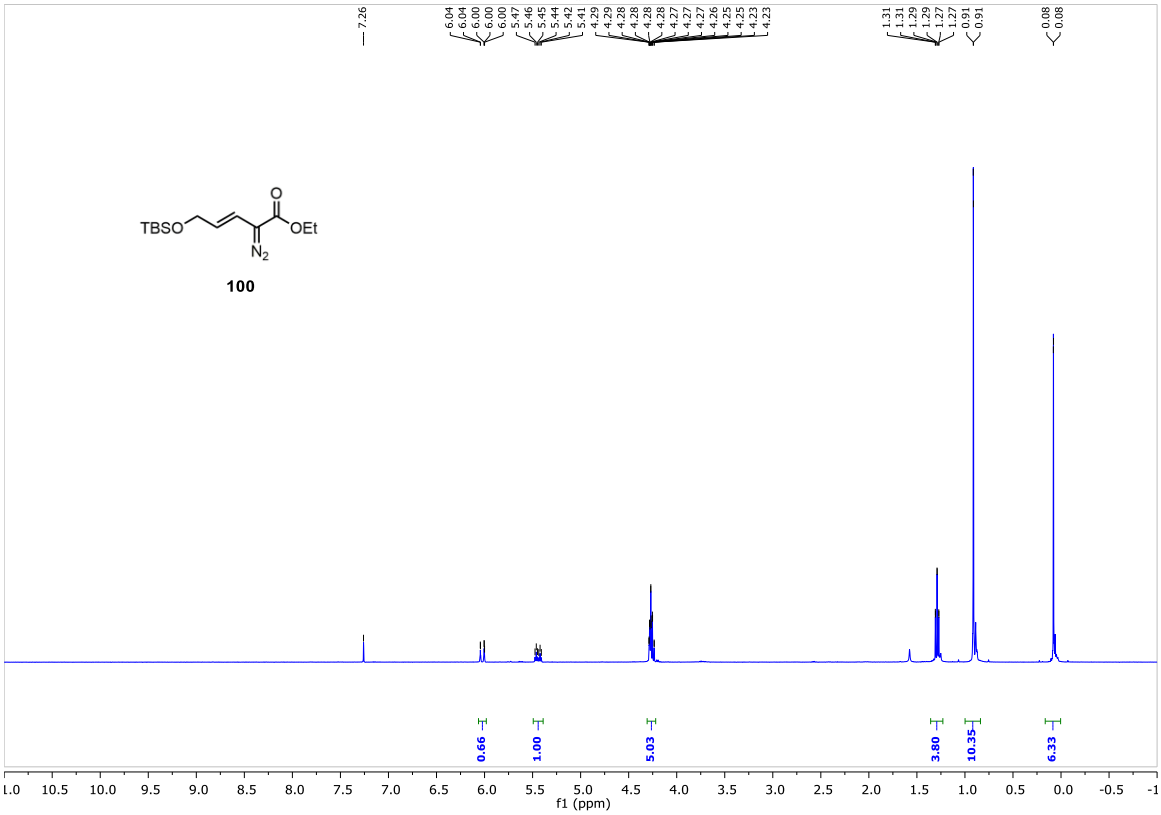
7.26
6.04
6.04
6.00
6.00
6.00
5.47
5.46
5.45
5.44
5.42
5.41
4.29
4.29
4.28
4.28
4.28
4.27
4.27
4.26
4.25
4.25
4.23
4.23
1.31
1.31
1.29
1.29
1.27
1.27
0.91
0.91
0.08
0.08
TBSO
O
OEt
N2
100
0.66
1.00
5.03
3.80
10.35
6.33
f1 (ppm)

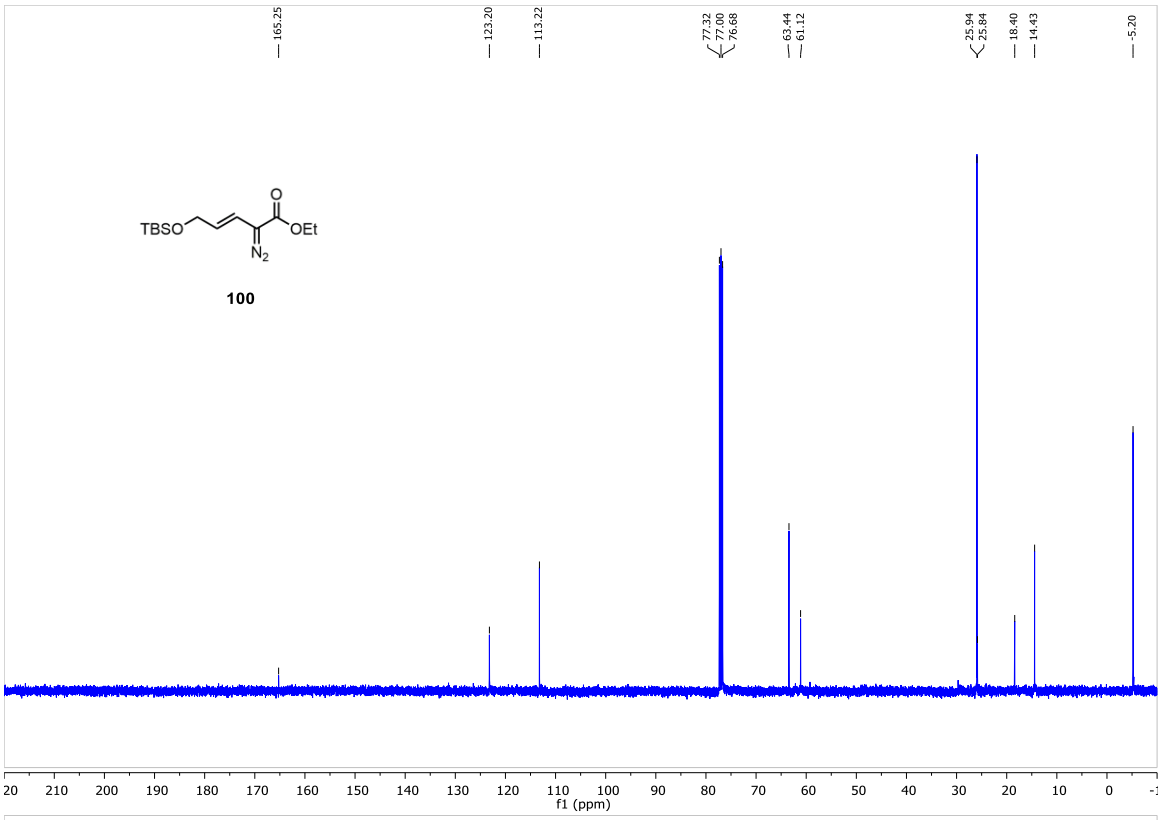
165.25
123.20
113.22
77.32
77.00
76.68
63.44
61.12
25.94
25.84
18.40
14.43
-5.20
TBSO
OEt
N2
O
100
f1 (ppm)

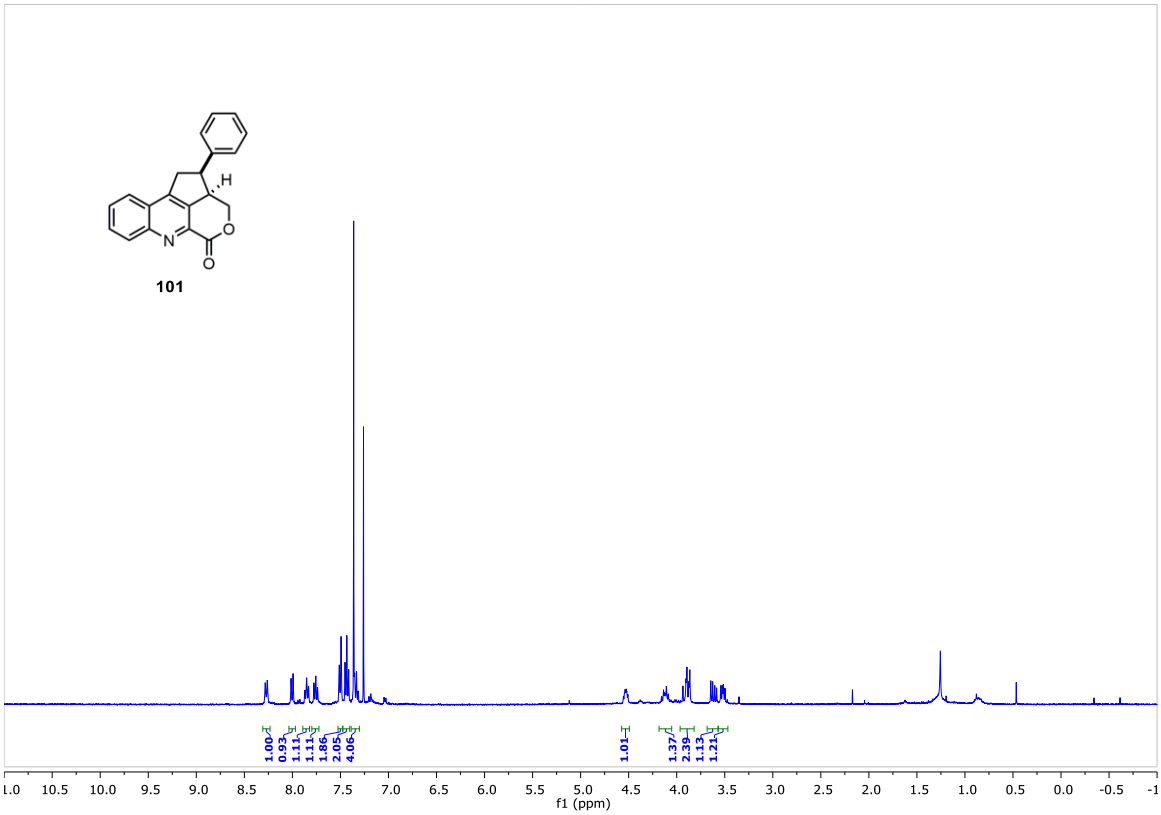
H
N
O
O
101
1.00
0.93
1.11
1.16
2.05
4.06
1.01
1.37
2.39
1.13
1.21
f1 (ppm)

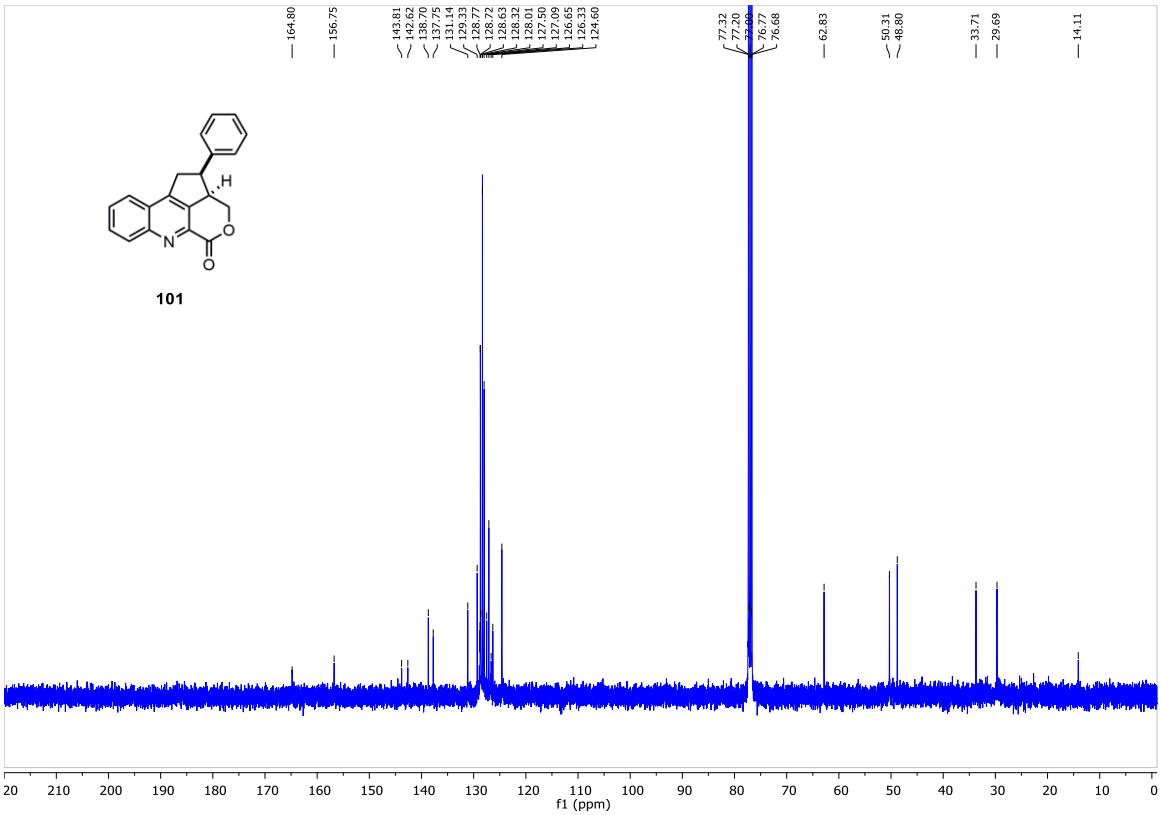
164.80
156.75
143.81
142.62
138.70
137.75
131.14
129.33
128.77
128.72
128.63
128.32
128.01
127.50
127.09
126.65
126.33
124.60
77.32
77.20
77.06
76.77
76.68
62.83
50.31
48.80
33.71
29.69
14.11
H
N
O
O
101
f1 (ppm)

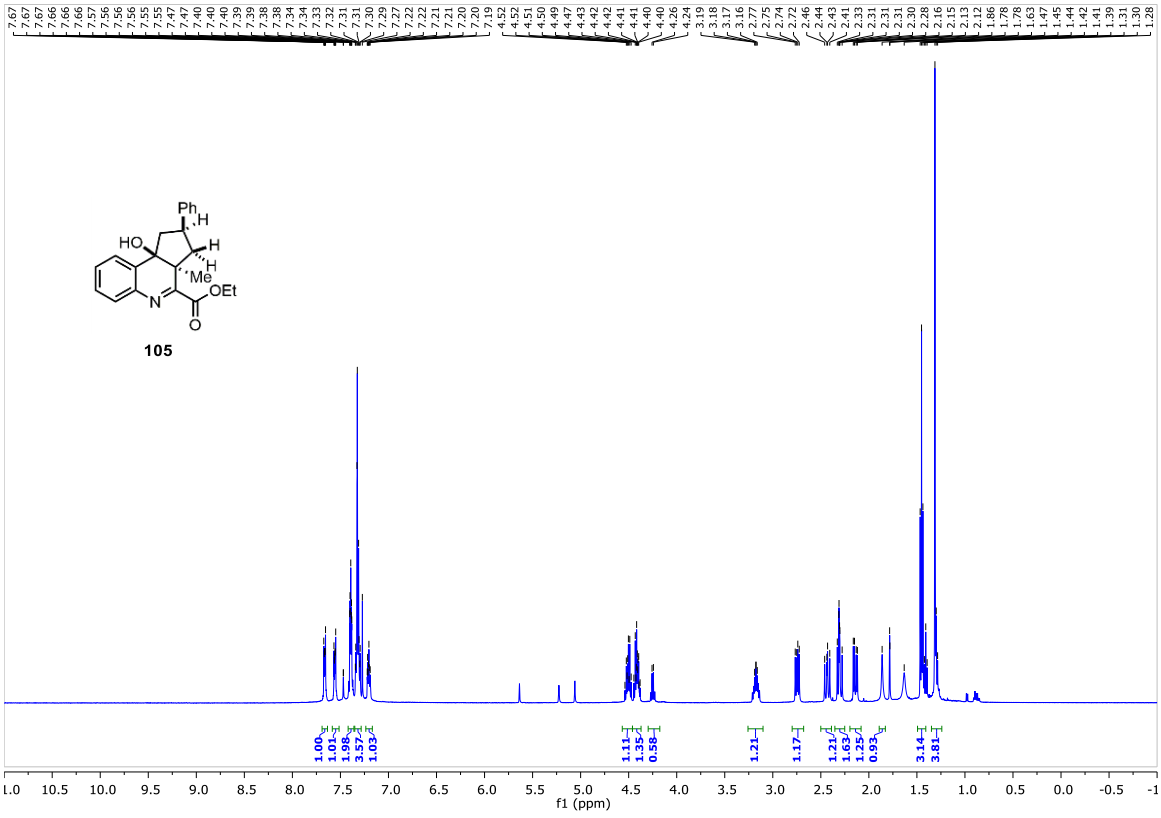
Ph
H
HO
H
H
Me
N
OEt
O
105
1.00
1.01
1.98
3.57
1.03
1.11
1.35
0.58
1.21
1.17
1.21
1.63
1.25
0.93
3.14
3.81
f1 (ppm)

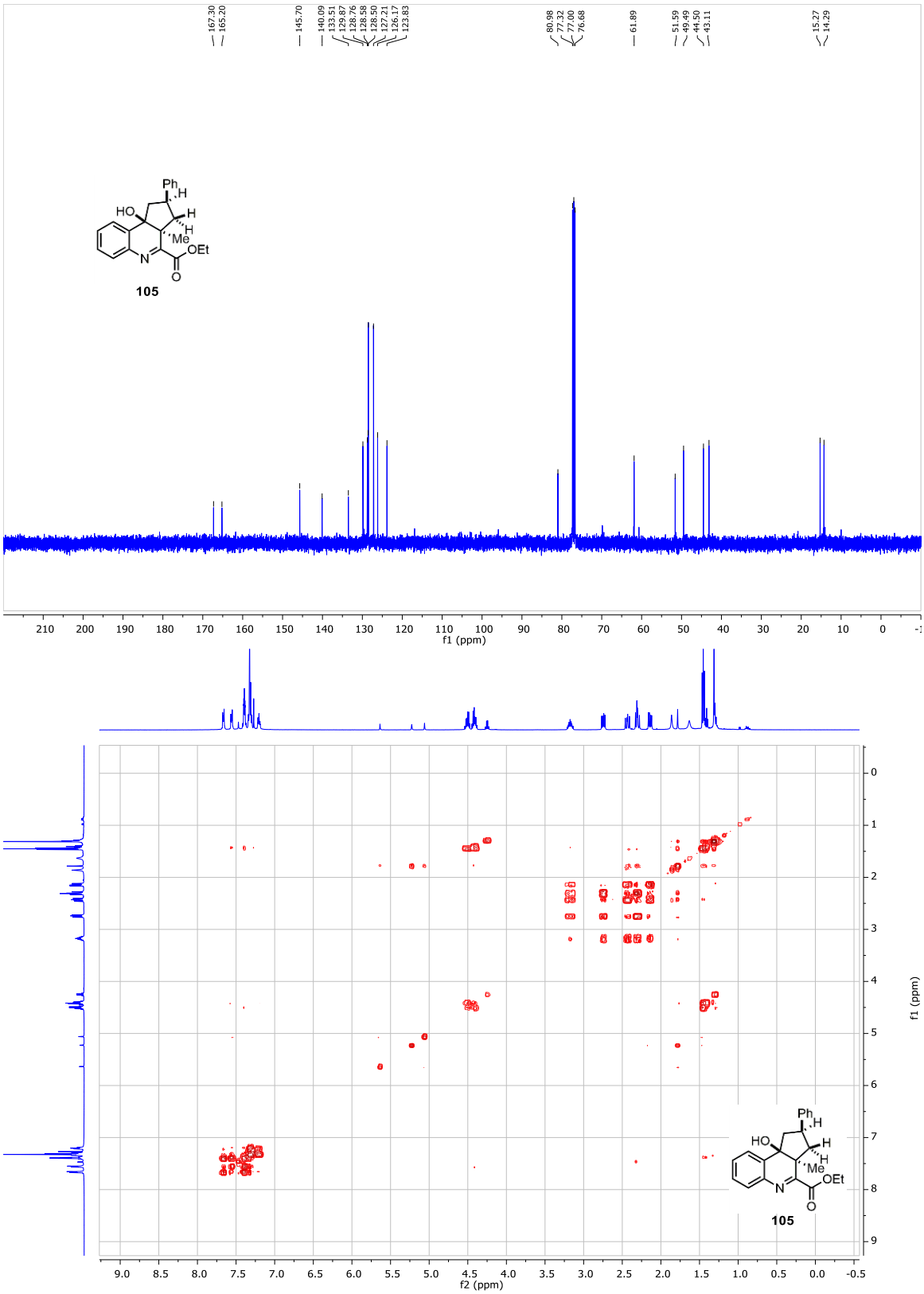
167.30
165.20
145.70
140.09
133.51
129.87
128.76
128.58
128.50
127.21
126.17
123.83
80.98
77.32
77.00
76.68
61.89
51.59
49.49
44.50
43.11
15.27
14.29
Ph
H
HO
H
H
Me
N
OEt
O
105
f1 (ppm)
f2 (ppm)

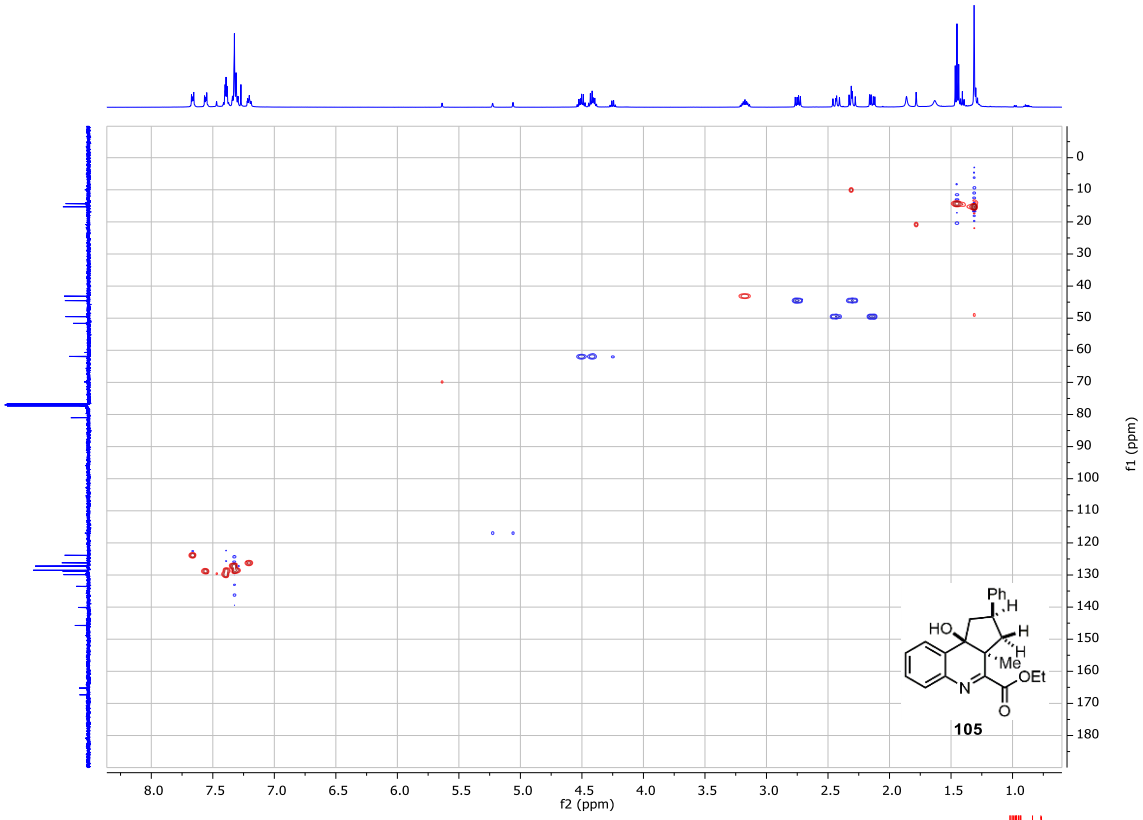
f2 (ppm)
f1 (ppm)
Ph
H
HO
H
H
Me
OEt
N
O
105

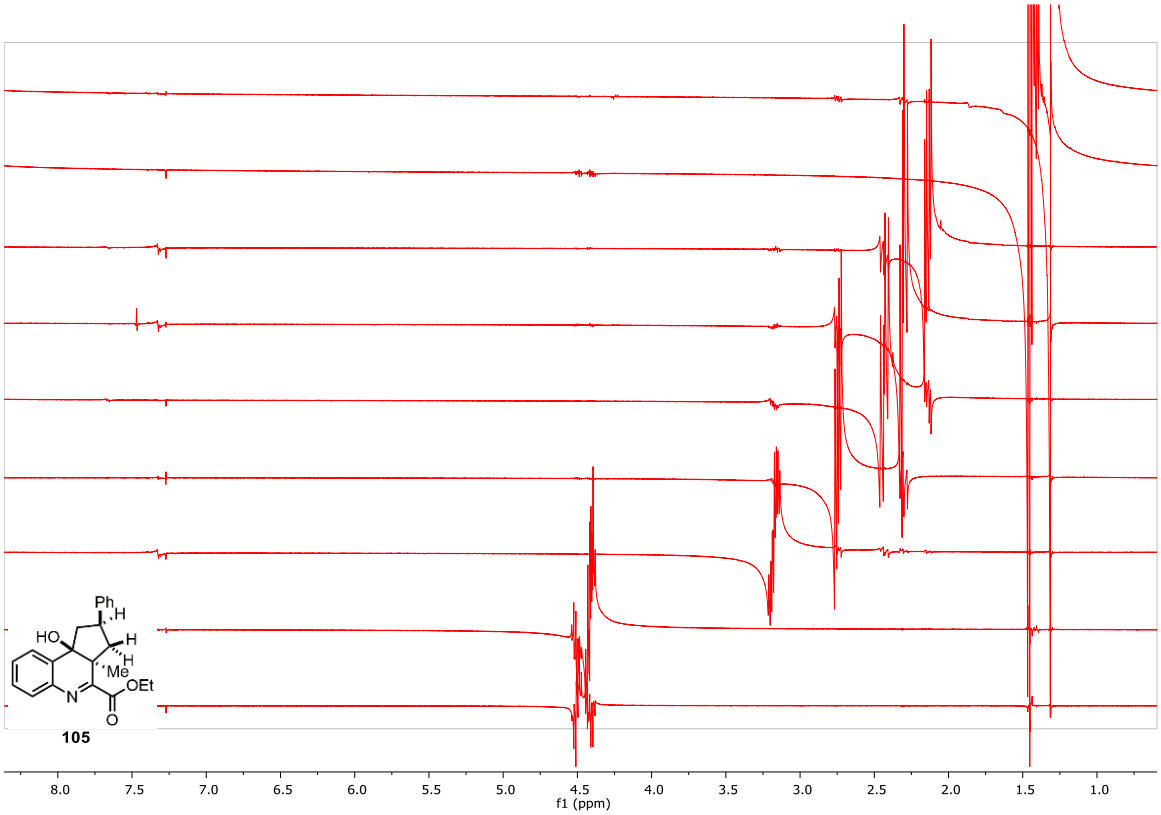
f1 (ppm)
Ph
H
HO
H
H
Me
OEt
N
O
105

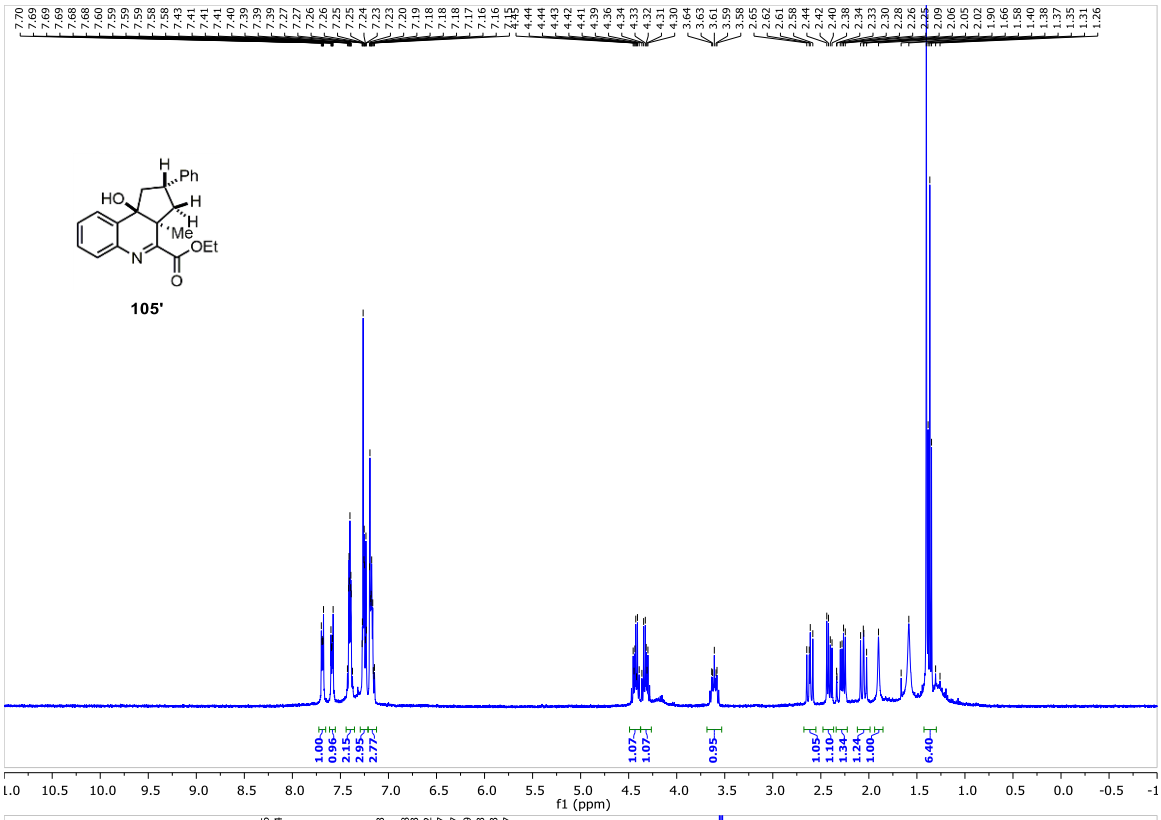
H
Ph
HO
H
H
Me
OEt
N
O
105'
1.00
0.96
2.15
2.95
2.77
1.07
1.07
0.95
1.05
1.10
1.34
1.24
1.00
6.40
f1 (ppm)

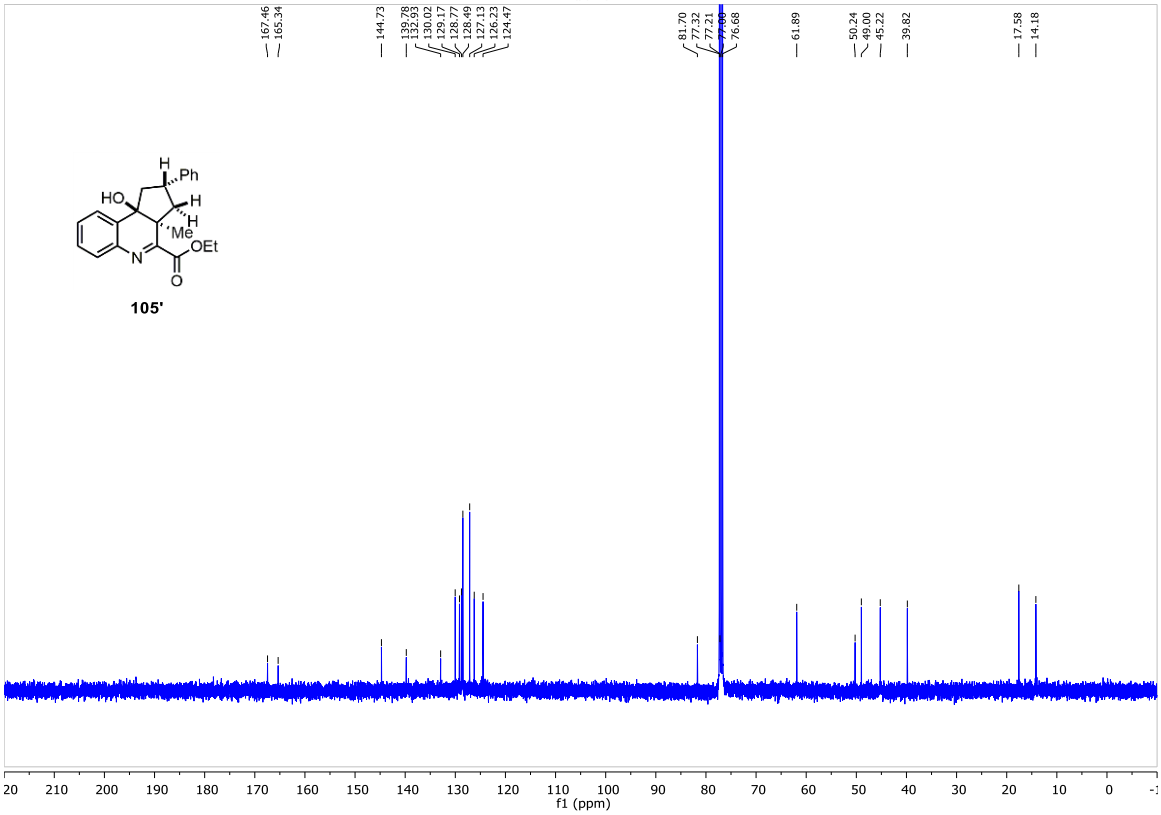
167.46
165.34
144.73
139.78
132.93
130.02
129.17
128.77
128.49
127.13
126.23
124.47
81.70
77.32
77.21
77.00
76.68
61.89
50.24
49.00
45.22
39.82
17.58
14.18
H
Ph
HO
H
H
Me
OEt
N
O
105'
f1 (ppm)

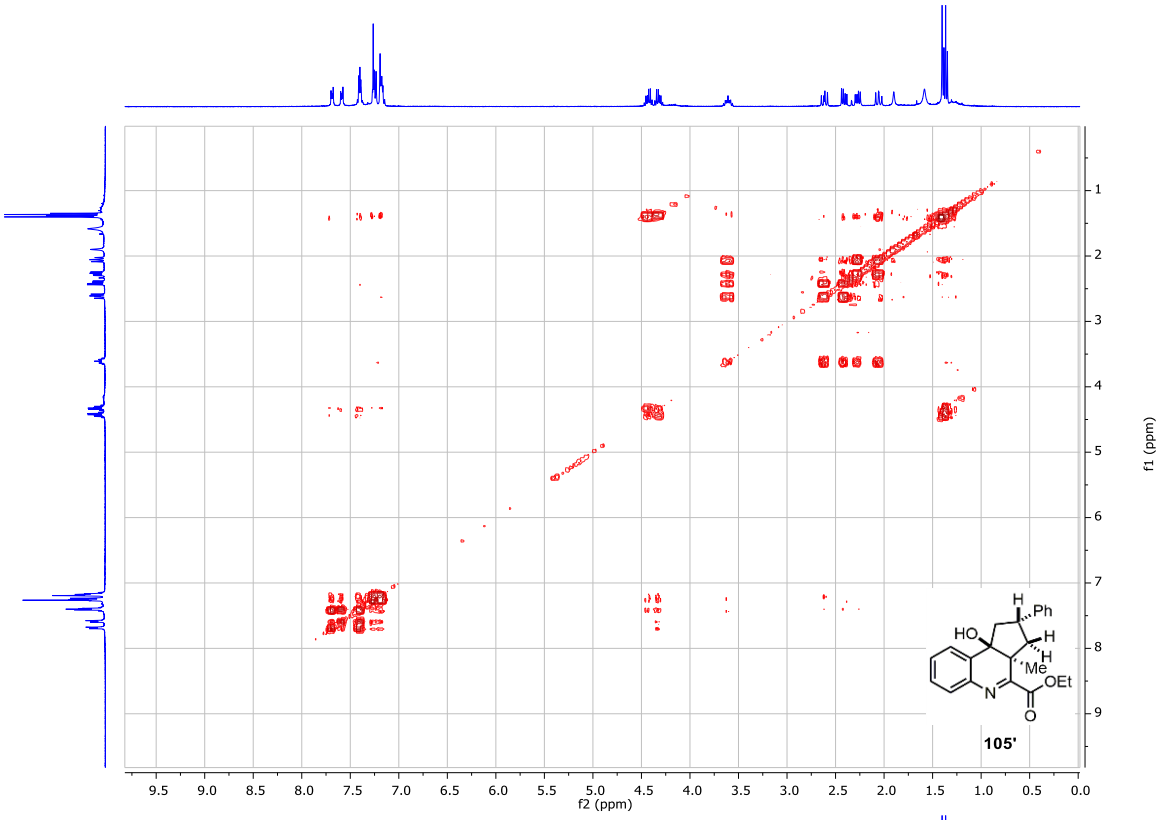
f2 (ppm)
f1 (ppm)
HO
H
Ph
H
H
Me
N
OEt
O
105'

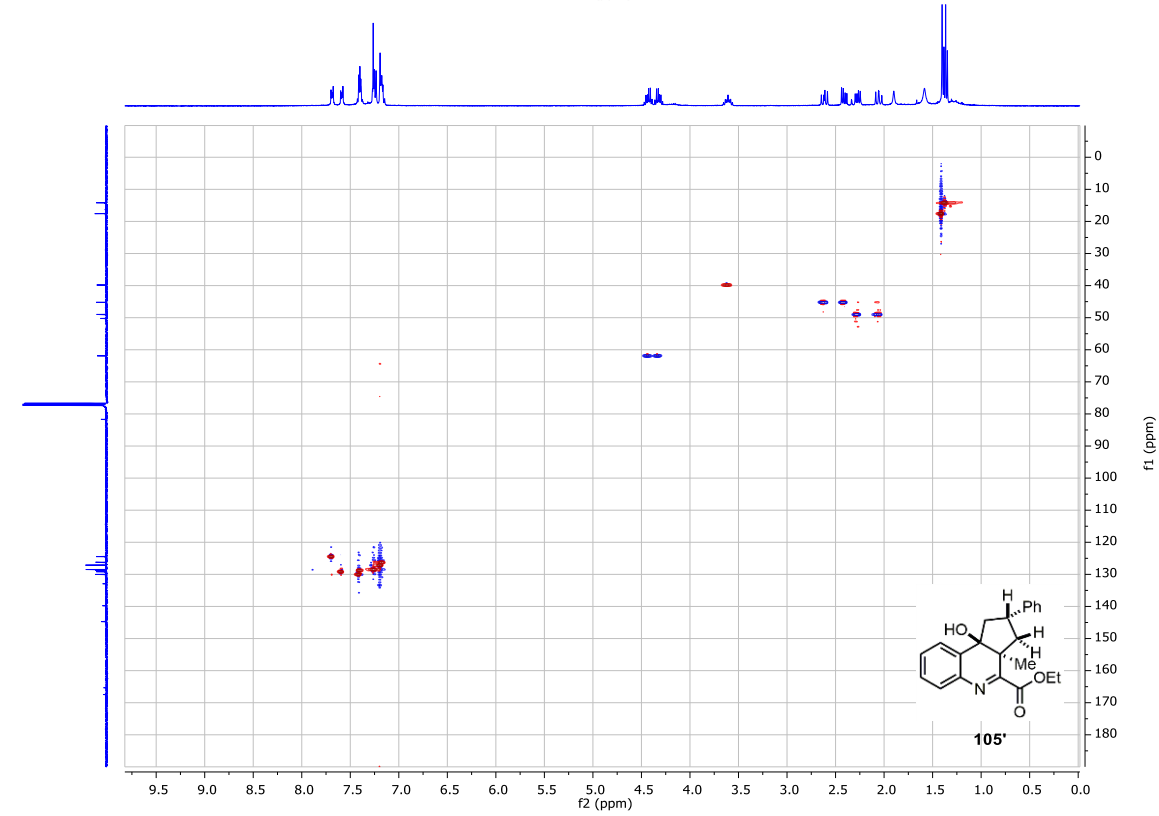
f2 (ppm)
f1 (ppm)
HO
H
Ph
H
H
Me
N
OEt
O
105'

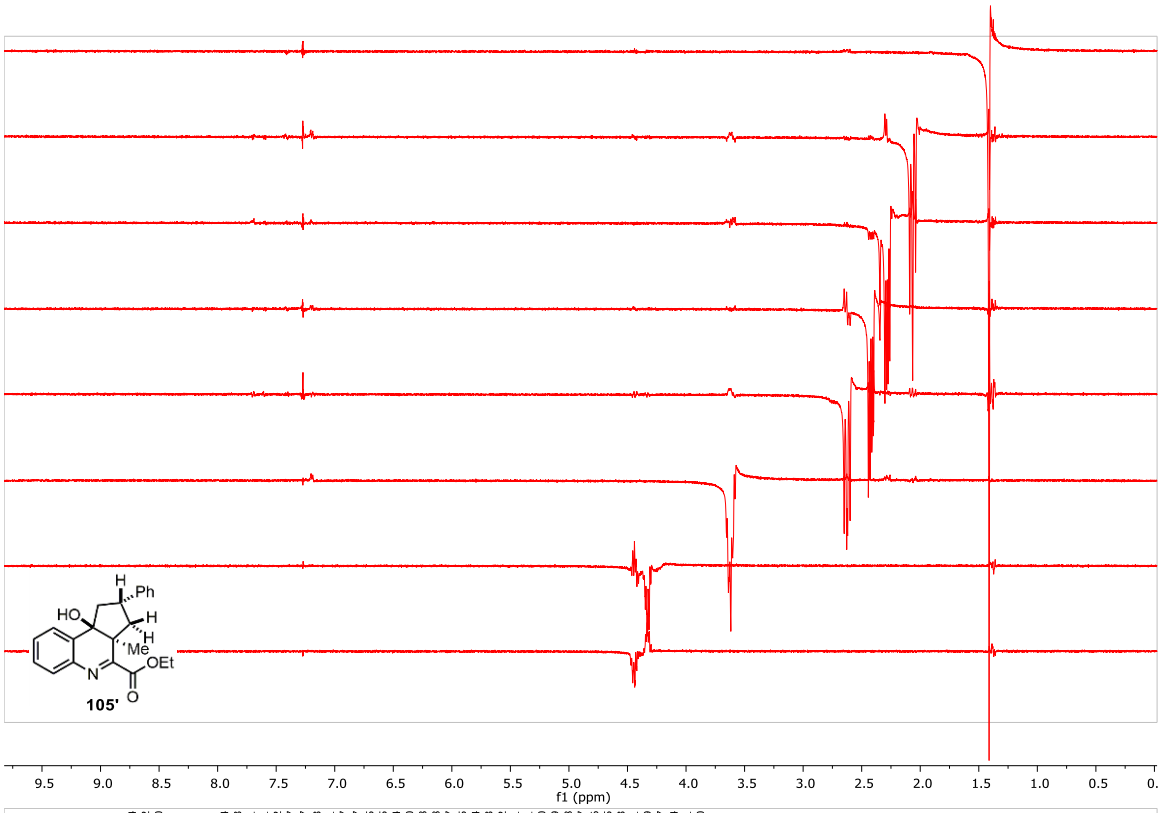
H
Ph
HO
H
H
Me
OEt
N
O
105'
9.5 9.0 8.5 8.0 7.5 7.0 6.5 6.0 5.5 5.0 4.5 4.0 3.5 3.0 2.5 2.0 1.5 1.0 0.5 0.
f1 (ppm)

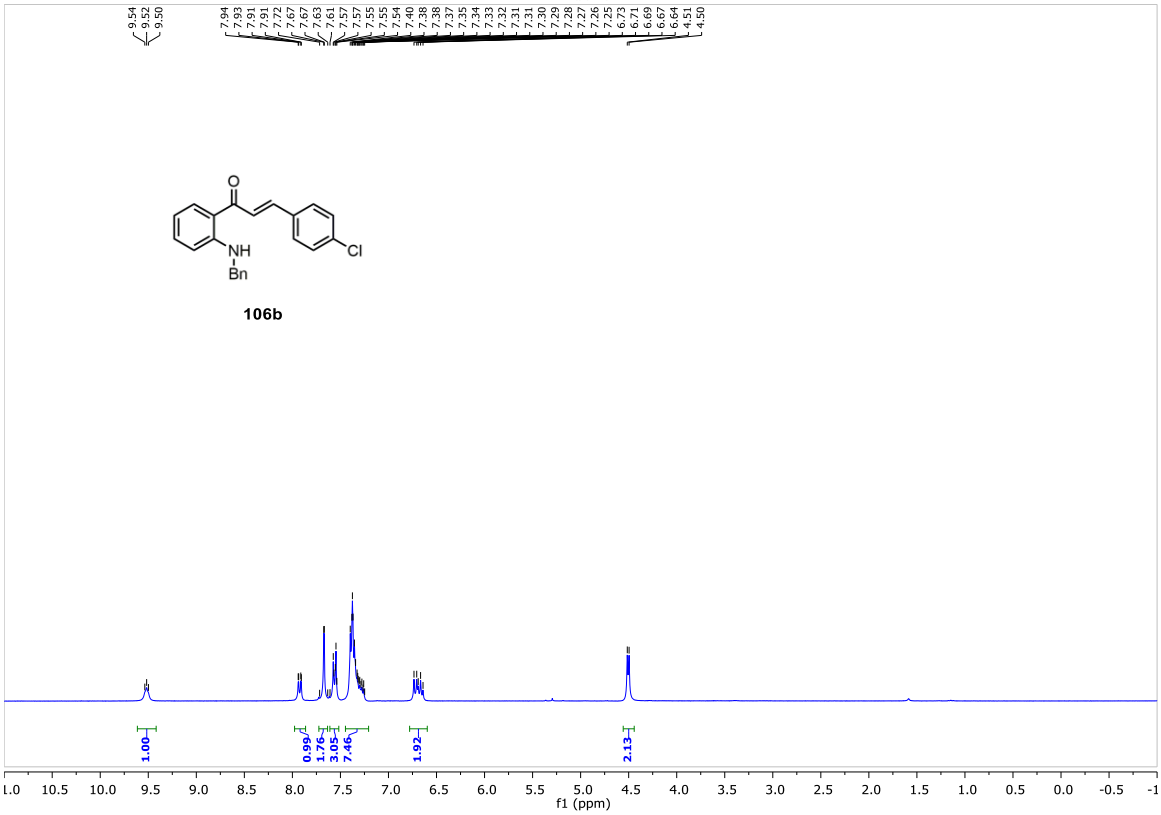
9.54
9.52
9.50
7.94
7.93
7.91
7.91
7.72
7.67
7.67
7.63
7.61
7.57
7.57
7.55
7.55
7.54
7.40
7.38
7.38
7.37
7.35
7.34
7.33
7.32
7.31
7.31
7.30
7.29
7.28
7.27
7.26
7.25
6.73
6.71
6.69
6.67
6.64
4.51
4.50
O
NH
Bn
Cl
106b
1.00
0.99
1.76
3.05
7.46
1.92
2.13
1.0 10.5 10.0 9.5 9.0 8.5 8.0 7.5 7.0 6.5 6.0 5.5 5.0 4.5 4.0 3.5 3.0 2.5 2.0 1.5 1.0 0.5 0.0 -0.5 -1
f1 (ppm)

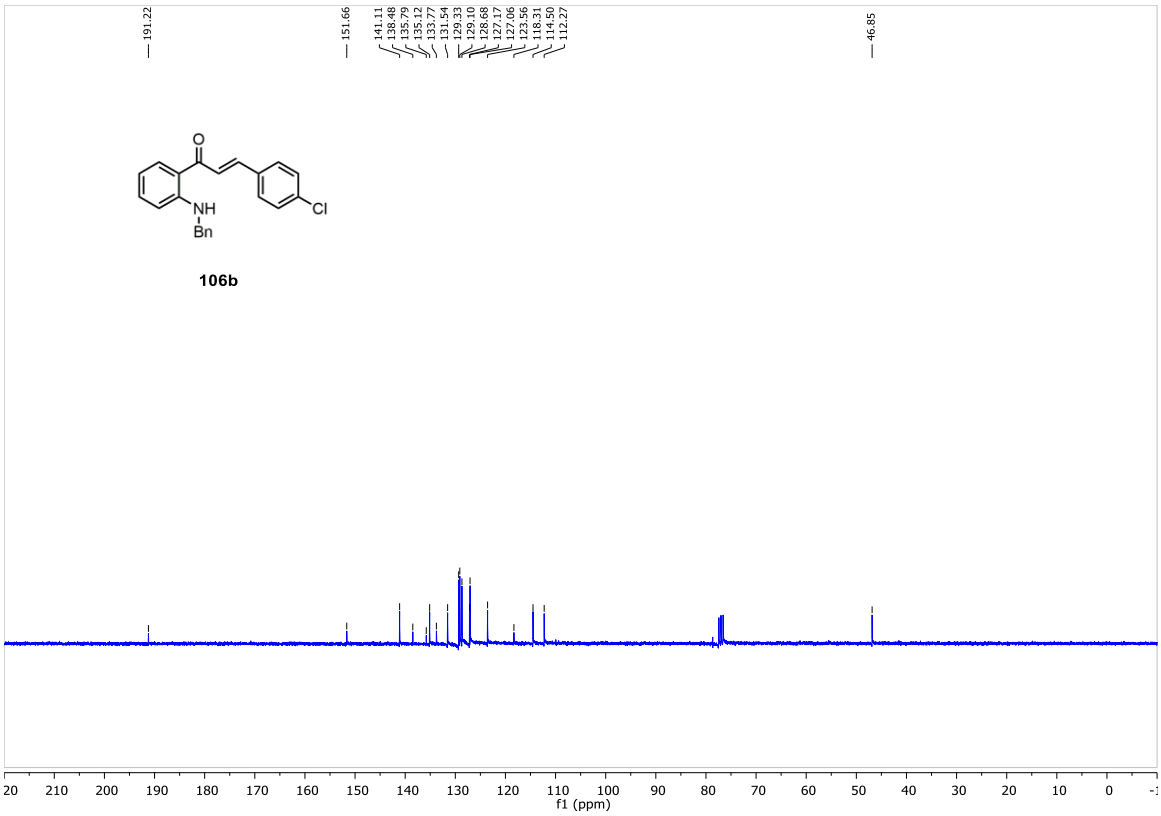
191.22
151.66
141.11
138.48
135.79
135.12
133.77
131.54
129.33
129.10
128.68
127.17
127.06
123.56
118.31
114.50
112.27
46.85
O
NH
Bn
Cl
106b
f1 (ppm)

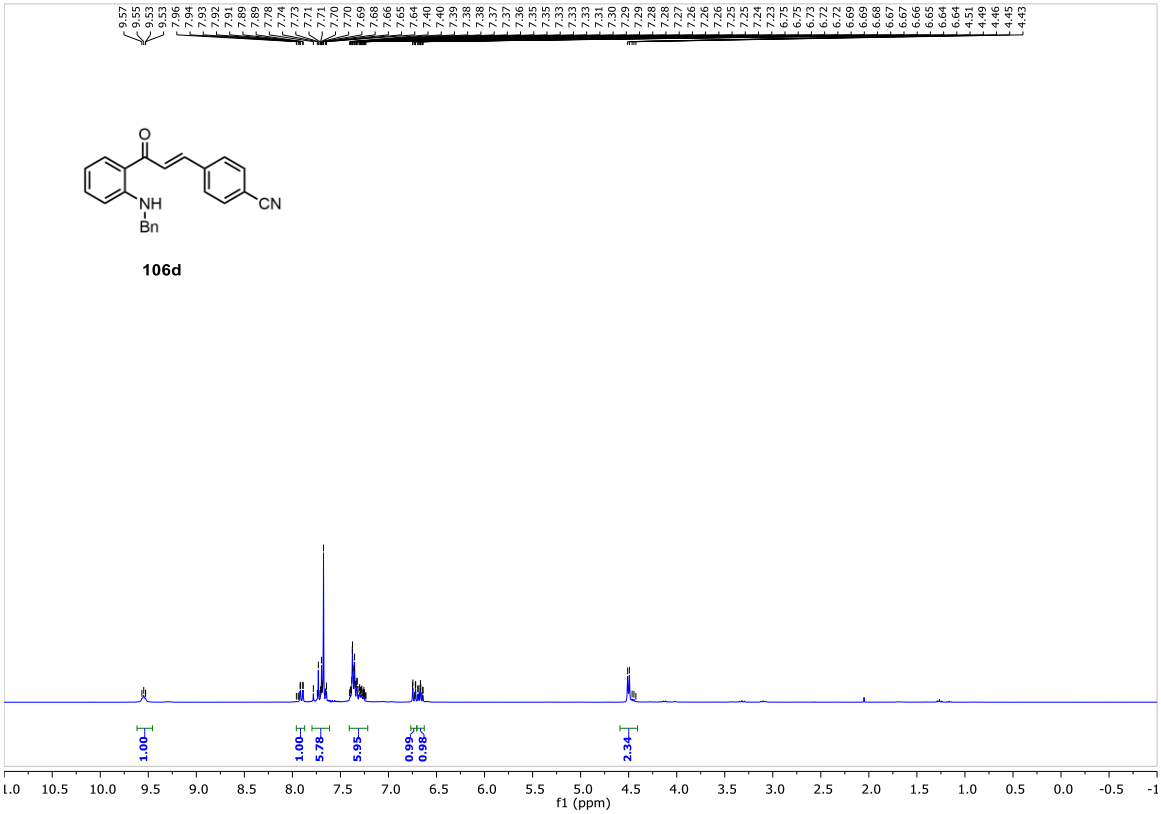
9.57
9.55
9.53
O
NH
Bn
CN
106d
1.00
1.00
5.78
5.95
0.99
0.98
2.34
f1 (ppm)

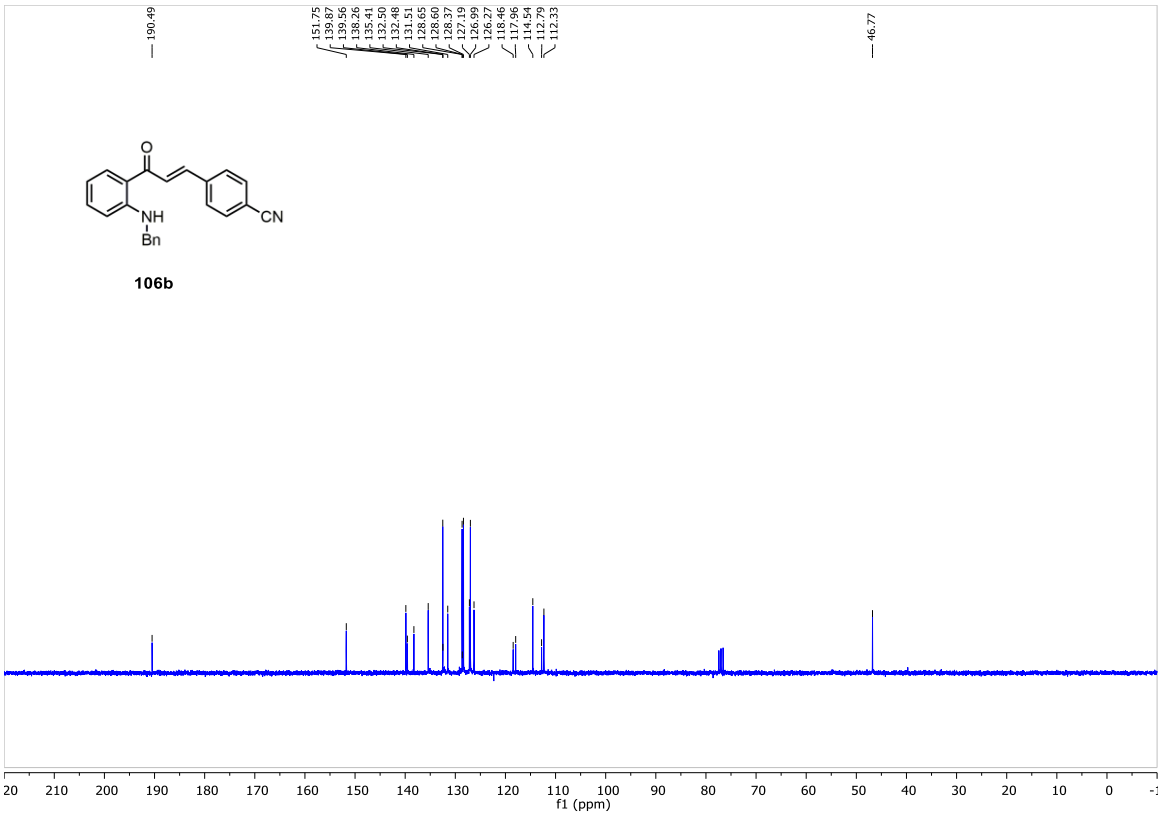
190.49
151.75
139.87
139.56
138.26
135.41
132.50
132.48
131.51
130.65
128.60
128.37
127.19
126.99
126.27
118.46
117.96
114.54
112.79
112.33
46.77
O
NH
Bn
CN
106b
f1 (ppm)

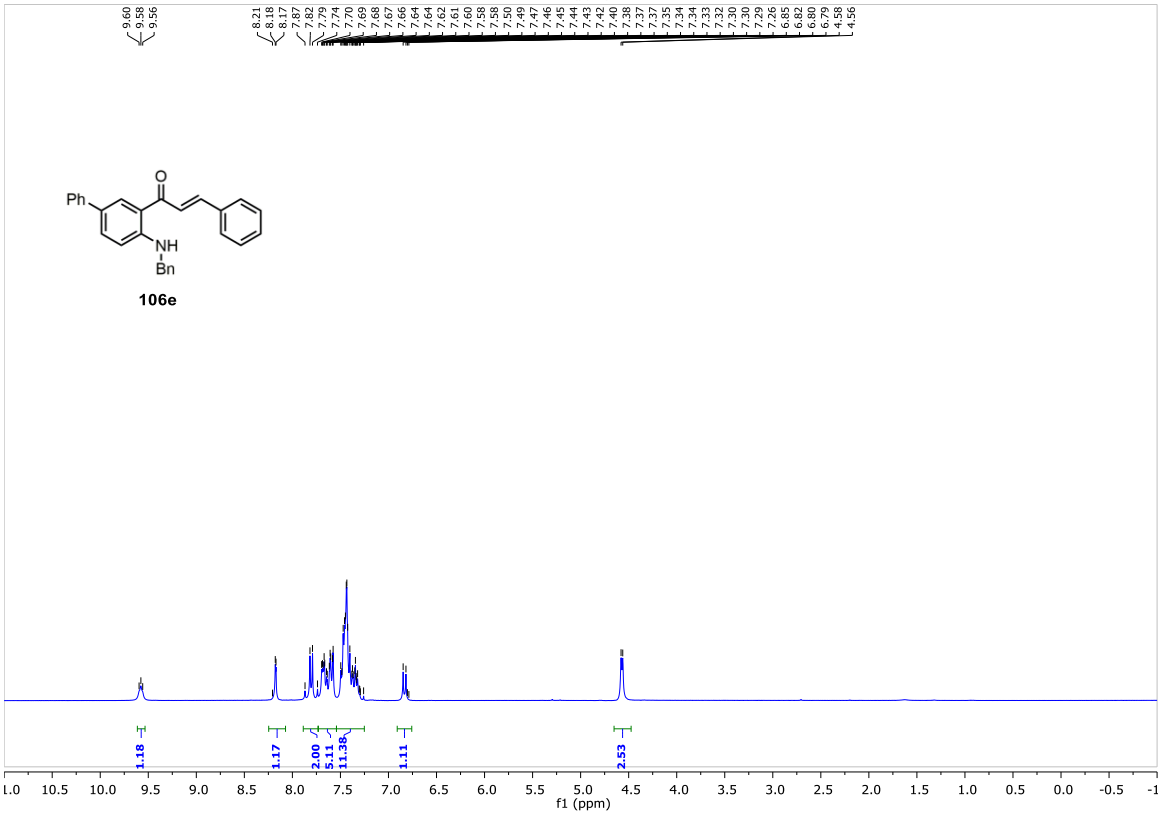
9.60
9.58
9.56
8.21
8.18
8.17
7.87
7.82
7.79
7.74
7.70
7.69
7.68
7.67
7.66
7.64
7.64
7.62
7.61
7.60
7.58
7.58
7.50
7.49
7.47
7.46
7.45
7.44
7.43
7.42
7.40
7.38
7.37
7.37
7.35
7.34
7.34
7.33
7.32
7.30
7.30
7.29
7.26
6.85
6.82
6.80
6.79
4.58
4.56
O
Ph
NH
Bn
106e
1.18
1.17
2.00
5.11
11.38
1.11
2.53
f1 (ppm)

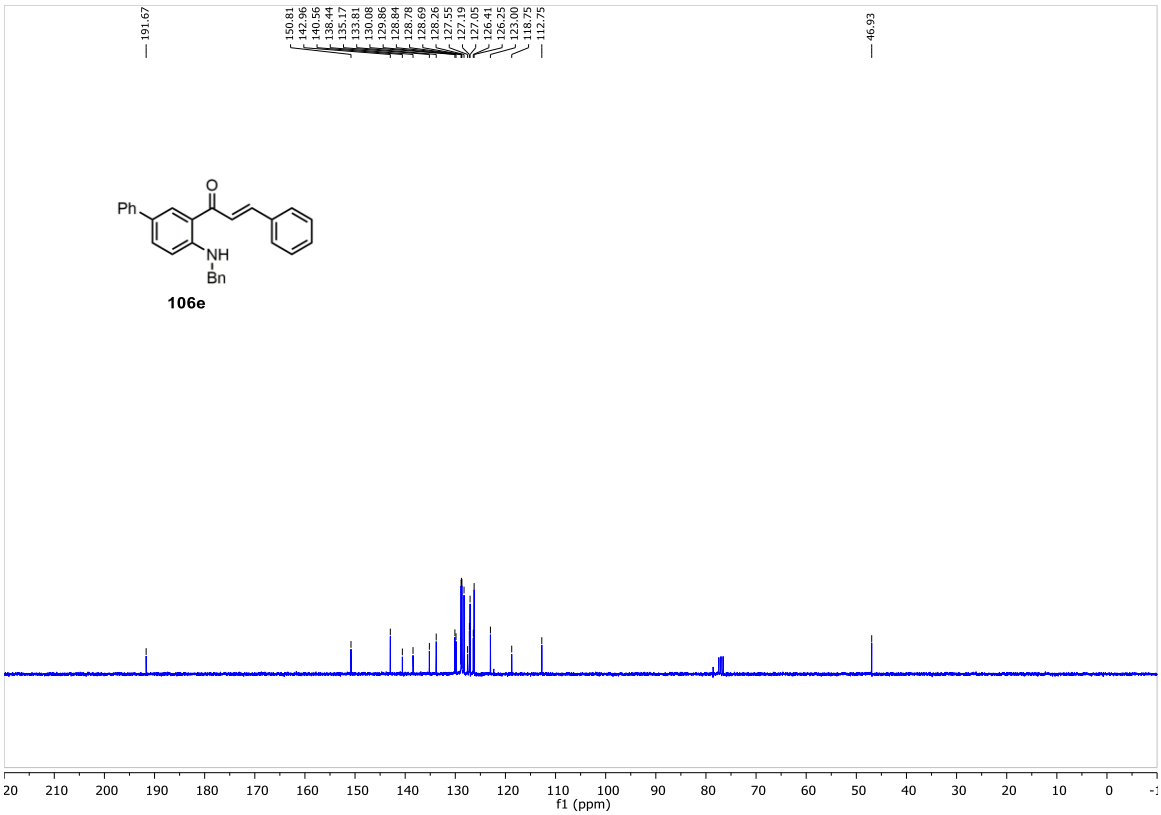
191.67
150.81
142.96
140.56
138.44
135.17
133.81
130.08
129.86
128.84
128.78
128.69
128.26
127.55
127.19
127.05
126.41
126.25
123.00
118.75
112.75
46.93
O
Ph
NH
Bn
106e
f1 (ppm)

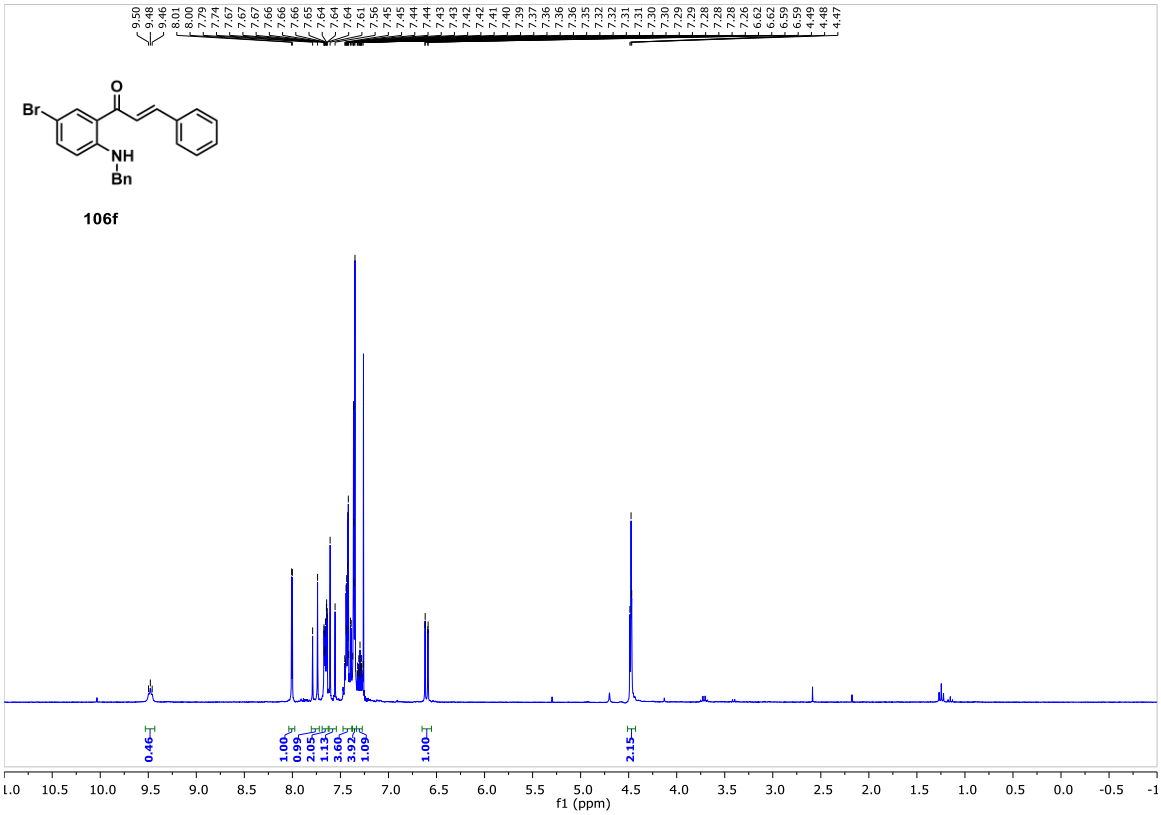
9.50
9.48
9.46
8.01
8.00
7.79
7.74
7.67
7.67
7.67
7.66
7.66
7.65
7.64
7.64
7.64
7.61
7.56
7.45
7.45
7.44
7.44
7.43
7.43
7.42
7.42
7.41
7.40
7.39
7.37
7.36
7.36
7.35
7.32
7.32
7.31
7.31
7.30
7.29
7.29
7.28
7.28
7.28
7.26
6.62
6.62
6.59
6.59
4.49
4.48
4.47
O
Br
NH
Bn
106f
0.46
1.00
0.99
2.05
1.13
3.60
3.32
1.09
1.00
2.15
f1 (ppm)

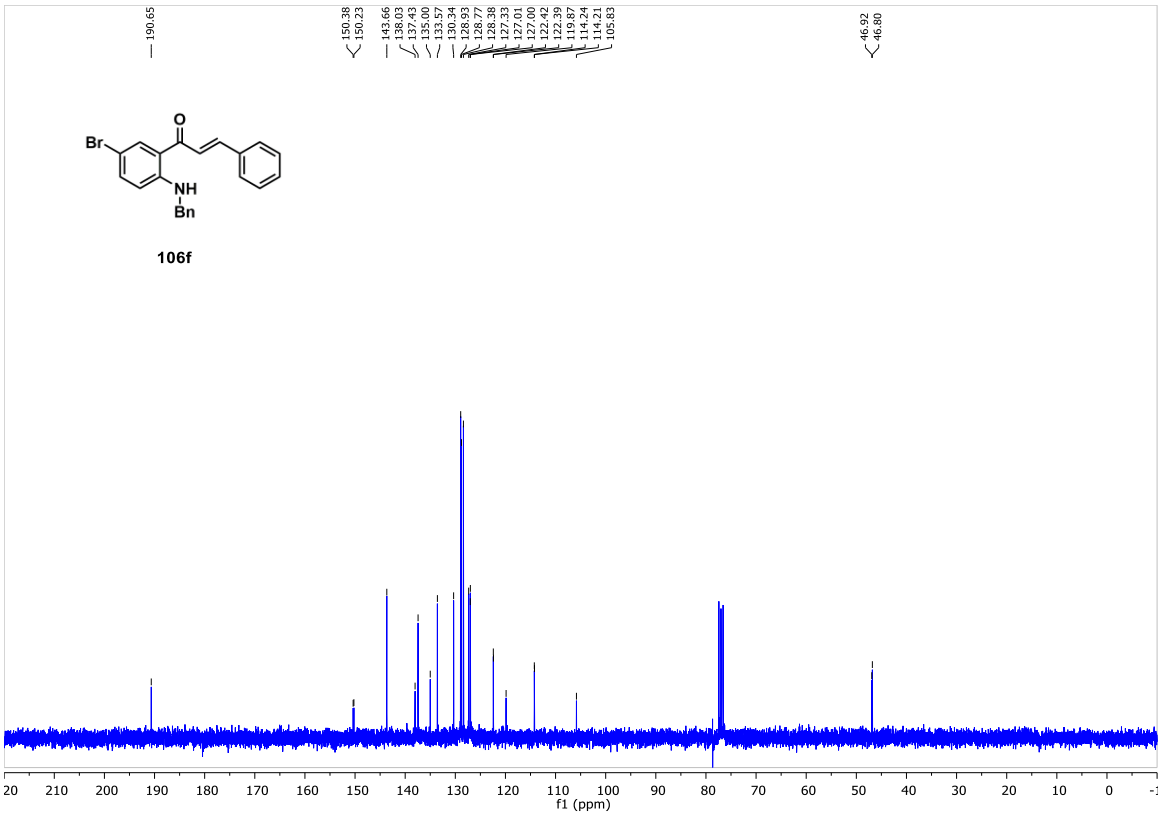
190.65
150.38
150.23
143.66
138.03
137.43
135.00
133.57
130.34
128.93
128.77
128.38
127.33
127.01
127.00
122.42
122.39
119.87
114.24
114.21
105.83
46.92
46.80
Br
O
NH
Bn
106f
f1 (ppm)

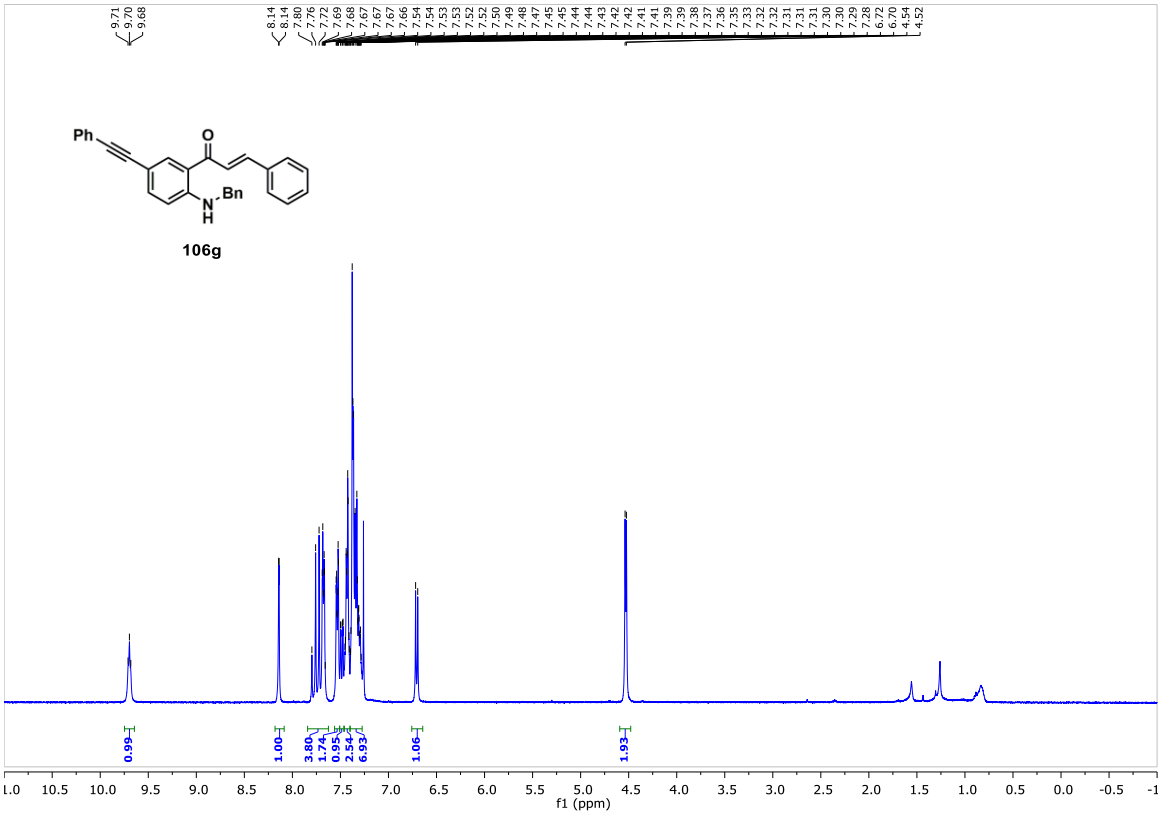
9.71
9.70
9.68
8.14
8.14
7.80
7.76
7.72
7.68
7.68
7.67
7.67
7.67
7.66
7.54
7.54
7.53
7.53
7.52
7.52
7.50
7.49
7.48
7.47
7.45
7.45
7.44
7.44
7.43
7.42
7.42
7.42
7.41
7.41
7.39
7.39
7.38
7.37
7.36
7.35
7.33
7.32
7.32
7.31
7.31
7.31
7.31
7.30
7.29
7.28
6.72
6.70
4.54
4.52
Ph
O
N
H
Bn
106g
0.99
1.00
3.80
1.74
0.95
2.54
6.93
1.06
1.93
f1 (ppm)

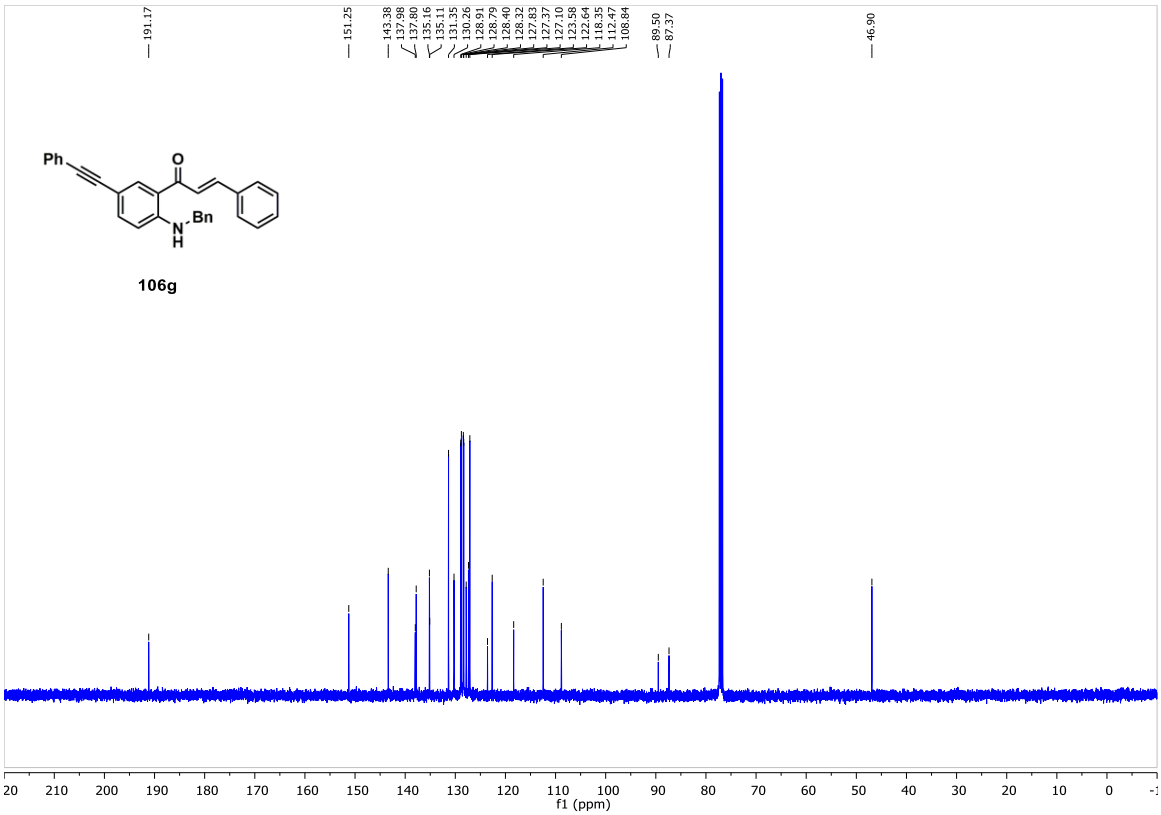
191.17
151.25
143.38
137.98
137.80
135.16
135.11
131.35
130.26
128.91
128.79
128.60
128.32
127.83
127.37
127.10
123.58
122.64
118.35
112.47
108.84
89.50
87.37
46.90
Ph
O
N
H
Bn
106g
f1 (ppm)

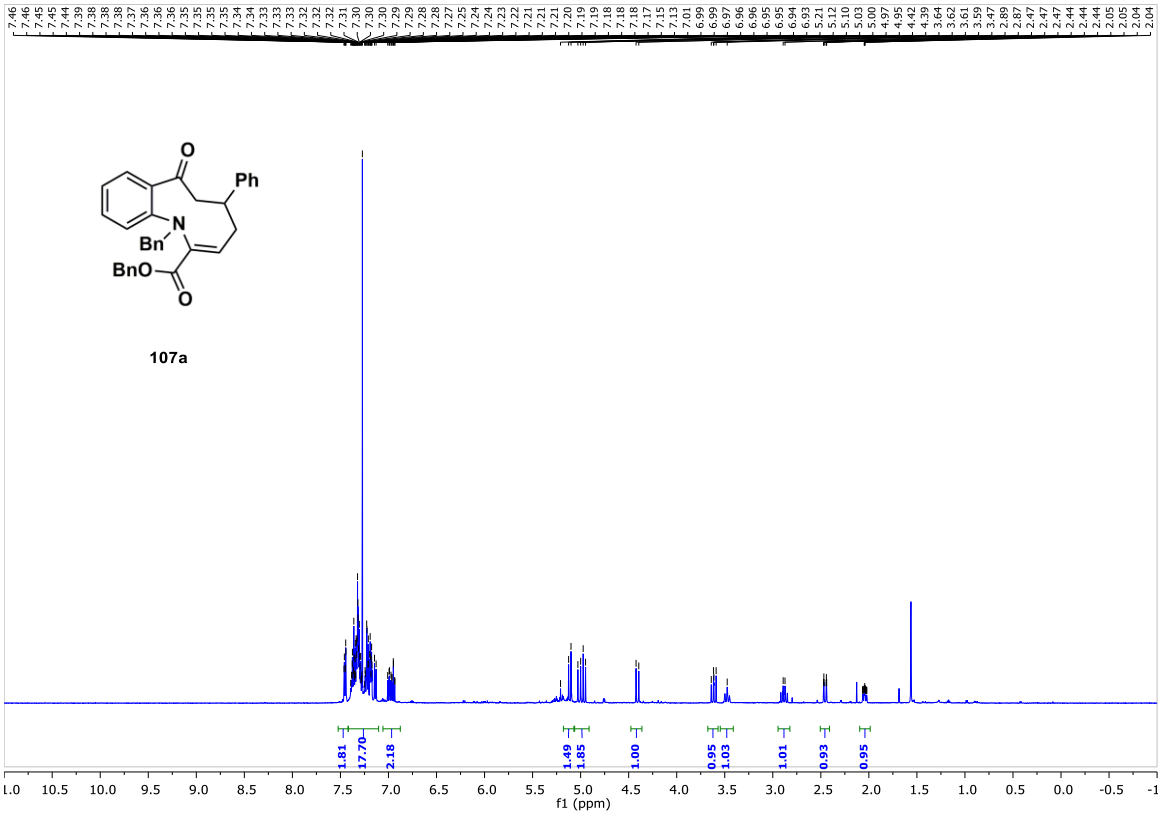
O
Ph
N
Bn
BnO
O
107a
1.81
17.70
2.18
1.49
1.85
1.00
0.95
1.03
1.01
0.93
0.95
f1 (ppm)

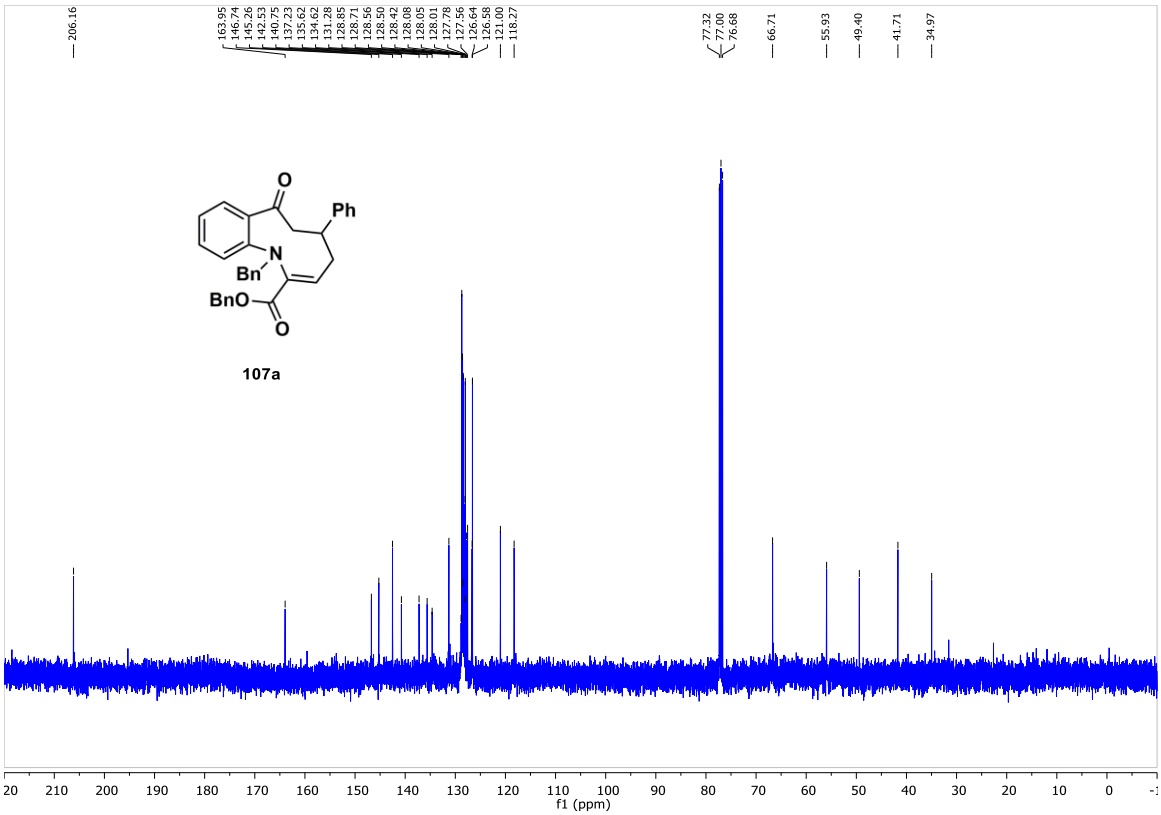
206.16
163.95
146.74
145.26
142.53
140.75
137.23
135.62
134.62
131.28
128.85
128.71
128.56
128.50
128.42
128.08
128.05
128.01
127.78
127.56
126.64
126.58
121.00
118.27
77.32
77.00
76.68
66.71
55.93
49.40
41.71
34.97
O
Ph
N
Bn
BnO
O
f1 (ppm)

107a

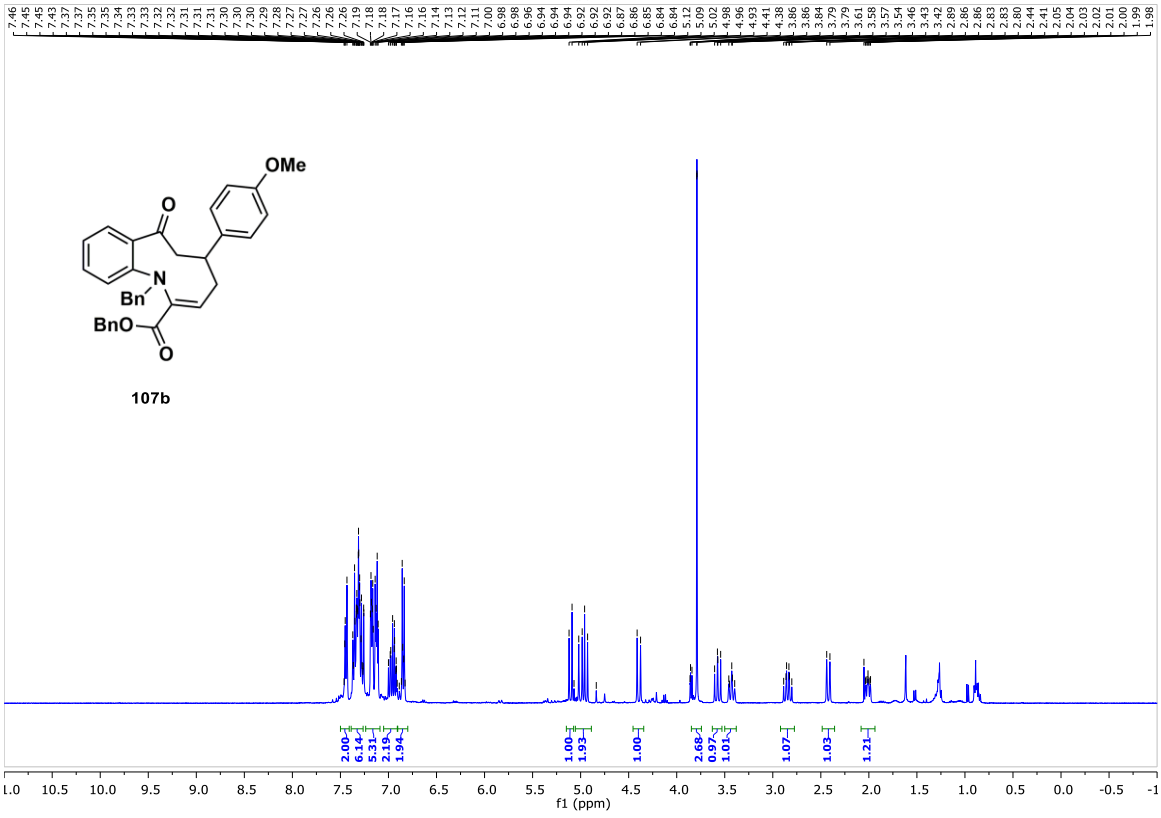
OMe
O
N
Bn
BnO
O
2.00
6.14
5.31
2.19
1.94
1.00
1.93
1.00
2.68
0.97
1.01
1.07
1.03
1.21
f1 (ppm)

107b

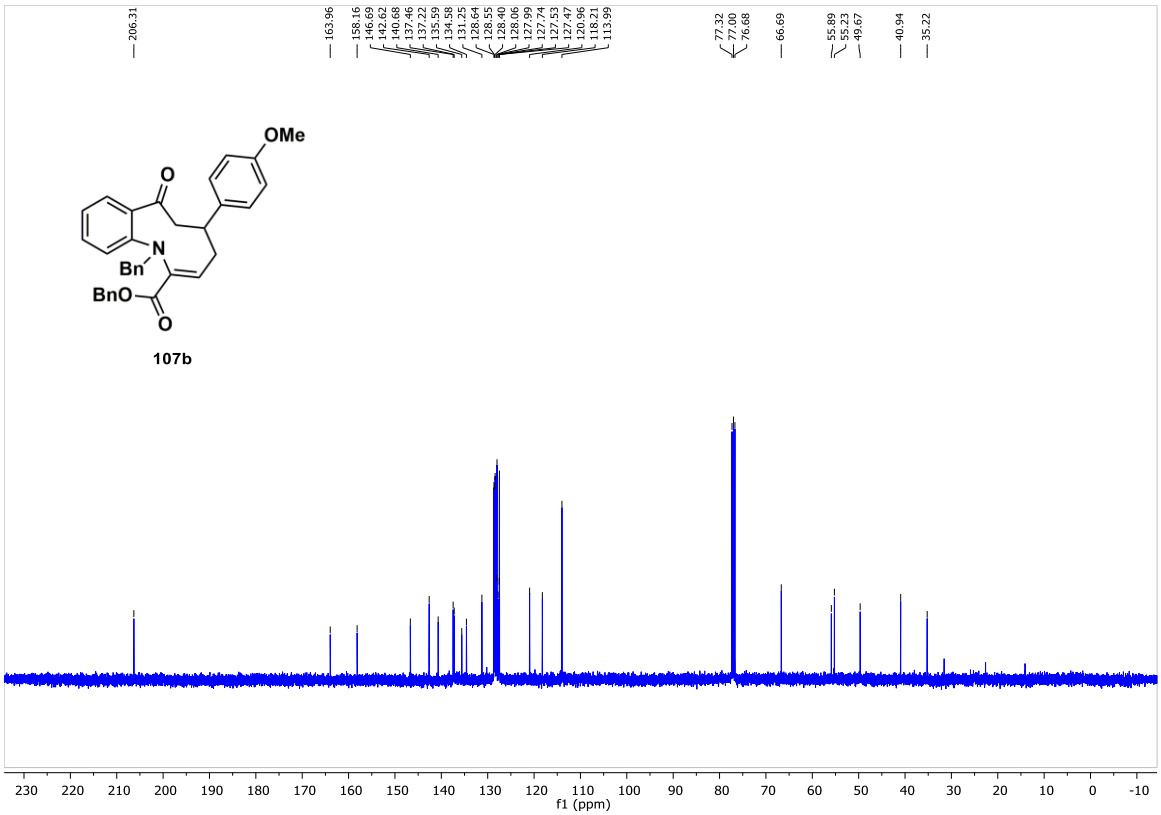
206.31
163.96
158.16
146.69
142.62
140.68
137.46
137.22
135.59
134.58
131.25
128.64
128.55
128.40
128.06
127.99
127.74
127.53
127.47
120.96
118.21
113.99
77.32
77.00
76.68
66.69
55.89
55.23
49.67
40.94
35.22
OMe
O
N
Bn
BnO
O
107b
f1 (ppm)

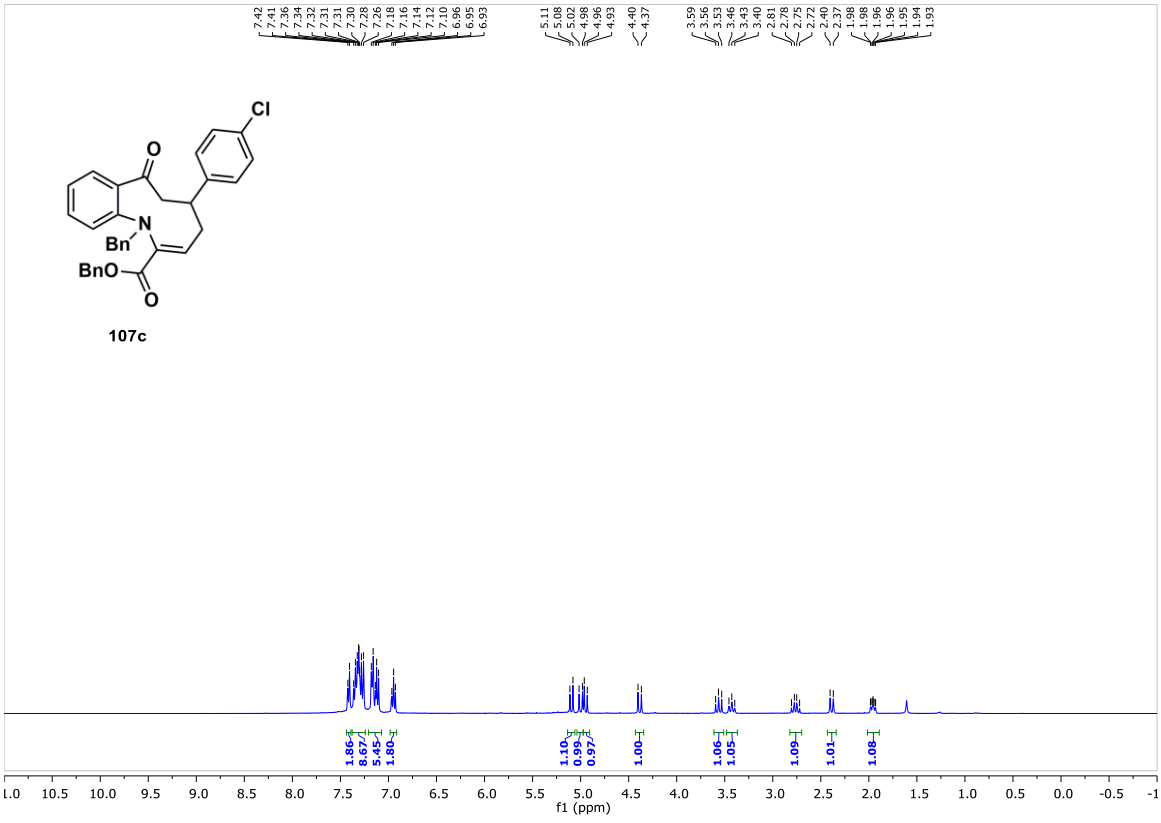
7.42
7.41
7.36
7.34
7.32
7.31
7.31
7.30
7.28
7.26
7.18
7.16
7.14
7.12
7.10
6.96
6.95
6.93
5.11
5.08
5.02
4.98
4.96
4.93
4.40
4.37
3.59
3.56
3.53
3.46
3.43
3.40
2.81
2.78
2.75
2.72
2.40
2.37
1.98
1.98
1.96
1.96
1.95
1.94
1.93
Cl
O
N
Bn
BnO
O
107c
1.86
8.57
5.45
1.80
1.10
0.99
0.97
1.00
1.06
1.05
1.09
1.01
1.08
f1 (ppm)

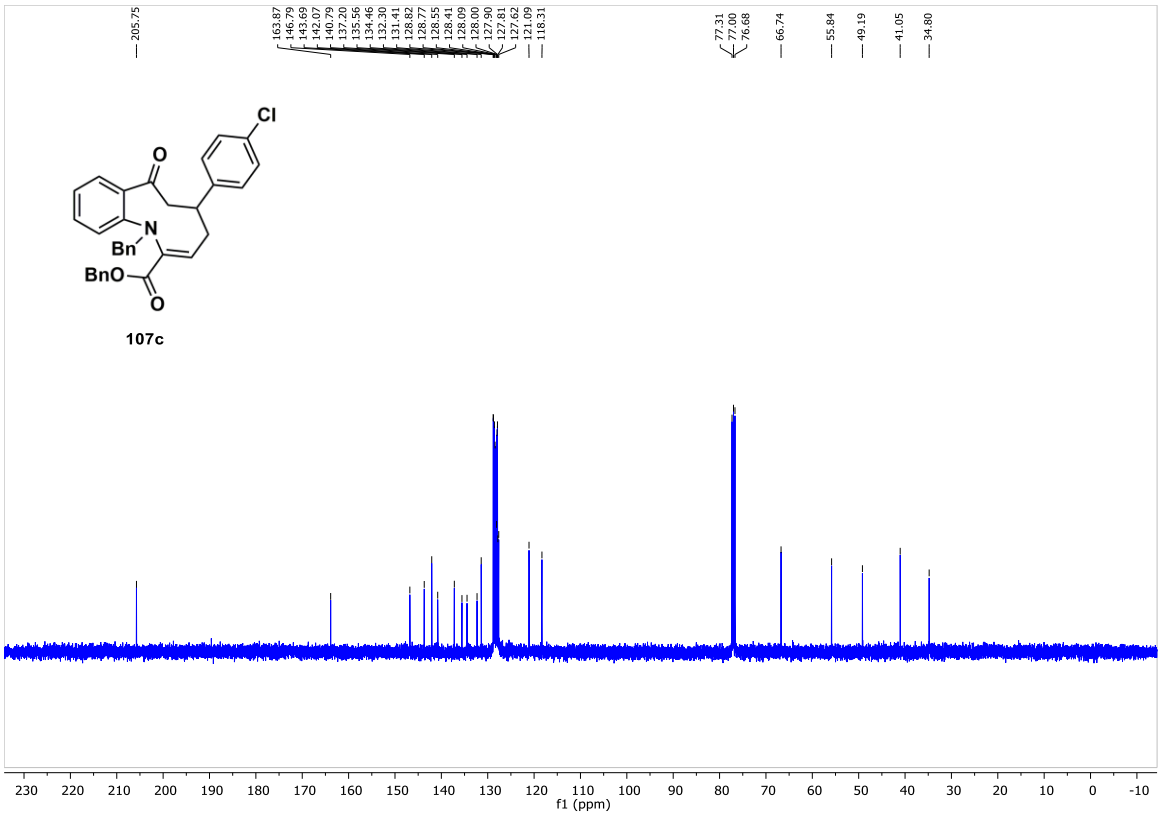
205.75
163.87
146.79
143.69
142.07
140.79
137.20
135.56
134.46
132.30
131.41
128.82
128.77
128.55
128.41
128.09
128.00
127.90
127.81
127.62
121.09
118.31
77.31
77.00
76.68
66.74
55.84
49.19
41.05
34.80
Cl
O
N
Bn
BnO
O
107c
f1 (ppm)

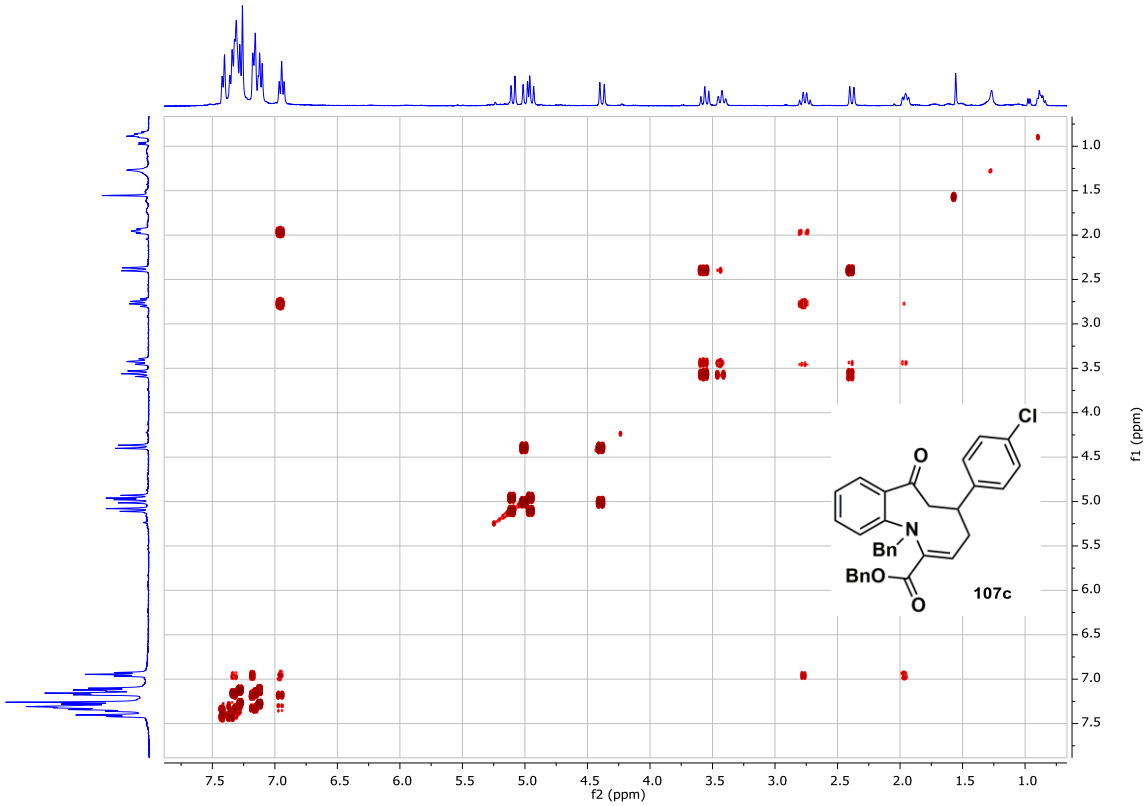
Cl
O
N
Bn
BnO
O
107c
f2 (ppm)
f1 (ppm)

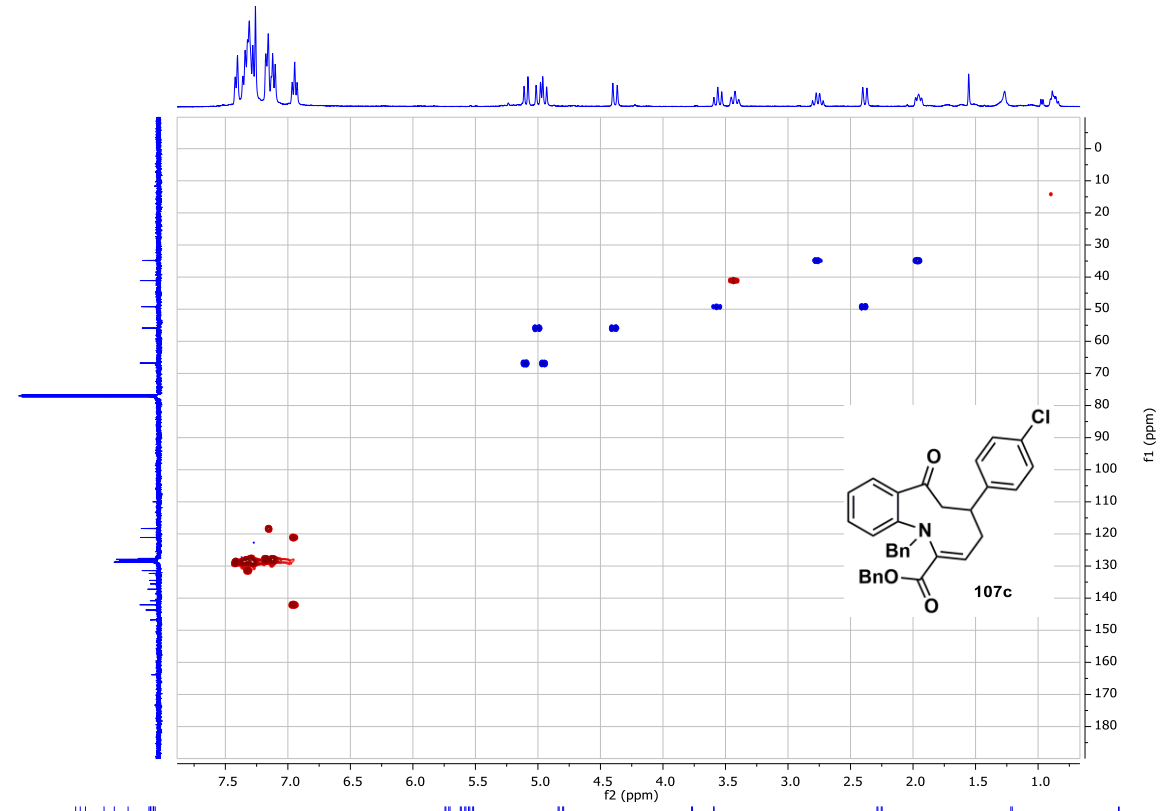
f2 (ppm)
f1 (ppm)
Cl
O
N
Bn
BnO
O
107c

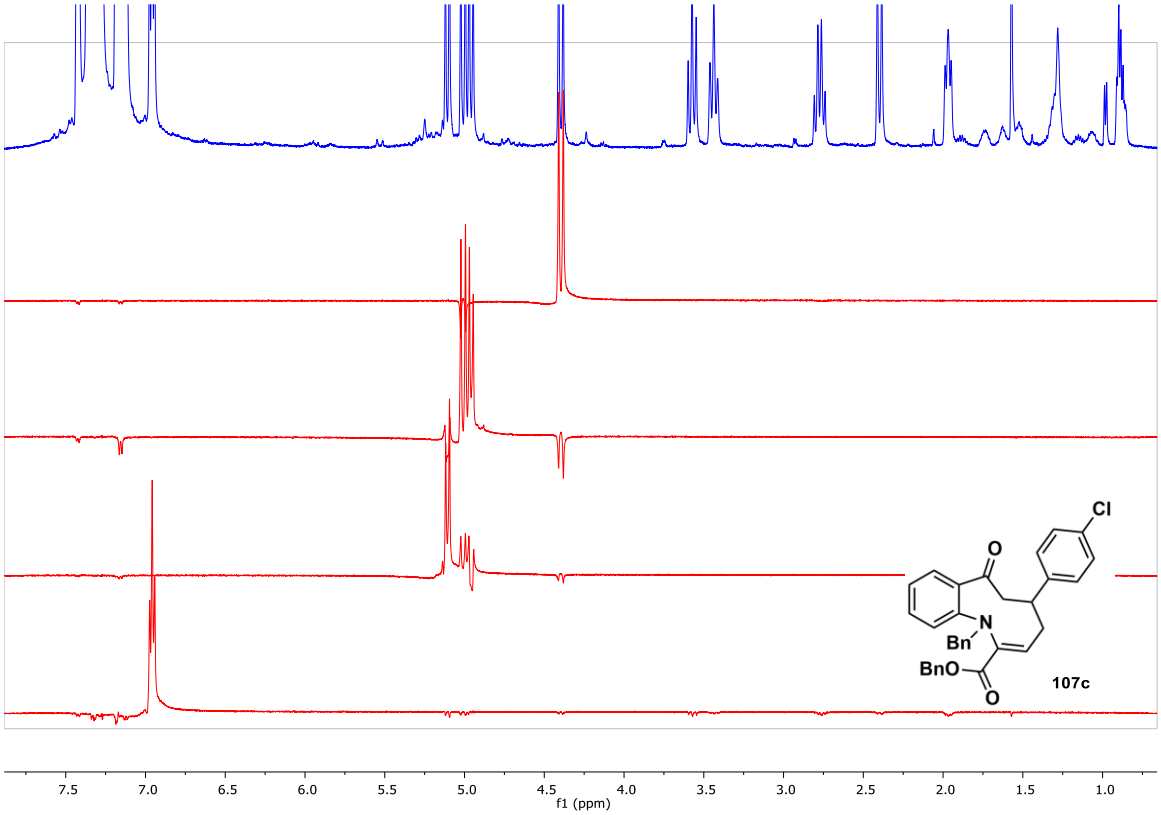
f1 (ppm)
Cl
O
N
Bn
BnO
O
107c

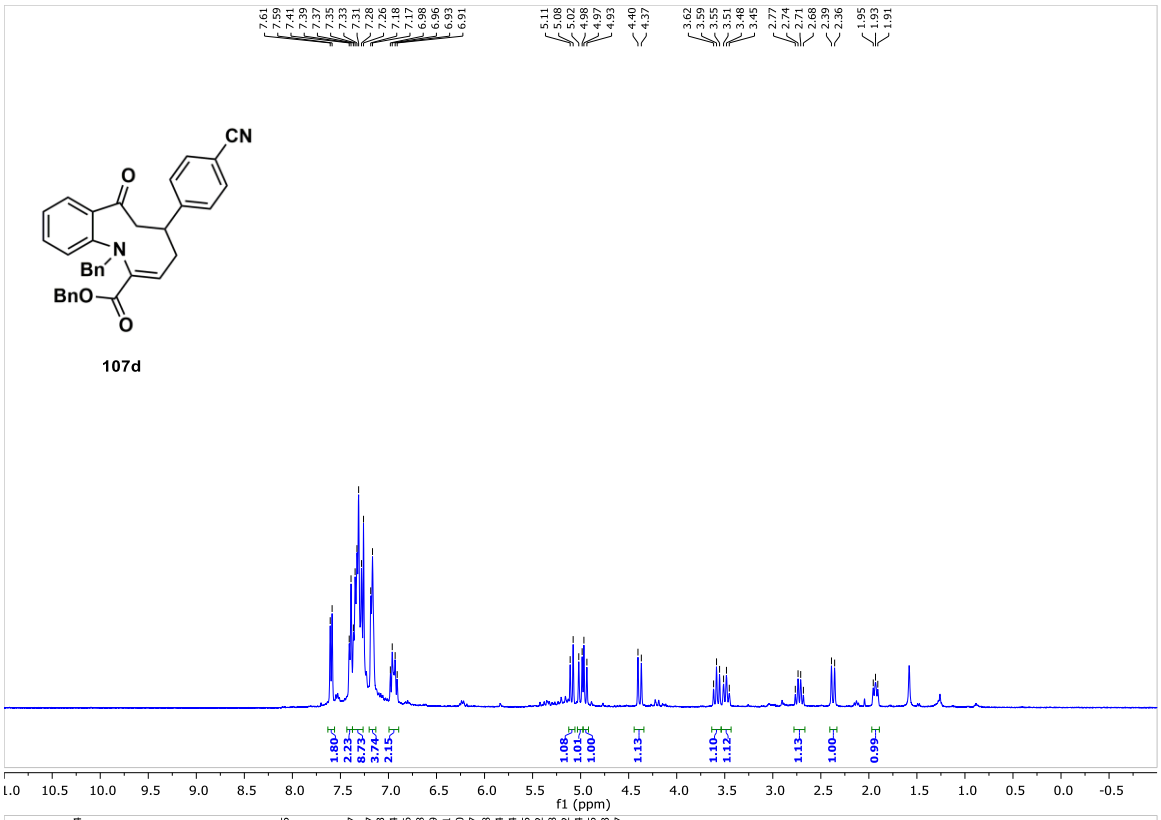
CN
O
N
Bn
BnO
O
107d
f1 (ppm)

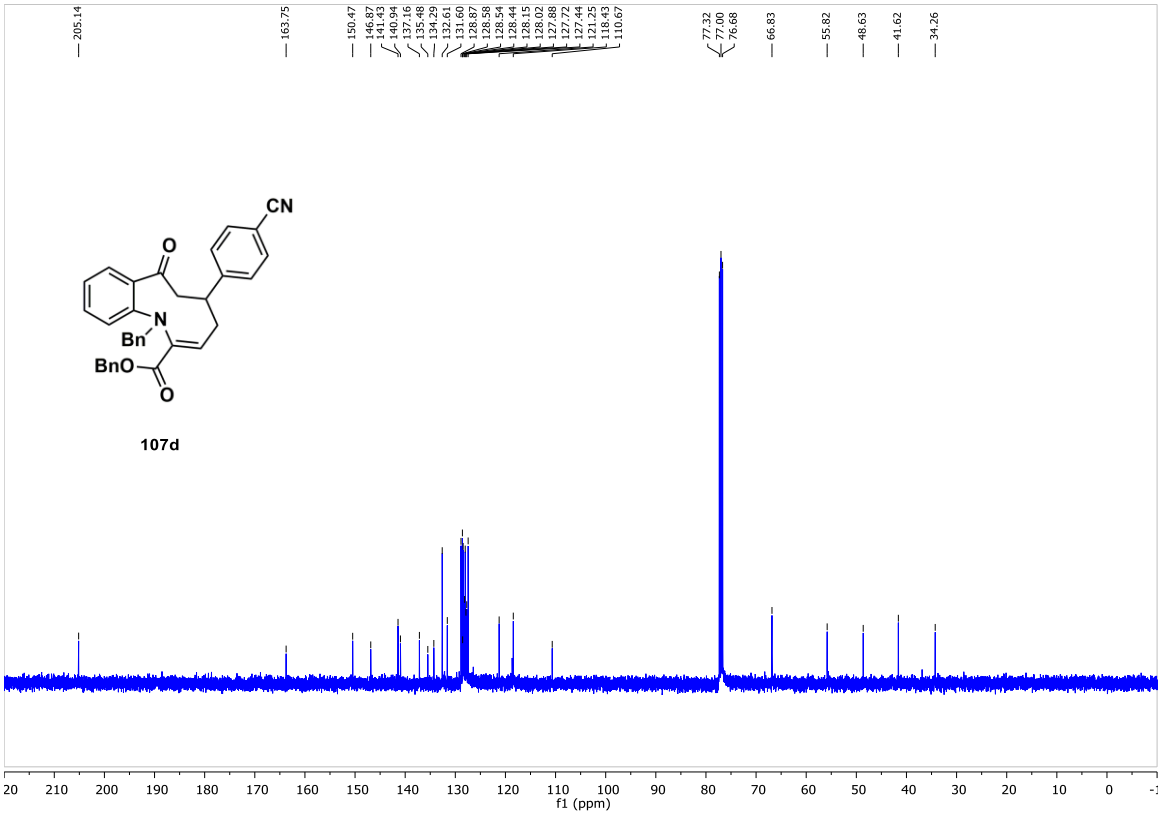
CN
O
N
Bn
BnO
O
107d
f1 (ppm)

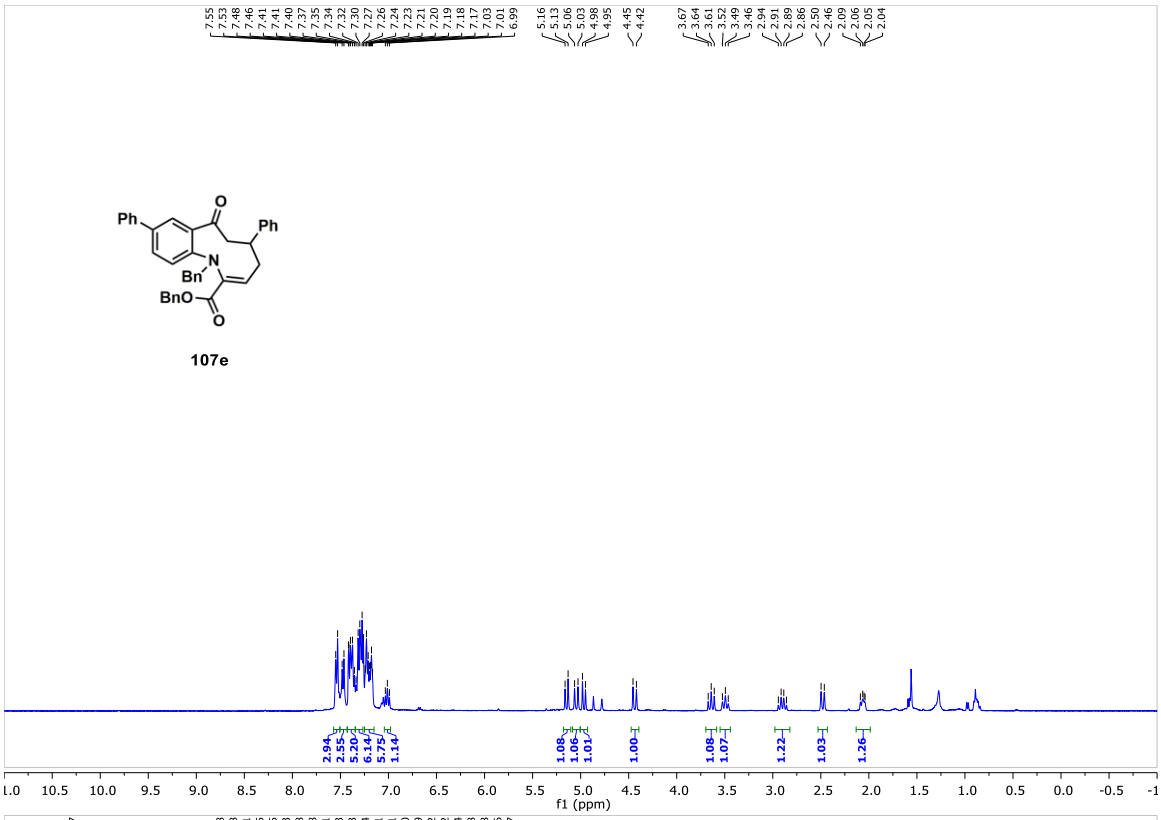
Ph
O
Ph
N
Bn
BnO
O
107e
f1 (ppm)

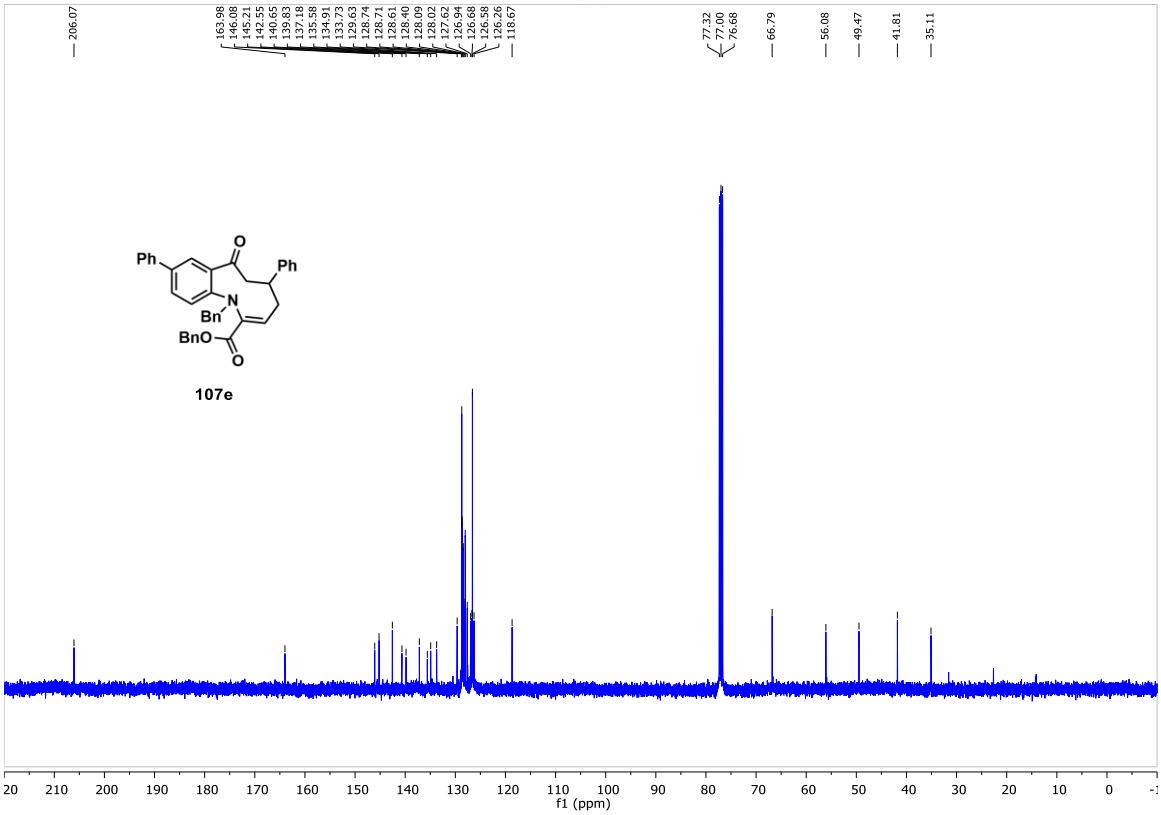
Ph
O
Ph
N
Bn
BnO
O
107e
f1 (ppm)

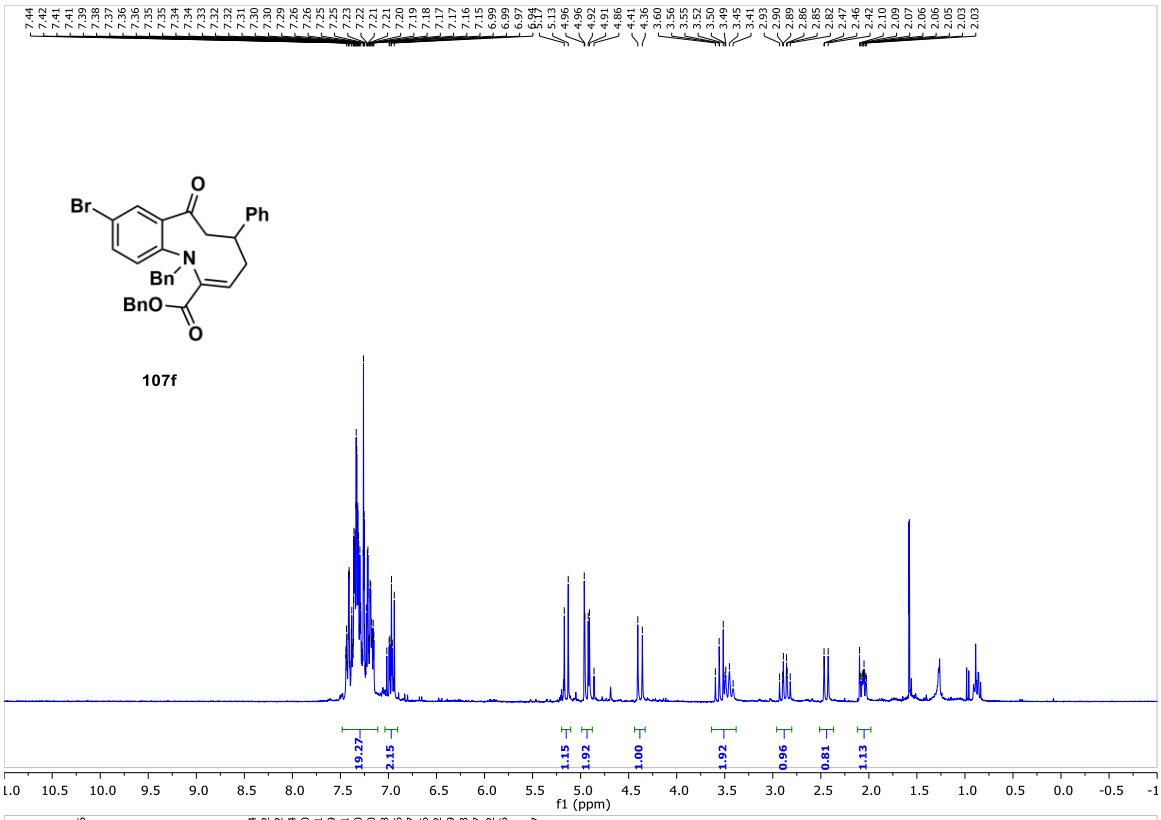
Br
O
Ph
N
Bn
BnO
O
107f
19.27
2.15
1.15
1.92
1.00
1.92
0.96
0.81
1.13
f1 (ppm)

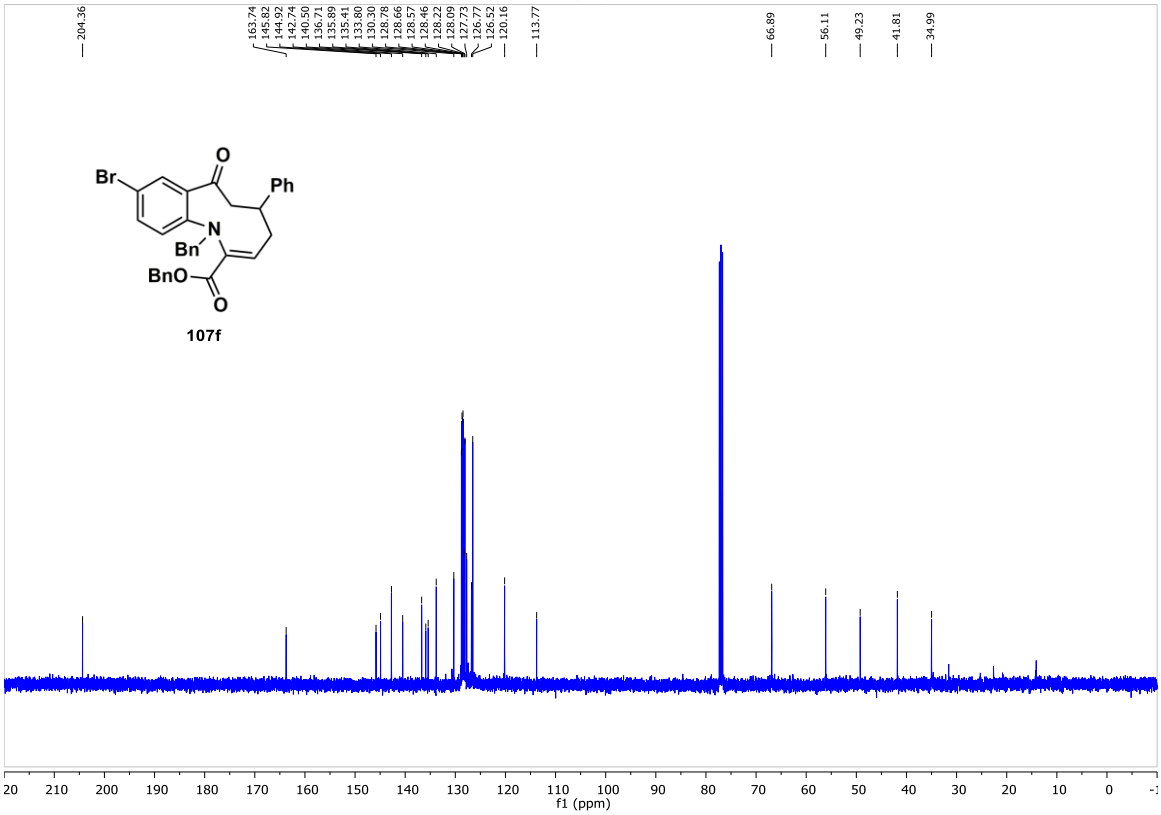
Br
O
Ph
N
Bn
BnO
O
107f
f1 (ppm)

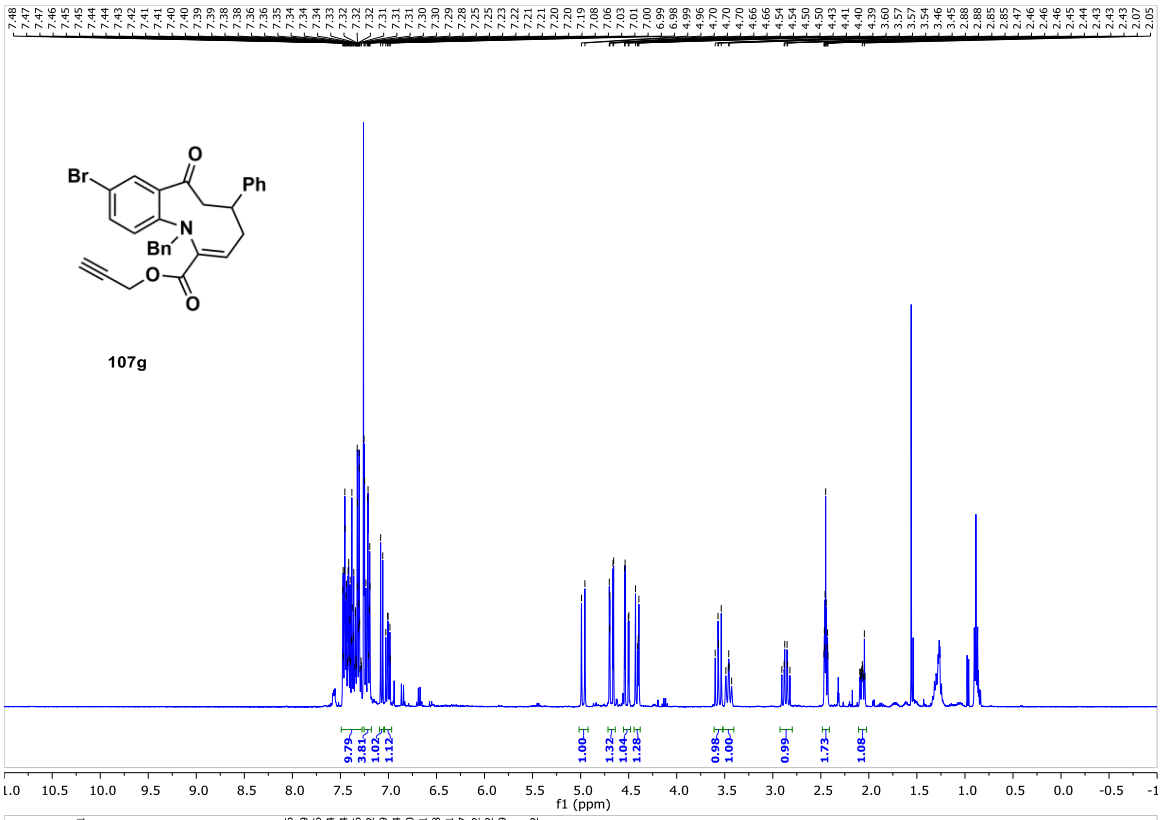
Br
O
Ph
N
Bn
O
O
107g
f1 (ppm)

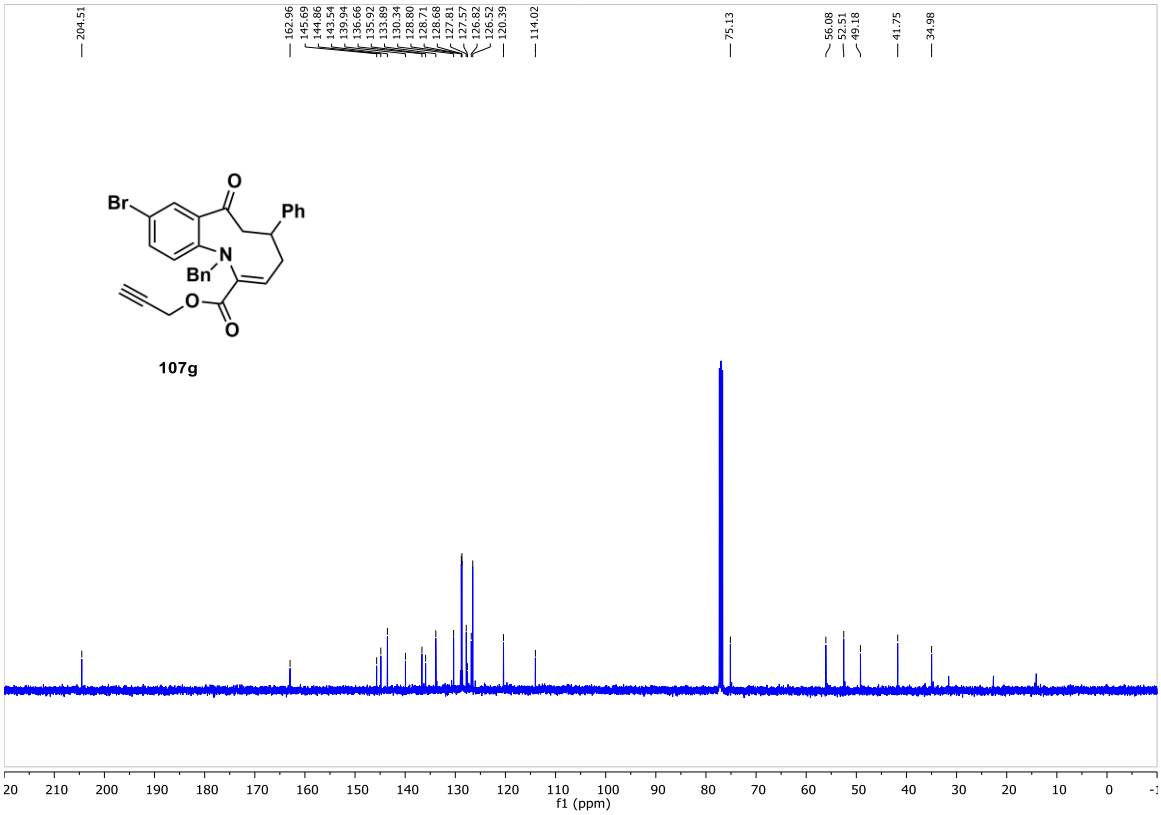
Br
O
Ph
N
Bn
O
O
107g
f1 (ppm)

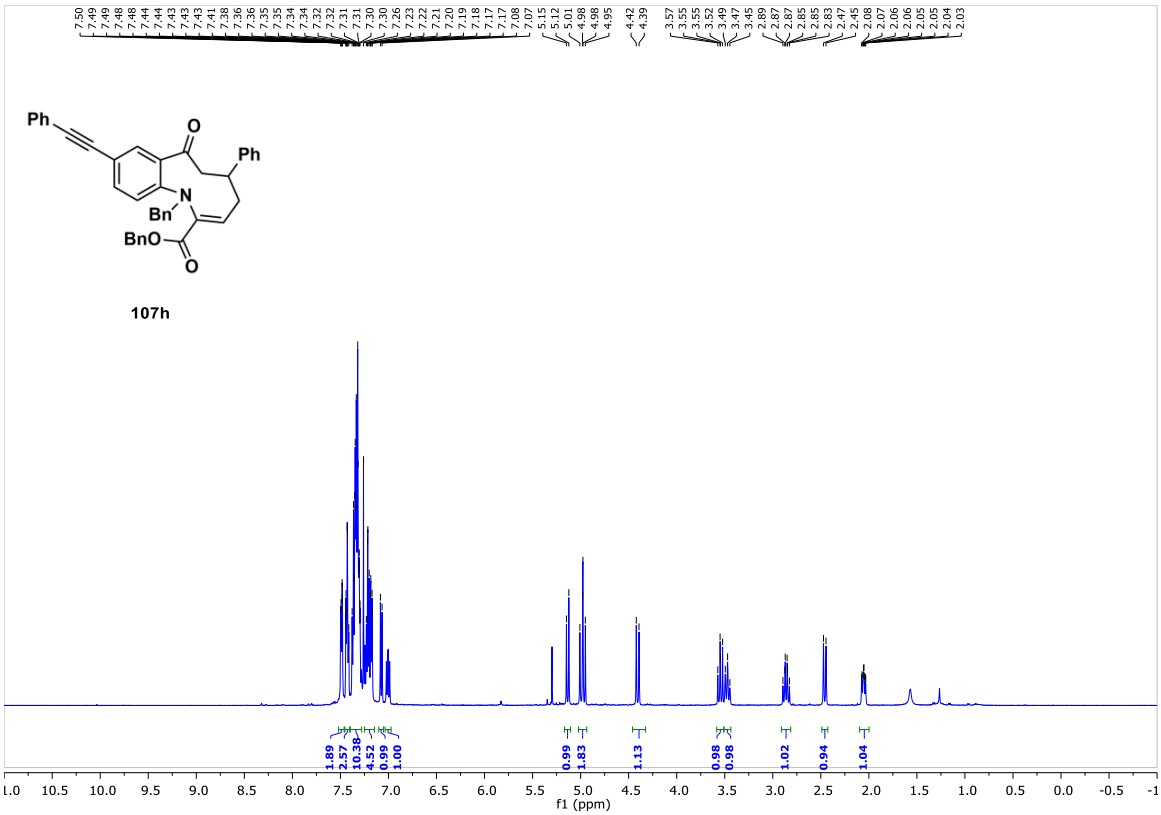
Ph
O
Ph
N
Bn
BnO
O
107h
f1 (ppm)

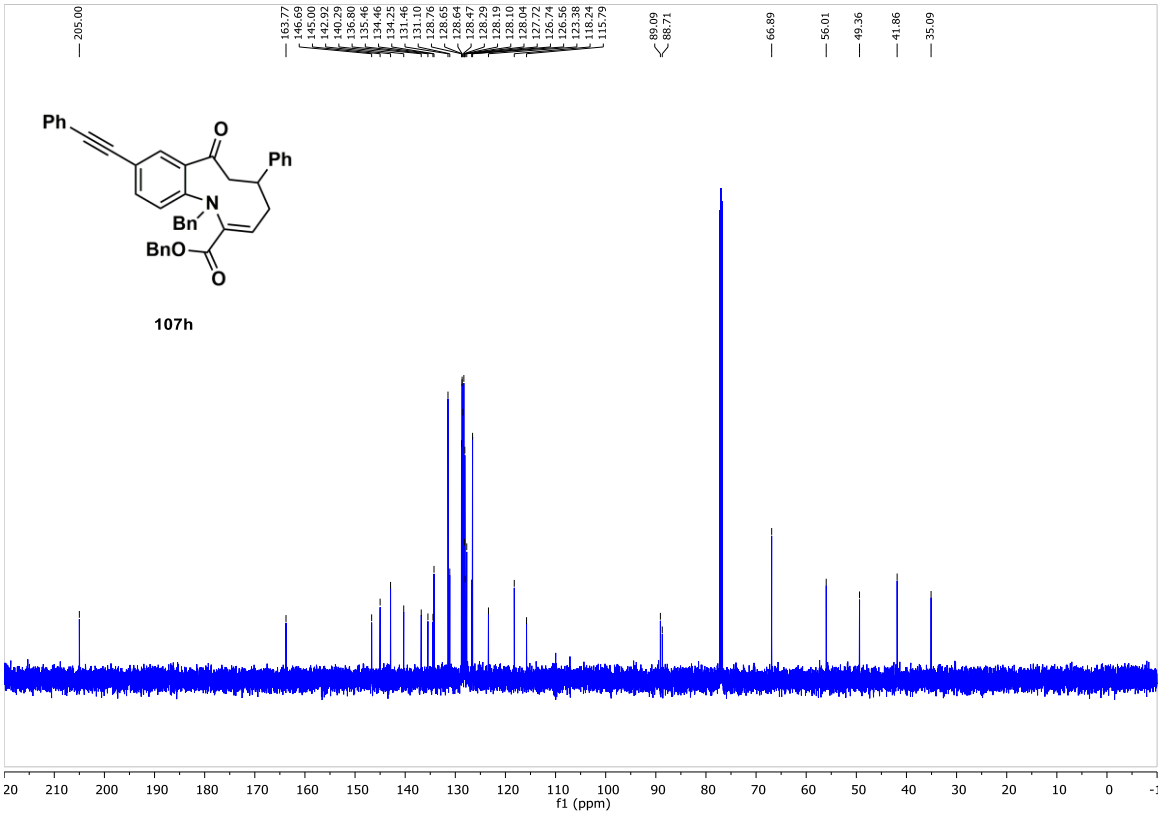
Ph
O
Ph
N
Bn
BnO
O
107h
f1 (ppm)

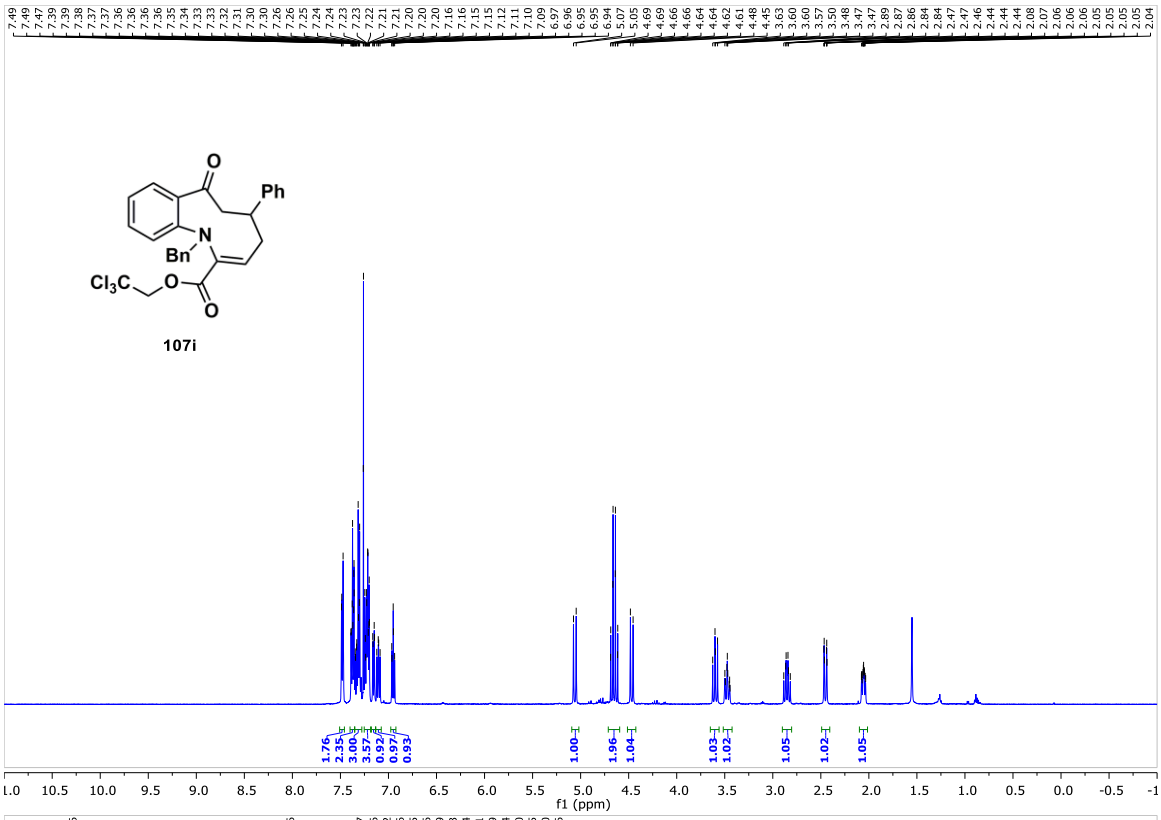
O
Ph
N
Bn
Cl3C
O
O
107i
f1 (ppm)

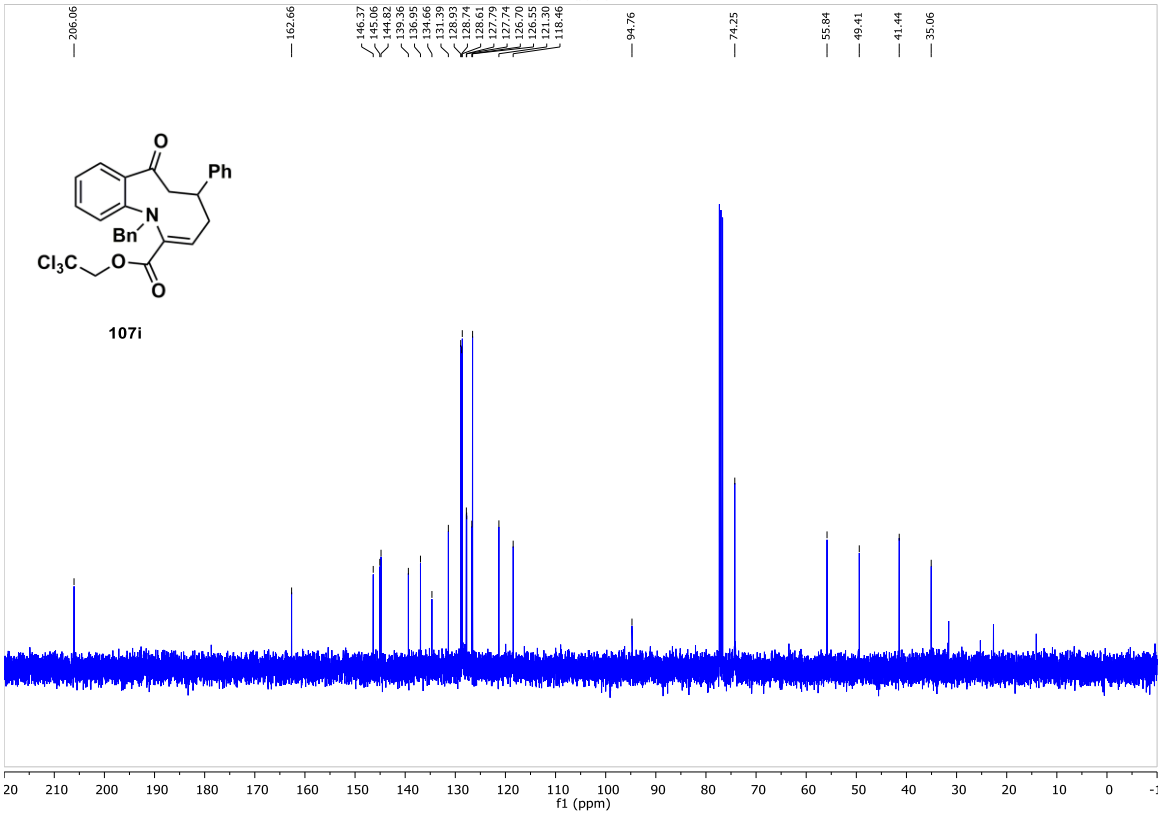
O
Ph
N
Bn
Cl3C
O
O
107i
f1 (ppm)

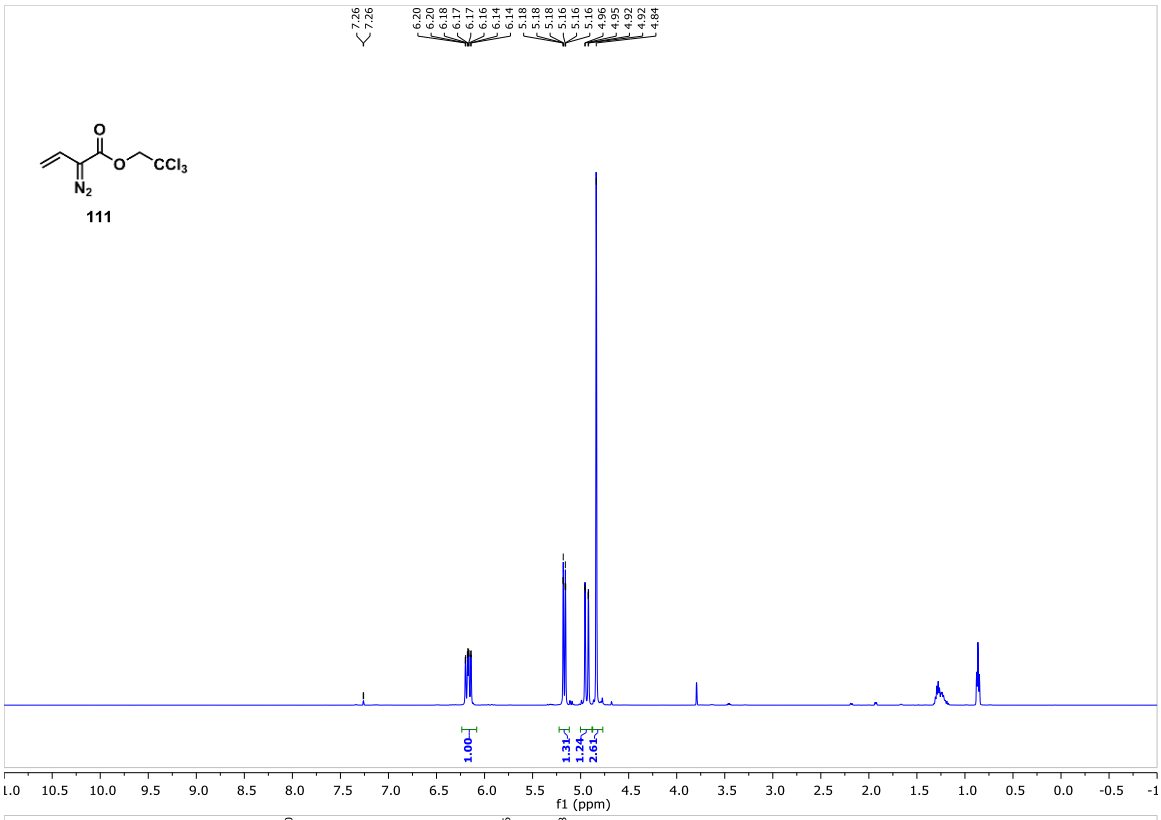
7.26
7.26
6.20
6.20
6.18
6.17
6.17
6.16
6.14
5.18
5.18
5.16
5.16
5.16
4.96
4.95
4.92
4.92
4.84
O
O
CCl3
N2
111
1.00
1.31
1.24
2.61
f1 (ppm)

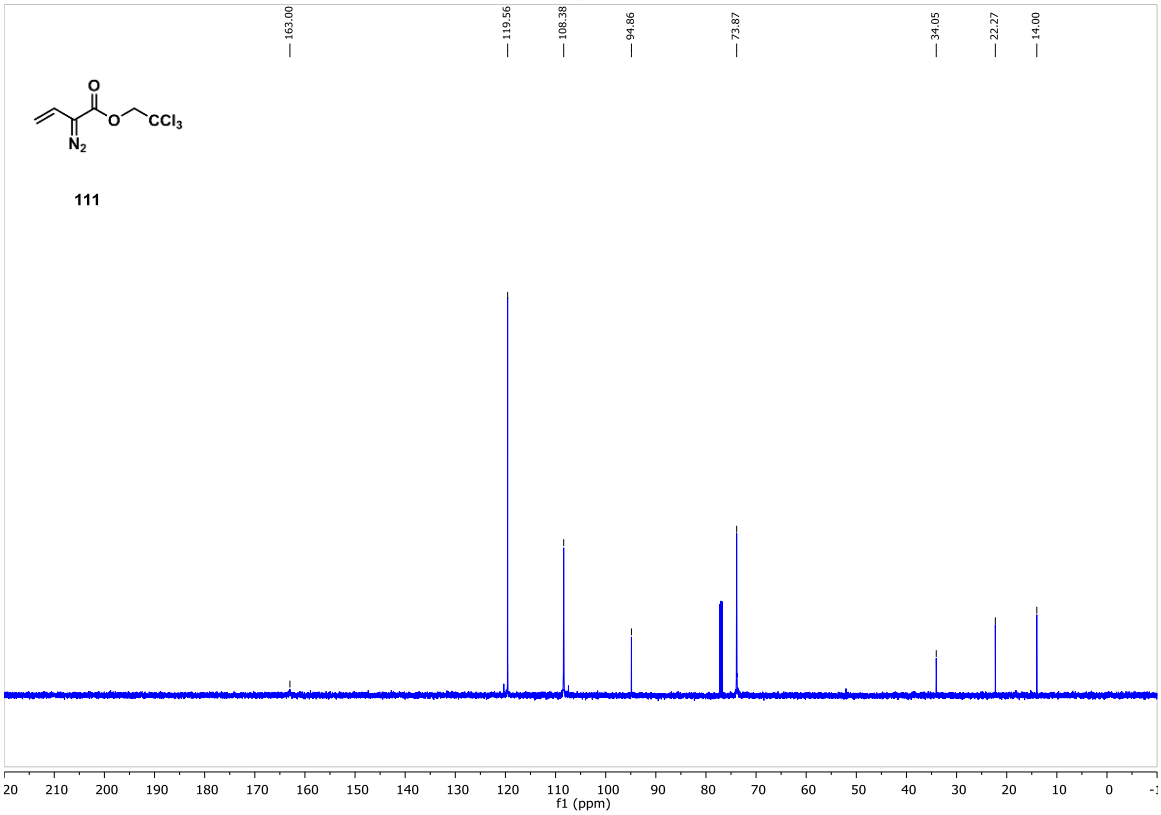
163.00
119.56
108.38
94.86
73.87
34.05
22.27
14.00
O
O
CCl3
N2
111
f1 (ppm)

References

1. Khan, A. R.; Parrish, J. C.; Fraser, M. E.; Smith, W. W.; Bartlett, P. A.; James, M. N. G., Lowering the Entropic Barrier for Binding Conformationally Flexible Inhibitors to Enzymes. *Biochemistry* **1998,** *37* (48), 16839-16845.
2. Rezai, T.; Yu, B.; Millhauser, G. L.; Jacobson, M. P.; Lokey, R. S., Testing the Conformational Hypothesis of Passive Membrane Permeability Using Synthetic Cyclic Peptide Diastereomers. *J. Am. Chem. Soc.* **2006,** *128* (8), 2510-2511.
3. Silvestri, R., New Prospects for Vinblastine Analogues as Anticancer Agents. *J. Med. Chem.* **2013,** *56* (3), 625-627.
4. Lin, L.-C.; Kuo, T.-T.; Chang, H.-Y.; Liu, W.-S.; Hsia, S.-M.; Huang, T.-C., Manzamine A Exerts Anticancer Activity against Human Colorectal Cancer Cells. *Mar. Drugs* **2018,** *16* (8), 252.
5. Baden, D. G.; Bourdelais, A. J.; Jacocks, H.; Michelliza, S.; Naar, J., Natural and Derivative Brevetoxins: Historical Background, Multiplicity, and Effects. *Environ. Health Perspect.* **2005,** *113* (5), 621-625.
6. Gordaliza, M., Natural products as leads to anticancer drugs. *Clinical and Translational Oncology* **2007,** *9* (12), 767-776.
7. McGrath, N. A.; Brichacek, M.; Njardarson, J. T., A Graphical Journey of Innovative Organic Architectures That Have Improved Our Lives. *J. Chem. Educ.* **2010,** *87* (12), 1348-1349.
8. Bauer, R. A.; Wenderski, T. A.; Tan, D. S., Biomimetic diversity-oriented synthesis of benzannulated medium rings via ring expansion. *Nat. Chem. Biol.* **2012,** *9*, 21.
9. Kingston, D. G. I., Recent Advances in the Chemistry of Taxol. *J. Nat. Prod.* **2000,** *63* (5), 726-734.
10. Choi, Y.; Kim, H.; Park, S. B., A divergent synthetic pathway for pyrimidine-embedded medium-sized azacycles through an N-quaternizing strategy. *Chemical Science* **2019,** *10* (2), 569-575.
11. Vo, C.-V. T.; Luescher, M. U.; Bode, J. W., SnAP reagents for the one-step synthesis of medium-ring saturated N-heterocycles from aldehydes. *Nat. Chem.* **2014,** *6*, 310.
12. Crimmins, M. T.; Emmitte, K. A., Total Synthesis of (+)-Laurencin: An Asymmetric Alkylation−Ring-Closing Metathesis Approach to Medium Ring Ethers. *Organic Letters* **1999,** *1* (12), 2029-2032.
13. Mukai, C.; Ohta, M.; Yamashita, H.; Kitagaki, S., Base-Catalyzed Endo-Mode Cyclization of Allenes: Easy Preparation of Five- to Nine-Membered Oxacycles. *The Journal of Organic Chemistry* **2004,** *69* (20), 6867-6873.
14. Majhi, T. P.; Neogi, A.; Ghosh, S.; Mukherjee, A. K.; Helliwell, M.; Chattopadhyay, P., An Efficient Synthesis of Novel Dibenzo-Fused Nine-Membered Oxacycles Using a Sequential Baylis-Hillman Reaction and Radical Cyclization. *Synthesis* **2008,** *2008* (01), 94-100.
15. Mendoza, A.; Ishihara, Y.; Baran, P. S., Scalable enantioselective total synthesis of taxanes. *Nat. Chem.* **2011,** *4*, 21.
16. Deiters, A.; Martin, S. F., Synthesis of Oxygen- and Nitrogen-Containing Heterocycles by Ring-Closing Metathesis. *Chem. Rev.* **2004,** *104* (5), 2199-2238.

17. Illuminati, G.; Mandolini, L., Ring closure reactions of bifunctional chain molecules. *Acc. Chem. Res.* **1981,** *14* (4), 95-102.
18. Blankenstein, J.; Zhu, J., Conformation-Directed Macrocyclization Reactions. *European J. Org. Chem.* **2005,** *2005* (10), 1949-1964.
19. Gradillas, A.; Pérez-Castells, J., Macrocyclization by Ring-Closing Metathesis in the Total Synthesis of Natural Products: Reaction Conditions and Limitations. *Angewandte Chemie International Edition* **2006,** *45* (37), 6086-6101.
20. Kaul, R.; Surprenant, S.; Lubell, W. D., Systematic Study of the Synthesis of Macrocyclic Dipeptide β-Turn Mimics Possessing 8-, 9-, and 10- Membered Rings by Ring-Closing Metathesis. *The Journal of Organic Chemistry* **2005,** *70* (10), 3838-3844.
21. Chemler, S. R.; Danishefsky, S. J., Transannular Macrocyclization via Intramolecular B-Alkyl Suzuki Reaction. *Organic Letters* **2000,** *2* (17), 2695-2698.
22. Galli, C.; Illuminati, G.; Mandolini, L.; Tamborra, P., Ring-closure reactions. 7. Kinetics and activation parameters of lactone formation in the range of 3- to 23-membered rings. *J. Am. Chem. Soc.* **1977,** *99* (8), 2591-2597.
23. Rendina, V. L.; Kaplan, H. Z.; Kingsbury, J. S., Highly Efficient and Enantioselective α-Arylation of Cycloalkanones by Scandium-Catalyzed Diazoalkane-Carbonyl Homologation. *Synthesis* **2012,** *44* (05), 686-693.
24. Corey, E. J.; Brunelle, D. J.; Nicolaou, K. C., A translactonization route to macrocyclic lactones. *J. Am. Chem. Soc.* **1977,** *99* (22), 7359-7360.
25. Yang, J.; Long, Y. O.; Paquette, L. A., Concise Total Syntheses of the Bioactive Mesotricyclic Diterpenoids Jatrophatrione and Citlalitrione. *J. Am. Chem. Soc.* **2003,** *125* (6), 1567-1574.
26. Stephens, T. C.; Lawer, A.; French, T.; Unsworth, W. P., Iterative Assembly of Macrocyclic Lactones using Successive Ring Expansion Reactions. *Chemistry – A European Journal* **2018,** *24* (52), 13947-13953.
27. Stephens, T. C.; Lodi, M.; Steer, A. M.; Lin, Y.; Gill, M. T.; Unsworth, W. P., Synthesis of Cyclic Peptide Mimetics by the Successive Ring Expansion of Lactams. *Chemistry – A European Journal* **2017,** *23* (54), 13314-13318.
28. Kitsiou, C.; Hindes, J. J.; I'Anson, P.; Jackson, P.; Wilson, T. C.; Daly, E. K.; Felstead, H. R.; Hearnshaw, P.; Unsworth, W. P., The Synthesis of Structurally Diverse Macrocycles By Successive Ring Expansion. *Angewandte Chemie International Edition* **2015,** *54* (52), 15794-15798.
29. Chen, C.; Layton, M. E.; Shair, M. D., Stereospecific Synthesis of the CP-263,114 Core Structure. *J. Am. Chem. Soc.* **1998,** *120* (41), 10784-10785.
30. Nicolle, S. M.; Lewis, W.; Hayes, C. J.; Moody, C. J., Stereoselective Synthesis of Highly Substituted Tetrahydrofurans through Diverted Carbene O□H Insertion Reaction. *Angewandte Chemie International Edition* **2015,** *54* (29), 8485-8489.
31. Nicolle, S. M.; Lewis, W.; Hayes, C. J.; Moody, C. J., Stereoselective Synthesis of Functionalized Pyrrolidines by the Diverted N−H Insertion Reaction of Metallocarbenes with β-Aminoketone Derivatives. *Angewandte Chemie International Edition* **2016,** *55* (11), 3749-3753.
32. Heines, S. V., Peter Griess—Discoverer of diazo compounds. *J. Chem. Educ.* **1958,** *35* (4), 187.

33. Horneff, T.; Chuprakov, S.; Chernyak, N.; Gevorgyan, V.; Fokin, V. V., Rhodium-Catalyzed Transannulation of 1,2,3-Triazoles with Nitriles. *J. Am. Chem. Soc.* **2008,** *130* (45), 14972-14974.
34. Doyle, M. P.; Duffy, R.; Ratnikov, M.; Zhou, L., Catalytic Carbene Insertion into C−H Bonds. *Chem. Rev.* **2010,** *110* (2), 704-724.
35. Ford, A.; Miel, H.; Ring, A.; Slattery, C. N.; Maguire, A. R.; McKervey, M. A., Modern Organic Synthesis with α-Diazocarbonyl Compounds. *Chem. Rev.* **2015,** *115* (18), 9981-10080.
36. Davies, H. M. L.; Smith, H. D.; Korkor, O., Tandem cyclopropanation/Cope rearrangement sequence. Stereospecific [3 + 4] cycloaddition reaction of vinylcarbenoids with cyclopentadiene. *Tetrahedron Lett.* **1987,** *28* (17), 1853-1856.
37. Davies, H. M. L.; Xiang, B.; Kong, N.; Stafford, D. G., Catalytic Asymmetric Synthesis of Highly Functionalized Cyclopentenes by a [3 + 2] Cycloaddition. *J. Am. Chem. Soc.* **2001,** *123* (30), 7461-7462.
38. Lian, Y.; Davies, H. M. L., Rhodium-Catalyzed [3 + 2] Annulation of Indoles. *J. Am. Chem. Soc.* **2010,** *132* (2), 440-441.
39. Lian, Y.; Miller, L. C.; Born, S.; Sarpong, R.; Davies, H., Catalyst-Controlled Formal [4 + 3] Cycloaddition Applied to the Total Synthesis of (+)-Barekoxide and (-)-Barekol. *J. Am. Chem. Soc.* **2010,** *132* (35), 12422-12425.
40. Qin, C.; Davies, H. M. L., Rh2(R-TPCP)4-Catalyzed Enantioselective [3+2]-Cycloaddition between Nitrones and Vinyldiazoacetates. *J. Am. Chem. Soc.* **2013,** *135* (39), 14516-14519.
41. Schwartz, B. D.; Denton, J. R.; Lian, Y.; Davies, H. M. L.; Williams, C. M., Asymmetric [4 + 3] Cycloadditions between Vinylcarbenoids and Dienes: Application to the Total Synthesis of the Natural Product (−)-5-epi-Vibsanin E. *J. Am. Chem. Soc.* **2009,** *131* (23), 8329-8332.
42. Wang, X.; Xu, X.; Zavalij, P. Y.; Doyle, M. P., Asymmeric Formal [3 + 3]-Cycloaddition Reactions of Nitrones with Electrophilic Vinylcarbene Intermediates. *J. Am. Chem. Soc.* **2011,** *133* (41), 16402-16405.
43. Davies, H. M. L.; Nikolai, J., Catalytic and enantioselective allylic C-H activation with donor-acceptor-substituted carbenoids. *Org. Biomol. Chem.* **2005,** *3* (23), 4176-4187.
44. Espino, C. G.; Fiori, K. W.; Kim, M.; Du Bois, J., Expanding the Scope of C−H Amination through Catalyst Design. *J. Am. Chem. Soc.* **2004,** *126* (47), 15378-15379.
45. Li, Z.; Parr, B. T.; Davies, H. M. L., Highly Stereoselective C–C Bond Formation by Rhodium-Catalyzed Tandem Ylide Formation/[2,3]-Sigmatropic Rearrangement between Donor/Acceptor Carbenoids and Chiral Allylic Alcohols. *J. Am. Chem. Soc.* **2012,** *134* (26), 10942-10946.
46. Gillingham, D.; Fei, N., Catalytic X-H insertion reactions based on carbenoids. *Chem. Soc. Rev.* **2013,** *42* (12), 4918-4931.
47. Chinthapally, K.; Massaro, N. P.; Padgett, H. L.; Sharma, I., A serendipitous cascade of rhodium vinylcarbenoids with aminochalcones for the synthesis of functionalized quinolines. *Chemical Communications* **2017,** *53* (90), 12205-12208.
48. Chinthapally, K.; Massaro, N. P.; Sharma, I., Rhodium Carbenoid Initiated O–H Insertion/Aldol/Oxy-Cope Cascade for the Stereoselective Synthesis of Functionalized Oxacycles. *Organic Letters* **2016,** *18* (24), 6340-6343.

49. Hunter, A. C.; Chinthapally, K.; Sharma, I., Rh2(esp)2: An Efficient Catalyst for O–H Insertion Reactions of Carboxylic Acids into Acceptor/Acceptor Diazo Compounds. *European J. Org. Chem.* **2016,** *2016* (13), 2260-2263.
50. Hunter, A. C.; Schlitzer, S. C.; Sharma, I., Synergistic Diazo-OH Insertion/Conia-Ene Cascade Catalysis for the Stereoselective Synthesis of γ-Butyrolactones and Tetrahydrofurans. *Chemistry – A European Journal* **2016,** *22* (45), 16062-16065.
51. Baum, J. S.; Shook, D. A.; Davies, H. M. L.; Smith, H. D., Diazotransfer Reactions with p-Acetamidobenzenesulfonyl Azide. *Synthetic Communications* **1987,** *17* (14), 1709-1716.
52. Briones, J. F.; Davies, H. M. L., Enantioselective Gold(I)-Catalyzed Vinylogous [3 + 2] Cycloaddition between Vinyldiazoacetates and Enol Ethers. *J. Am. Chem. Soc.* **2013,** *135* (36), 13314-13317.
53. Maier, T. C.; Fu, G. C., Catalytic Enantioselective O−H Insertion Reactions. *J. Am. Chem. Soc.* **2006,** *128* (14), 4594-4595.
54. Guo, X.; Hu, W., Novel Multicomponent Reactions via Trapping of Protic Onium Ylides with Electrophiles. *Acc. Chem. Res.* **2013,** *46* (11), 2427-2440.
55. Guo, X.; Yue, Y.; Hu, G.; Zhou, J.; Zhao, Y.; Yang, L.; Hu, W., Trapping of an Ammonium Ylide with Activated Ketones: Synthesis of β-Hydroxy-α-Amino Esters with Adjacent Quaternary Stereocenters. *Synlett* **2009,** *2009* (13), 2109-2114.
56. Medvedev, J. J.; Nikolaev, V. A., Recent advances in the chemistry of Rh carbenoids: multicomponent reactions of diazocarbonyl compounds. *Russian Chemical Reviews* **2015,** *84* (7), 737.
57. Davies, H. M. L.; Parr, B. T., Rhodium Carbenes. In *Contemporary Carbene Chemistry*, John Wiley & Sons, Inc: 2013; pp 363-403.
58. Wong, F. M.; Wang, J.; Hengge, A. C.; Wu, W., Mechanism of Rhodium-Catalyzed Carbene Formation from Diazo Compounds. *Organic Letters* **2007,** *9* (9), 1663-1665.
59. Xie, Z.-Z.; Liao, W.-J.; Cao, J.; Guo, L.-P.; Verpoort, F.; Fang, W., Mechanistic Insight into the Rhodium-Catalyzed O–H Insertion Reaction: A DFT Study. *Organometallics* **2014,** *33* (10), 2448-2456.
60. Padwa, A.; Hornbuckle, S. F., Ylide formation from the reaction of carbenes and carbenoids with heteroatom lone pairs. *Chem. Rev.* **1991,** *91* (3), 263-309.
61. Thumar, N. J.; Wei, Q. H.; Hu, W. H., Chapter Two - Recent Advances in Asymmetric Metal-Catalyzed Carbene Transfer from Diazo Compounds Toward Molecular Complexity. In *Advances in Organometallic Chemistry*, Pérez, P. J., Ed. Academic Press: 2016; Vol. 66, pp 33-91.
62. Zhang, D.; Zhou, J.; Xia, F.; Kang, Z.; Hu, W., Bond cleavage, fragment modification and reassembly in enantioselective three-component reactions. *Nature Communications* **2015,** *6*, 5801.
63. Padwa, A.; Kassir, J. M.; Semones, M. A.; Weingarten, M. D., A Tandem Cyclization-Onium Ylide Rearrangement-Cycloaddition Sequence for the Synthesis of Benzo-Substituted Cyclopentenones. *The Journal of Organic Chemistry* **1995,** *60* (1), 53-62.
64. Balakumar, A.; Janardhanam, S.; Rajagopalan, K., Studies in base-catalyzed allenic oxy-Cope rearrangement: an expedient synthesis of functionalized bicyclo[4.3.0] and -[4.4.0] systems and 3,5-cycloundecadien-1-one. *The Journal of Organic Chemistry* **1993,** *58* (20), 5482-5486.

65. Janardhanam, S.; Devan, B.; Rajagopalan, K., Ring enlargement-annulation via thermal oxy-Cope rearrangement. *Tetrahedron Lett.* **1993,** *34* (42), 6761-6764.
66. Carey, F. A.; Sundberg, R. J., *Advanced Organic Chemistry: Part B: Reaction and Synthesis*. Springer US: 2007.
67. Baumann, H.; Chen, P., Density Functional Study of the Oxy-Cope Rearrangement. *Helv. Chim. Acta* **2001,** *84* (1), 124-140.
68. Berson, J. A.; Jones, M., A Synthesis of Ketones by the Thermal Isomerization of 3-Hydroxy-1,5-hexadienes. The Oxy-Cope Rearrangement. *J. Am. Chem. Soc.* **1964,** *86* (22), 5019-5020.
69. Dewar, M. J. S.; Wade, L. E., A study of the mechanism of the Cope rearrangement. *J. Am. Chem. Soc.* **1977,** *99* (13), 4417-4424.
70. Evans, D. A.; Baillargeon, D. J.; Nelson, J. V., A general approach to the synthesis of 1,6-dicarbonyl substrates. New applications of base-accelerated oxy-Cope rearrangements. *J. Am. Chem. Soc.* **1978,** *100* (7), 2242-2244.
71. Paquette, L. A., Recent applications of anionic oxy-cope rearrangements. *Tetrahedron* **1997,** *53* (41), 13971-14020.
72. Paquette, L. A.; Combrink, K. D.; Elmore, S. W.; Rogers, R. D., Impact of substituent modifications on the atropselectivity characteristics of an anionic oxy-Cope ring expansion. *J. Am. Chem. Soc.* **1991,** *113* (4), 1335-1344.
73. Baud, L. G.; Manning, M. A.; Arkless, H. L.; Stephens, T. C.; Unsworth, W. P., Ring-Expansion Approach to Medium-Sized Lactams and Analysis of Their Medicinal Lead-Like Properties. *Chemistry – A European Journal* **2017,** *23* (9), 2225-2230.
74. Donald, J. R.; Unsworth, W. P., Ring-Expansion Reactions in the Synthesis of Macrocycles and Medium-Sized Rings. *Chemistry – A European Journal* **2017,** *23* (37), 8780-8799.
75. Ohnuma, T.; Hata, N.; Miyachi, N.; Wakamatsu, T.; Ban, Y., A synthesis of novel nine-membered dienones through a cyclic acetylenic oxy-cope rearrangement: The synthesis of dl-phoracantholide I. *Tetrahedron Lett.* **1986,** *27* (2), 219-222.
76. John Faulkner, D., Marine natural products. *Nat. Prod. Rep.* **1999,** *16* (2), 155-198.
77. Wang, D.-Z., Neurotoxins from marine dinoflagellates: a brief review. *Mar. Drugs* **2008,** *6* (2), 349-371.
78. Faulkner, D. J., Marine natural products. *Nat. Prod. Rep.* **2001,** *18* (1), 1R-49R.
79. Nicolaou, K. C.; Yang, Z.; Shi, G.-q.; Gunzner, J. L.; Agrios, K. A.; Gärtner, P., Total synthesis of brevetoxin A. *Nature* **1998,** *392* (6673), 264-269.
80. Crimmins, M. T.; Zuccarello, J. L.; Ellis, J. M.; McDougall, P. J.; Haile, P. A.; Parrish, J. D.; Emmitte, K. A., Total Synthesis of Brevetoxin A. *Organic Letters* **2009,** *11* (2), 489-492.
81. Soriano, E.; Marco-Contelles, J., Synthesis of Eight- to Ten-Membered Ring Ethers. In *Synthesis of Saturated Oxygenated Heterocycles II: 7- to 16-Membered Rings*, Cossy, J., Ed. Springer Berlin Heidelberg: Berlin, Heidelberg, 2014; pp 321-368.
82. Yasumoto, T.; Murata, M., Marine toxins. *Chem. Rev.* **1993,** *93* (5), 1897-1909.
83. Crimmins, M. T.; Powell, M. T., Enantioselective Total Synthesis of (+)-Obtusenyne. *J. Am. Chem. Soc.* **2003,** *125* (25), 7592-7595.
84. Denmark, S. E.; Yang, S.-M., Total Synthesis of (+)-Brasilenyne. Application of an Intramolecular Silicon-Assisted Cross-Coupling Reaction. *J. Am. Chem. Soc.* **2004,** *126* (39), 12432-12440.

85. Burton, J. W.; Anderson, E. A.; O'Sullivan, P. T.; Collins, I.; Davies, J. E.; Bond, A. D.; Feeder, N.; Holmes, A. B., The Claisen rearrangement approach to fused bicyclic medium-ring oxacycles. *Org. Biomol. Chem.* **2008,** *6* (4), 693-702.
86. Crimmins, M. T.; Ellis, J. M.; Emmitte, K. A.; Haile, P. A.; McDougall, P. J.; Parrish, J. D.; Zuccarello, J. L., Enantioselective Total Synthesis of Brevetoxin A: Unified Strategy for the B, E, G, and J Subunits. *Chemistry – A European Journal* **2009,** *15* (36), 9223-9234.
87. Kopp, F.; Stratton, C. F.; Akella, L. B.; Tan, D. S., A diversity-oriented synthesis approach to macrocycles via oxidative ring expansion. *Nat. Chem. Biol.* **2012,** *8*, 358.
88. Xu, X.; Han, X.; Yang, L.; Hu, W., Highly Diastereoselective Synthesis of Fully Substituted Tetrahydrofurans by a One-Pot Cascade Reaction of Aryldiazoacetates with Allyl Alcohols. *Chemistry – A European Journal* **2009,** *15* (46), 12604-12607.
89. Jing, C.; Xing, D.; Gao, L.; Li, J.; Hu, W., Divergent Synthesis of Multisubstituted Tetrahydrofurans and Pyrrolidines via Intramolecular Aldol-type Trapping of Onium Ylide Intermediates. *Chemistry – A European Journal* **2015,** *21* (52), 19202-19207.
90. Lu, C.-D.; Chen, Z.-Y.; Liu, H.; Hu, W.-H.; Mi, A.-Q.; Doyle, M. P., A Facile Three-Component One-Pot Synthesis of Structurally Constrained Tetrahydrofurans That Are t-RNA Synthetase Inhibitor Analogues. *The Journal of Organic Chemistry* **2004,** *69* (14), 4856-4859.
91. Hashimoto, Y.; Itoh, K.; Kakehi, A.; Shiro, M.; Suga, H., Diastereoselective Synthesis of Tetrahydrofurans by Lewis Acid Catalyzed Intermolecular Carbenoid–Carbonyl Reaction–Cycloaddition Sequences: Unusual Diastereoselectivity of Lewis Acid Catalyzed Cycloadditions. *The Journal of Organic Chemistry* **2013,** *78* (12), 6182-6195.
92. Wu, J.-Q.; Yang, Z.; Zhang, S.-S.; Jiang, C.-Y.; Li, Q.; Huang, Z.-S.; Wang, H., From Indoles to Carbazoles: Tandem Cp*Rh(III)-Catalyzed C–H Activation/Brønsted Acid-Catalyzed Cyclization Reactions. *ACS Catalysis* **2015,** *5* (11), 6453-6457.
93. Iosub, A. V.; Stahl, S. S., Palladium-Catalyzed Aerobic Oxidative Dehydrogenation of Cyclohexenes to Substituted Arene Derivatives. *J. Am. Chem. Soc.* **2015,** *137* (10), 3454-3457.
94. Thies, R. W., Siloxy-Cope and oxy-Cope rearrangements of the cis-1-vinylcyclonon-3-en-1-o1 system. Effective two-carbon ring expansion. *J. Am. Chem. Soc.* **1972,** *94* (20), 7074-7080.
95. Zhu, Y.; Zhai, C.; Yang, L.; Hu, W., Copper(ii)-catalyzed highly diastereoselective three-component reactions of aryl diazoacetates with alcohols and chalcones: an easy access to furan derivatives. *Chemical Communications* **2010,** *46* (16), 2865-2867.
96. Lutz, R. P., Catalysis of the Cope and Claisen rearrangements. *Chem. Rev.* **1984,** *84* (3), 205-247.
97. Front Matter. In *Natural Lactones and Lactams*.
98. Kim, E.; Lim, S.-M.; Kim, M.-S.; Yoo, S.-H.; Kim, Y., Phyllodulcin, a Natural Sweetener, Regulates Obesity-Related Metabolic Changes and Fat Browning-Related Genes of Subcutaneous White Adipose Tissue in High-Fat Diet-Induced Obese Mice. *Nutrients* **2017,** *9* (10), 1049.
99. Kitaura, T.; Endo, H.; Nakamoto, H.; Ishihara, M.; Kawai, T.; Nokami, J., Isolation and synthesis of a new natural lactone in apple juice (Malus × domestica var. Orin). *Flavour and Fragrance Journal* **2004,** *19* (3), 221-224.

100. Surburg, H., Panten, J., Individual Fragrance and Flavor Materials. In *Common Fragrance and Flavor Materials*, Panten, H. S. a. J., Ed. 2006.
101. Kenji Kinoshita, R. S., Masashi Awata, Masaki Takada, Satoshi Yaginuma, *The Journal of Antibiotics* **1997,** *50* (11), 4.
102. Jansen, R.; Kunze, B.; Reichenbach, H.; Höfle, G., Apicularen A and B, Cytotoxic 10-Membered Lactones with a Novel Mechanism of Action from Chondromyces Species (Myxobacteria): Isolation, Structure Elucidation, and Biosynthesis. *European J. Org. Chem.* **2000,** *2000* (6), 913-919.
103. Croston, G. E.; Olsson, R.; Currier, E. A.; Burstein, E. S.; Weiner, D.; Nash, N.; Severance, D.; Allenmark, S. G.; Thunberg, L.; Ma, J.-N.; Mohell, N.; O'Dowd, B.; Brann, M. R.; Hacksell, U., Discovery of the First Nonpeptide Agonist of the GPR14/Urotensin-II Receptor: 3-(4-Chlorophenyl)-3-(2- (dimethylamino)ethyl)isochroman-1-one (AC-7954). *J. Med. Chem.* **2002,** *45* (23), 4950-4953.
104. Lagoutte, R.; Besnard, C.; Alexakis, A., Direct Organocatalysed Double Michael Addition of α-Angelica Lactone to Enones. *European J. Org. Chem.* **2016,** *2016* (25), 4372-4381.
105. Rullière, P.; Cannillo, A.; Grisel, J.; Cividino, P.; Sébastien, C.; Poisson, J.-F., Total Synthesis of Proteasome Inhibitor (−)-Omuralide through Asymmetric Ketene [2 + 2]-Cycloaddition. *Organic Letters* **2018,** *20* (15), 4558-4561.
106. Owen, W. J.; Yao, C.; Myung, K.; Kemmitt, G.; Leader, A.; Meyer, K. G.; Bowling, A. J.; Slanec, T.; Kramer, V. J., Biological characterization of fenpicoxamid, a new fungicide with utility in cereals and other crops. *Pest Management Science* **2017,** *73* (10), 2005-2016.
107. Changcheng, J.; Dong, X.; Lixin, G.; Jia, L.; Wenhao, H., Divergent Synthesis of Multisubstituted Tetrahydrofurans and Pyrrolidines via Intramolecular Aldol-type Trapping of Onium Ylide Intermediates. *Chemistry – A European Journal* **2015,** *21* (52), 19202-19207.
108. Choi, S.; Song, C. W.; Shin, J. H.; Lee, S. Y., Biorefineries for the production of top building block chemicals and their derivatives. *Metabolic Engineering* **2015,** *28*, 223-239.
109. Lee, S.-H.; Park, O.-J., Uses and production of chiral 3-hydroxy-γ-butyrolactones and structurally related chemicals. *Appl. Microbiol. Biotechnol.* **2009,** *84* (5), 817-828.
110. Evidente, A.; Lanzetta, R.; Capasso, R.; Vurro, M.; Botralico, A., Pinolidoxin, a phytotoxic nonenolide from Ascochyta pinodes. *Phytochemistry* **1993,** *34* (4), 999-1003.
111. Hussain, A.; Yousuf, S. K.; Mukherjee, D., Importance and synthesis of benzannulated medium-sized and macrocyclic rings (BMRs). *RSC Advances* **2014,** *4* (81), 43241-43257.
112. Nicolaou, K. C.; Yang, Z.; Shi, G.-q.; Gunzner, J. L.; Agrios, K. A.; Gärtner, P., Total synthesis of brevetoxin A. *Nature* **1998,** *392*, 264.
113. Brown, B. R., The mechanism of thermal decarboxylation. *Quarterly Reviews, Chemical Society* **1951,** *5* (2), 131-146.
114. Ma, C.; Xing, D.; Zhai, C.; Che, J.; Liu, S.; Wang, J.; Hu, W., Iron Porphyrin-Catalyzed Three-Component Reaction of Ethyl Diazoacetate with Aliphatic Amines and β,γ-Unsaturated α-Keto Esters. *Organic Letters* **2013,** *15* (24), 6140-6143.
115. Tortoreto, C.; Rackl, D.; Davies, H. M. L., Metal-Free C–H Functionalization of Alkanes by Aryldiazoacetates. *Organic Letters* **2017,** *19* (4), 770-773.

116. Kaur, J.; Kumari, A.; Bhardwaj, V. K.; Chimni, S. S., Chiral Squaramide-Catalyzed Enantioselective Decarboxylative Addition of β-Keto Acids to Isatin Imines. *Advanced Synthesis & Catalysis* **2017,** *359* (10), 1725-1734.
117. Wang, S.; Cao, L.; Shi, H.; Dong, Y.; Sun, J.; Hu, Y., Preparation of 2-Pyridone-Containing Tricyclic Alkaloid Derivatives as Potential Inhibitors of Tumor Cell Proliferation by Regioselective Intramolecular N- and C-Acylation of 2-Pyridone. *Chem. Pharm. Bull. (Tokyo)* **2005,** *53* (1), 67-71.
118. Hu, M.; He, Z.; Gao, B.; Li, L.; Ni, C.; Hu, J., Copper-Catalyzed gem-Difluoroolefination of Diazo Compounds with TMSCF3 via C–F Bond Cleavage. *J. Am. Chem. Soc.* **2013,** *135* (46), 17302-17305.
119. Zhang, Z.; Sheng, Z.; Yu, W.; Wu, G.; Zhang, R.; Chu, W.-D.; Zhang, Y.; Wang, J., Catalytic asymmetric trifluoromethylthiolation via enantioselective [2,3]-sigmatropic rearrangement of sulfonium ylides. *Nat. Chem.* **2017,** *9*, 970.
120. Davis, O. A.; Croft, R. A.; Bull, J. A., Synthesis of diversely functionalised 2,2-disubstituted oxetanes: fragment motifs in new chemical space. *Chemical Communications* **2015,** *51* (84), 15446-15449.
121. Xu, B.; Zhu, S.-F.; Zuo, X.-D.; Zhang, Z.-C.; Zhou, Q.-L., Enantioselective N□H Insertion Reaction of α-Aryl α-Diazoketones: An Efficient Route to Chiral α-Aminoketones. *Angewandte Chemie International Edition* **2014,** *53* (15), 3913-3916.
122. Ošeka, M.; Kimm, M.; Kaabel, S.; Järving, I.; Rissanen, K.; Kanger, T., Asymmetric Organocatalytic Wittig [2,3]-Rearrangement of Oxindoles. *Organic Letters* **2016,** *18* (6), 1358-1361.
123. Mejuch, T.; Gilboa, N.; Gayon, E.; Wang, H.; Houk, K. N.; Marek, I., Axial Preferences in Allylation Reactions via the Zimmerman–Traxler Transition State. *Acc. Chem. Res.* **2013,** *46* (7), 1659-1669.
124. Meier, H.; Zeller, K.-P., The Wolff Rearrangement of α-Diazo Carbonyl Compounds. *Angewandte Chemie International Edition in English* **1975,** *14* (1), 32-43.
125. Parr, B. T.; Davies, H. M. L., Highly stereoselective synthesis of cyclopentanes bearing four stereocentres by a rhodium carbene-initiated domino sequence. *Nature Communications* **2014,** *5*, 4455.
126. Parr, B. T.; Davies, H. M. L., Stereoselective Synthesis of Highly Substituted Cyclohexanes by a Rhodium-Carbene Initiated Domino Sequence. *Organic Letters* **2015,** *17* (4), 794-797.
127. Minami, A.; Ozaki, T.; Liu, C.; Oikawa, H., Cyclopentane-forming di/sesterterpene synthases: widely distributed enzymes in bacteria, fungi, and plants. *Nat. Prod. Rep.* **2018,** *35* (12), 1330-1346.
128. Malinowski, J. T.; Sharpe, R. J.; Johnson, J. S., Enantioselective Synthesis of Pactamycin, a Complex Antitumor Antibiotic. *Science* **2013,** *340* (6129), 180.
129. Inman, M.; Moody, C. J., Indole synthesis – something old, something new. *Chemical Science* **2013,** *4* (1), 29-41.
130. Fairfax, D. J.; Austin, D. J.; Xu, S. L.; Padwa, A., Alternatives to α-diazo ketones for tandem cyclization–cycloaddition and carbenoid–alkyne metathesis strategies. Novel cyclic enol–ether formation via carbonyl ylide rearrangement reactions. *Journal of the Chemical Society, Perkin Transactions 1* **1992,** (21), 2837-2844.

131. Marien, N.; Reddy, B. N.; De Vleeschouwer, F.; Goderis, S.; Van Hecke, K.; Verniest, G., Metal-Free Cyclization of ortho-Nitroaryl Ynamides and Ynamines towards Spiropseudoindoxyls. *Angewandte Chemie* **2018,** *130* (20), 5762-5766.
132. Doyle, M. P.; Hu, W.; Chapman, B.; Marnett, A. B.; Peterson, C. S.; Vitale, J. P.; Stanley, S. A., Enantiocontrolled Macrocycle Formation by Catalytic Intramolecular Cyclopropanation. *J. Am. Chem. Soc.* **2000,** *122* (24), 5718-5728.
133. Zhang, Z.; Wang, J., Recent studies on the reactions of α-diazocarbonyl compounds. *Tetrahedron* **2008,** *64* (28), 6577-6605.
134. Casadei, M. A.; Galli, C.; Mandolini, L., Ring-closure reactions. 22. Kinetics of cyclization of diethyl (.omega.-bromoalkyl)malonates in the range of 4- to 21-membered rings. Role of ring strain. *J. Am. Chem. Soc.* **1984,** *106* (4), 1051-1056.
135. Brown, H. C.; Ichikawa, K., Chemical effects of steric strains—XIV: The effect of ring size on the rate of reaction of the cyclanones with sodium borohydride. *Tetrahedron* **1957,** *1* (3), 221-230.
136. Reetz, M. T.; Hugel, H.; Dresely, K., The relative reactivity of cyclic ketones towards methyltitanium reagents. *Tetrahedron* **1987,** *43* (1), 109-114.
137. Larsen, E. M.; Chang, C.-F.; Sakata-Kato, T.; Arico, J. W.; Lombardo, V. M.; Wirth, D. F.; Taylor, R. E., Conformation-guided analogue design identifies potential antimalarial compounds through inhibition of mitochondrial respiration. *Org. Biomol. Chem.* **2018,** *16* (30), 5403-5406.
138. Larsen, E. M.; Wilson, M. R.; Taylor, R. E., Conformation–activity relationships of polyketide natural products. *Nat. Prod. Rep.* **2015,** *32* (8), 1183-1206.
139. Paquette, L. A., Stereocontrolled Construction of Complex Cyclic Ketones via Oxy-Cope Rearrangement. *Angewandte Chemie International Edition in English* **1990,** *29* (6), 609-626.
140. Supurgibekov, M. B.; Cantillo, D.; Kappe, C. O.; Surya Prakash, G. K.; Nikolaev, V. A., Effect of configuration of 2-vinyldiazocarbonyl compounds on their reactivity: experimental and computational study. *Org. Biomol. Chem.* **2014,** *12* (4), 682-689.
141. Davies, H. M. L.; Mark Hodges, L.; Matasi, J. J.; Hansen, T.; Stafford, D. G., Effect of carbenoid structure on the reactivity of rhodium-stabilized carbenoids. *Tetrahedron Lett.* **1998,** *39* (25), 4417-4420.
142. Wolf, J. R.; Hamaker, C. G.; Djukic, J.-P.; Kodadek, T.; Woo, L. K., Shape and stereoselective cyclopropanation of alkenes catalyzed by iron porphyrins. *J. Am. Chem. Soc.* **1995,** *117* (36), 9194-9199.
143. Salomon, R. G.; Kochi, J. K., Copper(I) catalysis in cyclopropanations with diazo compounds. Role of olefin coordination. *J. Am. Chem. Soc.* **1973,** *95* (10), 3300-3310.
144. Jing, C.; Xing, D.; Hu, W., Highly diastereoselective synthesis of 3-hydroxy-2,2,3-trisubstituted indolines via intramolecular trapping of ammonium ylides with ketones. *Chemical Communications* **2014,** *50* (8), 951-953.
145. Manske, R. H., The Chemistry of Quinolines. *Chem. Rev.* **1942,** *30* (1), 113-144.
146. Chung, P.-Y.; Bian, Z.-X.; Pun, H.-Y.; Chan, D.; Chan, A. S.-C.; Chui, C.-H.; Tang, J. C.-O.; Lam, K.-H., Recent advances in research of natural and synthetic bioactive quinolines. *Future Med. Chem.* **2015,** *7* (7), 947–967.
147. Afzal, O.; Kumar, S.; Haider, M. R.; Ali, M. R.; Kumar, R.; Jaggi, M.; Bawa, S., A review on anticancer potential of bioactive heterocycle quinoline. *Eur. J. Med. Chem.* **2015,** *97*, 871–910.

148. Marella, A.; Tanwar, O. P.; Saha, R.; Ali, M. R.; Srivastava, S.; Akhter, M.; Shaquiquzzaman, M.; Alam, M. M., Quinoline: A versatile heterocyclic. *Saudi Pharmaceutical Journal* **2013,** *21* (1), 1-12.
149. Afzal, O.; Kumar, S.; Haider, M. R.; Ali, M. R.; Kumar, R.; Jaggi, M.; Bawa, S., A review on anticancer potential of bioactive heterocycle quinoline. *Eur. J. Med. Chem.* **2015,** *97*, 871-910.
150. Marella, A.; Tanwar, O. P.; Saha, R.; Ali, M. R.; Srivastava, S.; Akhter, M.; Shaquiquzzaman, M.; Alam, M. M., Quinoline: A versatile heterocyclic. *Saudi Pharm J* **2013,** *21* (1), 1–12.
151. Hunter, A. C.; Chinthapally, K.; Sharma, I., Rh2(esp)2: An Efficient Catalyst for O-H Insertion Reactions of Carboxylic Acids into Acceptor/Acceptor Diazo Compounds. *Eur. J. Org. Chem.* **2016,** *2016* (13), 2260–2263.
152. Hunter, A. C.; Schlitzer, S. C.; Sharma, I., Synergistic Diazo-OH Insertion/Conia-Ene Cascade Catalysis for the Stereoselective Synthesis of γ-Butyrolactones and Tetrahydrofurans. *Chem. - Eur. J.* **2016,** *22* (45), 16062–16065.
153. Zhao, X.; Zhang, Y.; Wang, J., Recent developments in copper-catalyzed reactions of diazo compounds. *Chem. Commun.* **2012,** *48* (82), 10162–10173.
154. Ma, C.; Xing, D.; Zhai, C.; Che, J.; Liu, S.; Wang, J.; Hu, W., Iron Porphyrin-Catalyzed Three-Component Reaction of Ethyl Diazoacetate with Aliphatic Amines and β,γ-Unsaturated α-Keto Esters. *Org. Lett.* **2013,** *15* (24), 6140–6143.
155. Yang, T.; Zhuang, H.; Lin, X.; Xiang, J.-N.; Elliott, J. D.; Liu, L.; Ren, F., A catalyst-free N-H insertion/Mannich-type reaction cascade of α-nitrodiazoesters. *Tetrahedron Lett.* **2013,** *54* (32), 4159–4163.
156. Davies, H. M. L.; Clark, D. M.; Alligood, D. B.; Eiband, G. R., Mechanistic aspects of formal [3 + 4] cycloadditions between vinyl carbenoids and furans. *Tetrahedron* **1987,** *43* (19), 4265–4270.
157. Davies, H. M. L.; Ahmed, G.; Churchill, M. R., Asymmetric Synthesis of Highly Functionalized 8-Oxabicyclo[3.2.1]octene Derivatives. *J. Am. Chem. Soc.* **1996,** *118* (44), 10774–10782.
158. Davies, H. M. L.; Hedley, S. J., Intermolecular reactions of electron-rich heterocycles with copper and rhodium carbenoids. *Chem. Soc. Rev.* **2007,** *36* (7), 1109–1119.
159. Goto, T.; Takeda, K.; Shimada, N.; Nambu, H.; Anada, M.; Shiro, M.; Ando, K.; Hashimoto, S.-I., Highly Enantioselective Cyclopropenation Reaction of 1-Alkynes with α-Alkyl-α-Diazoesters Catalyzed by Dirhodium(II) Carboxylates. *Angew. Chem., Int. Ed.* **2011,** *50* (30), 6803–6808.
160. Lou, Y.; Horikawa, M.; Kloster, R. A.; Hawryluk, N. A.; Corey, E. J., A New Chiral Rh(II) Catalyst for Enantioselective [2 + 1]-Cycloaddition. Mechanistic Implications and Applications. *J. Am. Chem. Soc.* **2004,** *126* (29), 8916-8918.
161. Zheng, Y.; Mao, J.; Weng, Y.; Zhang, X.; Xu, X., Cyclopentadiene Construction via Rh-Catalyzed Carbene/Alkyne Metathesis Terminated with Intramolecular Formal [3 + 2] Cycloaddition. *Org. Lett.* **2015,** *17* (22), 5638–5641.
162. Qiu, H.; Deng, Y.; Marichev, K. O.; Doyle, M. P., Diverse Pathways in Catalytic Reactions of Propargyl Aryldiazoacetates: Selectivity between Three Reaction Sites. *J. Org. Chem.* **2017,** *82* (3), 1584–1590.

163. Jansone-Popova, S.; May, J. A., Synthesis of Bridged Polycyclic Ring Systems via Carbene Cascades Terminating in C-H Bond Insertion. *J. Am. Chem. Soc.* **2012,** *134* (43), 17877–17880.
164. CCDC1.
165. Anderson, K.; Calo, F.; Pfaffeneder, T.; White, A. J. P.; Barrett, A. G. M., Biomimetic Total Synthesis of Angelicoin A and B via a Palladium-Catalyzed Decarboxylative Prenylation-Aromatization Sequence. *Org. Lett.* **2011,** *13* (21), 5748–5750.
166. Jing, C.; Xing, D.; Hu, W., Highly diastereoselective synthesis of 3-hydroxy-2,2,3-trisubstituted indolines via intramolecular trapping of ammonium ylides with ketones. *Chem. Commun.* **2014,** *50* (8), 951–953.
167. Janardhanam, S.; Devan, B.; Rajagopalan, K., Ring enlargement-annulation via thermal oxy-Cope rearrangement. *Tetrahedron Lett.* **1993,** *34* (42), 6761–6764.
168. Evans, D. A.; Baillargeon, D. J.; Nelson, J. V., A general approach to the synthesis of 1,6-dicarbonyl substrates. New applications of base-accelerated oxy-Cope rearrangements. *J. Am. Chem. Soc.* **1978,** *100* (7), 2242–2244.
169. Paquette, L. A.; Combrink, K. D.; Elmore, S. W.; Rogers, R. D., Impact of substituent modifications on the atropselectivity characteristics of an anionic oxy-Cope ring expansion. *J. Am. Chem. Soc.* **1991,** *113* (4), 1335–1344.
170. Verma, S. K.; Fleischer, E. B.; Moore, H. W., Synthesis of Angular Triquinanes from 1-Alkynylbicyclo[3.2.0]hept-2-en-7-ones. A Tandem Alkoxy-Cope Ring Expansion/Transannular Ring Closure Reaction. *J. Org. Chem.* **2000,** *65* (25), 8564–8573.
171. Chen, C.; Layton, M. E.; Shair, M. D., Stereospecific Synthesis of the CP-263,114 Core Structure. *J. Am. Chem. Soc.* **1998,** *120* (41), 10784–10785.
172. Miao, C.-B.; Zeng, Y.-M.; Shi, T.; Liu, R.; Wei, P.-F.; Sun, X.-Q.; Yang, H.-T., 2-Oxindole Acts as a Synthon of 2-Aminobenzoyl Anion in the K2CO3-Catalyzed Reaction with Enones: Preparation of 1,4-Diketones Bearing an Amino Group and Their Further Transformations. *J. Org. Chem.* **2016,** *81* (1), 43–50.
173. Snieckus, V.; Richardson, P., One-Pot Rhodium-Catalyzed Synthesis of Highly Substituted Quinolines. *Synfacts* **2018,** *14* (03), 0234.
174. Gerasimenko, I.; Sheludko, Y.; Stöckigt, J., 3-Oxo-rhazinilam: A New Indole Alkaloid from Rauvolfia serpentina × Rhazya stricta Hybrid Plant Cell Cultures. *J. Nat. Prod.* **2001,** *64* (1), 114-116.
175. Gigant, B.; Wang, C.; Ravelli, R. B. G.; Roussi, F.; Steinmetz, M. O.; Curmi, P. A.; Sobel, A.; Knossow, M., Structural basis for the regulation of tubulin by vinblastine. *Nature* **2005,** *435* (7041), 519-522.
176. Deutsch, H. F.; Evenson, M. A.; Drescher, P.; Sparwasser, C.; Madsen, P. O., Isolation and biological activity of aspidospermine and quebrachamine from an Aspidosperma tree source. *J. Pharm. Biomed. Anal.* **1994,** *12* (10), 1283-1287.
177. Szostak, M.; Aubé, J., Direct Synthesis of Medium-Bridged Twisted Amides via a Transannular Cyclization Strategy. *Organic Letters* **2009,** *11* (17), 3878-3881.
178. Hall, J. E.; Matlock, J. V.; Ward, J. W.; Gray, K. V.; Clayden, J., Medium-Ring Nitrogen Heterocycles through Migratory Ring Expansion of Metalated Ureas. *Angewandte Chemie International Edition* **2016,** *55* (37), 11153-11157.
179. Hill, J. E.; Matlock, J. V.; Lefebvre, Q.; Cooper, K. G.; Clayden, J., Consecutive Ring Expansion and Contraction for the Synthesis of 1-Aryl Tetrahydroisoquinolines and

Tetrahydrobenzazepines from Readily Available Heterocyclic Precursors. *Angewandte Chemie International Edition* **2018,** *57* (20), 5788-5791.
180. Roche, C.; Labeeuw, O.; Haddad, M.; Ayad, T.; Genet, J.-P.; Ratovelomanana-Vidal, V.; Phansavath, P., Synthesis of anti-1,3-Diols through RuCl3/PPh3-Mediated Hydrogenation of β-Hydroxy Ketones: An Alternative to Organoboron Reagents. *European J. Org. Chem.* **2009,** *2009* (23), 3977-3986.
181. Hong, B.-C.; Chin, S.-F., Lanthanide(III) Promoted Aldol Condensation of Enones and Aldehydes1. *Synthetic Communications* **1997,** *27* (7), 1191-1197.
182. Batt, F.; Bourcet, E.; Kassab, Y.; Fache, F., Selective Aerobic Oxidation of Allylic Alcohols to Carbonyl Compounds Using Catalytic Pd(OAc)2: High Intramolecular Selectivity. *Synlett* **2007,** *2007* (12), 1869-1872.
183. Prandi, C.; Venturello, P., 1,1-Diethoxybut-2-ene as a Precursor of (2-Hydroxyethyl)-Substituted Alkoxy Dienes: Convenient Intermediates for a New Synthesis of 2-Substituted and 2,6-Disubstituted Tetrahydro-4H-pyran-4-ones. *The Journal of Organic Chemistry* **1994,** *59* (12), 3494-3496.
184. M., N. S.; William, L.; J., H. C.; J., M. C., Stereoselective Synthesis of Highly Substituted Tetrahydrofurans through Diverted Carbene O□H Insertion Reaction. *Angewandte Chemie International Edition* **2015,** *54* (29), 8485-8489.
185. Loy, N. S. Y.; Singh, A.; Xu, X.; Park, C.-M., Synthesis of Pyridines by Carbenoid-Mediated Ring Opening of 2H-Azirines. *Angewandte Chemie International Edition* **2013,** *52* (8), 2212-2216.
186. Yaeghoobi, M.; Frimayanti, N.; Chee, C. F.; Ikram, K. K.; Najjar, B. O.; Zain, S. M.; Abdullah, Z.; Wahab, H. A.; Rahman, N. A., QSAR, in silico docking and in vitro evaluation of chalcone derivatives as potential inhibitors for H1N1 virus neuraminidase. *Med. Chem. Res.* **2016,** *25* (10), 2133-2142.
187. Lee, J. I.; Jung, H.-J., Effective synthesis of 2,3-dihydro-2-phenyl-4-quinolone from 2'-aminoacetophenone. *Journal of the Korean Chemical Society* **2007,** *51*, 4.
188. Climent, M. J.; Corma, A.; Iborra, S.; Martí, L., Process Intensification with Bifunctional Heterogeneous Catalysts: Selective One-Pot Synthesis of 2′-Aminochalcones. *ACS Catalysis* **2015,** *5* (1), 157-166.
189. Cheng, S.; Zhao, L.; Yu, S., Enantioselective Synthesis of Azaflavanones Using Organocatalytic 6-endo Aza-Michael Addition. *Advanced Synthesis & Catalysis* **2014,** *356* (5), 982-986.
190. Khoza, A. T.; Maluleka, M. M.; Mama, N.; Mphahlele, J. M., Synthesis and Photophysical Properties of 2-Aryl-6,8-bis(arylethenyl)-4-methoxyquinolines. *Molecules* **2012,** *17* (12).
191. Yang, X.-Y.; Tay, W. S.; Li, Y.; Pullarkat, S. A.; Leung, P.-H., Asymmetric 1,4-Conjugate Addition of Diarylphosphines to α,β,γ,δ-Unsaturated Ketones Catalyzed by Transition-Metal Pincer Complexes. *Organometallics* **2015,** *34* (20), 5196-5201.
192. Zhao, F.; Zhao, Q.-J.; Zhao, J.-X.; Zhang, D.-Z.; Wu, Q.-Y.; Jin, Y.-S., Synthesis and cdc25B inhibitory activity evaluation of chalcones. *Chemistry of Natural Compounds* **2013,** *49* (2), 206-214.
193. Dias, L. C.; de Lucca, E. C., Total Synthesis of (−)-Marinisporolide C. *The Journal of Organic Chemistry* **2017,** *82* (6), 3019-3045.

194. Pagar, V. V.; Jadhav, A. M.; Liu, R.-S., Gold-Catalyzed Formal [3 + 3] and [4 + 2] Cycloaddition Reactions of Nitrosobenzenes with Alkenylgold Carbenoids. *J. Am. Chem. Soc.* **2011,** *133* (51), 20728-20731.
195. Tang, E.; Chen, B.; Zhang, L.; Li, W.; Lin, J., ZnCl2-Catalyzed Intramolecular Cyclization Reaction of 2-Aminochalcones Using Polymer-Supported Selenium Reagent: Synthesis of 2-Phenyl-4-quinolones and 2-Phenyl-2,3-dihydroquinolin-4(1H)-one. *Synlett* **2011,** *2011* (05), 707-711.
196. Litkei, G.; Tkés, A. L., Oxidation of the 2′ -NHR Analogues of 2′ -OR-Chalcones; Conversion of 2′ -NHR-Chalcone Epoxides. *Synthetic Communications* **1991,** *21* (15-16), 1597-1609.

Autobiographical Statement

Education

08/2014-present	**Ph.D. in Chemistry** with Dr. Indrajeet Sharma at University of Oklahoma, OK "Metal Carbenoid Initiated Cascades for the Synthesis of Diverse Heterocycles"
08/2012-07/2014	**M.S. in Chemistry** with Dr. Fehmi Damkaci at the State University of New York at Oswego, NY "The attempted total synthesis of Trigonoine B"
08/2007-05/2012	**B.A. in Chemistry** with Dr. Fehmi Damkaci at the State University of New York at Oswego, NY "N-picolinamides as ligands for Ullmann-type homocoupling reactions."

Peer-Reviewed Publications

7. Chinthapally, K.; **Massaro, N. P.**; Sharma, I. "Rhodium Carbenoid Initiated Heteroatom Insertion/Aldol/oxy-Cope Cascade for the Stereoselective Synthesis of Benzannulated Medium-Sized Heterocycles." **2019**, (Manuscript in Preparation).

6. **Massaro, N. P.**; Chatterji, A.; Sharma, I. "An Efficient Three Component Approach to Pyridine Stabilized Ketenimines for the Synthesis of Diverse Heterocycles." **2019**, (Just submitted).

5. **Massaro, N. P.**; Stevens, J. C.; Chatterji, A.; Sharma, I. "Stereoselective Synthesis of Diverse Lactones through a Cascade Reaction of Rhodium Carbenoids with Ketoacids." *Org. Lett.* **2018**, *20*, 7585–7589. DOI: 10.1021/acs.orglett.8b03327

4. **Massaro, N. P.**.; Chinthapally, K.;(authors contributed equally) Sharma, I. "A serendipitous cascade of rhodium vinylcarbenoids with aminochalcones for the synthesis of functionalized quinolines" *Chem. Commun*., **2017**, *53*, 12205–12208.

- highlighted by Victor Snieckus and Paul Richardson (Pfizer) in *Synfacts*. *Synfacts* **2018**, *14*, 0234. DOI: 10.1055/s-0037-1609309.

3. Chinthapally, K.; **Massaro, N. P.**; Sharma, I. "Rhodium Carbenoid Initiated O–H Insertion/Aldol/Oxy-Cope Cascade for the Stereoselective Synthesis of Functionalized Oxacycles." *Org. Lett.* **2016**, *18*, 6340–6343. DOI: 10.1021/acs.orglett.6b03229.

- highlighted by Douglas F. Taber in Organic Chemistry Portal. See https://www.organic-chemistry.org/Highlights/2017/10April.shtm

2. Gupta, A.; Gomes, I.; Bobeck, E. N.; Fakira, A. K.; **Massaro, N. P.**; Sharma, I.; Cave, A.; Hamm, H. E.; Parello, J.; Devi, L. A. "Collybolide is a Novel Biased Agonist of κ-

Opioid Receptors with Potent Antipruritic Activity" *Proc. Natl. Acad. Sci. (PNAS), USA.* **2016**, *113*, 6041–6046. DOI: 10.1073/pnas.1521825113.

1. Damkaci, F.; Altay, E.; Waldron, M.; Knopp, M. A.; Snow, D.; **Massaro, N. P.** N-picolinamides as ligands for Ullmann-type homocoupling reactions. *Tetrahedron Letters* **2014**, *55* (3), 690–693 DOI: 10.1016/j.tetlet.2013.11.111.

Honors and Awards

05/2019	Selected for TexSyn IV speed talk; only 8 total selected within conference
04/2019	Roland Lehr Scholarship for outstanding performance in research and teaching.
07/2018	Selected for ACS, Division of Organic Chemistry sponsored Graduate Research Symposium among **top 50** chemistry 4th year graduate students
05/2018	Robberson Research and Creative Endeavors Grant
10/2017	Robberson Research Travel Award
05/2017	International Narcotics Research Conference Travel Award
04/2015	Michael R. Abraham Graduate Teaching Assistant Award
05/2014	Dr. H. Alan Ewart Memorial Scholarship
05/2013	Augustine Silveira, Jr. Research Award in Chemistry
2007-2011	NCAA Division III Wrestler

Presentation and Poster Sessions

05/2019	Oral and poster presentation at the TexSynIV 2019 hosted at Baylor University in Waco Texas.
04/2019	"A Metal Carbenoid Initiated Cascade for the Synthesis of Diverse Medium-sized Heterocycles." Oral presentation at the ACS 64th Annual Pentasectional Meeting hosted at the University of Oklahoma.
07/2018	"Metal Carbenoid Initiated Cascades for the Synthesis of Diverse Heterocycles." Research Poster Session at the Division of Organic Chemistry Graduate Research Symposium (Doc GRS) 2018 at the University of Indiana in Bloomington.
07/2017	"Design and Synthesis of Collybolide Probes for Kappa-Opioid Receptor." Research Presentation and Poster Session at International Narcotics Research Conference (INRC) 2017 in Chicago.
05/2017	Research Poster Session at the TexSynIII 2017 hosted at UT Southwestern in Dallas Texas.
07/2014	"The Total Synthesis of Trigonoine B." Research Presentation at the Master's Level Graduate Research Conference (MaRC) in Brockport New York 2014.

Professional and Leadership Experience

01/2019-present	**Lecturer for Organic Chemistry and Director of Organic Chemistry Labs for CHEM 3152** with Dr. Robyn Biggs at the University of Oklahoma
01/2016-present	**Graduate Research Assistant** with Dr. Indrajeet Sharma at the University of Oklahoma
01/2015-12/2015	**Head Graduate Teaching Assistant** with Dr. Laura Clifford at the University of Oklahoma for General Chemistry Course
08/2014-12/2014	**Graduate Teaching Assistant** with Dr. Laura Clifford at the University of Oklahoma for General Chemistry Course
08/2012-07/2014	**Graduate Teaching Assistant** at SUNY Oswego for General, Instrumental, and Introduction to Organic Chemistry Courses
08/2011-07/2012	**Volunteer Assistant Collegiate Wrestling Coach** at SUNY Oswego with coach Mike Howard

Memberships

Division of Organic Chemistry ACS
American Chemical Society

Teaching Workshops Attended

09/2016	Center for Teaching Excellence Workshop: Teaching Philosophy Statement
09/2016	Graduate Student Life Workshop: Digital Identity
03/2016	Center for Teaching Excellence Seminar: How Students Learn
04/2014	PKAL Upstate New York Regional Network, Improving Learning in Undergraduate STEM at Monroe Community College